ISSUED

DOE/WIPP-20-3610
Volume 1

Waste Isolation Pilot Plant

Geotechnical Analysis Report for July 2018 – June 2019

U.S. Department of Energy
Carlsbad Field Office

October 2020

This document has been submitted as required to:

U.S. Department of Energy
Office of Scientific and Technical Information
PO Box 62
Oak Ridge, TN 37831
(865) 576-8401

Additional information about this document may be obtained by calling 1-800-336-9477

Unlimited, publicly available full-text scientific and technical reports produced since 1991 are available online at Information Bridge (www.osti.gov/bridge).

U.S Department of Energy and its contractors may obtain full-text reports produced prior to 1991 in paper form for a processing fee from:

U.S. Department of Energy
Office of Scientific and Technical Information
P.O. Box 62
Oak Ridge, TN 37831-0062
Telephone: (865) 576-8401
E-mail: reports@osti.gov

Available for sale to the public from:

U.S. Department of Commerce
National Technical Information Service
5301 Shawnee Rd
Alexandria, VA 22312
Email: info@ntis.gov

Waste Isolation Pilot Plant

Geotechnical Analysis Report for July 2018 – June 2019

U.S. Department of Energy
Carlsbad Field Office

October 2020

Approved by: //signature of file// 10/29/2020
Michael R. Brown Date
Director, Office of Environmental Protection
Carlsbad Field Office

FOREWORD AND ACKNOWLEDGMENTS

This report contains an assessment of the geotechnical status of the Waste Isolation Pilot Plant (WIPP). During the excavation of the WIPP principal underground access and experimental areas, the status was reported quarterly. Since 1987, when the initial construction phase was completed, reports have been published annually. This report presents and analyzes data collected from July 1, 2018, to June 30, 2019.

This Geotechnical Analysis Report (GAR) was written to meet the needs of several audiences. It satisfies requirements contained in the WIPP Hazardous Waste Facility Permit[1] and the Certification of Compliance[2] with Subparts B and C, Title 40 *Code of Federal Regulations* (CFR) Part 191, "Environmental Radiation Protection Standards for Management and Disposal of Spent Nuclear Fuel, High-Level and Transuranic Radioactive Wastes." This report focuses on the geotechnical performance of the various components of the WIPP underground facility, including shaft stations, access drifts, and waste disposal areas. The results of investigations of excavation effects and other geotechnical studies are also included.

This report compares the geotechnical performance of the repository to the design criteria. It describes the techniques that were used to acquire the data. The depth and breadth of the evaluation of the different components of the underground facility vary according to the types and quantities of data available, and the complexity of the recorded geotechnical responses. Graphic documentation of data and tabular documentation of instrument history can be provided upon request.

This GAR was prepared by Nuclear Waste Partnership LLC for the U.S. Department of Energy (DOE), Carlsbad Field Office, in Carlsbad, New Mexico. Work was supported by the DOE under Contract No. DE-EM0001971.

[1] New Mexico Environment Department (NMED), 2016, Waste Isolation Pilot Plant Hazardous Waste Facility Permit, NM4890139088-TSDF, Santa Fe, NM

[2] U.S. Environmental Protection Agency, 1998, "Criteria for the Certification and Recertification of the Waste Isolation Pilot Plant's Compliance with the Disposal Regulations: Certification Decision," *Federal Register*, Vol. 63, No. 95, pp. 27354, May 18, 1998, Washington, DC

CHANGE HISTORY SUMMARY

Revision Number	Date Issued	Description of Changes
0	10/29/2020	• Initial issue.

This page was intentionally left blank.

TABLE OF CONTENTS

ACRONYMS AND ABBREVIATIONS x

1.0 INTRODUCTION 1
1.1 Location and Description 1
1.2 Mission 4
1.3 Development Status 4
1.4 Purpose and Scope of Geomechanical Monitoring Program 5
1.4.1 Instrumentation 6
1.4.2 Data Evaluation 8
1.4.3 Data Errors 9

2.0 GEOLOGY 9
2.1 Regional Stratigraphy 10
2.1.1 Permian 10
2.1.2 Triassic 11
2.1.3 Quaternary 12
2.2 Underground Facility Stratigraphy 14
2.2.1 Disposal Horizon Stratigraphy of Panels 1, 2, 7, and 8 14
2.2.2 Disposal Horizon Stratigraphy of Panels 3, 4, 5, 6 and 8 17
2.2.3 Northeast Area Stratigraphy 17

3.0 PERFORMANCE OF SHAFTS AND KEYS 19
3.1 Salt Shaft 19
3.1.1 Shaft Observations 21
3.1.2 Instrumentation 21
3.2 Waste Shaft 24
3.2.1 Shaft Observations 26
3.2.2 Instrumentation 26
3.3 Exhaust Shaft 29
3.3.1 Quarterly Exhaust Shaft Inspection 29
3.3.2 Instrumentation 35
3.4 Air Intake Shaft 38
3.4.1 Shaft Performance 38

4.0 PERFORMANCE OF SHAFT STATIONS 40
4.1 Salt Shaft Station 40
4.1.1 Modifications to Excavation and Ground Control Activities 40
4.1.2 Instrumentation 40
4.2 Waste Shaft Station 43
4.2.1 Modifications to Excavation and Ground Control Activities 43
4.2.2 Instrumentation 46
4.3 Air Intake Shaft Station 46
4.3.1 Modifications to Excavation and Ground Control Activities 46
4.3.2 Instrumentation 46

5.0 PERFORMANCE OF ACCESS DRIFTS 46
5.1 Modifications to Excavation and Ground Control Activities 46
5.2 Instrumentation 47
5.2.1 Extensometers 47
5.2.2 Convergence Points 48
5.3 Analysis of Convergence Point and Extensometer Data 48
5.4 Excavation Performance 49

6.0 PERFORMANCE OF THE WASTE DISPOSAL AREA 52
6.1 History 52
6.2 Modifications to Excavations and Ground Control Activities 53
6.3 Instrumentation 54
6.4 Analysis of Extensometer and Convergence Point Data 54
6.5 Excavation Performance 56

7.0 PERFORMANCE OF THE SALT DISPOSAL INVESTIGATIONS AND SALT DEFENSE DISPOSAL INVESTIGATIONS 56
7.1 Ground Control Program 56
7.2 Instrumentation 56
7.3 Analysis of Convergence Point Data 56
7.4 Excavation Performance 56

8.0 GEOSCIENCE PROGRAM 57
8.1 Observation Hole Inspections 57
8.2 Fracture Mapping 60
8.3 Stratigraphic Mapping 60
8.4 Drilling and Geologic Core Descriptions 60

9.0 SUMMARY 61

10.0 REFERENCES 63

LIST OF TABLES

Table 1-1 Geomechanical Instrumentation Data Acquisition 7
Table 4-1 Closure Rates in the Salt Shaft Station 43
Table 5-1 Summary of Modifications and Ground Control Activities in the Access 47
Table 5-2 Radial Convergence Point Installations in the Access Drifts: July 1, 2018 to June 30, 2019 51
Table 5-3 Vertical Closure Rate Changes in Excess of Twenty Percent in the Access Drifts 52
Table 9-1 Comparison of Excavation Performance to System Design Requirements .. 62

LIST OF FIGURES

Figure 1-1 WIPP Location 2
Figure 1-2 Underground Mining and Waste Disposal Configuration as of June 30, 2019 3
Figure 2-1 Regional Geology 13
Figure 2-2 Repository Level Stratigraphy of Panels 1, 2, and 7 16
Figure 2-3 Repository Level Stratigraphy of Panels 3, 4, 5, 6 and 8 18
Figure 3-1 Salt Shaft Stratigraphy 20
Figure 3-2 Salt Shaft Instrumentation 22
Figure 3-3 Salt Shaft Key Instrumentation 23
Figure 3-4 Waste Shaft Stratigraphy 25
Figure 3-5 Waste Shaft Instrumentation 27
Figure 3-6 Waste Shaft Key Instrumentation 28
Figure 3-7 Exhaust Shaft Stratigraphy 31
Figure 3-8 Sample Intake of Exhaust Shaft Air Monitoring System 32
Figure 3-9 Diagram of Exhaust Shaft Fixtures and Seepage Zones (Upper 200 ft) .. 33
Figure 3-10 Location of Interception Wells and Storage Tanks 34
Figure 3-11 Exhaust Shaft Instrumentation 36
Figure 3-12 Exhaust Shaft Key Instrumentation 37
Figure 3-13 Air Intake Shaft Stratigraphy 39
Figure 4-1 Salt Shaft Station Stratigraphy 41
Figure 4-2 Salt Shaft Station Instrumentation After Roof Beam Excavation 42
Figure 4-3 Waste Shaft Station Stratigraphy 44
Figure 4-4 Waste Shaft Station Instrumentation 45
Figure 5-1 Typical Convergence Point Array Configurations Showing Anchor Designations 50
Figure 6-1 Typical Waste Panel Instrument Layout 55
Figure 8-1 Example of Observation Hole Layout at Lower Horizon 58
Figure 8-2 Typical Fracture Pattern at Lower Horizon 59
Figure 8-3 Example Observation Hole Layout at Upper Horizon 59
Figure 8-4 Typical Fracture Patterns at Upper Horizon 60

ACRONYMS AND ABBREVIATIONS

ASTM	American Society for Testing and Materials
bp	before present
bsc	below shaft collar
CFR	Code of Federal Regulations
CH	contact-handled
cm	centimeter(s)
DOE	U.S. Department of Energy
EPA	U.S. Environmental Protection Agency
ft	foot (feet)
GAR	Geotechnical Analysis Report
GIS	geomechanical instrumentation system
in	inch(es)
km	kilometer(s)
kVA	kilovolt ampere(s)
lb(s)	pound(s)
m	meter(s)
Ma	million years
MB	marker bed
NMED	New Mexico Environment Department
OMB	orange marker bed
psi	pound(s) per square inch
RH	remote-handled
SDI	Salt Disposal Investigation
SDDI	Salt Defense Disposal Investigation
SPDV	Site and Preliminary Design Validation
TRU	Transuranic
WIPP	Waste Isolation Pilot Plant

1.0 INTRODUCTION

This Geotechnical Analysis Report (GAR) presents and interprets geotechnical data from the underground excavations at the Waste Isolation Pilot Plant (WIPP). The data, which are obtained as part of a regular monitoring program, are used to characterize conditions, to compare actual performance to the design criteria, and to evaluate and forecast the performance of the underground excavations.

WIPP GARs have been available to the public since 1983. During operation of the Site and Preliminary Design Validation (SPDV) Program, the architect/engineer for the project produced these reports quarterly to document the geomechanical performance during and immediately after early excavations of the underground facility. Since completion of the construction phase of the project in 1987, the management and operating contractor for the facility has prepared these reports annually. This report describes the performance and condition of selected areas of the WIPP for the period July 1, 2018, to June 30, 2019.

This report is divided into 10 sections. Section 1 provides background information on the WIPP, its mission, and the purpose and scope of the geomechanical monitoring program. Section 2 describes the local and regional geology of the WIPP site. Sections 3 and 4 describe the geomechanical instrumentation in the shafts and shaft stations, present the data collected by that instrumentation, and provide interpretation of these data. Sections 5 and 6 present the results of geomechanical monitoring in the two main portions of the WIPP underground (the access drifts and the waste disposal area). Section 7 introduces the Salt Disposal Investigation (SDI) and Salt Defense Disposal Investigation (SDDI) areas. Section 8 discusses the results of the Geoscience Program, which include fracture mapping and observation borehole information. Section 9 summarizes the results of geomechanical monitoring and compares the current excavation performance to the design requirements. Section 10 lists references.

1.1 Location and Description

The WIPP facility is located in southeastern New Mexico, 26 miles (42 kilometers [km]) east of Carlsbad (Figure 1-1). The surface facilities were built on flat to gently rolling terrain that is characteristic of the Los Medaños area. The underground facility is being excavated approximately 2,150 feet (ft) beneath the surface in the Salado Formation. Figure 1-2 shows a plan view of the underground configuration of the WIPP as of June 30, 2019.

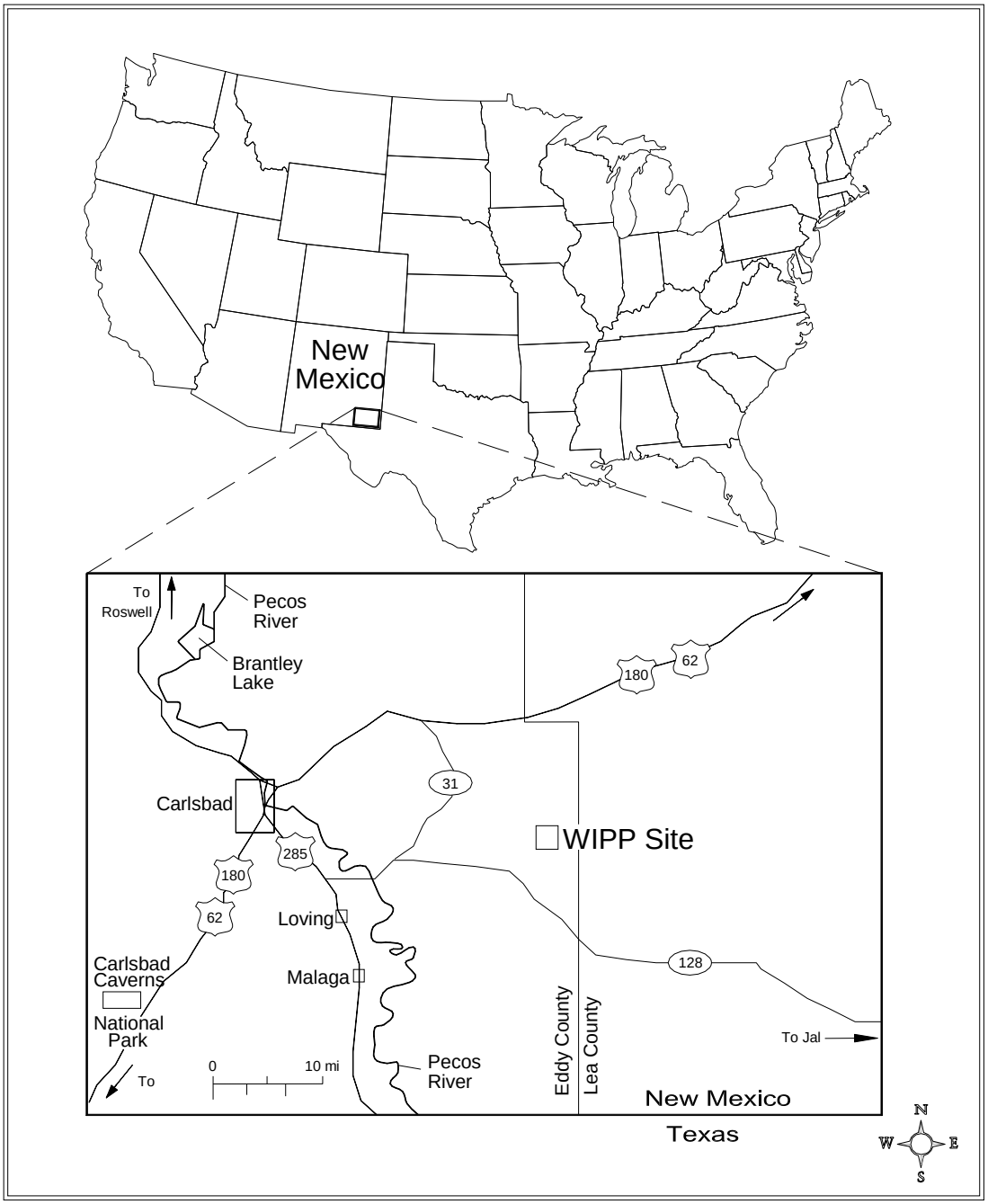

Figure 1-1 WIPP Location

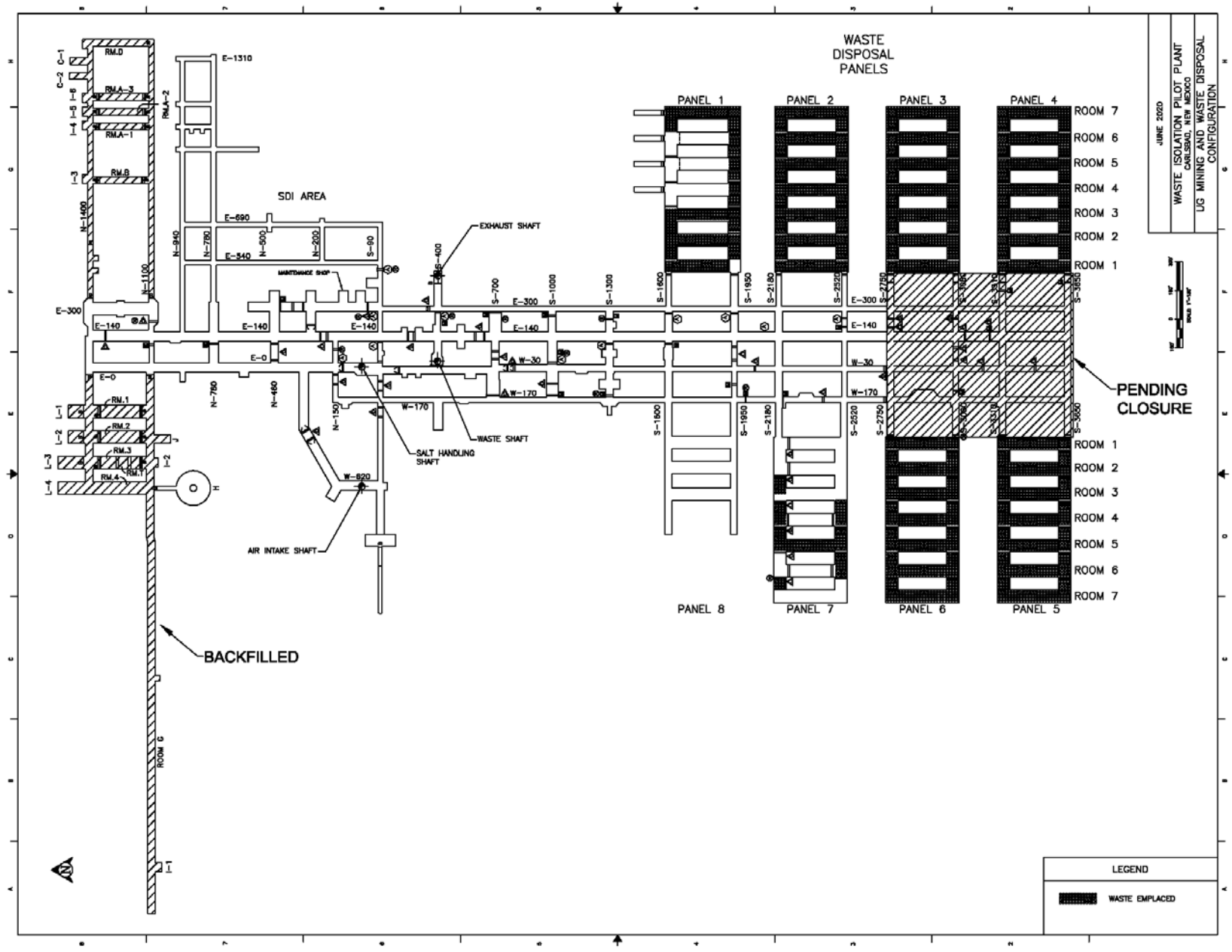

Figure 1-2 Underground Mining and Waste Disposal Configuration as of June 30, 2019

1.2 Mission

In 1979 Congress authorized the WIPP (Public Law 96-164, Department of Energy National Security and Military Applications of Nuclear Energy Authorization Act of 1980) to provide ". . . a research and development facility to demonstrate the safe disposal of radioactive wastes resulting from the defense activities and programs of the United States exempted from regulation by the Nuclear Regulatory Commission." To fulfill this mission, the U. S. Department of Energy (DOE) constructed a full-scale facility to demonstrate both technical and operational principles of the permanent disposal of transuranic (TRU) and TRU mixed wastes. Technical aspects are those concerned with the design, construction, and performance of the subsurface excavations. Operational aspects refer to the receiving, handling, and emplacement of TRU wastes in the facility. The facility was first used for *in situ* studies and experiments without the use of radioactive waste. The WIPP now receives, handles, and permanently disposes of TRU waste and TRU mixed waste.

1.3 Development Status

To fulfill its mission, the DOE developed the WIPP in a phased manner. The goal of the SPDV phase, begun in 1980, was to characterize the site and obtain *in situ* geotechnical data from underground excavations to determine whether site characteristics and *in situ* conditions were suitable for permanent waste disposal. During this phase, the Salt Shaft, a ventilation shaft, a drift to the southernmost extent of the proposed waste disposal area, a four-room experimental panel, and access drifts were excavated. Surface-based geological and hydrological investigations were also conducted. The data obtained from the SPDV investigations were reported in the Summary of the Results of the Evaluation of the WIPP Site and Preliminary Design Validation Program (DOE, 1983).

Based upon the favorable results of the SPDV investigations, additional activities were initiated in 1983. These included the construction of surface structures, conversion of the ventilation shaft for use as the Waste Shaft, excavation of the Exhaust Shaft, development of additional access drifts to the waste disposal area and excavation of additional experimental rooms to support research and development. Geotechnical data acquired during this phase were used to evaluate the performance of the excavations in the context of established design criteria (DOE, 1984). Results of these evaluations were reported in geotechnical field data reports (DOE, 1985; DOE, 1986a), and were summarized in the *WIPP Design Validation Final Report* (DOE, 1986b).

The *WIPP Design Validation Final Report* concluded that the facility, including waste disposal areas, could be developed and operated to fulfill the long-term mission of the WIPP (DOE, 1986b). All available information validated the design of underground openings to safely accommodate the permanent disposal of waste under routine operating conditions.

The Air Intake Shaft was constructed between March 1988 and November 1989. Panel 1 mining began in 1986 and was completed in 1988. Panel 1 was intended to receive waste for an initial operations demonstration and pilot plant phase that was scheduled to start in October 1988; however, the demonstration and pilot plant phase was not put into effect because waste could not be emplaced until permits were acquired.

In October 1996, the DOE submitted to the U.S. Environmental Protection Agency (EPA) a compliance certification application in accordance with Title 40 *Code of Federal Regulations* (CFR) Parts 191 and 194, which addressed the long-term (10,000-year) performance criteria for the disposal system. On May 18, 1998, the EPA published the final certification that allowed for the receipt of TRU waste at the WIPP. Immediately before this certification, the DOE Carlsbad Area Office completed an Operational Readiness Review, which is required by the DOE before the start-up or a process change of any nuclear facility. As a result of the review, the DOE Carlsbad Area Office notified the Energy Secretary on April 1, 1998, that the WIPP was operationally ready to receive waste. On March 26, 1999, the first shipment of TRU waste was received from Los Alamos National Laboratory. By the end of June 2013, many additional waste generator sites had shipped waste to the WIPP. The cleanup of several small-quantity waste generator sites, as well as one large-quantity site (Rocky Flats Environmental Technology Site), is now complete.

Waste disposal in Panels 1, 2, 3, 4, 5, and 6 is complete. Panels 1, 2, and 3 contain only contact-handled (CH) waste. The first remote-handled (RH) waste shipment arrived January 24, 2007. Panel 4 was the first to receive both CH and RH waste. CH and RH waste emplacement had commenced in Panel 7, but was halted initially by a truck fire in the underground which was quickly followed by a radioactive release in Panel 7. CH waste emplacement resumed in January 2017, and RH waste emplacement was resumed in Panel 7 in February 2019 using shielded containers only, no additional borehole emplacement occurred during this period.

1.4 Purpose and Scope of Geomechanical Monitoring Program

As specified in the WIPP Hazardous Waste Facility Permit (New Mexico Environment Department [NMED], 2016), the purpose of the geomechanical monitoring program is to obtain *in situ* data to support the continuous assessment of the design for underground facilities.

Specifically, the program provides for:

- Early detection of conditions that could affect operational safety.
- Evaluation of disposal room closure that ensures adequate access.
- Guidance for design modifications and remedial actions.
- Data for interpreting the behavior of underground openings, in comparison with the established design criteria.

Data taken by or input into the geomechanical instrumentation system (GIS) are evaluated and reported in this GAR. This annual report fulfills the requirements set forth in Part 4.6.1.2., Attachment A2, Section A2-5b (2) of the WIPP Hazardous Waste Facility Permit (NMED, 2016), and 40 CFR §191.14, "Assurance Requirements," implemented through the certification criteria, 40 CFR Part 194.

The Geomechanical Monitoring Program generates the data for four of the compliance monitoring parameters:

- Creep closure and stresses
- Extent of deformation
- Initiation of brittle deformation
- Displacement of deformation features

The instrumentation system for geomechanical monitoring provides data for routine evaluations of safety, stability, and performance of underground openings. *In situ* data are also used to model long-term disposal system performance. Changes resulting from excavations are monitored by routine inspections of selected observation borehole arrays and fracture mapping to detect and quantify occurrences of discontinuities such as fractures and bed separations. Analysis of data indicating areas of potential instability allows timely corrective action before the areas become unsafe. Other geoscience activities include geologic mapping and sampling, and seismic monitoring.

The GIS provides data that are collected, processed, and stored for analysis. The following subsections briefly describe the major components of the GIS.

1.4.1 Instrumentation

Instrumentation installed for measuring the geomechanical response of the shafts, drifts, and other underground openings includes convergence points, convergence meters, extensometers, rock bolt load cells, pressure cells, strain gauges, piezometers, and joint meters. Table 1-1 lists a summary of the specifications for geomechanical instrumentation.

Instrument Type	Measures	Range[2]	Resolution[2]
Convergence point (tape extensometer)	Cumulative deformation	250 feet	0.001 inch
Wire convergence meter	Cumulative deformation	0–40 inches	0.005 inch
Embedded strain gauge	Cumulative strain	0–3000 microstrain	1 microstrain
Spot-welded strain gauge	Cumulative strain	0–2500 microstrain	1 microstrain
Rock bolt load cell	Load	0–50 tons	40 pounds
Earth pressure cell	Pressure	0–1000 psi	1 psi
Piezometer	Fluid pressure	0–500 psi	0.5 psi
Joint meter	Cumulative deformation	0–4 inches	0.001 inch
Wire extensometer	Cumulative deformation	0–25 inches	0.005 inch

Table 1-1 Geomechanical Instrumentation Data Acquisition

Geomechanical instruments are read either manually, using portable devices, or remotely, by electronically polling the stations from the surface, in accordance with approved operating procedures. Remotely read instruments are connected to one of the underground data loggers, and readings are collected by initiating the appropriate polling routine. Upon completion of a verification process, data are transferred to a computer database. Manual readout devices are taken to instrument locations in the underground. Data are recorded on data sheets and later entered into an electronic database.

The underground data acquisition system consists of instruments, polling devices, and a communications network. Instruments are connected to polling devices that are installed in electrical enclosures near the instrument locations. Polling devices are connected by a data link to a surface computer.

[2] Manual readout boxes for the instruments were manufactured to render measurements in U.S. customary units. Range and resolution measurement units have not been converted to metric units. PSI denotes, pounds per square inch.

Whether acquired manually or remotely, geomechanical data are entered into the database files of the GIS data processing system. The data processing system consists of computer programs that are used to enter, reduce, and transfer the data to permanent storage files. Additional routines allow access to the permanent storage files for numerical analysis, tabular reporting, and graphical plotting. Copies of the report are available upon request[3].

1.4.2 Data Evaluation

Rounding and significant digits are used in the data tables of this document. The reference document is American Society for Testing and Materials (ASTM) document ASTM D 6026-06, "Standard Practice for Using Significant Digits in Geotechnical Data."

Closure measurements are acquired manually from convergence point anchors and remotely from convergence meters. Data are presented in plots of closure versus time. Closure rate data are calculated and presented as part of the data analysis. Extensometers provide displacement data from instrumented rods or wires anchored at various depths. Plots show displacement versus time for individual anchors.

Displacement rate data from the hole (collar) to the deepest anchor are presented in the data analysis.

The annual closure rate is calculated as follows:

$$Rate\left(\frac{inches}{year}\right) = \left[\frac{reading2 - reading1}{date2 - date1}\right] * 365.25\frac{days}{year}$$

reading = the change from the initial reading (inches)

reading1 = reading closest to the beginning of the reporting period

reading2 = reading closest to the end of the reporting period

Comparisons between closure rates of the previous and current reporting periods are presented as percent changes in rate and are calculated as follows:

$$percent\ change\ in\ rate = (Rate_{Current\ Period} - Rate_{Previous\ Period}) / (Rate_{Previous\ Period}) \times 100\%$$

Rock bolt load cells are used to determine bolt support performance. Plots show load versus time for each instrumented bolt.

[3] Instrumentation data and data plots are presented in "Geotechnical Analysis Report for July 2018 - June 2019 Supporting Data" (DOE/WIPP-20-3610 Volume 2). The document is available upon request from the National Technical Information Service. See page ii for details and addresses.

Earth pressure cells and strain gauges are used to determine the stresses and deformation in and around the shaft liners. Data are depicted in time-based plots. Piezometers are used to measure the gauge pressure of groundwater and are installed in the shafts at varying elevations to monitor the hydraulic head acting on the shaft liners. Data are plotted as pressure versus time.

Joint meters, installed perpendicular to a crack, monitor the dilation of the crack with time. Data are presented as displacement versus time.

1.4.3 Data Errors

GIS data are processed through a comprehensive database management system. Whether acquired manually or remotely, GIS data are processed and permanently stored according to approved procedures. On occasion, erroneous readings can occur. There are several possible explanations for erroneous readings, including the following:

- The measuring device was misread.
- The reading was recorded incorrectly.
- The measuring device was not functioning within specifications.

When a reading is believed to be erroneous, the suspect reading is evaluated, and, if necessary, a second reading is collected. If the second reading falls in line with the instrument trend, the first reading is discarded and the second reading is entered in the database. If the second reading and subsequent readings remain out of the instrument trend, the ground conditions in the vicinity of the instrument are assessed to determine the reason for the discrepancy. In addition, the reading frequency may be increased.

2.0 GEOLOGY

This section provides a summary of the stratigraphy of the WIPP region and the site. Readers desiring further geologic information may consult the *Geological Characterization Report, WIPP Site, Southeastern New Mexico* (Powers et al., 1978). This report was developed as a source document on the geology of the WIPP site for individuals, groups, or agencies seeking basic information on geologic history, hydrology, and geochemistry, or detailed information, such as physical and chemical properties of repository rocks. A more recent survey of WIPP stratigraphy is included in the *Geologic Mapping of the Air Intake Shaft at the Waste Isolation Pilot Plant* (Holt and Powers, 1990).

2.1 Regional Stratigraphy

The stratigraphy in the vicinity of the WIPP site includes rocks of Permian (295 to 250 million years [Ma] before present [bp]), Triassic (250 to 203 Ma), and Quaternary (1.75 Ma to present) ages. The descriptions of formations provided in this section are given in order of deposition (oldest to youngest), beginning with the Castile Formation (Figure 2-1).

2.1.1 Permian

The Permian system in southwestern North America is divided into four series. The last of these, the Ochoan Series, contains the host rock in which the WIPP repository is located.

The Ochoan Series is of mostly marine origin and consists of four formations: three evaporite formations (the Castile, the Salado, and the Rustler) and one redbeds formation (the Dewey Lake). The Ochoan evaporites overlie marine limestones and sandstones of the Guadalupian Series (Delaware Mountain Group). The younger redbeds represent a transition from the lower evaporite deposition to fluvial deposition on a broad, low-relief, fluvial plain. The Permian rocks are overlain by fluvial deposits of the Triassic and Quaternary periods.

2.1.1.1 Castile Formation

The Castile Formation, lowermost of the four Ochoan formations, is approximately 1,250 ft (380 meters [m]) thick in the WIPP vicinity. Lithologically, the Castile is the least complex of the evaporite formations and is composed chiefly of interbedded anhydrite and halite, with limestone present in minor amounts.

2.1.1.2 Salado Formation

The Salado Formation comprises nearly 2,000 ft of evaporites, primarily halite. The formation is subdivided into three informal members: the unnamed lower member, the McNutt potash zone, and the unnamed upper member. Each member contains similar amounts of halite, anhydrite, and polyhalite, and is differentiated on the basis of soluble potassium- and magnesium-bearing minerals. The WIPP disposal horizon is located within the unnamed lower member, 2,150 ft below the surface.

2.1.1.3 Rustler Formation

The Rustler Formation is subdivided into five members, starting from its base: the Los Medaños Member, the Culebra Dolomite Member, the Tamarisk Member, the Magenta Dolomite Member, and the Forty-niner Member.

In the vicinity of the WIPP site, the Rustler is approximately 310 ft thick and thickens to the east. The lower portion (Los Medaños Member) contains primarily fine sandstone to mudstone with lesser amounts of anhydrite, polyhalite, and halite. Bedded and burrowed siliciclastic sedimentary rocks with cross-bedding and fossil remains signify the transition from the strongly evaporitic environments of the Salado to the brackish lagoonal environments of the Rustler (Holt and Powers, 1990).

The upper portion of the Rustler contains interbeds of anhydrite, dolomite, and mudstone. The Culebra Dolomite Member is generally brown, finely crystalline, and locally argillaceous. The Culebra contains rare to abundant vugs with variable gypsum and anhydrite filling, and is the most transmissive hydrologic unit within the Rustler. The Tamarisk Member consists of lower and upper sulfate units separated by a unit that varies laterally from mudstone to mainly halite. The Magenta Dolomite Member is a gypsiferous dolomite with abundant primary sedimentary structures and well-developed algal features. The Forty-niner Member consists of lower and upper sulfate units separated by a mudstone that displays sedimentary features and bedding. East of the site area, halite correlates with the mudstone. The Culebra and Magenta Dolomite members are persistent and serve as important marker units.

2.1.1.4 Dewey Lake Redbeds

The Dewey Lake Redbeds is the uppermost of the Ochoan Series formations. Within the series, the Dewey Lake represents a transition from the lower marine evaporite deposition to fluvial deposition on a broad, low-relief, fluvial plain. The redbeds, approximately 475 ft thick, consist of predominantly reddish-brown interbedded fine-grained sandstone, siltstone, and claystone. This formation is differentiated from others by its lithology and distinctive color (both of which are remarkably uniform), and by sedimentary structures, including horizontal- and cross-laminae and ripple marks. The redbeds also contain locally abundant greenish-gray reduction spots and gypsum filled fractures. The formation thickens from west to east due to eastward dips and erosion to the west.

2.1.2 Triassic

The only Triassic rocks present in the WIPP region belong to the Dockum Group.

2.1.2.1 Dockum Group

The Dockum Group consists of fine-grained floodplain sediments and coarse alluvial debris of Triassic age. From a pinch-out near the center of the WIPP site it thickens eastward, forming an erosional wedge. Local subdivisions of the Dockum Group are the Santa Rosa Sandstone and the Chinle Formation; however, only the Santa Rosa occurs in the vicinity of the site. It consists primarily of poorly sorted sandstone with conglomerate lenses and thin mudstone partings, and contains impressions and remnants of fossils. These rocks have more variegated hues than the underlying uniformly colored Dewey Lake.

2.1.3 Quaternary

Quaternary Period deposits include the Gatuña Formation, Mescalero Caliche, and surficial sediments.

2.1.3.1 Gatuña Formation, Mescalero Caliche, and Surficial Sediments

The Gatuña Formation (ranging in age from approximately 1.3 million to 600,000 years bp) (Powers and Holt, 1993) is a stream-laid deposit overlying the Dockum Group in the WIPP vicinity. At the site center, the formation consists of poorly consolidated sand, gravel, and silty clay at a thickness of approximately 13 ft. The Gatuña Formation is light red and mottled with dark stains. The unit contains abundant calcium carbonate, but is poorly cemented. Sedimentary structures are abundant (Powers and Holt, 1993, 1995).

The Mescalero Caliche (approximately 500,000 years bp) is approximately 4 ft thick in the WIPP vicinity. The Mescalero is a hard, resistant soil horizon that lies beneath a cover of wind-blown sand. The horizon is petrocalcic (i.e., very strongly cemented with calcium carbonate). Petrocalcic horizons form slowly beneath a stable landscape at the average depth of infiltration of soil moisture, and indicate stability and integrity of the land surface. Many of the surface buildings at the WIPP are founded on top of the Mescalero Caliche.

Surficial sediments include sandy soils developed from eolian material and active dune areas. The Berino Series (a soil type) covers about 50 percent of the site and consists of deep sandy soils that developed from wind-worked material of mixed origin. Based on sample analyses, the Berino soil from the WIPP site formed 330,000 ± 75,000 years bp.

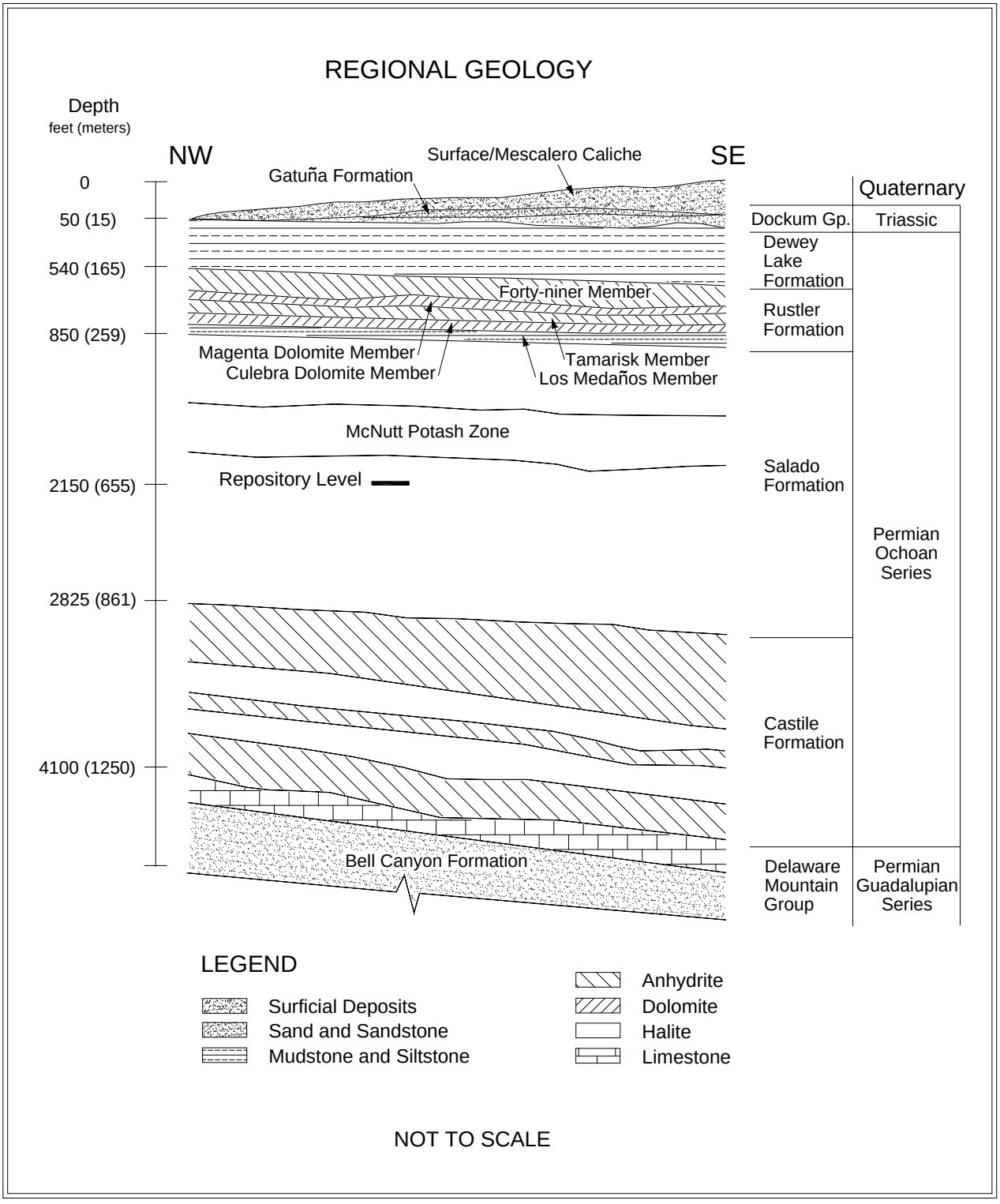

Figure 2-1 Regional Geology

2.2 Underground Facility Stratigraphy

The WIPP disposal horizon lies near the midpoint of the Salado Formation. The Salado was deposited in a shallow saline lagoon environment, which progressed through numerous inundation and desiccation cycles that are reflected in the formation. An "ideal" cycle progresses upward as follows: a basal layer consisting predominantly of claystone, followed by a layer of sulfate, which is in turn followed by a layer of halite. The entire sequence is capped by a bed of argillaceous (clay-rich) halite accumulated during a period of mainly subaerial exposure.

A regional system used for numbering the more significant sulfate beds within the Salado designates these beds as marker beds (MBs), counted from MB100 near the top of the formation to MB144 near the base. The repository is located between MB138 and MB139 within a sequence of laterally continuous depositional cycles as described above. Within this sequence, layers of clay and anhydrite that are locally designated (as shown) can have a significant impact on the geomechanical performance of the excavations. Clay layers provide surfaces along which slip and separation can occur, whereas anhydrites form brittle layers that do not deform plastically.

In the vicinity of the WIPP, the stratigraphy is fairly continuous and uniform. Beds generally dip toward the south-southeast at a slope of approximately 3 percent.

2.2.1 Disposal Horizon Stratigraphy of Panels 1, 2, 7, and 8

This disposal horizon contains Panels 1, 2 and 7, all the shaft areas, the shop areas, the SPDV areas (which are now closed), and all the access drifts north of S-2520. Farther south, the four main entries rise in a ramp that starts at S-2520 and ends at S2750. Panel 7 excavation was completed in January 2013. Most underground excavations are located within this disposal horizon (Figure 2-2). In it, the Orange Marker Bed (OMB) lies near the middle of the rib (i.e., the excavation wall). The OMB is a laterally consistent unit of moderate to light reddish-orange translucent halite, about 6 inches (in) (15 centimeters [cm]) thick, that is used as a point of reference during excavation.

MB139 lies approximately 11.5 ft (3.5 m) below the OMB. MB139 is a 20- to 32-in (50- to 80-cm)-thick layer of polyhalitic anhydrite. The top of the anhydrite undulates up to 15 in (38 cm), while the bottom is sub-horizontal and is underlain by Clay E.

Above MB139, a unit of halite terminates at the base of the OMB. Within this unit, polyhalite is locally abundant and decreases upward, while argillaceous material increases upward.

Above the OMB, a thin band of argillaceous halite gives way to a thick sequence of clear halite that becomes increasingly argillaceous upward and is capped by Clay F. This constitutes a thin layer occasionally interrupted by partings and breaks and is readily visible in the upper ribs. Above Clay F, another sequence of halite begins that, as in lower sequences, becomes increasingly argillaceous upward. This sequence terminates at the Clay G/Anhydrite "b" interface, approximately 6.5 ft (2 m) above the roof of most disposal horizon excavations, forming a roof beam that typically acts as a structural unit.

The roof of some disposal horizon excavations (e.g., the E-140 drift between S-1000 and S-1950) has been excavated to the upper contact of Anhydrite "b." In this case, a roof beam is formed by the next depositional sequence beginning with Anhydrite "b" and progressing upward to the Clay H/Anhydrite "a" interface, approximately 6.5 ft (2 m) above the upper contact of Anhydrite "b."

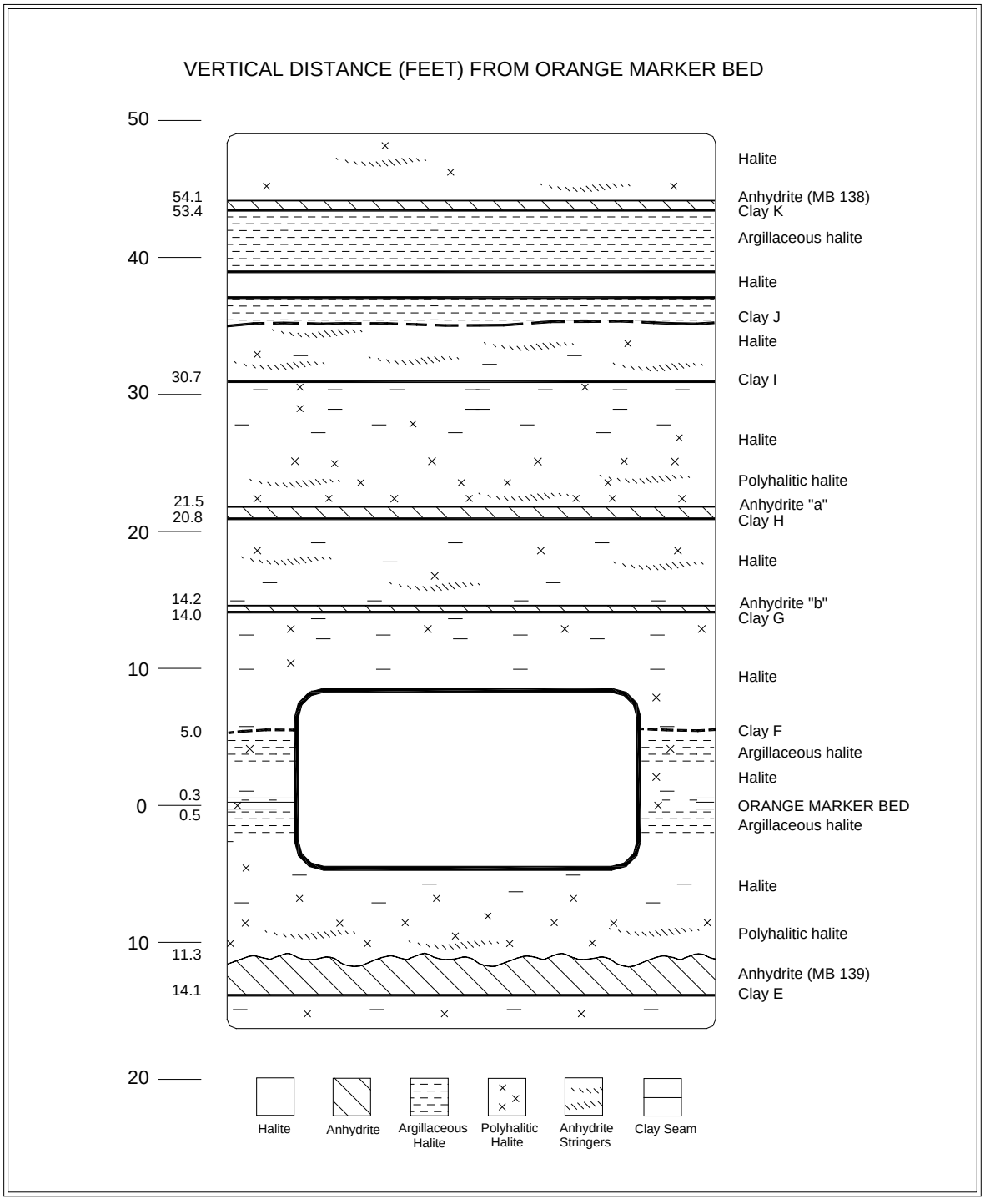

Figure 2-2 Repository Level Stratigraphy of Panels 1, 2, and 7

2.2.2 Disposal Horizon Stratigraphy of Panels 3, 4, 5, 6 and 8

Field observations and computer modeling indicated that moving the disposal horizon stratigraphically upward (so that the roof was located at Clay G) would improve long-term ground conditions and provide a more stable roof configuration without significantly impacting repository performance. In 2000, the decision was made to implement this change by moving the mining horizon up approximately 6 ft. Subsequently, in 2000 and 2001, ramps were mined in the W-170, W-30, E-140, and E-300 drifts between S-2520 and S-2750 (Figure 1-2). As a result, the disposal horizon for Panels 3, 4, 5, and 6, and the associated connecting drifts, lies above the horizon for the other panels (Figure 2-3).

Panel 8 was originally planned to be mined on the lower horizon, but due to the interruption in mining, which resulted in significant low angle shear and separation in the immediate back; it is now being mined to the upper horizon. Ramps are in place both in the intake and exhaust drifts (S1600 and S1950) west of W170.

In this horizon, the OMB lies at or below the floor. MB139 lies about 12 ft (3.7 m) below the floor. The roof lies at or slightly above Anhydrite "b." Clay G/Anhydrite "b" is used as the mining reference during excavation of this disposal horizon. Locally continuous anhydrite stringers are found within this horizon that extend to Clay H at Anhydrite “a,” generally concentrated in the lower portion toward Anhydrite "b." These effectively divide the roof beam itself into a series of thinner, independent beams, thereby weakening the overall beam strength.

2.2.3 Northeast Area Stratigraphy

The Northeast Area, formerly an experimental area, is now deactivated and closed for access. These excavations lie at a higher stratigraphic level than the disposal excavations. Floors are at Anhydrite "b." As in the lower units, the halite intervals between the clay seams/anhydrite beds contain relatively pure halite that becomes increasingly argillaceous upward. Above Clay I, two more halite intervals complete the underground facility stratigraphy. Clay J, at the top of the first of these intervals, may consist of a distinct seam or merely an argillaceous zone. Clay K tops the second interval and is overlain by MB138.

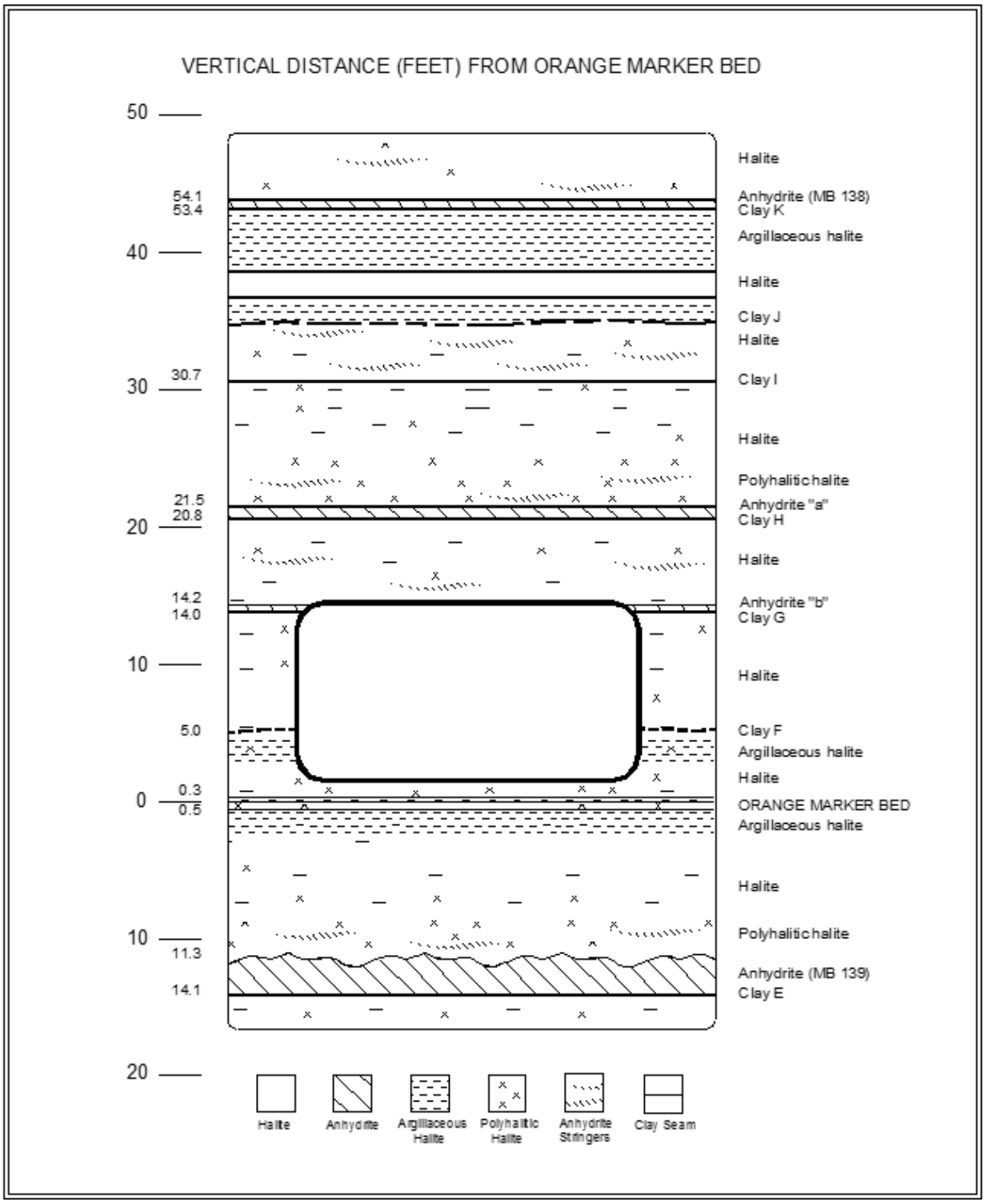

Figure 2-3 Repository Level Stratigraphy of Panels 3, 4, 5, 6 and 8

3.0 PERFORMANCE OF SHAFTS AND KEYS

Four shafts connect the surface with the underground at the WIPP. They are the Salt Shaft, which is used primarily for removing excavated salt from the underground and for transporting personnel and materials; the Waste Shaft, which is used primarily for transporting TRU waste to the underground and for transporting personnel and materials; the Exhaust Shaft, which is used to exhaust the ventilation air from the underground; and the Air Intake Shaft, which is the primary source of fresh air ventilation to the underground. This section describes the geomechanical performance of these shafts.

Although much of the instrumentation installed in the shafts has failed through the years, there are no plans to replace it. The project has a good understanding of the expected movements in the shafts. Monitoring results up to the point of instrument failure did not indicate unusual shaft movements or displacements. Continued periodic visual inspections confirm the expected shaft performance and provide necessary observations to evaluate shaft performance. Replacement of failed instrumentation will not provide significant additional information.

3.1 Salt Shaft

The first construction activity undertaken by the SPDV Program was the excavation of the Exploratory Shaft. This shaft was subsequently referred to as the Construction and Salt Shaft, and is currently designated the Salt Shaft (see Figure 1-2). The shaft was drilled from July 4, to October 24, 1981, and geologically mapped in the spring of 1982 (DOE, 1983). Figure 3-1 presents the stratigraphy in the shaft.

The Salt Shaft is lined from the surface to 846 ft (258 m) with steel casing having an inside diameter of 10 ft (3 m). The thickness of the steel liner (including external stiffener rings) increases from 0.62 in (1.6 cm) at the top to 1.5 in (3.8 cm) at the key. Cement grout was placed between the liner and the rock face. The 10-ft (3-m)-diameter steel liner extends through the concrete shaft key to 880 ft (268 m). The shaft key is a 37.5-ft (11.4-m)-long, reinforced concrete structure that begins 3.5 ft (1.07 m) above the bottom of the steel liner. From the key to the bottom at 2,298 ft (700 m), the shaft has a nominal diameter of 12 ft (4 m).

Wire mesh anchored by rock bolts is installed in sections of the lower shaft as a safety screen to contain rock fragments that may become detached. The shaft extends approximately 140 ft (43 m) below the repository horizon in order to accommodate the skip loading equipment and a sump.

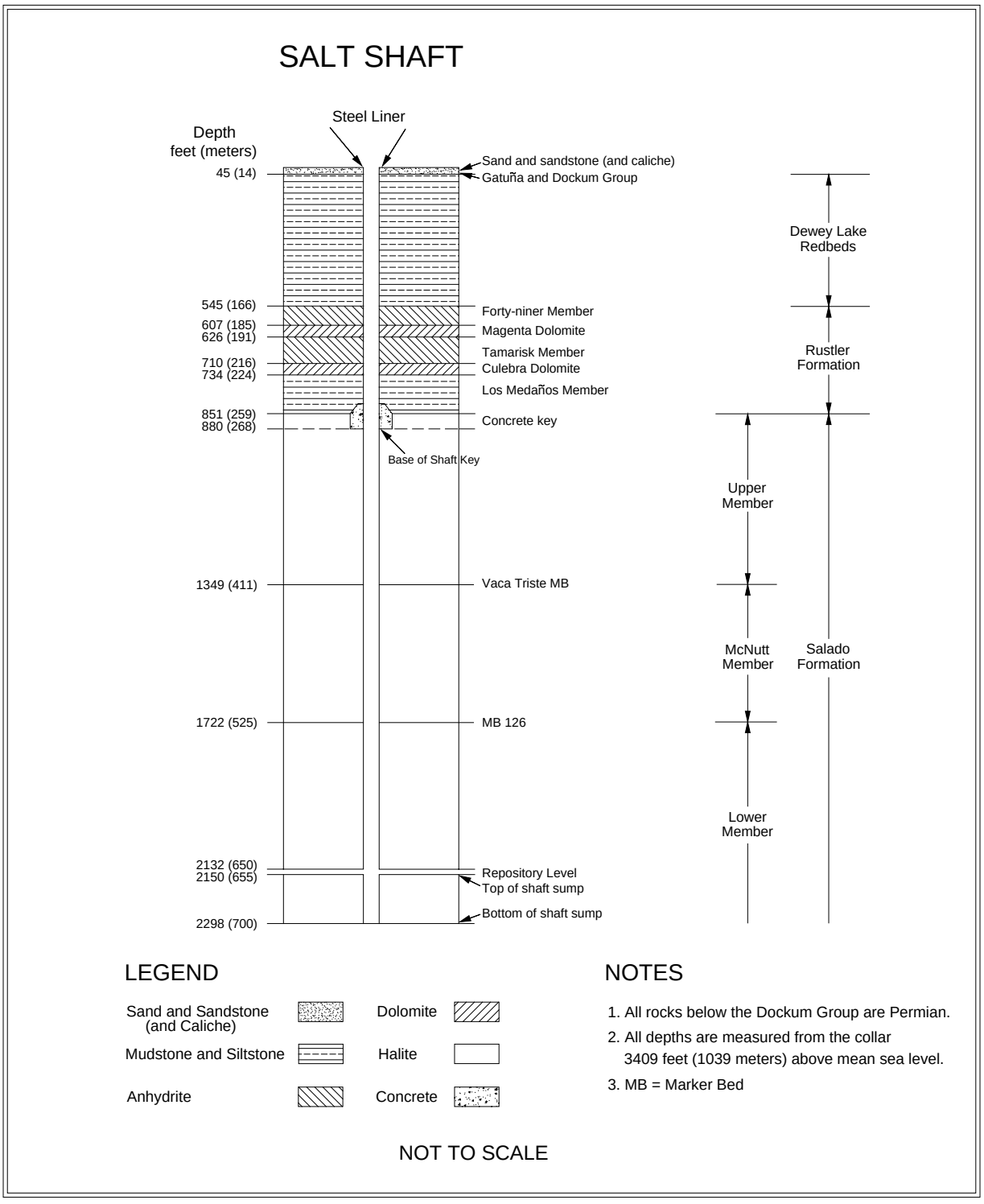

Figure 3-1 Salt Shaft Stratigraphy

3.1.1 Shaft Observations

Underground operations personnel conduct weekly visual inspections. These inspections are performed principally to assess the condition of the hoisting and mechanical systems, but they also include examining the shaft walls for water seepage, loose rock, or sloughing. Visual inspections during this reporting period found that the shaft remains in satisfactory condition. Only routine ground control activities were required.

3.1.2 Instrumentation

Geomechanical instruments (radial convergence points, extensometers, and piezometers) were installed at various levels in the shaft from April through July 1982 (Figures 3-2 and 3-3). Instruments in the shaft key included strain gauges, pressure cells, and piezometers. Radial convergence points were installed prior to outfitting. Upon completion of shaft outfitting, no more readings were taken.

Nine piezometers continue to provide data. The fluid pressures recorded at the end of this reporting period range from approximately 0 pounds per square inch (psi) at the 802-ft (259-m) level (upper section of the shaft key) to 164 psi at the 691-ft (211-m) level in the Tamarisk Member. The recorded pressures for this reporting period are generally consistent with the readings from the previous reporting period.

Four earth pressure cells were installed in the key section during concrete emplacement at the 860-ft (262-m) level. These instruments measure the normal stress between the concrete key and the Salado Formation as salt creep loads up the key structure. Two of the earth pressure cells continue to provide data. These instruments have indicated essentially no contact pressure since their installation (readings resemble instrument drift at a zero pressure).

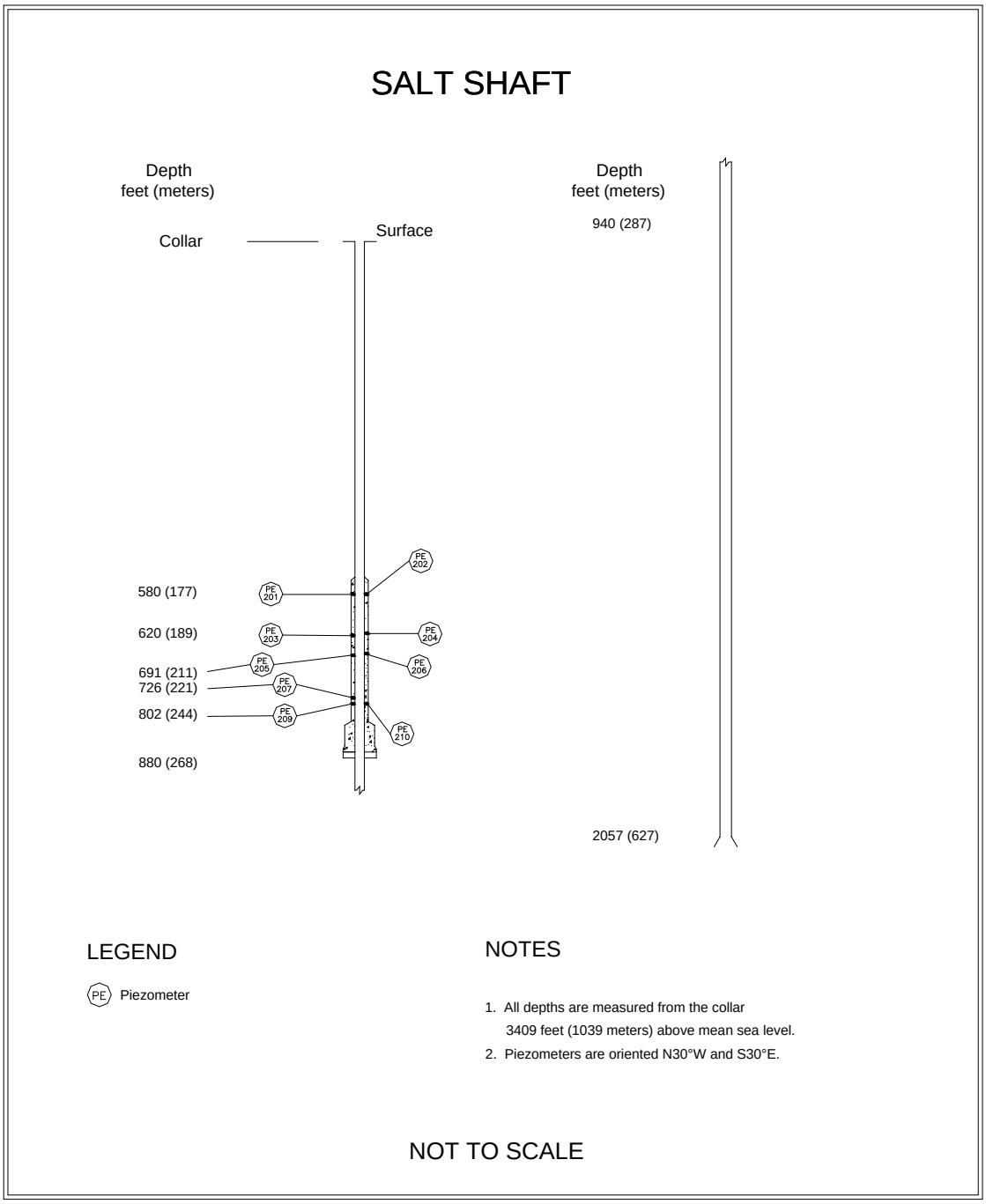

Figure 3-2 Salt Shaft Instrumentation

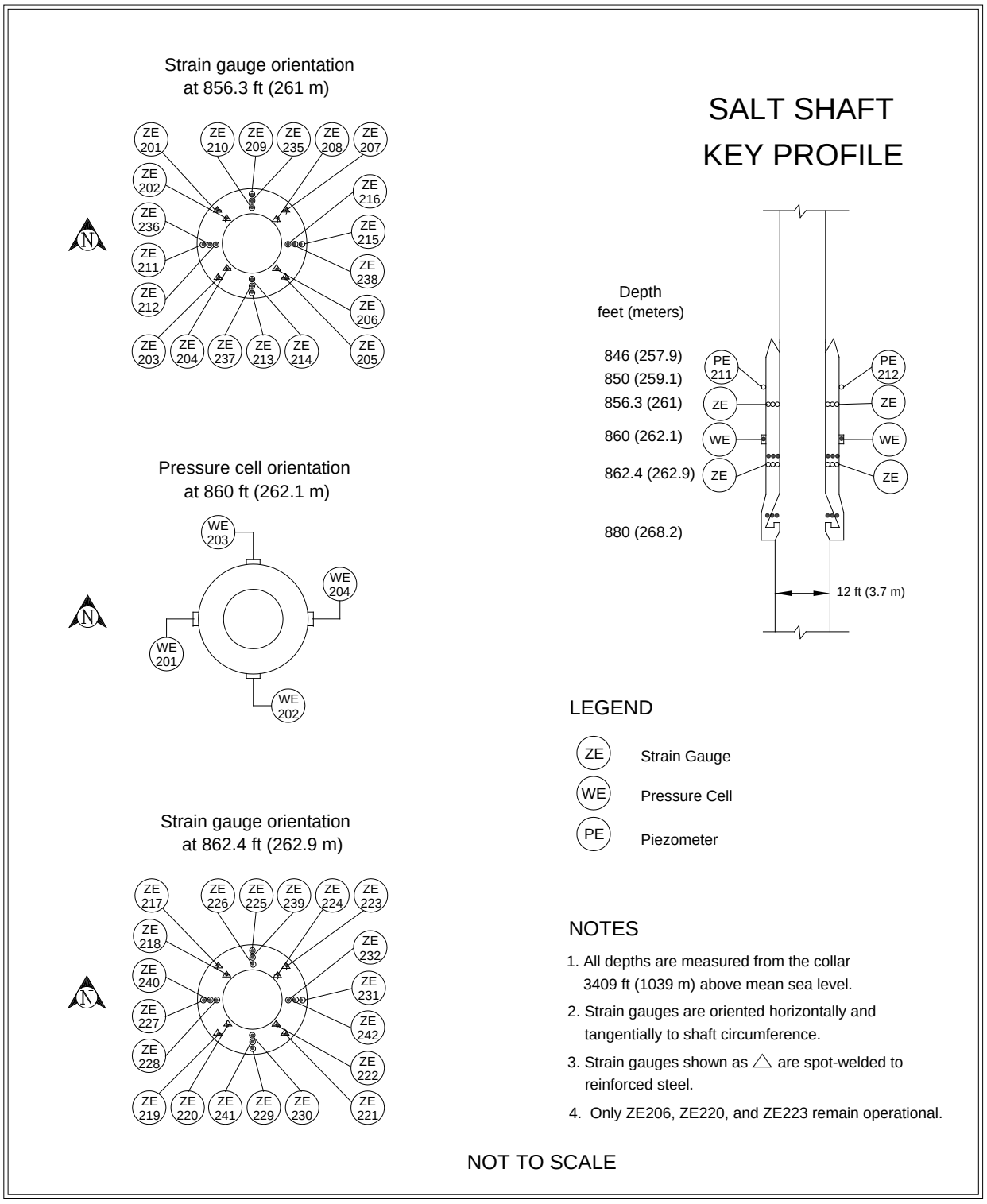

Figure 3-3 Salt Shaft Key Instrumentation

Sixteen spot-welded and 24 embedment strain gauges were installed on and in the shaft key concrete at both the 856.3-ft (261-m) level and at the 862.4-ft (263-m) level. One spot-welded strain gauge is still functioning at the 856.3-ft (261-m) level. The maximum strain this period is 663 microstrain and the maximum the previous period was 677 microstrain.

Eighteen embedment strain gauges are still functioning. The strains at the 856.3-ft (261-m) level ranged from -826 to 1,007 microstrain. The strains from the 6 embedment strain gauges at the 862.4-ft (263-m) level were 64 to 948 microstrain. The strain recorded by the spot-welded strain gauge and the embedment strain gauges during this reporting period are similar to the strains recorded by these instruments at the end of the previous reporting period.

3.2 Waste Shaft

As part of the SPDV Program, a 6-ft (2-m)-diameter ventilation shaft, now referred to as the Waste Shaft, was excavated from December 1981 through February 1982 (see Figure 1-2). This shaft and the Salt Shaft created a two-shaft underground air circulation system. From October 11, 1983, to June 11, 1984, the shaft was enlarged to a diameter of 20 to 23 ft (6 to 7 m) and lined above the key. Stratigraphic mapping (Figure 3-4) was conducted during shaft enlargement from December 9, 1983, to June 5, 1984 (Holt and Powers, 1984).

The Waste Shaft is lined with non-reinforced concrete having a 19-ft (6-m) inside diameter from the surface to the top of the key at 837 ft (255 m). Liner thickness increases from 10 in (25 cm) at the surface to 20 in (51 cm) at the key. The key is 63 ft (19 m) long and 4.25 ft (1.3 m) thick, and is constructed of reinforced concrete. The bottom of the key is 900 ft (274 m) below the surface. The diameter of the shaft is 20 ft (6 m) at the bottom of the key and increases to 23 ft (7 m) just above the shaft station. The shaft below the key is lined with wire mesh anchored by rock bolts. The diameter of 23 ft (7 m) extends to a depth of approximately 2,286 ft (697 m), with the shaft sump comprising the lower 119 ft (36 m) of that interval.

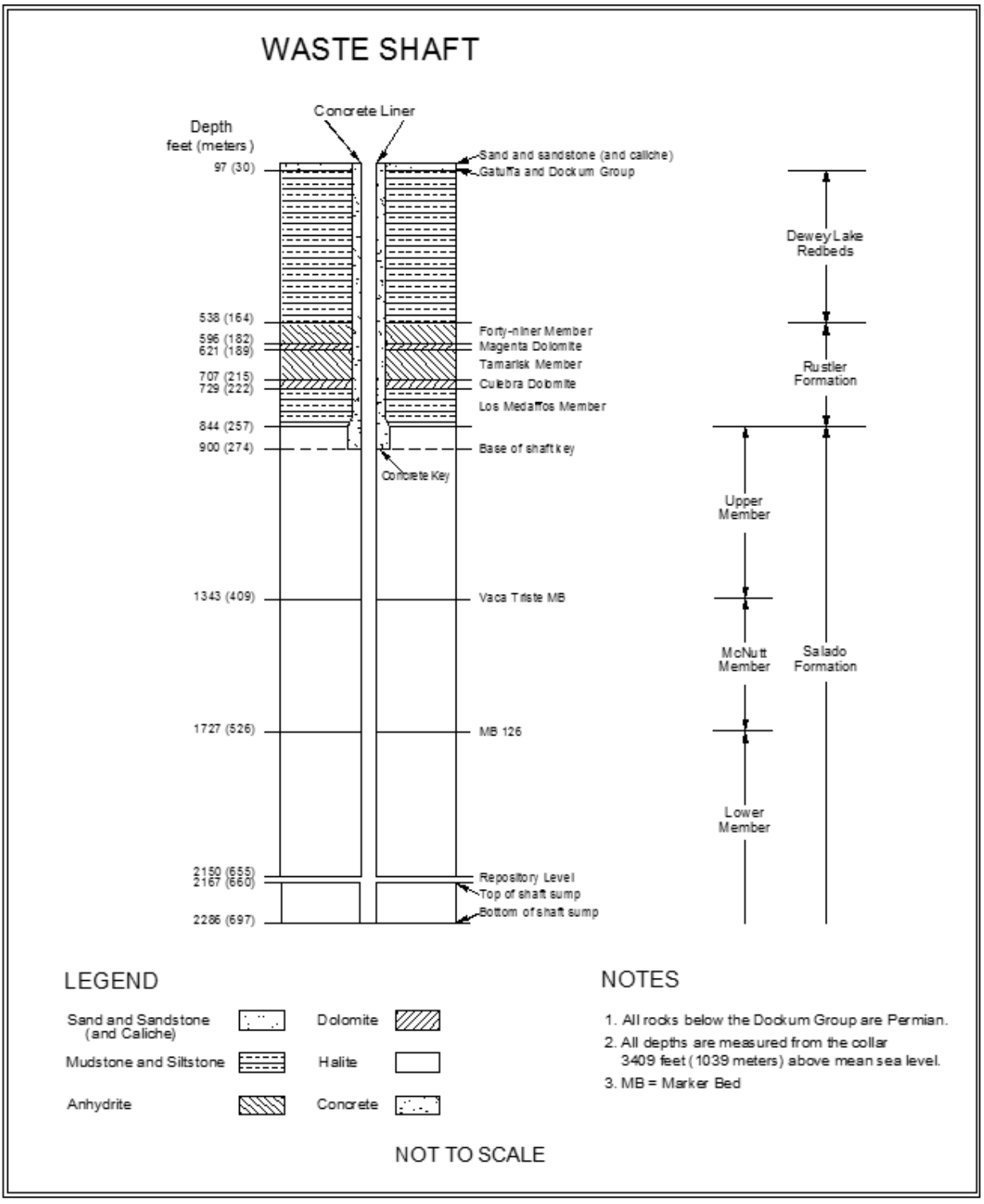

Figure 3-4 Waste Shaft Stratigraphy

3.2.1 Shaft Observations

Underground operations personnel conduct weekly visual inspections, principally to assess the condition of the hoisting and mechanical systems, but also to examine the shaft walls for water seepage, loose rock, or sloughing. The visual inspections found that the shaft was in satisfactory condition. No ground control activities other than routine maintenance were required.

3.2.2 Instrumentation

Radial convergence points, extensometers, piezometers, and earth pressure cells were installed in the Waste Shaft between August 27, and September 10, 1984. Radial convergence points were installed prior to the outfitting. Upon completion of shaft outfitting, no more radial convergence readings were taken. Figure 3-5 and Figure 3-6 show the instrument locations.

Nine multi-position extensometers were installed in arrays 1,071 ft (326 m), 1,566 ft (477 m), and 2,059 ft (628 m) below the surface, as shown in Figure 3-5. Each array consists of three extensometers. No extensometer data have been collected in recent years due to the malfunction of the data acquisition equipment. Since the extensometer type installed in the shaft over 30 years ago is no longer manufactured, remote data acquisition equipment for these extensometers is also unavailable.

Twelve piezometers were installed in the lined section of the Waste Shaft on September 7, and 8, 1984, to monitor fluid pressure behind the shaft liner and the key section. As of this reporting period, data is no longer being received from any of the piezometers.

Four earth pressure cells were installed in the key section of the Waste Shaft during concrete emplacement, which occurred between March 23, and April 3, 1984. Earth pressure cells measure the normal stress between the concrete key and the Salado Formation as salt creep loads the key structure. As of this reporting period, data is no longer being received from any of the Earth pressure cells.

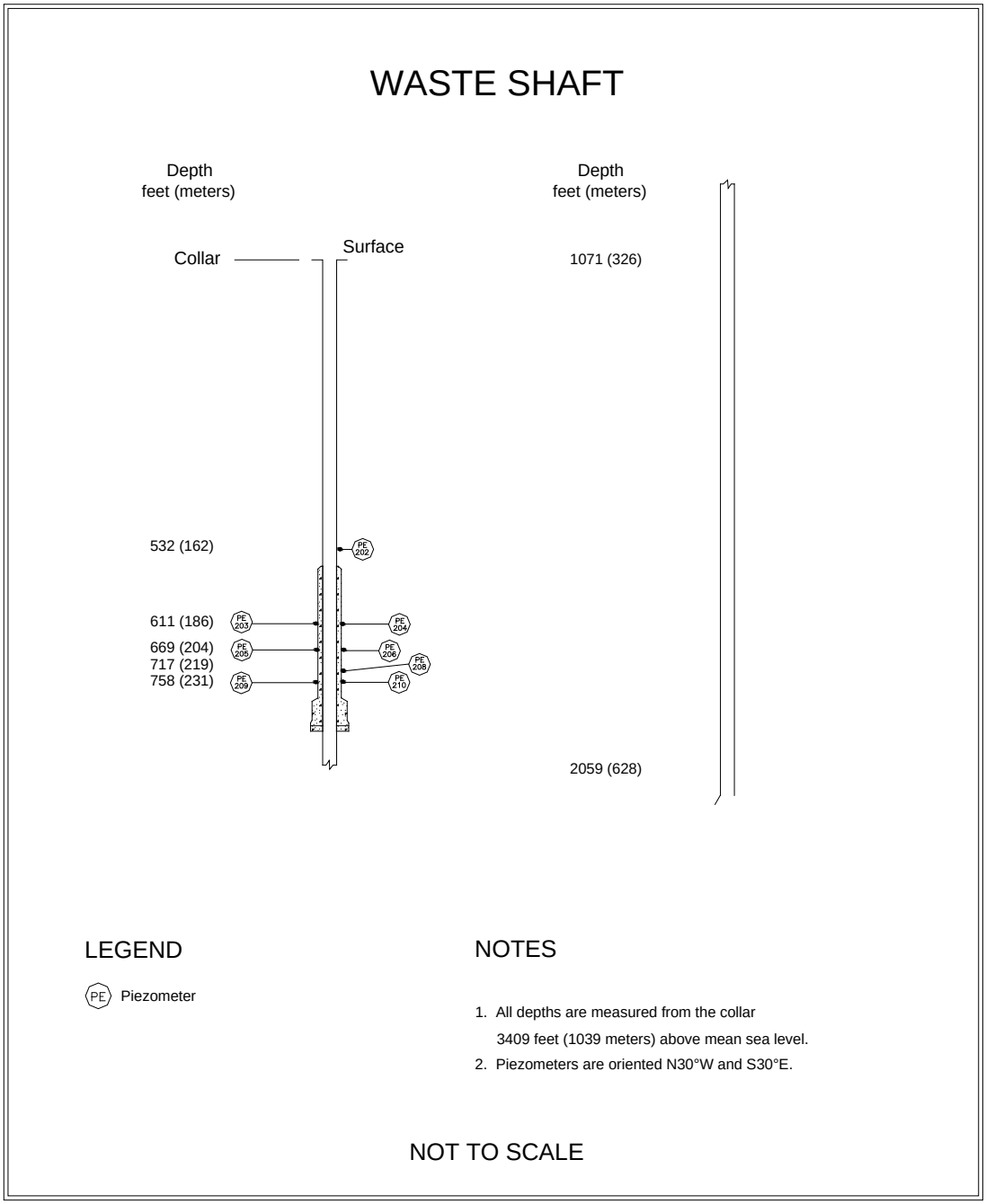

Figure 3-5 Waste Shaft Instrumentation

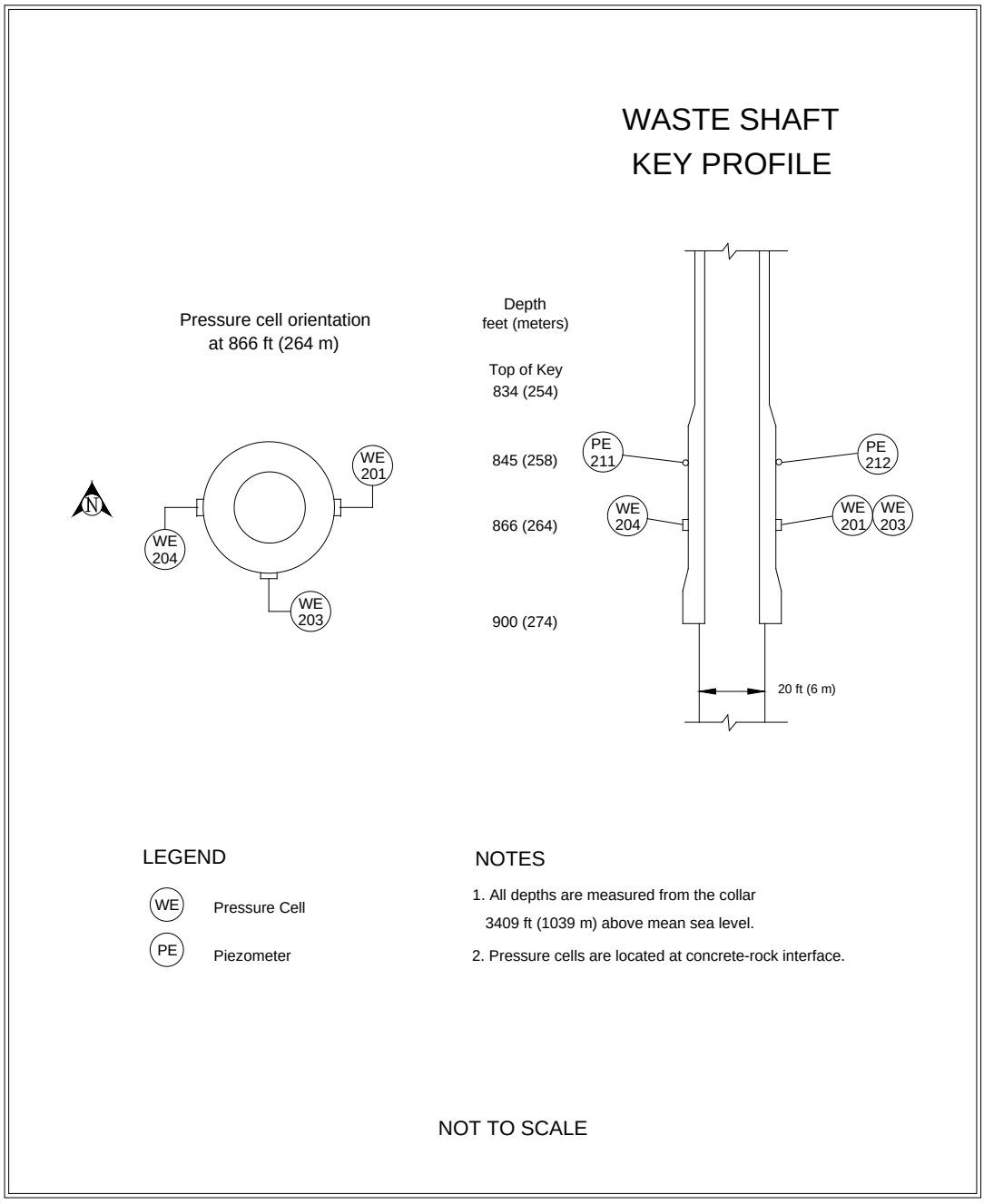

Figure 3-6 Waste Shaft Key Instrumentation

3.3 Exhaust Shaft

The Exhaust Shaft was drilled from September 22, 1983, to November 29, 1984, to establish a route from the underground to the surface for exhaust air (Figure 1-2). Stratigraphic mapping was conducted from July 16, 1984, to January 18, 1985 (DOE, 1986). Figure 3-7 illustrates the shaft stratigraphy.

The Exhaust Shaft is lined with non-reinforced concrete from the surface to the top of the shaft key at 844 ft (257 m). The liner thickness increases from 10 to 16 in (25 to 41 cm) over that interval. The key is 63 ft (19 m) long and 3.5 ft (1 m) thick. The shaft diameter below the key is 15 ft (5 m), and the interval below the key is lined with wire mesh anchored by rock bolts. The shaft terminates at the facility horizon, approximately 2,150 ft (655 m) deep. This shaft has no sump.

3.3.1 Quarterly Exhaust Shaft Inspection

Quarterly video inspections of the Exhaust Shaft are conducted according to approved WIPP procedures. Inspections are performed to evaluate the condition and to verify the integrity of the shaft. The shaft is examined for cracks, corrosion, salt buildup, seeps, and debris. In addition, inspections examine the condition of anchors, brackets, and down-hole equipment. Exhaust Shaft video inspections were performed this reporting period in September 2018, November 2018, and June 2019. The 2019 Q1 inspection could not be performed due to repairs being made to the cable winch.

3.3.1.1 Video Camera

Video inspections use a custom-designed, vertical-drop color camera in an aerodynamic housing, with pan, tilt, and zoom capability. The camera is suspended by a dual-armored cable. The cable contains five copper conductors and two multi-mode optical fibers. It is reeled out by a winch mounted in a control trailer. Inspections are recorded electronically.

3.3.1.2 Shaft Inspection Observations

Quarterly video inspection observations concentrate on four major areas: air-monitoring components, shaft liner, shaft walls, and equipment support and cabling. The air-monitoring components consist of one tube that provides a conduit for air-velocity measurements, and three tubes for monitoring possible radionuclides within the exhaust air stream, as shown in Figure 3-8. The video inspection includes examination of each device, including the transport assembly, guide tubes, the sample intake, and the support brackets that extend from Station "A" above the shaft to the shaft collar. Air-monitoring components extend from the collar 21 ft into the shaft. Video inspections indicate that the air-sampling components can accumulate salt buildup of up to several inches thick.

The Exhaust Shaft liner is examined for cracks, seepage, and general shaft stability. Currently, there are three principal zones of seepage in the shaft. The first is about 50 to 55 ft below the shaft collar (bsc), the second is about 60 to 65 ft bsc, and the third is about 80 to 85 ft bsc, as shown in Figure 3-9. Monitoring of seepage horizons started before 1995. Water entering the shaft through these cracks is believed to originate from a perched-shallow-water-bearing horizon at the base of the Santa Rosa Formation. The fluid level in the Santa Rosa near the shaft is about 48 to 49 ft below the surface. Based on examination of inspection videos, the flow rate into the shaft has been estimated to be about 1 to 1½ gallons per minute. Seepage cracks are confined primarily to the eastern side of the shaft wall.

When fluid was detected seeping into the shaft, a catch basin was designed and installed at the base of the Exhaust Shaft to intercept water and prevent it from draining into the Waste Shaft sump. Fluid was removed from the catch basin from March 1996 through October 2005, as needed. The catch basin was damaged in 2004 by fallen debris, either salt or instrumentation cables or both. A new catch basin was fabricated and installed in December 2004. This basin was damaged in August 2005, most likely the result of fallen debris. An interception well system was installed between November 2005 and March 2006 to replace the catch basin. Interception wells were drilled down gradient in S-400 between E-140 and E-300 (Figure 3-10). The interception well system initially consisted of four 30-ft-deep 9-7/8-in-diameter fluid collection holes with a submersible pump and pressure transducer in each. Fluid was pumped from each hole to a series of storage containers in S-550. A data-acquisition system monitors the fluid level in each hole, turning the pump on and off between set limits, as needed.

Between February 2, and 6, 2008, two additional fluid collection holes, OH631 and OH632, were drilled in S-400 to improve the total volume of fluid recovered by the interception well system. They replaced OH613 and OH614, which generated little fluid. As with the previous four holes, the additional holes were drilled at 9-7/8-in diameter to a total depth of 30 ft. Pumps were pulled from OH613 and OH614 and installed in OH631 and OH632. Figure 3-10 shows the location of the interception well system.

The catch basin and the interception well system collected fluid from July 1997 through June 2006 and from July 2006 through June 2018, respectively. The largest reported volumes are typically associated with periods of reduced ventilation and increased humidity. No fluid was collected by the system during this reporting period due to the relocation of the components from S-550 to S-300. For a discussion of the factors affecting the quantity of fluid produced in the Exhaust Shaft, refer to DOE/WIPP-00-2000, *Brine Generation Study* (DOE, 2000).

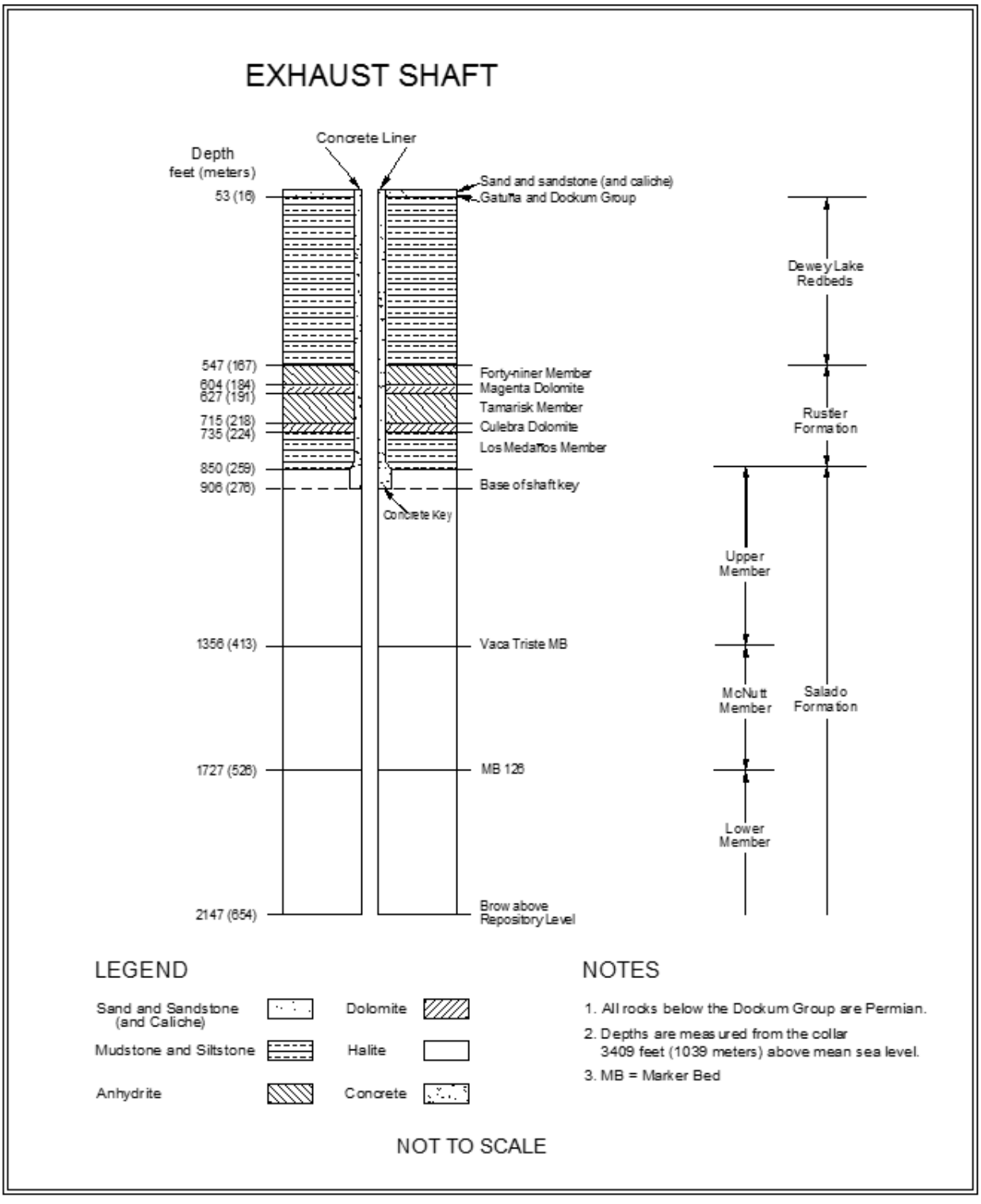

Figure 3-7 Exhaust Shaft Stratigraphy

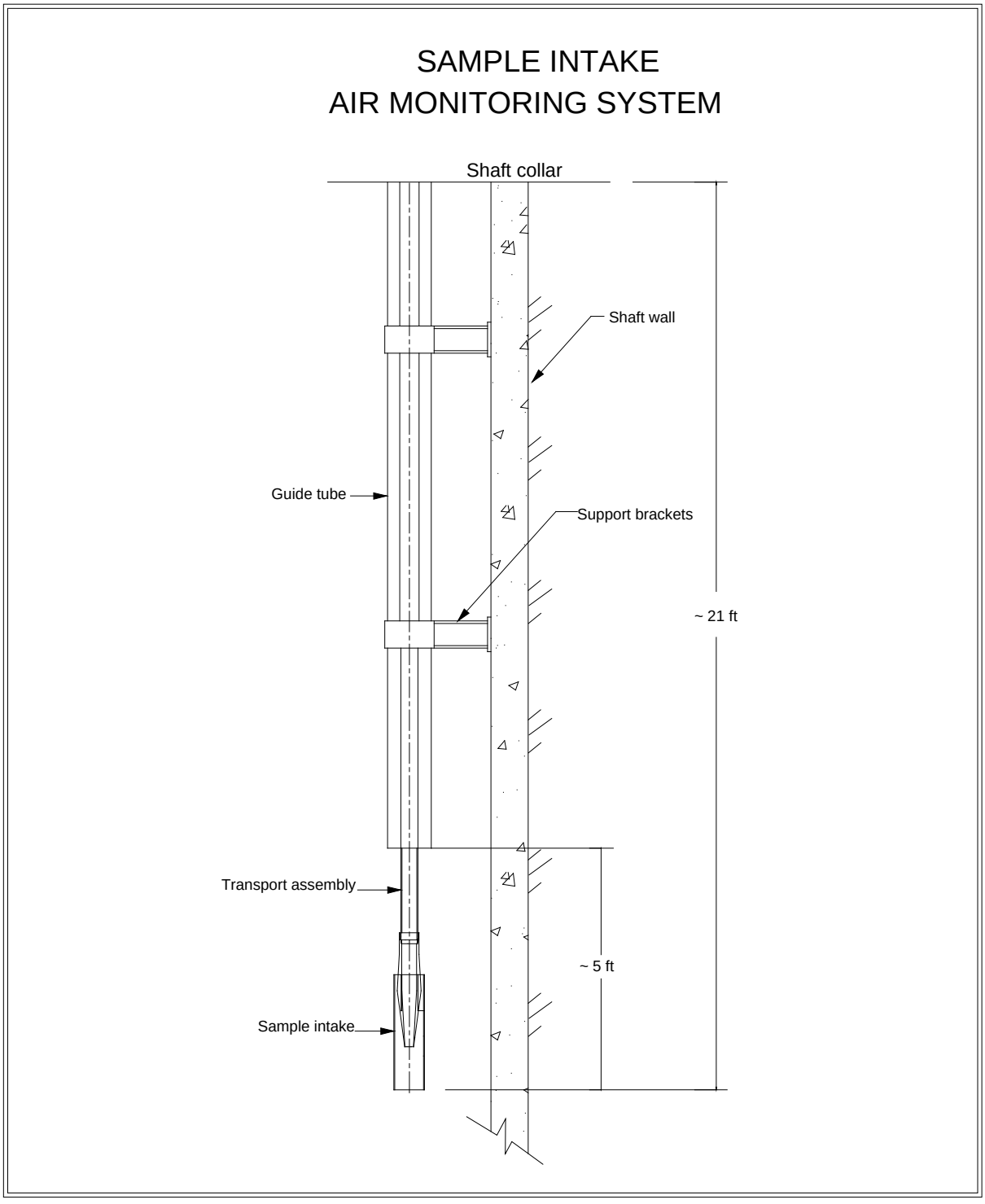

Figure 3-8 Sample Intake of Exhaust Shaft Air Monitoring System

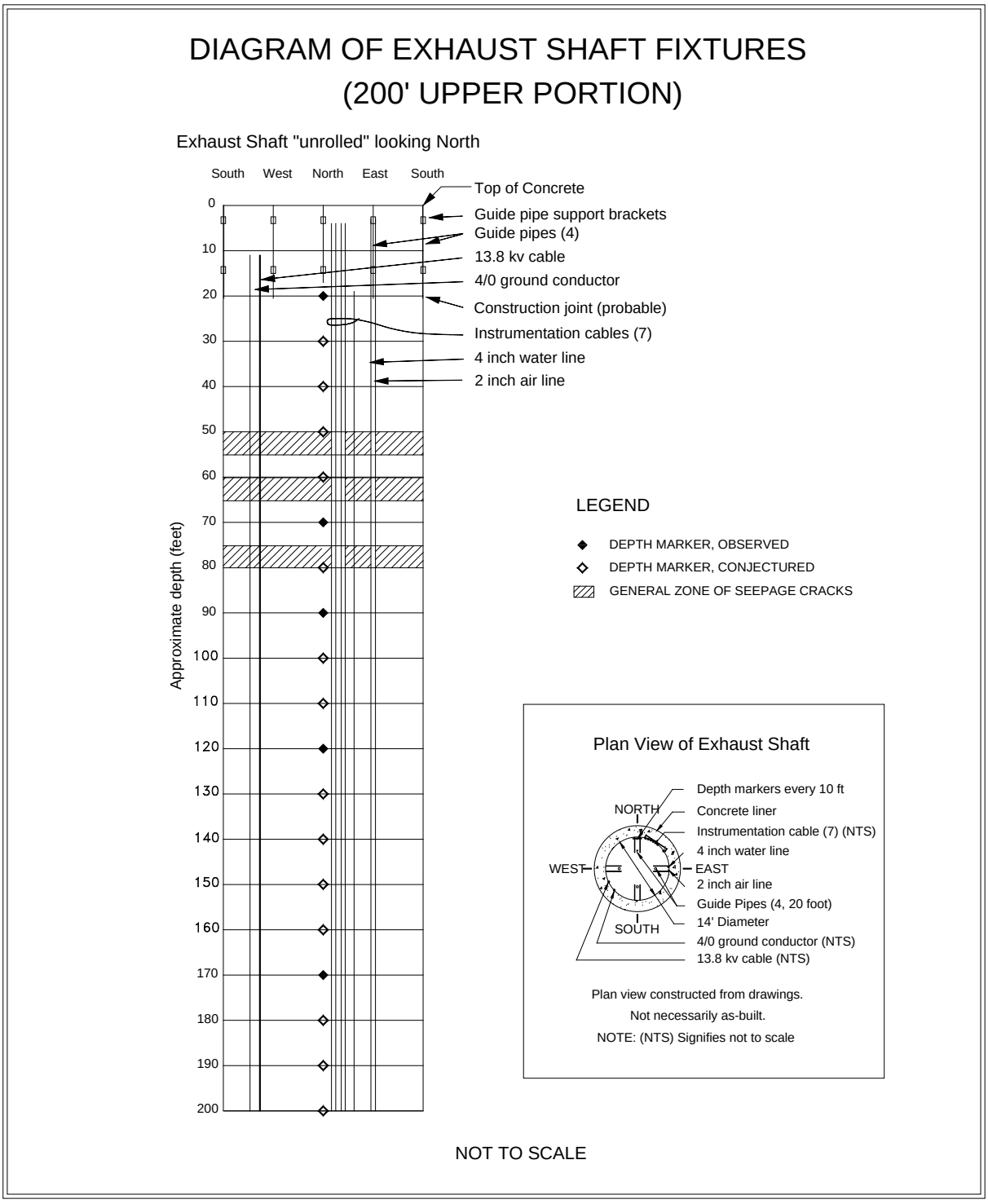

Figure 3-9 Diagram of Exhaust Shaft Fixtures and Seepage Zones (Upper 200 ft)

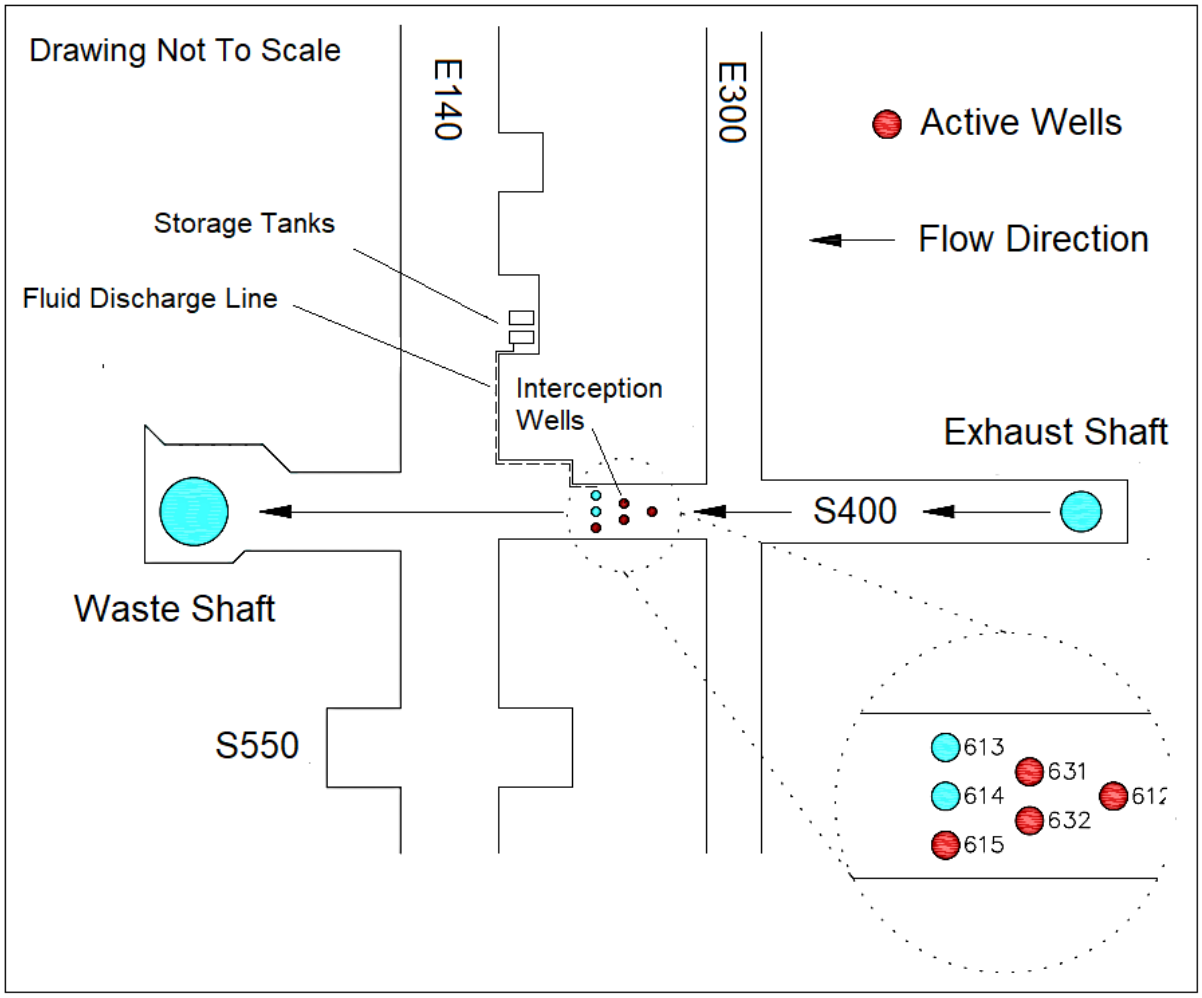

Figure 3-10 Location of Interception Wells and Storage Tanks

The shaft walls were examined for salt buildup, cracks, moisture, and encrustations, with particular attention paid to power cables, instrument cables, air and water lines, and the three water rings occurring at the base of the Magenta and Culebra members of the Rustler Formation and at the bottom of the shaft key. The condition of the shaft wall with respect to salt buildup varies depending on airflow, humidity, temperature, and underground mining activities. The shaft conditions for this reporting period largely mirror the conditions during the previous reporting period. There were no significant changes in the thickness of the salt in the shaft plenum, ranging from zero to several feet thick. The principle seepage in the shaft liner this period was located at about 60-65 ft and 80-85 ft bsc. At the same time, there continues to be an increase in the buildup of salt along the shaft walls in the form of stalactites in the lower portion of the shaft.

Similar to numerous previous inspections, sporadic salt buildup continues on the remaining cables in the shaft. The long-term implication of salt buildup is increased loading on cables and cable hangers, accompanied by intermittent falls of debris. The 4-in compressed air line and the 2-in water line extend from the surface to the bottom of the shaft. At present, neither line is being used. The integrity of the brackets holding the air and water lines continues to be essentially impossible to assess because of salt

buildup. Many instrumentation cables and much of the abandoned 13.8 kilovolt ampere(s) (kVA) power cables have broken off and fallen to the base of the shaft. There are no visible signs of dissolution of the salt below the key.

3.3.2 Instrumentation

The Exhaust Shaft was equipped with geomechanical instrumentation in two stages. Earth pressure cells were installed behind the liner key in November 1984. Piezometers and nine multi-position extensometers were installed during November and December 1985. Figure 3-11 and Figure 3-12 show the instrument locations. None of these instruments continue to provide data.

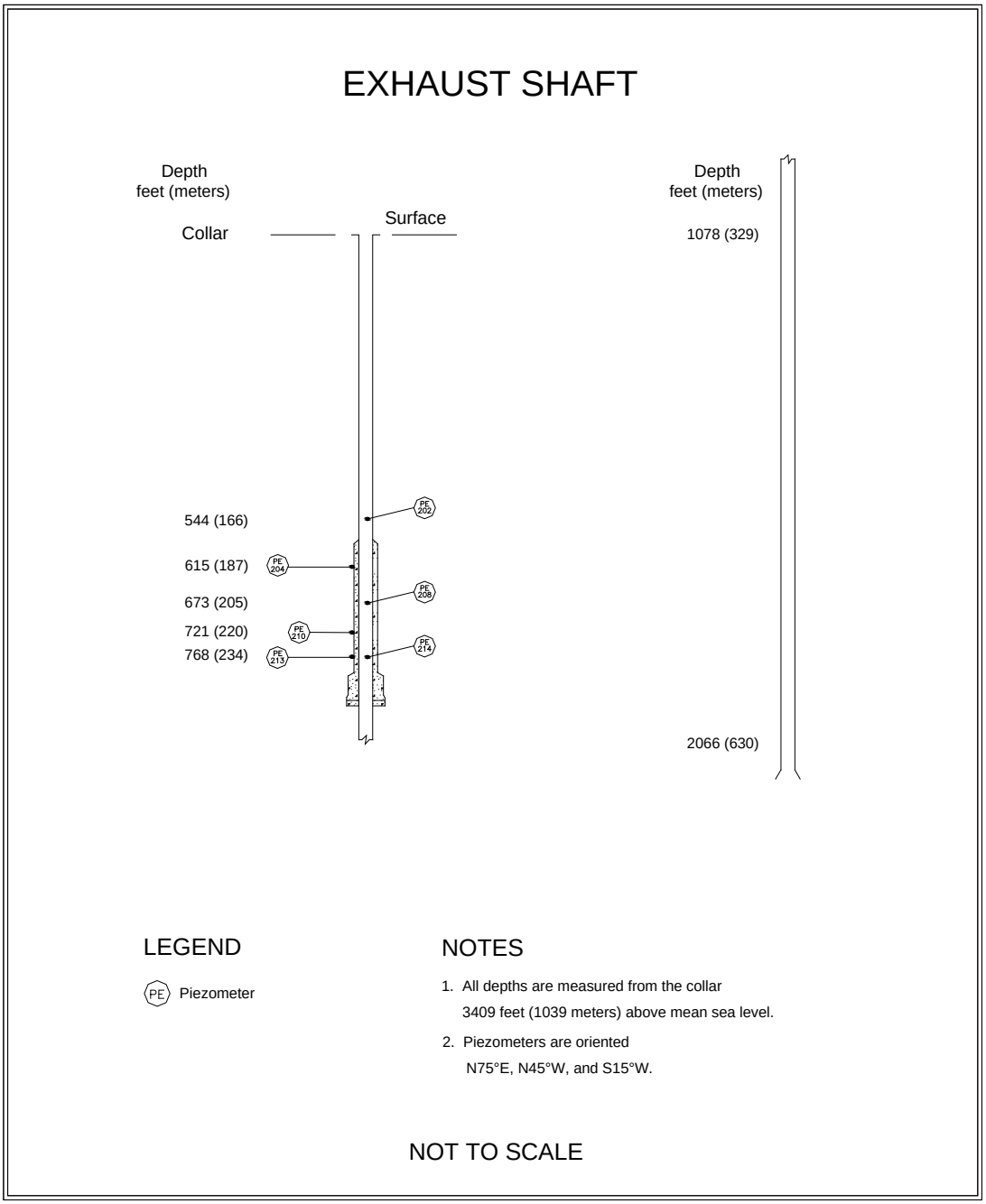

Figure 3-11 Exhaust Shaft Instrumentation

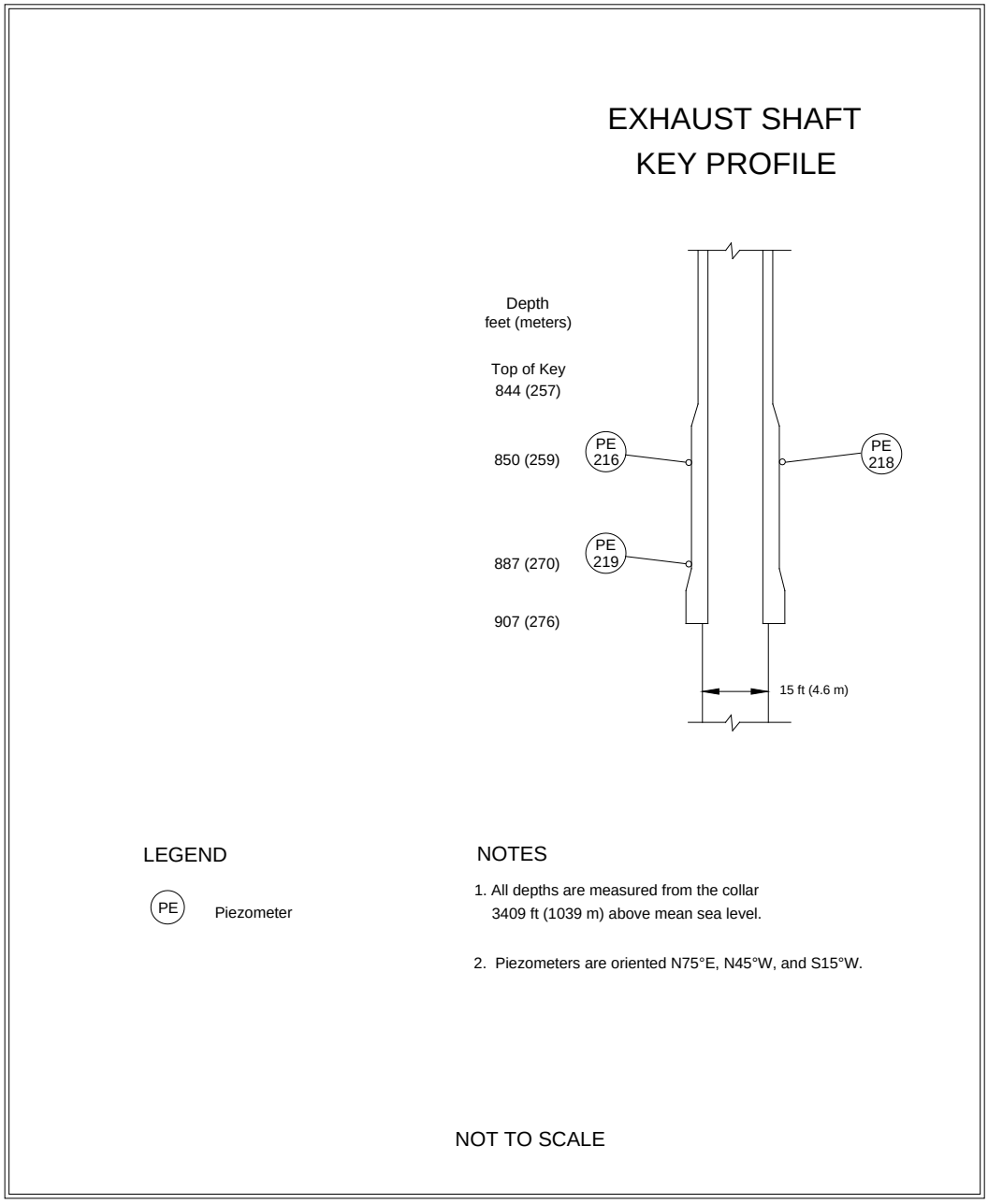

Figure 3-12 Exhaust Shaft Key Instrumentation

3.4 Air Intake Shaft

The Air Intake Shaft was drilled from December 4, 1987, to August 31, 1988, to establish a primary route for surface air to enter the repository (see Figure 1-2). The stratigraphy was mapped from September 14, 1988, to November 14, 1989 (Holt and Powers, 1990). Figure 3-14 summarizes the shaft stratigraphy.

The Air Intake Shaft is lined with non-reinforced concrete from the surface to the bottom of the shaft key at 903 ft (275 m). The key is 81 ft (25 m) long with an inside diameter of 16 ft (5 m). The shaft diameter below the key is 20 ft (6 m), and the shaft below the key is unlined to the facility horizon at 2,150 ft (655 m). The shaft walls are bolted and meshed from just below the key all the way down to the shaft station. This shaft has no sump.

3.4.1 Shaft Performance

Weekly visual inspections were performed on the Air Intake Shaft during this reporting period, and the shaft was found to be in satisfactory condition. No ground control activities other than routine maintenance were required during this reporting period.

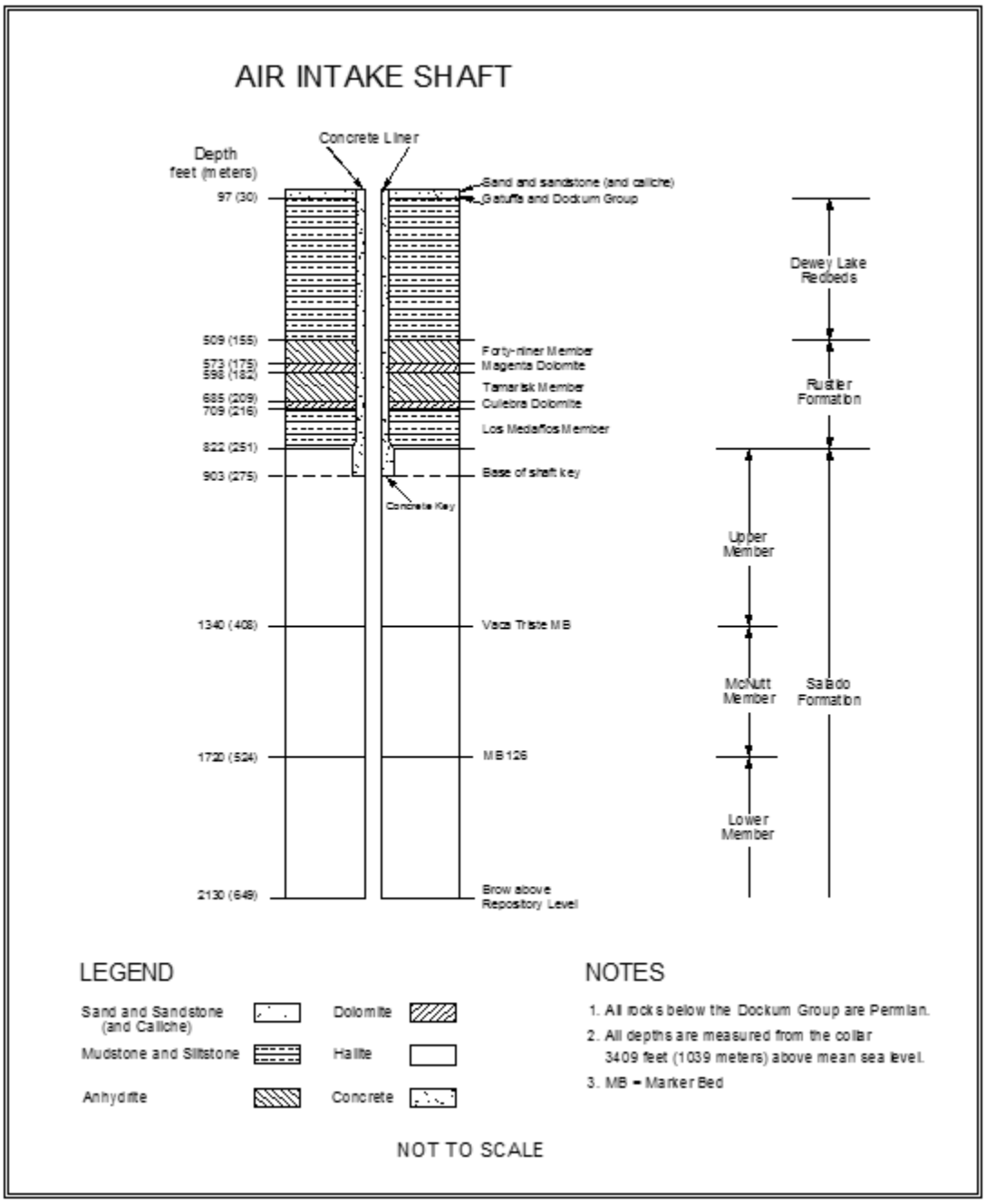

Figure 3-13 Air Intake Shaft Stratigraphy

4.0 PERFORMANCE OF SHAFT STATIONS

This section describes the instrumentation and geomechanical performance of the shaft stations at the base of the Salt Shaft, the Waste Shaft, and the Air Intake Shaft. The Exhaust Shaft does not have an enlarged shaft station; therefore, it is not included in this section.

4.1 Salt Shaft Station

The Salt Shaft Station was excavated by drilling and blasting between May 2, and June 3, 1982. In 1987, the station was enlarged by removing the roof beam up to Anhydrite "b" between S-90 and N-20 using a mechanical scaler. In 1995, the remaining roof beam at the north end of the station was also removed up to Anhydrite "b." The station area south of the shaft is 90 ft (27.5 m) long and 32 to 38 ft (10 to 12 m) wide. The height of the station south of the shaft is 18 ft (5.5 m). The station dimensions north of the shaft are approximately 30 ft (9 m) long, 32 to 35 ft (10 to 11 m) wide, and 18 ft (5.5 m) high. The shaft extends approximately 140 ft (43 m) below the facility horizon to accommodate the skip loading equipment and a sump. Figure 4-1 shows a cross section of the station.

4.1.1 Modifications to Excavation and Ground Control Activities

The Salt Shaft Station was not modified during this reporting period. Ground control activities were limited to routine maintenance.

4.1.2 Instrumentation

Geomechanical instrumentation was installed in the Salt Shaft Station between June 1982 and February 1983, with subsequent re-installation of extensometers and convergence points, as necessary. Figure 4-2 shows the instrument locations after the roof beam was taken down.

Four vertical convergence points are currently monitored. Table 4-1 summarizes the vertical closure rates in the Salt Shaft Station from July 2018 through June 2019. The closure rates for this reporting period are less that the rates for the previous reporting period.

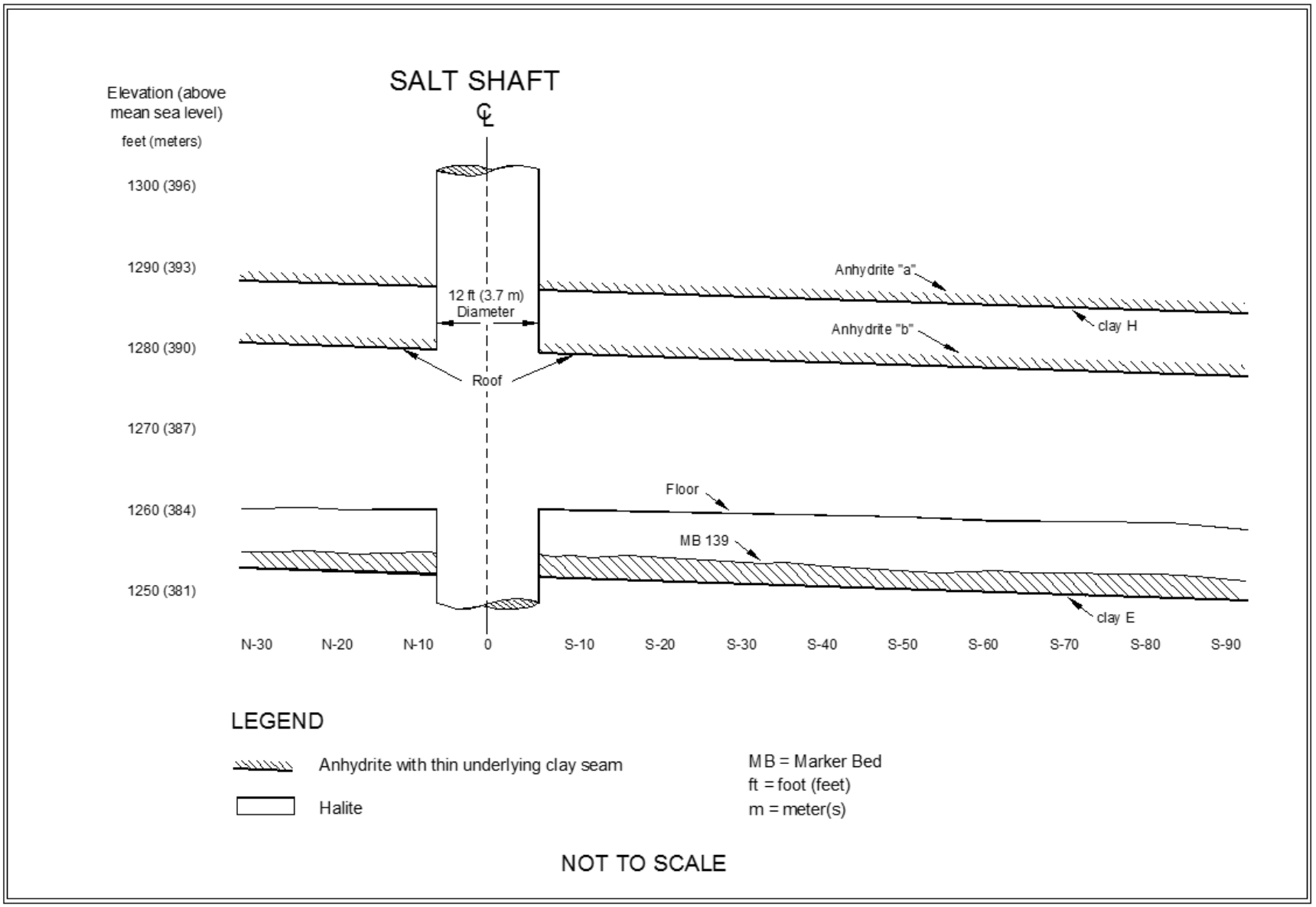

Figure 4-1 Salt Shaft Station Stratigraphy

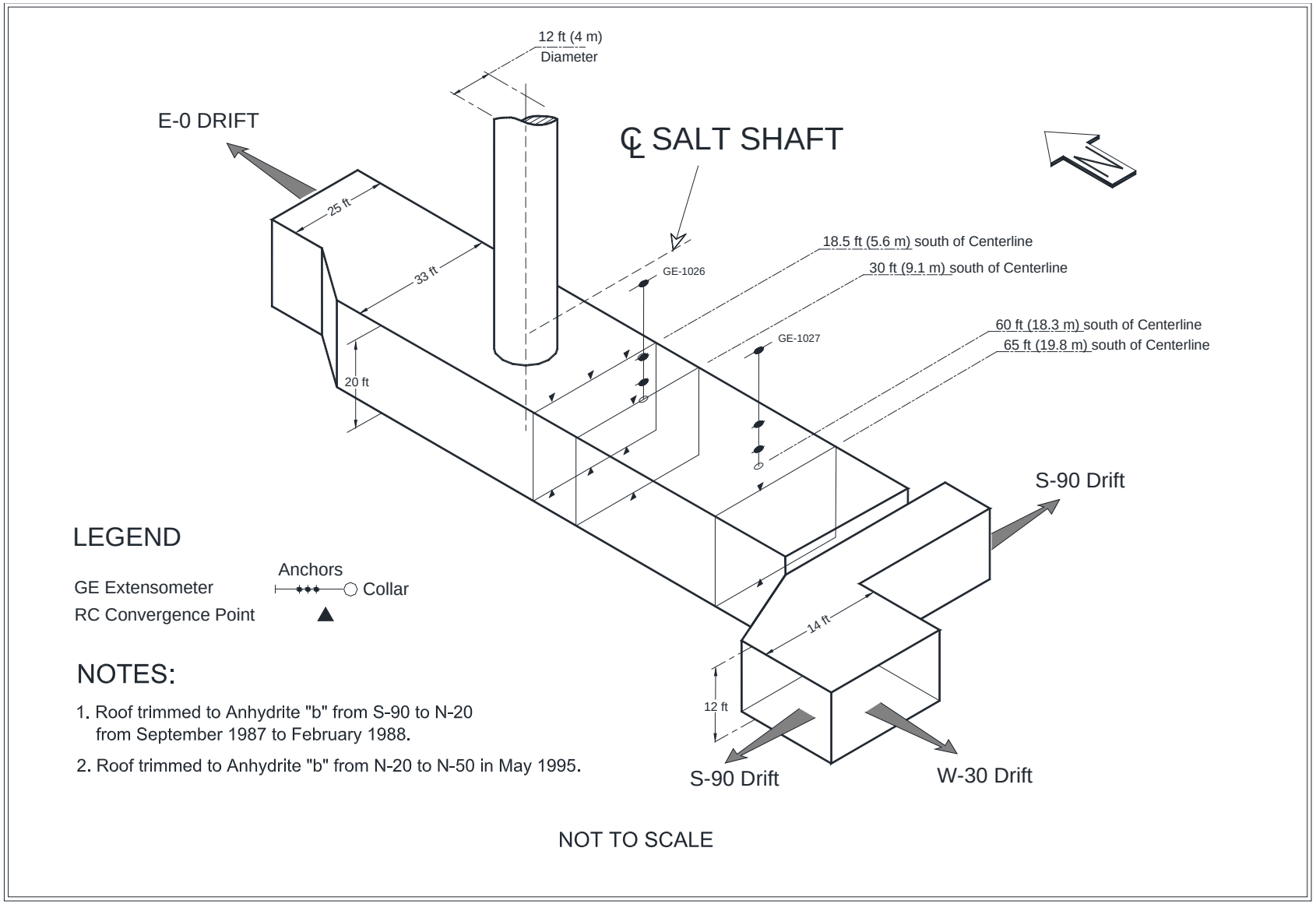

Figure 4-2 Salt Shaft Station Instrumentation After Roof Beam Excavation

Location	Chord[4]	Last Reading	Total Cumulative Displacement (in)	Closure Rate 2018-2019 (in/yr)	Closure Rate 2017-2018 (in/yr))	Rate Change (%)
E0-S18	A-E	02/26/19	33.275	1.3	1.8	-28
E0-S18	H-F	02/26/19	21.986	0.8	1.1	-27
E0-S30	A-C	02/26/19	34.168	1.4	1.8	-22
E0-S65	A-C	02/26/19	23.560	0.9	1.2	-25

Table 4-1 Closure Rates in the Salt Shaft Station

4.2 Waste Shaft Station

The Waste Shaft Station was initially excavated with a continuous miner in November 1982 to serve as a ventilation connection to a 6-ft (2-m)-diameter exhaust shaft. In 1984, the station was enlarged to a height of 15 to 20 ft (4.5 to 6 m) and a width of 20 to 30 ft (6 to 9 m). The station is approximately 150 ft (46 m) long. In 1988, the station walls were trimmed, and concrete was placed on the floor. Since 1988, the Waste Shaft Station has undergone five major floor renovations. A 53-ft (16-m)-long section of the reinforced concrete was removed in February 1991. In 1995, an additional 30-ft (9-m) section of concrete was removed. In 2000, floor maintenance included trimming of the floor and reinstallation of the rails supported by segmented concrete panels on a crushed rock backfill. The roof of the Waste Shaft Station was mined up to Clay G in December 2008 to assure adequate operational clearance. Chain link fencing and 12-ft resin-anchored roof bolts were installed for ground support. Figure 4-3 shows a cross section of the Waste Shaft Station stratigraphy.

4.2.1 Modifications to Excavation and Ground Control Activities

No modifications to the Waste Shaft Station were made during this reporting period. Ground control activities were limited to routine maintenance.

[4] Chord is defined in Section 5.2 and illustrated in Figure 5-1.

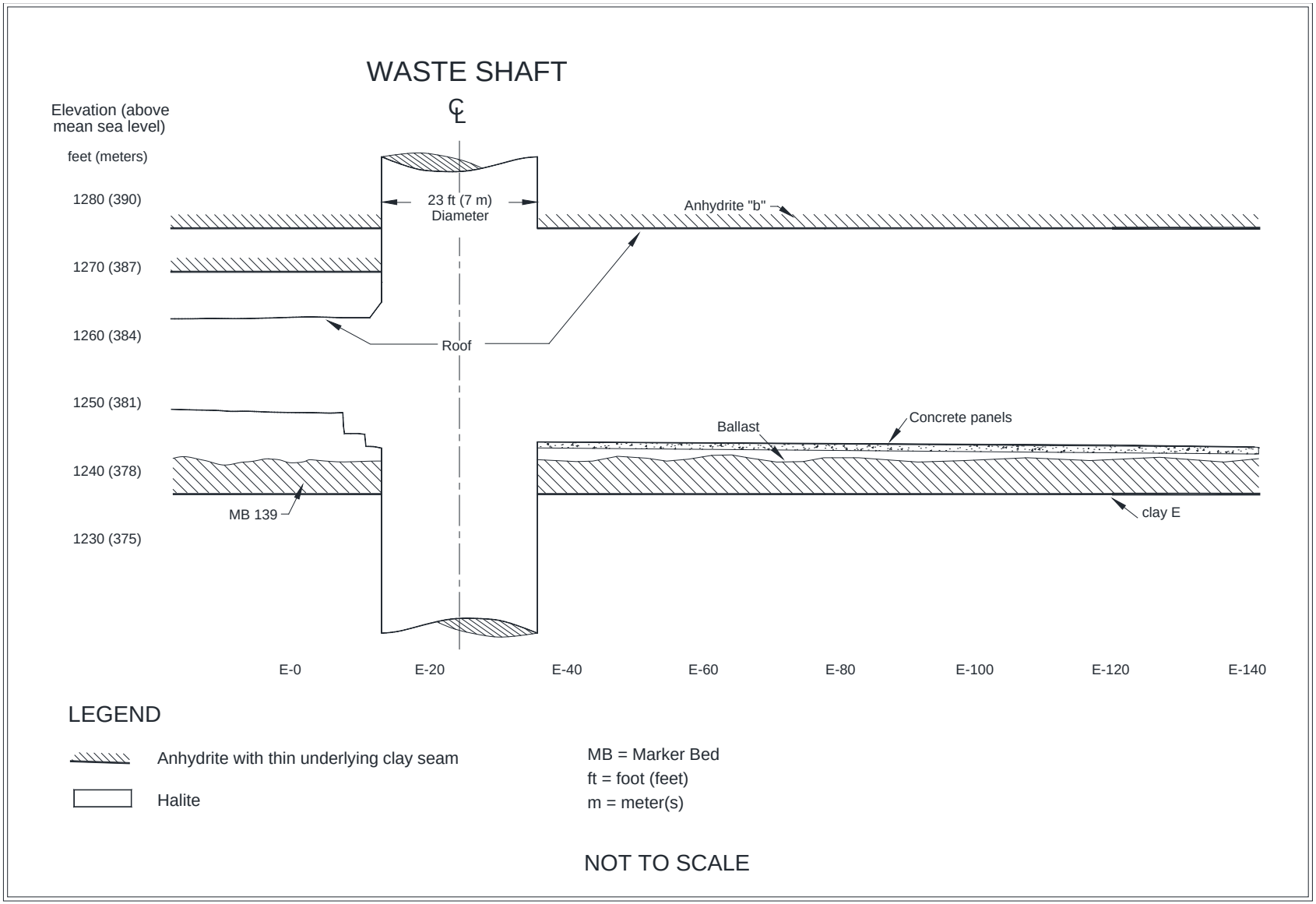

Figure 4-3 Waste Shaft Station Stratigraphy

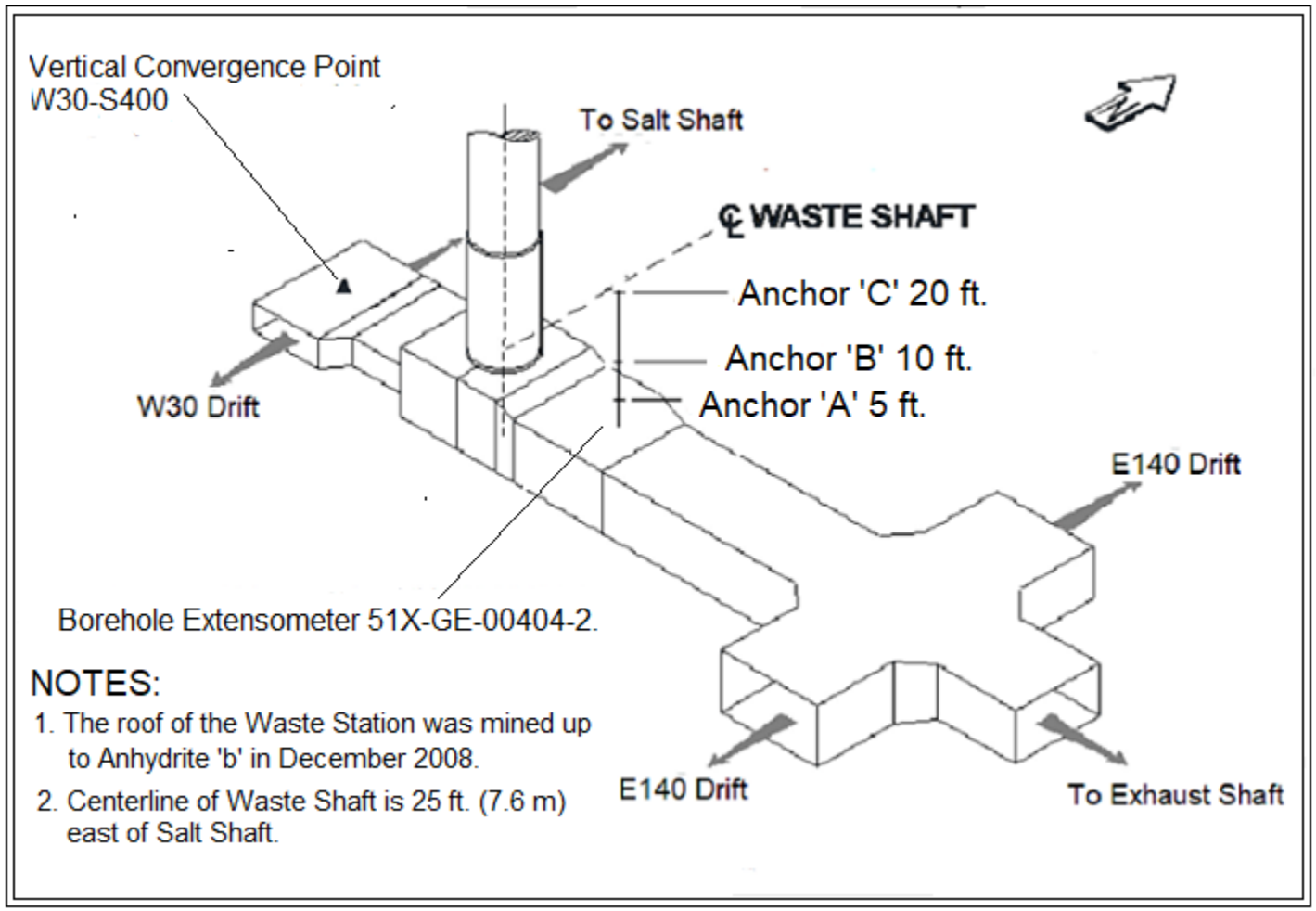

Figure 4-4 Waste Shaft Station Instrumentation

4.2.2 Instrumentation

The Waste Shaft Station geomechanical instrumentation, as depicted in Figure 4-4, consists of a vertical convergence point in W30-S400 and a borehole extensometer east of the Waste Shaft at S400-E35. The convergence rate this reporting period was 0.8 in/yr. The beam expansion rate as measured by the extensometer was 0.28 in/yr. The data are representative of a very stable back.

4.3 Air Intake Shaft Station

The Air Intake Shaft Station was excavated in late 1987 and early 1988, using a continuous miner. The Air Intake Shaft is furnished with a work platform and a small cage that can be raised and lowered to perform routine ground maintenance. The principal purpose of the cage is to provide emergency ingress and egress.

4.3.1 Modifications to Excavation and Ground Control Activities

The Air Intake Shaft Station was not modified during this reporting period. Ground control activities were limited to routine maintenance.

4.3.2 Instrumentation

Radial convergence point and extensometer instrumentation data near the Air Intake Shaft Station are presented in Section 5.0 as part of the discussion on the performance of the access drifts

5.0 PERFORMANCE OF ACCESS DRIFTS

This section describes the geomechanical performance of the underground access drifts. The Waste Disposal Area is discussed in Section 6.0 and the Salt Disposal Investigation areas are discussed in Section 7.0. Four major north-south drifts in the WIPP underground are intersected by shorter east-west cross-drifts. Drift dimensions range from 13 ft (4 m) to 21 ft (6.4 m) high, and from 14 ft (4.3 m) to 33 ft (9.2 m) wide.

5.1 Modifications to Excavation and Ground Control Activities

Floor trimming and rock bolting were performed during this reporting period. Table 5-1 summarizes these activities.

Location	Work Activity
E0 Salt Shaft Station	Installed 14-ft resin anchored roof bolt pattern.
E0 N150-N1400	Installed 14-ft resin anchored roof bolt pattern.
E140 drift from S700-S2520	Replaced 14-ft Dywidag roof bolts
E140 drift from N150 to S400	Replaced broken 14-ft resin anchored roof bolts.
E140 drift from N920 to N1100	Replaced broken 14-ft resin anchored roof bolts.
E140 drift from N1200 to N1300	Replaced broken 14-ft resin anchored roof bolts.
E300 drift from N250 to N460	Replaced broken 14-ft resin anchored roof bolts.
E300 drift from N1250 to N1420	Replaced broken 14-ft resin anchored roof bolts.
W30 drift from S1300 to S1950	Replaced broken 14-ft resin anchored roof bolts.
W30 drift, S1150 "High Back"	Replaced broken 14-ft resin anchored roof bolts.
W30 drift from S90 to S700	Installed 14-ft resin anchored roof bolt pattern.
W170 drift from S2180 to S2520	Replaced broken 14-ft resin anchored roof bolts.
S700 drift from E140 to E300	Installed 14-ft resin anchored roof bolt pattern.
S700 W30-W170	Extended the 14-ft resin anchored pattern to the south rib.
S1000 drift from E140 to E300	Installed 14-ft resin anchored roof bolt pattern.
S1000 drift from W30 to E140	Replaced broken 14-ft resin anchored roof bolts.
S1000 drift from W30 to W170	Replaced broken 14-ft resin anchored roof bolts.
S1300 drift from E140 to E300	Installed 14-ft resin anchored roof bolt pattern.
S1600 drift from W30 to W170	Replaced broken 14-ft resin anchored roof bolts.
S2180 drift W30-W170	Replaced broken 14-ft resin anchored roof bolts.
S2520 drift from E140 to W170	Replaced broken 14-ft resin anchored roof bolts.
N460 North and East Alcoves	Replaced broken 14-ft resin anchored roof bolts.
Maintenance Shop	Replaced broken 14-ft resin anchored roof bolts.
AIS (N215 & N300)	Replaced broken 14-ft resin anchored roof bolts.
Panel 7	Replaced broken 14-ft resin anchored roof bolts.
Panel 8	Installed 5-ft resin anchored roof bolt pattern.
Mine Wide	Drilled 20-ft Observation Holes.

Table 5-1 Summary of Modifications and Ground Control Activities in the Access Drifts: July 1, 2018, to June 30, 2019

5.2 Instrumentation

This section discusses instrumentation details in the access drifts.

5.2.1 Extensometers

Thirteen extensometers continue to be monitored at various locations in the access drifts. Where displacement data were available, annual displacement rates were calculated (see Section 1.4.3) for each active installation and compared to the annual displacement rates from the previous reporting period. Extensometer data are obtained by measuring the displacement from the reference head anchor (collar) to each fixed anchor of the extensometer. These measurements are scheduled to be made at least monthly throughout the WIPP underground.

Many of the E-140 extensometers indicate movement in the roof beam that may be attributed to shallow fracturing and the effects of anhydrite stringer separations in the roof. Lateral deformation in the roof beam may influence the extensometer readings, causing an increase in the measured displacement. Although the extensometer data indicate continued deformation and breakup of the lower beam, the roof bolt anchorage zone remains competent.

5.2.2 Convergence Points

Convergence point data are obtained by measuring the change in distance between fixed points anchored into the rock across an opening, either from rib to rib or from roof to floor. The measurement end-points constitute a "chord." Figure 5-1 shows typical convergence point array configurations along with typical chord designations.

Convergence points are routinely installed following new mining and in areas where ground maintenance has been performed and previously installed convergence points have been removed. A listing of convergence point installations performed in the access drifts during this reporting period are shown in Table 5-2, Convergence Point Installations in the Access Drifts: July 1, 2018, to June 30, 2019.

Where possible, annual closure rates were calculated from convergence point array data gathered in the access drifts. During this reporting period the active convergence points in the underground were distributed as follows: 175 convergence points in the access drifts, 25 accessible convergence points in Panel 7 and 55 convergence points in the SDI area. However, access restrictions are in place in SDI for areas south of N780 until regular ground control maintenance can be performed, preventing access to 27 of the 55 convergence arrays. A complete tabulation of the accessible convergence point data and calculated closure rates is presented in the supporting data document for this report.

Locations with increases in annual vertical closure rates of greater than 20 percent are shown in Table 5-3, Vertical Closure Rate Changes in Excess of Twenty Percent in the Access Drifts.

5.3 Analysis of Convergence Point and Extensometer Data

Vertical loading on mine pillars results in lateral stresses on the roof and floor beams. The composition of those beams, in part, determines how these structures will react to the horizontal stresses. In particular, horizontally continuous anhydrite stringers (see Section 2.2.2) divide the beam itself into a series of smaller independent beams.

Lateral strain on the beam imposed by vertical loading on the pillars is accommodated by vertical displacement over the mined opening. This requires that the horizontally oriented beam separate along the most favorable, or weakest, planes.

Where anhydrite stringers interpose the beam, they constitute a plane of weakness, and delamination occurs. The material is confined in the plane above, so that the roof accommodates the lateral strain by bending convex into the mined opening.

Two distinct results develop from this action. First, voids form within the beam as the portions closer to the opening move away from those deeper within the beam. Second, the convex portion of the bended plane is subjected to tensile loading perpendicular to the axis of the drift and superficial tears known as "tensile fractures" develop generally parallel to the axis of the drift.

Where anhydrite stringers are small and discontinuous or absent within the beam, horizontal loading is accommodated along shear planes. These develop at angles of approximately 35 degrees with respect to the horizontal. In some cases, a plane develops preferentially on one side of the drift, and the bulk of material is pushed into the mined opening on that side. This may be thought of as a cantilevered beam.

Whatever mechanism is used, vertical displacement into the mined opening is measured by convergence monitoring. Convergence points consider the displacement between two opposing surfaces: either the roof and floor or the two ribs. Extensometers consider the displacement between one surface (usually the back) and one or more points within the beam. Where a convergence point and an extensometer are adjacent to one another, it is possible to determine the individual displacements of both floor and roof beams.

These data are used to analyze the stability and mechanics of the beam, and to determine what actions may be taken to ensure the safety of personnel and equipment consistent with the safe operation of the facility.

5.4 Excavation Performance

Approximately 238 readings were collected and assessed regularly from convergence point arrays throughout the WIPP underground this reporting period. Due to the effect rock temperature has on salt creep, convergence rates vary seasonally, typically increasing during the warmer summer months and decreasing during the cooler and drier winter months. These temperature effects are more pronounced nearer the fresh air intake.

The performance of the access drift excavations during this reporting period was within acceptable criteria. "Acceptable criteria" means that a drift remains accessible, and the ground can be controlled by routine maintenance. Standard remedial ground control in some areas was required to maintain the performance of the excavations. The accessible drifts remain stable and controlled. Of the 185 convergence locations measured in the access drifts, only two locations had annual closure rates in excess of 20 percent from the previous year’s value. See Table 5-3, Vertical Closure Rate Changes in Excess of Twenty Percent in the Access Drifts.

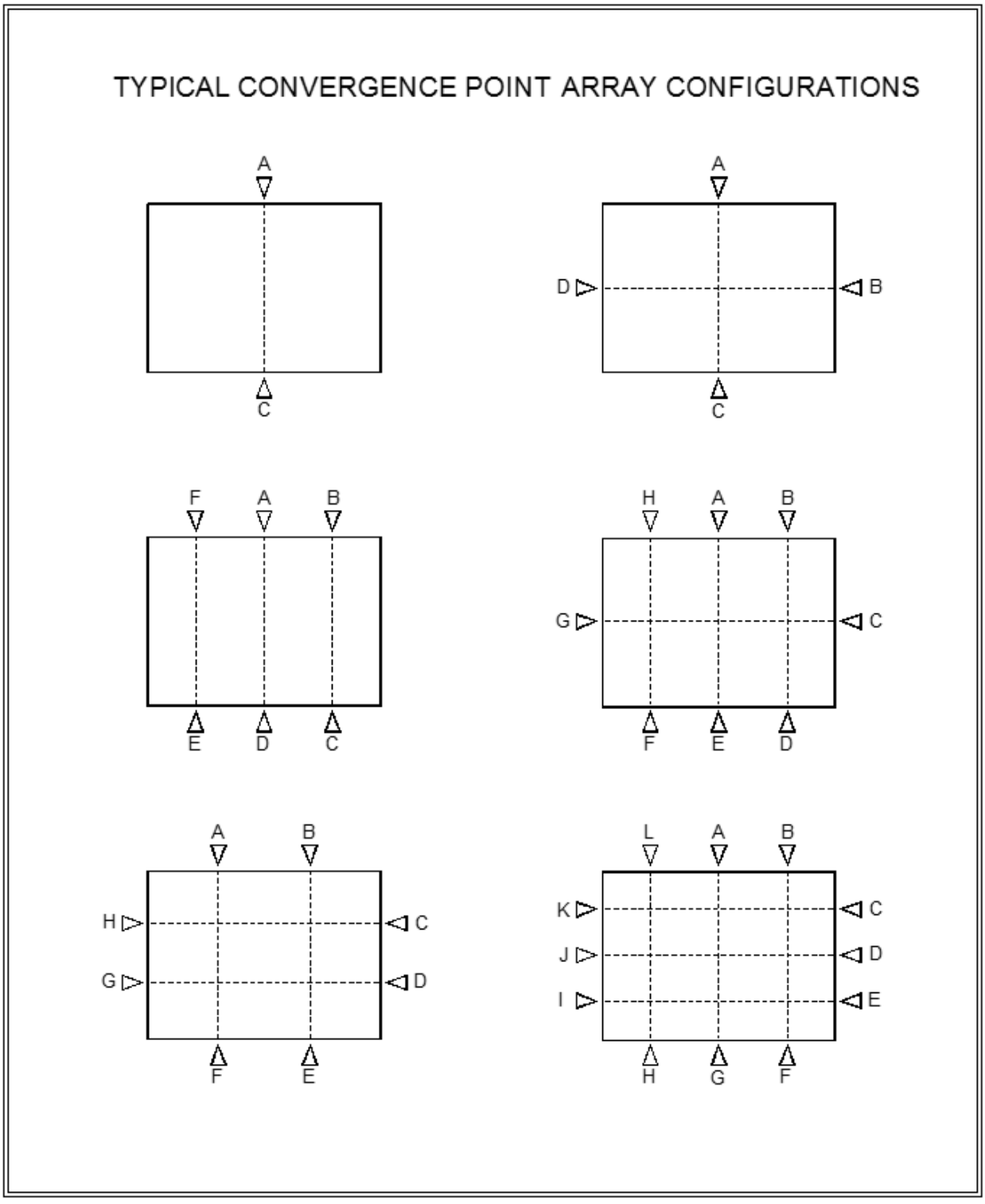

Figure 5-1 Typical Convergence Point Array Configurations Showing Anchor Designations

Location	Installation Date	Type of Installation[5]	Field Tag[6]
E0-N225	02/26/19	R	E0-N225-5 A-C
E0-N460	02/26/19	R	E0-N460-4 A-C
E0-S18	02/26/19	R	E0-S18-7 B-D
E140-S1496	06/20/19	N	E140-S1496 B-D
E140-S1496	06/28/19	N	E140-S1496 H-F
E140-S1496	06/03/19	N	E140-S1496 A-E
E140-S1524	06/20/19	N	E140-S1524 B-D
E140-S1524	06/28/19	N	E140-S1524 H-F
E140-S1524	06/03/19	N	E140-S1524 A-E
E140-S1534	04/01/19	R	E140-S1534-5 A-E
E140-S1534	04/01/19	R	E140-S1534-5 H-F
E140-S1534	04/01/19	R	E140-S1534-6 B-D
E140-S1548	06/20/19	N	E140-S1548 B-D
E140-S1548	06/28/19	N	E140-S1548 H-F
E140-S1548	06/03/19	N	E140-S1548 A-E
E140-S1578	04/01/19	R	E140-S1378-7 B-D
E140-S1667	06/03/19	N	E140-S1667 A-E
E140-S1667	06/03/19	N	E140-S1667 B-D
E140-S1667	06/03/19	N	E140-S1667 H-F
E140-S1699	06/03/19	N	E140-S1699 A-E
E140-S1699	06/03/19	N	E140-S1699 B-D
E140-S1699	06/03/19	N	E140-S1699 H-F
E140-S1717	06/20/19	N	E140-S1717 H-F
E140-S1717	06/03/19	N	E140-S1717 A-E
E140-S1717	06/03/19	N	E140-S1717 B-D
S1600-E170	04/01/19	R	S1600-E170-3 A-C
W30-S1150	07/17/18	R	W30-S1150-3 A-C
W30-S1150	11/13/18	R	W30-S1150-3 A-C
W30-S1775	04/15/19	R	W30-S1775-9 A-C

Table 5-2 Radial Convergence Point Installations in the Access Drifts: July 1, 2018, to June 30, 2019

[5] R - denotes a replacement installation, e.g., roof or floor point(s) could have been mined out, damaged, etc. N – represents a new installation at that location.
[6] Field Tag (aka fieldtag) is a string consisting of 'location' + '- number of times a reinstall was conducted at that location' + ' chord'. Note that new installations do not have a reinstallation number.

Location	Chord[7]	Last Reading Date	Closure Rate 2018 to 2019 (in/yr)	Closure Rate 2017 to 2018 (in/yr)	Rate Change (%)
E140-S1025	A-C	05/14/19	2.9	2.0	45
E140-S1600	A-C	05/15/19	4.5	3.6	25

Table 5-3 Vertical Closure Rate Changes in Excess of Twenty Percent in the Access Drifts

6.0 PERFORMANCE OF THE WASTE DISPOSAL AREA

The Waste Disposal Area as of June 30, 2019, consisted of Panels 1, 2, 3, 4, 5, 6, 7, and a partially mined Panel 8. Panels 1, 2, 3, 4, 5, and 6 were closed during previous reporting periods.

6.1 History

Excavation of Panel 1 began in May 1986 with the mining of the access entries. Initially, the disposal rooms and drifts were developed as pilot drifts that were later excavated to nominal operational dimensions of 13 ft (4 m) high, 33 ft (10 m) wide, and 300 ft (91 m) long. Room 1 was completed to these dimensions in August 1986, and pilot drifts for Rooms 2 and 3 were excavated in January and February 1987. Rooms 2 and 3 were completed in February and March 1988, and Rooms 4 through 7 were completed in May 1988. Four short access drifts designed to lead to smaller test alcoves were excavated north off the S-1600 drift and Rooms 4-7 in June 1989. Only the access drifts to the alcoves were completed; the alcoves themselves were not excavated. Panel 1 waste emplacement (in Rooms 1, 2, 3, 7, adjacent areas of S-1600, and all of S-1950) was completed during a prior reporting period, and the panel is closed to all access

Excavation of Panel 2 began in September 1999 with the mining of access entries. Initially, the disposal rooms and drifts were developed as pilot drifts that were trimmed to finished dimensions. Room 1 was completed in January 2000, and pilot drifts for Rooms 2 and 3 were excavated in February 2000. Pilot drifts were completed for Rooms 4 through 6 in April 2000. The pilot drift for Room 7 was excavated in May 2000. All the rooms were excavated to final dimensions by August 2000. Waste emplacement in Panel 2 was completed during a prior reporting period, and the panel is closed to all access.

[7] Chord is defined in Section 5.2.2 and illustrated in Figure 5-1.

Excavation of Panel 3 began in May 2002 with the mining of access entries. As with Panel 2, the disposal rooms and drifts were initially developed as pilot drifts that were trimmed to finished dimensions. All the rooms were excavated to final dimensions by the end of March 2004. Waste emplacement in Panel 3 was completed in February 2007. Substantial barriers and bulkheads were installed in the exhaust and intake drifts of Panel 3 to prevent access into the panel and to isolate it from the ventilation circuit.

Panel 4 access drift mining began in January 2005. The disposal rooms were initially developed as pilot drifts and were later trimmed to final dimensions. Mining was completed by June 2006. Waste emplacement in Panel 4 was completed in March 2009. Substantial barriers and bulkheads were installed in the exhaust and intake drifts of Panel 4 to prevent access into the panel and to isolate it from the ventilation circuit.

Panel 5 excavation activities began in June 2006. The panel was initially mined to less-than-final dimensions and later trimmed to specification. Mining was complete by February 2008. Waste emplacement was conducted from March 2009 through July 2011. Isolation walls were completed in November 2011

Panel 6 mining began in April 2008. The panel was initially mined to less-than-final dimensions and later trimmed to specification. Mining was complete by April 2010. Waste emplacement began in March 2011 and was completed in January 2014.

Panel 7 mining began in April 2010 and was completed in August 2011.
Initial mining placed the floor within 2 ft of a polyhalitic halite bed (designated PH-4), which sits atop a thick anhydrite bed designated MB-139. Horizontal stresses caused significant uplift and the floor was then mined down through MB-139 and backfilled with run of mine salt. The remediation of the floor was completed in January 2013. Subsequent geomechanical monitoring indicates stable vertical convergence. RH waste emplacement began in Panel 7 in September 2013 and CH waste emplacement began in January 2014. Waste emplacement and ground control activities were suspended in February 2014 due to a truck fire in the underground followed by a radiation release in Panel 7. Ground control activities resumed in 2015. Waste emplacement resumed in January 2017 at the intersection of Room 6 and S2520.

Panel 8 mining resumed in February 2018. The back has been mined to Clay G in the S1600 access drifts from Room 1 to Room 3, S1950 drift from Room 1 to Room 4, Room 2, and the north half of Room 3.

6.2 Modifications to Excavations and Ground Control Activities

No planned excavation modifications were performed this reporting period in Panel 7. However, a roof fall in Room 6 of Panel 7 occurred on November 11, 2018. The potential for a roof fall was first identified in September 2017 and access to the room had been closed since September 2016. The roof fall did not impact the accessible areas of the panel.

Routine ground control activities were performed in Panel 7 to include scaling and meshing, as needed, and the replacement of broken roof bolts with 14-ft resin anchored bolts.

A very significant modification to Panel 8 (as detailed in Section 6.1) is the mining of the back up to the upper horizon. Also initiated during this reporting period in Panel 8 was the installation of 6-foot resin anchor roof bolts. The bolts were installed within two weeks of mining to slow the development of separations along anhydrite stringers within the roof beam and subsequent surface tension crack development.

6.3 Instrumentation

Panel 7 instrumentation originally consisted of the following:

- Forty-nine vertical convergence points, distributed as 14 in each of the intake and exhaust drifts and three in each of the rooms; and
- Eleven wire extensometers, distributed as two in each of the intake and exhaust drifts and one in each of the rooms.

A schematic of the geomechanical instrumentation layout found in Panel 7 is shown in Figure 6-1. This figure presents what has been a typical Waste Panel instrumentation layout since emplacement began in Panel 1.

6.4 Analysis of Extensometer and Convergence Point Data

Similar to last year Panel 7 is continuing to experience age-appropriate roof beam and floor deformation. Extensometer data in Panel 7, Room 5 indicates a constant roof beam acceleration of approximately 1 in/yr/yr. Convergence rates in Room 3 indicate all three measurement locations had closure rates less than 4 in/yr and extensometer readings indicate a steady roof beam acceleration of 1.6 in/yr/yr.

Extensometer readings from Room 2 show a beam dilation of approximately 2 in/yr. Convergence rates in Rooms 1 and 2 are less than 5 in/yr with no acceleration. The Room 1 extensometer indicates a steady bean expansion rate of less than 4 in/yr. The intersection of Room 3 and the S-2520 drift for much of the reporting period had a roof-to-floor closure rate slightly over 5 in/yr, largely due to floor heave. Following floor remediation and some bolting, the intersection ended the reporting period with a closure rate of less than a 3 in/yr. Closure rates in S-2180 indicate steady rates of closure, with most less than 4 in/yr. The Panel 7 convergence stations had an average closure rate of 3.3 in/yr down from a 3.9 in/yr average during the 2017 to 2018 reporting period. Twenty-two of the 25 convergence stations had a negative percent change in rate, two had no change and one had a three percent increase in rate. Convergence monitoring in Panel 8, Room 1 indicates closure rates of less than 4 in/yr with no accelerations. The S-1600 access drift shows an average rate of 4 in/yr.

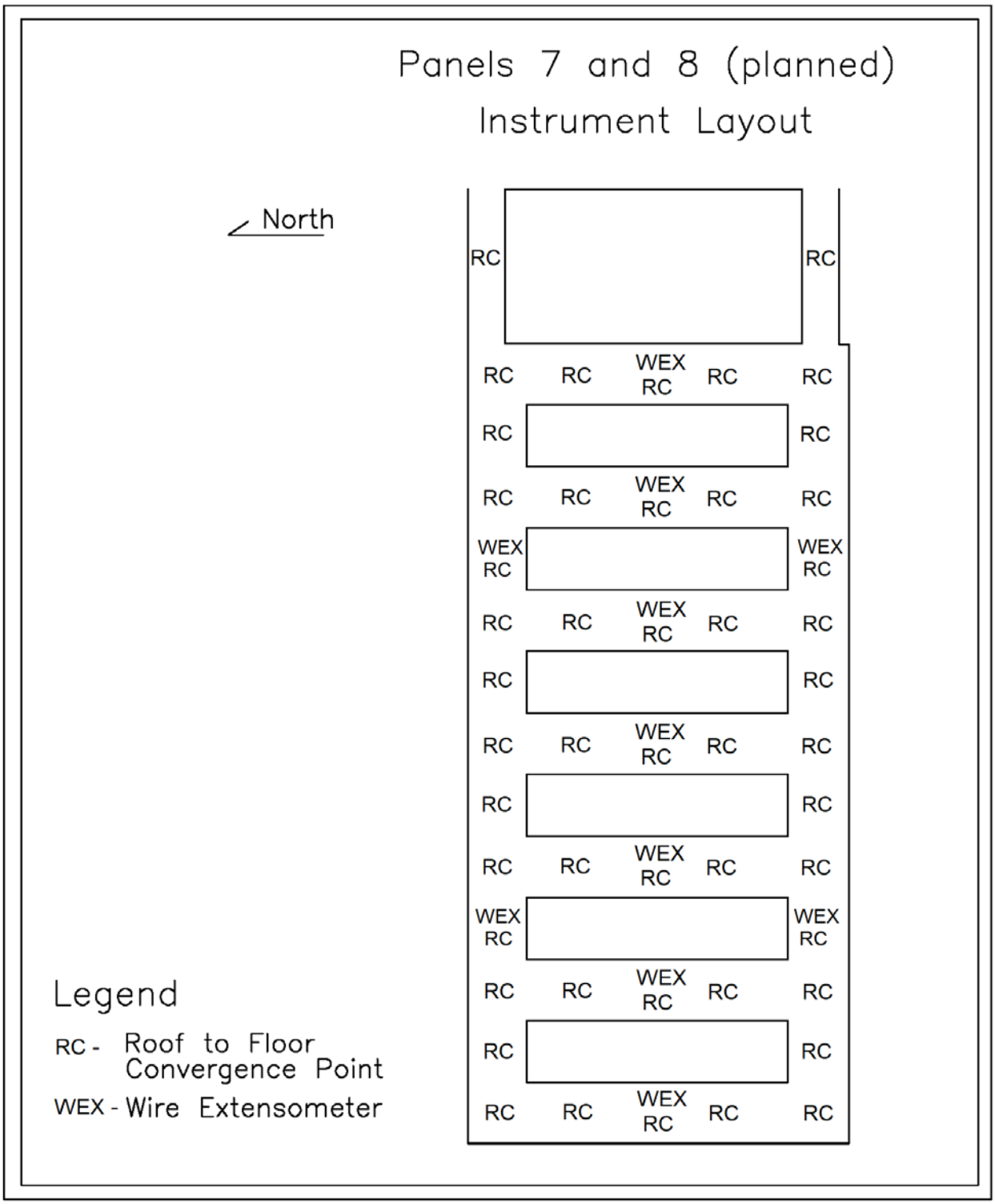

Figure 6-1 Typical Waste Panel Instrument Layout

6.5 Excavation Performance

Panel 7 is performing as expected considering its age and history. The panel should fulfill its intended purpose as long as ground control efforts can continue.

7.0 PERFORMANCE OF THE SALT DISPOSAL INVESTIGATIONS AND SALT DEFENSE DISPOSAL INVESTIGATIONS

This chapter describes the geomechanical performance of the SDI and SDDI areas (hereafter referred to as SDI). Development of the area began in January 2012. When completed, most of the area will have nominal dimensions of 13 ft high and 16 ft wide.

7.1 Ground Control Program

Due to the relatively narrow drifts (nominally 16 ft across) and favorable mining horizon, ground control plans in the SDI area are confined to routine maintenance, such as spot-bolting where localized drummy surface features develop. More substantial engineered ground control systems may be applied in the event that ongoing geomechanical monitoring and analysis of the area identify a need.

7.2 Instrumentation

Fifty-five convergence arrays have been installed in the SDI area. The arrays are read on a periodic basis, when accessible. During this reporting period twenty-eight arrays were accessible.

7.3 Analysis of Convergence Point Data

The twenty-eight convergence points for this period had a mean roof-to-floor closure rate of 1.5 in/yr with a standard deviation of 0.3. Low rates of closure are expected for this area due to the factors described in beginning of Section 7.1.

7.4 Excavation Performance

A combination of ground control, and to some extent ventilation challenges, led the Operations Department to prohibit access to the SDI area during the previous reporting period so the resources could be channeled to address more significant ground control remediation in other areas. The same operational challenges apply to this reporting period, although, the inaccessibility is primarily limited to twenty-seven convergence stations in the areas in SDI south of the N-780 drift.

Since closure readings were not taken during the last reporting period, a comparison between the rates of closure between the two most recent reporting periods could not be obtained. However, a comparison of closure rates was performed using the data from the 2016 to 2017 reporting periods compared against this reporting period. The 2016 to 2017 reporting period also had a mean closure rate of 1.5 in/yr with a standard deviation of 0.3. The statistics for the 28 convergence stations are representative of steady state behavior with low rates of closure.

8.0 GEOSCIENCE PROGRAM

The activities of the geoscience program were not performed during this reporting period, primarily due to the difficulty in filling a geotechnical engineering position. A description of the various aspects of the geoscience program is presented in the remainder of Section 8.0.

The geoscience program confirms the suitability of the site through the collection of various geologic data and excavation characteristics from the underground. These include the inspection of open observation holes for fractures (separations) and offsets (lateral displacements) in roof beams, and the mapping of fracture development on roof surfaces. Data collected through these activities support the design and evaluation of ground support systems.

Normally, the following activities are performed:

- Observation hole inspections
- Fracture mapping
- Stratigraphic mapping
- Drilling and Geologic Core Descriptions

Fracture development in the roof is primarily caused by the concentration of compressive stresses in the roof beam and is influenced by the size and shape of the excavation and the stratigraphy in the immediate vicinity of the opening. In a thick roof beam, pillar deformations induce lateral compressive stresses into the immediate roof and floor. With time, the buildup of stress causes differential movement along stratigraphic boundaries. This differential movement is identified as offsets in observation holes and by the bends in failed rock bolts. Large strains associated with lateral movements can induce fracturing in the roof, which is frequently seen near the ribs. However, this process may take years to develop.

At the upper repository horizon, clay or anhydrite stringers exert significant influence over the effective thickness of the roof beam. The presence of these stringers causes the roof beam to behave as a series of thin independent beams. Little or no tensile support is provided across the stringer interface. As horizontal end-loading continues, each beam can deflect downward causing a tensile fracture to develop along the bottom of the beam. These tensile fractures can develop in relatively new excavations soon after separation occurs along the stringer interface.

8.1 Observation Hole Inspections

Geotechnical observation holes are drilled at various locations throughout the underground facility. A location may contain one or more holes arranged in an array. These holes are drilled to depths that allow the monitoring of fracture development and offsetting and are inspected for the development of those features. Roof observation holes usually extend up past Clays G and H (Figure 8-1 and Figure 8-2).

The clay seams nearest the excavation surfaces define the immediate roof beam. The roof beam is bounded by Clay G in most of the access drifts and Panels 1, 2, 7, and 8. Some areas, such as the Salt Shaft Station, portions of the E-0 and E-140 drifts, the south mains south of S-2620, and Panels 3, 4, 5, and 6, are excavated to Clay G and have roof beams bounded by Clay H.

The offset in an observation hole is determined by visually estimating the degree of occlusion. The direction of offset along clay seams is observed as the movement of the strata nearer to the observer relative to the strata farther away. Typically, the nearer strata move toward the center of the excavation (Figure 8-3 and Figure 8-4). Based on previous observations in the underground, the magnitude of offset is usually greater in holes located near ribs than in those located along excavation centerlines. Offsetting along the clay layers is observable until total offset is reached or visibility is obstructed by intervening offsets at other clay seams or fractures.

Observation holes are inspected for fractures using an aluminum rod with a flattened steel wire probe attached to one end perpendicular to the rod (referred to as a "scratch rod"). Fractures and clay seams are located by moving the probe along the inside of the hole until it is snagged in one of these features. Depth to each feature is recorded, as is the magnitude of separations encountered. A fiber scope camera is available for use in addition to the scratch rod to visually document features of interest in a hole.

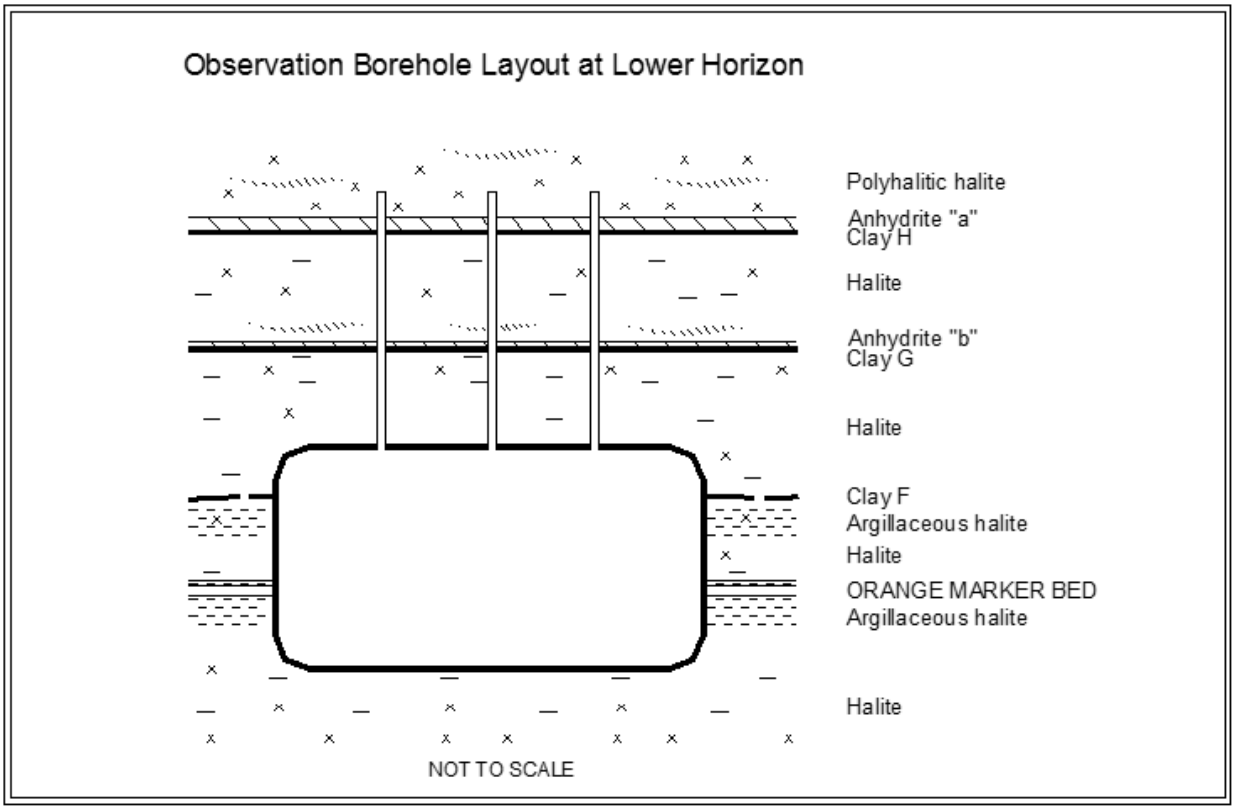

Figure 8-1 Example of Observation Hole Layout at Lower Horizon

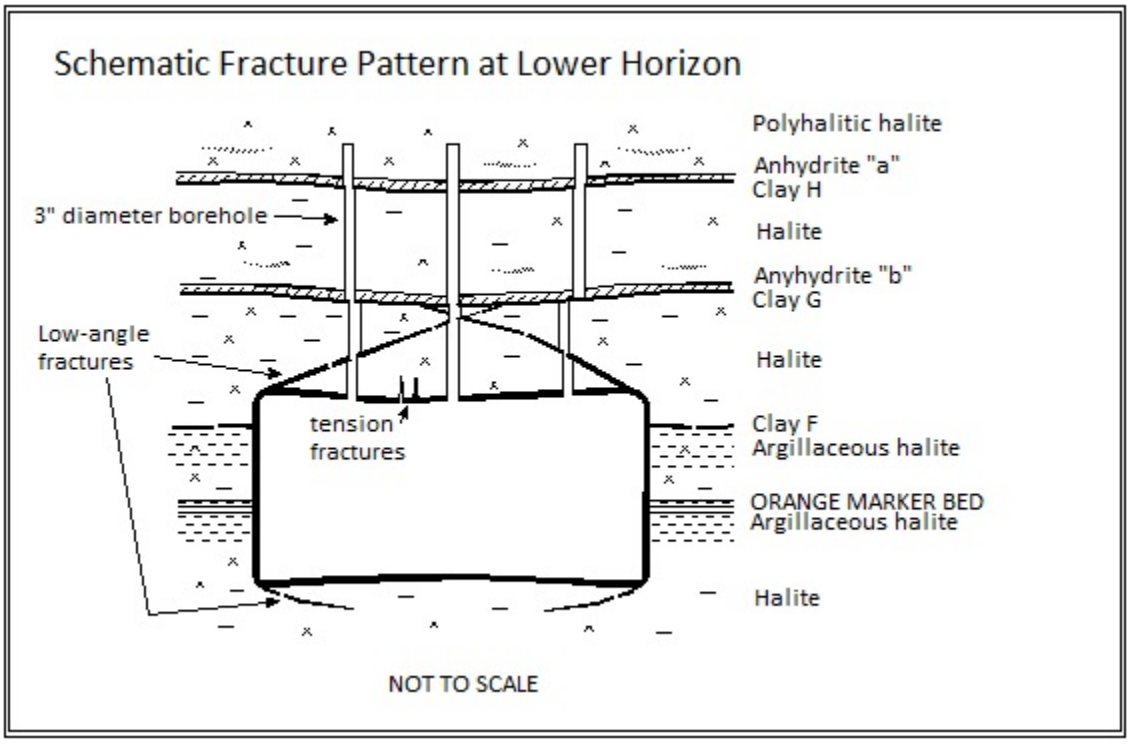

Figure 8-2 Typical Fracture Pattern at Lower Horizon

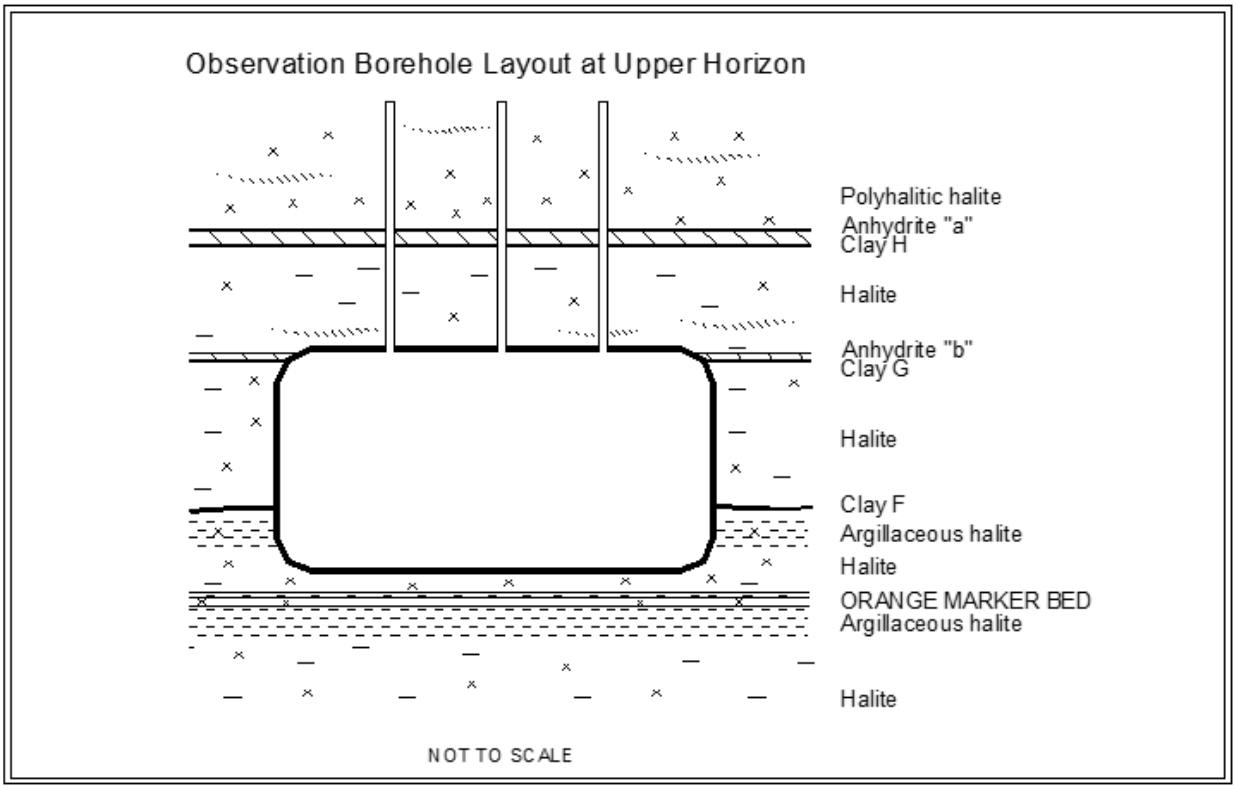

Figure 8-3 Example Observation Hole Layout at Upper Horizon

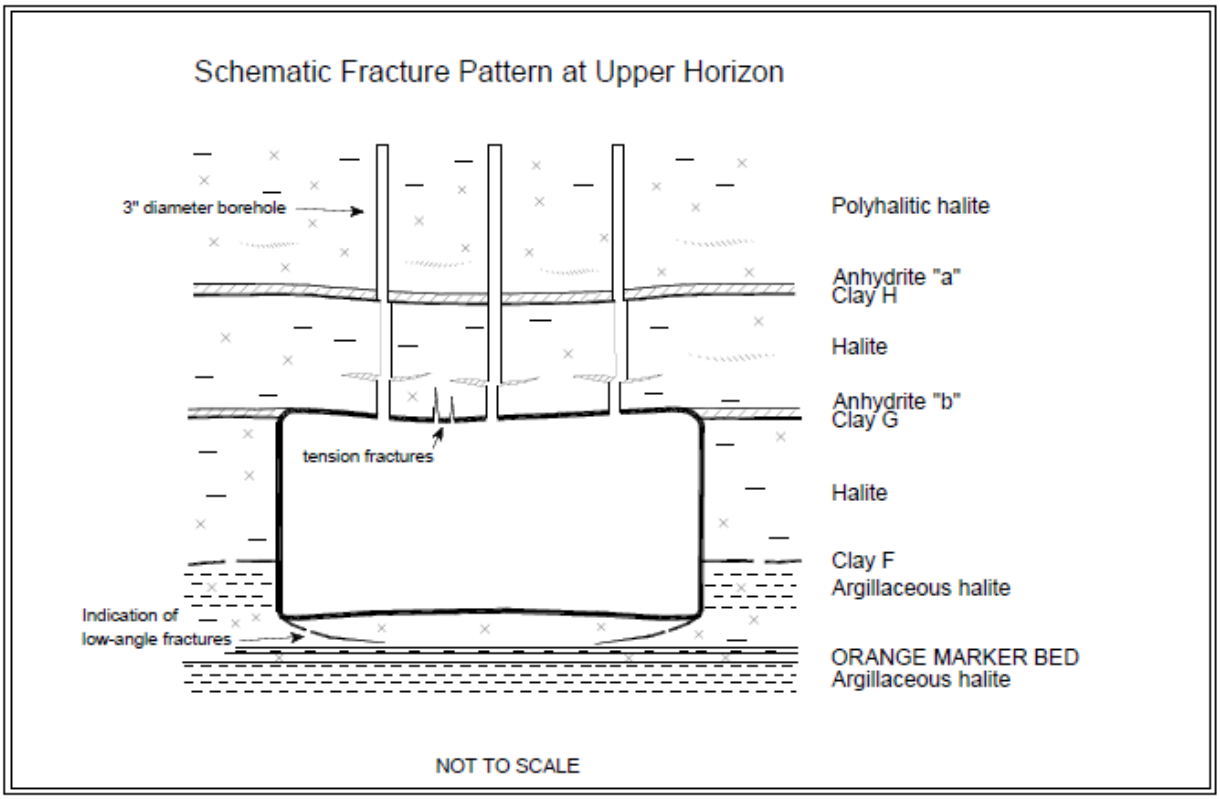

Figure 8-4 Typical Fracture Patterns at Upper Horizon

8.2 Fracture Mapping

Routine mapping documents the progression of fractures in the roof exposed on the excavation surfaces of the drifts and rooms in the underground repository. The fracture surveys are generally performed on an annual basis, and the fracture maps are updated. The fracture maps facilitate the analysis of strain in the immediate roof-beam because they document the development and propagation of fractures through time.

8.3 Stratigraphic Mapping

Stratigraphic mapping is the identification and partitioning of the sequence of rock strata based on their form, distribution, and lithologic composition. It is used to verify that there are no nonconformities in the geology within the waste disposal horizon at the WIPP.

8.4 Drilling and Geologic Core Descriptions

As new panels and new experimental areas are excavated, holes are typically drilled and cored vertically into the back and into the floor to depths of 50 ft to identify and describe the stratigraphic units present.

9.0 SUMMARY

At the inception of the WIPP, criteria were developed that addressed the design requirements (DOE, 1984). They pertained to all aspects of the mined facility and its operation as a pilot plant for the demonstration of technical and operational methods for permanent disposal of CH and RH TRU waste. In 1994, as the WIPP focus moved toward the permanent disposal of TRU waste, these design requirements were reassessed and replaced by a new set of requirements called system design descriptions. Table 9-1 shows the comparison of these design requirements with conditions actually observed in the underground from July 2018 through June 2019.

Replacement of failed rock bolts was performed at various locations during this reporting period. The pace of bolt replacement maintained before the radiological release event could not be met due to an increase in personal protection equipment requirement and the reduction in ventilation. An anticipated roof fall is thought to have occurred in Panel 7, Room 6 (a prohibited area closed to personnel access) around January 1, 2019. The potential for a fall to occur was predicted by increasing room closure rates. The data obtained from the instrument on January 2, 2019, was not indicative of a fully operational instrument, inferring a roof fall had occurred damaging the instrument. Due to waste emplacement in the entries leading to Room 6, a visual confirmation of the roof fall was not possible. Interestingly, the predicted roof fall mentioned above was anticipated to occur before January 3, 2019. The date was obtained from a nonlinear regression of the inverse closure rates contacting the x-axis just before 1/3/2019. The regression has an R^2 greater than 0.99.

The *in situ* performances of the accessible and bolted excavations generally continue to satisfy the appropriate design criteria. Although improvements to ground control maintenance activities in accessible areas in the underground have been made, additional efforts are still needed. Future changes to the planned life of some of the openings may require a change to the geometry of the access drifts, thus by removing unstable roof beam or rib spalls, milling the floor for added clearance, and installing roof bolts with mesh or straps.

In addition to underground instrumentation, qualitative assessments of fracture development are documented through mapping the underground repository and inspecting the observation holes. Although, as indicated in Section 8.0, no significant geoscience activities occurred during the current reporting period, the accumulation of many years of collected information acquired from these programs contributes to the understanding of the dynamic geomechanical processes in the WIPP underground. This aids in the design of effective ground control and support systems.

Requirement	Comments
"The lining shall be designed for a hydrostatic pressure. . . ."	Water pressure observed on piezometers located behind the shaft liners remains below design levels.
"The key shall be designed to resist the lateral pressure generated by salt creep."	Visual inspections of all shaft keys do not indicate any deterioration due to creep loading.
"The key shall be designed to retain the rock formation and will be provided with chemical seal rings and a water collection ring with drains to prevent water from flowing down the unlined shaft from the lining above."	Shaft inspection observations show no indication of instability due to salt dissolution. No water has been observed flowing along the rock-liner interface.
"The underground waste disposal facilities shall be designed to provide space and adequate access for the underground equipment and temporary storage space to support underground operations."	Geomechanical instrument data and visual observations indicate that the current design provides adequate access and storage and disposal space. Ground control maintenance is performed as necessary to maintain access. If ground control activities cannot be performed in a timely manner and the geomechanical data suggest potential instability, access to the drift is to be restricted or even prohibited until ground remediation can occur.
"Entries and subentries to the underground disposal area and the experimental areas shall be provided and sized for personnel safety, adequate air flow, and space for equipment."	Deformation of excavation remains within the required limits. Normal periodic maintenance consisting of rock bolting, wire meshing, trimming, and scaling continue throughout accessible areas of the repository. Areas such as the waste transport route undergo periodic floor trims in order to maintain adequate operating height.
"Geomechanical instrumentation shall be provided to measure the cumulative deformation of the rock mass surrounding mined drifts. . . ."	Geomechanical instrumentation is operated and maintained to meet this requirement. This annual report provides a summary and analysis of the geomechanical data.

Table 9-1 Comparison of Excavation Performance to System Design Requirements

10.0 REFERENCES

ASTM, 2006, D6026-06, *Standard Practice for Using Significant Digits in Geotechnical Data*.

Public Law 96-164, *Department of Energy National Security and Military Applications of Nuclear Energy Authorization Act of 1980*.

Title 40 CFR Part 191, *Environmental Radiation Protection Standards for Management and Disposal of Spent Nuclear Fuel, High-Level and Transuranic Radioactive Wastes.*

Title 40 CFR Part 194, *Criteria for the Certification and Re-certification of the Waste Isolation Pilot Plant's Compliance with the 40 CFR Part 191 Disposal Regulations.*

Holt, R. M., and D. W. Powers, 1990, *Geologic Mapping of the Air Intake Shaft at the Waste Isolation Pilot Plant*, DOE/WIPP 90-051, Waste Isolation Pilot Plant, Carlsbad, New Mexico.

Holt, R. M., and D. W. Powers, 1984, *Geotechnical Activities in the Waste Handling Shaft, Waste Isolation Pilot Plant (WIPP) Project, Southeastern New Mexico*, WTSD TME 038, Waste Isolation Pilot Plant, Carlsbad, New Mexico.

New Mexico Environment Department (NMED), 2016, Waste Isolation Pilot Plant Hazardous Waste Facility Permit, NM4890139088-TSDF, Santa Fe, New Mexico.

Powers, D. W., and R. M. Holt, 1993, *The Upper Cenozoic Gatuña Formation of Southeastern New Mexico, New Mexico Geological Society Guidebook*, 44th Field Conference, Carlsbad Region, New Mexico and West Texas, D. W. Love et al., Eds., pp 271-282.

Powers, D. W., and R. M. Holt, 1995, *Gatuña Formation (Miocene to Pleistocene) Geology and Paleohydrology*, prepared for Westinghouse Waste Isolation Division by International Technology Corporation, Albuquerque, New Mexico.

Powers, D. W., S. J. Lambert, S. E. Shaffer, L. R. Hill, and W. D. Weart, Eds.,1978, *Geological Characterization Report, Waste Isolation Pilot Plant (WIPP) Site, Southeastern New Mexico, Vols. I and II*, SAND 78 1596; Sandia National Laboratories, Albuquerque, New Mexico.

U.S. Department of Energy (DOE), 2000, *Brine Generation Study,* DOE/WIPP 00-2000, Waste Isolation Pilot Plant, Carlsbad, New Mexico.

U.S. Department of Energy (DOE), 1986a, *Interim Geotechnical Field Data Report,* DOE/WIPP 86-012, Waste Isolation Pilot Plant, Carlsbad, New Mexico.

U.S. Department of Energy (DOE), 1986b, *Waste Isolation Pilot Plant Design Validation Final Report*, DOE/WIPP 86-010; Prepared by Bechtel National, Inc., for the U.S. Department of Energy, San Francisco, California.

U.S. Department of Energy (DOE), 1985, *Quarterly Geotechnical Field Data Report*, DOE/WIPP-221, Waste Isolation Pilot Plant, Carlsbad, New Mexico.

U.S. Department of Energy (DOE), 1984, *Design Criteria, Waste Isolation Pilot Plant (WIPP) Revised Mission Concept-IIA*, DOE/WIPP-071; Waste Isolation Pilot Plant, Carlsbad, New Mexico.

U.S. Department of Energy (DOE), 1983, *Summary of the Results of the Evaluation of the WIPP Site and Preliminary Design Validation Program*, DOE/WIPP-161; Waste Isolation Pilot Plant, Carlsbad, New Mexico.

U.S. Environmental Protection Agency, 1998, "Criteria for the Certification and Recertification of the Waste Isolation Pilot Plant's Compliance with the Disposal Regulations: Certification Decision," *Federal Register*, Vol. 63, No. 95, pp. 27354, May 18, 1998, Washington, DC.

ISSUED

DOE/WIPP- 20-3610
Volume 2

Waste Isolation Pilot Plant

Geotechnical Analysis Report For July 2018– June 2019

Supporting Data

U.S. Department of Energy

October 2020

This document has been submitted as required to:

U.S. Department of Energy
Office of Scientific and Technical Information
PO Box 62
Oak Ridge, TN 37831
(865) 576-8401

Additional information about this document may be obtained by calling 1-800-336-9477

Unlimited, publicly available full-text scientific and technical reports produced since 1991 are available online at Information Bridge (www.osti.gov/bridge).

U.S Department of Energy and its contractors may obtain full-text reports produced prior to 1991 in paper form for a processing fee from:

U.S. Department of Energy
Office of Scientific and Technical Information
P.O. Box 62
Oak Ridge, TN 37831-0062
Telephone: (865) 576-8401
E-mail: reports@osti.gov

Available for sale to the public from:

U.S. Department of Commerce
National Technical Information Service
5301 Shawnee Rd
Alexandria, VA 22312
Email: info@ntis.gov

Waste Isolation Pilot Plant

Geotechnical Analysis Report For July 2018– June 2019

Supporting Data

U.S. Department of Energy
Carlsbad Field Office

October 2020

Approved by: //signature of file// 10/29/2020
Michael R. Brown Date
Director, Office of Environmental Protection
Carlsbad Field Office

This page was intentionally left blank.

FOREWORD AND ACKNOWLEDGMENTS

This report contains an assessment of the geotechnical status of the Waste Isolation Pilot Plant (WIPP). During the excavation of the WIPP principal underground access and experimental areas, the status was reported quarterly. Since 1987, when the initial construction phase was completed, reports have been published annually. This report presents and analyzes data collected from July 1, 2018, to June 30, 2019.

This Geotechnical Analysis Report (GAR) was written to meet the needs of several audiences. It satisfies requirements contained in the WIPP Hazardous Waste Facility Permit[1] (HWFP) and the Certification of Compliance[2] with Subparts B and C, Title 40 *Code of Federal Regulations* (CFR) Part 191, "Environmental Radiation Protection Standards for Management and Disposal of Spent Nuclear Fuel, High-Level and Transuranic Radioactive Wastes." This report focuses on the geotechnical performance of the various components of the WIPP underground facility, including the shafts, shaft stations, access drifts, and waste disposal areas. The results of investigations of excavation effects and other geotechnical studies are also included.

The report compares the geotechnical performance of the repository to the design criteria. It describes the techniques that were used to acquire the data. The depth and breadth of the evaluation of the different components of the underground facility vary according to the types and quantities of data available and the complexity of the recorded geotechnical responses. Graphic documentation of data and tabular documentation of instrument history can be provided upon request.

This GAR was prepared by Nuclear Waste Partnership LLC for the U.S. Department of Energy (DOE), Carlsbad Field Office in Carlsbad, New Mexico. Work was supported by the DOE under Contract No. DE-EM0001971.

[1] New Mexico Environment Department (NMED), 2017, Waste Isolation Pilot Plant Hazardous Waste Facility Permit, NM4890139088-TSDF, Santa Fe, NM

[2] U.S. Environmental Protection Agency (EPA), 1998, "Criteria for the Certification and Recertification of the Waste Isolation Pilot Plant's Compliance with the Disposal Regulations: Certification Decision," Federal Register, Vol. 63, No. 95, pp. 27354, May 18, 1998, Washington, DC

This page was intentionally left blank.

TABLE OF CONTENTS

1.0 Introduction 17
1.1 Instrumentation 17
1.2 Data Plot Explanation 18
1.3 Report Organization 18
2.0 Instrumentation Summary for Shafts 19
3.0 Instrumentation Summary for Shaft Stations 28
4.0 Instrumentation Summary for the Access Drifts 32
5.0 Instrumentation Summary for the Waste Disposal Area 145
6.0 Instrumentation Summary for the SDI Area 168
7.0 Geoscience Summary 184

LIST OF TABLES

Table 2-1 Salt Handling Shaft Data Analysis 20
Table 3-1 Salt Handling Shaft Station Data Analysis 29
Table 4-1 Access Drifts Data Analysis 33
Table 5-1 Panel 7 Data Analysis 146
Table 5-2 Panel 8 Data Analysis 147
Table 6-1 SDI Data Analysis 169

LIST OF FIGURES

Salt Handling Shaft and Key

Figure 2-1 Piezometers Salt Handling Shaft – Level 580 at the Forty-niner Member 22
Figure 2-2 Piezometer Salt Handling Shaft – Level 620 at the Magenta Dolomite Member 22
Figure 2-3 Piezometers Salt Handling Shaft – Level 691 at the Tamarisk Member 23
Figure 2-4 Piezometer Salt Handling Shaft – Level 802 at the Los Medaños Member 23
Figure 2-5 Piezometer Salt Handling Shaft – Level 850 at the Rustler-Salado Contact 24
Figure 2-6 Earth Pressure Cells – Salt Handling Shaft Key – Level 862.4 24
Figure 2-7 Spot Welded Strain Gauge – Salt Handling Shaft Key – Level 856.3 25
Figure 2-8 Embedment Strain Gauge – Salt Handling Shaft Key – Level 856.3 25
Figure 2-9 Embedment Strain Gauge – Salt Handling Shaft Key – Level 862.4 26
Figure 2-10 Embedment Strain Gauge – Salt Handling Shaft Key – Level 856.3 26
Figure 2-11 Embedment Strain Gauge – Salt Handling Shaft Key – Level 862.4 27

Salt Handling Shaft Station

Figure 3-1 Convergence Point Array – Salt Handling Shaft Station at S18 – Centerline – Roof to Floor 30
Figure 3-2 Convergence Point Array – Salt Handling Shaft Station at S18 – Quarter Points – Roof to Floor 30
Figure 3-3 Convergence Point Array – Salt Handling Shaft Station at S30 – Roof to Floor 31
Figure 3-4 Convergence Point Array – Salt Handling Shaft Station at S65 – Roof to Floor 31

Access Drifts

Figure 4-1 Wire Convergence Meter 51X-CW-01037 – E140 S2750 – Roof to Floor 43
Figure 4-2 Convergence Meter 51X-PG-01049 – E300-N1273 – Roof to Floor 43
Figure 4-3 Convergence Meter 51X-PG-01048 – E300-N1303 – Roof to Floor 44
Figure 4-4 Wire Convergence Meter 51X-CW-01048 – E300-S2635 – Roof to Floor 44
Figure 4-5 Convergence Meter 51X-PG-00442 – E300 S2750 – Roof to Floor 45
Figure 4-6 Convergence Meter 51X-PG-00446 – N460-E320 – Roof to Floor 45
Figure 4-7 Convergence Meter 51X-PG-00445 – S700-E220 – Roof to Floor 46
Figure 4-8 Wire Convergence Meter 51X-CW-01039 – W170 S2735 – Roof to Floor 46
Figure 4-9 Wire Convergence Meter 51X-CW-01038 – W30 S2750 – Roof 47
Figure 4-10 Extensometer 51X-GE-00355 – E0 N300 – Roof 47
Figure 4-11 Extensometer 51X-GE-00353 – E0 N626 – Roof 48
Figure 4-12 Extensometer 51X-GE-00352-2 – E0 N940 – Roof 48
Figure 4-13 Extensometer 51X-GE-00364 – E140 N1266 – Roof 49
Figure 4-14 Extensometer 51X-GE-00372-2 – E140 S146 – Roof 49

Access Drifts, continued

Figure 4-15 Extensometer 51X-GE-00374 – E300 N1186 – Roof 50
Figure 4-16 Extensometer 51X-GE-00388 – E300 N1266 – Roof 50
Figure 4-17 Extensometer 51X-GE-00373 – E300 N1341 – Roof 51
Figure 4-18 Extensometer 51X-GE-00440 – AIS North Brow – Roof..... 51
Figure 4-19 Extensometer 51X-GE-00441 – AIS South Brow – Roof 52
Figure 4-20 Extensometer 41X-GE-00401 –-W620-N20 – Roof 52
Figure 4-21 Extensometer 41X-GE-00123 –-W620-N93 – Roof 53
Figure 4-22 Extensometer 41X-GE-00122 –-W620-S65 – Roof 53
Figure 4-23 Core Storage Library – Roof to Floor – Centerline..... 54
Figure 4-24 Convergence Point Array – E0 N75 – All Chords 54
Figure 4-25 Convergence Point Array – E0 N225 – All Chords 55
Figure 4-26 Convergence Point Array – E0 N300 – All Chords 55
Figure 4-27 Convergence Point Array – E0 N460 – Roof to Floor – Centerline 56
Figure 4-28 Convergence Point Array – E0 N562 – All Chords 56
Figure 4-29 Convergence Point Array – E0 N626 – All Chords 57
Figure 4-30 Convergence Point Array – E0 N686 – All Chords 57
Figure 4-31 Convergence Point Array – E0 N780 – Roof to Floor – Centerline 58
Figure 4-32 Convergence Point Array – E0 N940 – All Chords 58
Figure 4-33 Convergence Point Array – E0 N1100 – Roof to Floor – Centerline 59
Figure 4-34 Convergence Point Array – E0 N1266 – All Chords 59
Figure 4-35 Convergence Point Array – E0 N1420 – Roof to Floor – Centerline 60
Figure 4-36 Convergence Point Array – E140 N5 – All Chords 60
Figure 4-37 Convergence Point Array – E140 N150 – Roof to Floor – Centerline 61
Figure 4-38 Convergence Point Array – E140 N220 – Roof to Floor – Centerline 61
Figure 4-39 Convergence Point Array – E140 N355 – All Chords 62
Figure 4-40 Convergence Point Array – E140 N460 – Roof to Floor – Centerline 62
Figure 4-41 Convergence Point Array – E140 N562 – All Chords 63
Figure 4-42 Convergence Point Array – E140 N626 – All Chords 63
Figure 4-43 Convergence Point Array – E140 N686 – All Chords 64
Figure 4-44 Convergence Point Array – E140 N780 – Roof to Floor – Centerline 64
Figure 4-45 Convergence Point Array – E140 N940 – All Chords 65
Figure 4-46 Convergence Point Array – E140 N1100 – Roof to Floor – Centerline 65
Figure 4-47 Convergence Point Array – E140 N1266 – All Chords 66
Figure 4-48 Convergence Point Array – E140 N1420 – Roof to Floor – Centerline 66
Figure 4-49 Convergence Point Array – E140 S90 – Roof to Floor – Centerline 67
Figure 4-50 Convergence Point Array – E140 S262 – All Chords..... 67
Figure 4-51 Convergence Point Array – E140 S460 – All Chords..... 68
Figure 4-52 Convergence Point Array – E140 S550 – All Chords..... 68
Figure 4-53 Convergence Point Array – E140 S700 – Roof to Floor – Centerline 69
Figure 4-54 Convergence Point Array – E140 S700 – Roof to Floor – East Quarter Point..... 69
Figure 4-55 Convergence Point Array – E140 S700 – Roof to Floor – West Quarter Point..... 70
Figure 4-56 Convergence Point Array – E140 S850 – Roof to Floor – Centerline 70
Figure 4-57 Convergence Point Array – E140 S1000 – Roof to Floor – Centerline 71

Access Drifts, continued

Figure 4-58 Convergence Point Array – E140 S1025 – Roof to Floor – Centerline 71
Figure 4-59 Convergence Point Array – E140 S1075 – Roof to Floor – Centerline 72
Figure 4-60 Convergence Point Array – E140 S1075 – Roof to Floor – East Quarter Point.... 72
Figure 4-61 Convergence Point Array – E140 S1075 – Roof to Floor – West Quarter Point.... 73
Figure 4-62 Convergence Point Array – E140 S1150 – Roof to Floor – Centerline 73
Figure 4-63 Convergence Point Array – E140 S1150 – Rib to Rib 74
Figure 4-64 Convergence Point Array – E140 S1150 – Roof-to-Floor – East Quarter Point.... 74
Figure 4-65 Convergence Point Array – E140 S1150 – Roof to Floor – West Quarter Point.... 75
Figure 4-66 Convergence Point Array – E140 S1225 – Roof to Floor – Centerline and Rib-to-Rib.... 75
Figure 4-67 Convergence Point Array – E140 S1225 – Roof to Floor – Quarter Points 76
Figure 4-68 Convergence Point Array – E140 S1300 – Roof to Floor – Centerline 76
Figure 4-69 Convergence Point Array – E140 S1378 – Roof to Floor – Centerline 77
Figure 4-70 Convergence Point Array – E140 S1378 – Roof to Floor – East Quarter Point.... 77
Figure 4-71 Convergence Point Array – E140 S1378 – Roof to Floor – West Quarter Point.... 78
Figure 4-72 Convergence Point Array – E140 S1450 – Roof to Floor – Centerline 78
Figure 4-73 Convergence Point Array – E140 S1450 – Roof to Floor – East Quarter Point.... 79
Figure 4-74 Convergence Point Array – E140 S1450 – Rib to Rib 79
Figure 4-75 Convergence Point Array – E140 S1450 – Roof to Floor – West Quarter Point.... 80
Figure 4-76 Convergence Point Array – E140 S1496 Test Area – Roof to Floor – East Quarter Point 80
Figure 4-77 Convergence Point Array – E140 S1524 Test Area – Roof to Floor – Centerline 81
Figure 4-78 Convergence Point Array – E140 S1524 Test Area – East Quarter Point 81
Figure 4-79 Convergence Point Array – E140 S1534 – Roof-to-Floor Centerline & Rib to Rib 82
Figure 4-80 Convergence Point Array – E140 S1534 – Roof to Floor – East Quarter Point.... 82
Figure 4-81 Convergence Point Array – E140 S1534 – Roof to Floor – West Quarter Point.... 83
Figure 4-82 Convergence Point Array – E140 S1600 – Roof to Floor – Centerline 83
Figure 4-83 Convergence Point Array – E140 S1667 Test Area – Roof to Floor – Centerline 84
Figure 4-84 Convergence Point Array – E140 S1667 Test Area – East Quarter Point 84
Figure 4-85 Convergence Point Array – E140 S1687– Roof-to-Floor – Centerline and Rib to Rib.... 85

Access Drifts, continued

Figure 4-86 Convergence Point Array – E140 S1687 – Roof to Floor – Quarter Points 85
Figure 4-87 Convergence Point Array – E140 S1699 Test Area – Roof to Floor – Centerline & Quarter Points 86
Figure 4-88 Convergence Point Array – E140 S1717 Test Area – Roof to Floor – Centerline 86
Figure 4-89 Convergence Point Array – E140 S1717 Test Area – Roof to Floor – East Quarter Point 87
Figure 4-90 Convergence Point Array – E140 S1717 Test Area – Roof to Floor – West Quarter Point 87
Figure 4-91 Convergence Point Array – E140 S1775 – Roof to Floor – Centerline 88
Figure 4-92 Convergence Point Array – E140 S1775 – Roof to Floor – Quarter Points 88
Figure 4-93 Convergence Point Array – E140 S1775 – Rib to Rib 89
Figure 4-94 Convergence Point Array – E140 S1862 – Roof to Floor – Centerline & Rib-to-Rib..... 89
Figure 4-95 Convergence Point Array – E140 S1862 – Roof to Floor – Quarter Points 90
Figure 4-96 Convergence Point Array – E140 S1950 – Roof to Floor – Centerline 90
Figure 4-97 Convergence Point Array – E140 S2007 – Roof to Floor – Centerline 91
Figure 4-98 Convergence Point Array – E140 S2065 – Roof to Floor – Centerline 91
Figure 4-99 Convergence Point Array – E140 S2122 – Roof to Floor – Centerline 92
Figure 4-100 Convergence Point Array – E140 S2275 – Roof to Floor – Centerline ... 92
Figure 4-101 Convergence Point Array – E140 S2350 – Roof to Floor – Centerline ... 93
Figure 4-102 Convergence Point Array – E140 S2425 – All Chords 93
Figure 4-103 Convergence Point Array – E140 S2520 – Roof to Floor – Centerline .. 94
Figure 4-104 Convergence Point Array – E300 N45 – Roof to Floor – Centerline & Quarter Points 94
Figure 4-105 Convergence Point Array – E300 N170 – Roof to Floor – Centerline and Quarter Points 95
Figure 4-106 Convergence Point Array – E300 N250 – Roof to Floor – Centerline..... 95
Figure 4-107 Convergence Point Array – E300 N280 – Roof to Floor – Centerline..... 96
Figure 4-108 Convergence Point Array – E300 N360 – Roof to Floor – Centerline..... 96
Figure 4-109 Convergence Point Array – E300 N440 – Roof to Floor – Centerline..... 97
Figure 4-110 Convergence Point Array – E300 N500 – Roof to Floor – Centerline..... 97
Figure 4-111 Convergence Point Array – E300 N1100 – Roof to Floor – Centerline... 98
Figure 4-112 Convergence Point Array – E300 N1262 – All Chords 98
Figure 4-113 Convergence Point Array – E300 N1341 – All Chords 99
Figure 4-114 Convergence Point Array – E300 S45 – Roof to Floor – All Chords..... 99
Figure 4-115 Convergence Point Array – E300 S90 – Roof to Floor – Centerline..... 100
Figure 4-116 Convergence Point Array – E300 S250 – All Chords 100
Figure 4-117 Convergence Point Array – N140 E90 – All Chords 101
Figure 4-118 Convergence Point Array – N215 W500 – All Chords 101
Figure 4-119 Convergence Point Array – N215 W620 – Roof to Floor – Centerline.. 102
Figure 4-120 Convergence Point Array – N250 E220 – Roof to Floor – Centerline... 102

Access Drifts, continued

Figure 4-121 Convergence Point Array – N250 E220 – Roof to Floor – Quarter Points 103
Figure 4-122 Convergence Point Array – N300 W170 – All Chords 103
Figure 4-123 Convergence Point Array – N460 E70 – All Chords 104
Figure 4-124 Convergence Point Array – N460 E310 – Roof to Floor – Centerline 104
Figure 4-125 Convergence Point Array – N780 E70 – All Chords 105
Figure 4-126 Convergence Point Array – N780 E220 – Roof to Floor – Centerline 105
Figure 4-127 Convergence Point Array – N780 E300 – Roof to Floor – Centerline 106
Figure 4-128 Convergence Point Array – N940 E220 – Roof to Floor – Centerline 106
Figure 4-129 Convergence Point Array – N940 E300 – Roof to Floor – Centerline 107
Figure 4-130 Convergence Point Array – N1420 E79 – Roof to Floor – Centerline 107
Figure 4-131 Convergence Point Array – N1420 E212 – Roof to Floor – Centerline 108
Figure 4-132 Convergence Point Array – N1420 E300 – Roof to Floor – Centerline 108
Figure 4-133 Convergence Point Array – S90 E220 – Roof to Floor – Centerline 109
Figure 4-134 Convergence Point Array – S90 W120 – All Chords 109
Figure 4-135 Convergence Point Array – S90 W400 – All Chords 110
Figure 4-136 Convergence Point Array – S90 W590 – All Chords 110
Figure 4-137 Convergence Point Array – S90 W620 – Roof to Floor – Centerline 111
Figure 4-138 Convergence Point Array – S700 E180 – All Chords 111
Figure 4-139 Convergence Point Array – S700 E205 – All Chords 112
Figure 4-140 Convergence Point Array – S700 W98 – Roof to Floor – Centerline 112
Figure 4-141 Convergence Point Array – S1000 E58 – All Chords 113
Figure 4-142 Convergence Point Array – S1000 E120 – Roof to Floor – Centerline 113
Figure 4-143 Convergence Point Array – S1000 E160 – Roof to Floor – Centerline 114
Figure 4-144 Convergence Point Array – S1000 W98 – All Chords 114
Figure 4-145 Convergence Point Array – S1300 E24 – Roof to Floor – Centerline 115
Figure 4-146 Convergence Point Array – S1300 E120 – Roof to Floor – Centerline 115
Figure 4-147 Convergence Point Array – S1300 E160 – Roof to Floor – Centerline 116
Figure 4-148 Convergence Point Array – S1300 W100 – Roof to Floor – Centerline 116
Figure 4-149 Convergence Point Array – S1600 E110 – Roof to Floor – Centerline 117
Figure 4-150 Convergence Point Array – S1600 E170 – Roof to Floor – Centerline 117
Figure 4-151 Convergence Point Array – S1600 W100 – Roof to Floor – Centerline 118
Figure 4-152 Convergence Point Array – S1950 E113 – Roof to Floor – Centerline 118
Figure 4-153 Convergence Point Array – S1950 E160 – Roof to Floor – Centerline 119
Figure 4-154 Convergence Point Array – S1950 E226 – Roof to Floor – Centerline 119
Figure 4-155 Convergence Point Array – S1950 W100 – Roof to Floor – Centerline 120
Figure 4-156 Convergence Point Array – S2180 W100 – All Chords 120
Figure 4-157 Convergence Point Array – S2520 E55 – All Chords 121
Figure 4-158 Convergence Point Array – S2520 W100 – All Chords 121
Figure 4-159 Convergence Point Array – W30 S90 – Roof to Floor – Centerline 122
Figure 4-160 Convergence Point Array – W30 S120 – Roof to Floor – Centerline 122
Figure 4-161 Convergence Point Array – W30 S250 – All Chords 123
Figure 4-162 Convergence Point Array – W30 S400 – Roof to Floor – Centerline 123
Figure 4-163 Convergence Point Array – W30 S500 – All Chords 124

Access Drifts, continued

Figure 4-164 Convergence Point Array – W30 S700 – Roof to Floor – Centerline 124
Figure 4-165 Convergence Point Array – W30 S850 – Roof to Floor – Centerline 125
Figure 4-166 Convergence Point Array – W30 S850 – Quarter Points 125
Figure 4-167 Convergence Point Array – W30 S1000 – Roof to Floor – Centerline .. 126
Figure 4-168 Convergence Point Array – W30 S1150 – Roof to Floor – Centerline .. 126
Figure 4-169 Convergence Point Array – W30 S1300 – Roof to Floor – Centerline .. 127
Figure 4-170 Convergence Point Array – W30 S1453 – All Chords 127
Figure 4-171 Convergence Point Array – W30 S1600 – Roof to Floor – Centerline .. 128
Figure 4-172 Convergence Point Array – W30 S1775 – All Chords 128
Figure 4-173 Convergence Point Array – W30 S1950 – Roof to Floor – Centerline .. 129
Figure 4-174 Convergence Point Array – W30 S2520 – Roof to Floor – Centerline .. 129
Figure 4-175 Convergence Point Array – W30 S2635 – All Chords 130
Figure 4-176 Convergence Point Array – W170 N150 – Roof to Floor – Centerline .. 130
Figure 4-177 Convergence Point Array – W170 S5 – All Chords 131
Figure 4-178 Convergence Point Array – W170 S90 – Roof to Floor – Centerline 131
Figure 4-179 Convergence Point Array – W170 S232 – All Chords 132
Figure 4-180 Convergence Point Array – W170 S400 – Roof to Floor – Centerline .. 132
Figure 4-181 Convergence Point Array – W170 S560 – All Chords 133
Figure 4-182 Convergence Point Array – W170 S700 – Roof to Floor – Centerline .. 133
Figure 4-183 Convergence Point Array – W170 S850 – Roof to Floor – Centerline .. 134
Figure 4-184 Convergence Point Array – W170 S850 – Rib to Rib 134
Figure 4-185 Convergence Point Array – W170 S1000 – Roof to Floor – Centerline 135
Figure 4-186 Convergence Point Array – W170 S1150 – Roof to Floor – Centerline 135
Figure 4-187 Convergence Point Array – W170 S1150 – Rib to Rib 136
Figure 4-188 Convergence Point Array – W170 S1300 – Roof to Floor – Centerline 136
Figure 4-189 Convergence Point Array – W170 S1445 – All Chords 137
Figure 4-190 Convergence Point Array – W170 S1600 – Roof to Floor – Centerline 137
Figure 4-191 Convergence Point Array – W170 S1779 – All Chords 138
Figure 4-192 Convergence Point Array – W170 S1950 – Roof to Floor – Centerline 138
Figure 4-193 Convergence Point Array – W170 S2060 – All Chords 139
Figure 4-194 Convergence Point Array – W170 S2180 – Roof to Floor – Centerline 139
Figure 4-195 Convergence Point Array – W170 S2350 – All Chords 140
Figure 4-196 Convergence Point Array – W170 S2520 – Roof to Floor – Centerline 140
Figure 4-197 Joint Meter – E140 S1505 141
Figure 4-198 Joint Meter – E140 S1529 141
Figure 4-199 Joint Meter – E140 S1545 142
Figure 4-200 Joint Meter – E140 S1795 142
Figure 4-201 Rock Bolt Load Cells 1-5 – AIS North Brow 143
Figure 4-202 Rock Bolt Load Cells 6-10 – AIS North Brow 143
Figure 4-203 Rock Bolt Load Cells 1-5 – AIS South Brow 144
Figure 4-204 Rock Bolt Load Cells 6-10 – AIS South Brow 144

Waste Disposal Panel 7

Figure 5-1 Extensometer 51X-GE-00416 – S2180 W585 – Roof 149

Waste Disposal Panel 7, continued

Figure 5-2 Extensometer 51X-GE-00417 – S2180 W985 – Roof 149
Figure 5-3 Extensometer 51X-GE-00423 – S2520 W585 – Roof 150
Figure 5-4 Extensometer 51X-GE-00424 – S2520 W985 – Roof 150
Figure 5-5 Extensometer 51X-GE-00425 – W390-S2350 – Roof 151
Figure 5-6 Extensometer 51X-GE-00426-2 – W520-S2350 – Roof 151
Figure 5-7 Extensometer 51X-GE-00418 – W660-S2350 – Roof 152
Figure 5-8 Extensometer 51X-GE-00420-1 – W920 S2350 – Roof 152
Figure 5-9 Convergence Point Array – S2180 W285 – Roof to Floor 153
Figure 5-10 Convergence Point Array – S2180 W390 – Roof to Floor 153
Figure 5-11 Convergence Point Array – S2180 W460 – Roof to Floor 154
Figure 5-12 Convergence Point Array – S2180 W520 – Roof to Floor 154
Figure 5-13 Convergence Point Array – S2180 W585 – Roof to Floor 155
Figure 5-14 Convergence Point Array – S2180 W660 – Roof to Floor 155
Figure 5-15 Convergence Point Array – W390 S2275 – Roof to Floor 156
Figure 5-16 Convergence Point Array – W390 S2350 – Roof to Floor 156
Figure 5-17 Convergence Point Array – W390 S2425 – Roof to Floor 157
Figure 5-18 Convergence Point Array – W520 S2275 – Roof to Floor 157
Figure 5-19 Convergence Point Array – W520 S2350 – All Chords 158
Figure 5-20 Convergence Point Array – W520 S2425 – Roof to Floor 158
Figure 5-21 Convergence Point Array – W660 S2275 – Roof to Floor 159
Figure 5-22 Convergence Point Array – W660 S2350 – Roof to Floor 159
Figure 5-23 Convergence Point Array – W660 S2425 – Roof to Floor 160
Figure 5-24 Convergence Point Array – S2520 W285 – Roof to Floor 160
Figure 5-25 Convergence Point Array – S2520 W390 – Roof to Floor 161
Figure 5-26 Convergence Point Array – S2520 W455 – Roof to Floor 161
Figure 5-27 Convergence Point Array – S2520 W520 – Roof to Floor 162
Figure 5-28 Convergence Point Array – S2520 W585 – Roof to Floor 162
Figure 5-29 Convergence Point Array – S2520 W660 – Roof to Floor 163
Figure 5-30 Convergence Point Array – S2520 W725 – Roof to Floor 163
Figure 5-31 Convergence Point Array – S2520 W790 – Roof to Floor 164
Figure 5-32 Convergence Point Array – S2520 W855 – Roof to Floor 164
Figure 5-33 Convergence Point Array – S2520 W920 – Roof to Floor 165

Waste Disposal Panel 8

Figure 5-34 Extensometer 51X-GE-00443 – W390 S1775 165
Figure 5-35 Convergence Point Array – W390-S1700 – Roof to Floor 166
Figure 5-36 Convergence Point Array – W390-S1775 – Roof to Floor 166
Figure 5-37 Convergence Point Array – S1600-W455 – Roof to Floor 167
Figure 5-38 Convergence Point Array – S1600-W520 – Roof to Floor 167

Salt Disposal Investigations

Figure 6-1 Convergence Point Array – E1300 N860 – Roof to Floor 170
Figure 6-2 Convergence Point Array – N780 E420 – Roof to Floor 170

Salt Disposal Investigations, continued

Figure 6-3 Convergence Point Array – N780 E540 – Roof to Floor 171
Figure 6-4 Convergence Point Array – N780 E615 – Roof to Floor 171
Figure 6-5 Convergence Point Array – N780 E690 – Roof to Floor 172
Figure 6-6 Convergence Point Array – N780 E768 – Roof to Floor 172
Figure 6-7 Convergence Point Array – N780 E845 – Roof to Floor 173
Figure 6-8 Convergence Point Array – N780 E922 – Roof to Floor 173
Figure 6-9 Convergence Point Array – N780 E1050 – Roof to Floor 174
Figure 6-10 Convergence Point Array – N780 E1100 – Roof to Floor 174
Figure 6-11 Convergence Point Array – N780 E1150 – Roof to Floor 175
Figure 6-12 Convergence Point Array – N780 E1200 – Roof to Floor 175
Figure 6-13 Convergence Point Array – N780 E1250 – Roof to Floor 176
Figure 6-14 Convergence Point Array – N780 E1300 – Roof to Floor 176
Figure 6-15 Convergence Point Array – N940 E420 – Roof to Floor 177
Figure 6-16 Convergence Point Array – N940 E540 – Roof to Floor 177
Figure 6-17 Convergence Point Array – N940 E615 – Roof to Floor 178
Figure 6-18 Convergence Point Array – N940 E690 – Roof to Floor 178
Figure 6-19 Convergence Point Array – N940 E768 – Roof to Floor 179
Figure 6-20 Convergence Point Array – N940 E845 – Roof to Floor 179
Figure 6-21 Convergence Point Array – N940 E922 – Roof to Floor 180
Figure 6-22 Convergence Point Array – N940 E1000 – Roof to Floor 180
Figure 6-23 Convergence Point Array – N940 E1050 – Roof to Floor 181
Figure 6-24 Convergence Point Array – N940 E1100 – Roof to Floor 181
Figure 6-25 Convergence Point Array – N940 E1150 – Roof to Floor 182
Figure 6-26 Convergence Point Array – N940 E1200 – Roof to Floor 182
Figure 6-27 Convergence Point Array – N940 E1250 – Roof to Floor 183
Figure 6-28 Convergence Point Array – N940 E1300 – Roof to Floor 183

1.0 INTRODUCTION

This report is a compilation of geotechnical data presented as plots for each active instrument installed in the underground at the Waste Isolation Pilot Plant (WIPP) through June 30, 2019. A summary of the geotechnical analyses that were performed using the compiled data is provided in Volume 1 of the Geotechnical Analysis Report (GAR).

1.1 Instrumentation

Geomechanical instrument data included in this report reflect the measurements of the geomechanical response of the underground within the mine. The instruments consist of convergence points, borehole extensometers, rock bolt load cells, pressure cells, strain gauges, piezometers, and joint meters.

Closure measurements are taken at convergence points. Rock displacement is calculated by measuring the distance between two opposing points. Displacement is monitored over time and is plotted as closure versus time. Annual rates of closure are calculated for the convergence data and are compared with annual closure rates from previous reporting periods.

Borehole extensometers are used to determine the absolute movements of the ground around the openings within the mine. With these instruments, stainless steel cables are installed into a hole and anchored at various depths. The displacement at the extensometer head (located near the excavation face) is measured relative to each of the fixed anchors. These data are used in the extensometer *displacement* plots presented in this report. Annual rates of displacement are calculated for each extensometer and are compared with the annual displacement rate reported during the previous reporting period.

Rock bolt load cells are used to measure the load exerted by the overburden and the effectiveness of rock bolts. Plots for each instrumented rock bolt are presented as load versus time.

Earth pressure cells and strain gauges are used in and around the shaft liners to determine their loads. These are also depicted in time-based plots. Monitoring of these instruments indicate whether there are stress buildup in the shaft lining systems.

Piezometers are used to measure the gauge pressure of groundwater. They have been installed in the shafts at varying elevations to monitor the hydraulic head acting on the shaft liners. Plots from piezometers are presented as pressure versus time.

Joint meters are installed perpendicular to a crack and monitor changes in separation of the crack which may occur over time.

1.2 Data Plot Explanation

Data are presented in graphical form for ease of interpretation. Time-based plots are used in this report. Each plot generally displays a legend in the upper right-hand corner that gives the array name and specific location of the instrument or point evaluated. The legend ties the graphical cross-sectional representation of the drift or shaft typically presented in the lower right-hand corner to the symbols on the curve in the graph. For extensometers, each anchor is designated with an alpha character "A" closest to the collar and "B," "C," "D," or "E" for the furthest point from the collar (the deepest anchor). For convergence points, the horizontal and vertical sections of the drift are referred to as chords. Breaks in the graph for convergence data and a numeric designator added to the legend typically indicate that the convergence point was lost due to normal mine maintenance activities and later reinstalled.

1.3 Report Organization

Chapter 1.0 provides an introduction to this Supporting Data volume of the GAR. Chapter 2.0 provides instrument data analysis for the Salt Shaft, followed by data plots for the piezometers, earth pressure cells, spot welded strain gauges, and embedment strain gauges installed in the Salt Shaft. Chapter 3.0 provides instrument data analysis for the Salt Shaft Station and data plots for convergence points located within the station. Chapter 4.0 provides instrument data analysis for the access drifts followed by data plots for the extensometers, convergence points, joint meters and rock bolt load cells. Chapter 5.0 provides instrument data analysis for the Waste Disposal Area followed by data plots for the extensometers and convergence points. Chapter 6.0 provides convergence point instrument data analysis for the Salt Disposal Investigations (SDI) area. Chapter 7.0 provides geologic data collected through the mapping of fractures, stratigraphic mapping and the observed displacements in vertical boreholes.

2.0 Instrumentation Summary for Shafts

Originally, the Salt, Waste, and Exhaust Shafts were instrumented with Geomechanical instrumentation. The instrument readings from the Waste and Exhaust Shafts are no longer available due to failed instruments, broken cabling, and/or inoperable/obsolete data acquisition equipment. Although much of the instrumentation installed in the shafts has failed through the years, there are no plans to replace it. The project has a good understanding of the expected movements in the shafts. Monitoring results up to the point of instrument failure did not indicate unusual shaft movements or displacements. Continued periodic visual inspections confirm the expected shaft performance and provide necessary observations to evaluate shaft performance. Replacement of failed instrumentation will not provide significant additional information.

Table 2-1 presents data and analysis of the Salt Shaft instrumentation. Plots of the instrument data are presented as Figures 2-1 through 2-11.

Table 2-1 Salt Handling Shaft Data Analysis

Piezometers

Field Tag	Level feet	Figure Number	Date of 2018-2019 Max. Reading	2018-2019 Maximum Pressure Readings (psi)	Date of 2017-2018 Max. Reading	2017-2018 Maximum Pressure Readings (psi)	Change in Maximum Pressure From Previous Year (psi)	Comments
37X-PE-00201	580	2-1	12/18/18	74	02/19/18	85	-10	
37X-PE-00202	580	2-1	12/18/18	85	05/29/18	110	-25	
37X-PE-00203	620	2-2	12/18/18	146	03/26/18	171	-25	
37X-PE-00205	691	2-3	07/26/18	164	05/29/18	195	-31	
37X-PE-00206	691	2-3	07/26/18	159	05/29/18	190	-31	
37X-PE-00210	802	2-4	10/09/18	-1	04/24/18	8	-9	
37X-PE-00211	850	2-5	10/09/18	37	10/10/17	34	2	
37X-PE-00212	850	2-5	08/07/18	65	07/11/17	77	-12	

Earth Pressure Cells

Field Tag	Level feet	Figure Number	Date of 2018-2019 Max. Reading	2018-2019 Maximum Pressure Readings (psi)	Date of 2017-2018 Max. Reading	2017-2018 Maximum Pressure Readings (psi)	Change in Maximum Pressure From Previous Year (psi)	Comments
37X-WE-00201	862.4	2-6	08/07/18	-12	09/18/17	-11	-2	
37X-WE-00202	862.4	2-6	07/26/18	-28	06/26/18	-27	-1	

Spot-Welded Strain Gauges

Field Tag	Level feet	Figure Number	Date of 2017-2018 Max. Reading	2017-2018 Maximum Strain Readings (με)	Date of 2016-2017 Max. Reading	2016-2017 Maximum Strain Readings (με)	Change in Maximum Strain From Previous Year (με)	Comments
37X-ZE-00206	856.3	2-7	07/26/18	663	07/11/17	677	-14	

Table 2-1 Salt Handling Shaft Data Analysis (continued)

Embedment Strain Gauges								
Field Tag	Level feet	Figure Number	Date of 2018-2019 Max. Reading	2018-2019 Maximum Strai999n Readings (με)	Date of 2017-2018 Maximum Strain Readings (με)	2017-2018 Maximum Strain Readings (με)	Change in Maximum Strain From Previous Year (με)	Comments
37X-ZE-00209	856.3	2-8	01/21/19	-537	01/08/18	-549	12	
37X-ZE-00210	856.3	2-8	07/26/18	1007	07/11/17	1021	-14	
37X-ZE-00211	856.3	2-8	08/07/18	347	08/01/17	356	-9	
37X-ZE-00212	856.3	2-8	01/15/19	-826	01/02/18	-970	144	
37X-ZE-00213	856.3	2-8	08/07/18	430	08/01/17	434	-4	
37X-ZE-00214	856.3	2-8	07/26/18	151	07/11/17	171	-20	
37X-ZE-00215	856.3	2-8	08/07/18	157	08/01/17	161	-4	
37X-ZE-00216	856.3	2-8	07/26/18	689	06/26/18	699	-10	
37X-ZE-00225	862.4	2-9	08/07/18	334	08/01/17	340	-6	
37X-ZE-00226	862.4	2-9	08/07/18	64	08/01/17	78	-14	
37X-ZE-00229	862.4	2-9	08/07/18	948	08/01/17	961	-13	
37X-ZE-00230	862.4	2-9	07/26/18	740	05/29/18	736	4	
37X-ZE-00235	856.3	2-10	01/21/19	-388	01/08/18	-401	13	
37X-ZE-00236	856.3	2-10	08/07/18	202	06/26/18	208	-6	
37X-ZE-00237	856.3	2-10	07/26/18	131	07/11/17	146	-15	
37X-ZE-00238	856.3	2-10	07/26/18	572	08/01/17	581	-9	
37X-ZE-00239	862.4	2-11	08/07/18	434	08/01/17	443	-9	
37X-ZE-00242	862.4	2-11	08/07/18	144	08/01/17	161	-17	

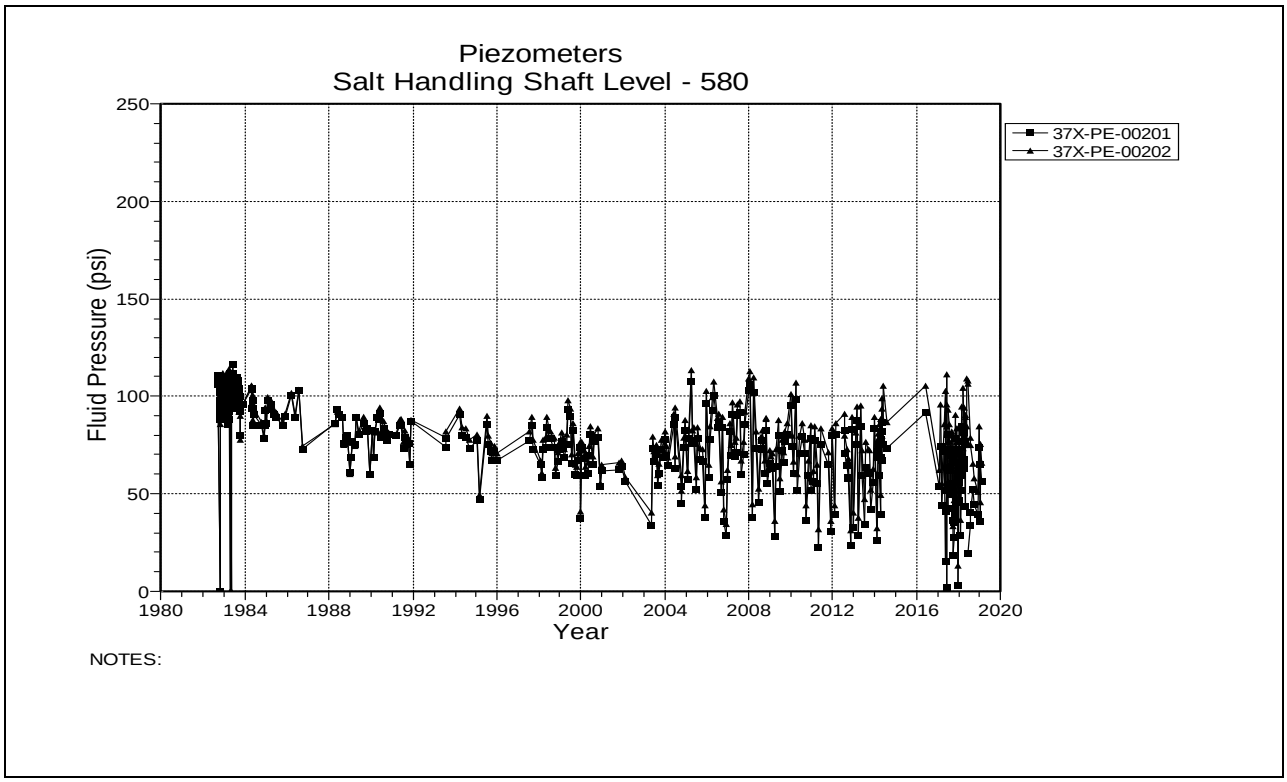

Figure 2-1 Piezometers Salt Handling Shaft – Level 580 at the Forty-niner Member

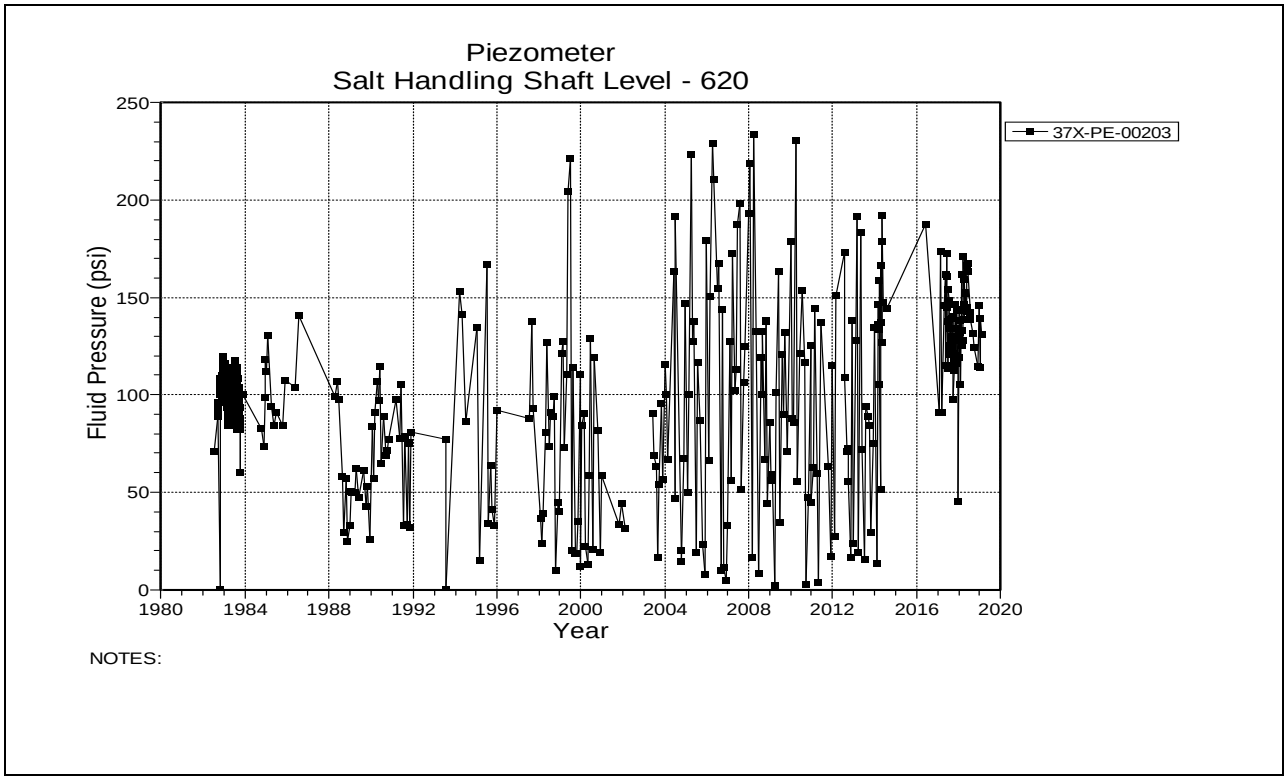

Figure 2-2 Piezometer Salt Handling Shaft – Level 620 at the Magenta Dolomite Member

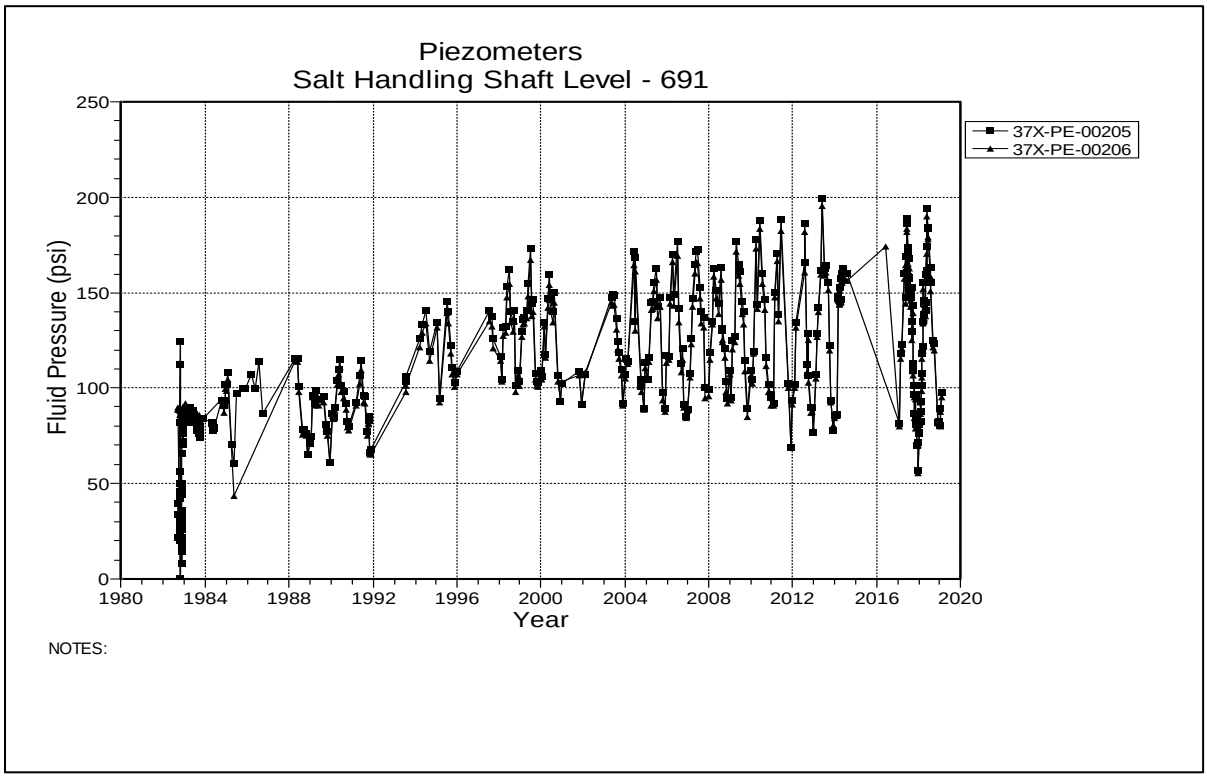

Figure 2-3 Piezometers Salt Handling Shaft – Level 691 at the Tamarisk Member

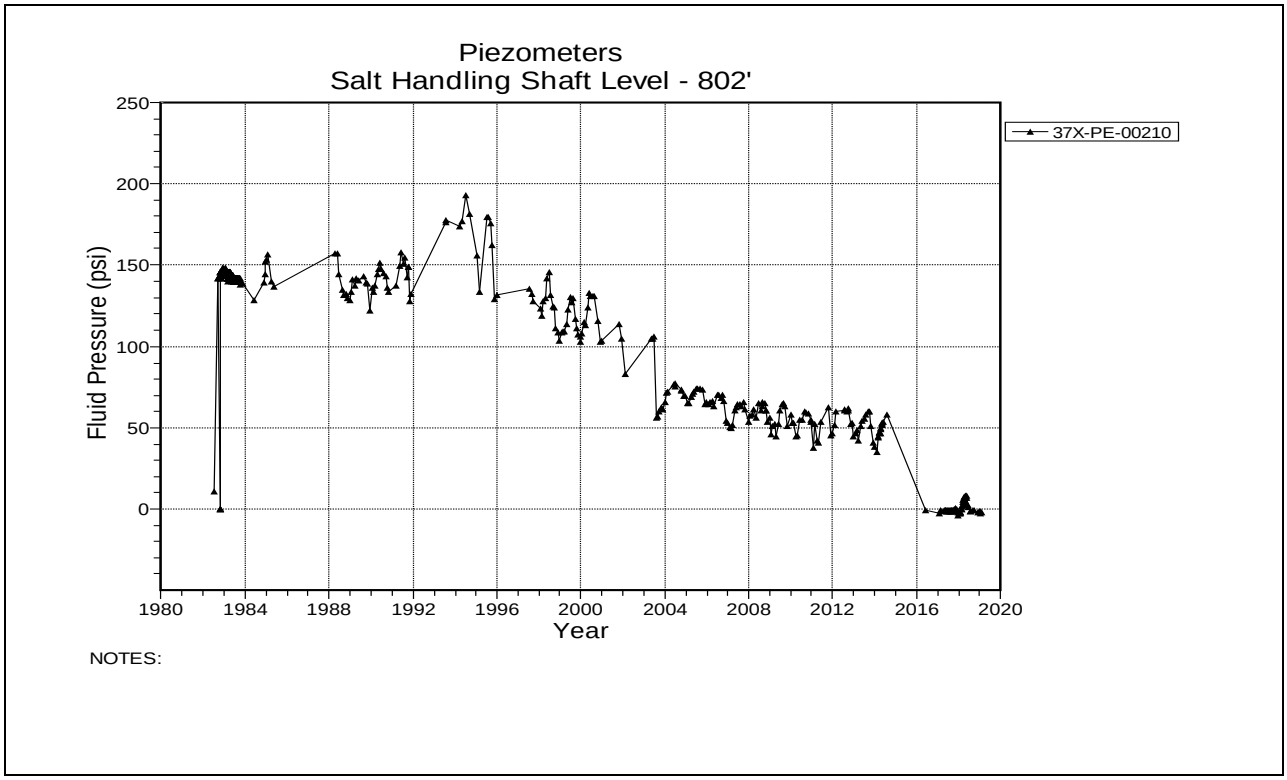

Figure 2-4 Piezometer Salt Handling Shaft – Level 802 at the Los Medaños Member

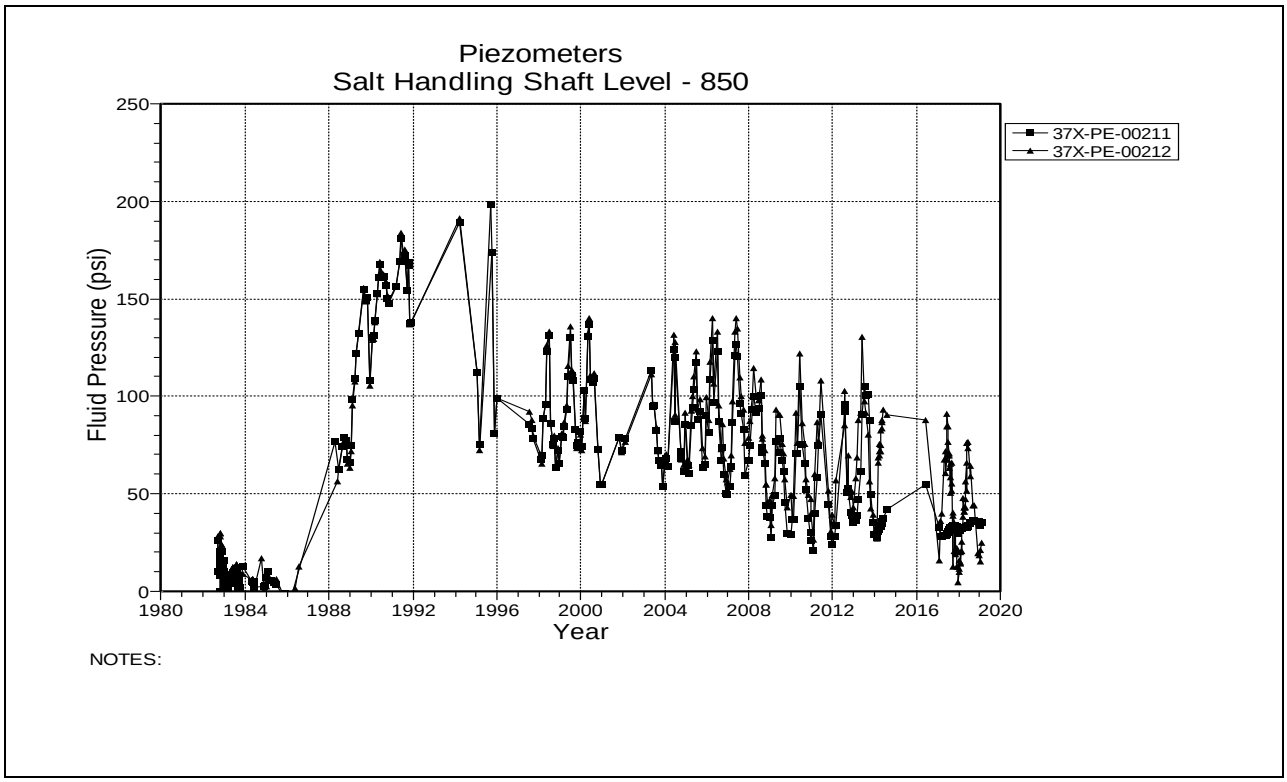

Figure 2-5 Piezometer Salt Handling Shaft – Level 850 at the Rustler-Salado Contact

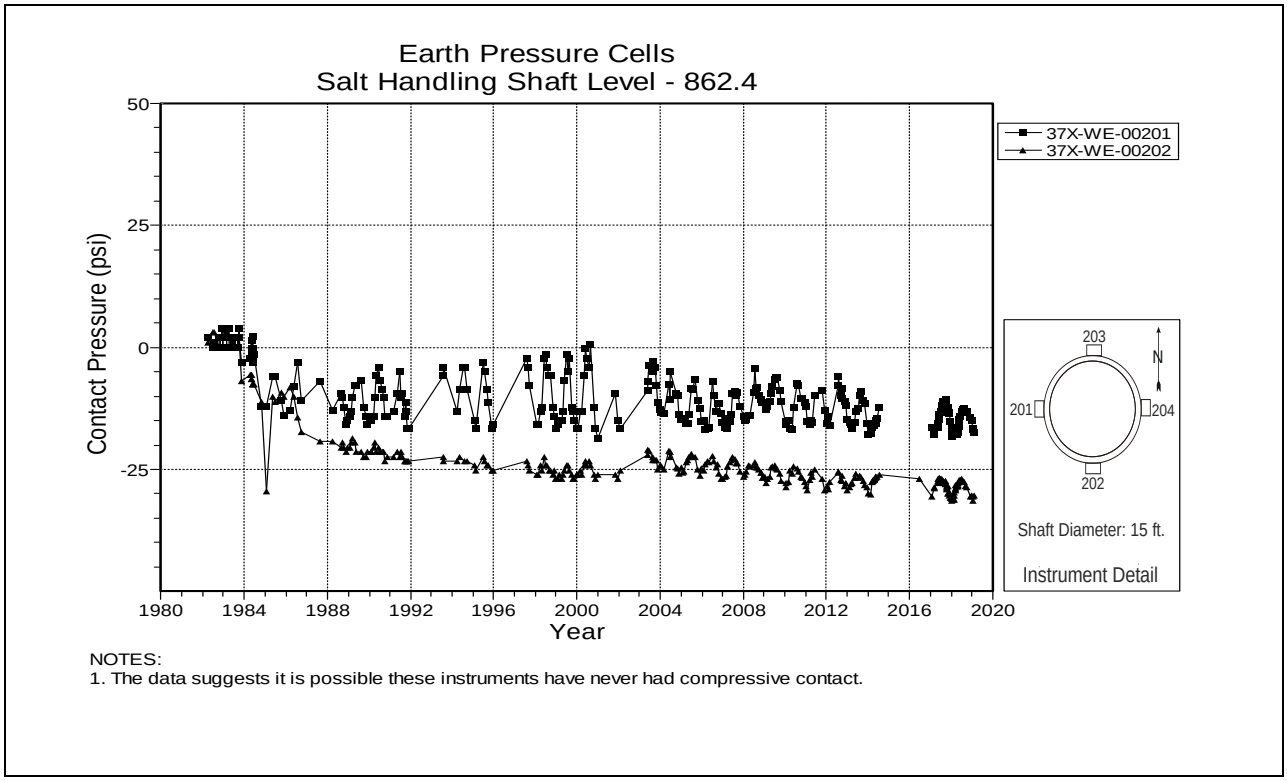

Figure 2-6 Earth Pressure Cells – Salt Handling Shaft Key – Level 862.4

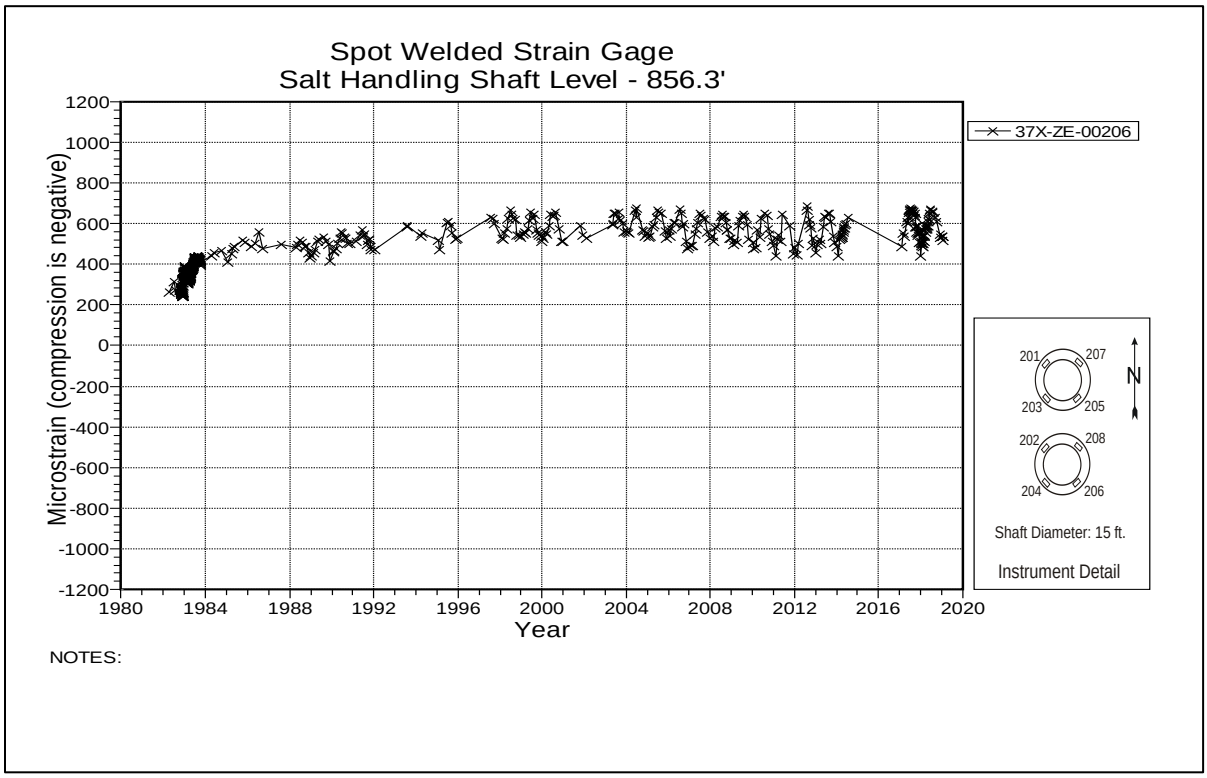

Figure 2-7 Spot Welded Strain Gauge – Salt Handling Shaft Key – Level 856.3

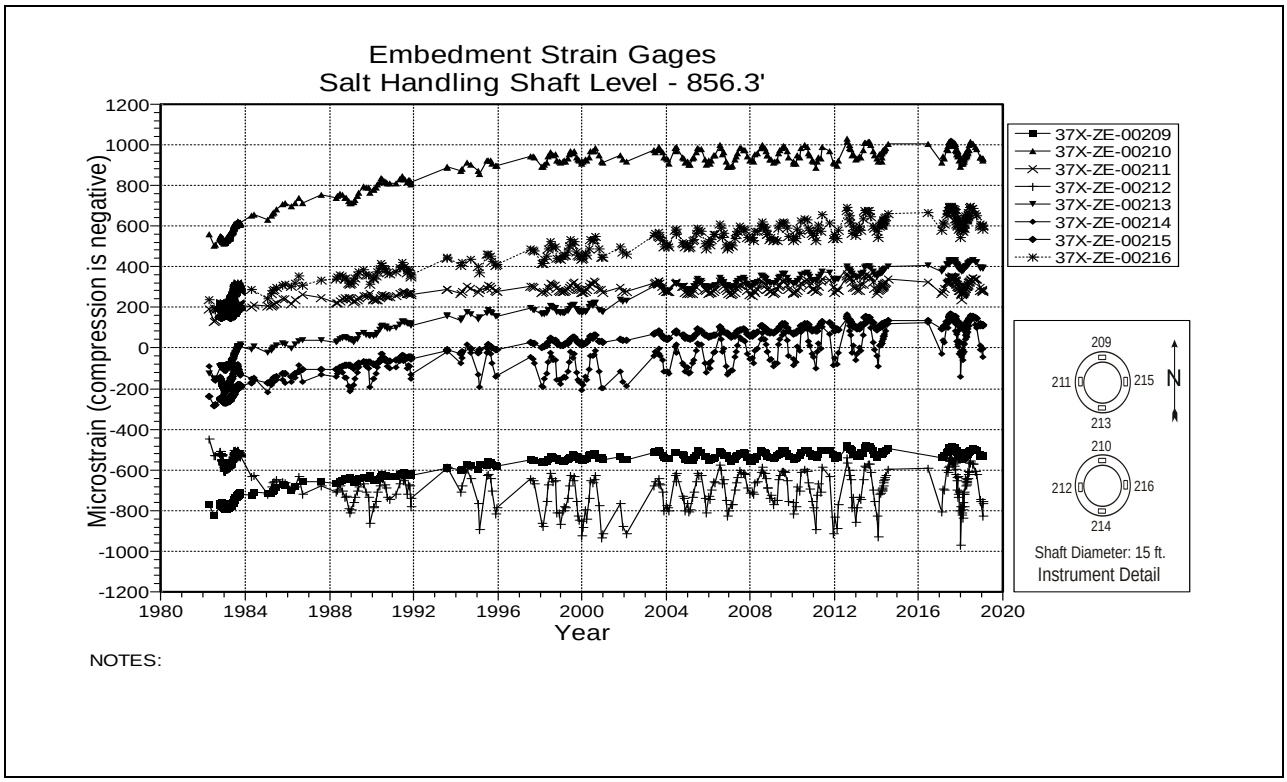

Figure 2-8 Embedment Strain Gauge – Salt Handling Shaft Key – Level 856.3

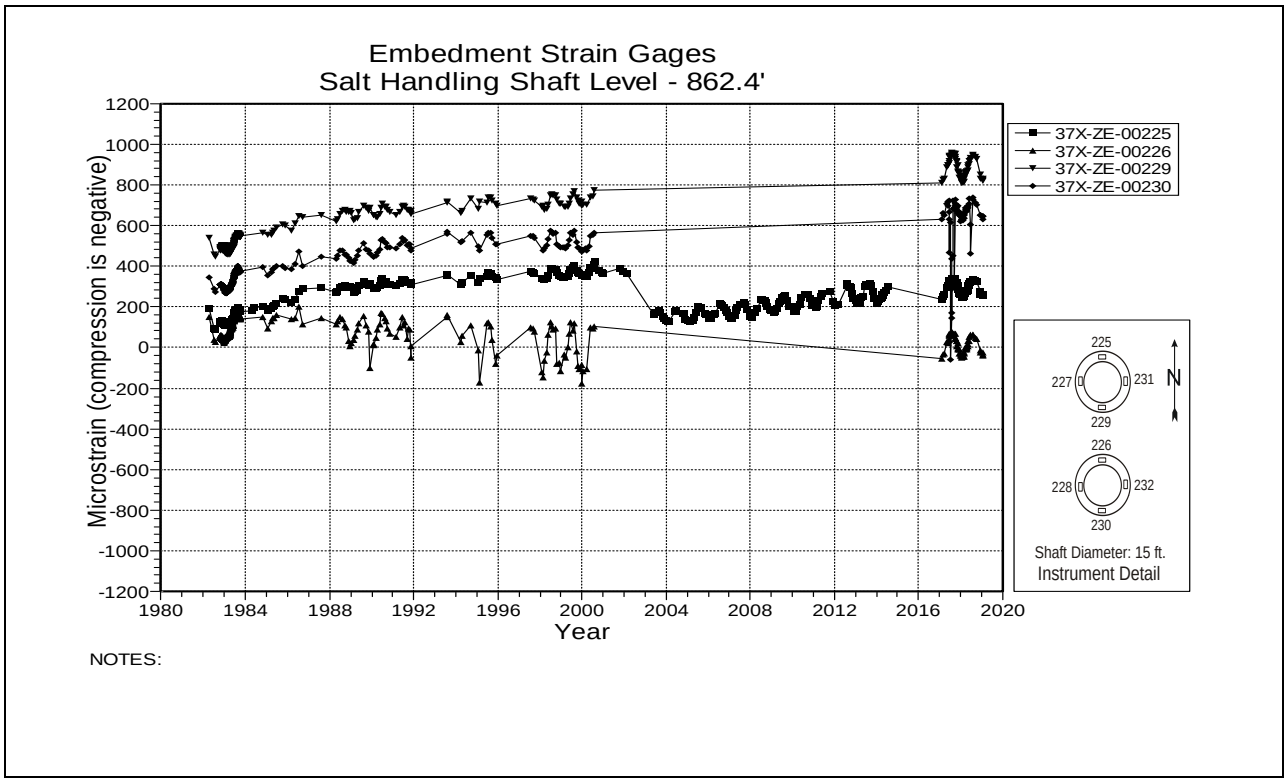

Figure 2-9 Embedment Strain Gauge – Salt Handling Shaft Key – Level 862.4

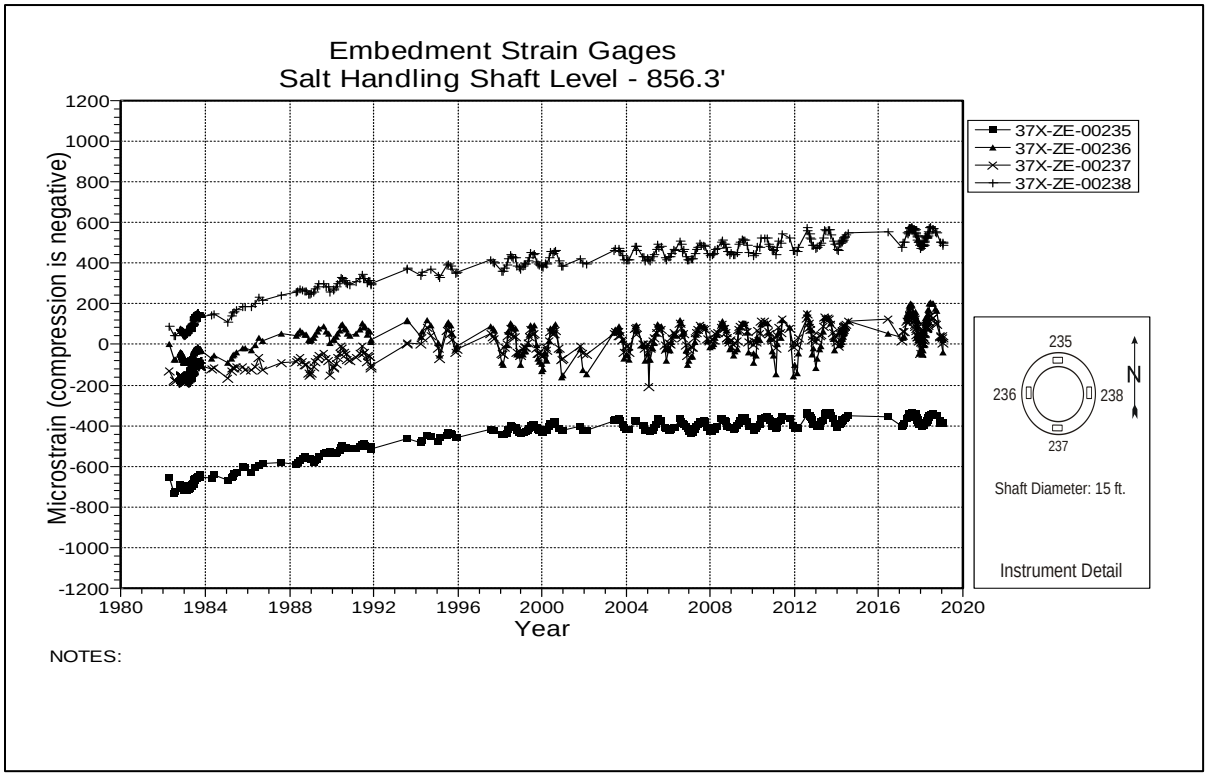

Figure 2-10 Embedment Strain Gauge – Salt Handling Shaft Key – Level 856.3

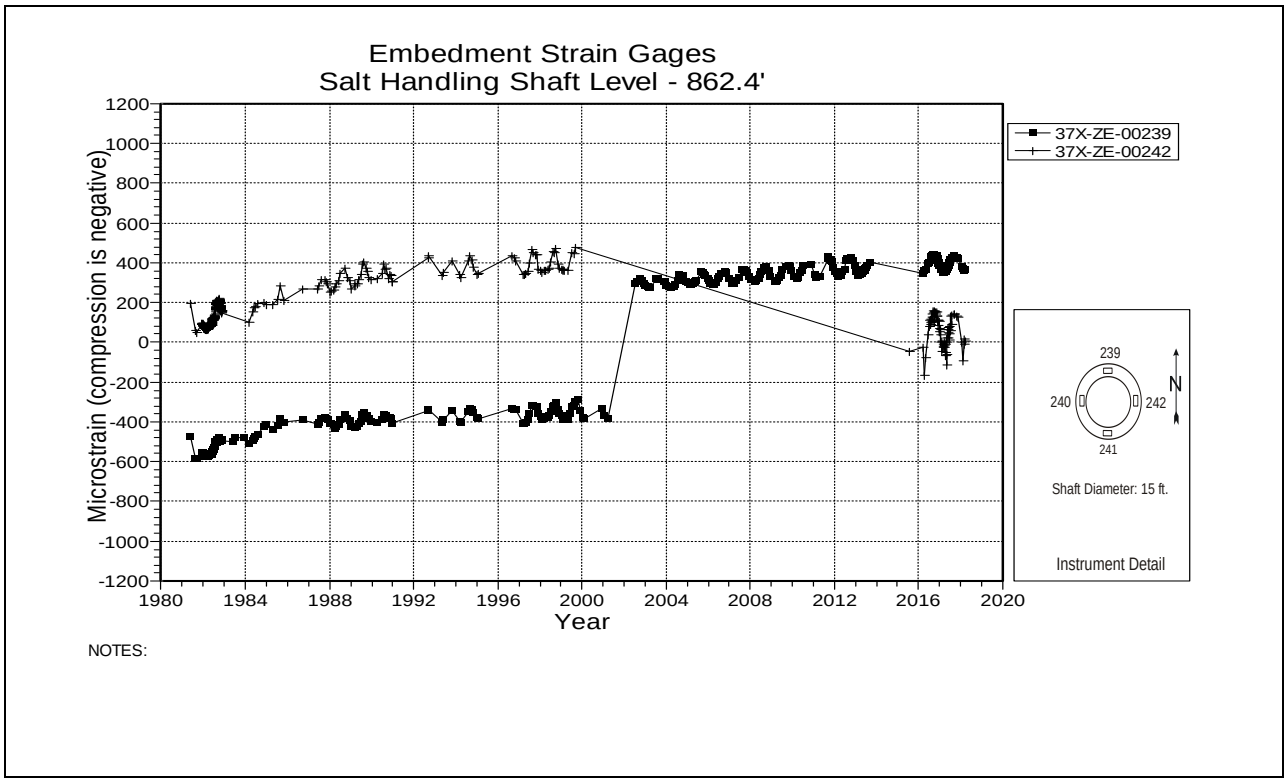

Figure 2-11 Embedment Strain Gauge – Salt Handling Shaft Key – Level 862.4

3.0 INSTRUMENTATION SUMMARY FOR SHAFT STATIONS

The following Instrumentation data analysis is for the Salt Handling Shaft Station. The Waste Shaft Station, and the area around the Air Intake Shaft are presented in Section 4.0. Table 3-1 presents data analyses for each of the Salt Handling Shaft Station instruments. Figures 3-1 through 3-4 present plots of the instrumentation data for the Salt Handling Shaft Station.

Table 3-1
Salt Handling Shaft Station Data Analysis

Convergence Points									
			Last Reading 2018-2019						
Field Tag	Location	Figure Number	Date	Inches	Cumulative Displacement (inches)	Closure Rate 2018 to 2019 (in/year)	Closure Rate 2017 to 2018 (in/year)	Rate Change Percent	Comments
E0-S18-8 A-E	E0-S18	3-1	02/26/19	12.123	33.275	1.3	1.8	-28	
E0-S18-5 H-F	E0-S18	3-2	02/26/19	7.525	21.986	0.8	1.1	-27	
E0-S30-6 A-C	E0-S30	3-3	02/26/19	12.137	34.168	1.4	1.8	-22	
E0-S65-5 A-C	E0-S65	3-4	02/26/19	8.200	23.560	0.9	1.2	-25	

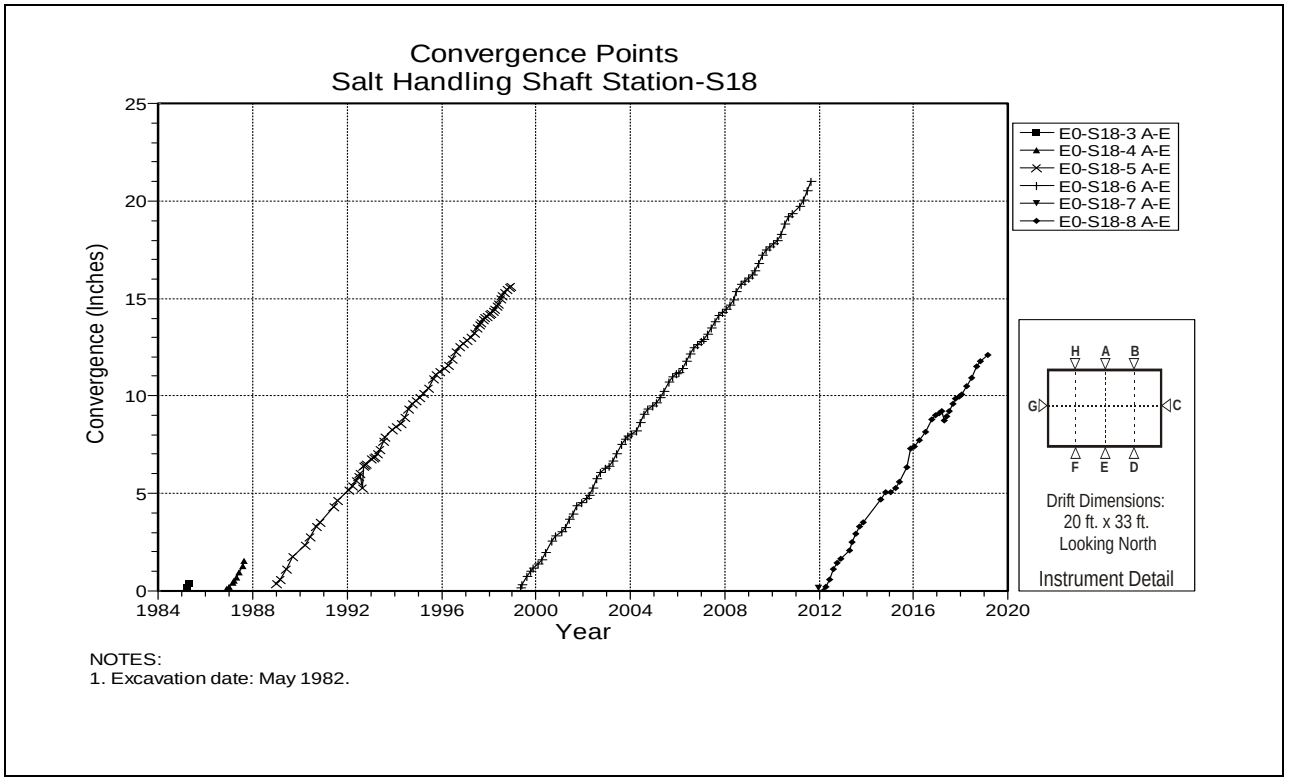

NOTES:
1. Excavation date: May 1982.

Figure 3-1 Convergence Point Array – Salt Handling Shaft Station at S18 – Centerline – Roof to Floor

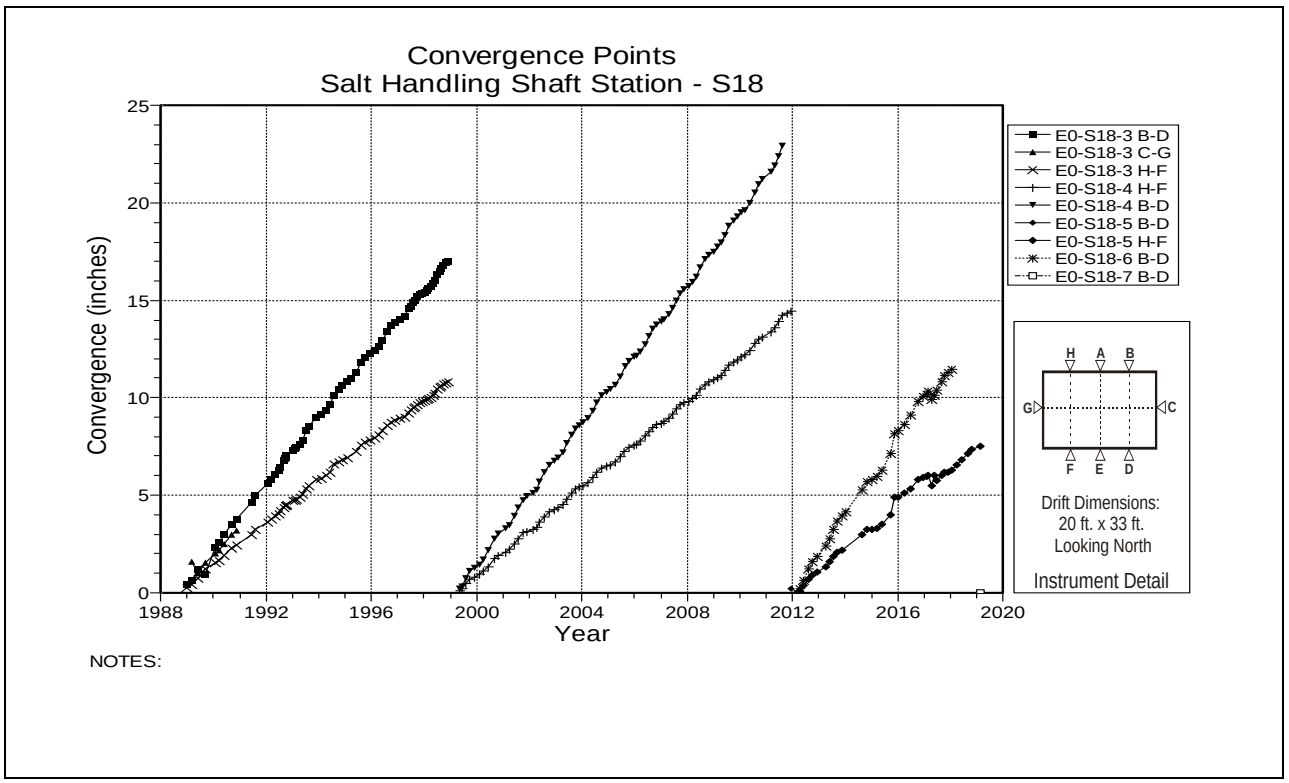

NOTES:

Figure 3-2 Convergence Point Array – Salt Handling Shaft Station at S18 – Quarter Points – Roof to Floor

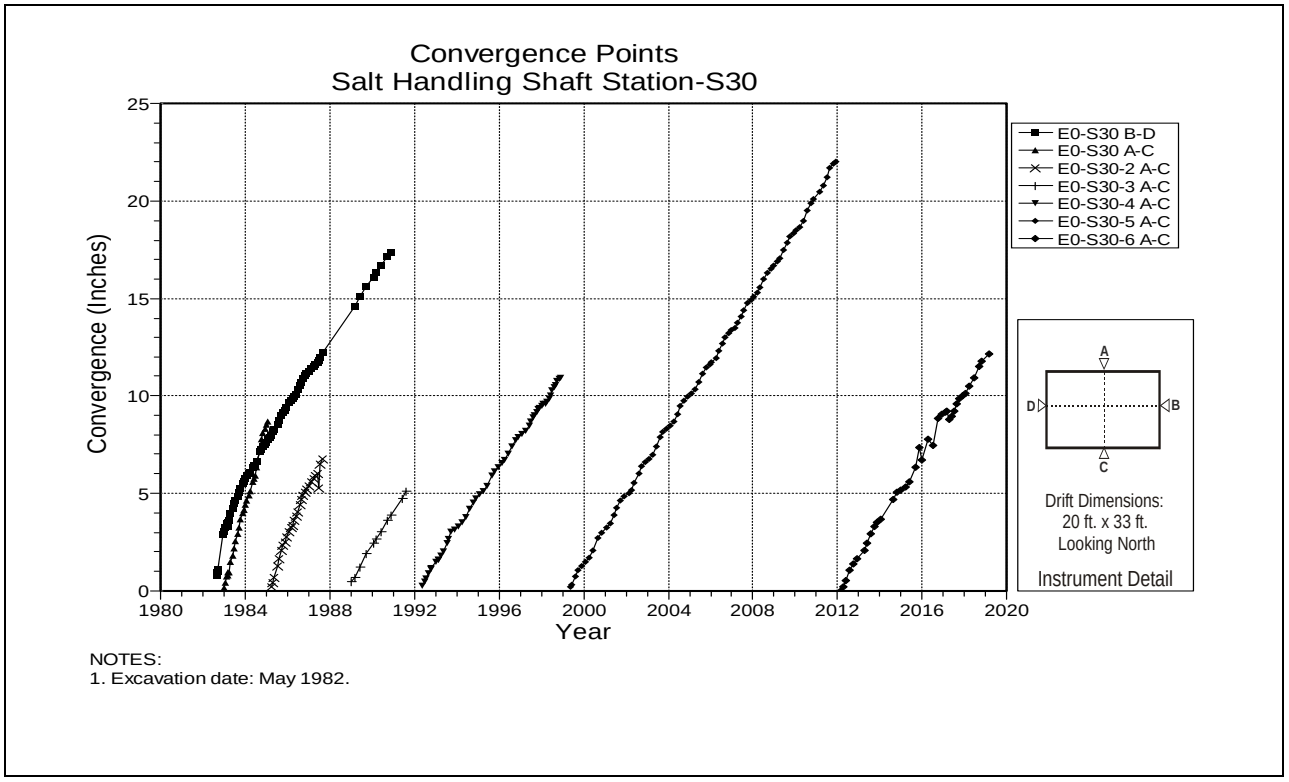

Figure 3-3 Convergence Point Array – Salt Handling Shaft Station at S30 – Roof to Floor

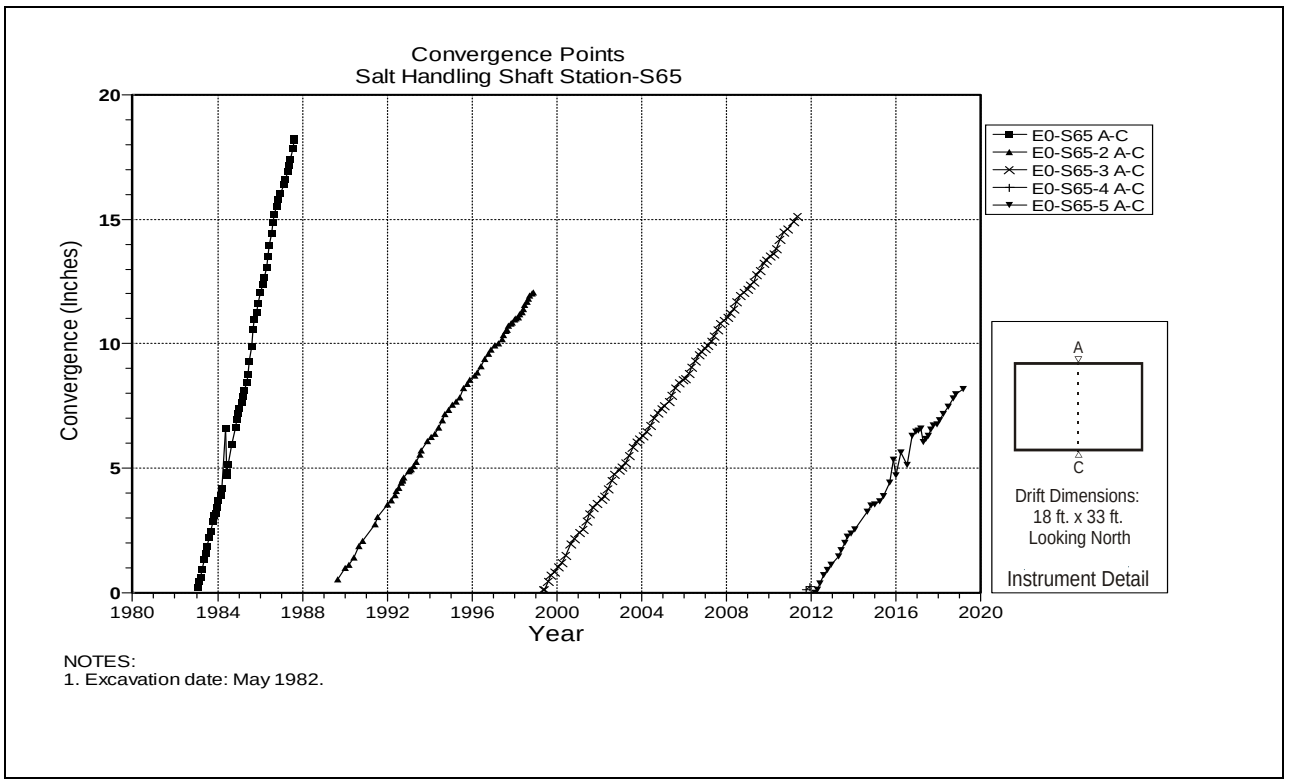

Figure 3-4 Convergence Point Array – Salt Handling Shaft Station at S65 – Roof to Floor

4.0 INSTRUMENTATION SUMMARY FOR THE ACCESS DRIFTS

This chapter presents the instrumentation data and data analyses for the access drifts throughout the WIPP underground. Table 4-1 provides the results of analyses performed on the instrument data including displacement, convergence rates, and rock bolt loading.

Figures 4-1 through 4-9 present data from convergence meters in the access drifts. Figure 4-10 through 4-20 present data from borehole extensometers installed in the access drifts while Figures 4-21 through 4-186 present the convergence point data. Figure 4-187 through 4-190 present data from joint meters installed at the S1950-E300 overcast and the access drifts. AIS brow support rock bolt load cell data are presented in Figures 4-191 through 4-194.

Table 4-1 Access Drifts Data Analysis

Convergence Meters								
Field Tag	Location	Figure Number	Date of Last Reading	Displacement (inches)	Displacement Rate 2018 to 2019 (in/year)	Displacement Rate[3] 2017 to 2018 (in/year)	Rate Change Percent[3]	Comments
51X-CW-01037	E140-S2750	4-1	06/13/19	8.345	4.0	3.5	14	
51X-PG-01049	E300-N1273	4-2	05/02/19	3.327	3.7	5.6	-34	
51X-PG-01048	E300-N1303	4-3	05/02/19	3.338	3.5	6.8	-49	
51X-CW-01048	E300-S2635	4-4	06/13/19	2.463	2.2	N/A	N/A	Installed end of previous period.
51X-PG-00442	E300-S2750	4-5	04/23/19	1.959	2.0	1.5	33	
51X-PG-00446	N460-E320	4-6	04/15/19	0.389	1.2	N/A	N/A	Installed this period.
51X-PG-00445	S700-E220	4-7	05/08/19	0.488	1.6	N/A	N/A	Installed this period.
51X-CW-01039	W170-S2735	4-8	06/13/19	4.356	2.3	2.5	-8	
51X-CW-01038	W30-S2750	4-9	06/13/19	14.533	7.8	6.6	18	
Extensometers								
Field Tag	Location	Figure Number	Date of Last Reading	Collar Displacement Relative to Deepest Anchor (inches)	Displacement Rate 2018 to 2019 (in/year)	Displacement Rate[3] 2017 to 2018 (in/year)	Rate Change Percent[3]	Comments
51X-GE-00355	E0-N300	4-10	06/24/19	2.691	0.3	0.2	50	Calculations on anchor 'A'.
51X-GE-00353	E0-N626	4-11	06/24/19	14.949	1.6	1.6	0	
51X-GE-00352-2	E0-N940	4-12	06/24/19	0.212	2.0	N/A	N/A	Reinstalled this period.
51X-GE-00364	E140-N1266	4-13	06/24/19	11.543	0.8	1.2	-33	
51X-GE-00372-2	E140-S146	4-14	06/24/19	0.114	0.8	N/A	N/A	Reinstalled this period.
51X-GE-00374	E300-N1186	4-15	06/24/19	12.833	1.0	2.1	-52	
51X-GE-00388	E300-N1266	4-16	06/24/19	9.822	1.0	1.3	-23	
51X-GE-00373	E300-N1341	4-17	06/24/19	11.112	1.6	1.6	0	
51X-GE-00440	AIS North Brow	4-18	04/23/19	0.523	0.2	0.2	0	
51X-GE-00441	AIS South Brow	4-19	04/23/19	0.646	0.2	0.3	-33	
51X-GE-00401	W620- N20	4-20	06/24/19	2.615	0.2	0.2	0	
41X-GE-00123	W620- N93	4-21	06/25/19	5.161	0.3	0.3	0	Calculations on anchor 'A'.
41X-GE-00122	W620- S65	4-22	06/25/19	4.888	0.2	0.3	-33	Calculations on anchor 'B'.

Table 4-1 Access Drifts Data Analysis (continued)

Convergence Points									
			Last Reading 2018-2019						
Field Tag	Location	Figure Number	Date	Inches	Cumulative Displacement (inches)	Closure Rate 2018 to 2019 (in/year)	Closure Rate[3] 2017 to 2018 (in/year)	Rate Change Percent[3]	Comments
CORE-W20 A-C	CORE STORAGE W20	4-23	02/01/19	28.405	28.405	1.1	1.1	0	
CORE-W30 A-C	CORE STORAGE W30	4-23	11/30/18	29.782	29.782	1.1	1.1	0	
CORE-W51 A-C	CORE STORAGE W51	4-23	07/18/18	35.237	35.237	N/A	1.3	N/A	One reading this period; cable in way.
E0-N75-3 A-C	E0-N75	4-24	02/26/19	33.882	50.860	1.9	2.7	-30	
E0-N225-2 A-C	E0-N225	4-25	10/30/18	30.134	30.181	1.8	1.7	6	-3 A-C new install, read once this period
E0-N300-6 A-C	E0-N300	4-26	10/30/18	14.242	30.579	N/A	1.9	N/A	One reading this period; floor point covered with muck.
E0-N460-3 A-C	E0-N460	4-27	10/30/18	38.591	58.680	2.5	2.6	-4	-4 A-C new install, read once this period
E0-N562 A-C	E0-N562	4-28	02/26/19	32.428	32.428	2.8	2.6	8	
E0-N626-5 A-C	E0-N626	4-29	02/26/19	7.616	79.012	3.4	3.3	3	
E0-N686 A-C	E0-N686	4-30	02/26/19	39.538	39.538	2.7	2.8	-4	
E0-N780-2 A-C	E0-N780	4-31	02/26/19	33.197	53.619	1.9	2.3	-17	
E0-N940-5 A-C	E0-N940	4-32	02/26/19	38.328	86.380	3.4	3.8	-11	
E0-N1110-5 A-C	E0-N1110	4-33	02/26/19	23.834	58.258	1.7	1.8	-6	
E0-N1266-4 A-C	E0-N1266	4-34	02/26/19	36.923	73.830	2.5	3.0	-17	
E0-N1420-2 A-C	E0-N1420	4-35	02/26/19	18.138	32.602	1.1	1.4	-21	
E140-N5-7 A-C	E140-N5	4-36	06/13/19	18.248	65.141	2.9	3.1	-6	
E140-N150-6 A-C	E140-N150	4-37	06/13/19	11.880	42.626	1.8	2.1	-14	
E140-N220-4 A-C	E140-N220	4-38	06/13/19	18.485	60.642	3.0	3.0	0	
E140-N355-2 A-C	E140-N355	4-39	06/13/19	30.236	38.780	2.3	2.6	-12	
E140-N460-3 A-C	E140-N460	4-40	06/13/19	38.326	59.157	2.3	2.7	-15	
E140-N562-2 A-C	E140-N562	4-41	06/13/19	41.811	53.628	3.2	3.3	-3	
E140-N626-3 A-C	E140-N626	4-42	06/13/19	54.656	87.226	4.1	4.1	0	
E140-N686-2 A-C	E140-N686	4-43	06/13/19	41.767	54.906	2.8	2.9	-3	

Table 4-1 Access Drifts Data Analysis (continued)

Convergence Points (continued)									
Field Tag	Location	Figure Number	Last Reading 2018-2019		Cumulative Displacement (inches)	Closure Rate 2018 to 2019 (in/year)	Closure Rate[3] 2017 to 2018 (in/year)	Rate Change Percent[3]	Comments
			Date	Inches					
E140-N780-3 A-C	E140-N780	4-44	06/13/19	7.744	75.877	2.6	3.0	-13	
E140-N940-2 A-C	E140-N940	4-45	11/02/18	52.557	81.956	4.6	4.9	-6	
E140-N1100-2 A-C	E140-N1100	4-46	06/13/19	25.575	45.298	1.5	2.2	-32	
E140-N1266-3 A-C	E140-N1266	4-47	06/13/19	40.493	78.248	2.8	3.5	-20	
E140-N1420-2 A-C	E140-N1420	4-48	06/13/19	27.452	43.922	1.9	2.3	-17	
E140-S90-4 A-C	E140-S90	4-49	06/13/19	25.560	43.273	2.1	2.3	-9	
E140-S262-5 A-C	E140-S262	4-50	05/14/19	13.757	50.778	2.1	2.3	-9	
E140-S460-7 A-C	E140-S460	4-51	05/14/19	5.354	65.628	2.1	2.2	-5	
E140-S460-2 B-D	E140-S460	4-51	05/14/19	35.613	41.557	1.2	1.3	-8	
E140-S550-6 A-C	E140-S550	4-52	05/14/19	16.133	58.100	2.1	1.9	11	
E140-S700-8 A-D	E140-S700	4-53	05/14/19	19.620	49.660	2.4	2.5	-4	
E140-S700-7 B-C	E140-S700	4-54	05/14/19	6.476	51.076	1.8	2.0	-10	
E140-S700-7 E-F	E140-S700	4-55	05/14/19	3.065	32.649	1.4	1.5	-7	
E140-S850-10 A-C	E140-S850	4-56	05/14/19	15.973	73.709	2.6	2.7	-4	
E140-S1000-4 A-C	E140-S1000	4-57	05/14/19	10.586	50.933	1.7	1.7	0	
E140-S1025-6 A-C	E140-S1025	4-58	05/14/19	5.126	39.990	2.9	2.0	45	
E140-S1075-5 A-E	E140-S1075	4-59	05/14/19	18.522	47.324	3.0	3.1	-3	
E140-S1075-5 B-D	E140-S1075	4-60	05/14/19	8.063	30.154	1.2	1.4	-14	
E140-S1075-6 H-F	E140-S1075	4-61	02/12/19	4.097	33.561	2.2	2.3	-4	
E140-S1150-6 A-G	E140-S1150	4-62	05/14/19	6.446	91.358	2.9	3.0	-3	
E140-S1150-2 E-I	E140-S1150	4-63	04/02/19	27.083	27.944	1.4	1.4	0	
E140-S1150-7 B-F	E140-S1150	4-64	05/14/19	16.882	49.339	1.9	2.1	-10	
E140-S1150-6 L-H	E140-S1150	4-65	05/14/19	10.670	36.468	1.5	1.7	-12	
E140-S1225-6 A-E	E140-S1225	4-65	05/14/19	7.310	58.519	3.2	3.9	-18	
E140-S1225-6 B-D	E140-S1225	4-66	05/14/19	2.880	47.356	1.4	1.6	-13	
E140-S1225-4 H-F	E140-S1225	4-67	05/14/19	12.480	37.863	1.5	1.9	-21	
E140-S1300-5 A-C	E140-S1300	4-68	05/14/19	9.843	47.786	1.4	1.7	-18	

Table 4-1 Access Drifts Data Analysis (continued)

Convergence Points (continued)

Field Tag	Location	Figure Number	Last Reading 2018-2019		Cumulative Displacement (inches)	Closure Rate 2018 to 2019 (in/year)	Closure Rate[3] 2017 to 2018 (in/year)	Rate Change Percent[3]	Comments
			Date	Inches					
E140-S1378-4 A-E	E140-S1375	4-69	05/14/19	21.083	63.624	2.9	3.0	-3	
E140-S1378-6 B-D	E140-S1378	4-70	05/14/19	3.656	41.180	1.7	1.8	-6	
E140-S1378-4 H-F	E140-S1378	4-71	05/14/19	24.877	70.739	4.2	4.3	-2	
E140-S1450-6 A-G	E140-S1450	4-72	05/14/19	23.000	103.807	3.4	3.3	3	
E140-S1450-4 B-F	E140-S1450	4-73	05/15/19	10.464	57.952	1.4	1.6	-13	
E140-S1450-3 I-E	E140-S1450	4-74	05/14/19	13.314	31.406	1.5	1.6	-6	
E140-S1450-4 L-H	E140-S1450	4-75	05/14/19	18.784	60.604	3.0	2.9	3	
E40-S1496 B-D	E40-S1496	4-76	06/25/19	0.019	0.019	1.4	N/A	N/A	New installation in E140 Test Area.
E140-S1524- A-E	E140-S1524	4-77	06/25/19	0.175	0.175	2.9	N/A	N/A	New installation in E140 Test Area.
E140-S1524 B-D	E140-S1524	4-78	06/25/19	0.034	0.034	2.5	N/A	N/A	New installation in E140 Test Area.
E140-S1534-5 A-E	E140-S1534	4-79	05/15/19	0.365	70.879	3.0	2.8	7	
E140-S1534-6 B-D	E140-S1534	4-80	05/15/19	0.312	49.199	2.6	2.4	8	
E140-S1534-4 H-F	E140-S1534	4-81	02/12/19	6.548	53.050	3.0	2.9	3	-5 H-F new install, read once this period.
E140-S1600-7 A-C	E140-S1600	4-82	05/15/19	19.014	60.960	4.5	3.6	25	
E140-S1667 A-E	E140-S1667	4-83	06/25/19	0.189	0.189	3.1	N/A	N/A	New installation in E140 Test Area.
E140-S1667 B-D	E140-S1667	4-84	06/25/19	0.214	0.214	3.6	N/A	N/A	New installation in E140 Test Area.
E140-S1687-5 A-E	E140-S1687	4-85	05/15/19	4.837	68.291	3.3	3.1	6	
E140-S1687-4 B-D	E140-S1687	4-86	05/15/19	14.530	51.272	2.3	2.5	-8	
E140-S1687-4 H-F	E140-S1687	4-87	05/15/19	18.915	55.683	3.0	2.8	7	
E140-S1699 A-E	E140-S1699	4-87	06/25/19	0.211	0.211	3.5	N/A	N/A	New installation in E140 Test Area.
E140-S1699 B-D	E140-S1699	4-87	06/25/19	0.136	0.136	2.3	N/A	N/A	New installation in E140 Test Area.
E140-S1699 H-F	E140-S1699	4-87	06/03/19	0.186	0.186	3.1	N/A	N/A	New installation in E140 Test Area.
E140-S1717 A-E	E140-S1717	4-88	06/25/19	0.192	0.192	3.2	N/A	N/A	New installation in E140 Test Area.
E140-S1717 B-D	E140-S1717	4-89	06/25/19	0.181	0.181	3.0	N/A	N/A	New installation in E140 Test Area.
E140-S1717 H-F	E140-S1717	4-90	06/25/19	0.040	0.040	2.9	N/A	N/A	New installation in E140 Test Area.
E140-S1775-4 A-G	E140-S1775	4-91	05/15/19	24.264	92.450	3.7	3.6	3	

Table 4-1 Access Drifts Data Analysis (continued)

Convergence Points (continued)									
Field Tag	Location	Figure Number	Last Reading 2018-2019		Cumulative Displacement (inches)	Closure Rate 2018 to 2019 (in/year)	Closure Rate[3] 2017 to 2018 (in/year)	Rate Change Percent[3]	Comments
			Date	Inches					
E140-S1775-6 B-F	E140-S1775	4-92	05/15/19	9.647	79.997	3.8	3.7	3	
E140-S1775-4 L-H	E140-S1775	4-92	05/15/19	13.939	46.524	2.4	2.3	4	
E140-S1775-3 I-E	E140-S1775	4-93	05/15/19	23.301	37.522	2.1	2.0	5	
E140-S1862-4 A-E	E140-S1862	4-94	05/15/19	22.200	75.198	3.4	3.3	3	
E140-S1862-4 B-D	E140-S1862	4-95	05/15/19	25.169	73.830	4.1	4.2	-2	
E140-S1862-4 H-F	E140-S1862	4-95	05/15/19	12.581	38.934	2.0	2.0	0	
E140-S1950-7 A-C	E140-S1950	4-96	05/15/19	25.438	81.828	4.1	3.8	8	
E140-S2007-8 A-C	E140-S2007	4-97	03/19/19	28.483	73.010	4.4	4.3	2	
E140-S2065-8 A-C	E140-S2065	4-98	03/19/19	7.076	70.826	3.6	3.6	0	
E140-S2122-8 A-C	E140-S2122	4-99	03/19/19	7.625	67.578	3.8	3.9	-3	
E140-S2275-7 A-C	E140-S2275	4-100	03/19/19	33.190	112.127	5.8	5.7	2	
E140-S2350-7 A-C	E140-S2350	4-101	03/19/19	32.199	114.912	5.7	5.5	4	
E140-S2425-6 A-C	E140-S2425	4-102	03/19/19	27.855	83.361	4.5	4.6	-2	
E140-S2520-4 A-C	E140-S2520	4-103	03/19/19	23.720	64.496	3.9	3.9	0	
E300-N45-2 A-E	E300-N45	4-104	04/29/19	11.333	44.214	1.7	2.0	-15	
E300-N45-2 H-F	E300-N45	4-104	04/29/19	10.005	39.544	1.5	1.8	-17	
E300-N170-3 A-E	E300-N170	4-105	04/29/19	13.383	46.857	2.4	2.5	-4	
E300-N170-3 H-F	E300-N170	4-105	04/29/19	11.163	41.458	2.1	2.1	0	
E300-N250-5 A-C	E300-N250	4-106	04/29/19	4.324	56.245	2.1	3.0	-30	
E300-N280 A-C	E300-N280	4-107	06/13/19	3.404	3.404	1.5	1.6	-6	
E300-N360 A-C	E300-N360	4-108	06/13/19	3.121	3.121	1.3	1.5	-13	
E300-N440 A-C	E300-N440	4-109	06/13/19	3.373	3.373	1.4	1.6	-13	
E300-N500 A-C	E300-N500	4-110	06/13/19	2.406	2.406	0.9	1.3	-31	
E300-N1100-2 A-C	E300- N1100	4-111	06/13/19	14.333	16.558	2.1	2.9	-28	
E300-N1262-4 A-C	E300-N1262	4-112	06/13/19	22.946	45.009	3.1	4.1	-24	

Table 4-1 Access Drifts Data Analysis (continued)

Convergence Points (continued)									
Field Tag	Location	Figure Number	Last Reading 2018-2019		Cumulative Displacement (inches)	Closure Rate 2018 to 2019 (in/year)	Closure Rate[3] 2017 to 2018 (in/year)	Rate Change Percent[3]	Comments
			Date	Inches					
E300-N1341-3 A-C	E300-N1341	4-113	06/13/19	21.903	42.501	3.1	4.3	-28	
E300-S45-3 A-E	E300-S45	4-114	04/29/19	9.183	36.387	1.3	1.7	-24	
E300-S45-3 B-D	E300-S45	4-114	04/29/19	9.469	34.660	1.2	1.4	-14	
E300-S45-3 H-F	E300-S45	4-114	04/29/19	7.928	31.177	1.1	1.5	-27	
E300-S90-3 A-C	E300-S90	4-115	04/29/19	7.734	28.011	1.4	1.5	-7	
E300-S250-2 A-C	E300-S250	4-116	04/29/19	14.981	19.366	1.0	1.0	0	
E300-S250-2 B-D	E300-S250	4-116	03/07/19	16.056	20.102	1.1	0.6	83	
N140-E90-3 A-C	N140-E90	4-117	06/13/19	4.400	23.035	0.8	1.0	-20	
N215-W500-2 A-C	N215-W500	4-118	04/08/19	20.534	38.863	1.3	1.3	0	
N215-W500-2 B-D	N215-W500	4-118	04/08/19	18.547	25.365	0.8	0.6	33	
N215-W620-2 A-C	N215-W620	4-119	04/08/19	16.086	32.304	1.1	1.1	0	
N250-E220-4 A-E	N250-E220	4-120	04/29/19	3.535	56.286	2.7	3.0	-10	
N250-E220-3 B-D	N250-E220	4-121	04/29/19	9.752	45.892	1.7	1.7	0	
N250-E220-4 H-F	N250-E220	4-121	04/29/19	2.135	38.203	1.7	1.8	-6	
N300-W170-2 A-C	N300-W170	4-122	04/08/19	25.565	47.825	1.8	1.7	6	
N300-W170-2 B-D	N300-W170	4-122	04/08/19	24.768	32.963	1.1	0.9	22	
N460-E70-3 A-C	N460-E70	4-123	02/26/19	26.489	42.935	1.6	1.8	-11	
N460-E310 A-C	N460-E310	4-124	06/13/19	4.040	4.040	1.6	2.0	-20	
N780-E70 A-C	N780-E70	4-125	02/26/19	22.486	22.486	1.5	1.6	-6	
N780-E220-4 A-C	N780-E220	4-126	02/19/19	16.687	30.113	2.7	N/A	N/A	Inaccessible previous period.
N780-E300-3 A-C	N780-E300	4-127	02/19/19	12.491	15.120	2.1	N/A	N/A	Inaccessible previous period.
N940-E220-2 A-C	N940-E220	4-128	02/19/19	6.658	8.093	1.1	N/A	N/A	Inaccessible previous period.
N940-E300-2 A-C	N940-E300	4-129	02/19/19	7.916	9.682	1.3	N/A	N/A	Inaccessible previous period.
N1420-E79 A-C	N1420-E79	4-130	02/26/19	3.004	3.004	1.3	1.9	-32	

Table 4-1 Access Drifts Data Analysis (continued)

Convergence Points (continued)

Field Tag	Location	Figure Number	Last Reading 2018-2019		Cumulative Displacement (inches)	Closure Rate 2018 to 2019 (in/year)	Closure Rate[3] 2017 to 2018 (in/year)	Rate Change Percent[3]	Comments
			Date	Inches					
N1420-E212 A-C	N1420-E212	4-131	06/13/19	3.263	3.263	1.5	1.7	-12	
N1420-E300 A-C	N1420-E300	4-132	06/13/19	27.009	27.009	1.9	2.5	-24	
S90-E220 A-C	S90-E220	4-133	04/29/19	5.924	5.924	0.8	1.2	-33	
S90-W120 A-C	S90-W120	4-134	04/18/19	12.115	12.115	0.5	0.6	-17	
S90-W120 B-D	S90-W120	4-134	04/18/19	13.193	13.193	0.7	0.7	0	
S90-W400-3 A-C	S90-W400	4-135	04/08/19	3.097	21.949	0.6	0.6	0	
S90-W400-3 B-D	S90-W400	4-135	04/08/19	3.101	21.438	0.5	0.6	-17	
S90-W590-2 A-C	S90-W590	4-136	04/08/19	8.286	17.615	0.6	0.6	0	
S90-W590-2 B-D	S90-W590	4-136	04/08/19	12.851	16.658	0.5	0.5	0	
S90-W620 A-C	S90-W620	4-137	04/08/19	33.015	33.015	1.0	1.0	0	
S700-E180 A-C	S700-E180	4-138	05/14/19	24.665	24.665	1.6	1.7	-6	
S700-E205-3 A-C	S700-E205	4-139	05/14/19	24.980	42.409	1.7	2.0	-15	
S700-W98-3 A-C	S700-W98	4-140	02/08/19	14.690	39.031	2.2	2.1	5	
S1000-E58-4 A-C	S1000-E58	4-141	05/14/19	18.744	34.210	1.5	1.4	7	
S1000-E120-3 A-C	S1000-E120	4-142	05/14/19	16.352	24.792	1.2	1.2	0	
S1000-E160 -3 A-C	S1000-E160	4-143	05/14/19	10.277	18.487	1.0	0.9	11	
S1000-W98-2 A-C	S1000-W98	4-144	04/15/19	29.744	48.492	2.1	2.1	0	
S1300-E24-2 A-C	S1300-E24	4-145	04/15/19	3.151	29.134	1.6	1.5	7	
S1300-E120 A-C	S1300-E120	4-146	05/14/19	22.049	22.049	1.1	1.0	10	
S1300-E160 A-C	S1300-E160	4-147	05/14/19	39.162	39.162	2.6	2.3	13	
S1300-W100-3 A-C	S1300-W100	4-148	02/08/19	30.273	54.276	2.6	2.6	0	
S1600-E110-2 A-C	S1600-E110	4-149	05/15/19	6.709	23.431	1.1	1.2	-8	
S1600-E170-2 A-C	S1600-E170	4-150	07/10/18	6.306	24.617	N/A	1.2	N/A	-2 A-C was read once this period, -3 A-C read during installation only.
S1600-W100-2 A-C	S1600-W100	4-151	04/15/19	7.900	8.917	3.4	N/A	N/A	
S1950-E113-4 A-C	S1950-E113	4-152	05/15/19	18.287	22.163	1.2	1.3	-8	

Table 4-1 Access Drifts Data Analysis (continued)

Convergence Points (continued)									
Field Tag	Location	Figure Number	Last Reading 2018-2019 Date	Last Reading 2018-2019 Inches	Cumulative Displacement (inches)	Closure Rate 2018 to 2019 (in/year)	Closure Rate[3] 2017 to 2018 (in/year)	Rate Change Percent[3]	Comments
S1950-E160 A-C	S1950-E160	4-153	05/15/19	3.770	3.770	1.7	1.8	-6	
S1950-E226 A-C	S1950-E226	4-154	05/15/19	3.608	3.608	1.6	1.8	-11	
S1950-W100-2 A-C	S1950-W100	4-155	04/15/19	7.566	8.537	3.6	3.6	0	
S2180-W100-3 A-C	S2180-W100	4-156	04/24/19	30.108	48.291	3.0	N/A	N/A	Inaccessible previous period.
S2520-E55-2 A-C	S2520-E55	4-157	03/19/19	13.933	34.333	2.7	2.6	4	
S2520-W100-2 A-C	S2520-W100	4-158	02/21/19	23.044	42.724	3.4	3.4	0	
W30-S90 A-C	W30-S90	4-159	04/15/19	2.053	2.053	0.8	0.9	-11	
W30-S120-3 A-C	W30-S120	4-160	04/15/19	4.996	32.642	0.9	0.9	0	
W30-S250-5 A-C	W30-S250	4-161	04/15/19	15.155	41.388	0.9	1.3	-31	
W30-S400-2 A-C	W30-S400	4-162	04/15/19	11.953	29.781	0.8	1.1	-27	
W30-S500-3 A-C	W30-S500	4-163	04/15/19	5.912	36.319	1.0	1.2	-17	
W30-S700-5 A-C	W30-S700	4-164	04/15/19	18.889	53.166	2.1	2.2	-5	
W30-S850-6 A-E	W30-S850	4-165	02/07/19	10.565	40.582	2.2	2.2	0	
W30-S850-5 B-D	W30-S850	4-166	04/15/19	6.598	27.007	1.4	1.3	8	
W30-S850-4 H-F	W30-S850	4-166	02/07/19	10.496	32.693	2.1	2.1	0	
W30-S1000-5 A-C	W30-S1000	4-167	04/15/19	17.182	55.361	1.9	2.0	-5	
W30-S1150-3 A-C	W30-S1150	4-168	04/15/19	1.179	35.818	2.8	3.4	-18	
W30-S1300-2 A-C	W30-S1300	4-169	04/15/19	18.325	39.563	2.2	2.3	-4	
W30-S1453-3 A-C	W30-S1453	4-170	04/15/19	6.858	36.086	2.9	2.8	4	
W30-S1600-4 A-C	W30-S1600	4-171	04/15/19	4.260	41.958	2.9	3.0	-3	
W30-S1775-5 A-C	W30-S1775	4-172	02/07/19	9.679	37.693	4.2	4.2	0	-6 A-C new install, read once this period.
W30-S1950-3 A-C	W30-S1950	4-173	04/15/19	17.051	46.725	2.9	3.3	-12	
W30-S2520-4 A-C	W30-S2520	4-174	03/19/19	17.729	46.718	3.5	3.4	3	
W30-S2685-3 A-C	W30-S2685	4-175	06/26/19	22.214	41.104	2.0	2.4	-17	

Table 4-1 Access Drifts Data Analysis (continued)

Convergence Points (continued)									
			Last Reading 2018-2019						
Field Tag	Location	Figure Number	Date	Inches	Cumulative Displacement (inches)	Closure Rate[3] 2018 to 2019 (in/year)	Closure Rate[3] 2017 to 2018 (in/year)	Rate Change Percent[3]	Comments
W170-N150-3 A-C	W170-N150	4-176	04/18/19	7.003	15.355	0.6	0.6	0	
W170-S5-2 A-C	W170-S5	4-177	04/18/19	3.240	19.436	0.7	0.6	17	
W170-S5-2 B-D	W170-S5	4-177	11/30/18	14.828	22.594	0.8	0.8	0	
W170-S90-3 A-C	W170-S90	4-178	04/18/19	15.249	22.451	0.8	0.9	-11	
W170-S232-2 A-C	W170-S232	4-179	04/18/19	11.033	16.622	0.5	0.7	-29	
W170-S232-2 B-D	W170-S232	4-179	04/18/19	14.664	17.306	0.6	0.7	-14	
W170-S400 A-C	W170-S400	4-180	04/18/19	20.838	20.838	0.9	0.8	13	
W170-S560-4 A-C	W170-S560	4-181	11/30/18	7.981	18.800	0.8	0.9	-11	
W170-S560-5 B-D	W170-S560	4-181	04/18/19	1.046	21.253	0.7	1.0	-30	
W170-S700-3 A-C	W170-S700	4-182	04/18/19	5.408	30.686	0.9	1.1	-18	
W170-S850-8 A-E	W170-S850	4-183	04/18/19	3.982	24.936	0.6	0.8	-25	
W170-S850-3 C-G	W170-S850	4-184	11/30/18	18.522	29.335	0.8	1.1	-27	
W170-S1000-3 A-C	W170-S1000	4-185	04/18/19	12.386	35.299	1.1	1.2	-8	
W170-S1150-5 A-E	W170-S1150	4-186	04/18/19	4.814	29.855	0.8	0.8	0	
W170-S1150-2 C-G	W170-S1150	4-187	04/18/19	22.269	33.846	1.3	1.3	0	
W170-S1300-4 A-C	W170-S1300	4-188	04/18/19	23.247	44.205	2.2	2.4	-8	
W170-S1445-4 A-C	W170-S1445	4-189	04/18/19	20.440	31.732	2.1	2.4	-13	
W170-S1600-4 A-C	W170-S1600	4-190	04/18/19	27.369	42.134	3.5	3.6	-3	
W170-S1779-3 A-C	W170-S1779	4-191	04/18/19	22.281	37.252	2.6	2.7	-4	
W170-S1950-3 A-C	W170-S1950	4-192	04/18/19	18.555	31.736	2.1	1.9	11	
W170-S2060-3 A-C	W170-S2060	4-193	04/23/19	12.695	30.939	1.8	1.9	-5	
W170-S2180-3 A-C	W170-S2180	4-194	04/24/19	15.858	39.422	2.1	2.4	-13	
W170-S2350 A-C	W170-S2350	4-195	10/24/18	36.415	36.415	N/A	N/A	N/A	Inaccessible after one reading.
W170-S2520-2 A-C	W170-S2520	4-196	02/21/19	25.398	45.993	3.4	3.4	0	

Table 4-1 Access Drifts Data Analysis (continued)

Joint Meters

Field Tag	Location	Figure Number	Date	Cumulative Displacement (inches)	Closure Rate 2018 to 2019 (in/year)	Closure Rate 2017 to 2018 (in/year)	Rate Change Percent	Comments
51X-CG-02876-2	E140-S1505	4-197	05/15/19	-0.280	0	0	0	
51X-CG-02883-3	E140-S1529	4-198	05/15/19	-0.293	0	0	0	
51X-CG-02885-2	E140-S1545	4-199	05/15/19	0.912	0.03	0.01	200	
51X-CG-02875-2	E140-S1795	4-200	05/15/19	0.709	-0.02	0.04	-150	

Rock Bolt Load Cells

Field Tag	Location	Figure Number	Date of Last Reading	Load (kips)	Comments
51X-WG-00246	AIS North Brow	4-201	06/26/18	28.0	
51X-WG-00248	AIS North Brow	4-201	06/26/18	32.6	
51X-WG-00250	AIS North Brow	4-201	06/26/18	11.4	
51X-WG-00251	AIS North Brow	4-201	06/26/18	24.7	
51X-WG-00254	AIS North Brow	4-202	06/26/18	5.5	
51X-WG-00255	AIS North Brow	4-202	06/26/18	15.3	
51X-WG-00238	AIS South Brow	4-203	06/26/18	0.0	
51X-WG-00239	AIS South Brow	4-203	06/26/18	48.3	
51X-WG-00240	AIS South Brow	4-203	06/26/18	1.0	
51X-WG-00242	AIS South Brow	4-204	06/26/18	55.2	
51X-WG-00243	AIS South Brow	4-204	06/26/18	29.5	
51X-WG-00244	AIS South Brow	4-204	06/26/18	26.3	

[3] N/A – Insufficient data available to perform the calculation. This is usually due to the inability to read the instruments because of activities such as the removal of an instrument due to floor, rib, or back trimming; locations blocked by equipment or waste disposal; installation timing, access issues, etc.

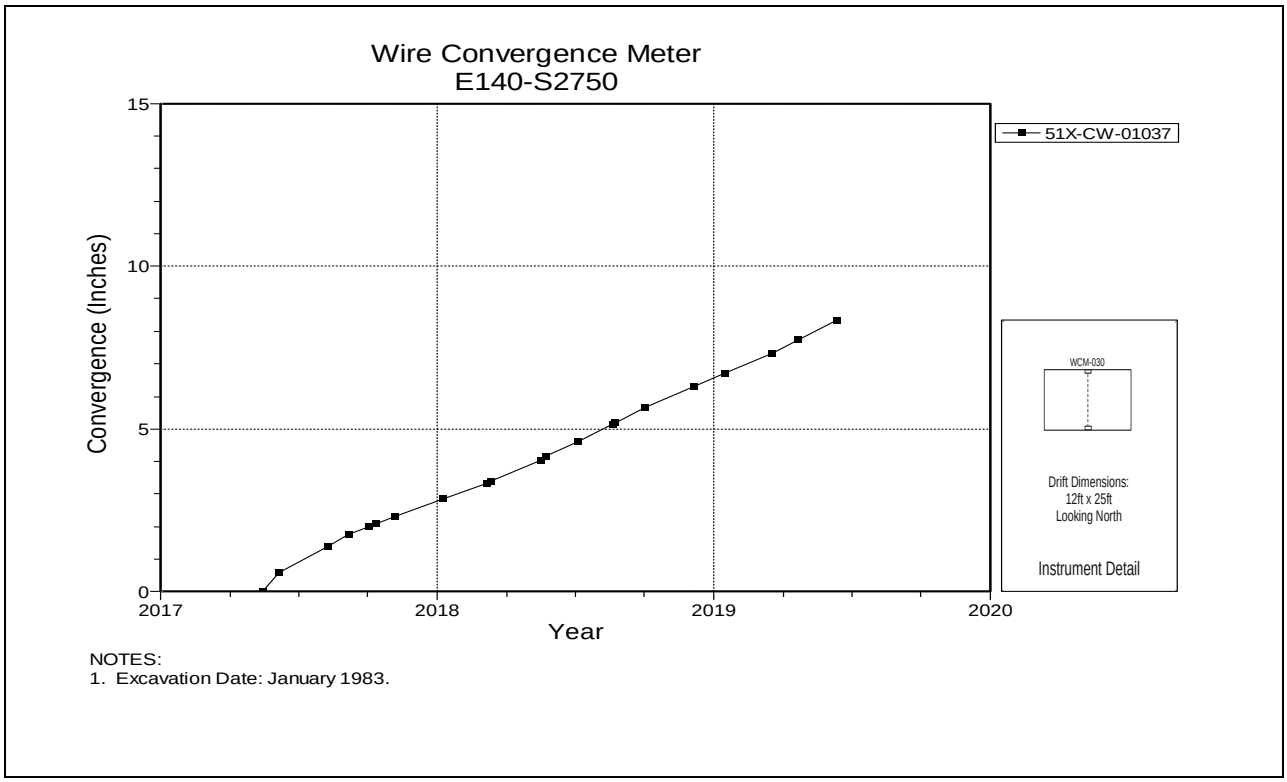

Figure 4-1 Wire Convergence Meter 51X-CW-01037 – E140 S2750 – Roof to Floor

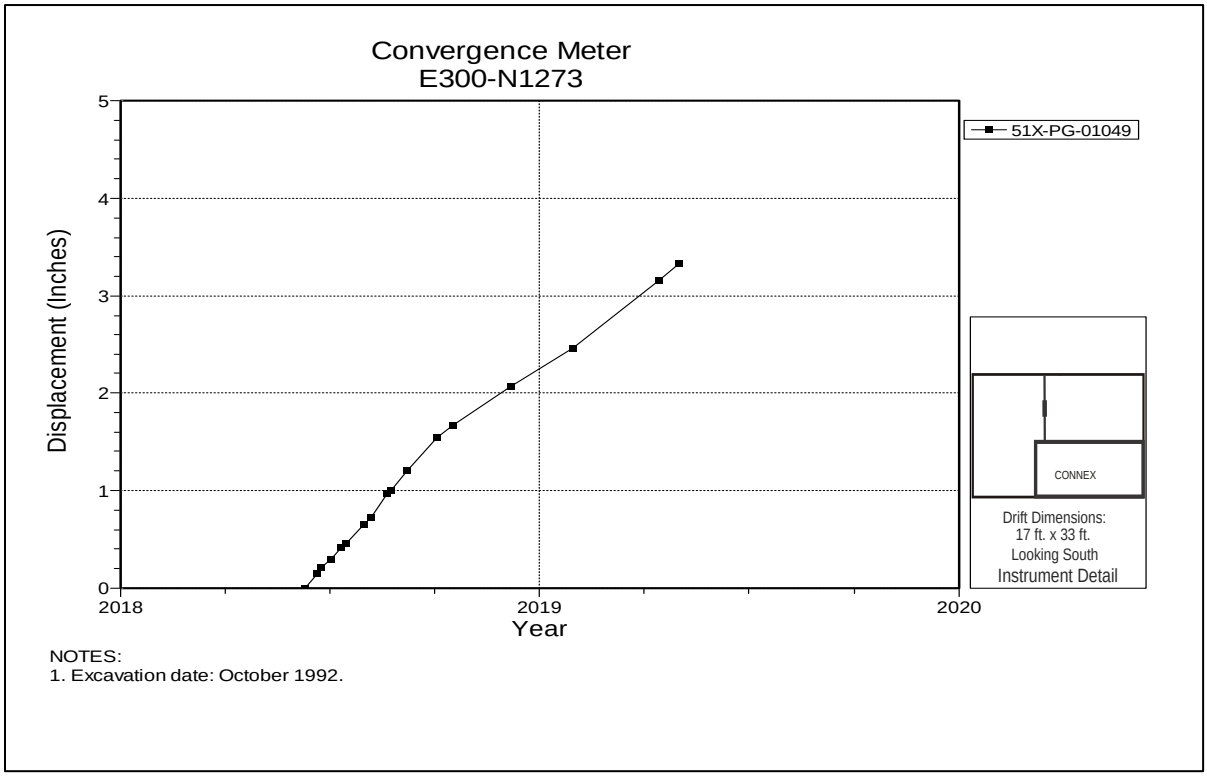

Figure 4-2 Convergence Meter 51X-PG-01049 – E300-N1273 – Roof to Floor

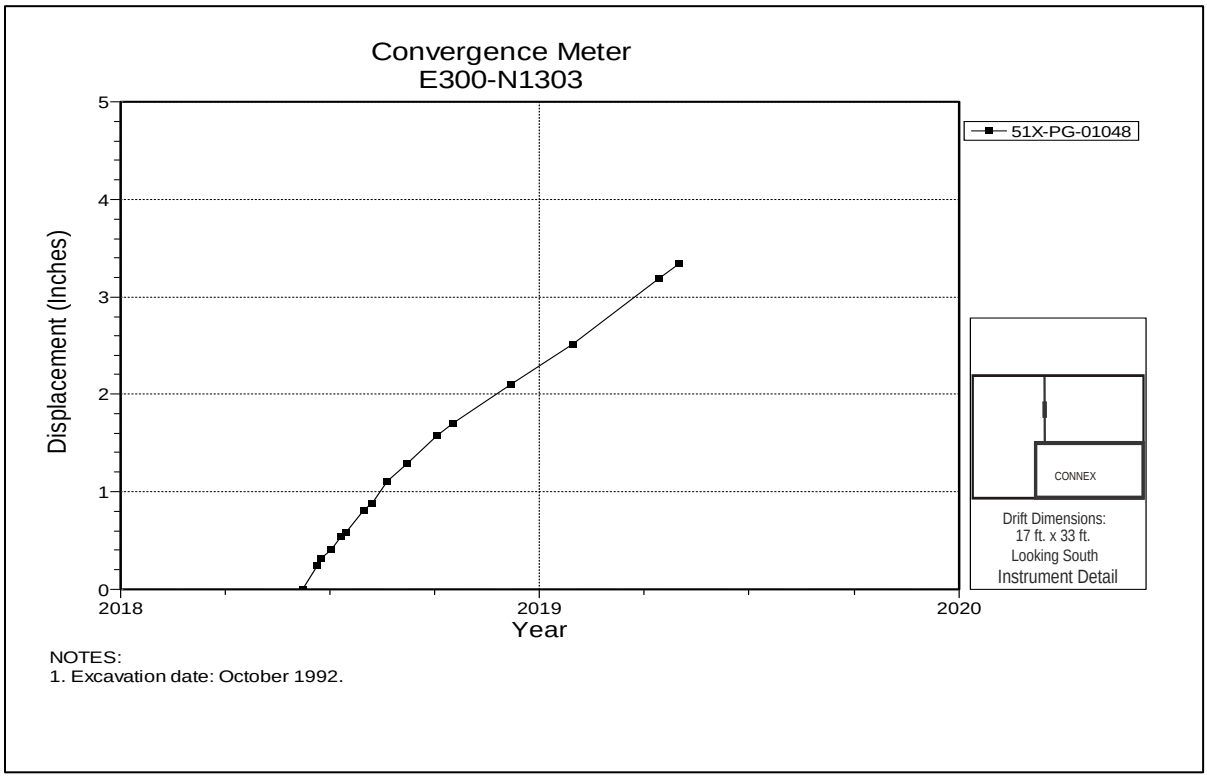

Figure 4-3 Convergence Meter 51X-PG-01048 – E300-N1303 – Roof to Floor

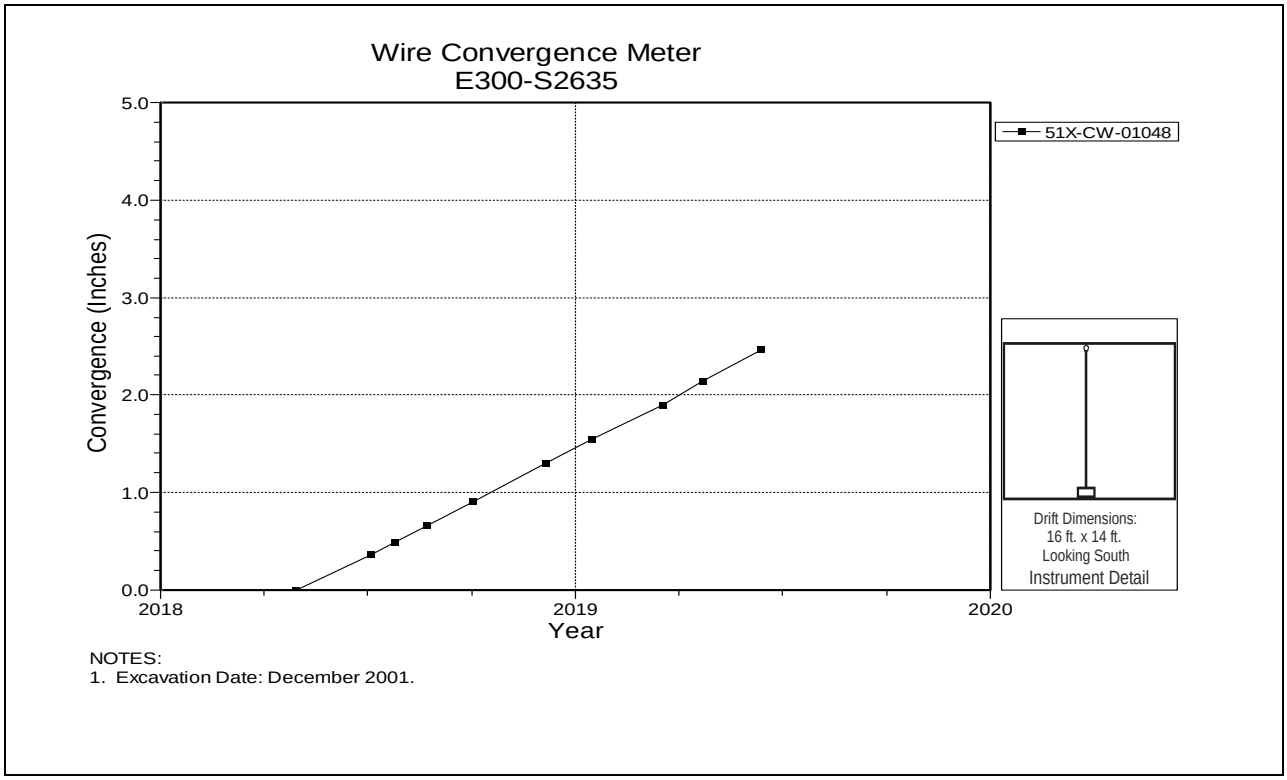

Figure 4-4 Wire Convergence Meter 51X-CW-01048 – E300-S2635 – Roof to Floor

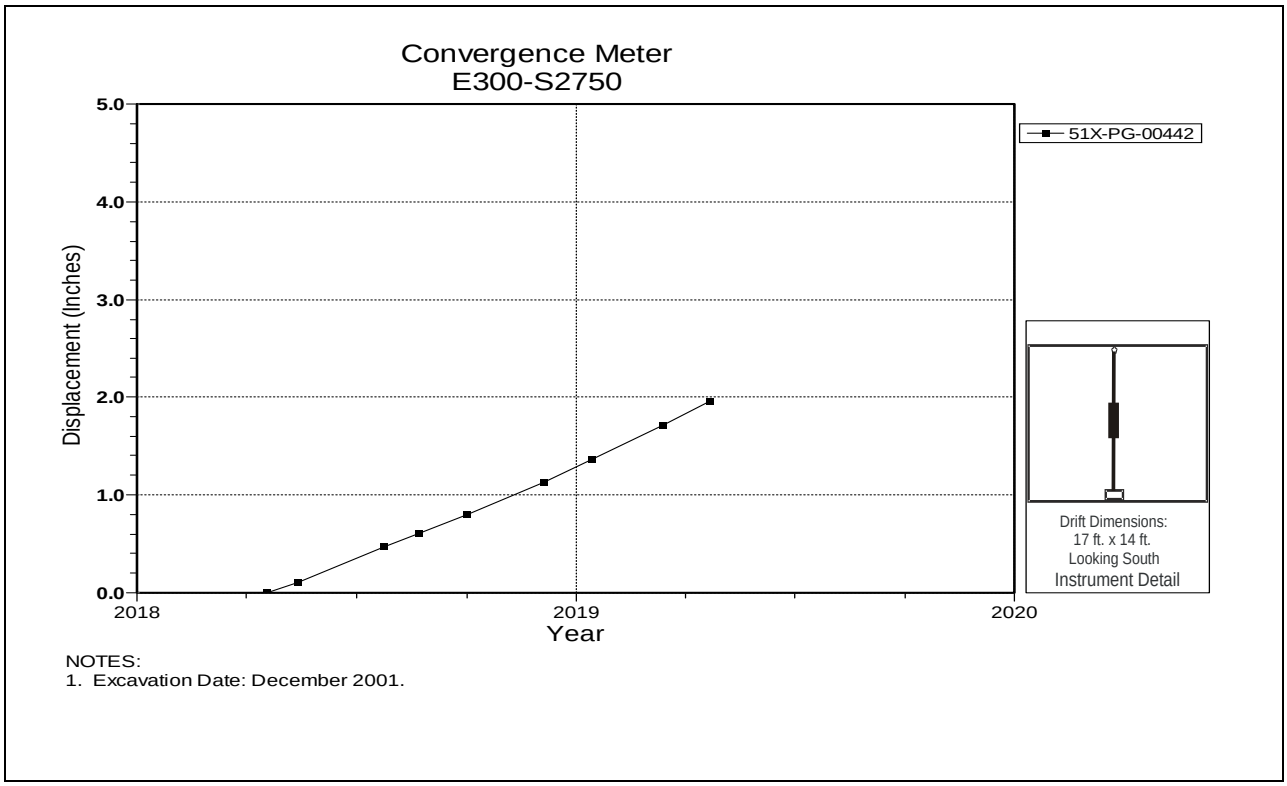

Figure 4-5 Convergence Meter 51X-PG-00442 – E300 S2750 – Roof to Floor

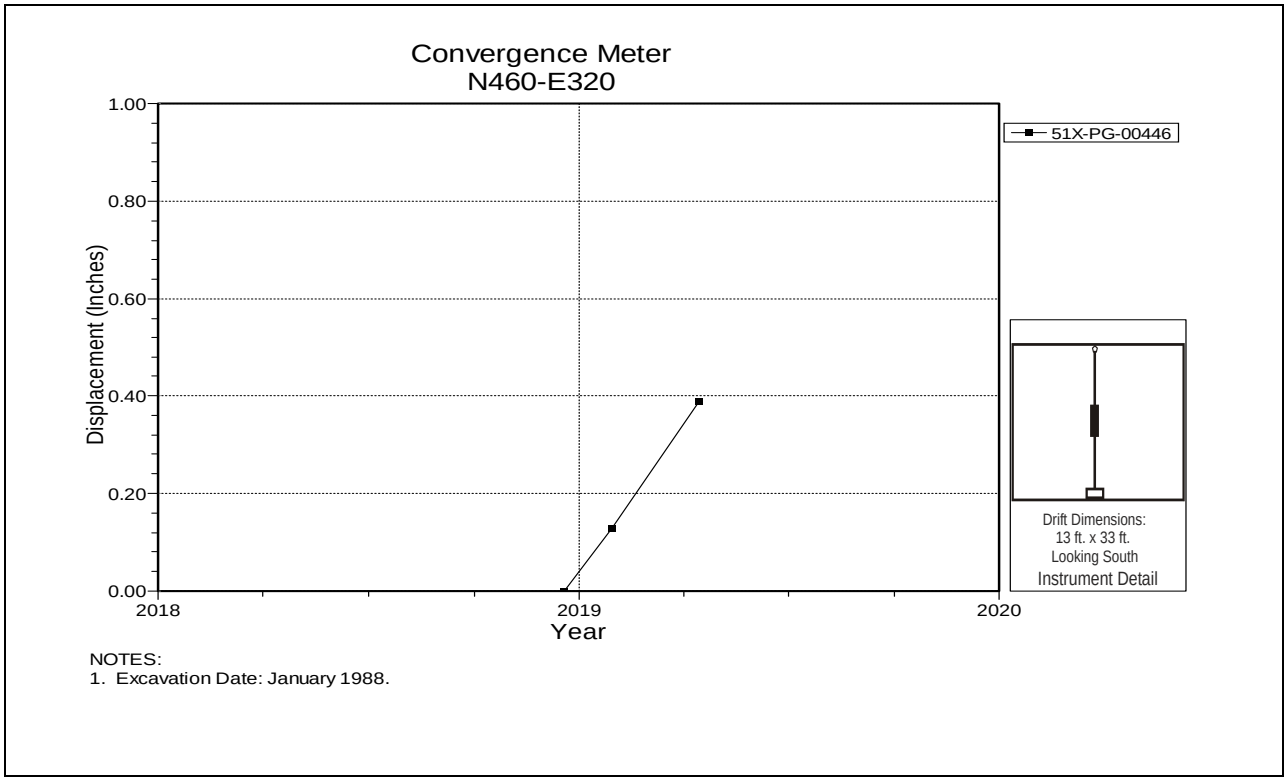

Figure 4-6 Convergence Meter 51X-PG-00446 – N460-E320 – Roof to Floor

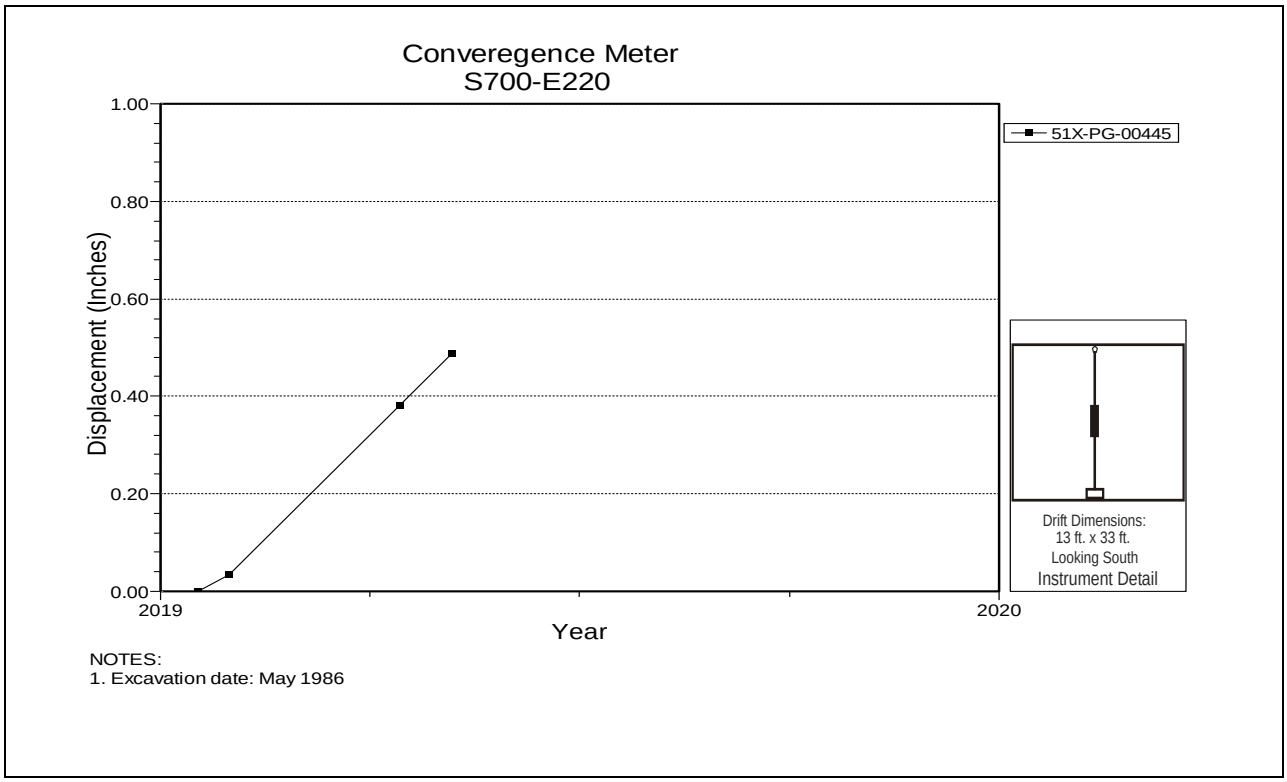

Figure 4-7 Convergence Meter 51X-PG-00445 – S700-E220 – Roof to Floor

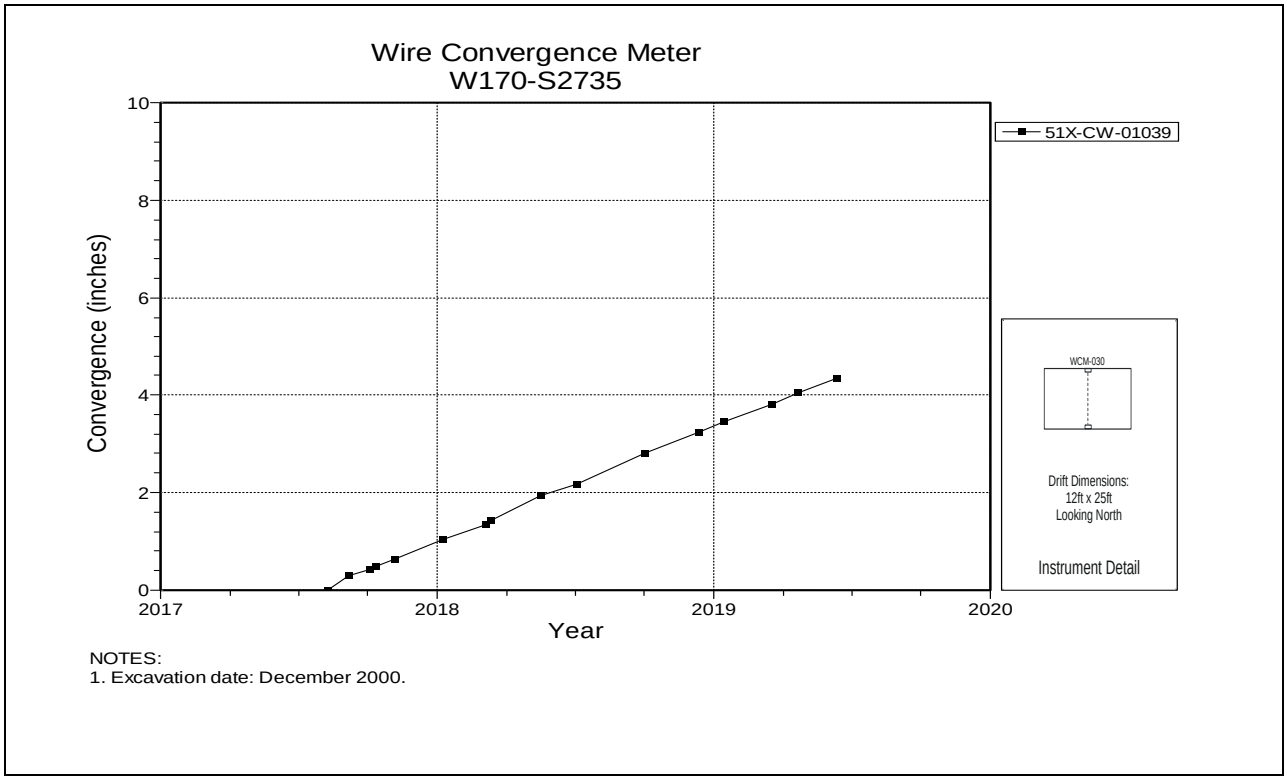

Figure 4-8 Wire Convergence Meter 51X-CW-01039 – W170 S2735 – Roof to Floor

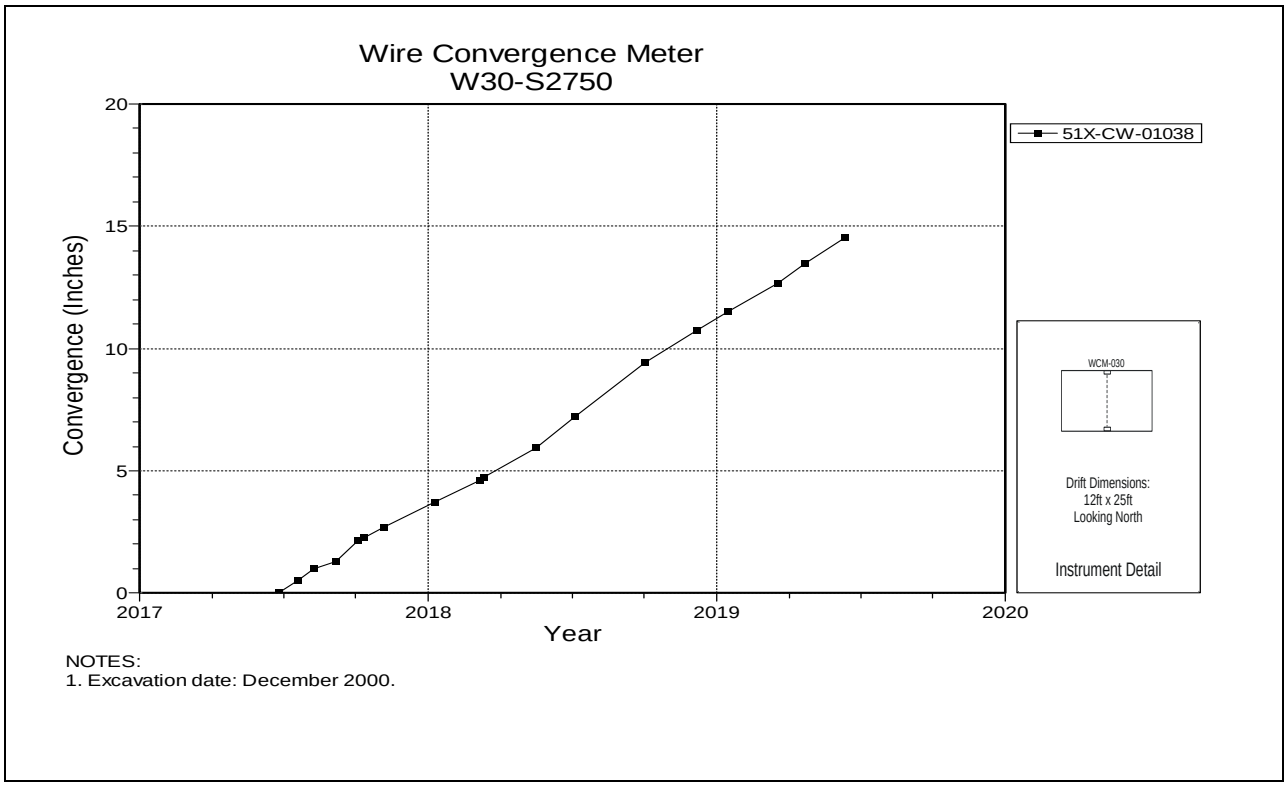

Figure 4-9 Wire Convergence Meter 51X-CW-01038 – W30 S2750 – Roof

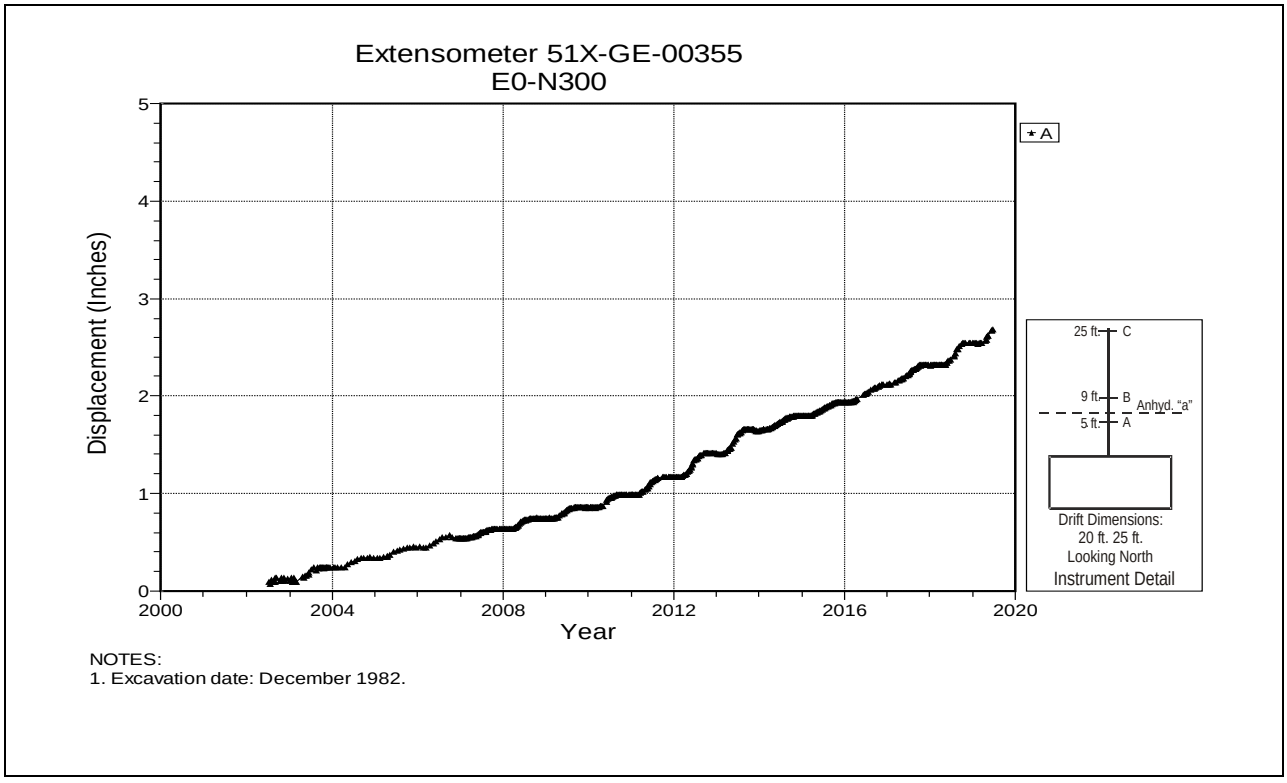

Figure 4-10 Extensometer 51X-GE-00355 – E0 N300 – Roof

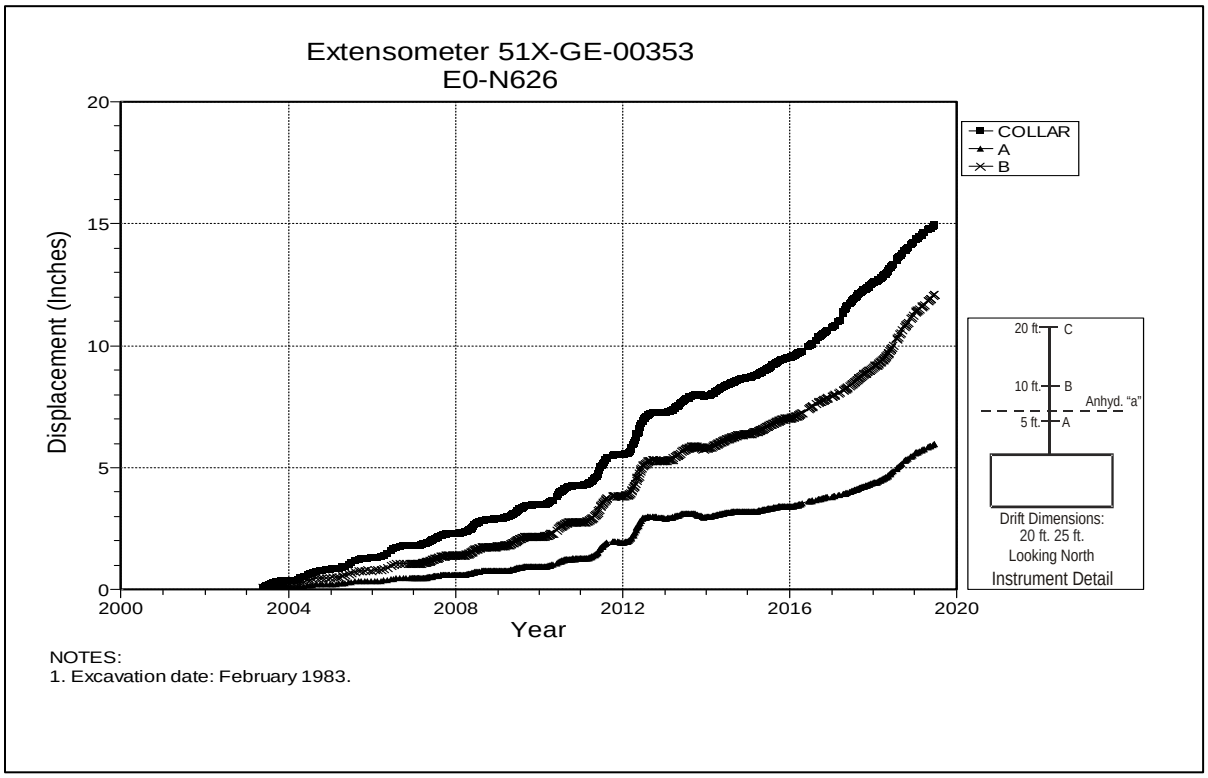

Figure 4-11 Extensometer 51X-GE-00353 – E0 N626 – Roof

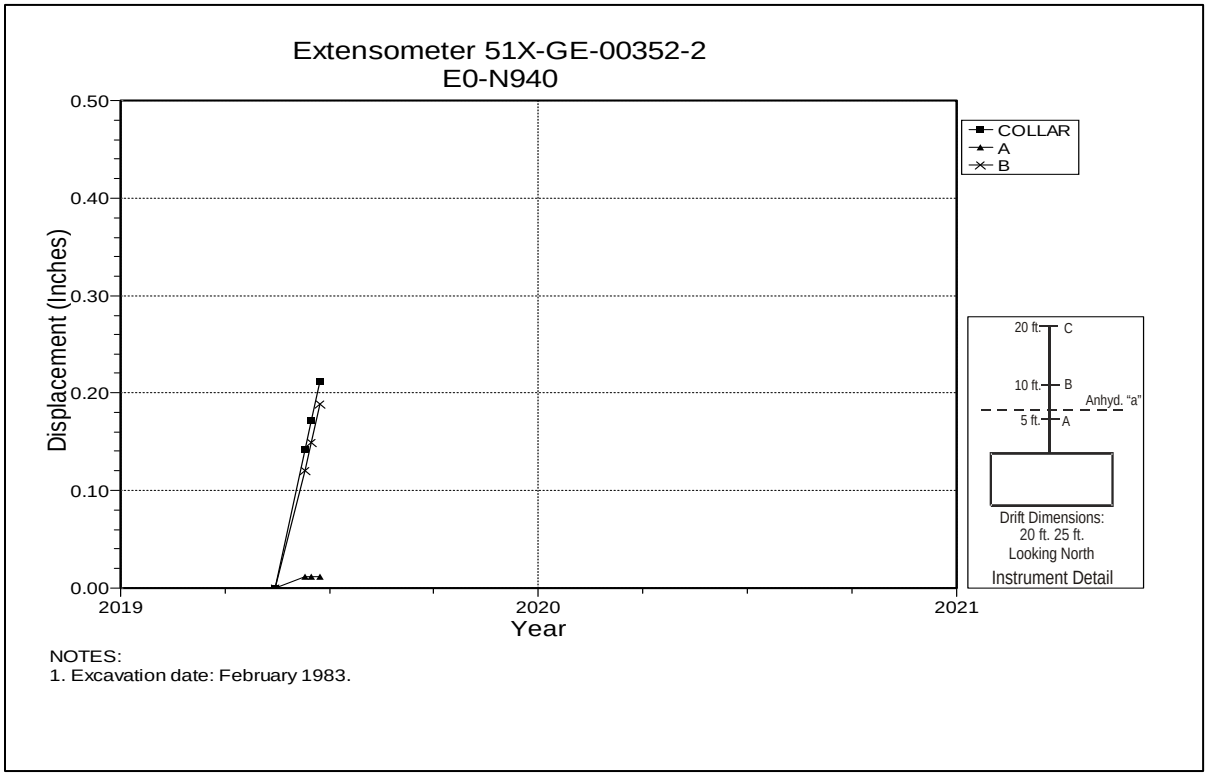

Figure 4-12 Extensometer 51X-GE-00352-2 – E0 N940 – Roof

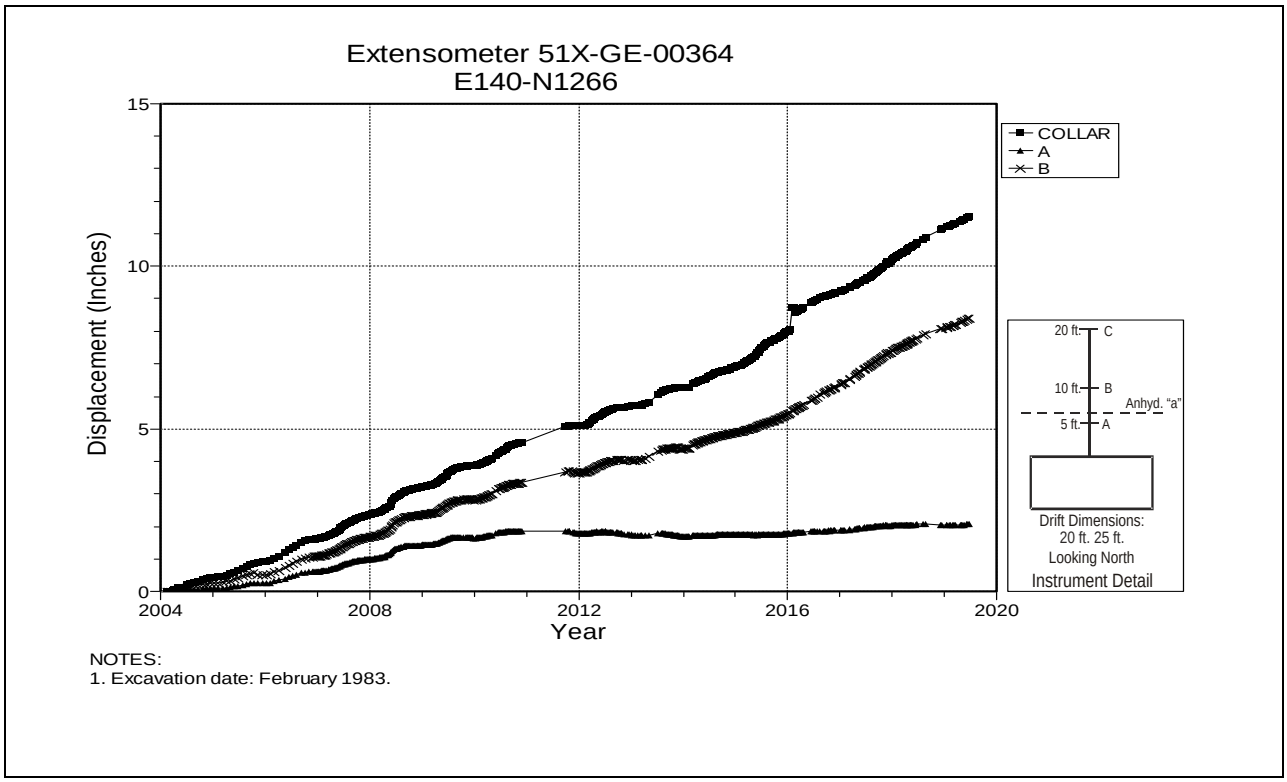

Figure 4-13 Extensometer 51X-GE-00364 – E140 N1266 – Roof

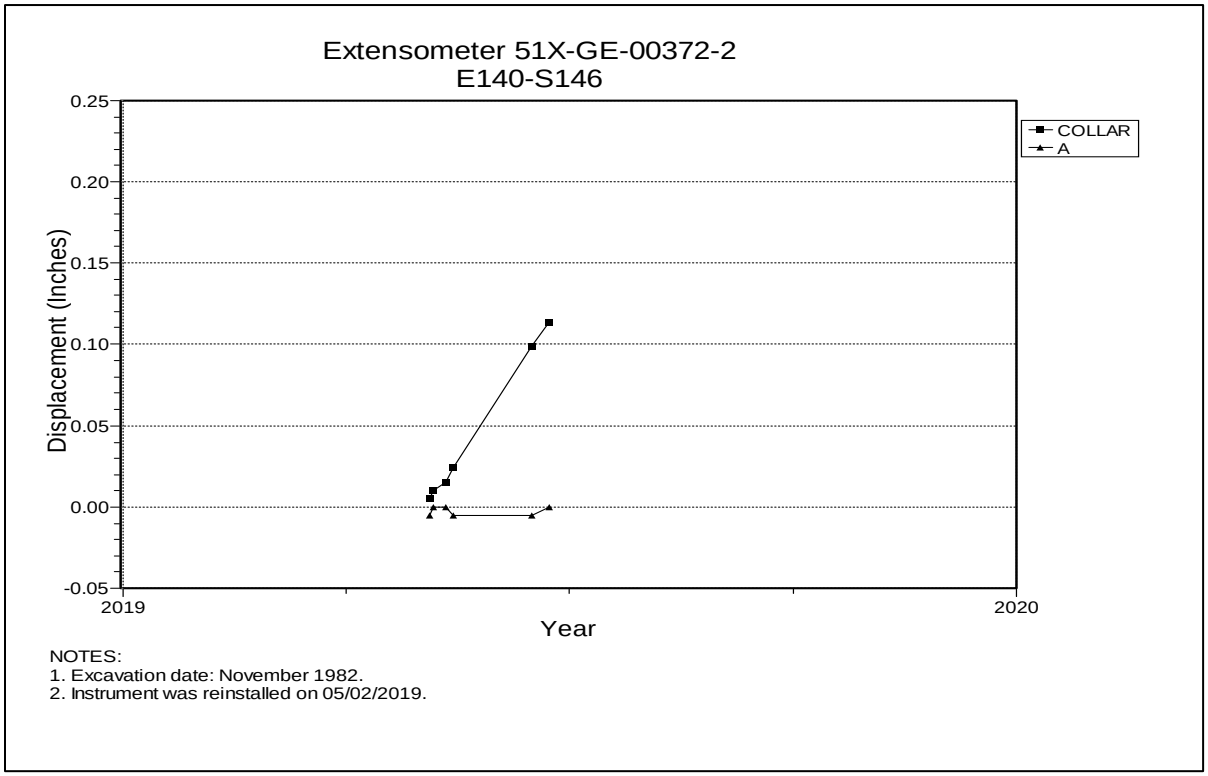

Figure 4-14 Extensometer 51X-GE-00372-2 – E140 S146 – Roof

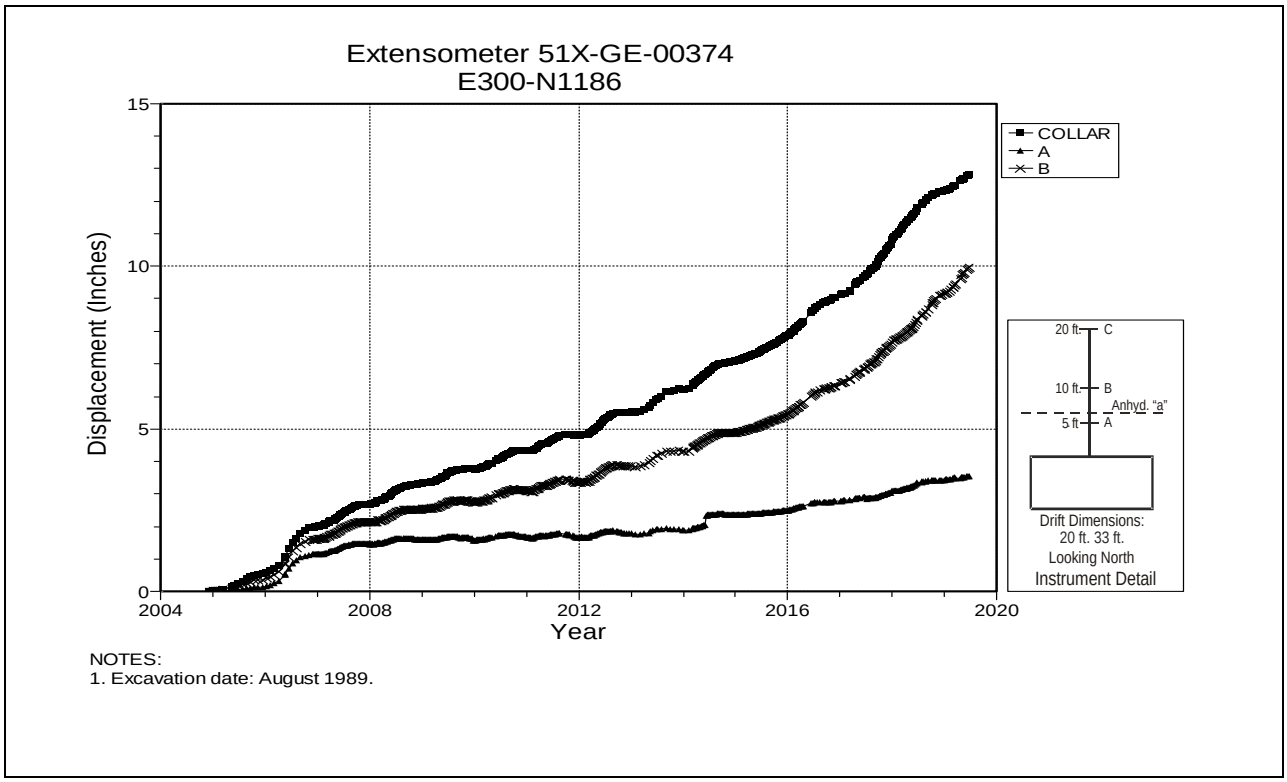

Figure 4-15 Extensometer 51X-GE-00374 – E300 N1186 – Roof

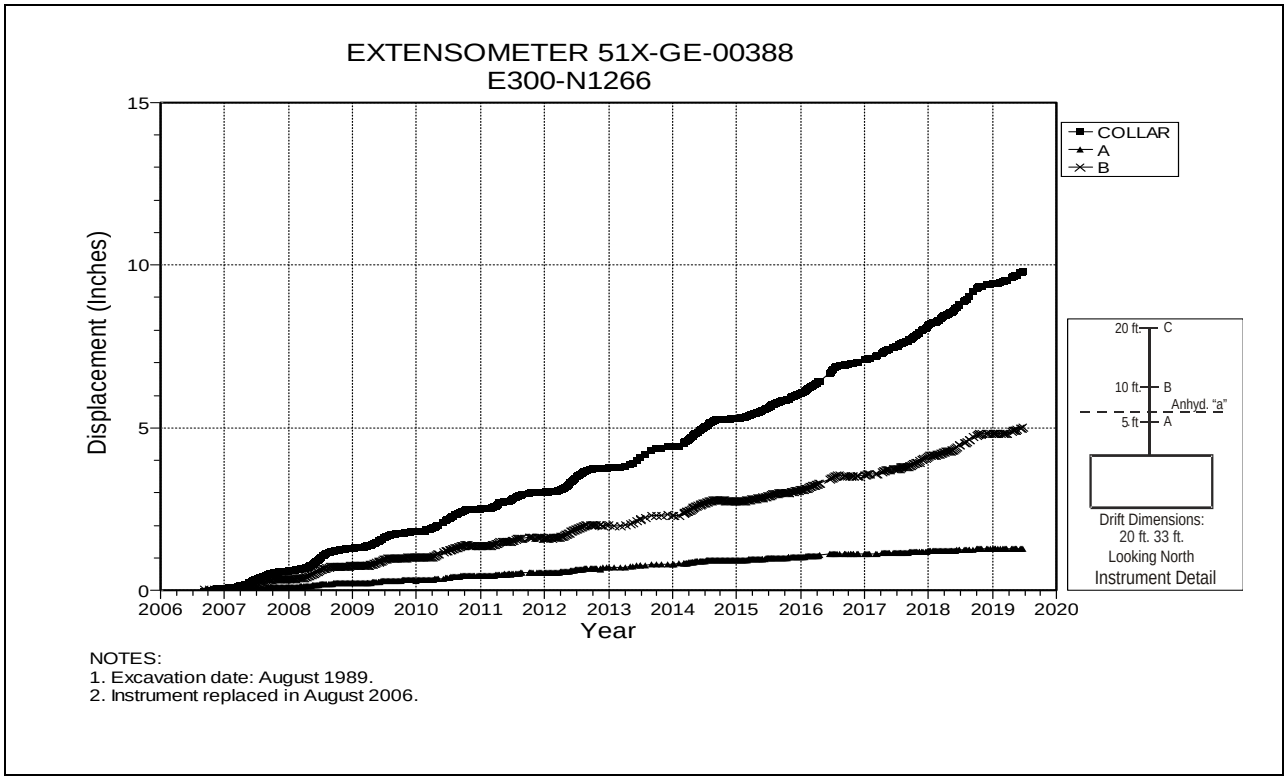

Figure 4-16 Extensometer 51X-GE-00388 – E300 N1266 – Roof

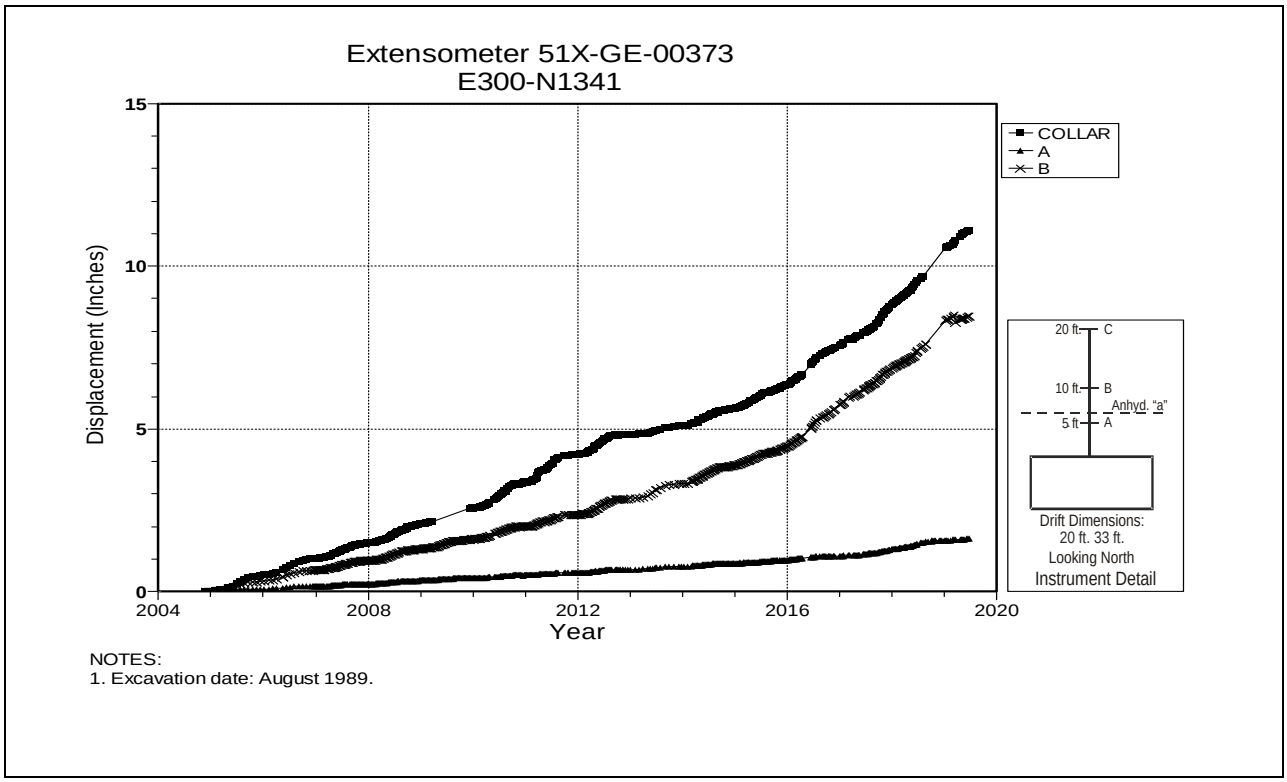

Figure 4-17 Extensometer 51X-GE-00373 – E300 N1341 – Roof

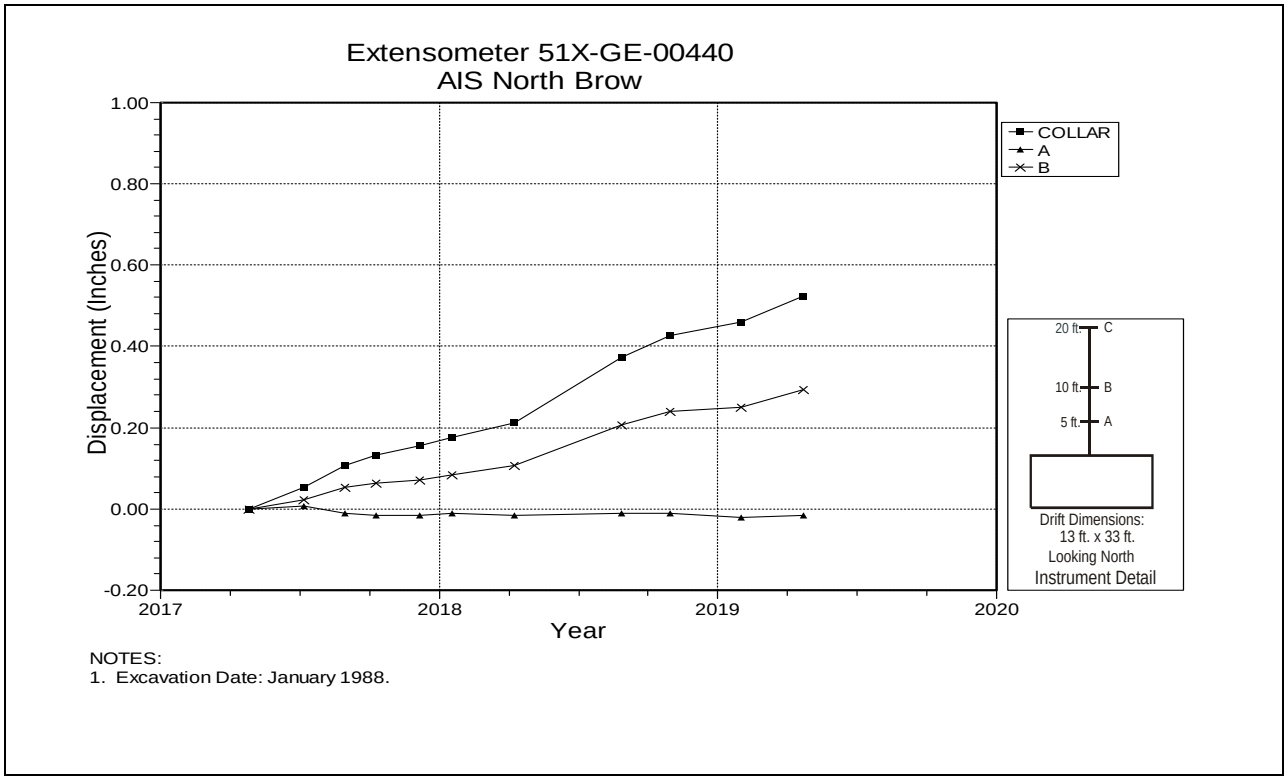

Figure 4-18 Extensometer 51X-GE-00440 – AIS North Brow – Roof

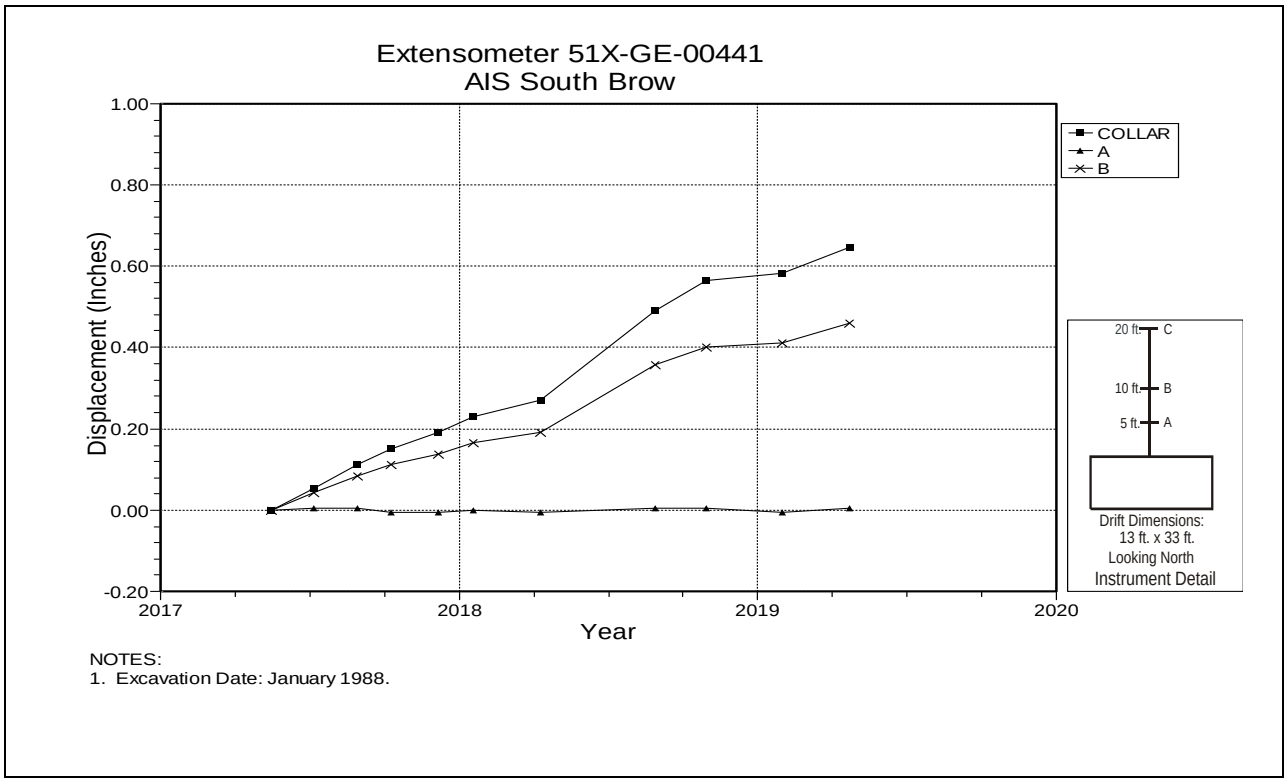

Figure 4-19 Extensometer 51X-GE-00441 – AIS South Brow – Roof

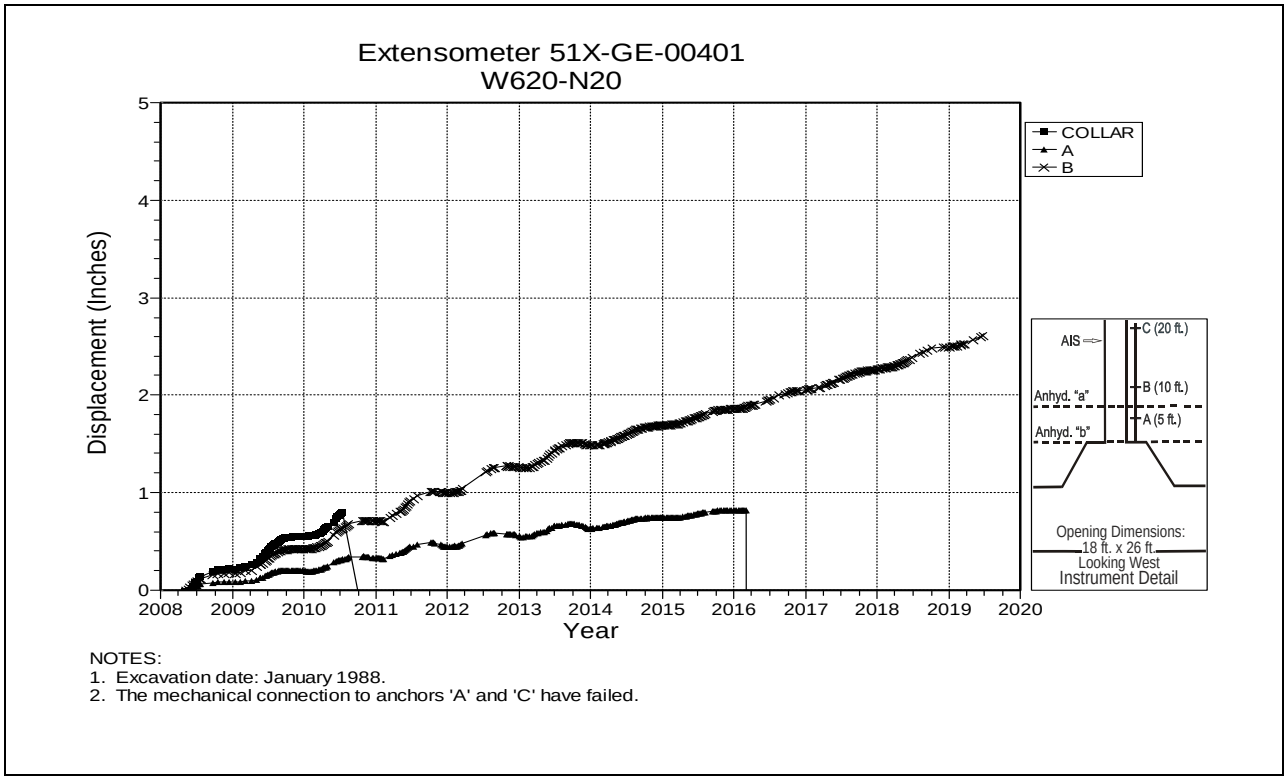

Figure 4-20 Extensometer 41X-GE-00401 –-W620-N20 – Roof

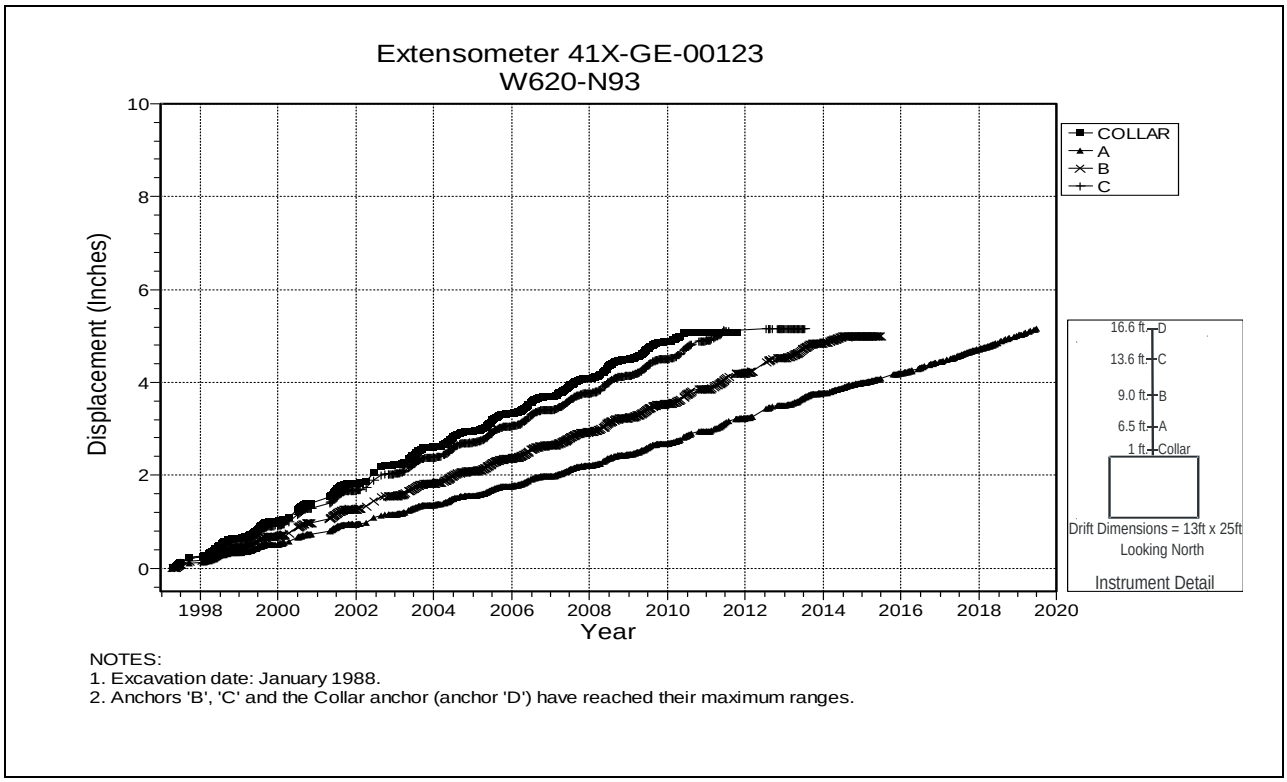

Figure 4-21 Extensometer 41X-GE-00123 –-W620-N93 – Roof

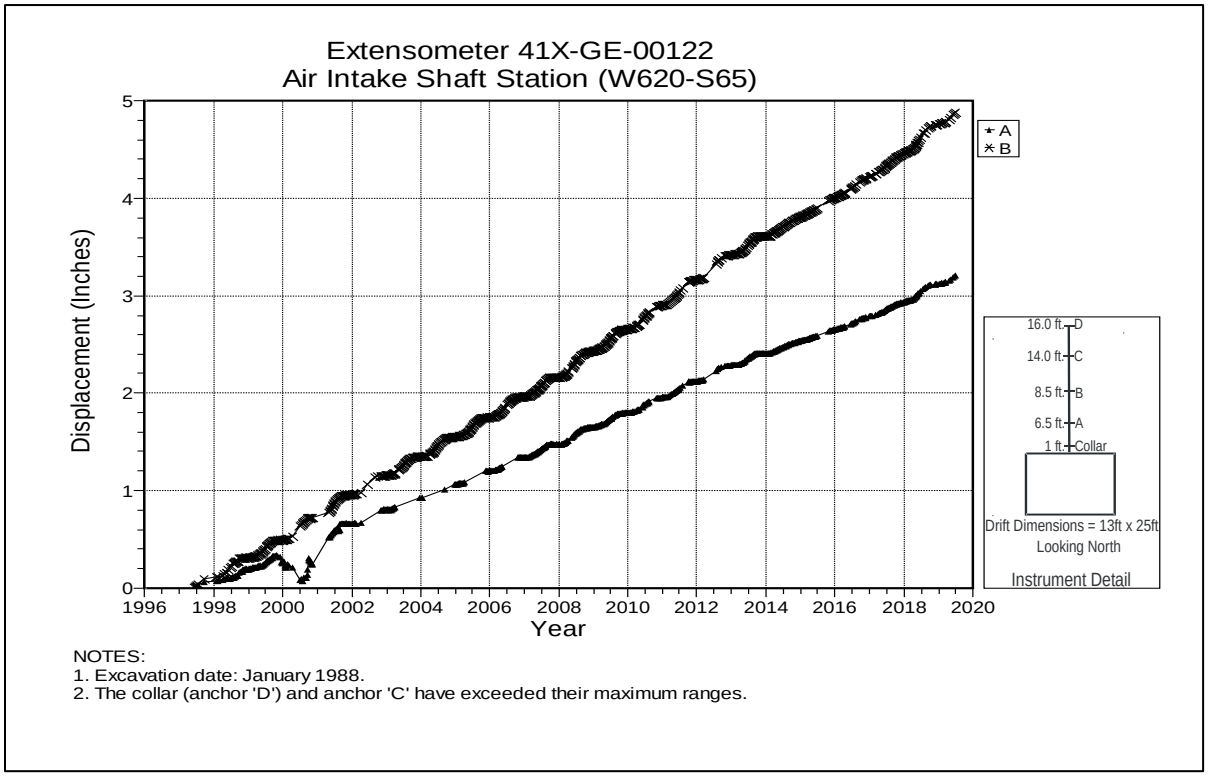

Figure 4-22 Extensometer 41X-GE-00122 –-W620-S65 – Roof

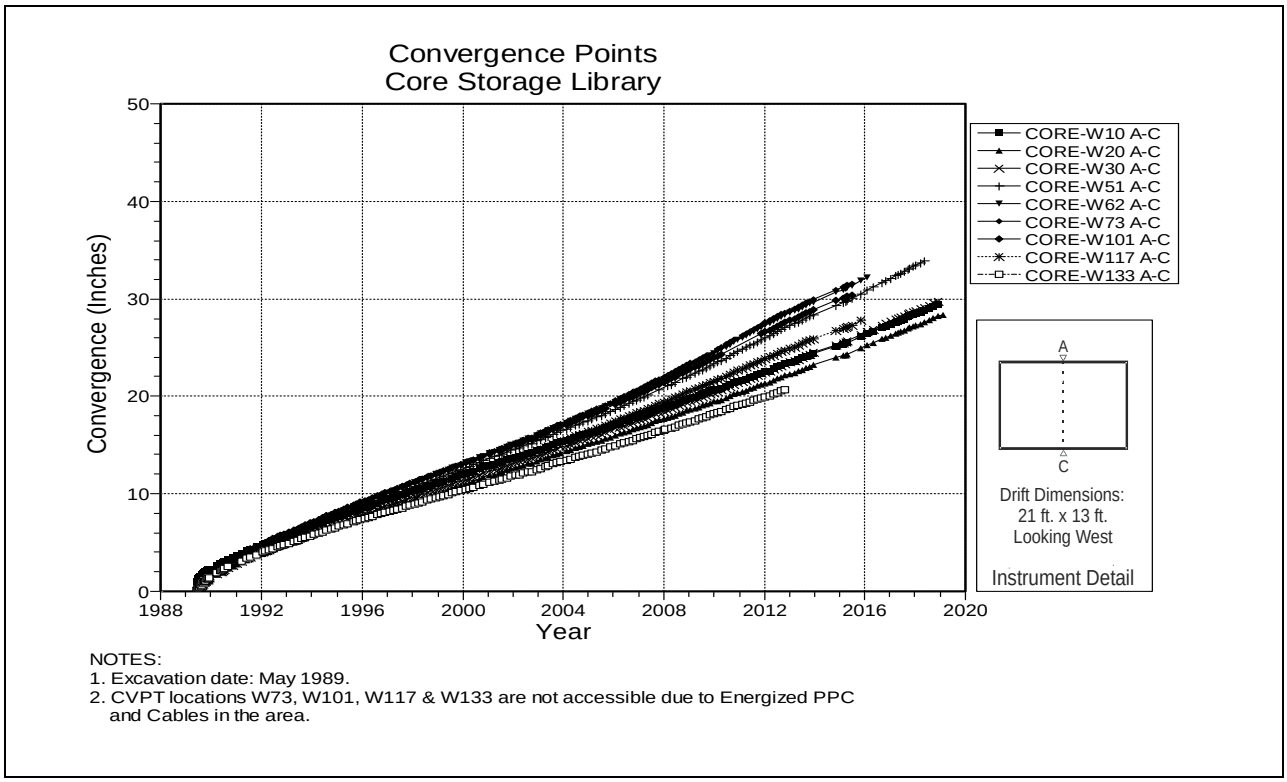

NOTES:
1. Excavation date: May 1989.
2. CVPT locations W73, W101, W117 & W133 are not accessible due to Energized PPC and Cables in the area.

Figure 4-23 Core Storage Library – Roof to Floor – Centerline

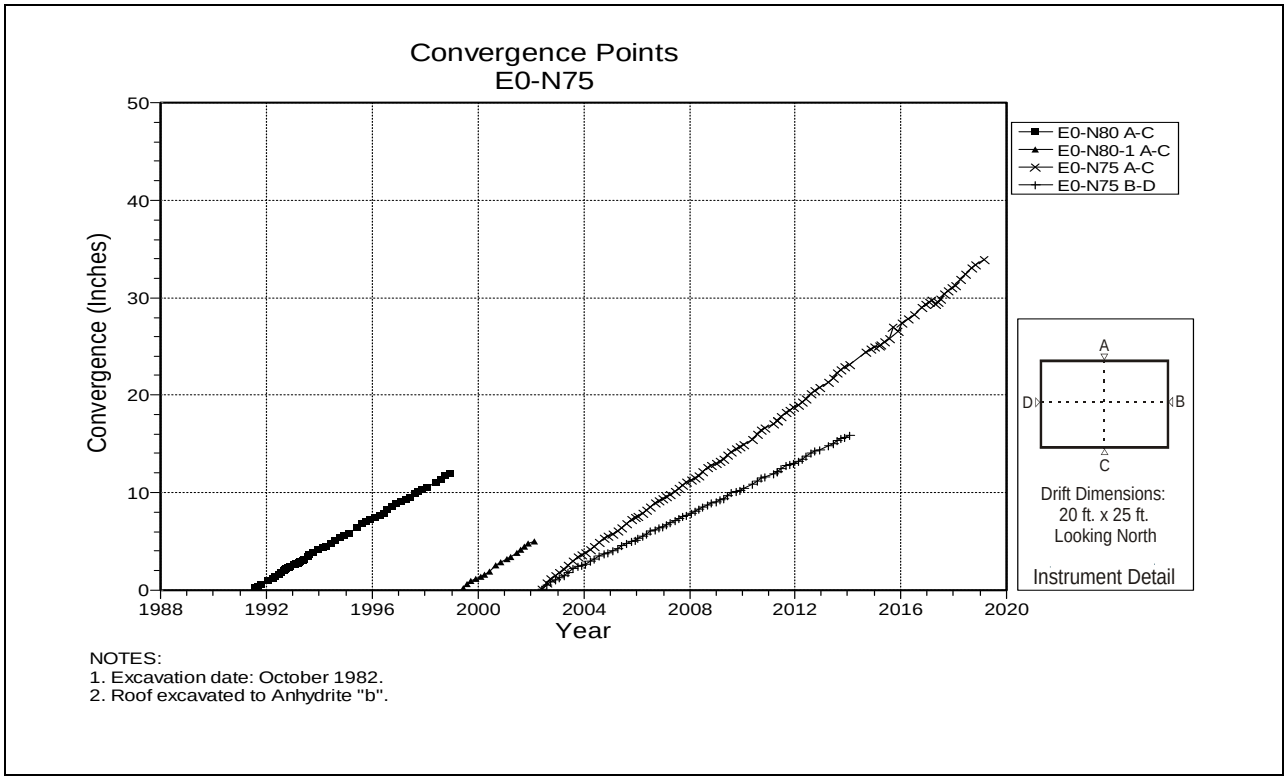

NOTES:
1. Excavation date: October 1982.
2. Roof excavated to Anhydrite "b".

Figure 4-24 Convergence Point Array – E0 N75 – All Chords

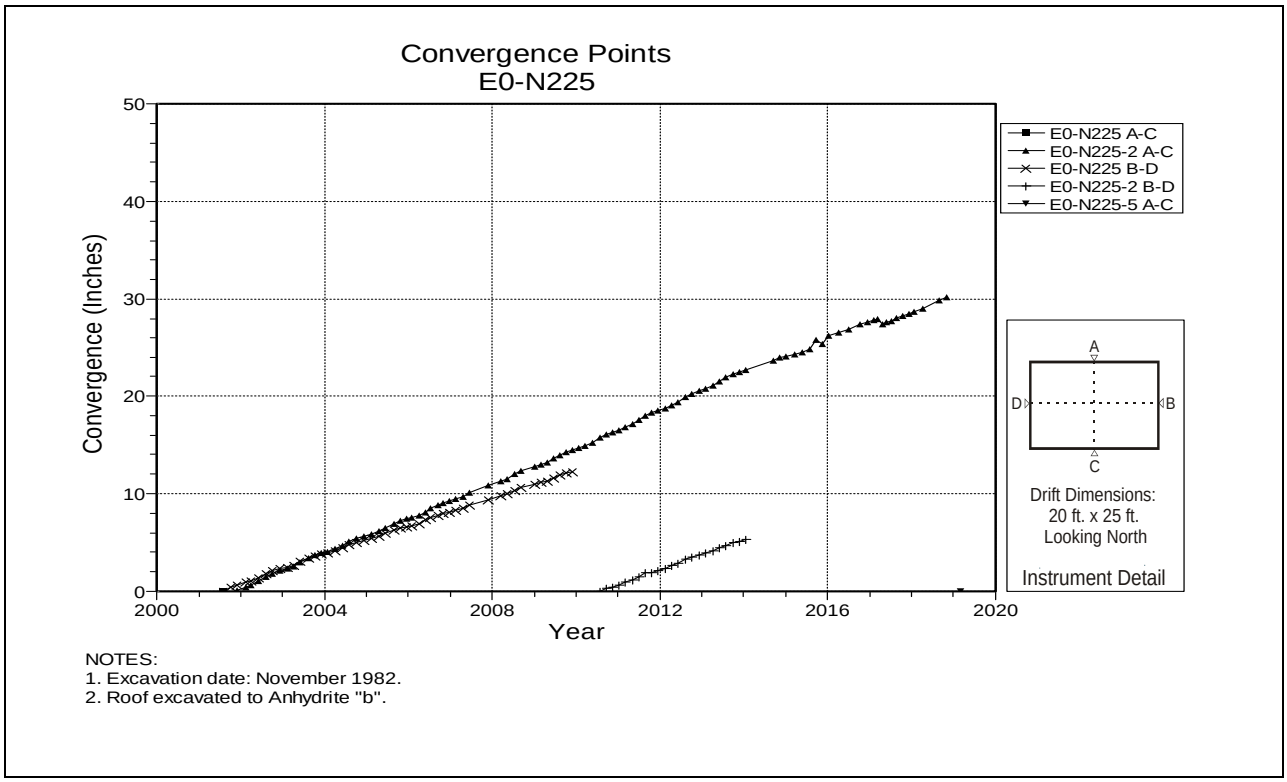

Figure 4-25 Convergence Point Array – E0 N225 – All Chords

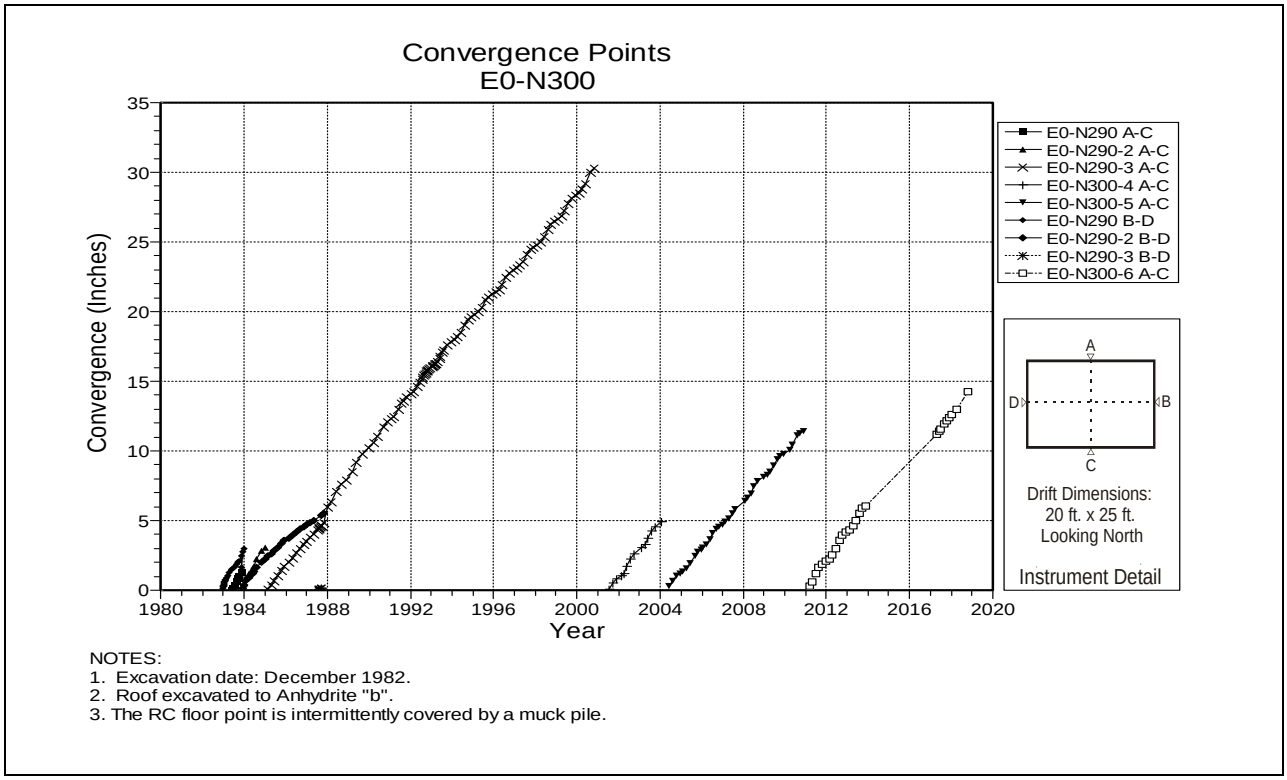

Figure 4-26 Convergence Point Array – E0 N300 – All Chords

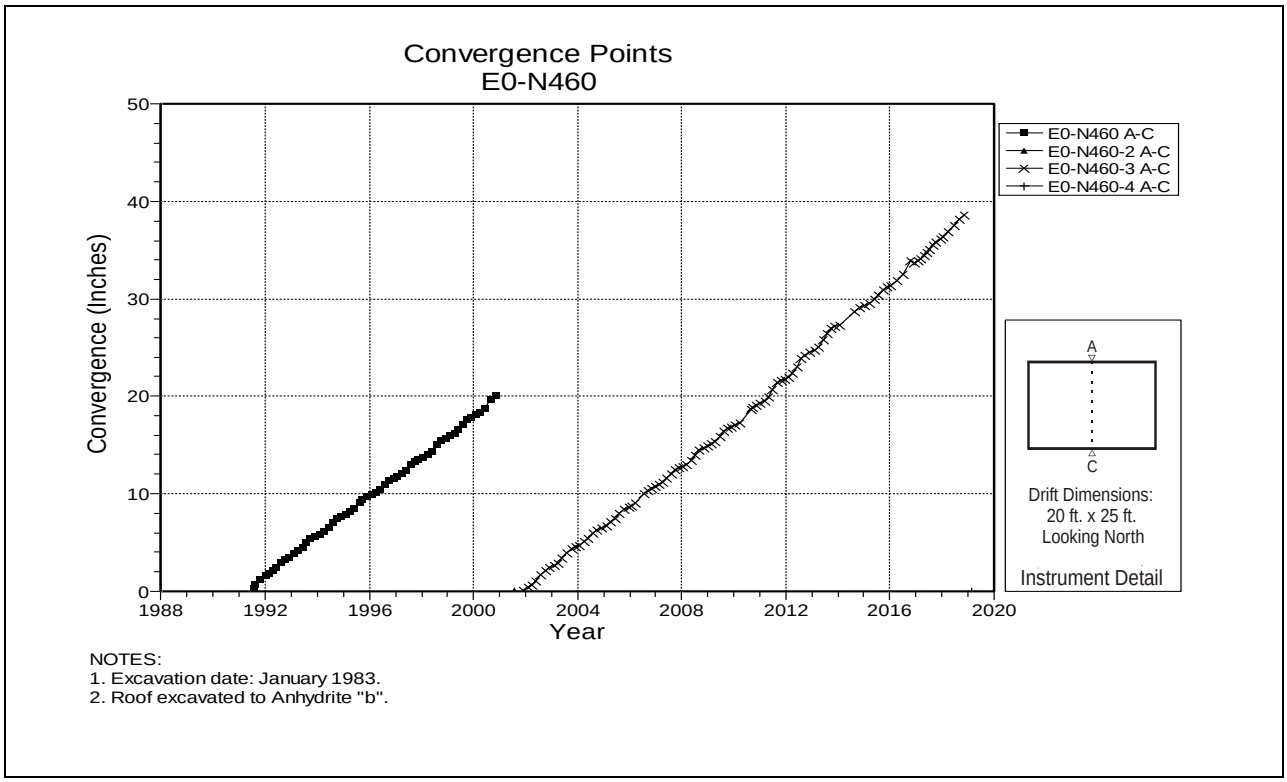

Figure 4-27 Convergence Point Array – E0 N460 – Roof to Floor – Centerline

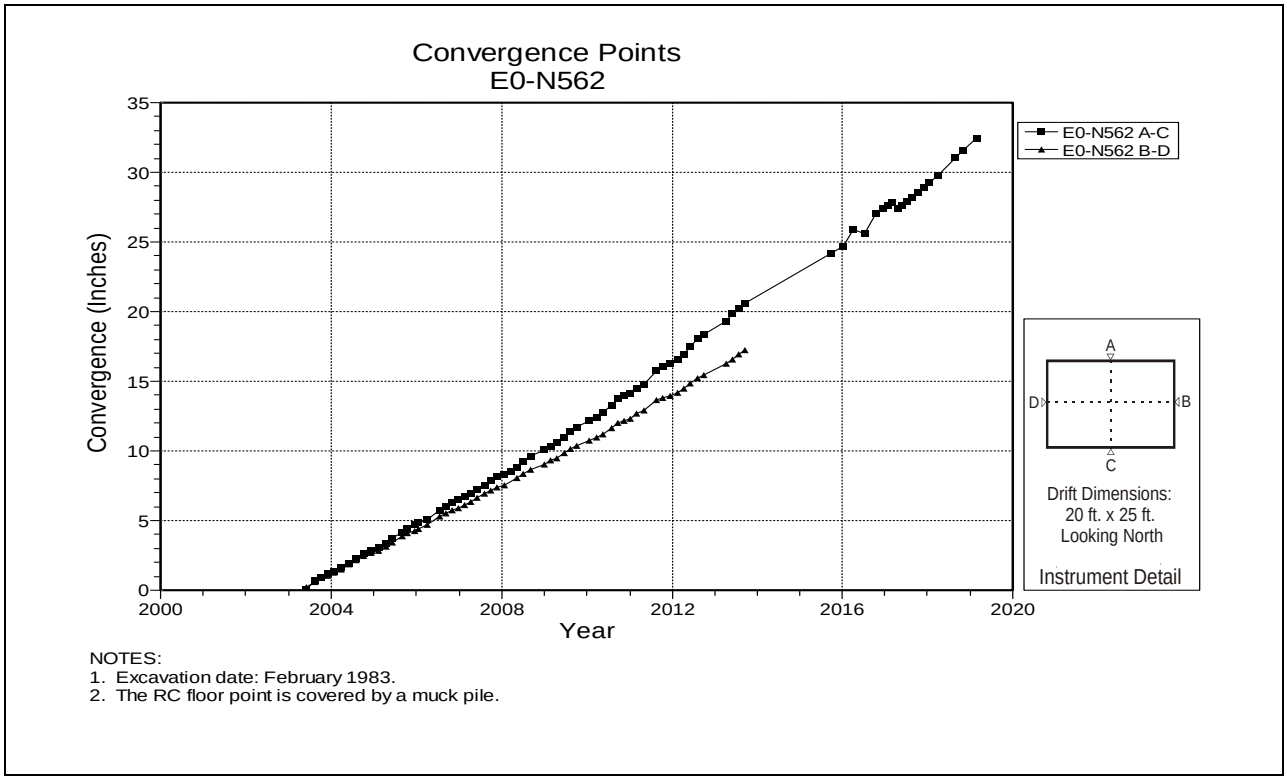

Figure 4-28 Convergence Point Array – E0 N562 – All Chords

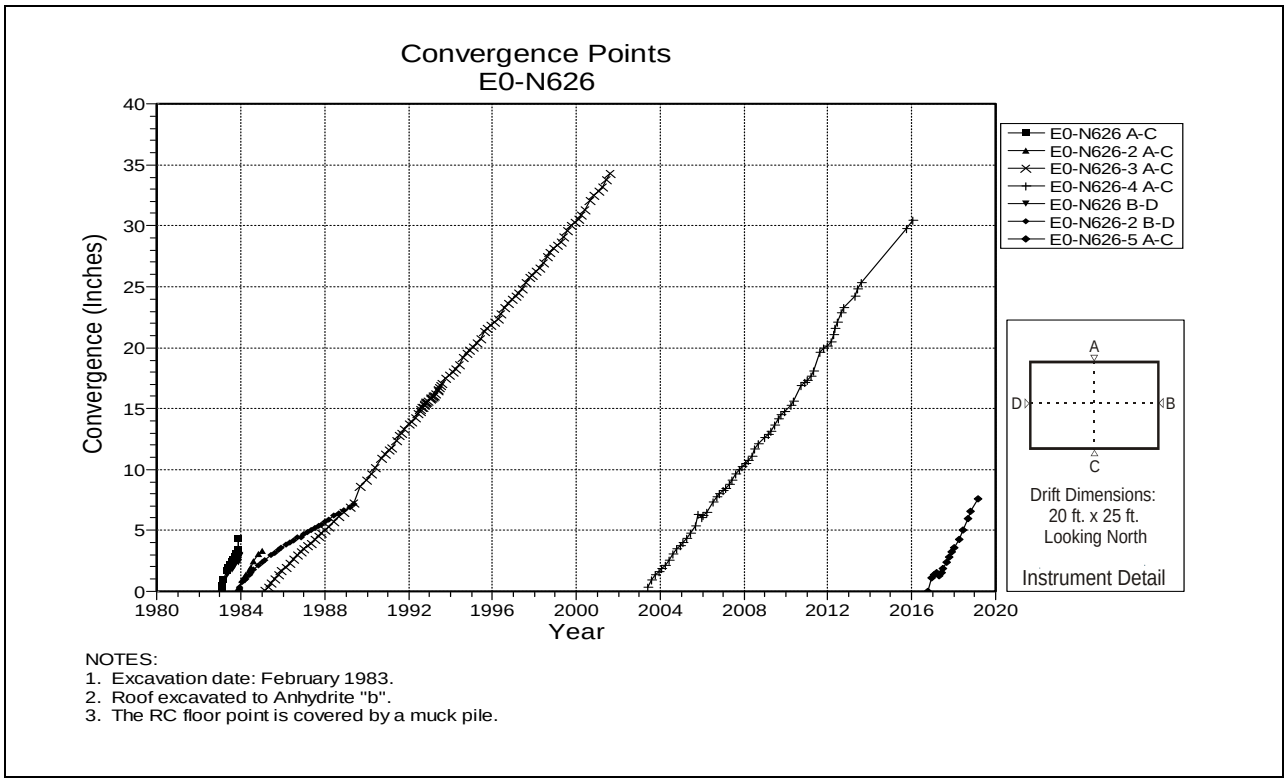

Figure 4-29 Convergence Point Array – E0 N626 – All Chords

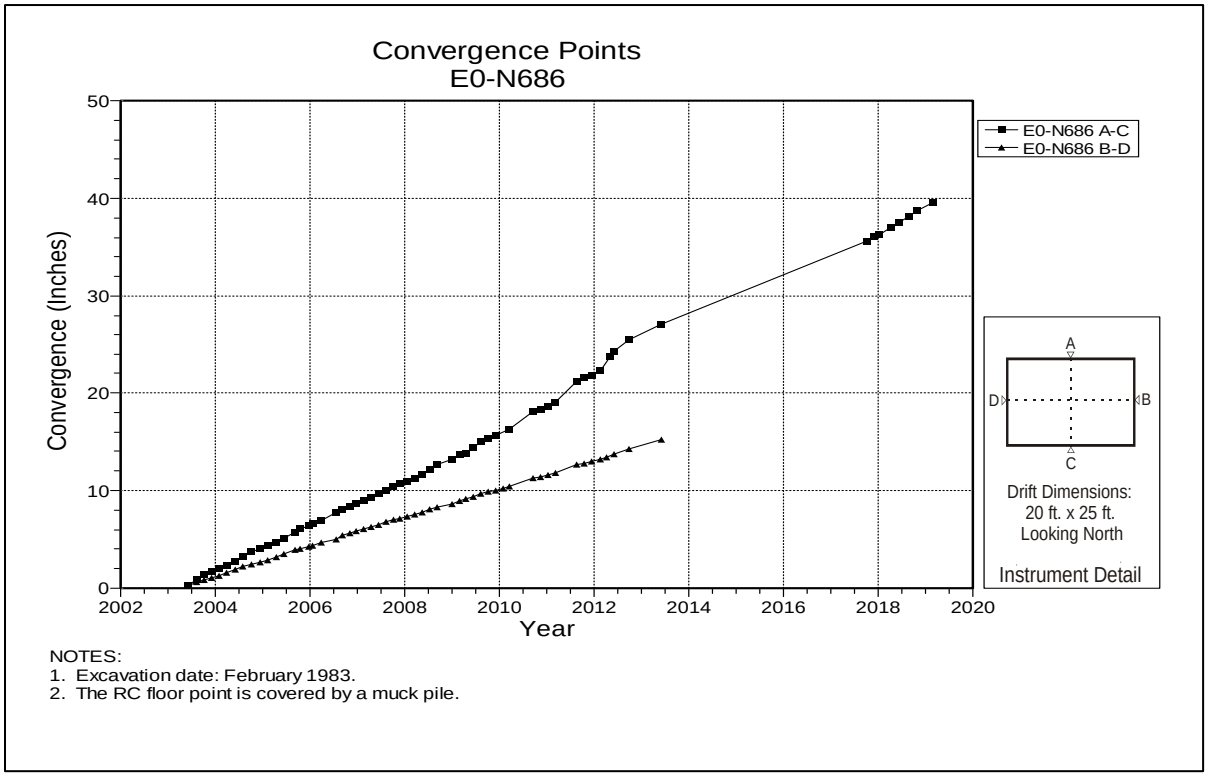

Figure 4-30 Convergence Point Array – E0 N686 – All Chords

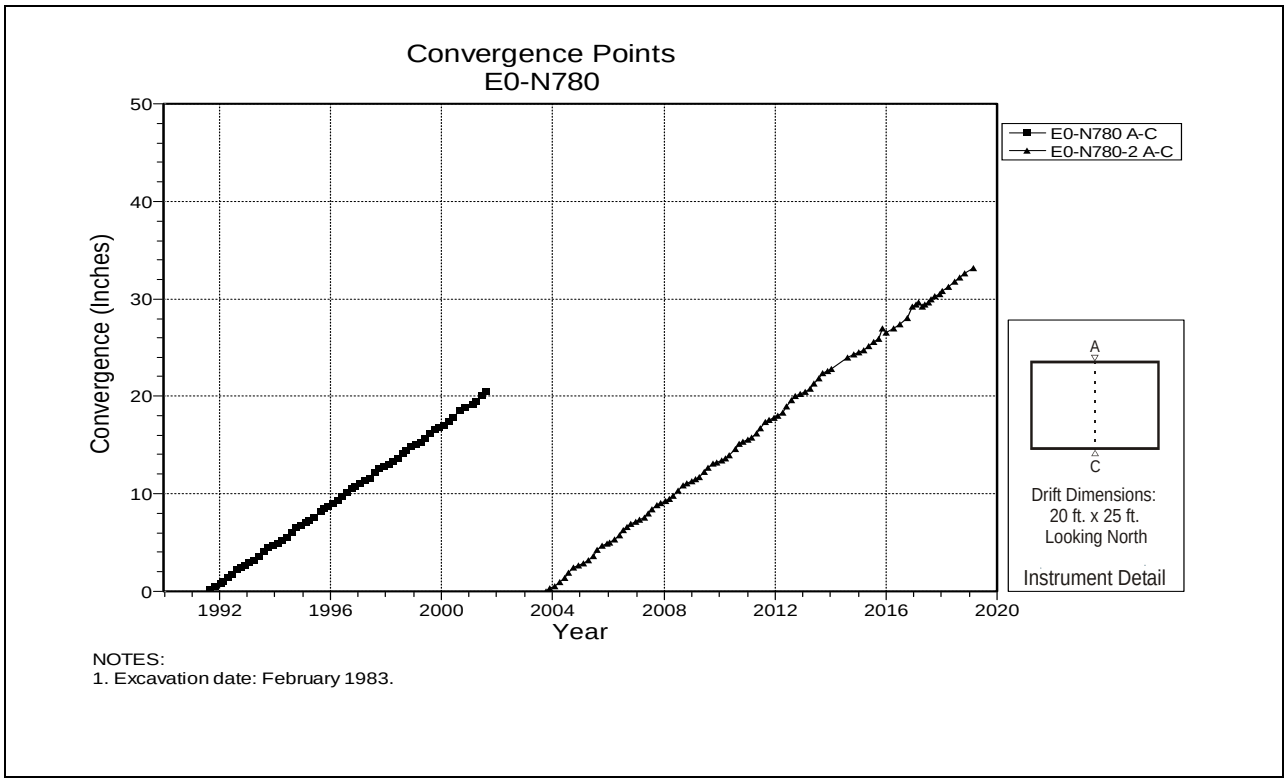

Figure 4-31 Convergence Point Array – E0 N780 – Roof to Floor – Centerline

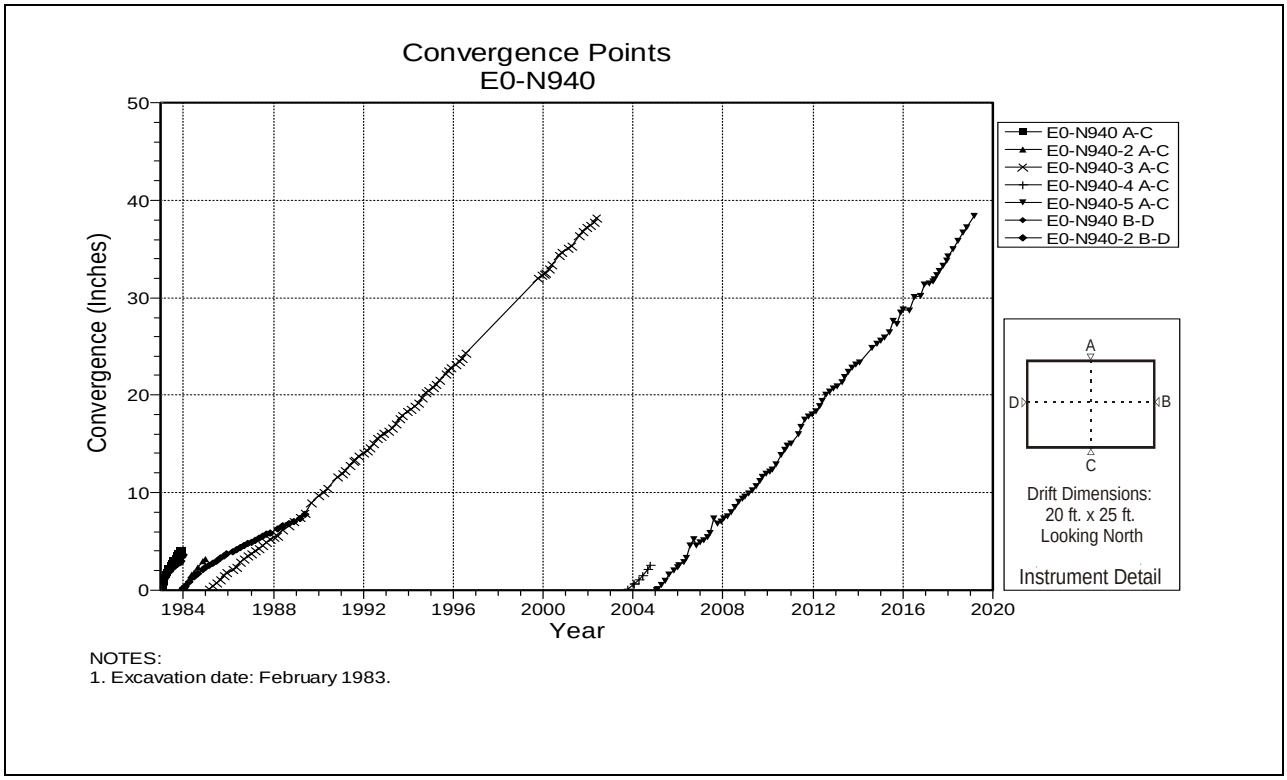

Figure 4-32 Convergence Point Array – E0 N940 – All Chords

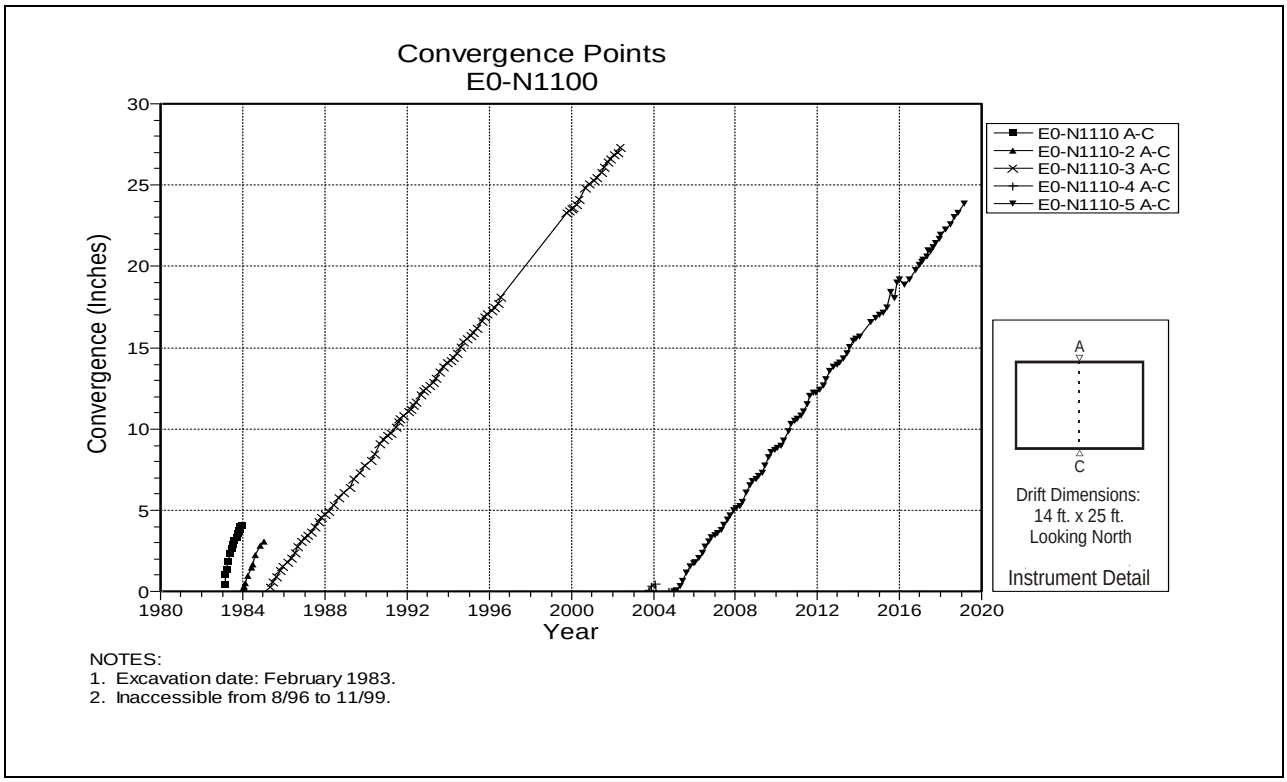

Figure 4-33 Convergence Point Array – E0 N1100 – Roof to Floor – Centerline

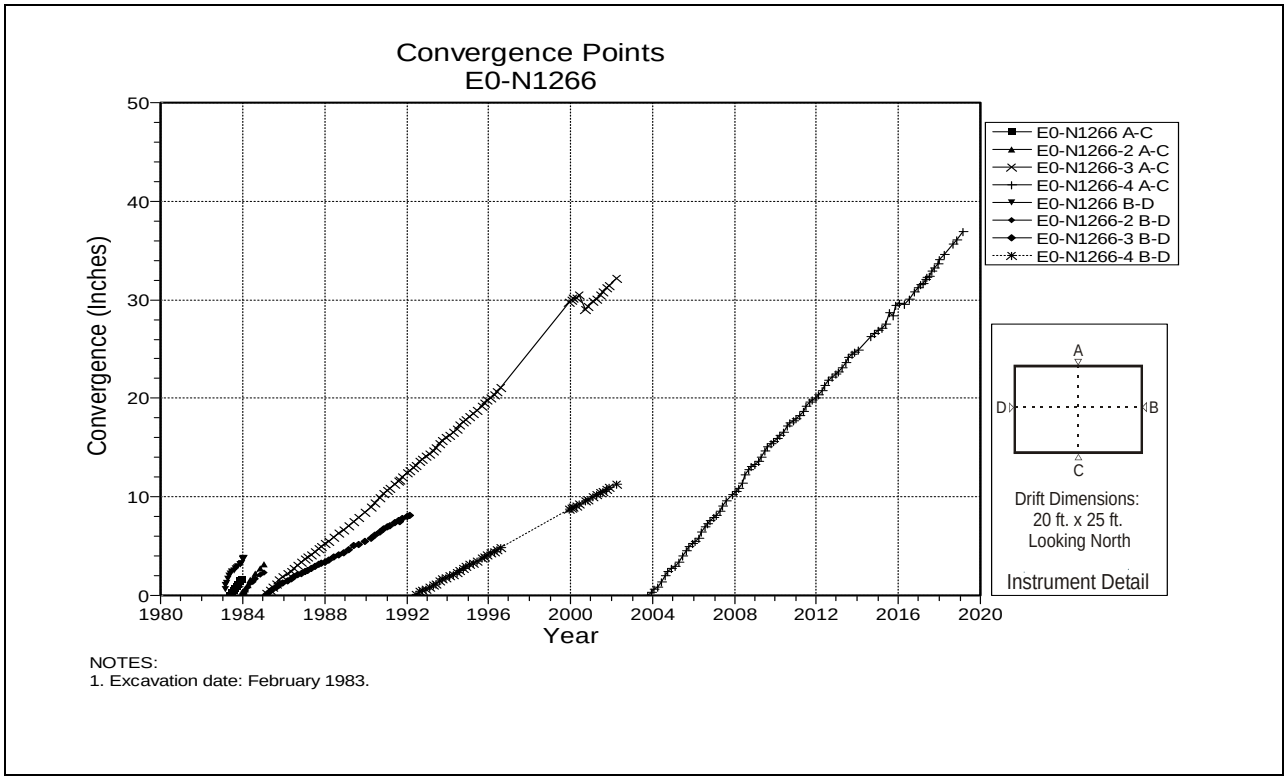

Figure 4-34 Convergence Point Array – E0 N1266 – All Chords

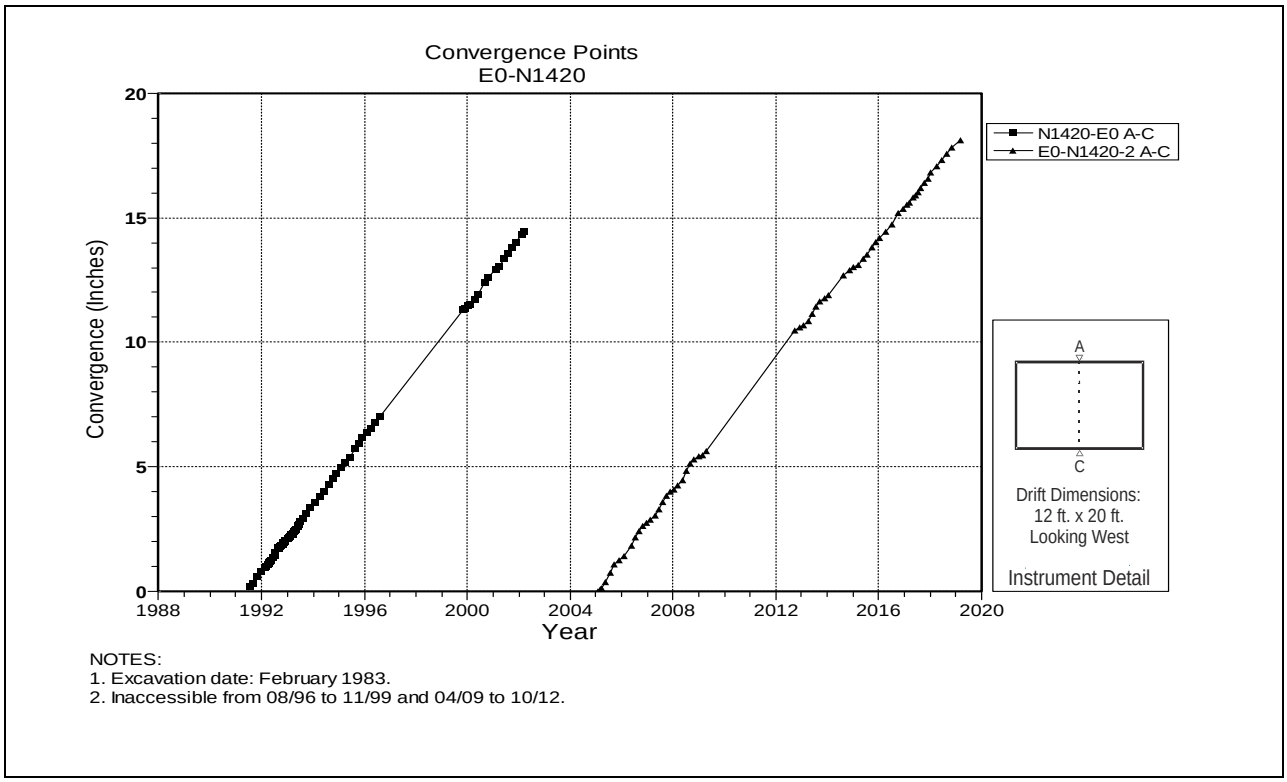

NOTES:
1. Excavation date: February 1983.
2. Inaccessible from 08/96 to 11/99 and 04/09 to 10/12.

Figure 4-35 Convergence Point Array – E0 N1420 – Roof to Floor – Centerline

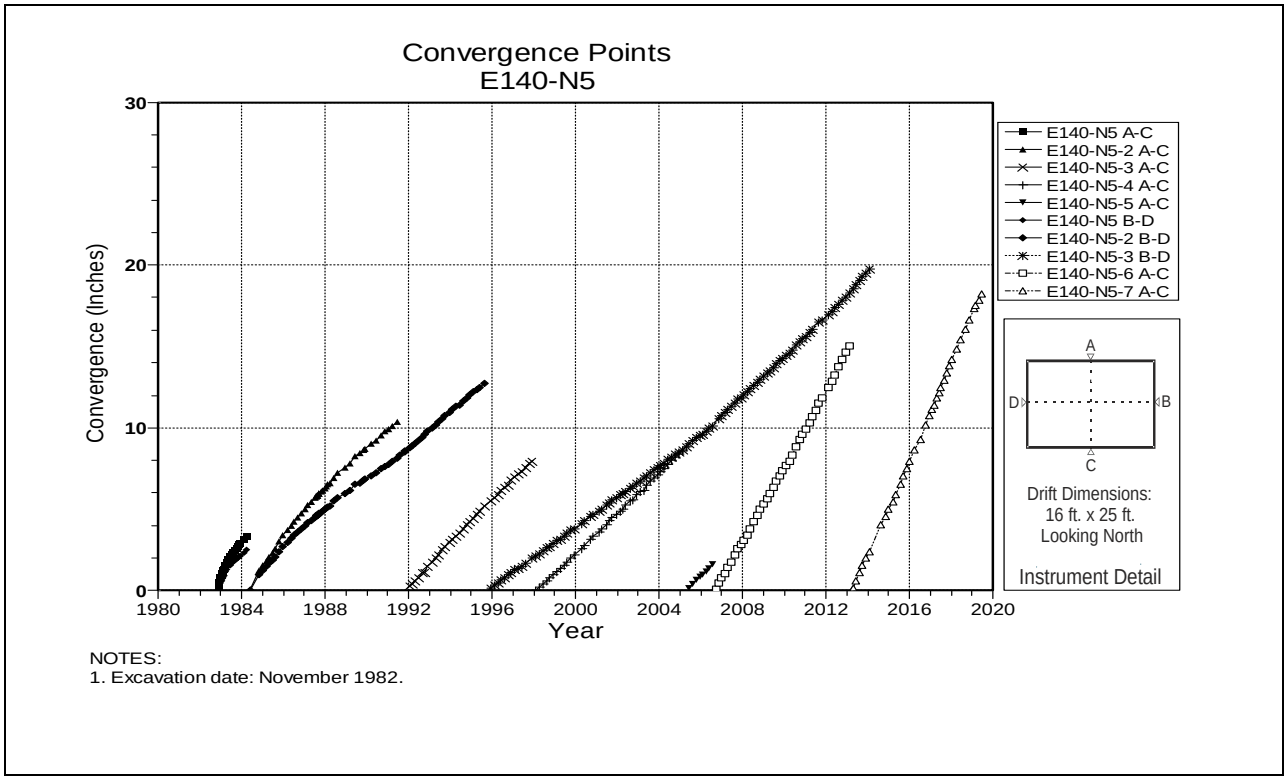

NOTES:
1. Excavation date: November 1982.

Figure 4-36 Convergence Point Array – E140 N5 – All Chords

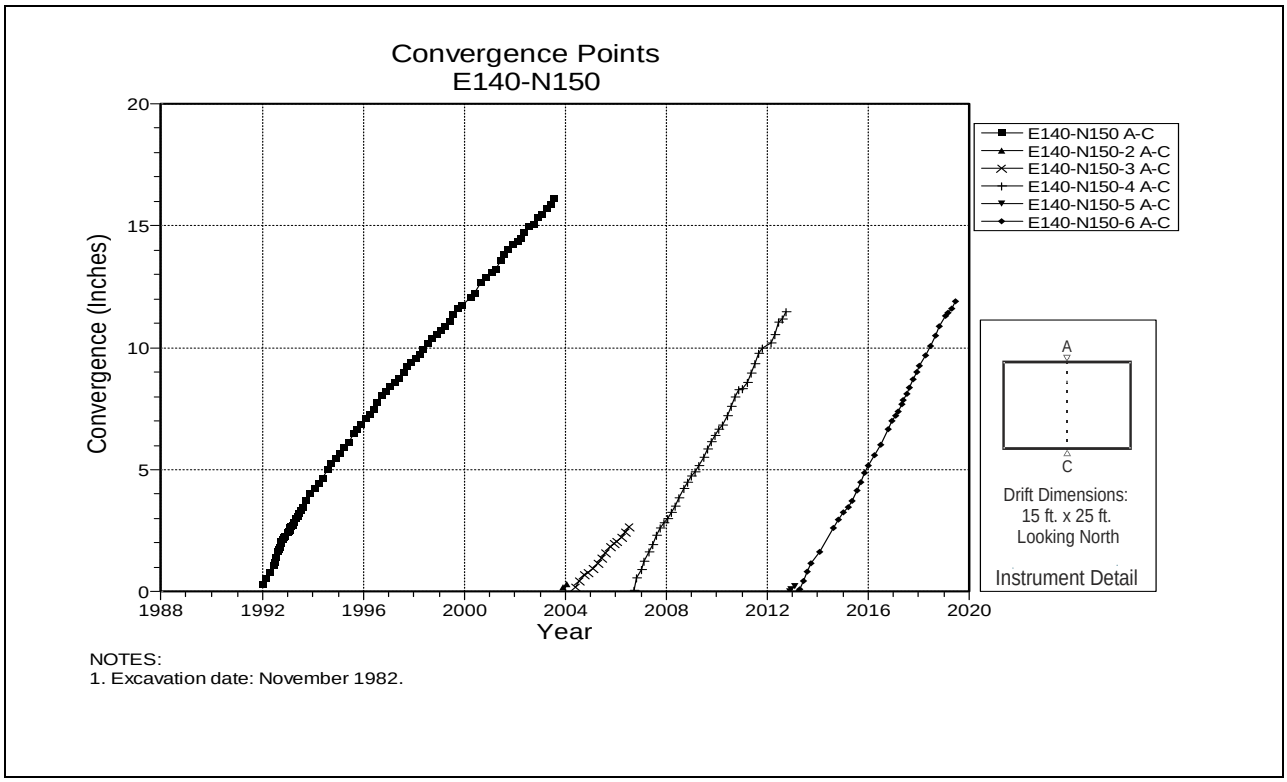

Figure 4-37 Convergence Point Array – E140 N150 – Roof to Floor – Centerline

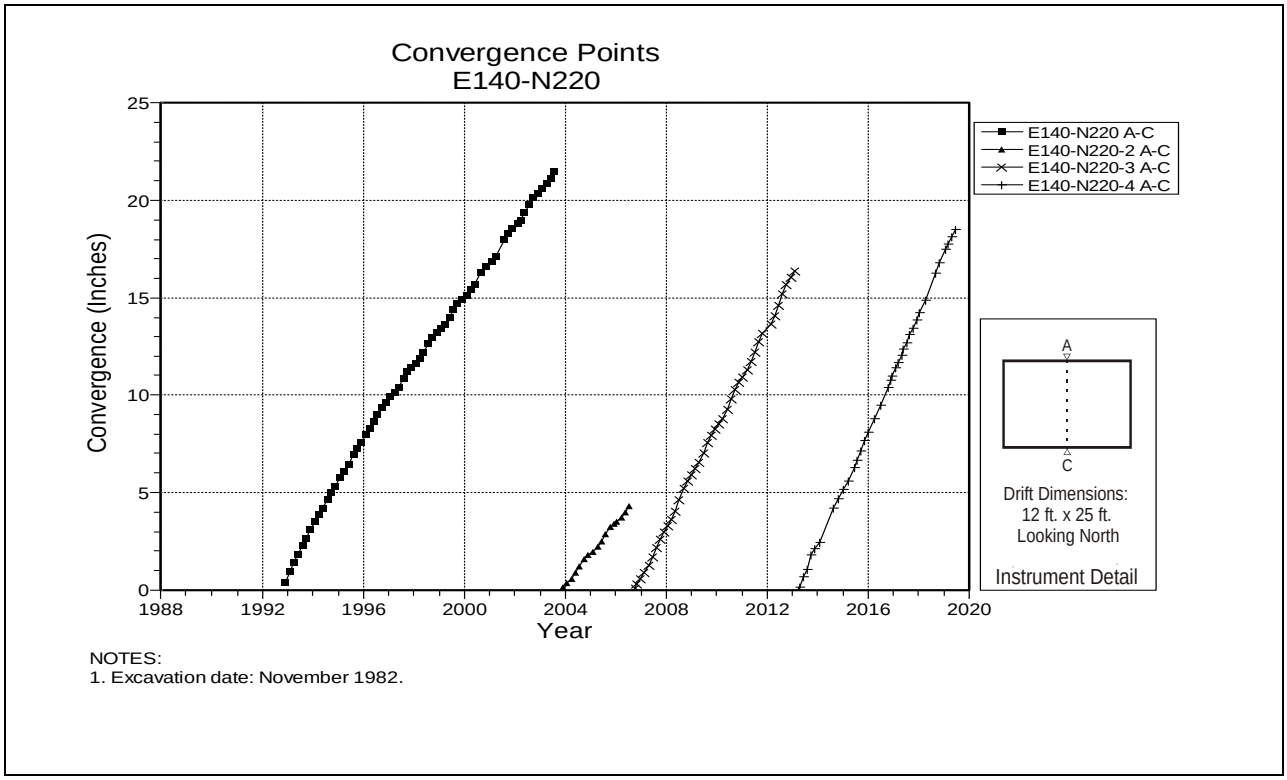

Figure 4-38 Convergence Point Array – E140 N220 – Roof to Floor – Centerline

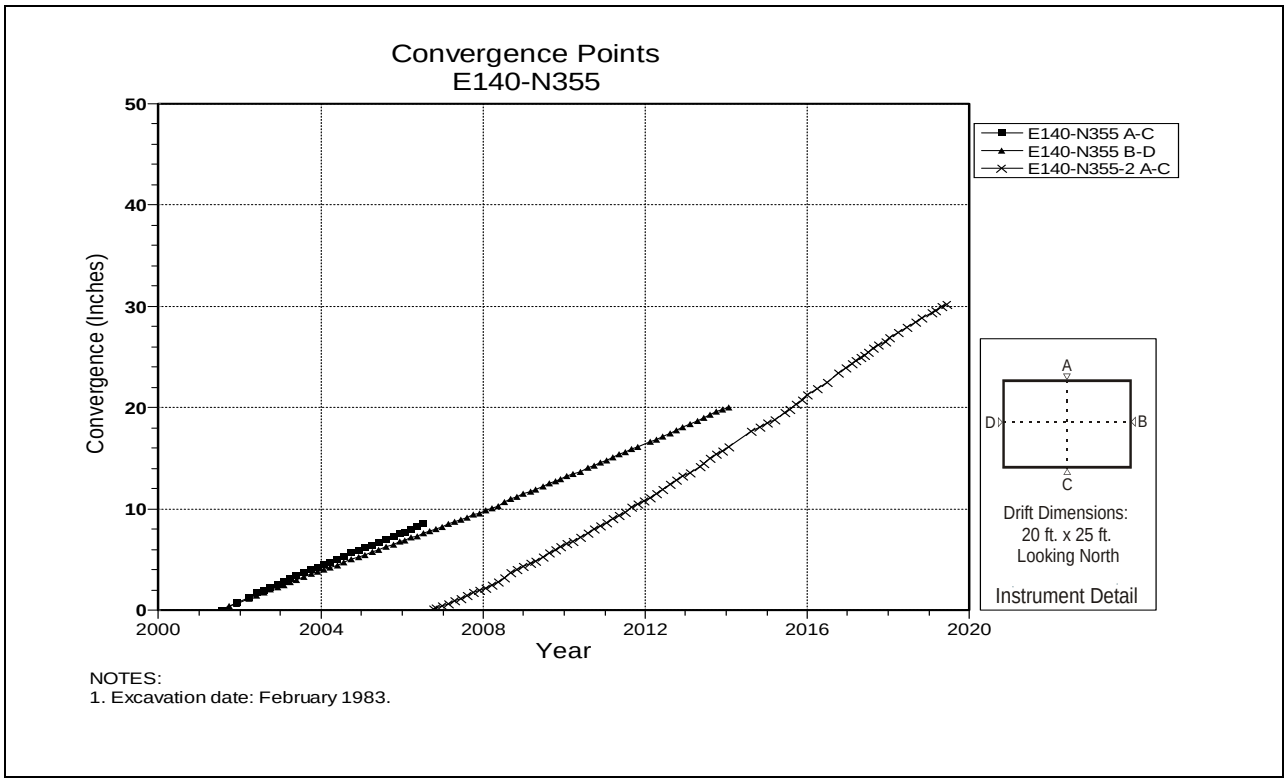

Figure 4-39 Convergence Point Array – E140 N355 – All Chords

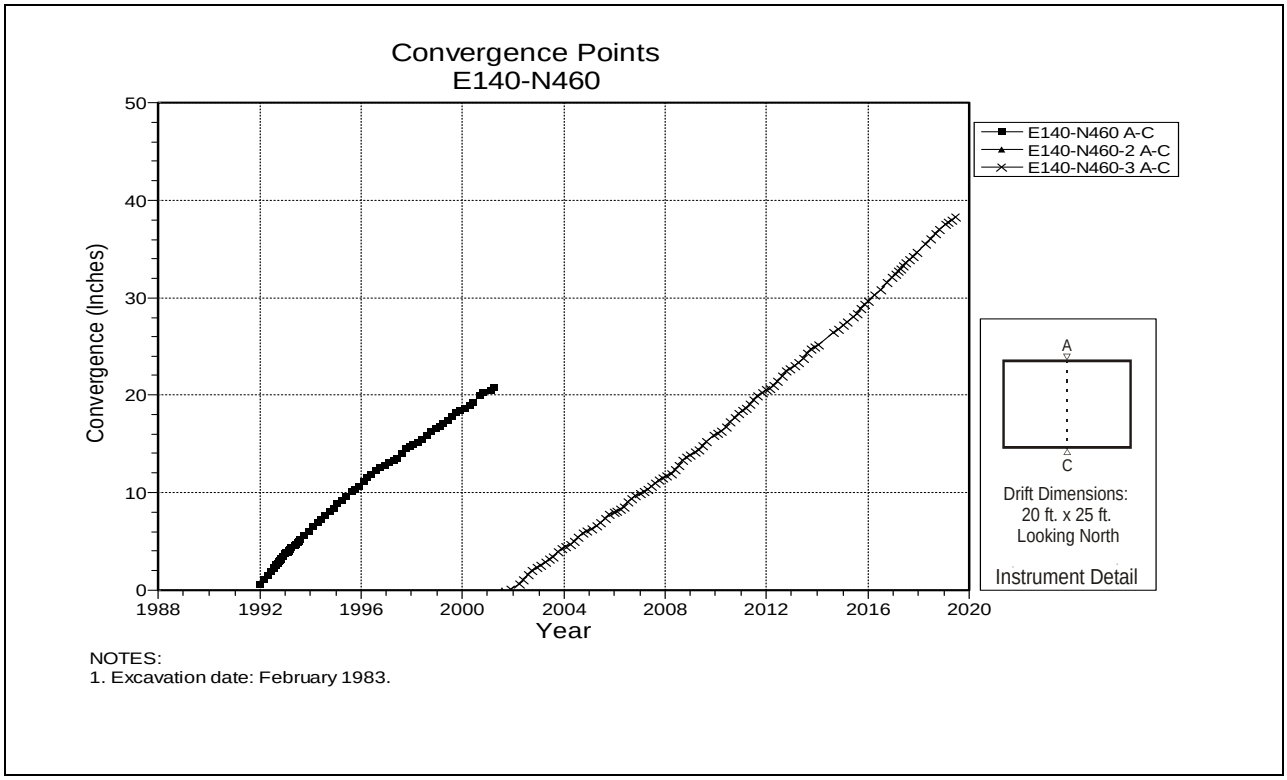

Figure 4-40 Convergence Point Array – E140 N460 – Roof to Floor – Centerline

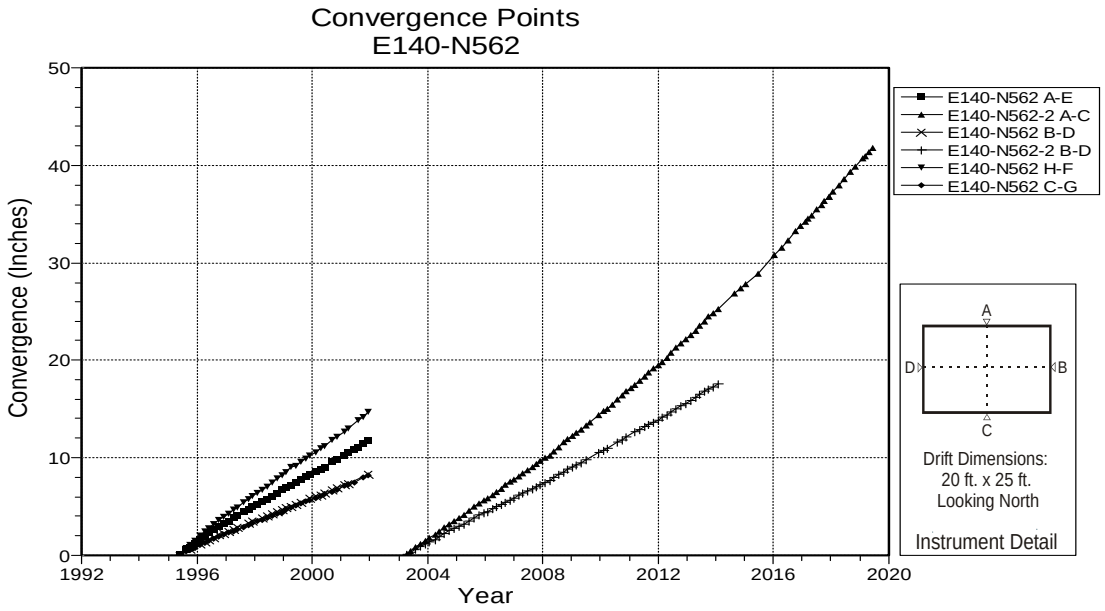

NOTES:
1. Excavation date: February 1983.
2. Roof excavated to Anhydrite "b" in early 2002.
3. Initially this location had three vertical chords: A-E, B-D, and H-F and a horizontal chord, G-G.

Figure 4-41 Convergence Point Array – E140 N562 – All Chords

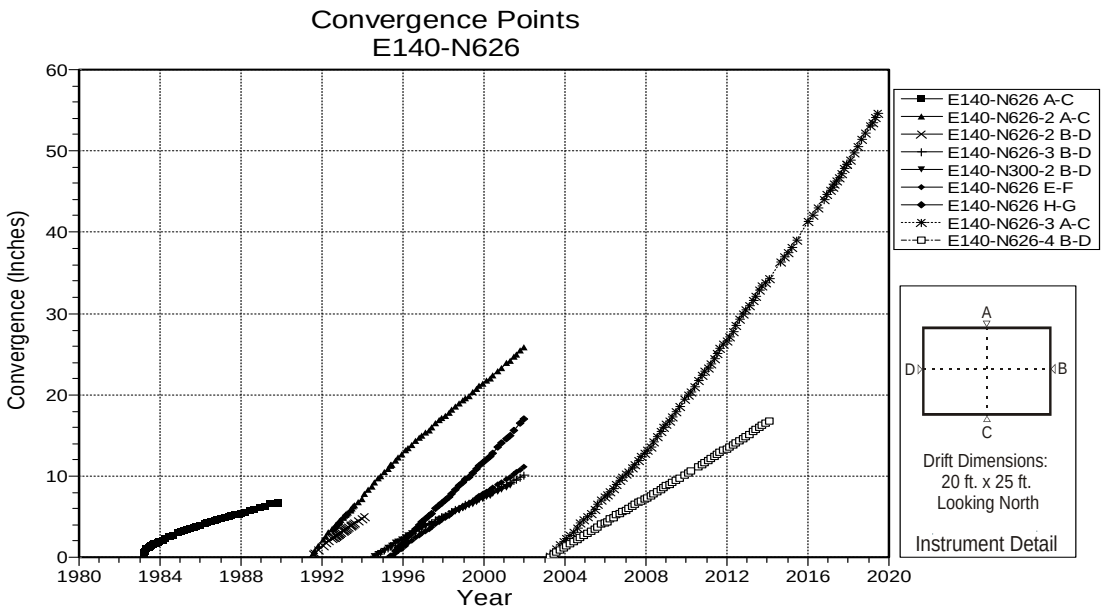

NOTES:
1. Excavation date: February 1983.

Figure 4-42 Convergence Point Array – E140 N626 – All Chords

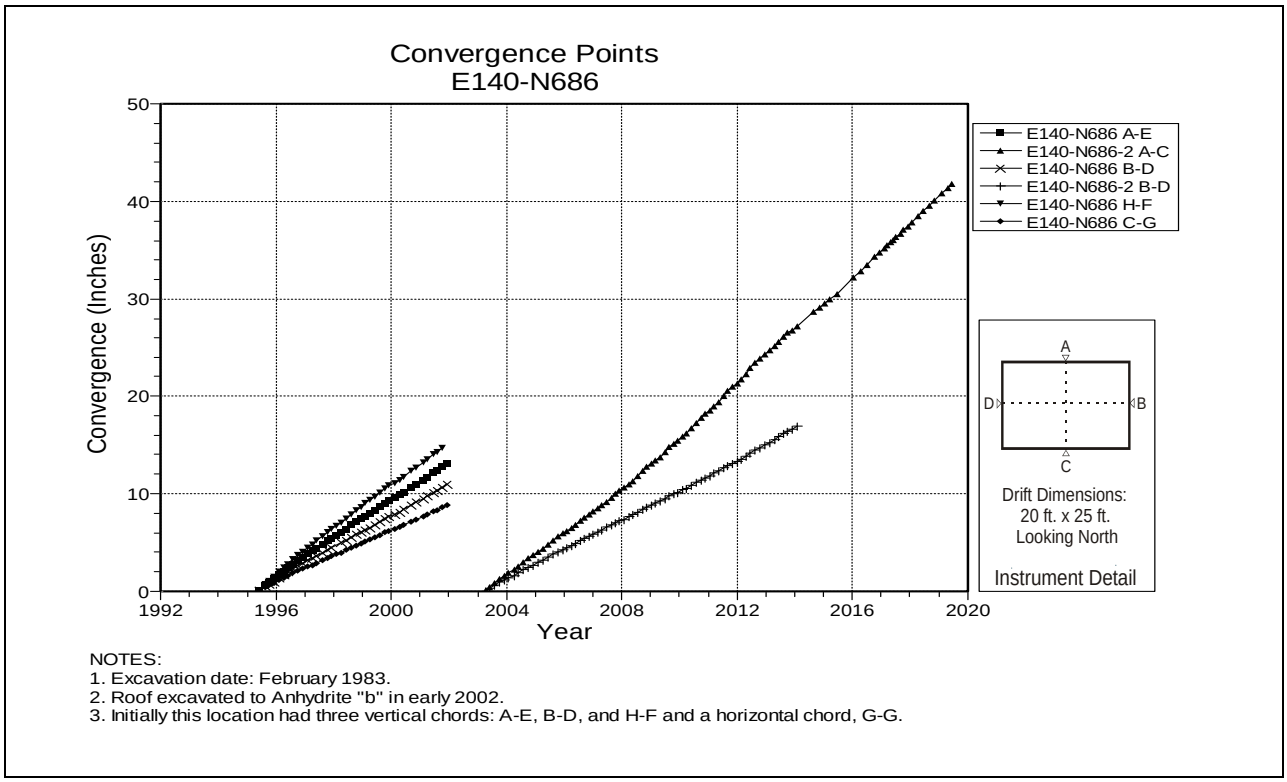

NOTES:
1. Excavation date: February 1983.
2. Roof excavated to Anhydrite "b" in early 2002.
3. Initially this location had three vertical chords: A-E, B-D, and H-F and a horizontal chord, G-G.

Figure 4-43 Convergence Point Array – E140 N686 – All Chords

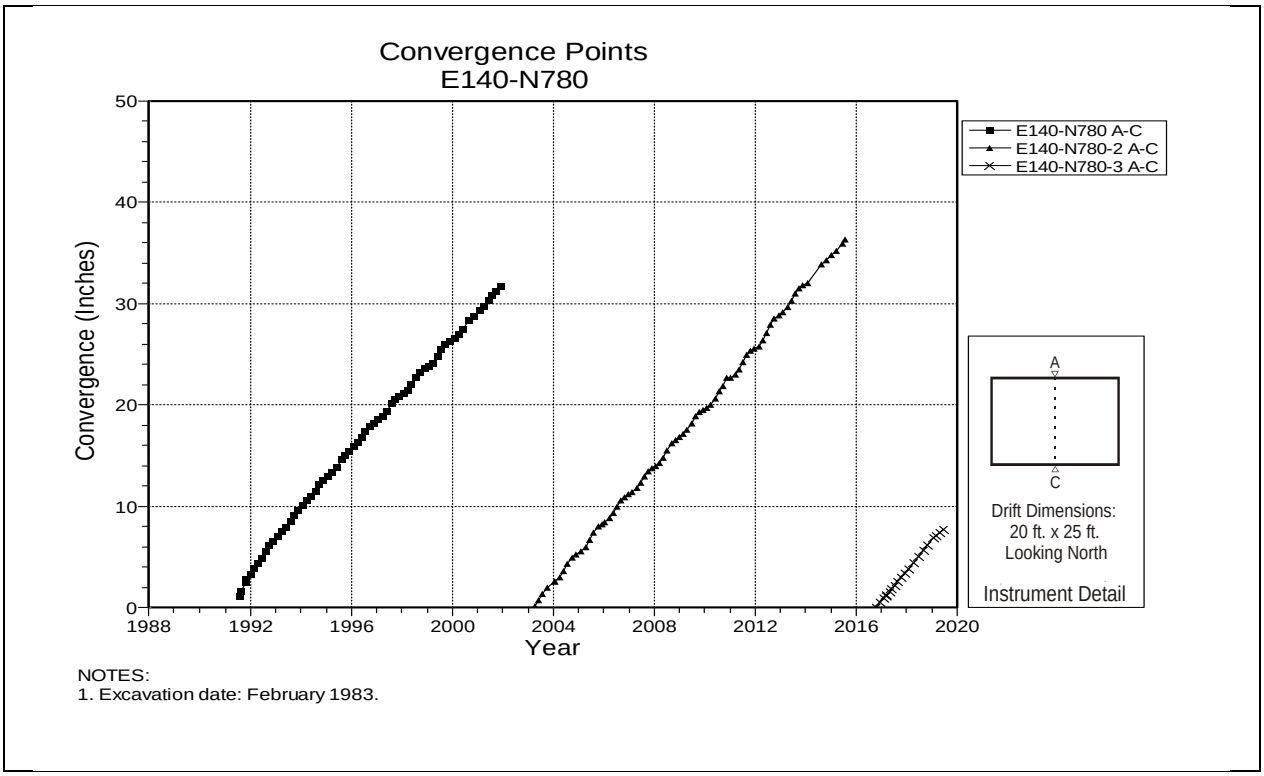

NOTES:
1. Excavation date: February 1983.

Figure 4-44 Convergence Point Array – E140 N780 – Roof to Floor – Centerline

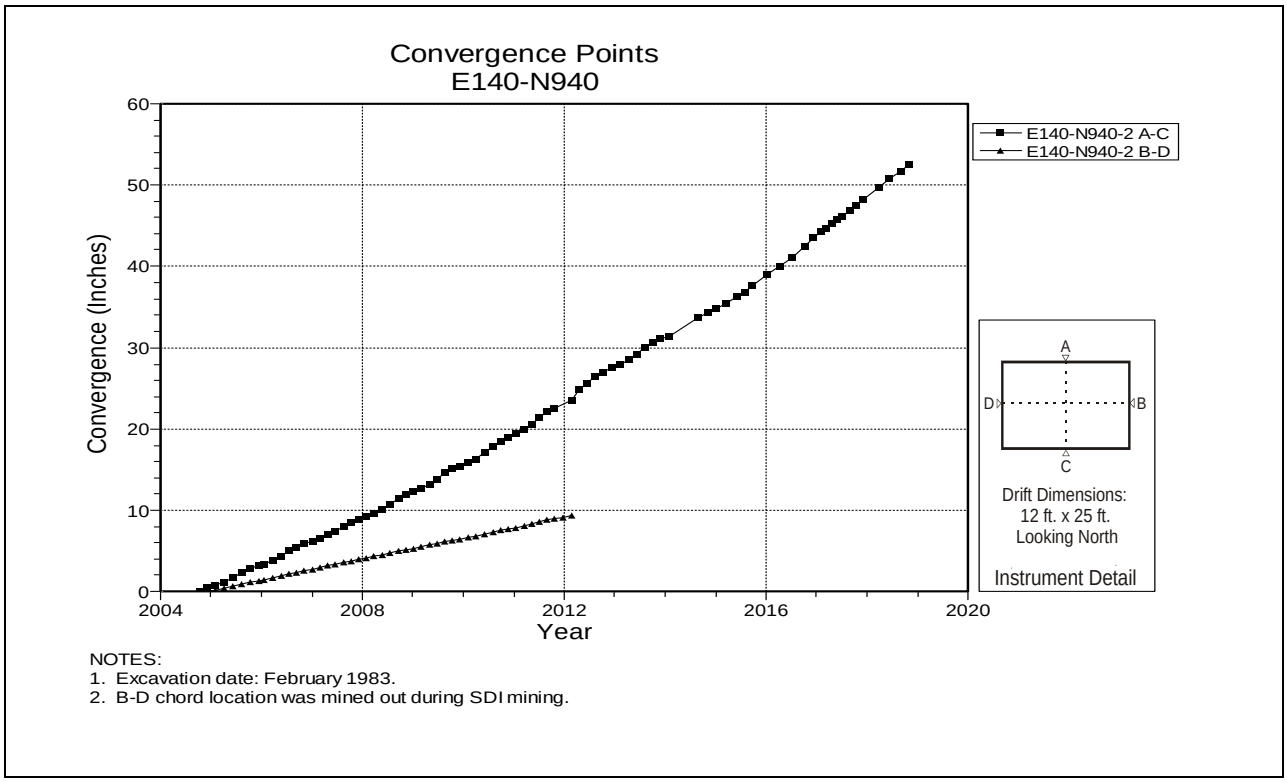

Figure 4-45 Convergence Point Array – E140 N940 – All Chords

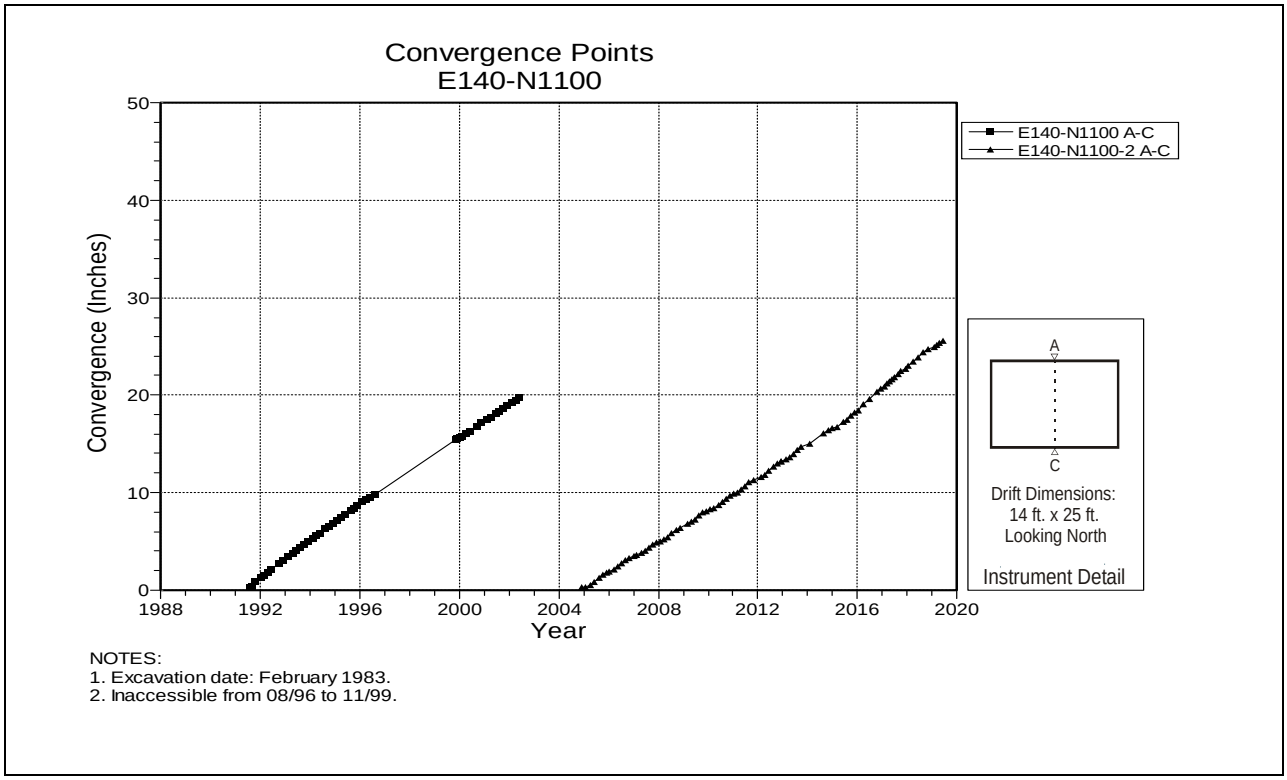

Figure 4-46 Convergence Point Array – E140 N1100 – Roof to Floor – Centerline

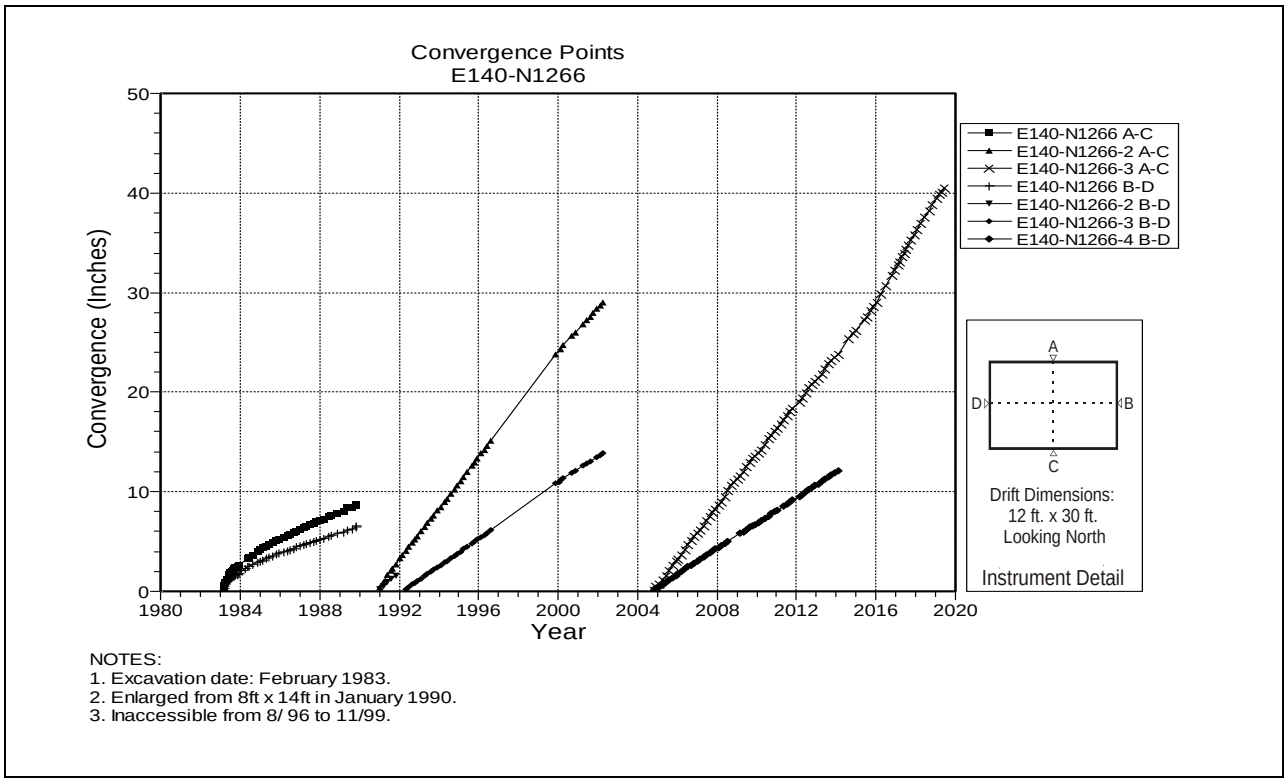

Figure 4-47 Convergence Point Array – E140 N1266 – All Chords

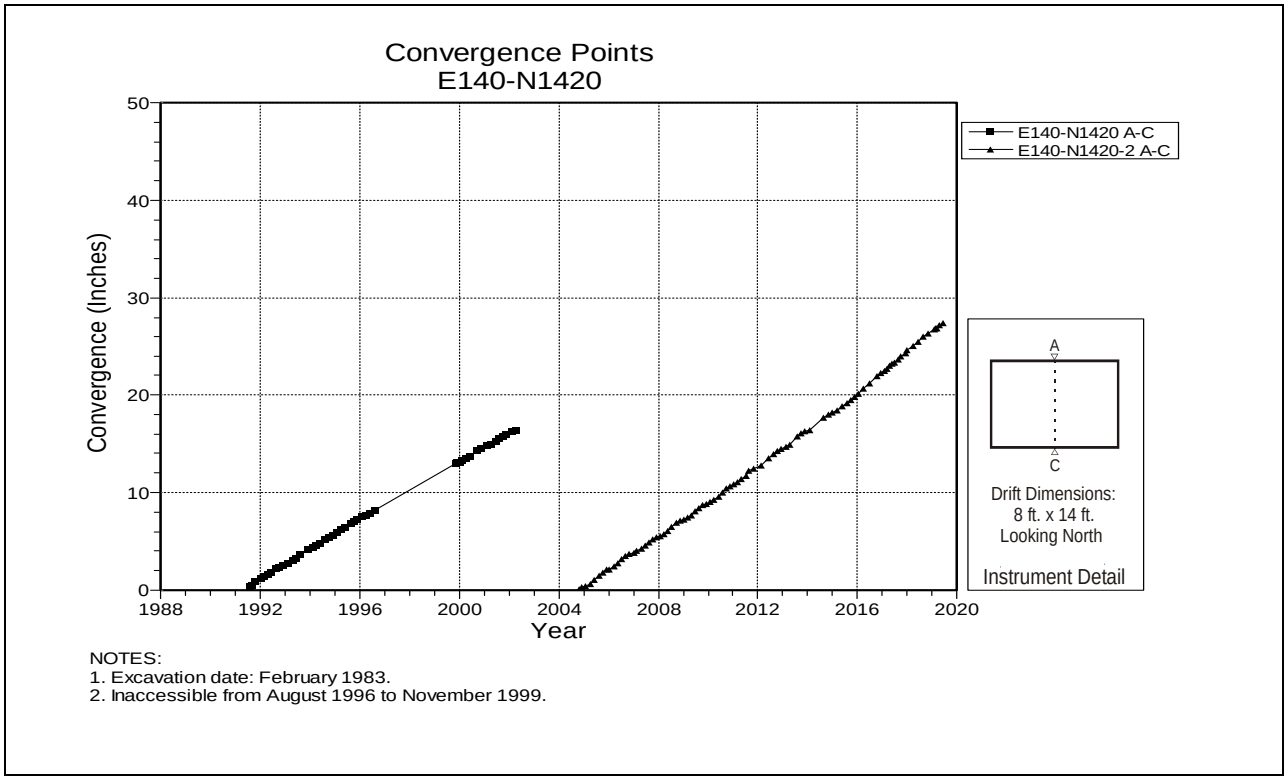

Figure 4-48 Convergence Point Array – E140 N1420 – Roof to Floor – Centerline

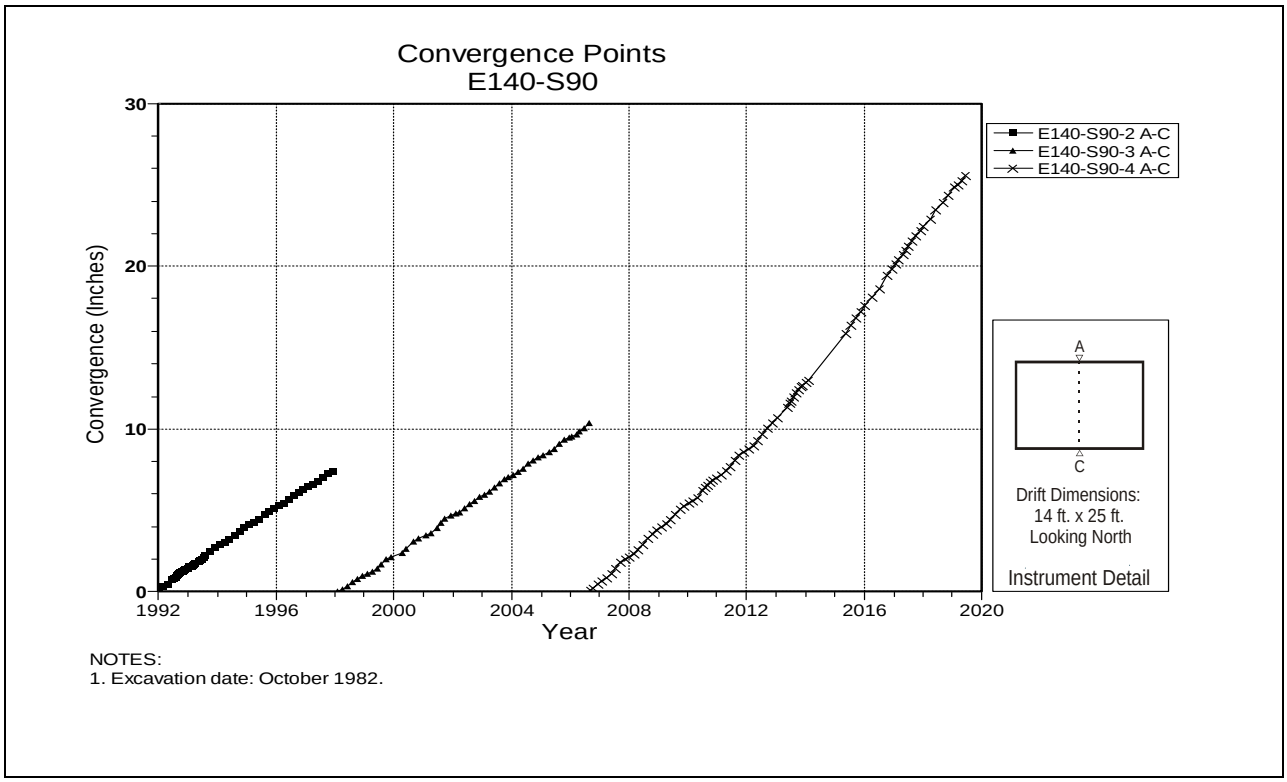

Figure 4-49 Convergence Point Array – E140 S90 – Roof to Floor – Centerline

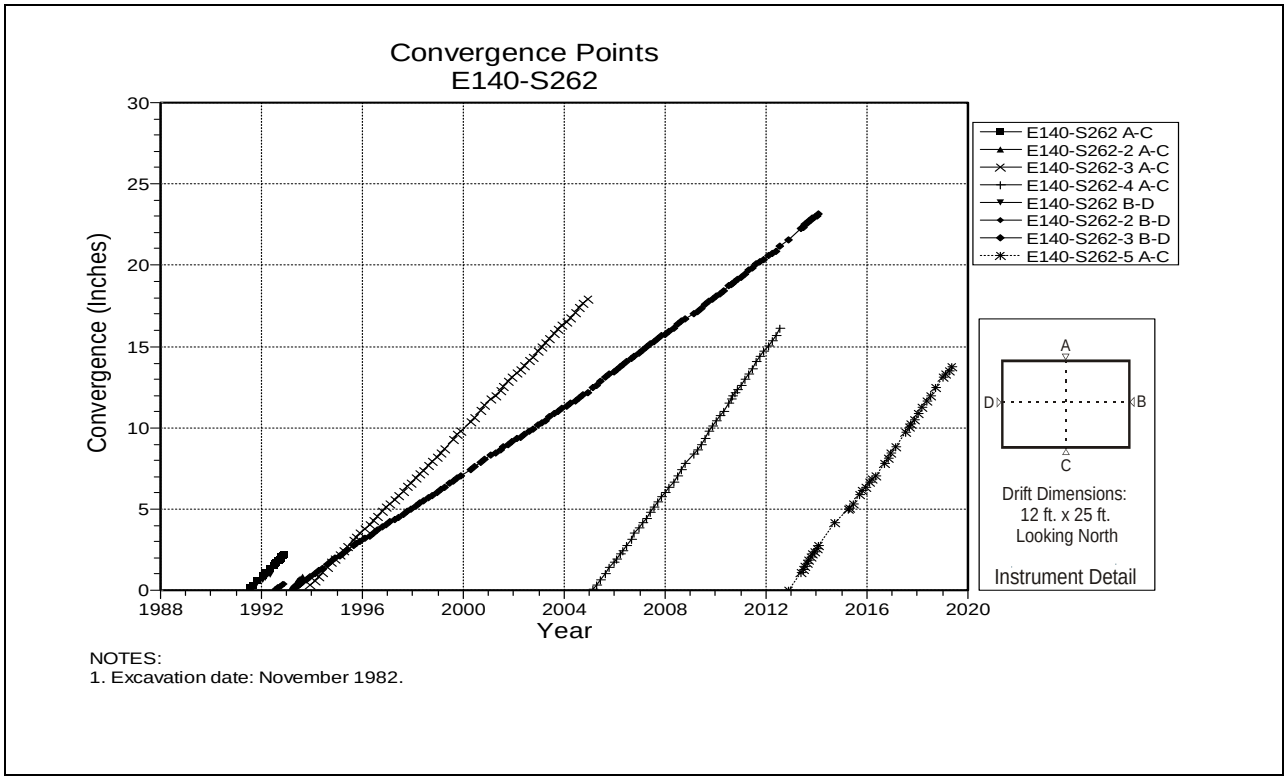

Figure 4-50 Convergence Point Array – E140 S262 – All Chords

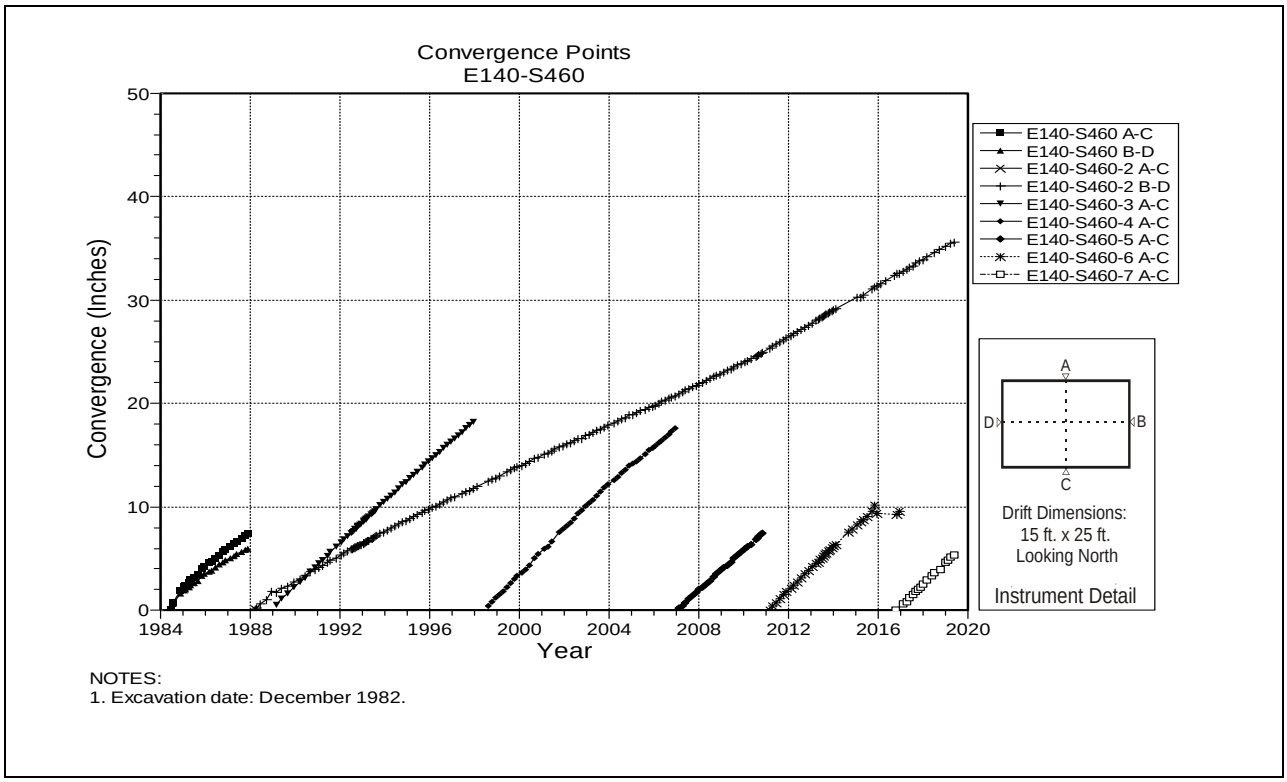

Figure 4-51 Convergence Point Array – E140 S460 – All Chords

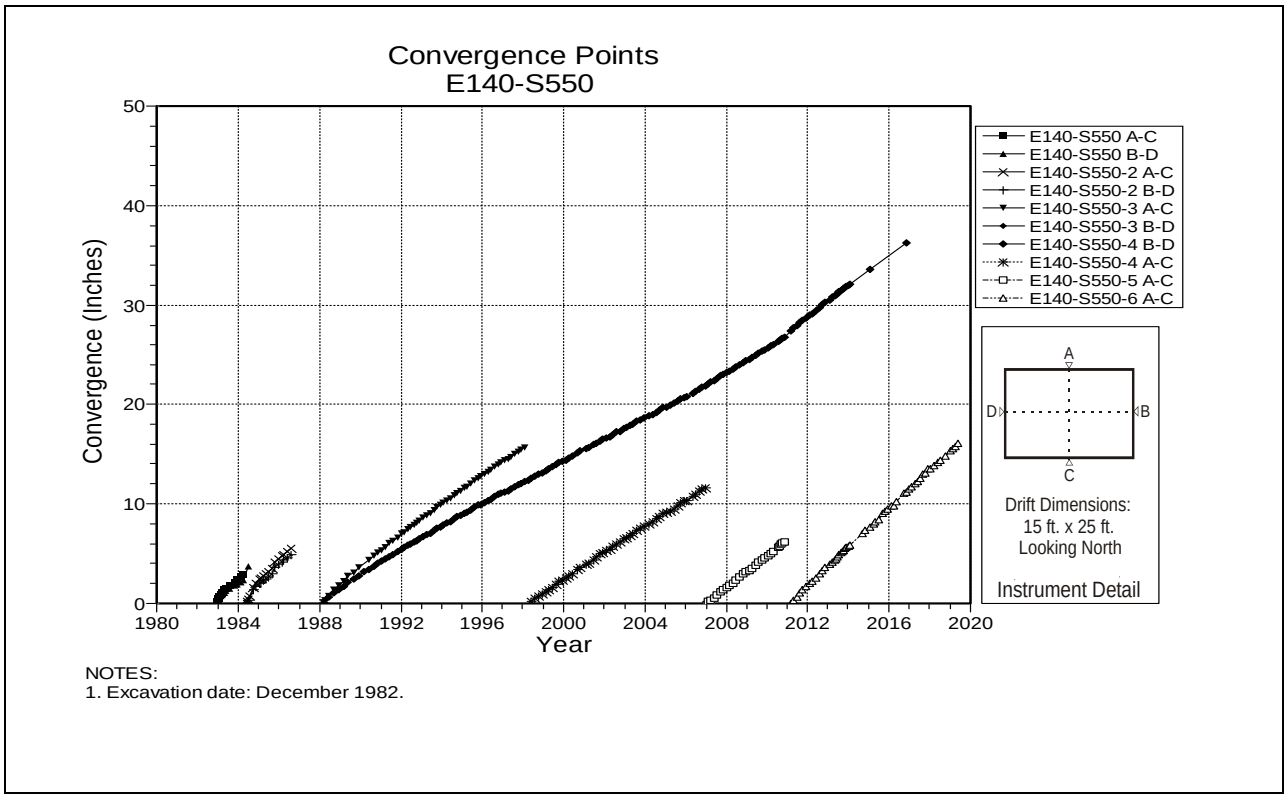

Figure 4-52 Convergence Point Array – E140 S550 – All Chords

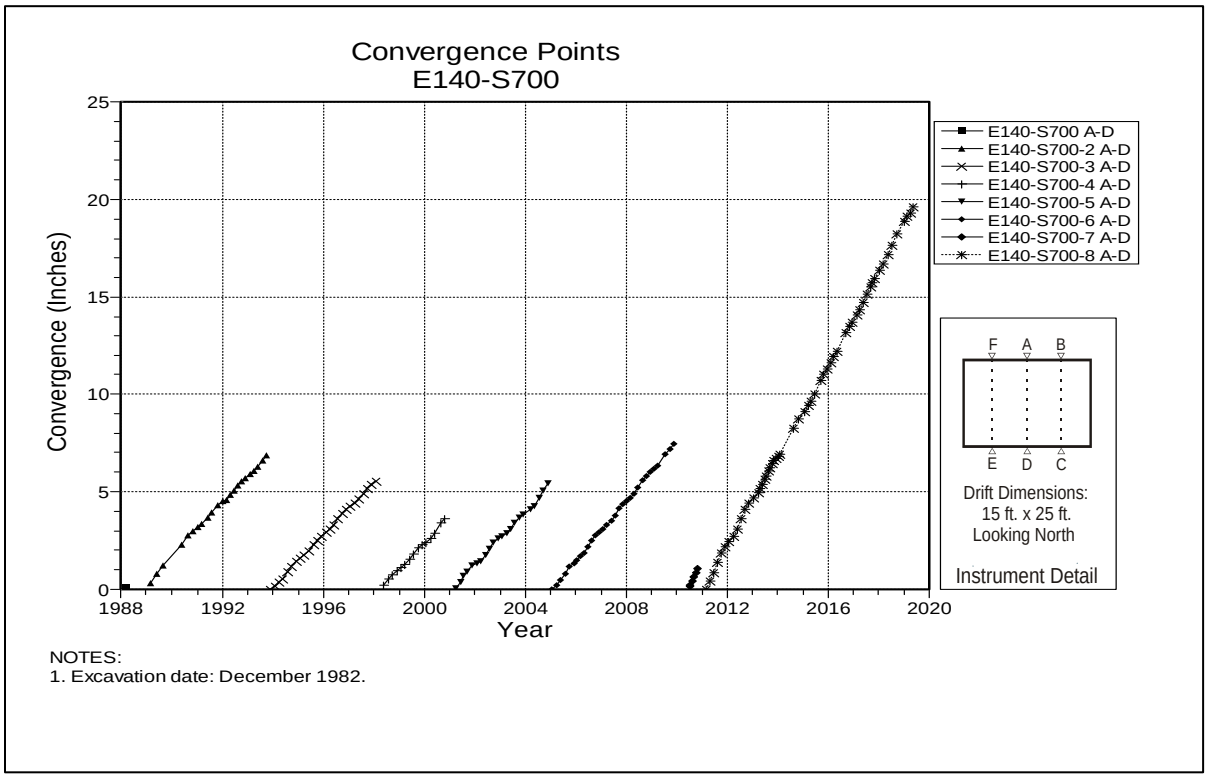

Figure 4-53 Convergence Point Array – E140 S700 – Roof to Floor – Centerline

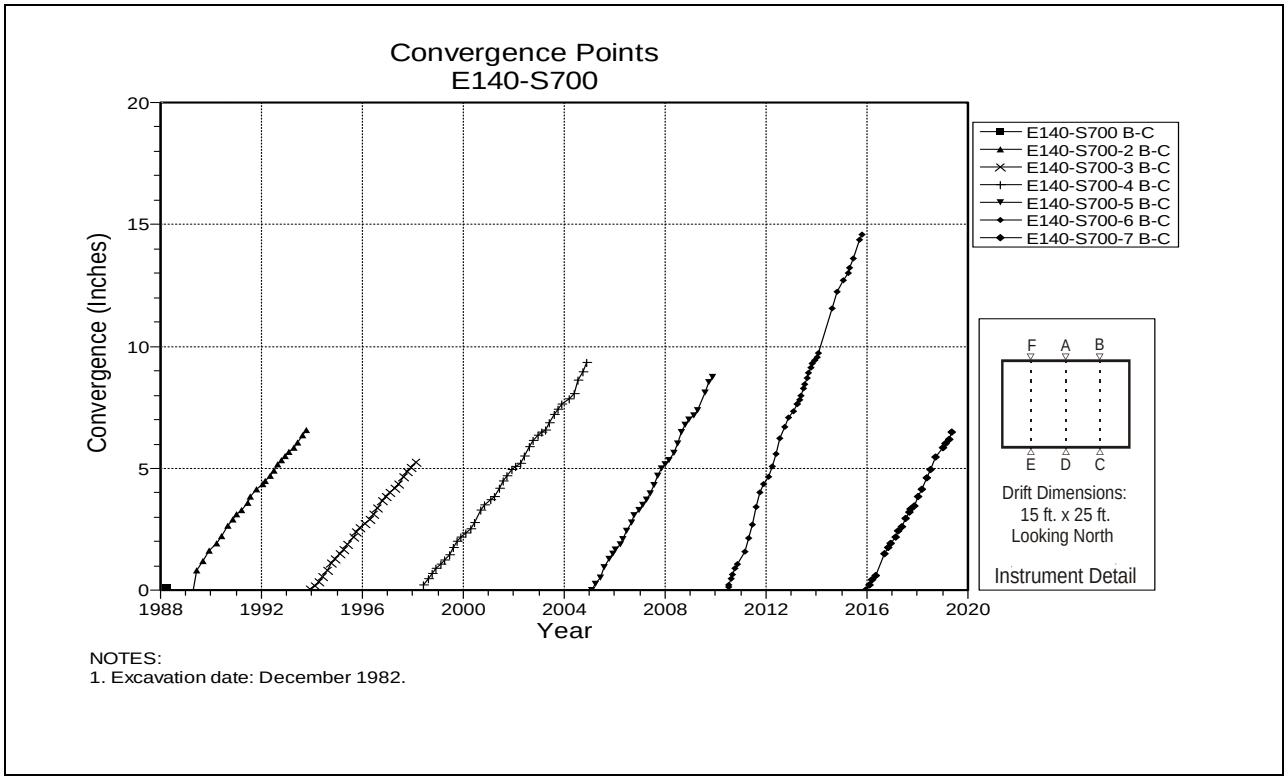

Figure 4-54 Convergence Point Array – E140 S700 – Roof to Floor – East Quarter Point

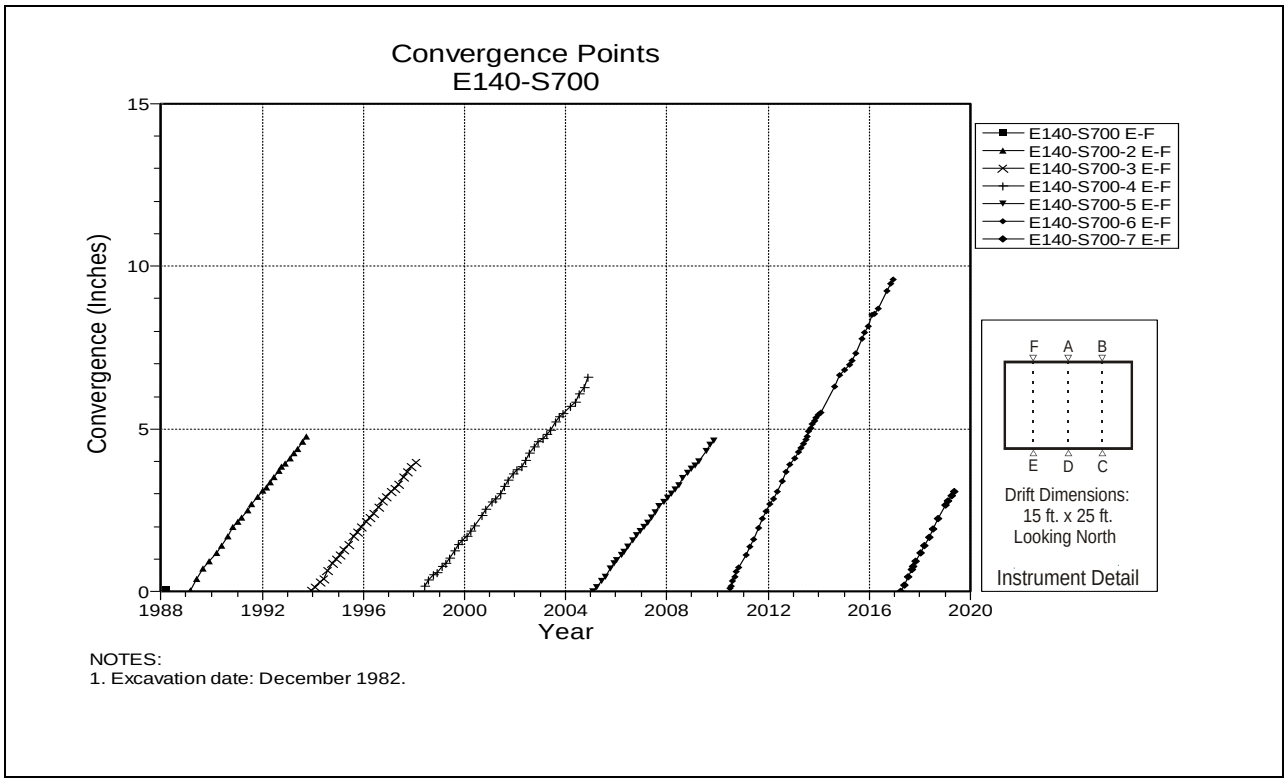

Figure 4-55 Convergence Point Array – E140 S700 – Roof to Floor – West Quarter Point

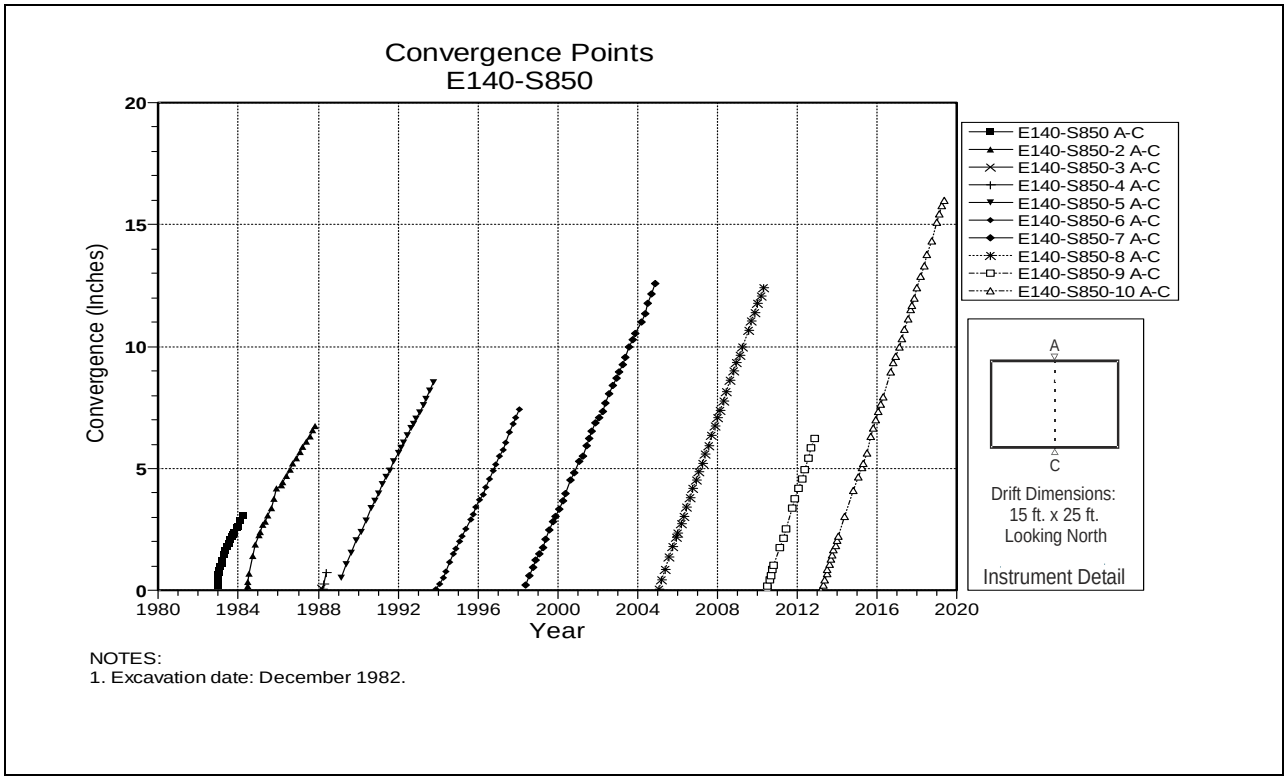

Figure 4-56 Convergence Point Array – E140 S850 – Roof to Floor – Centerline

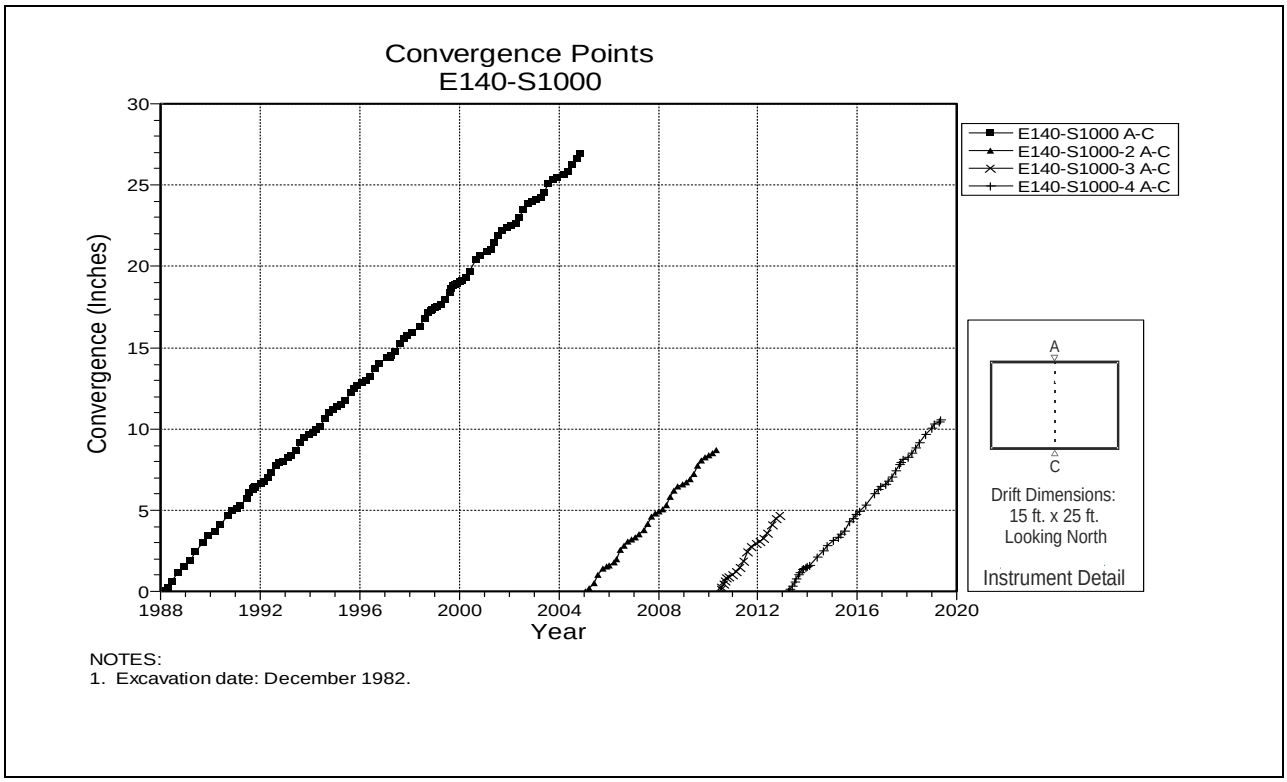

NOTES:
1. Excavation date: December 1982.

Figure 4-57 Convergence Point Array – E140 S1000 – Roof to Floor – Centerline

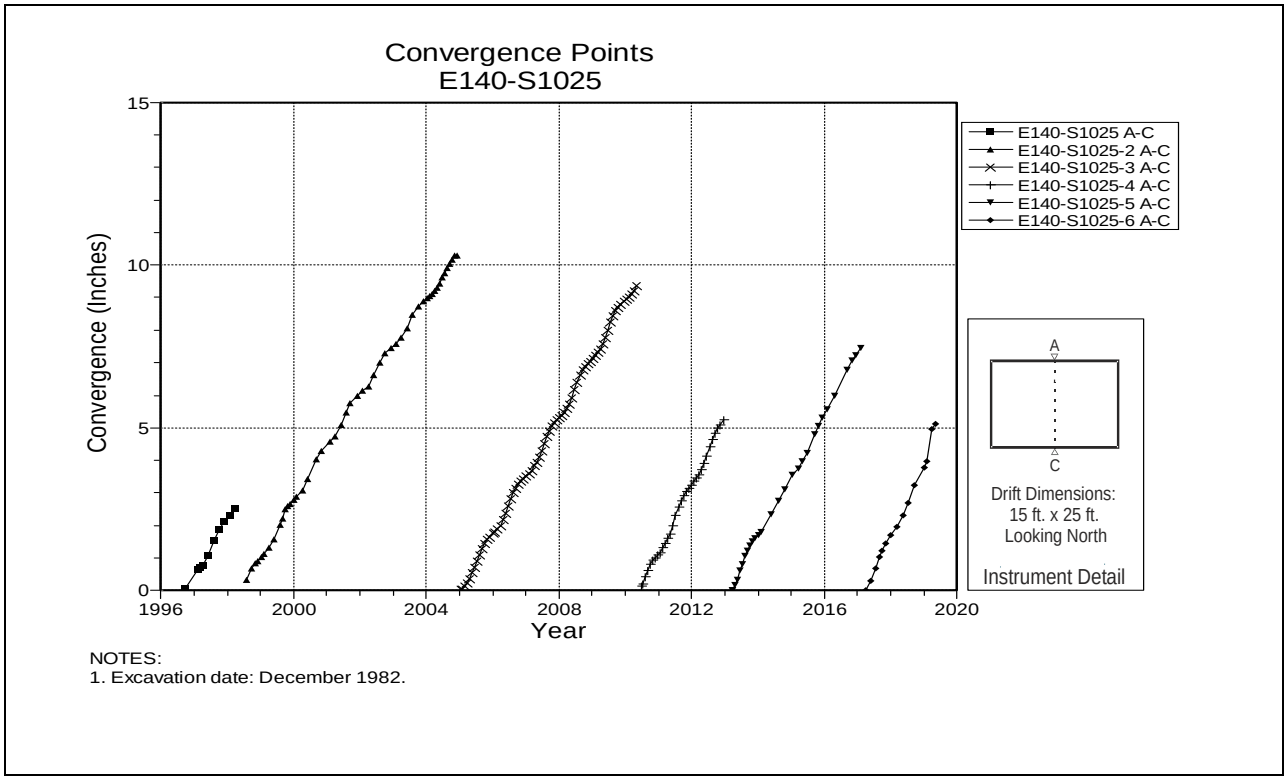

NOTES:
1. Excavation date: December 1982.

Figure 4-58 Convergence Point Array – E140 S1025 – Roof to Floor – Centerline

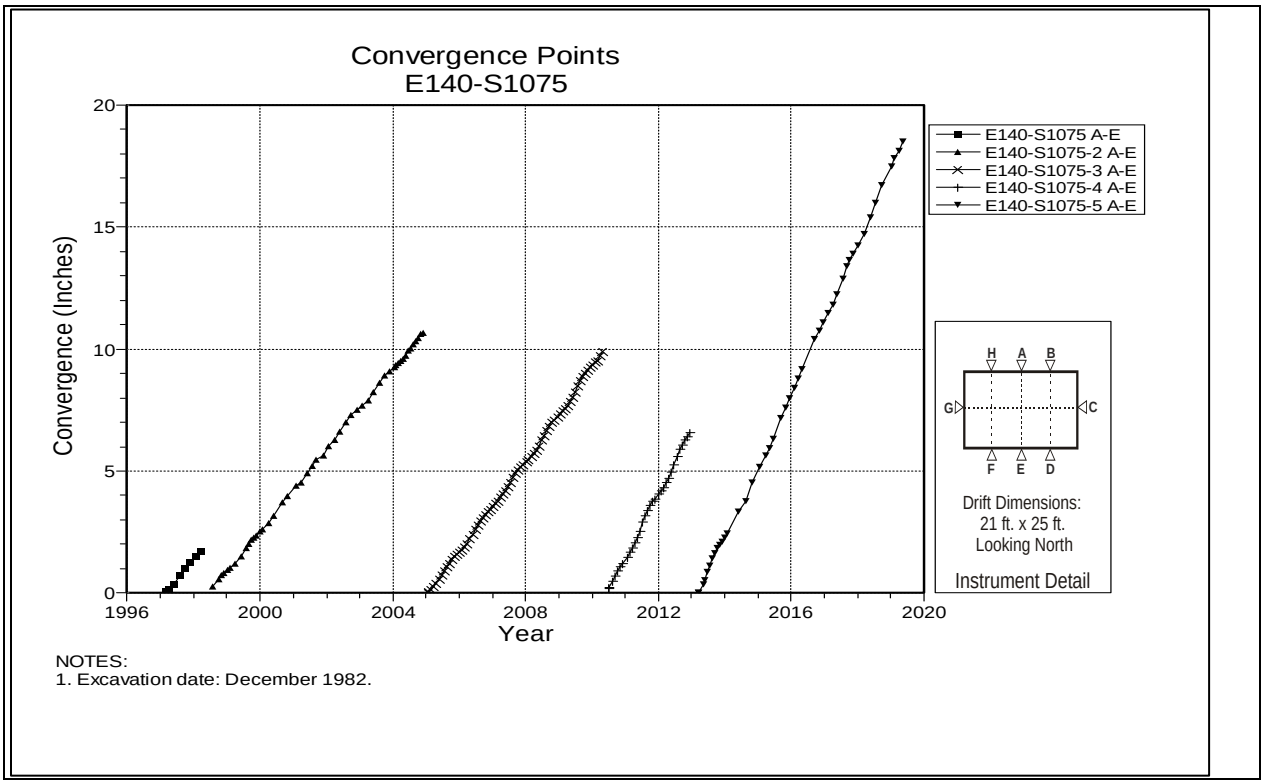

Figure 4-59 Convergence Point Array – E140 S1075 – Roof to Floor – Centerline

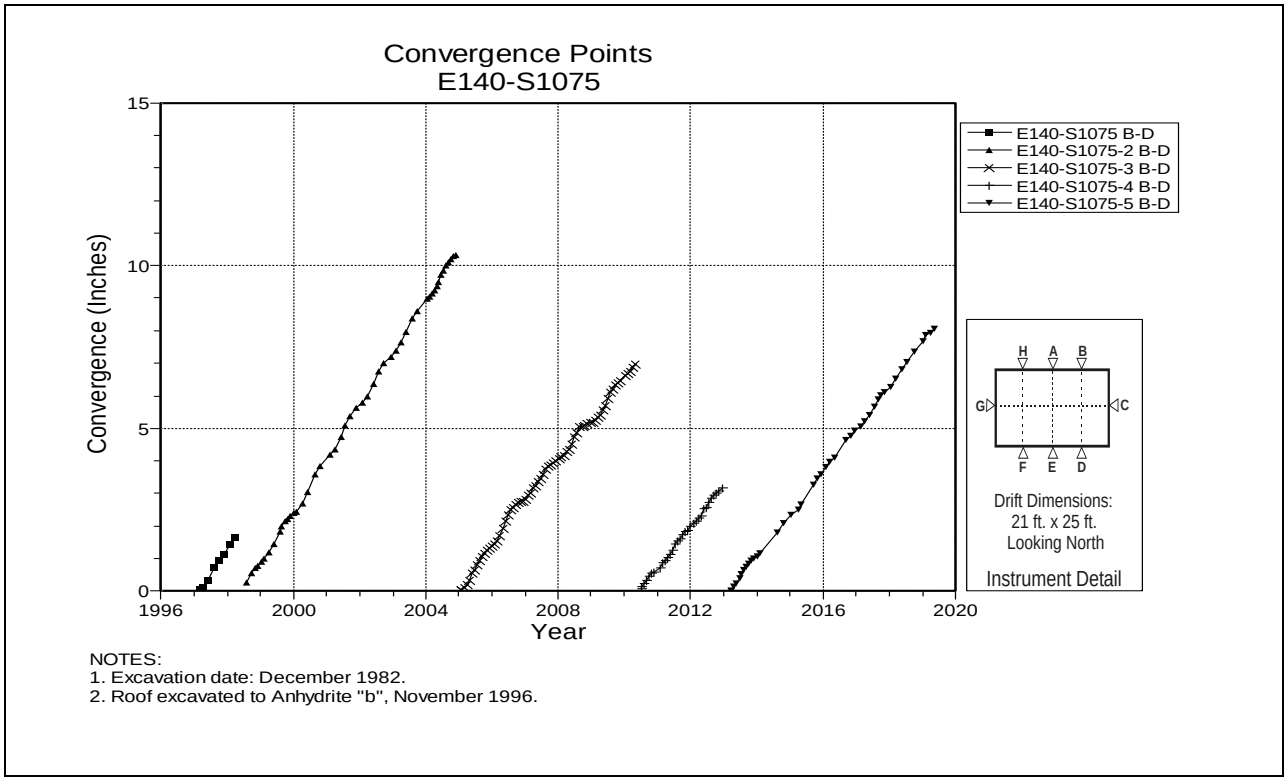

Figure 4-60 Convergence Point Array – E140 S1075 – Roof to Floor – East Quarter Point

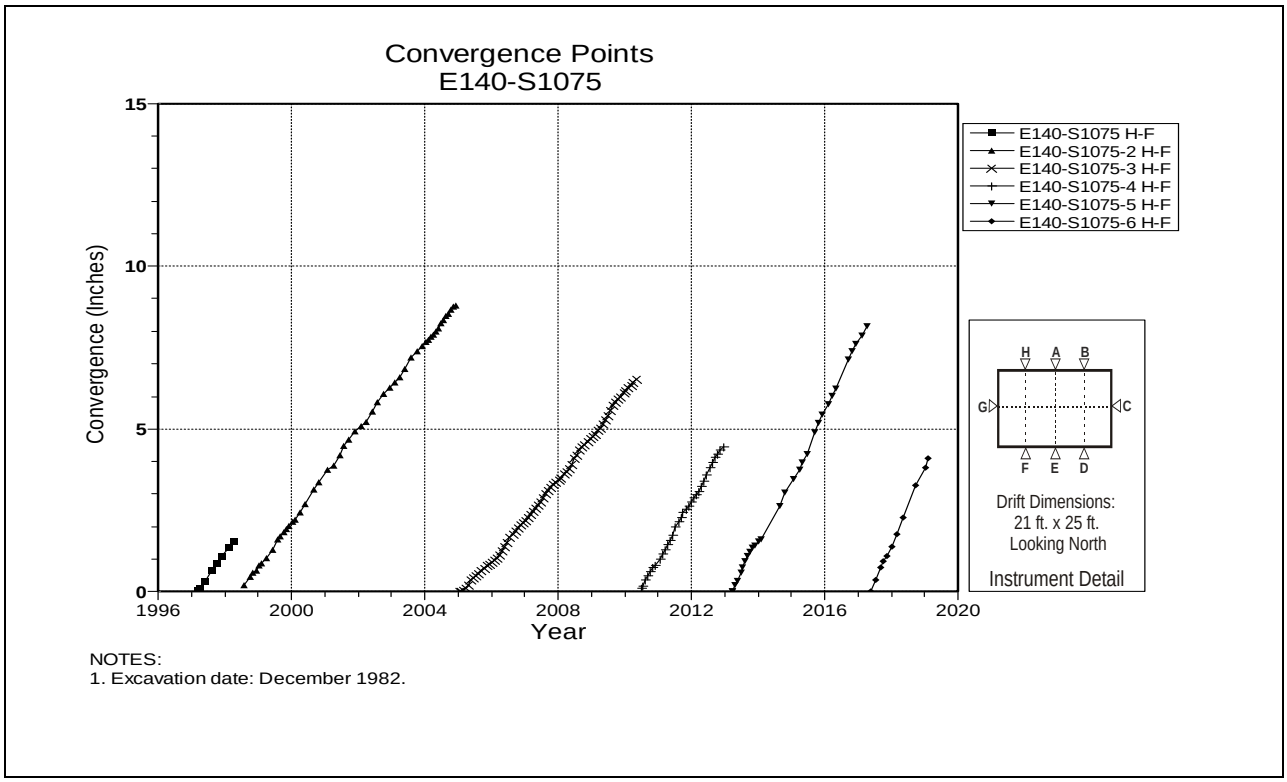

Figure 4-61 Convergence Point Array – E140 S1075 – Roof to Floor – West Quarter Point

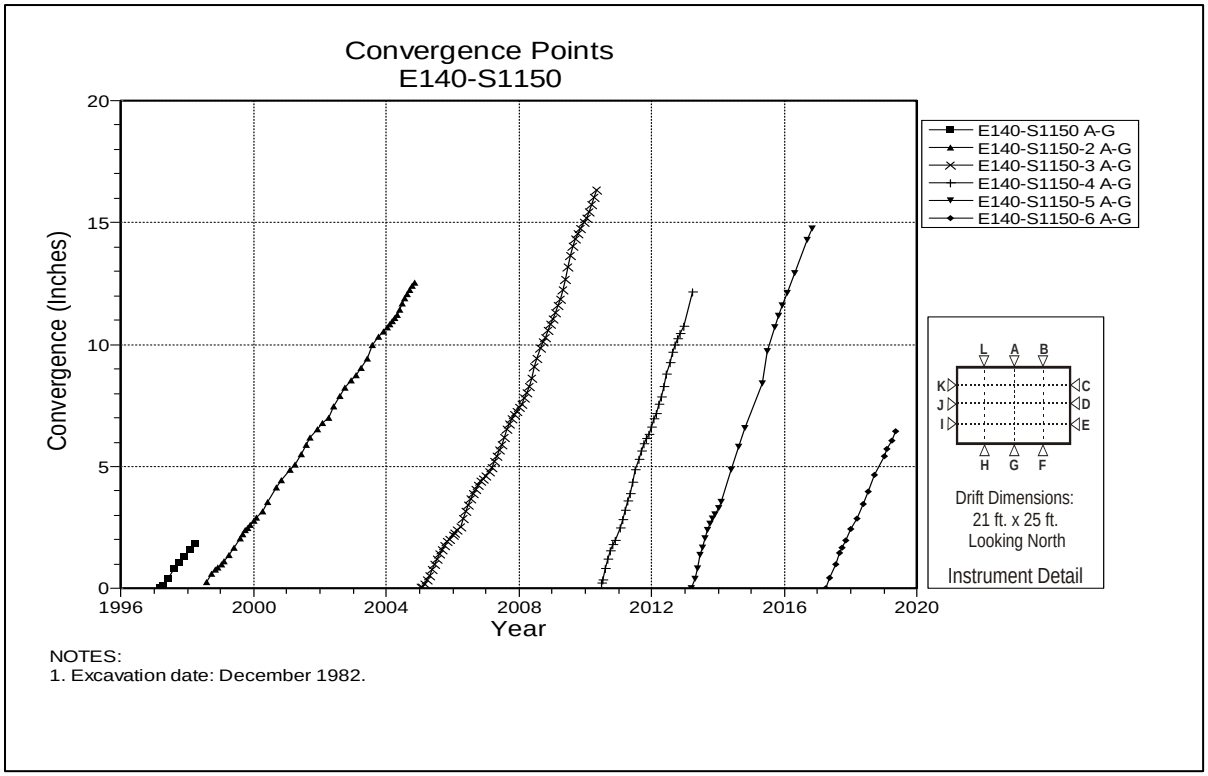

Figure 4-62 Convergence Point Array – E140 S1150 – Roof to Floor – Centerline

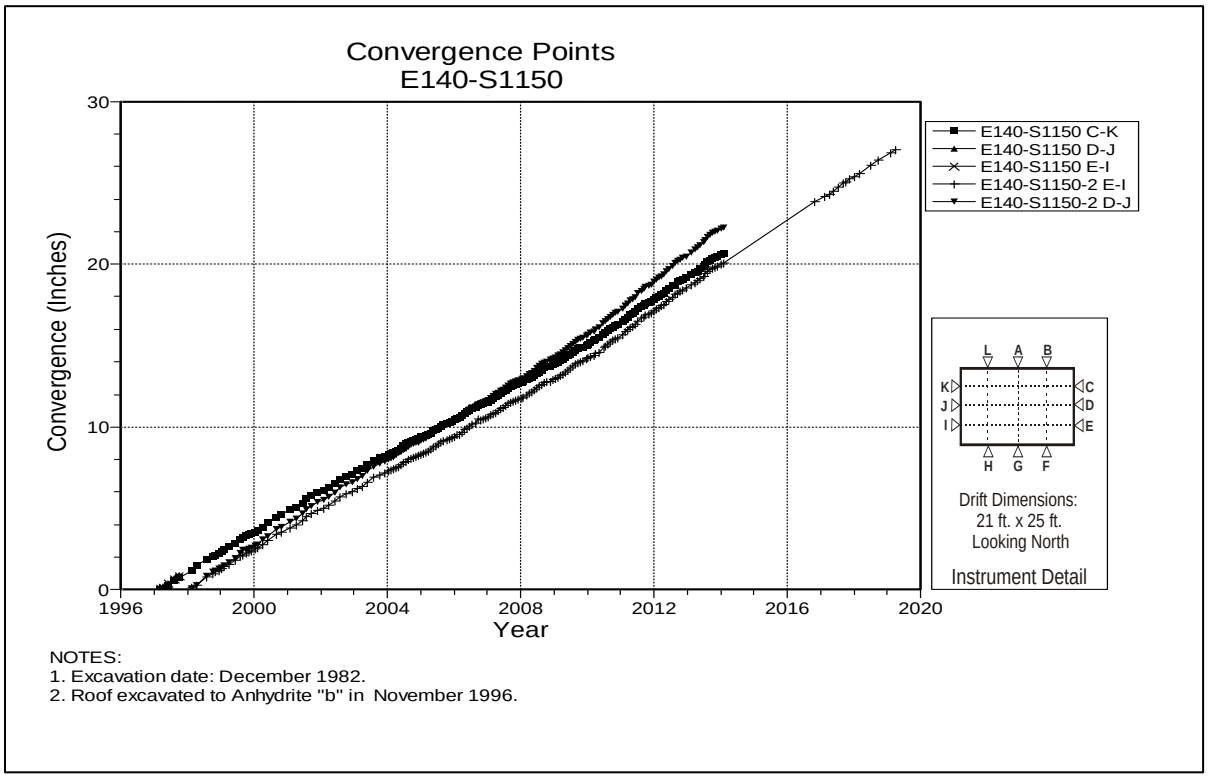

Figure 4-63 Convergence Point Array – E140 S1150 – Rib to Rib

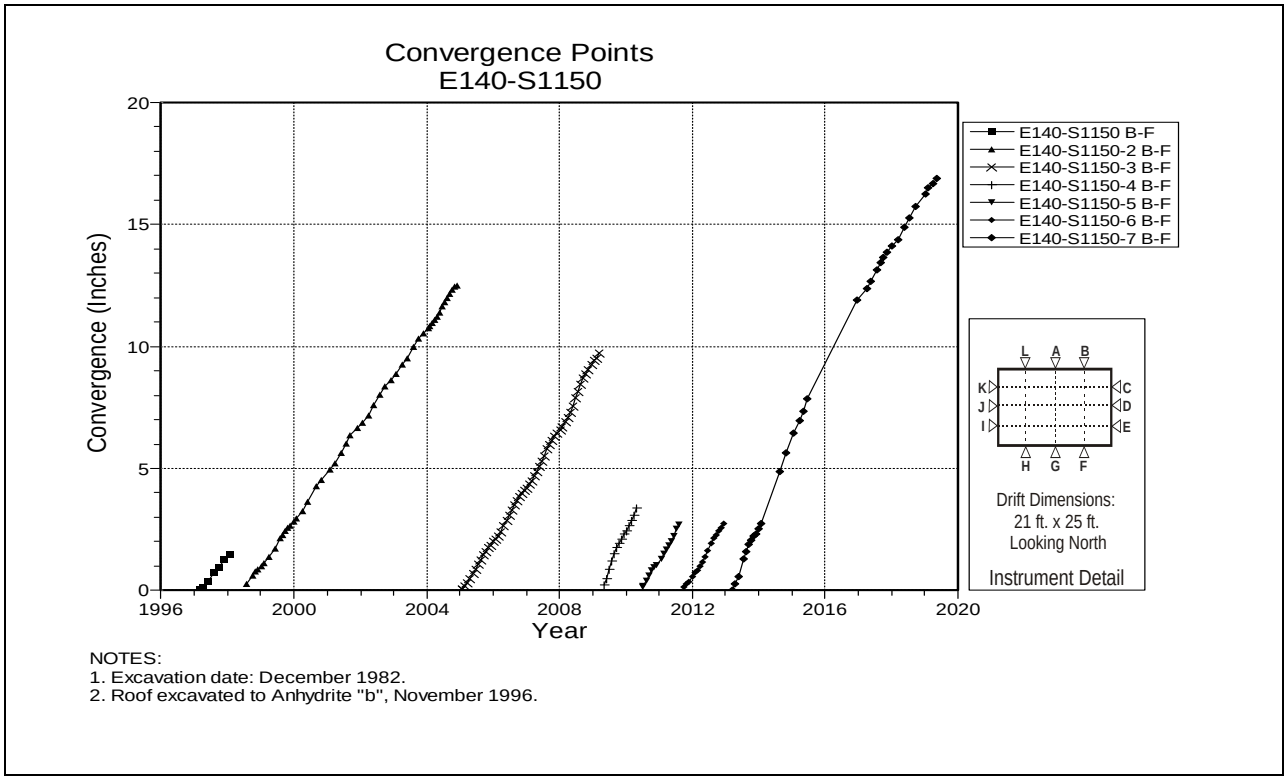

Figure 4-64 Convergence Point Array – E140 S1150 – Roof-to-Floor – East Quarter Point

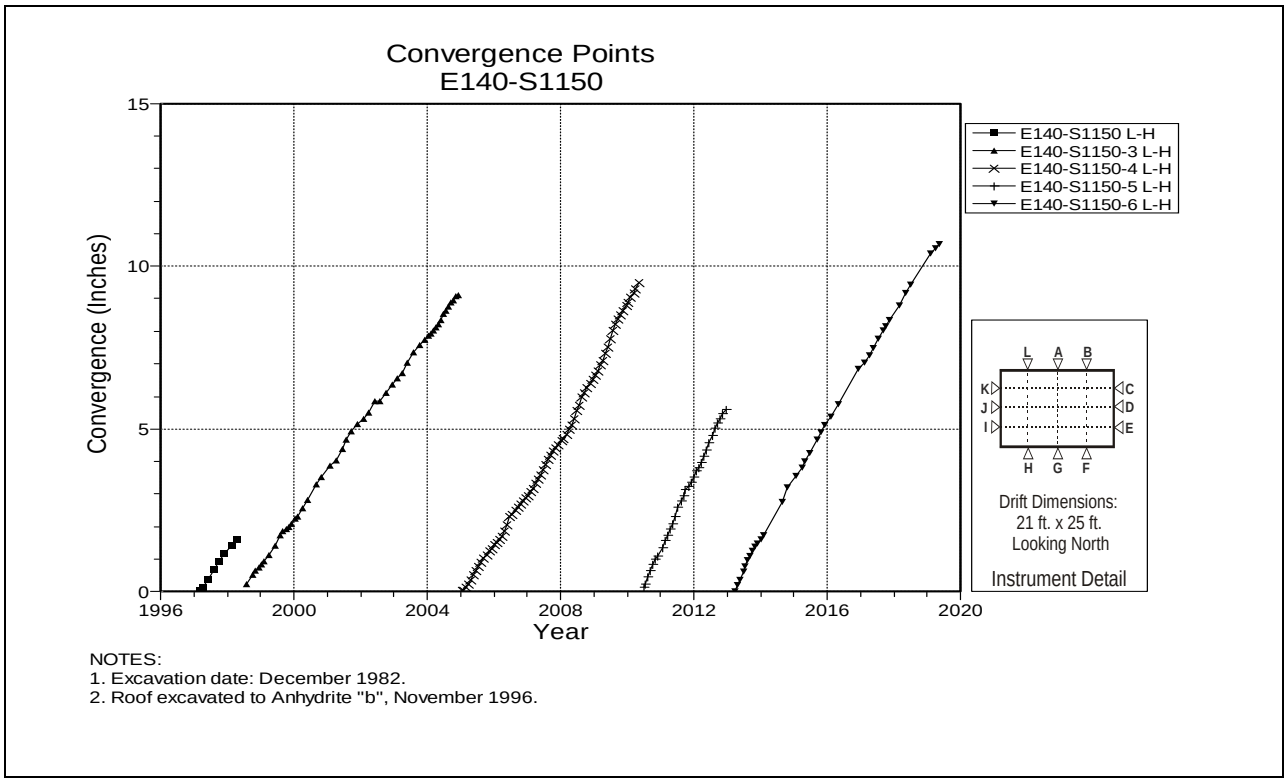

Figure 4-65 Convergence Point Array – E140 S1150 – Roof to Floor – West Quarter Point

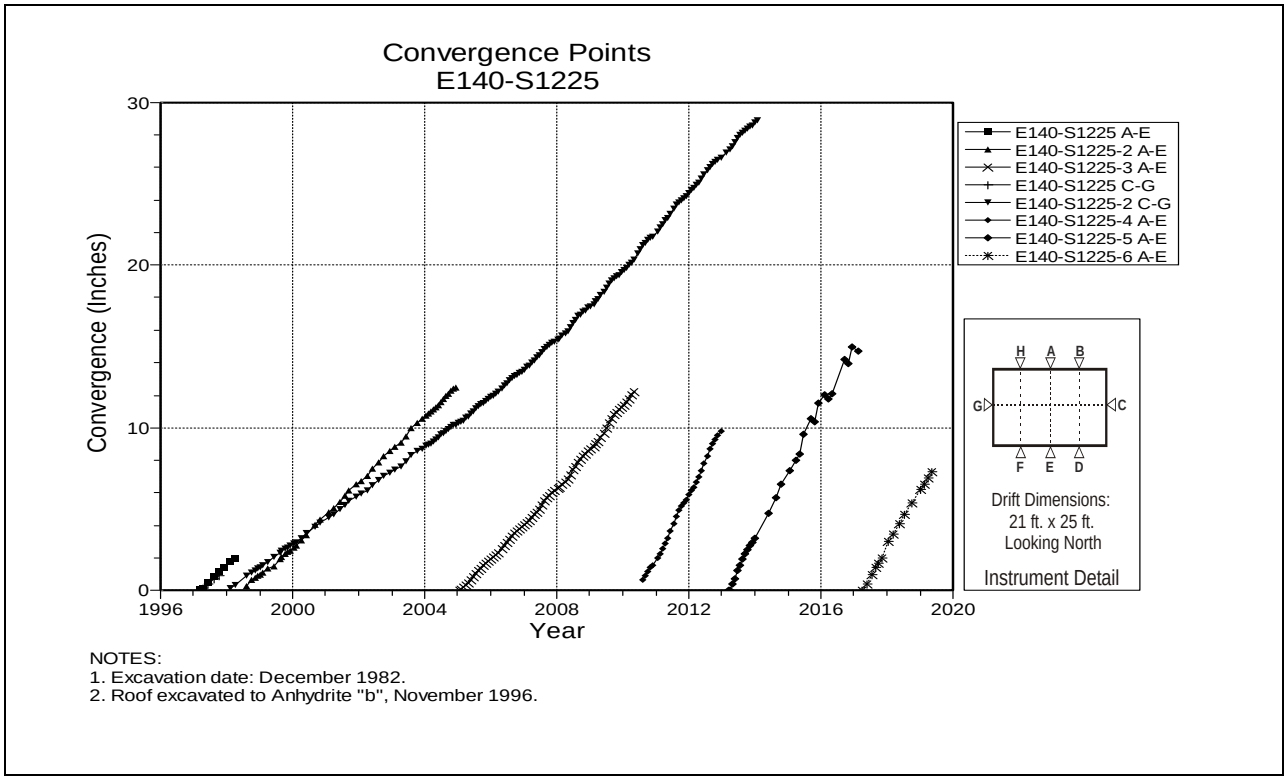

Figure 4-66 Convergence Point Array – E140 S1225 – Roof to Floor – Centerline and Rib-to-Rib

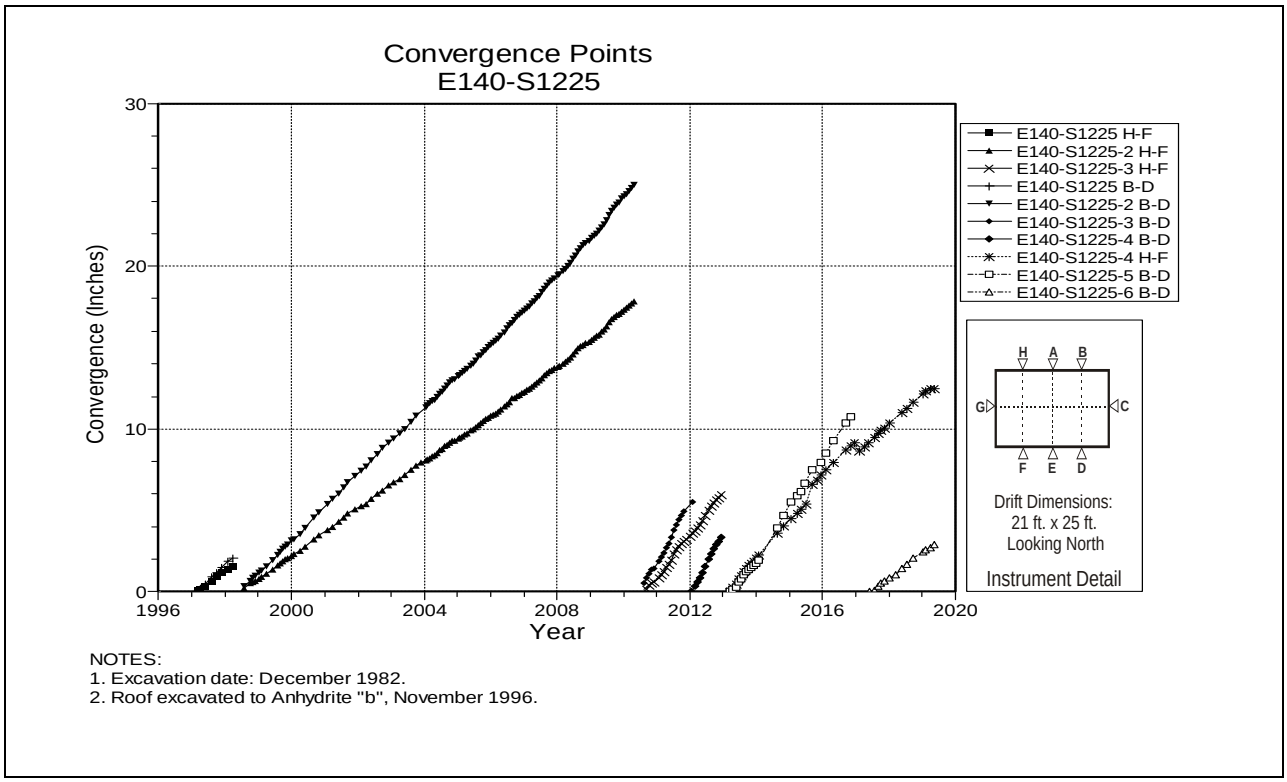

Figure 4-67 Convergence Point Array – E140 S1225 – Roof to Floor – Quarter Points

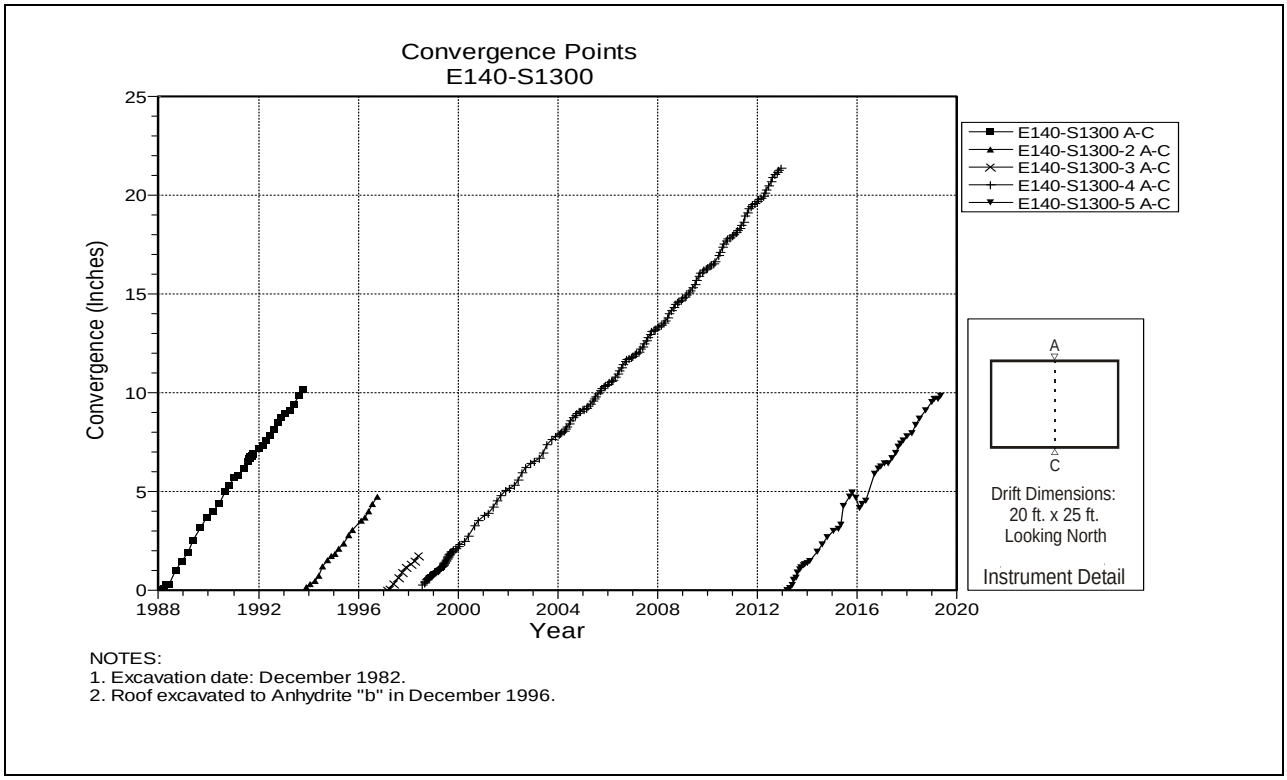

Figure 4-68 Convergence Point Array – E140 S1300 – Roof to Floor – Centerline

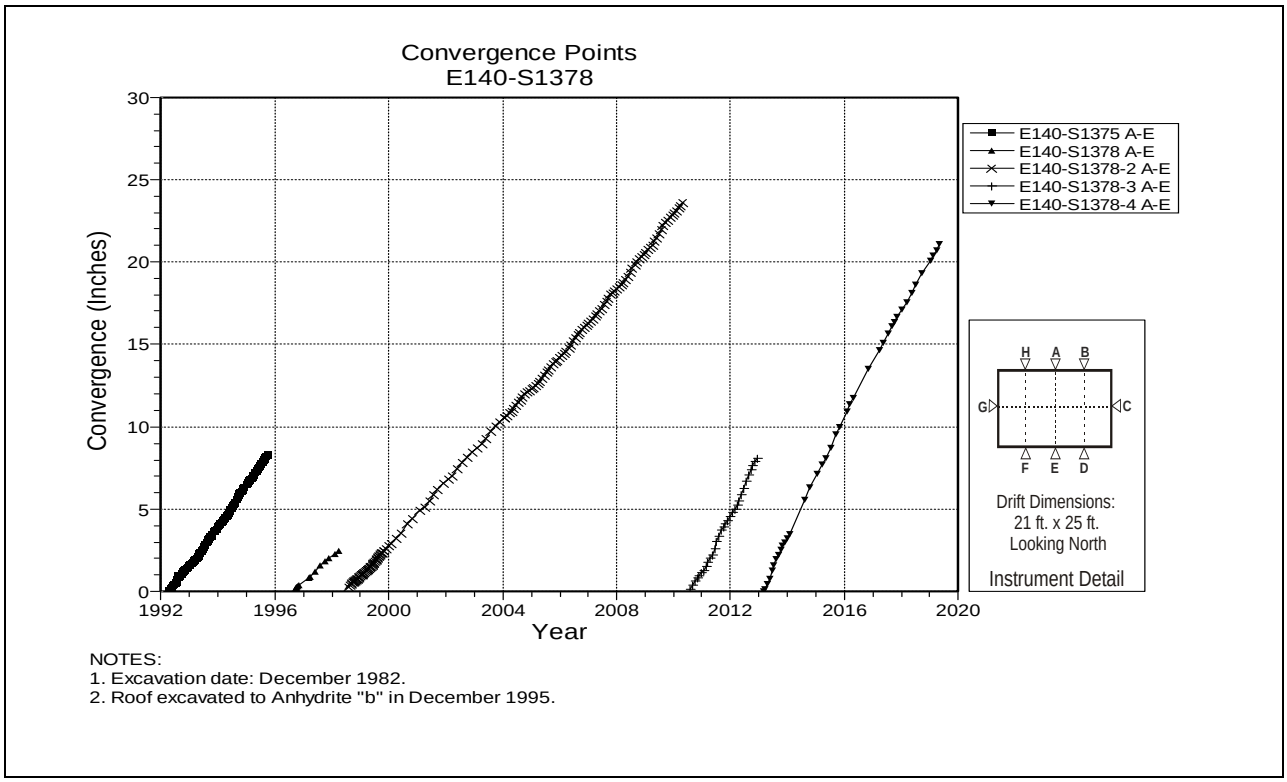

Figure 4-69 Convergence Point Array – E140 S1378 – Roof to Floor – Centerline

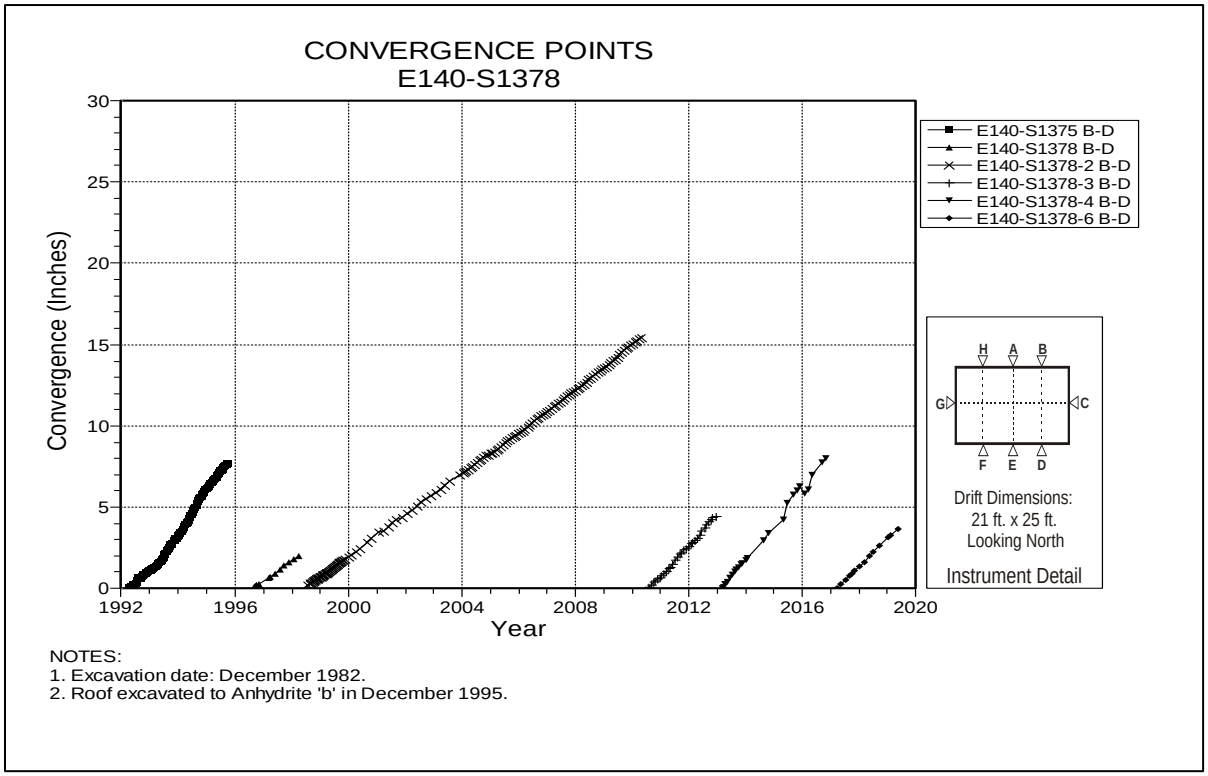

Figure 4-70 Convergence Point Array – E140 S1378 – Roof to Floor – East Quarter Point

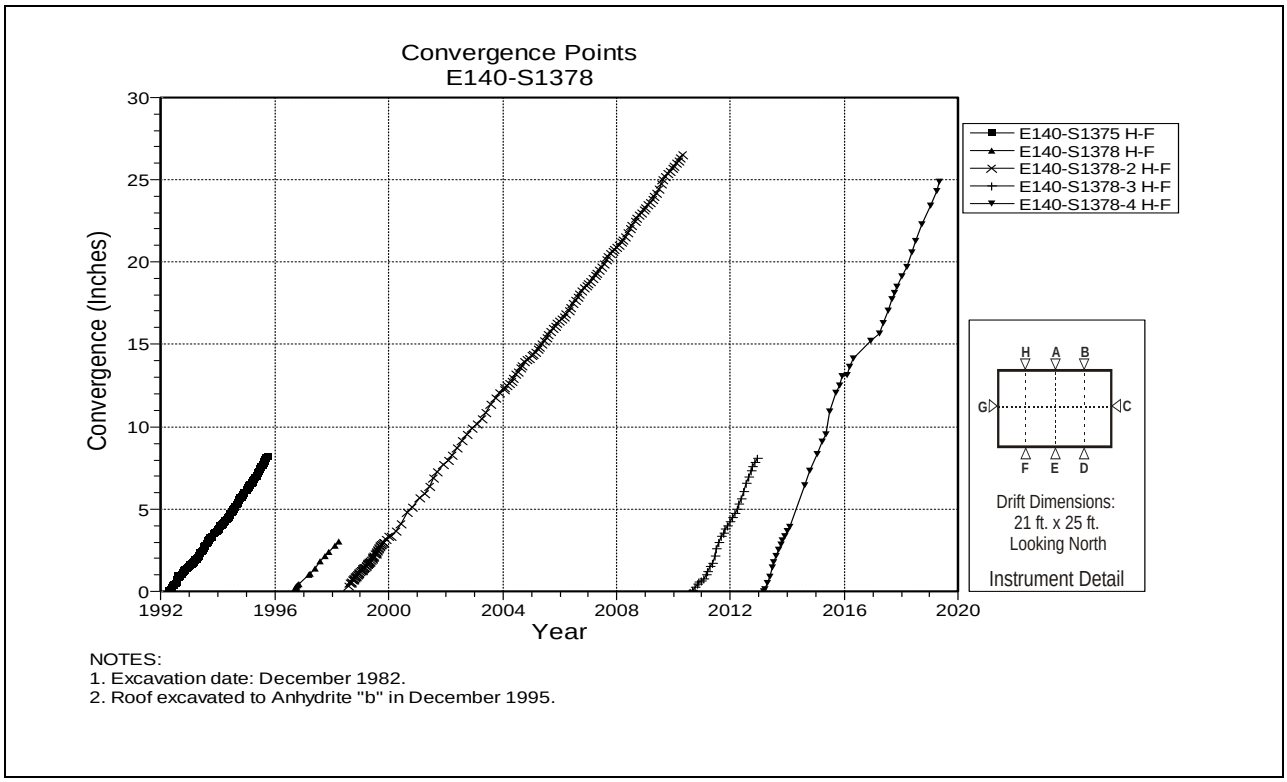

Figure 4-71 Convergence Point Array – E140 S1378 – Roof to Floor – West Quarter Point

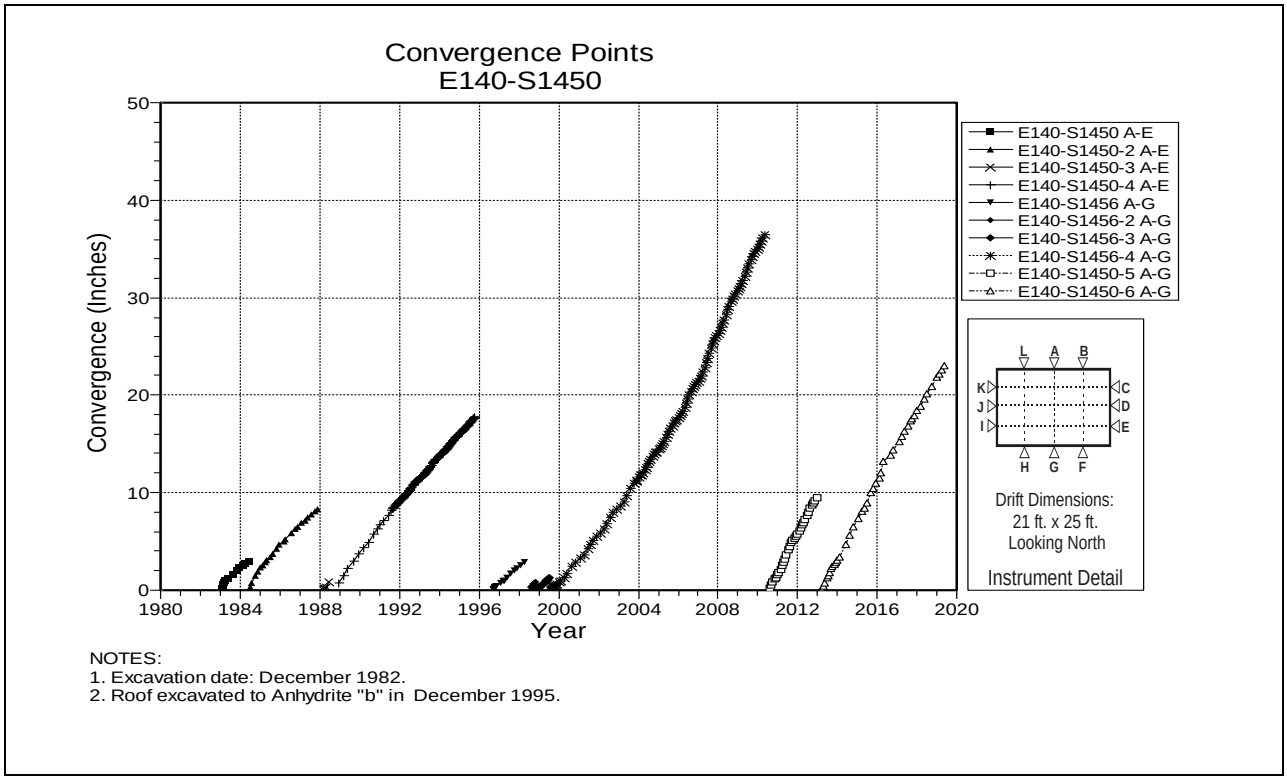

Figure 4-72 Convergence Point Array – E140 S1450 – Roof to Floor – Centerline

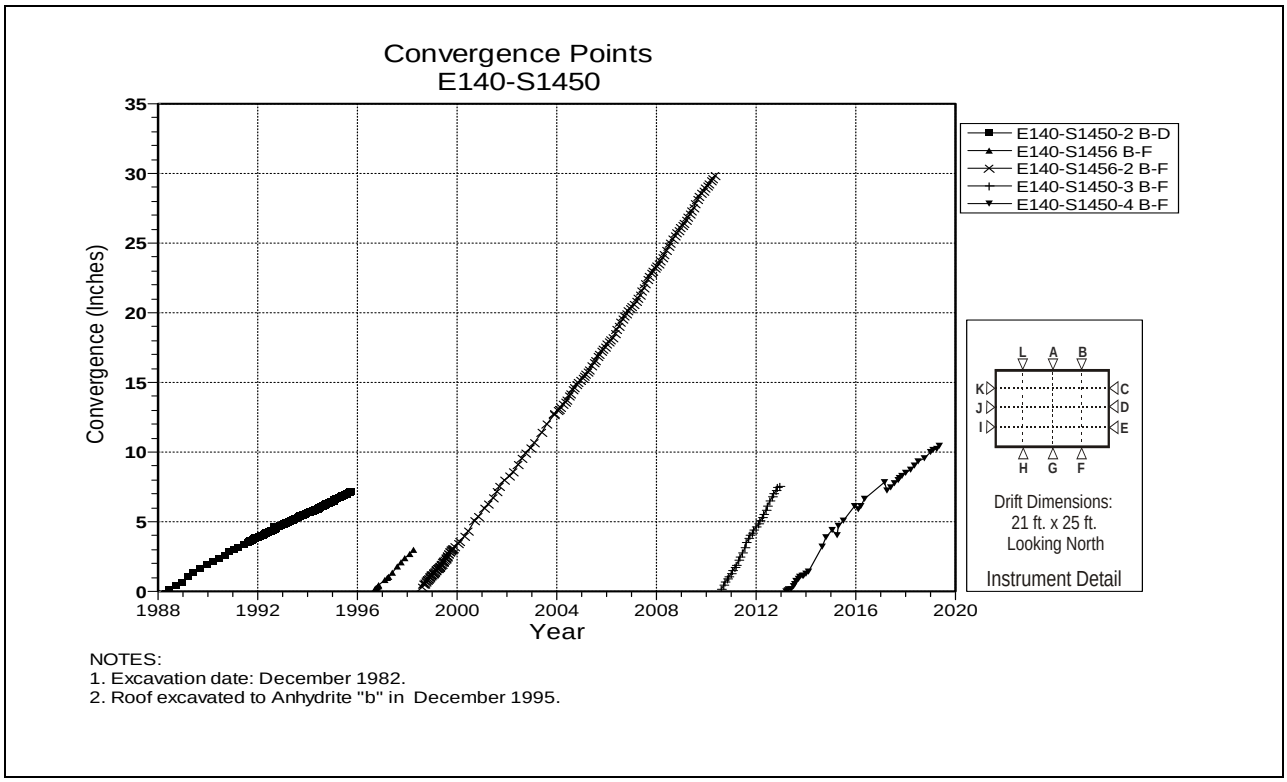

NOTES:
1. Excavation date: December 1982.
2. Roof excavated to Anhydrite "b" in December 1995.

Figure 4-73 Convergence Point Array – E140 S1450 – Roof to Floor – East Quarter Point

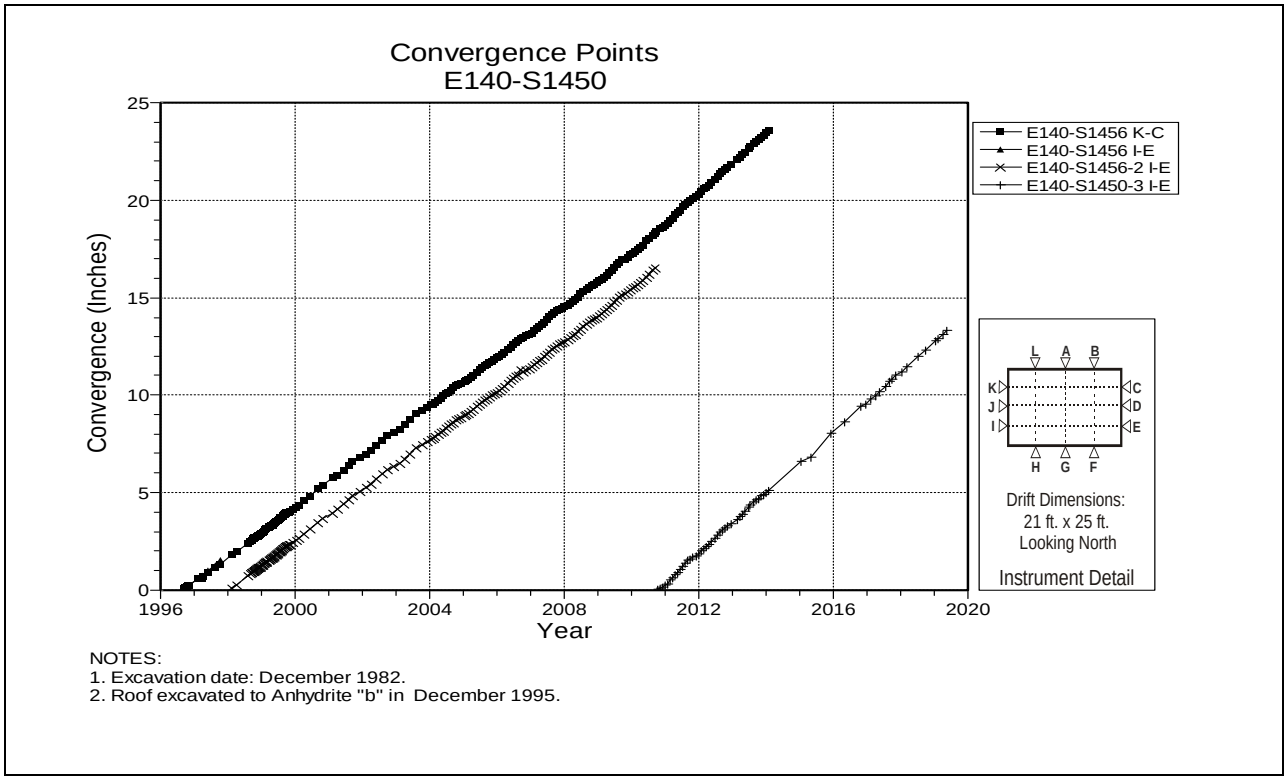

NOTES:
1. Excavation date: December 1982.
2. Roof excavated to Anhydrite "b" in December 1995.

Figure 4-74 Convergence Point Array – E140 S1450 – Rib to Rib

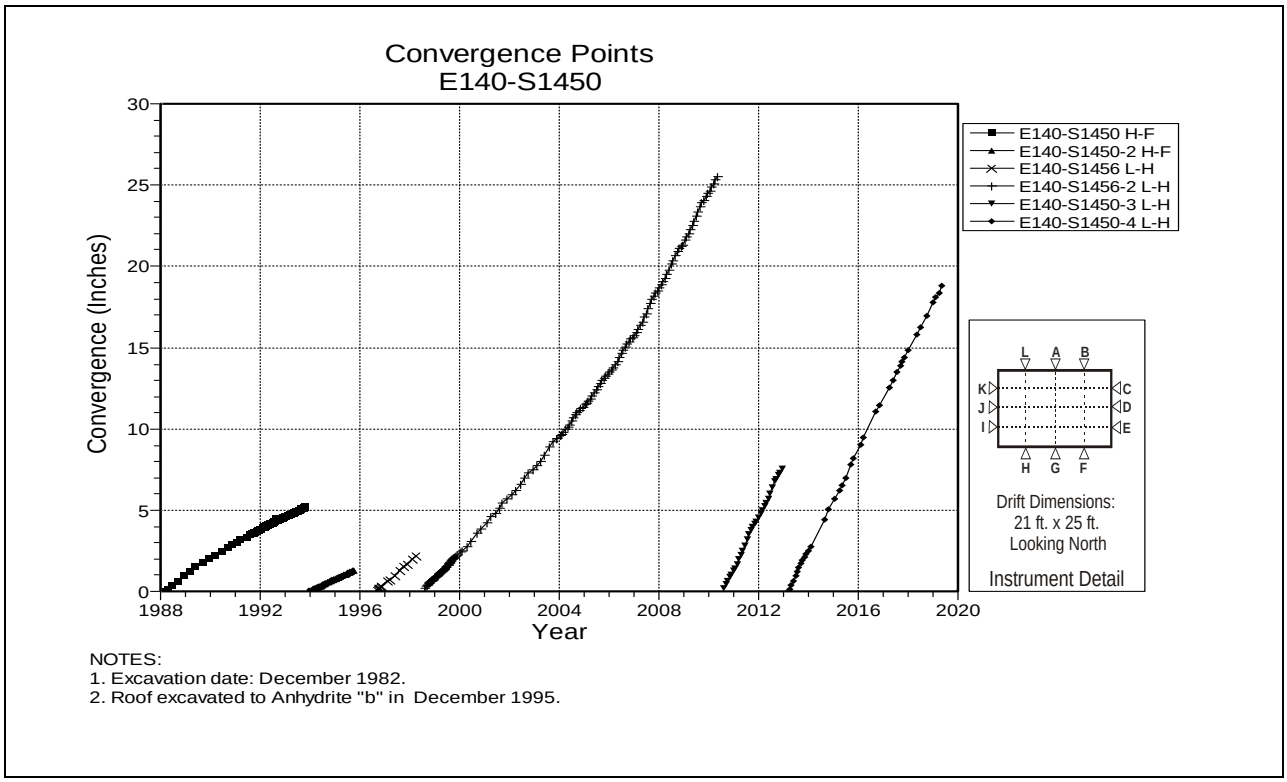

Figure 4-75 Convergence Point Array – E140 S1450 – Roof to Floor – West Quarter Point

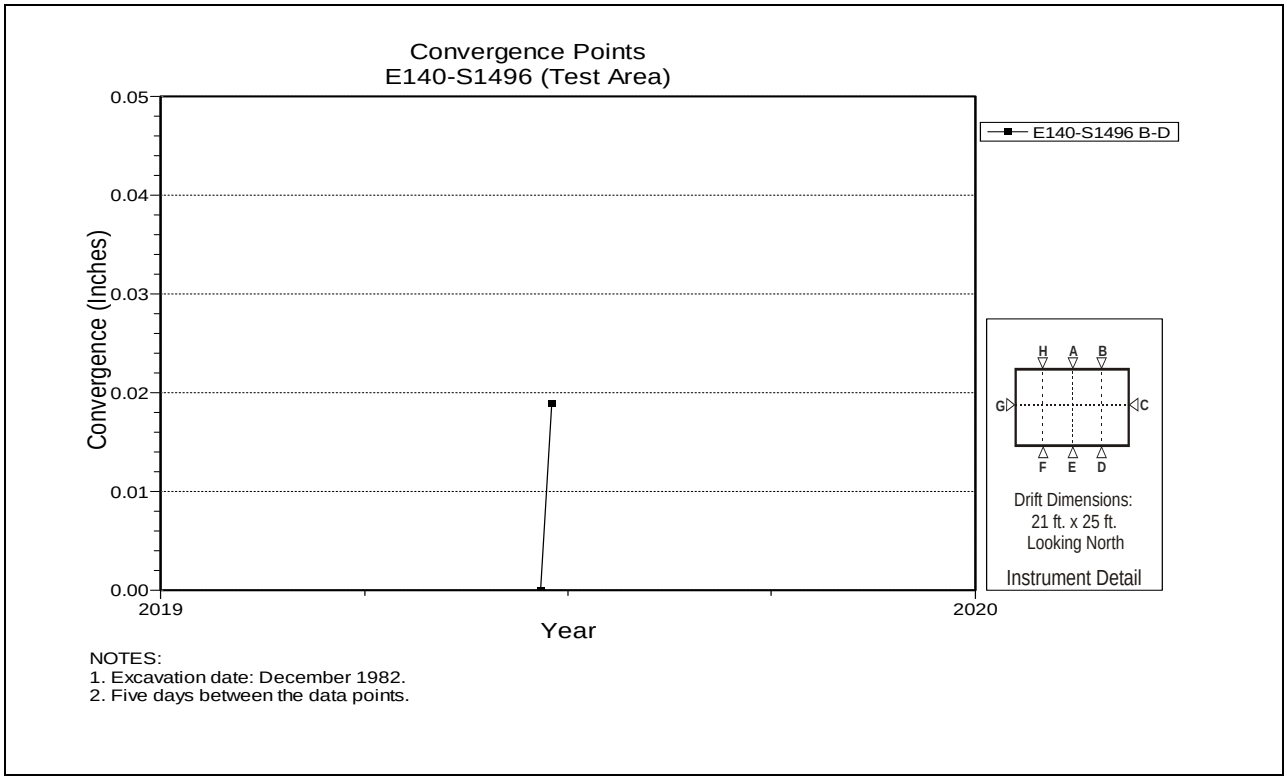

Figure 4-76 Convergence Point Array – E140 S1496 Test Area – Roof to Floor – East Quarter Point

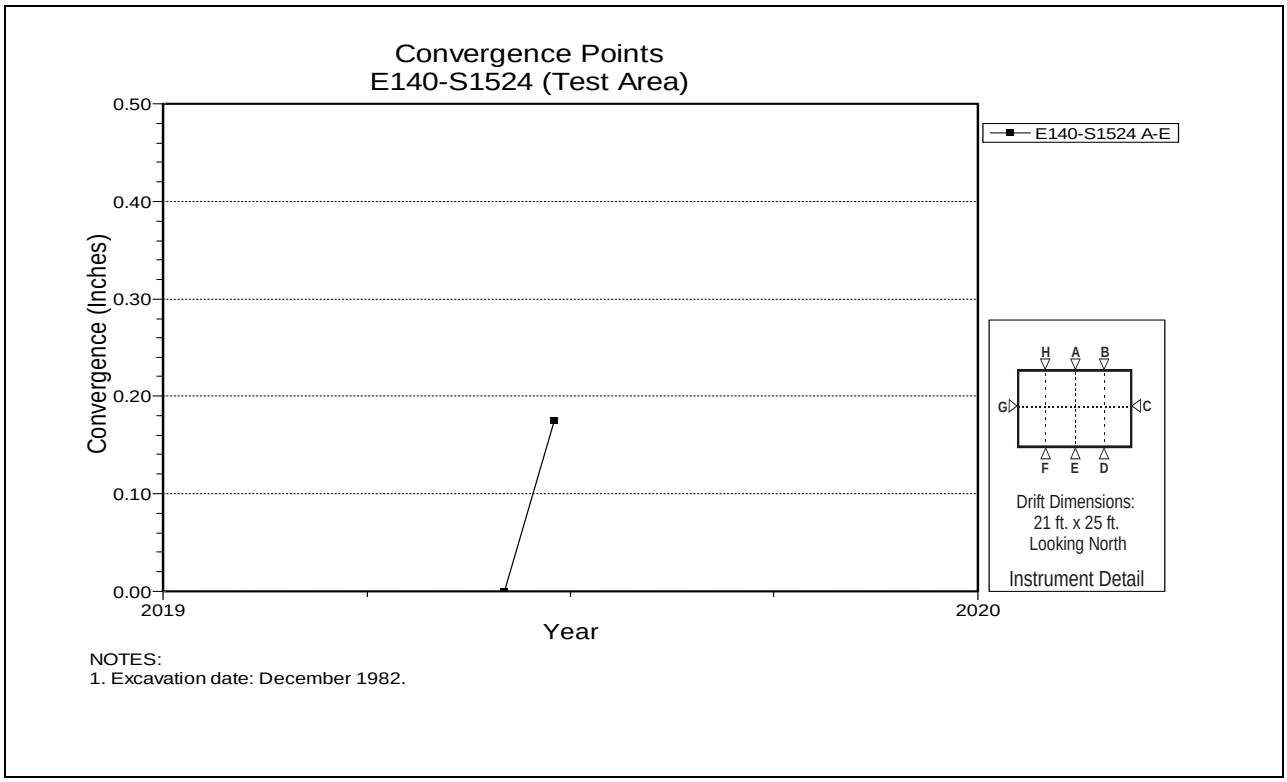

NOTES:
1. Excavation date: December 1982.

Figure 4-77 Convergence Point Array – E140 S1524 Test Area – Roof to Floor – Centerline

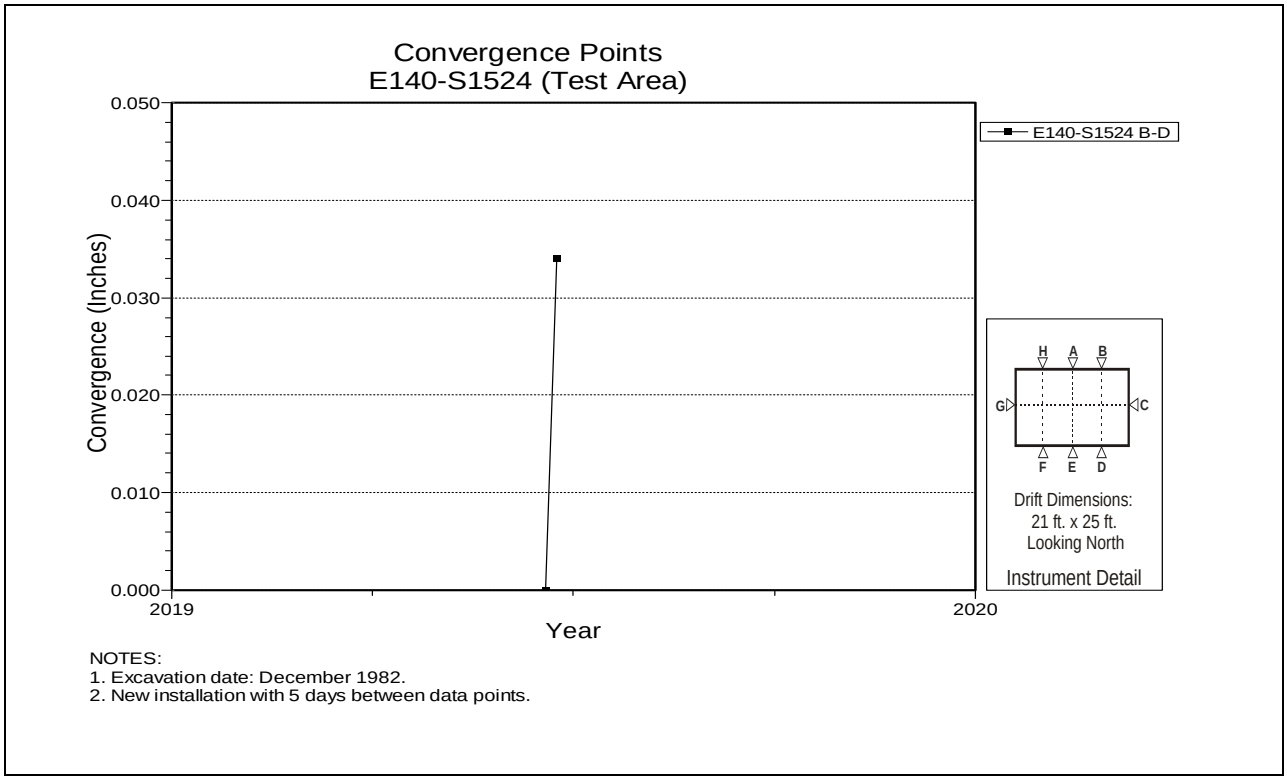

NOTES:
1. Excavation date: December 1982.
2. New installation with 5 days between data points.

Figure 4-78 Convergence Point Array – E140 S1524 Test Area – East Quarter Point

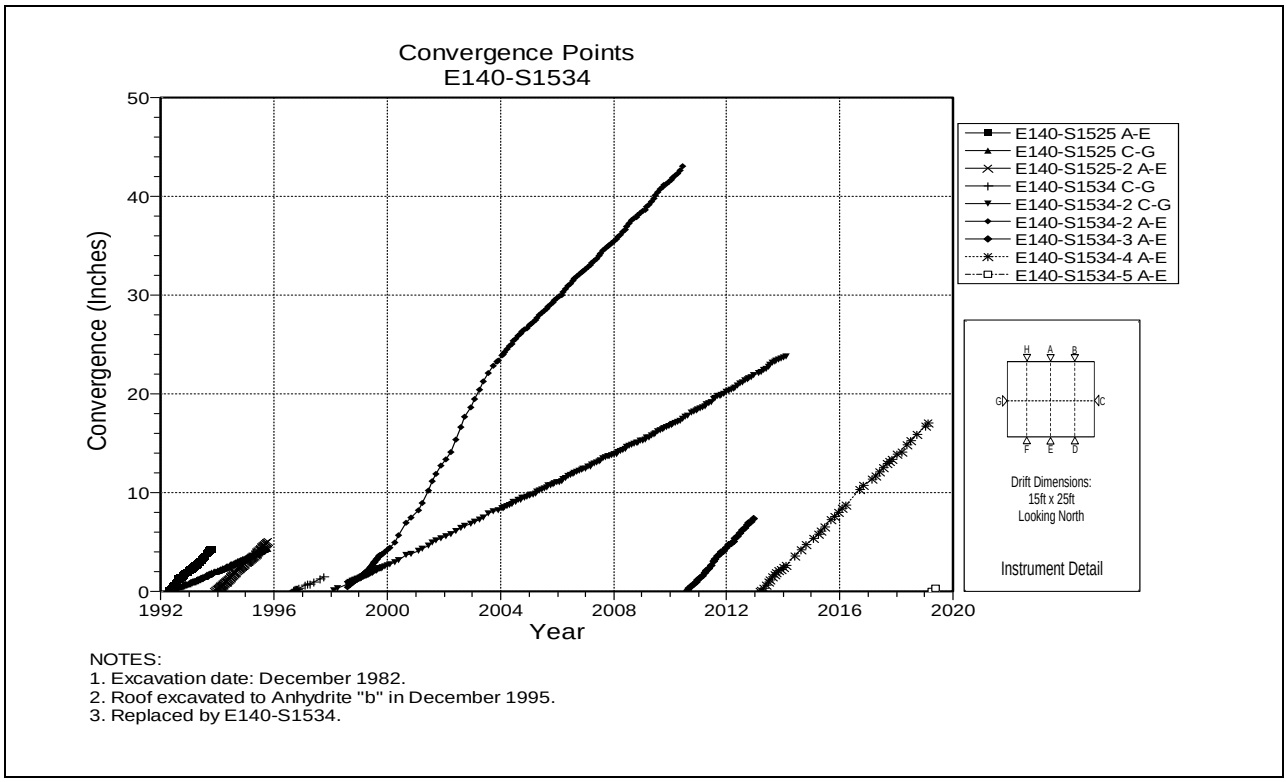

NOTES:
1. Excavation date: December 1982.
2. Roof excavated to Anhydrite "b" in December 1995.
3. Replaced by E140-S1534.

Figure 4-79 Convergence Point Array – E140 S1534 – Roof-to-Floor Centerline & Rib to Rib

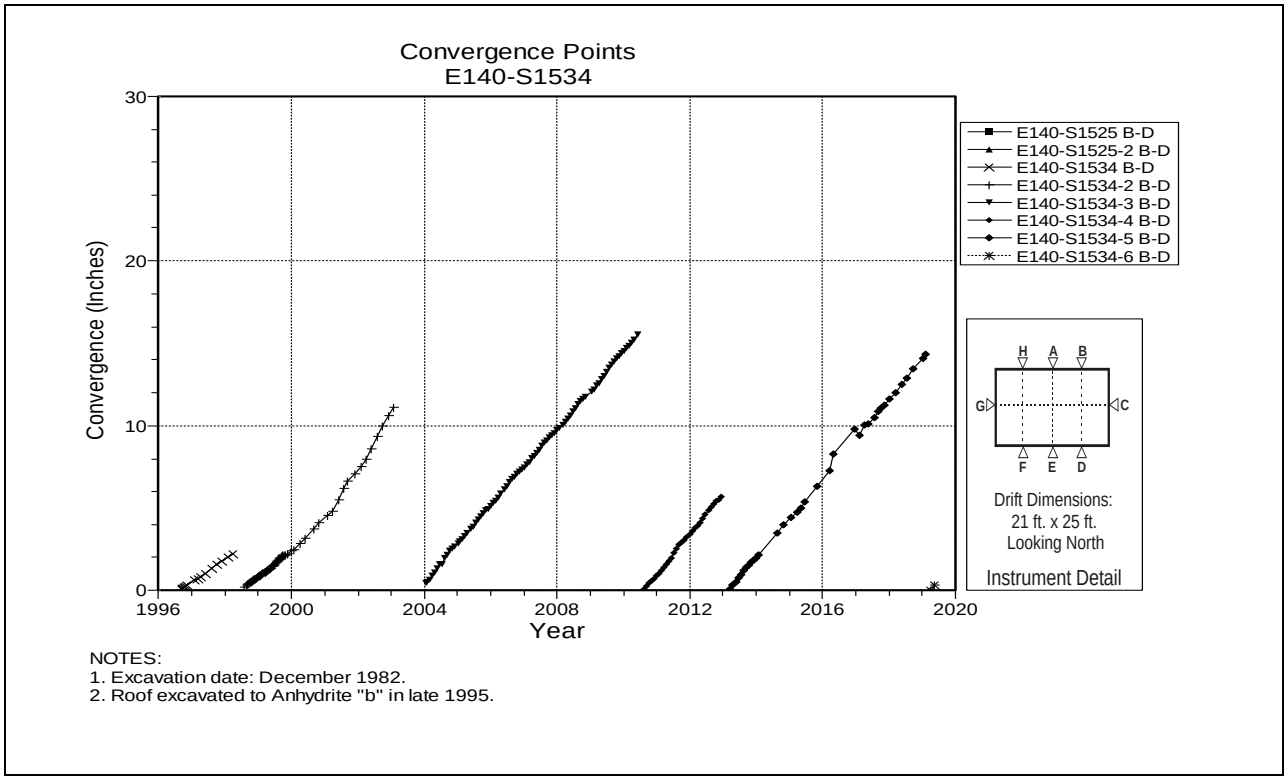

NOTES:
1. Excavation date: December 1982.
2. Roof excavated to Anhydrite "b" in late 1995.

Figure 4-80 Convergence Point Array – E140 S1534 – Roof to Floor – East Quarter Point

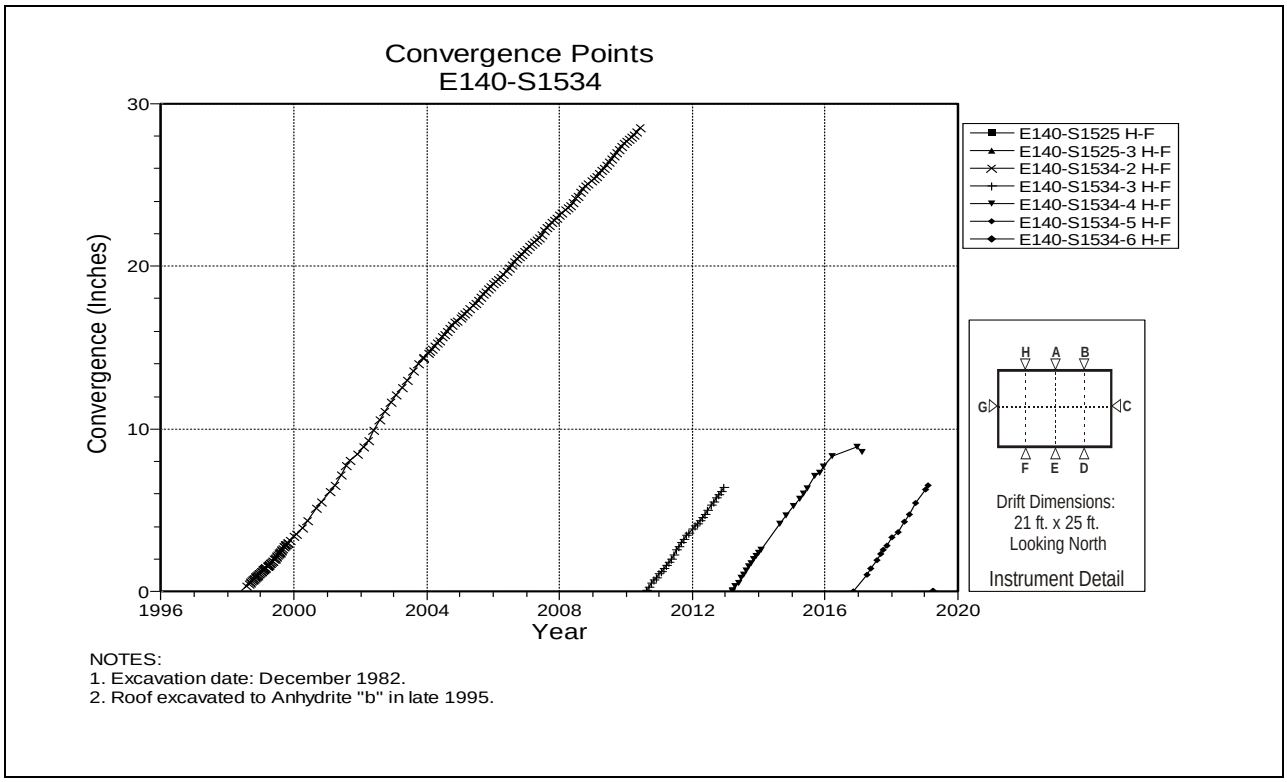

Figure 4-81 Convergence Point Array – E140 S1534 – Roof to Floor – West Quarter Point

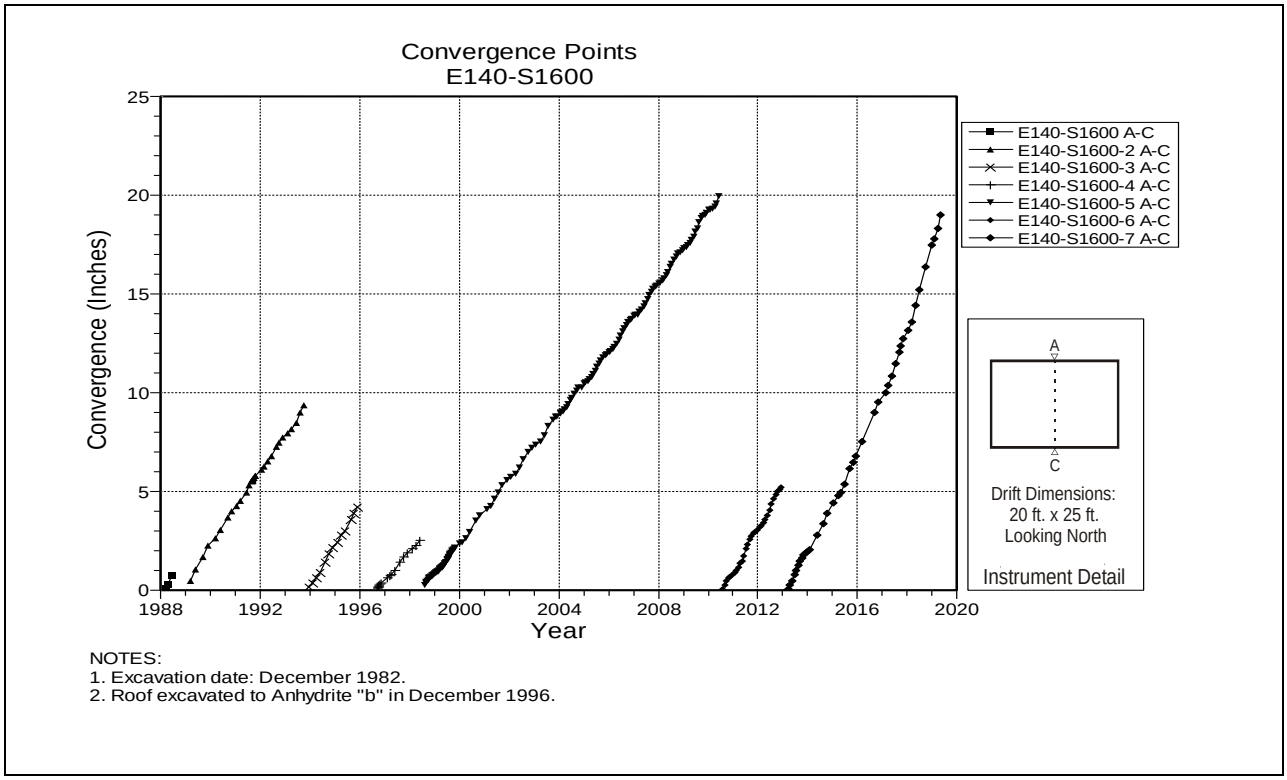

Figure 4-82 Convergence Point Array – E140 S1600 – Roof to Floor – Centerline

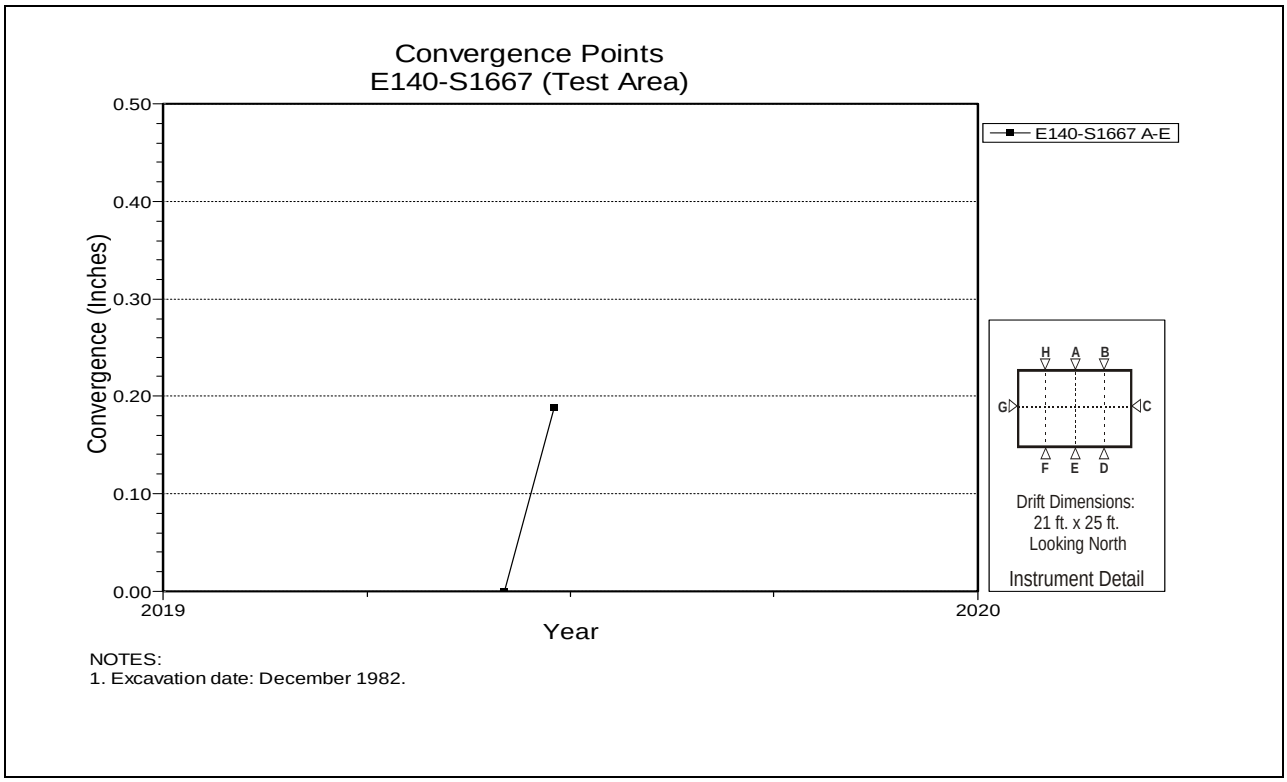

Figure 4-83 Convergence Point Array – E140 S1667 Test Area – Roof to Floor – Centerline

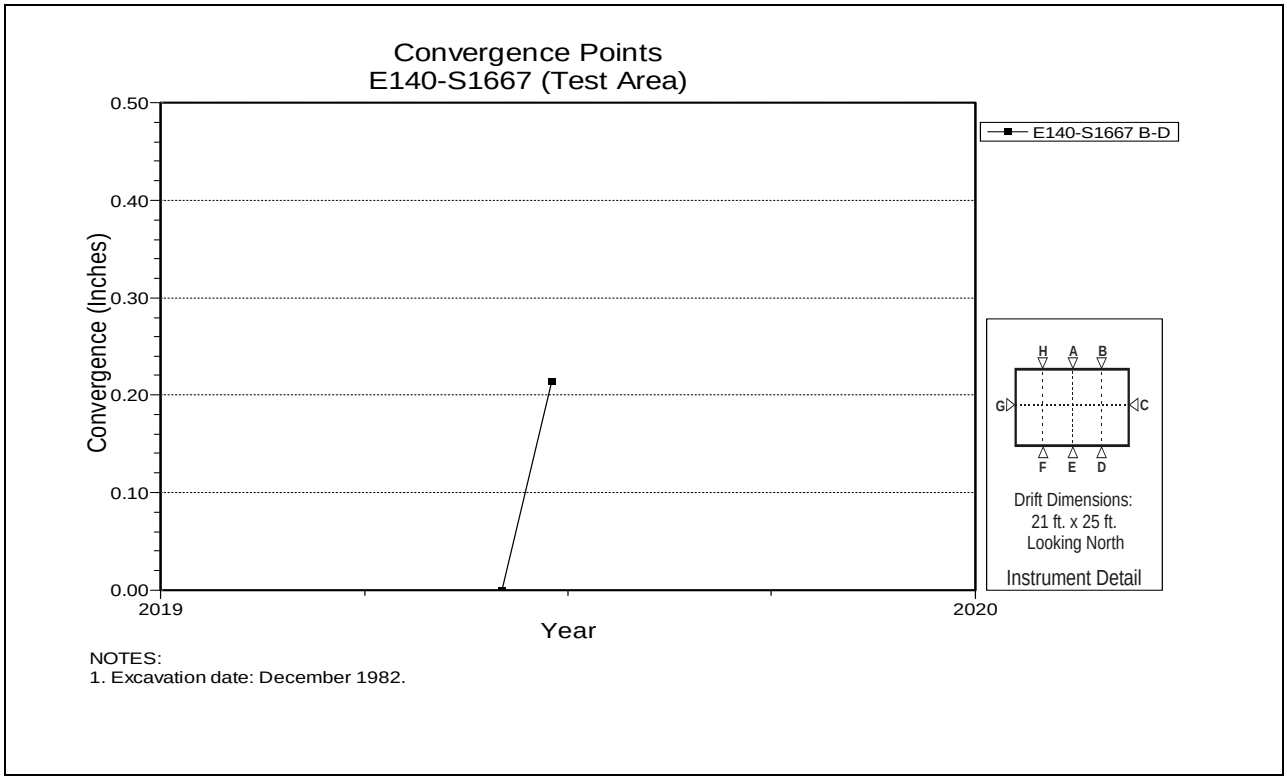

Figure 4-84 Convergence Point Array – E140 S1667 Test Area – East Quarter Point

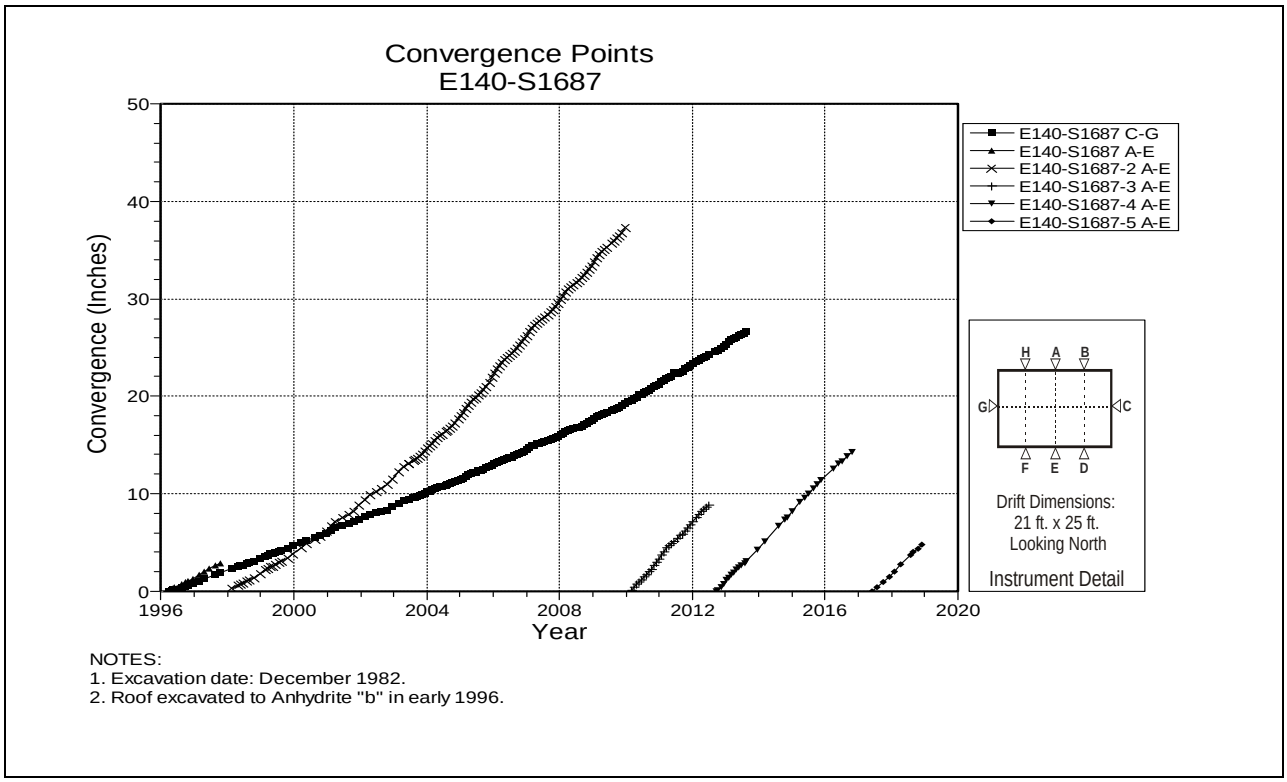

Figure 4-85 Convergence Point Array – E140 S1687– Roof-to-Floor – Centerline and Rib to Rib

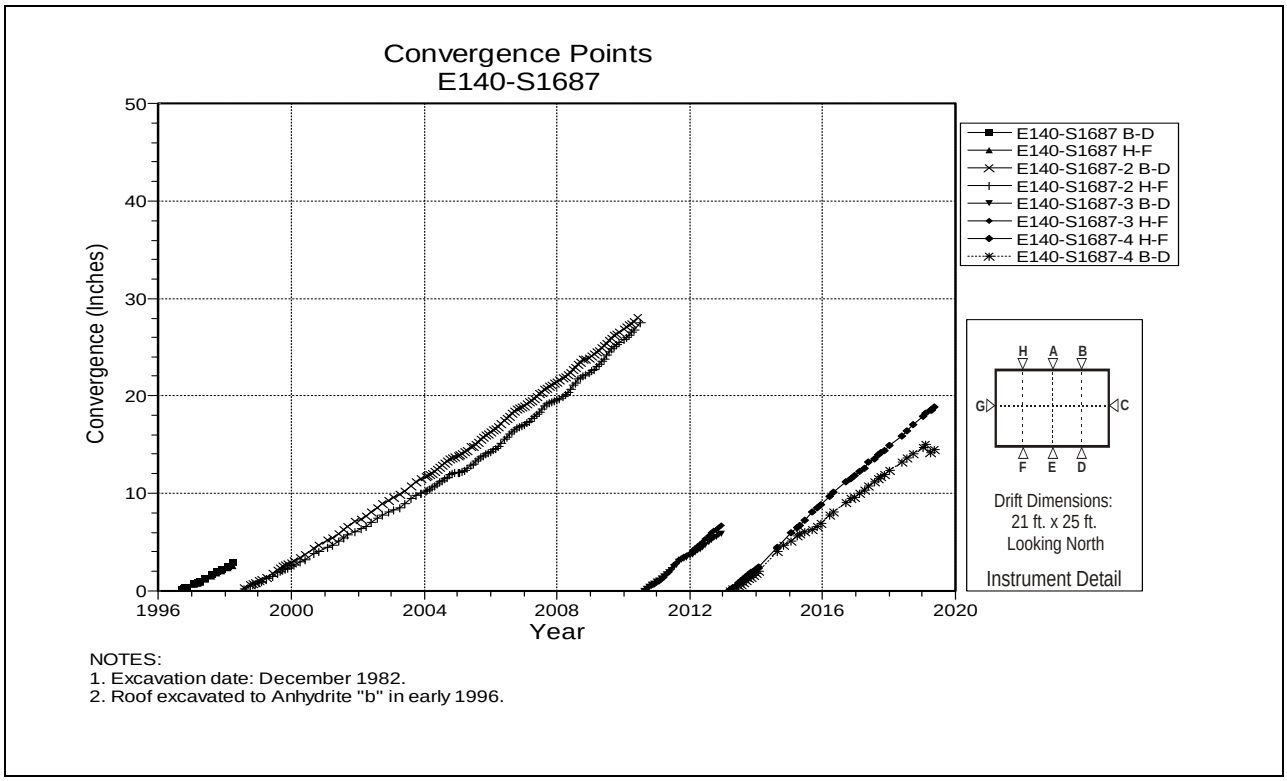

Figure 4-86 Convergence Point Array – E140 S1687 – Roof to Floor – Quarter Points

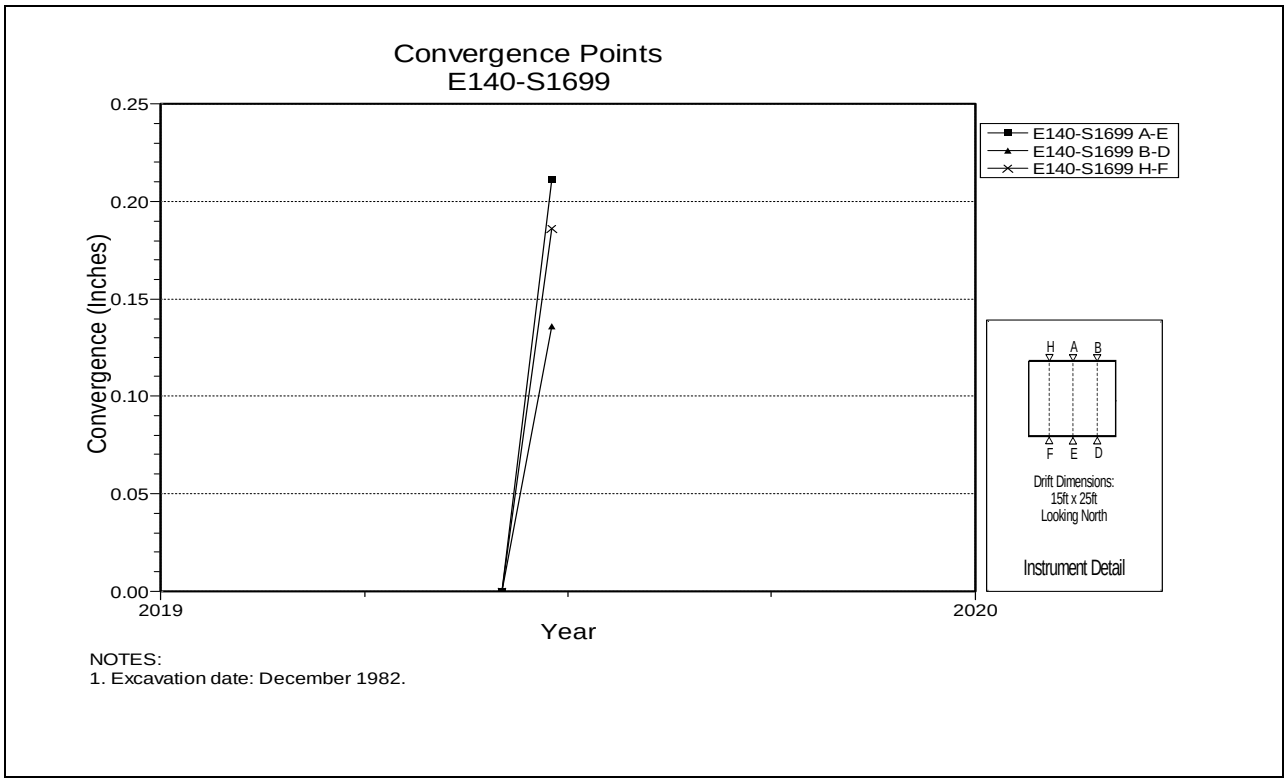

NOTES:
1. Excavation date: December 1982.

Figure 4-87 Convergence Point Array – E140 S1699 Test Area – Roof to Floor – Centerline & Quarter Points

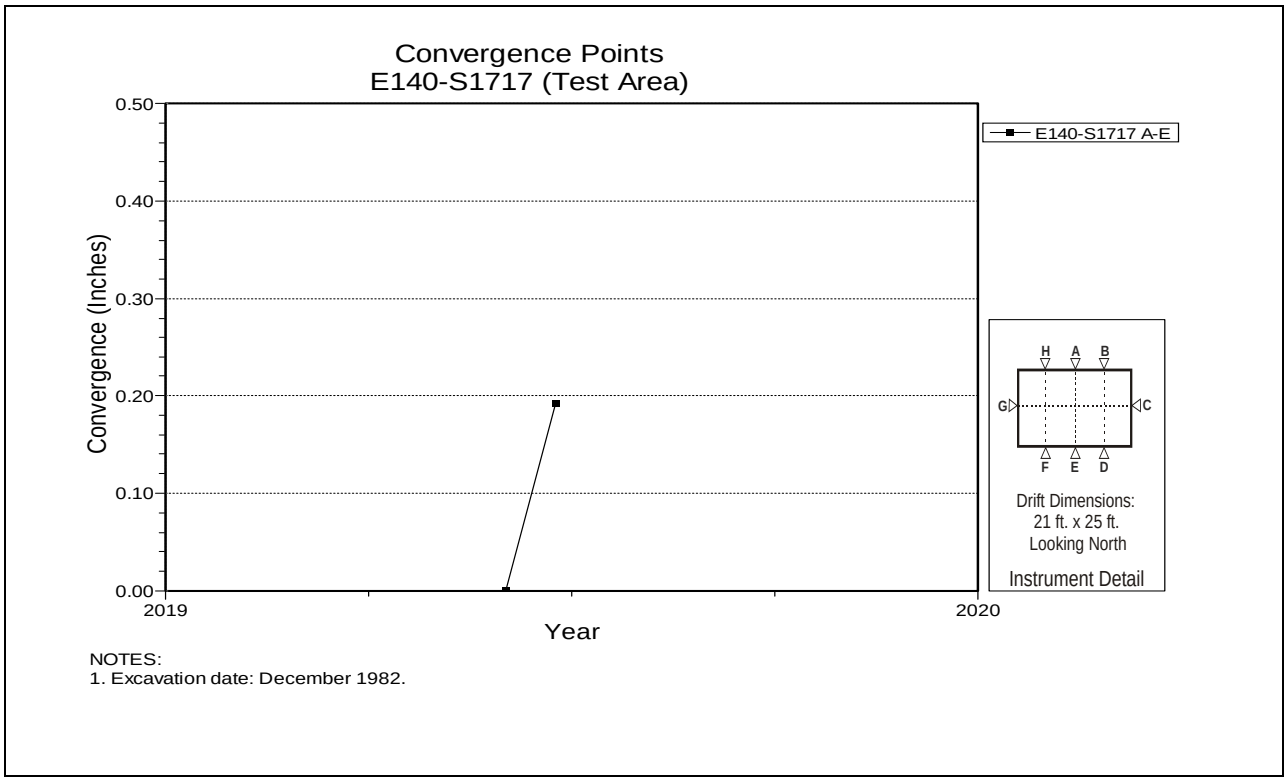

NOTES:
1. Excavation date: December 1982.

Figure 4-88 Convergence Point Array – E140 S1717 Test Area – Roof to Floor – Centerline

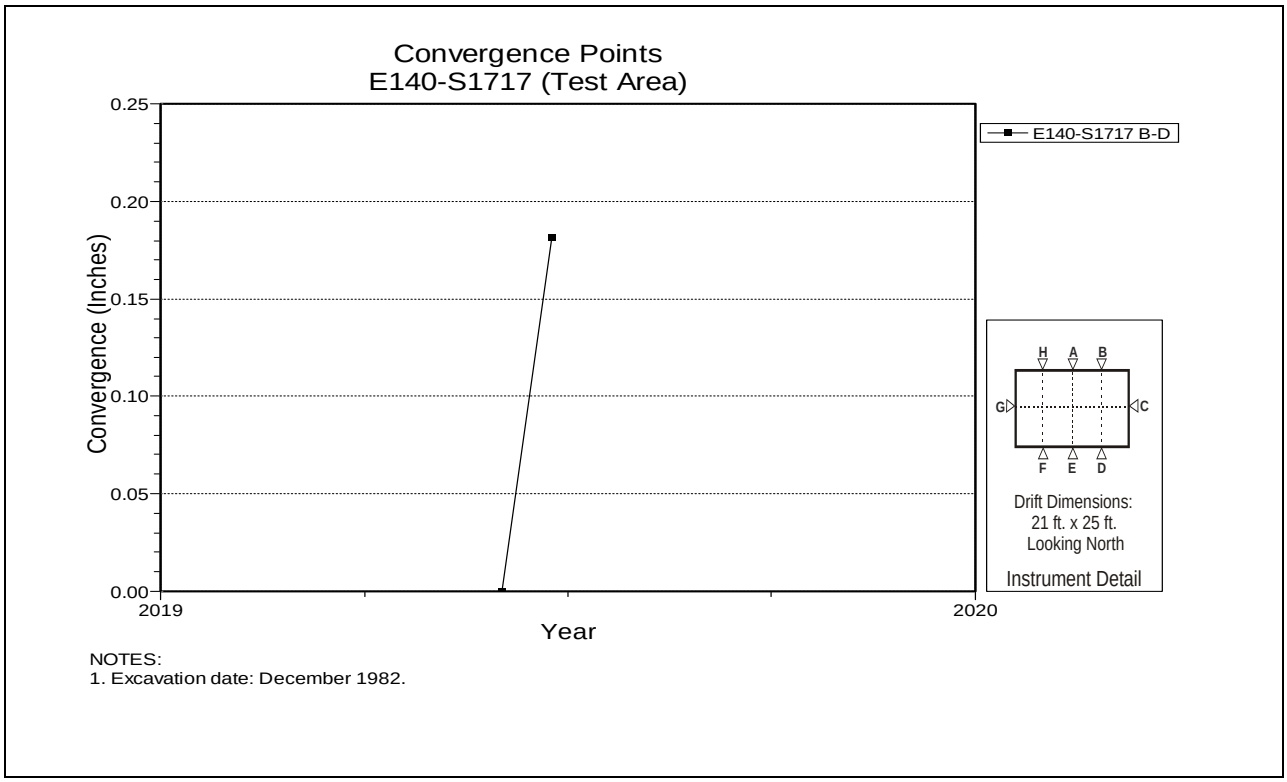

Figure 4-89 Convergence Point Array – E140 S1717 Test Area – Roof to Floor – East Quarter Point

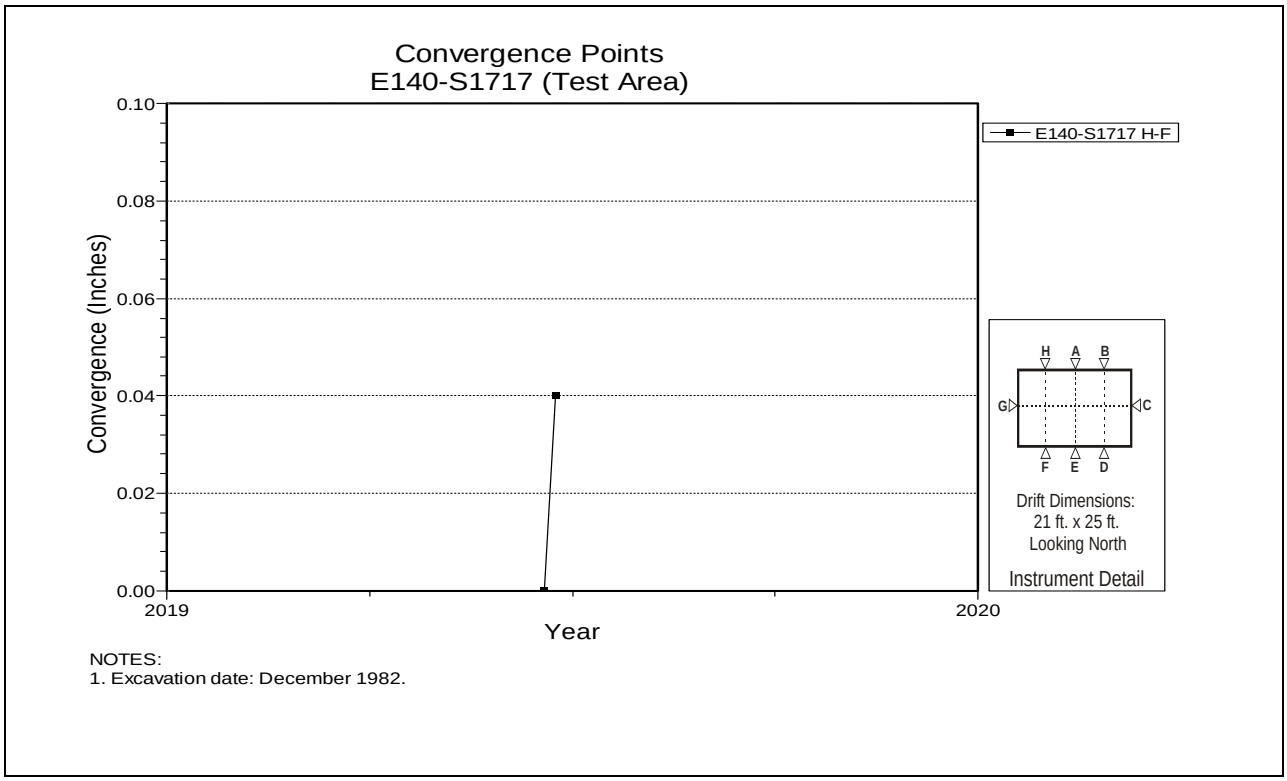

Figure 4-90 Convergence Point Array – E140 S1717 Test Area – Roof to Floor – West Quarter Point

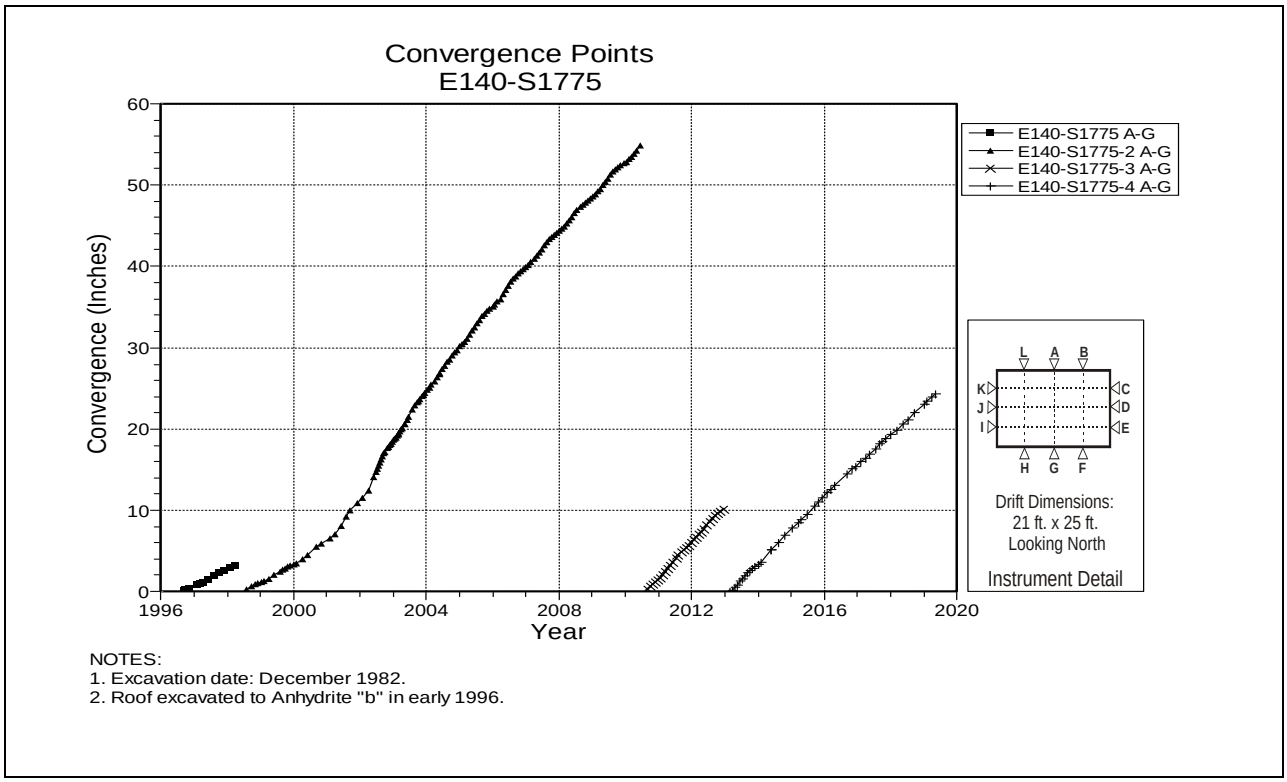

Figure 4-91 Convergence Point Array – E140 S1775 – Roof to Floor – Centerline

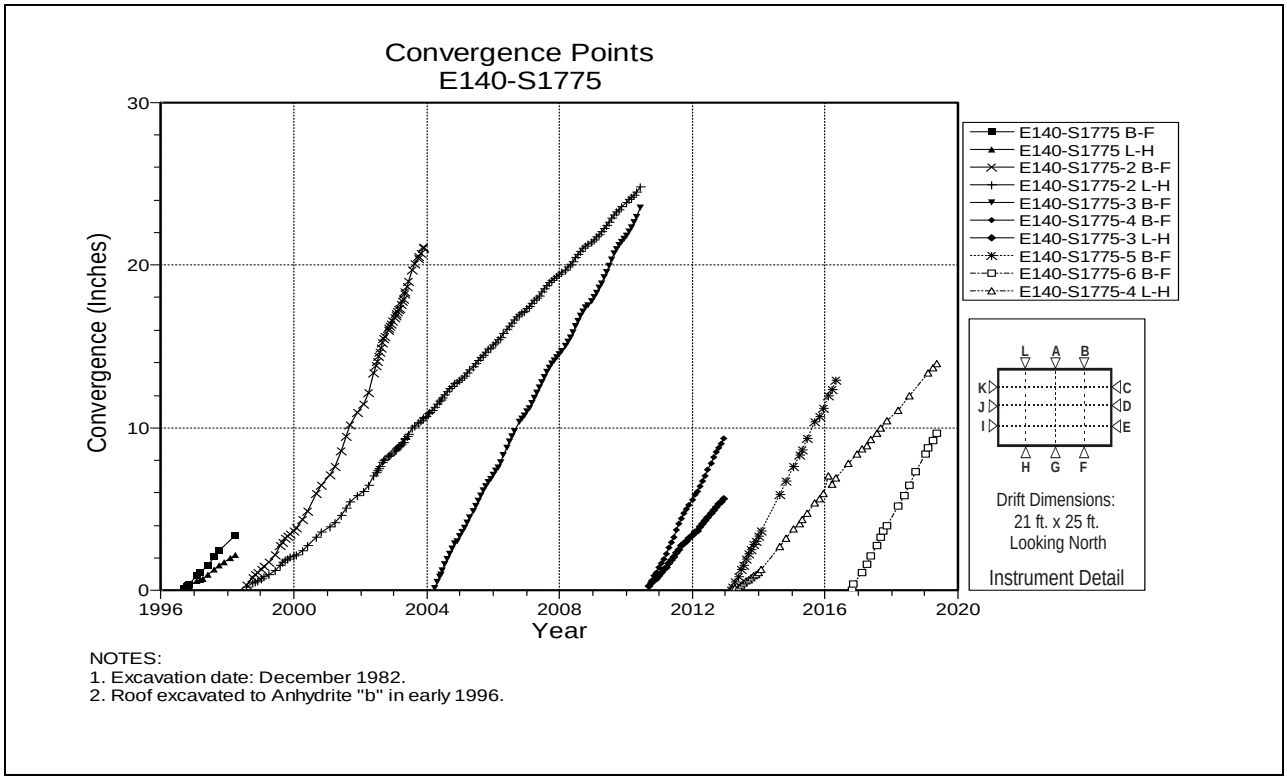

Figure 4-92 Convergence Point Array – E140 S1775 – Roof to Floor – Quarter Points

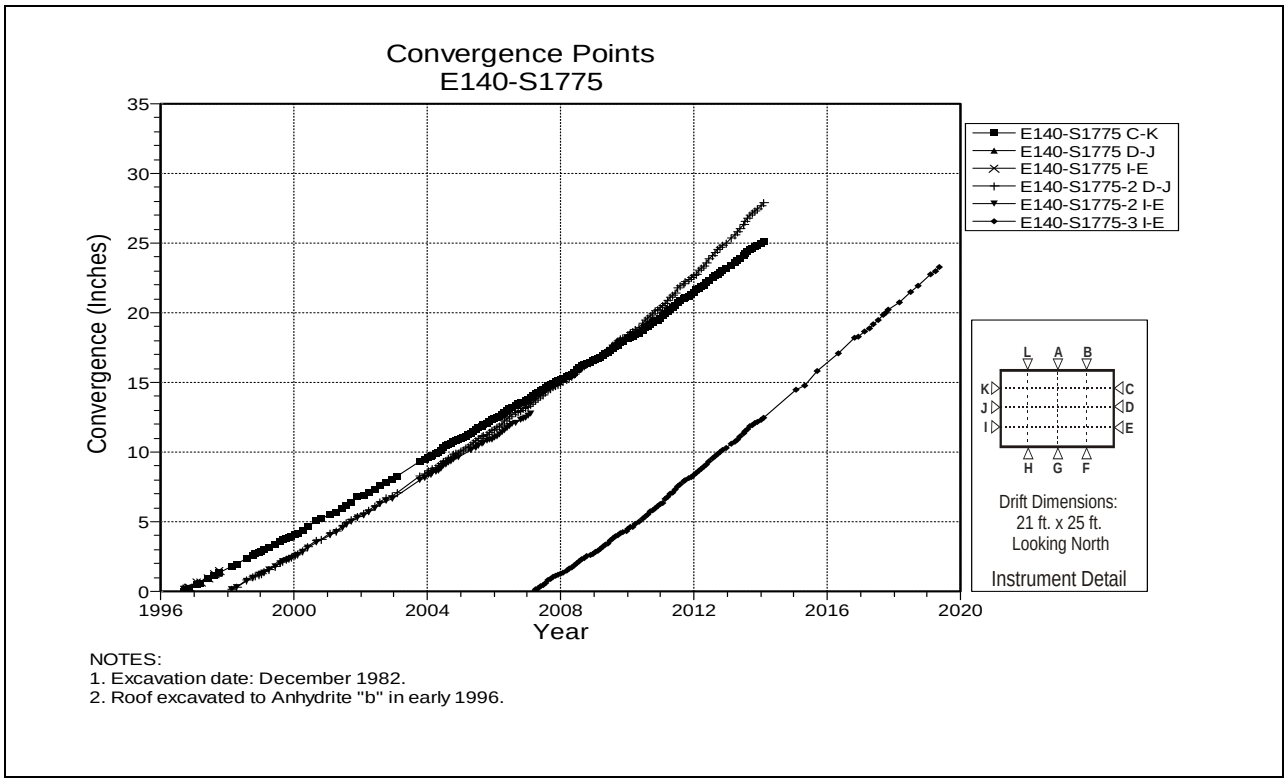

Figure 4-93 Convergence Point Array – E140 S1775 – Rib to Rib

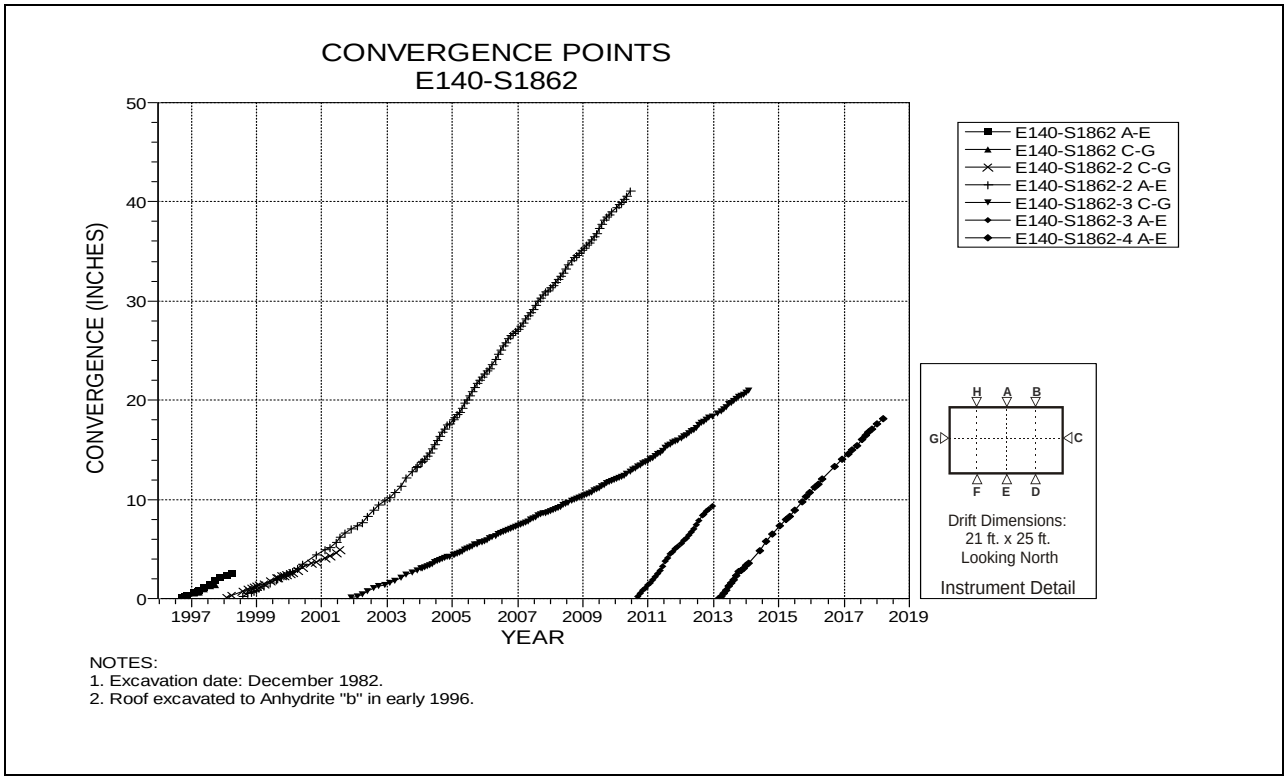

Figure 4-94 Convergence Point Array – E140 S1862 – Roof to Floor – Centerline & Rib-to-Rib

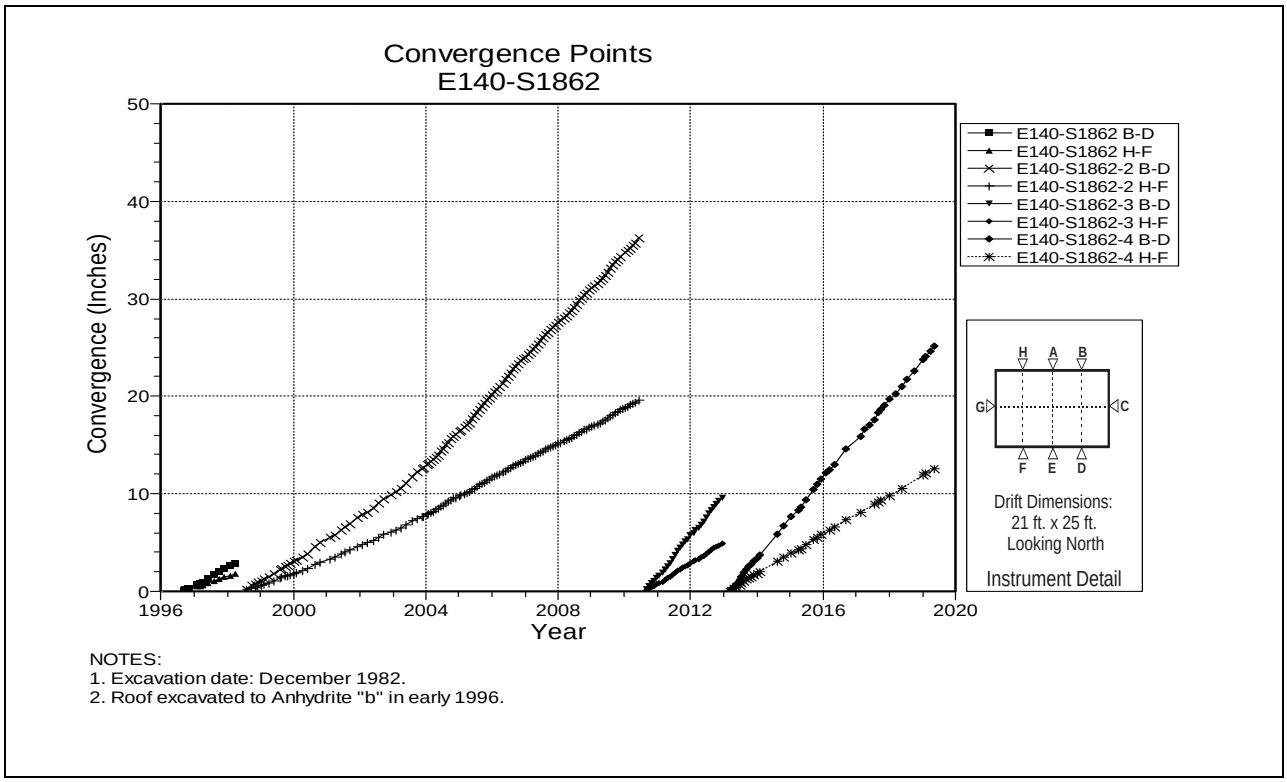

Figure 4-95 Convergence Point Array – E140 S1862 – Roof to Floor – Quarter Points

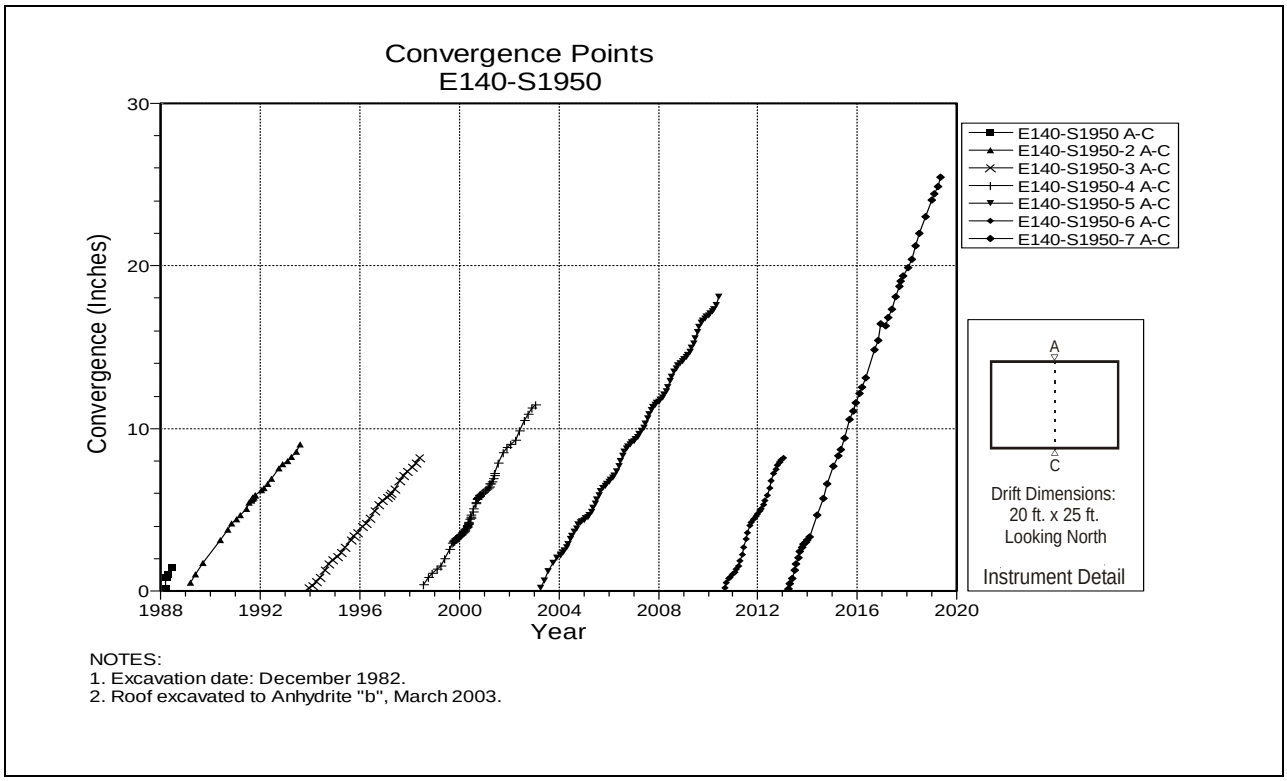

Figure 4-96 Convergence Point Array – E140 S1950 – Roof to Floor – Centerline

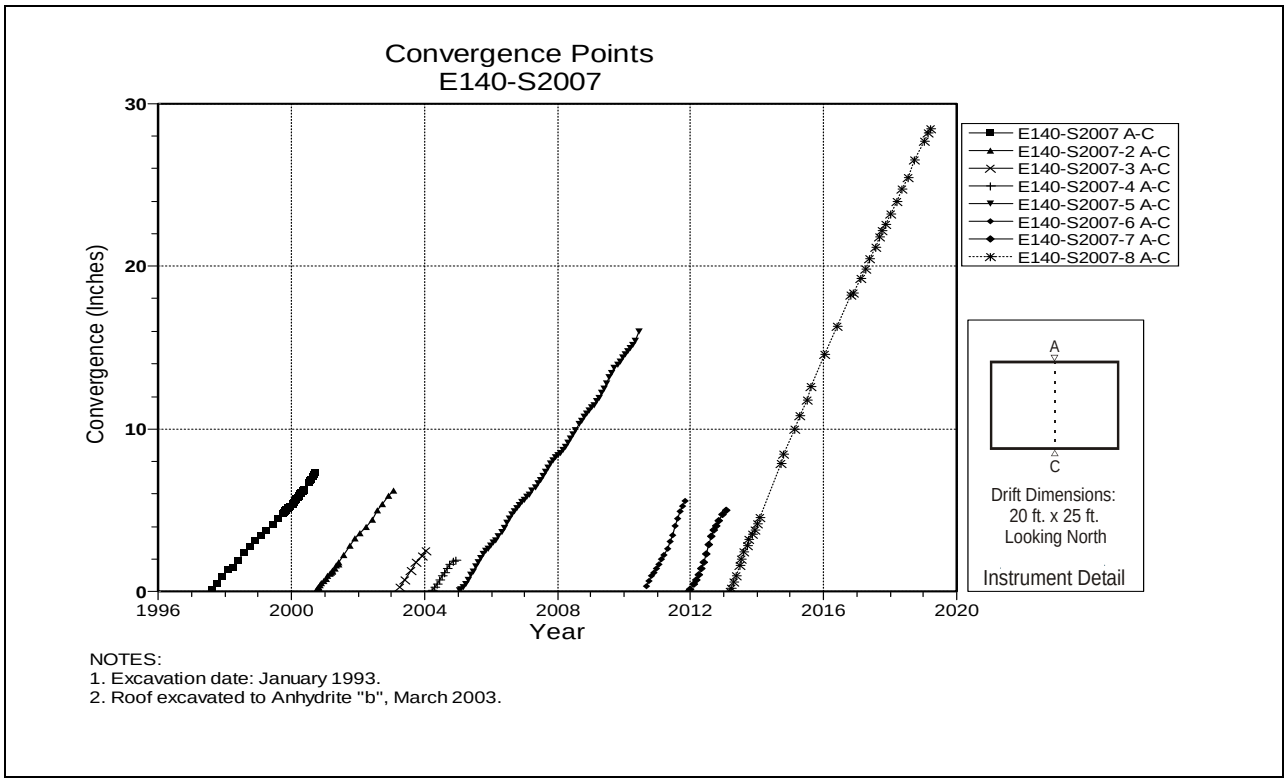

Figure 4-97 Convergence Point Array – E140 S2007 – Roof to Floor – Centerline

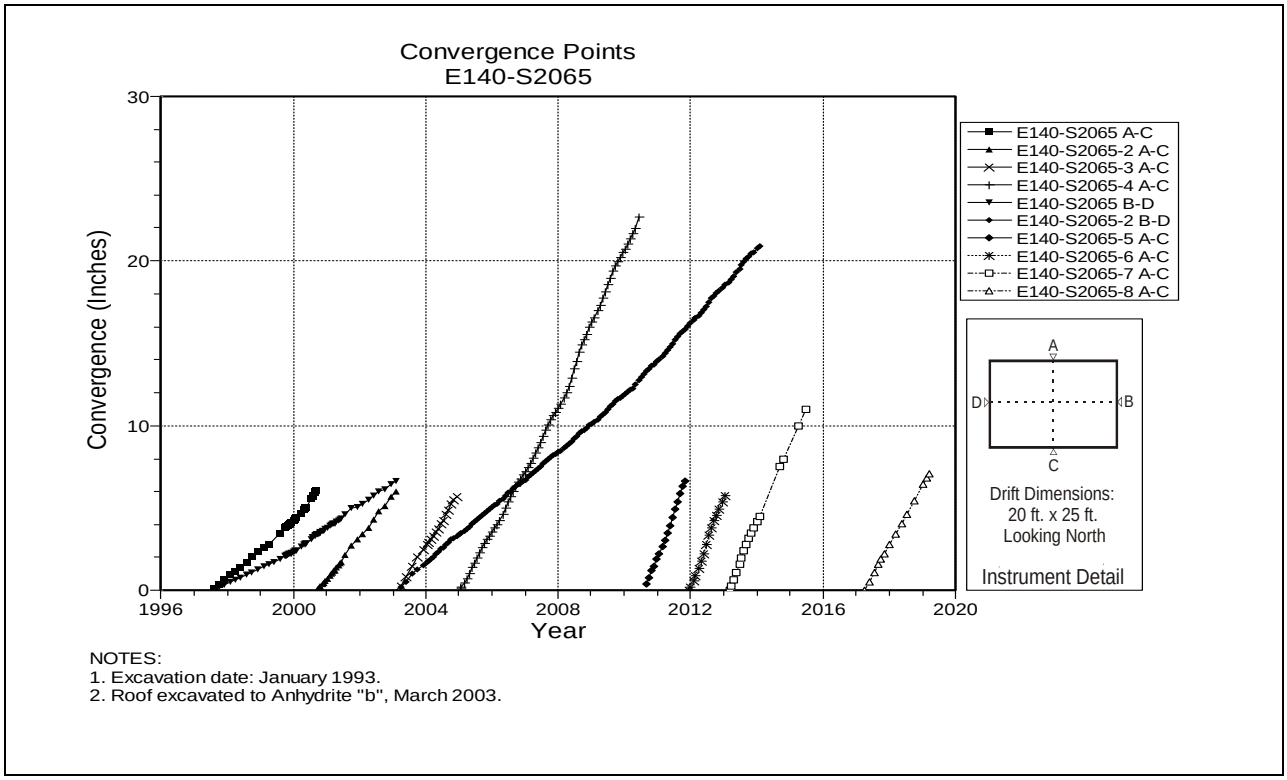

Figure 4-98 Convergence Point Array – E140 S2065 – Roof to Floor – Centerline

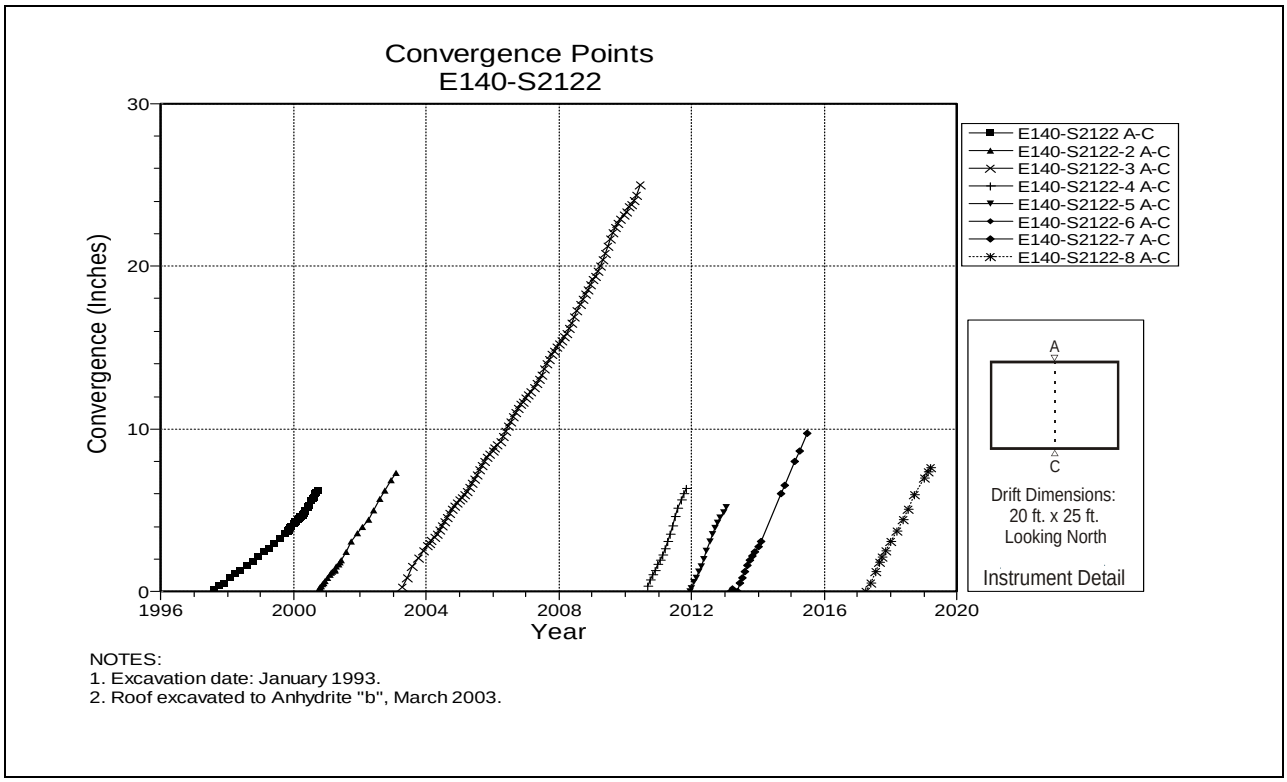

Figure 4-99 Convergence Point Array – E140 S2122 – Roof to Floor – Centerline

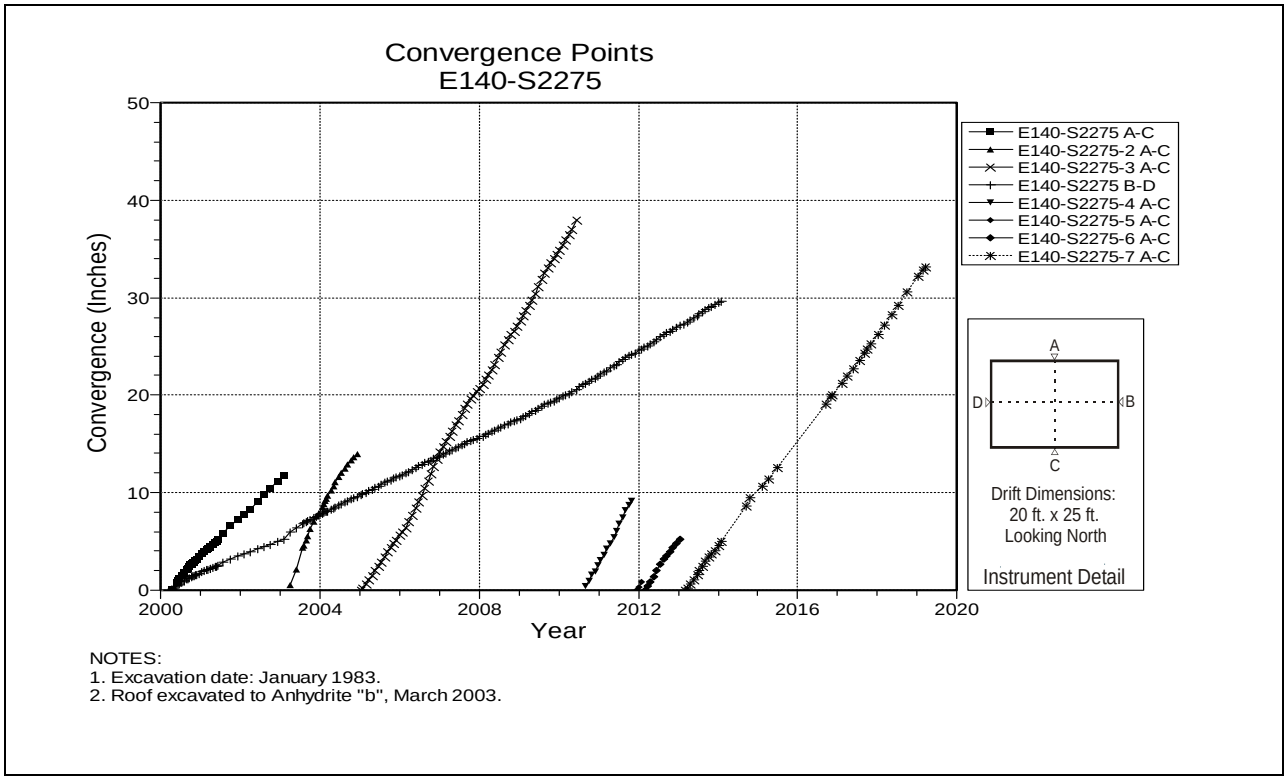

Figure 4-100 Convergence Point Array – E140 S2275 – Roof to Floor – Centerline

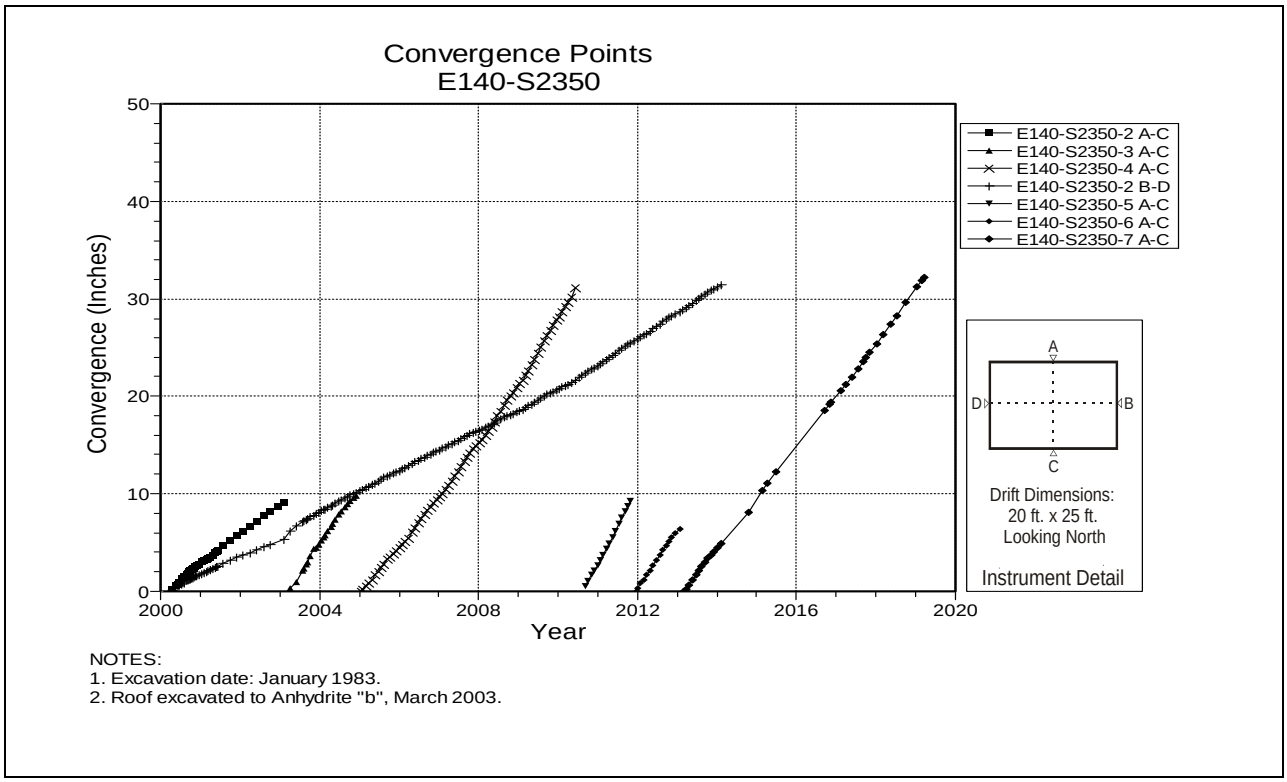

Figure 4-101 Convergence Point Array – E140 S2350 – Roof to Floor – Centerline

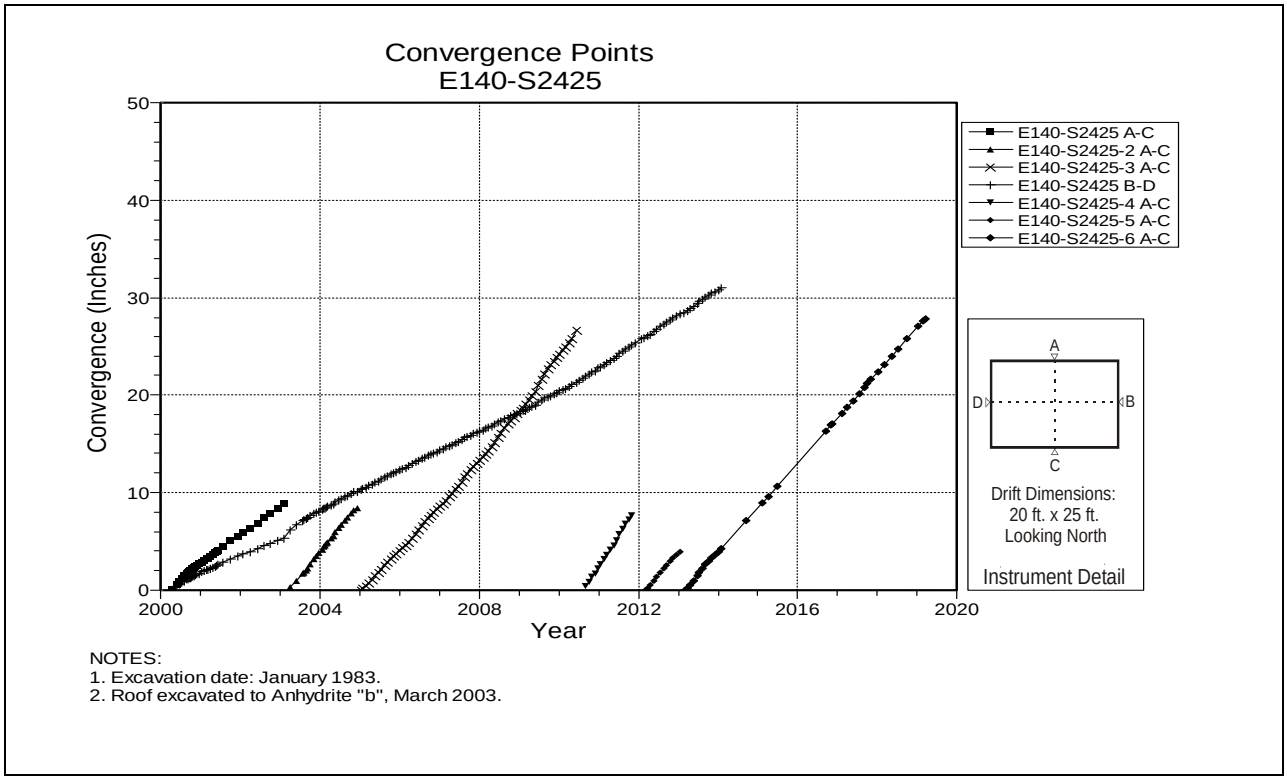

Figure 4-102 Convergence Point Array – E140 S2425 – All Chords

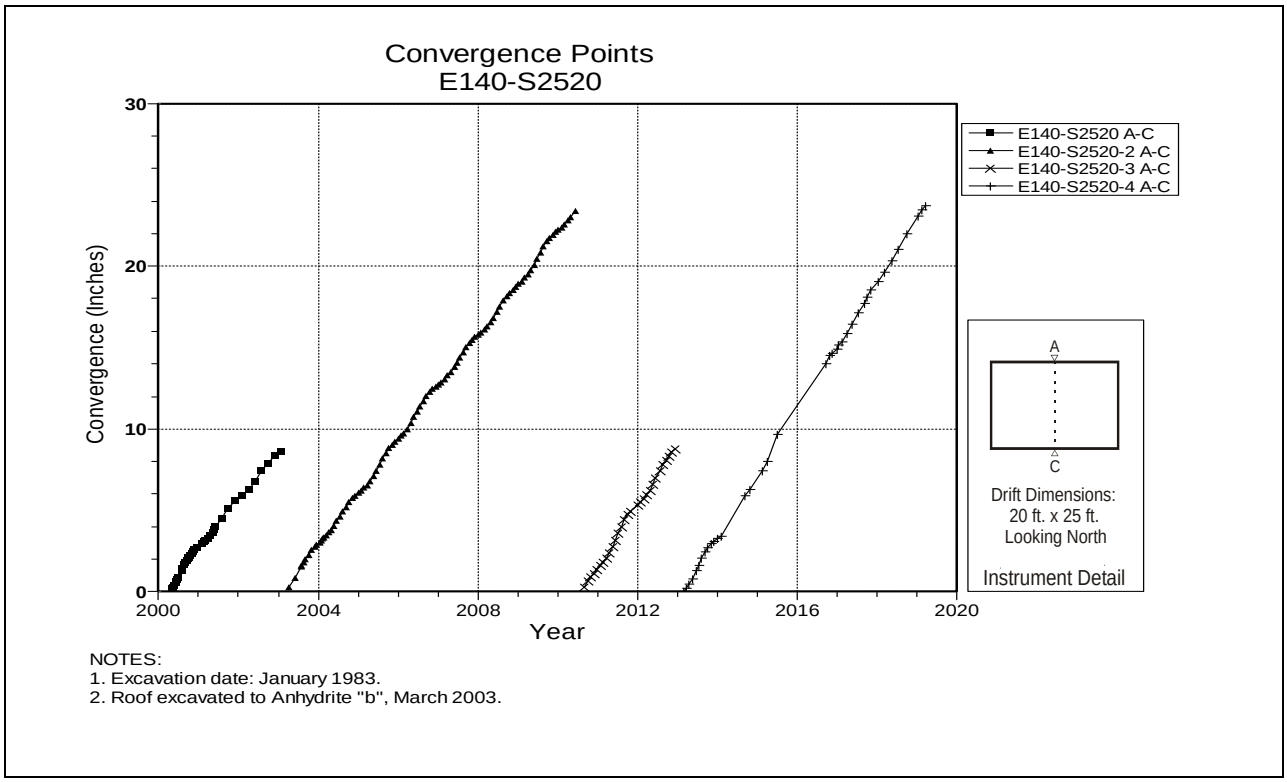

Figure 4-103 Convergence Point Array – E140 S2520 – Roof to Floor – Centerline

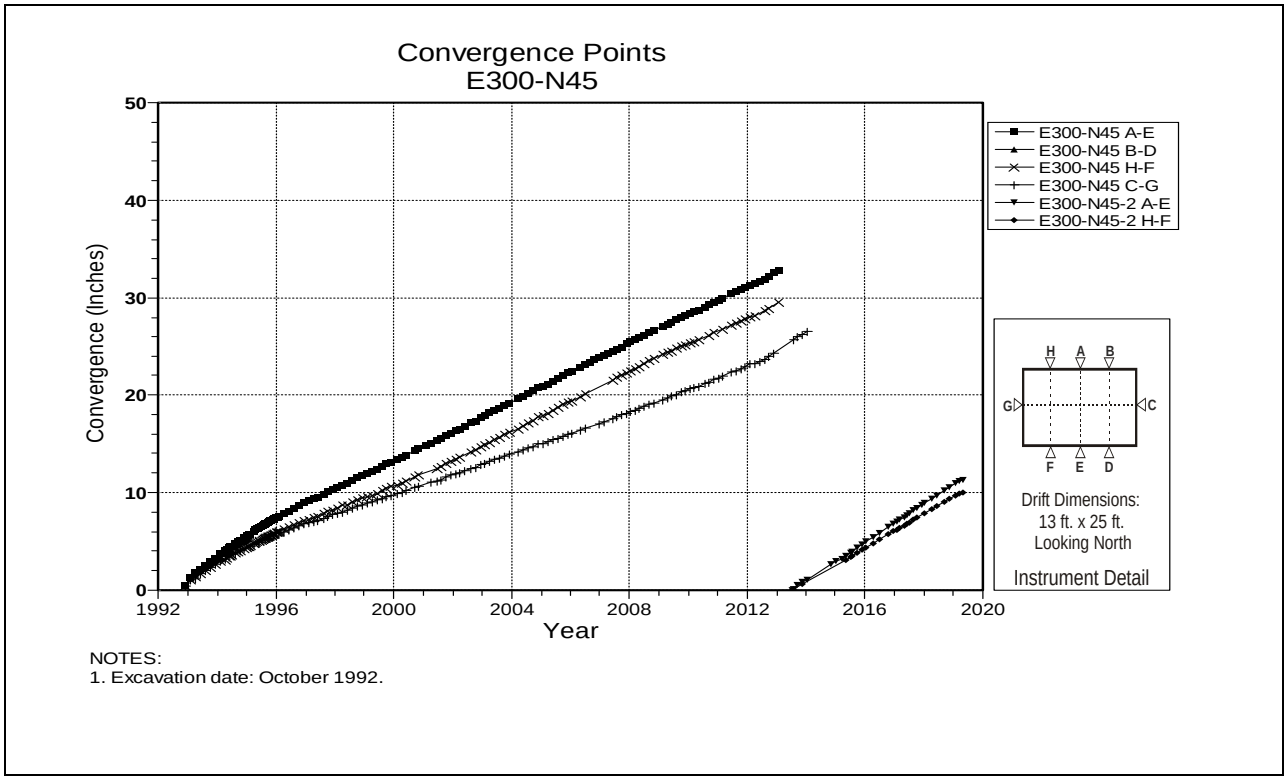

Figure 4-104 Convergence Point Array – E300 N45 – Roof to Floor – Centerline & Quarter Points

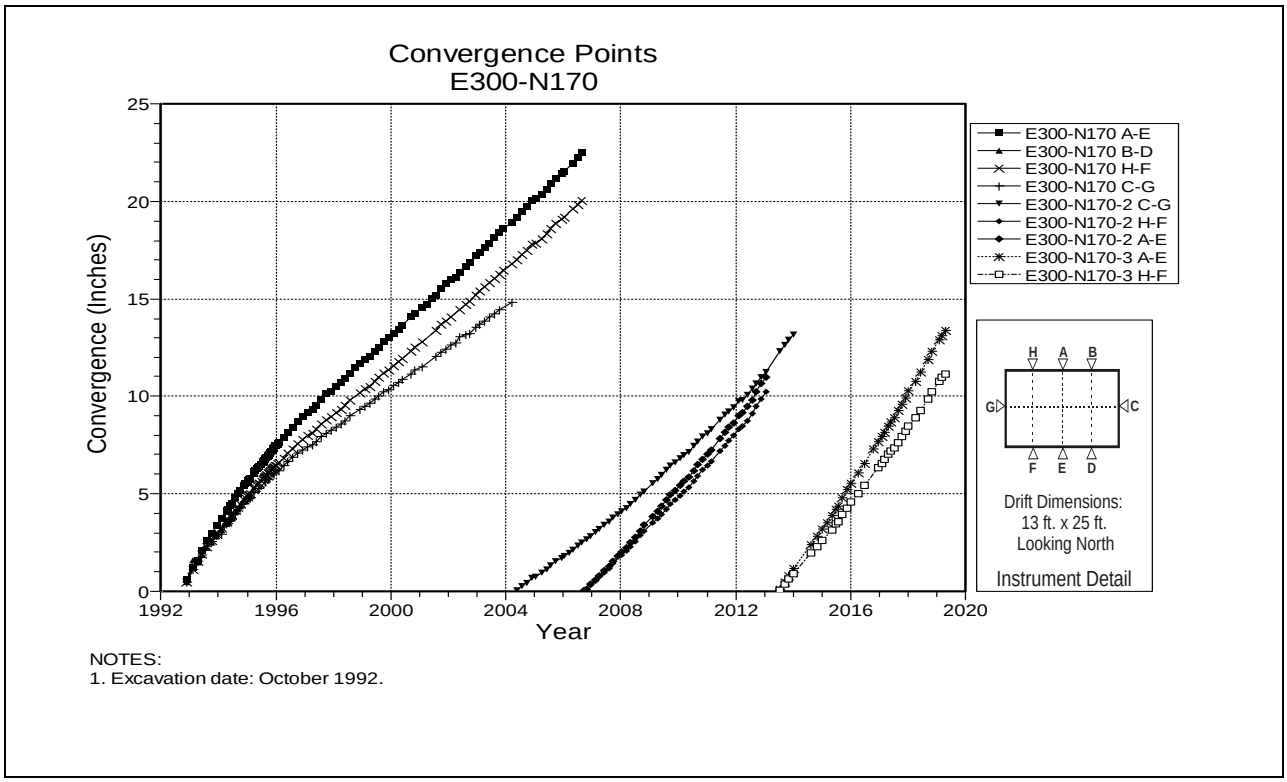

Figure 4-105 Convergence Point Array **–** E300 N170 – Roof to Floor – Centerline and Quarter Points

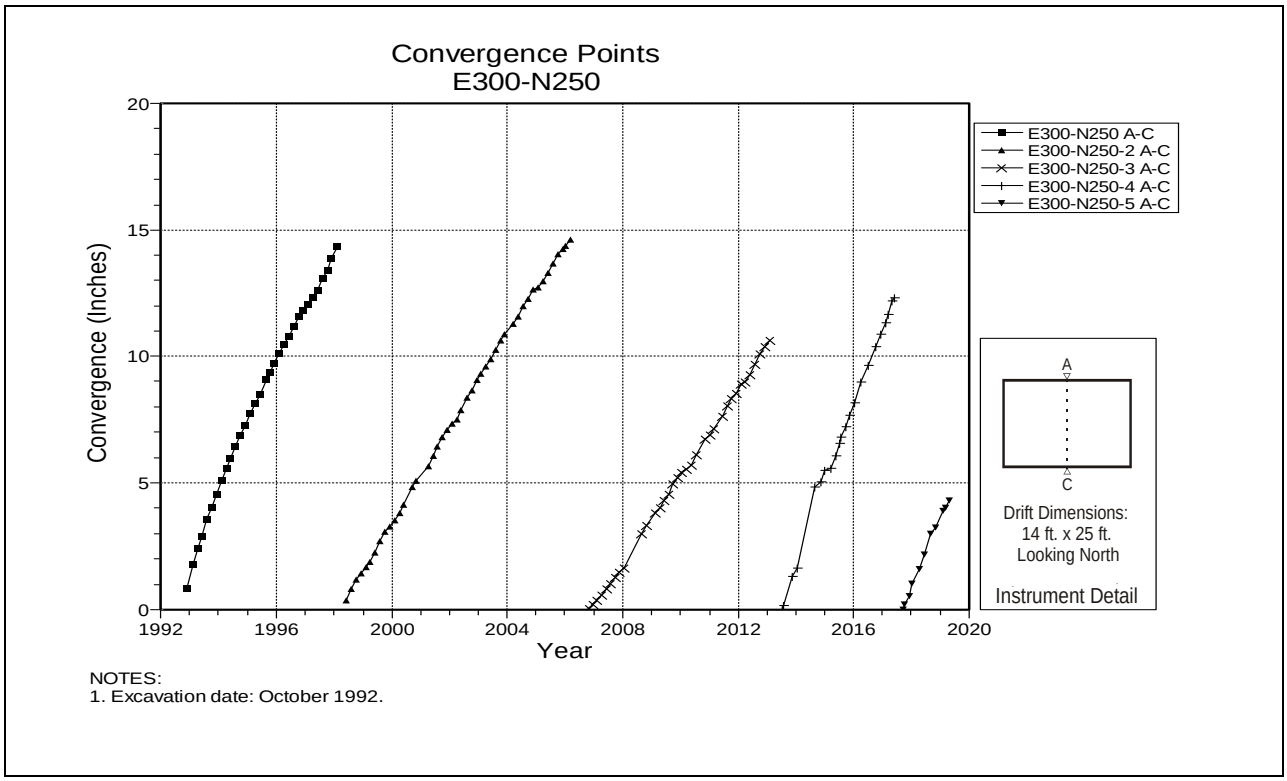

Figure 4-106 Convergence Point Array – E300 N250 – Roof to Floor – Centerline

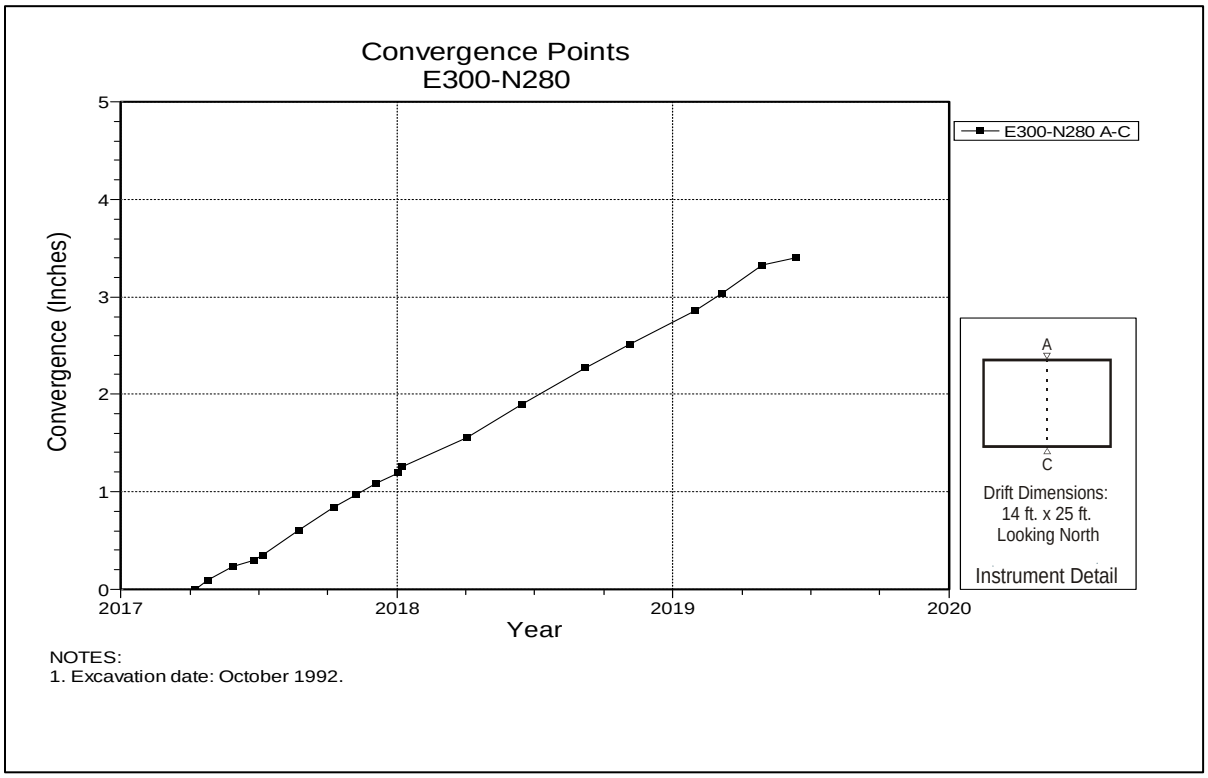

Figure 4-107 Convergence Point Array – E300 N280 – Roof to Floor – Centerline

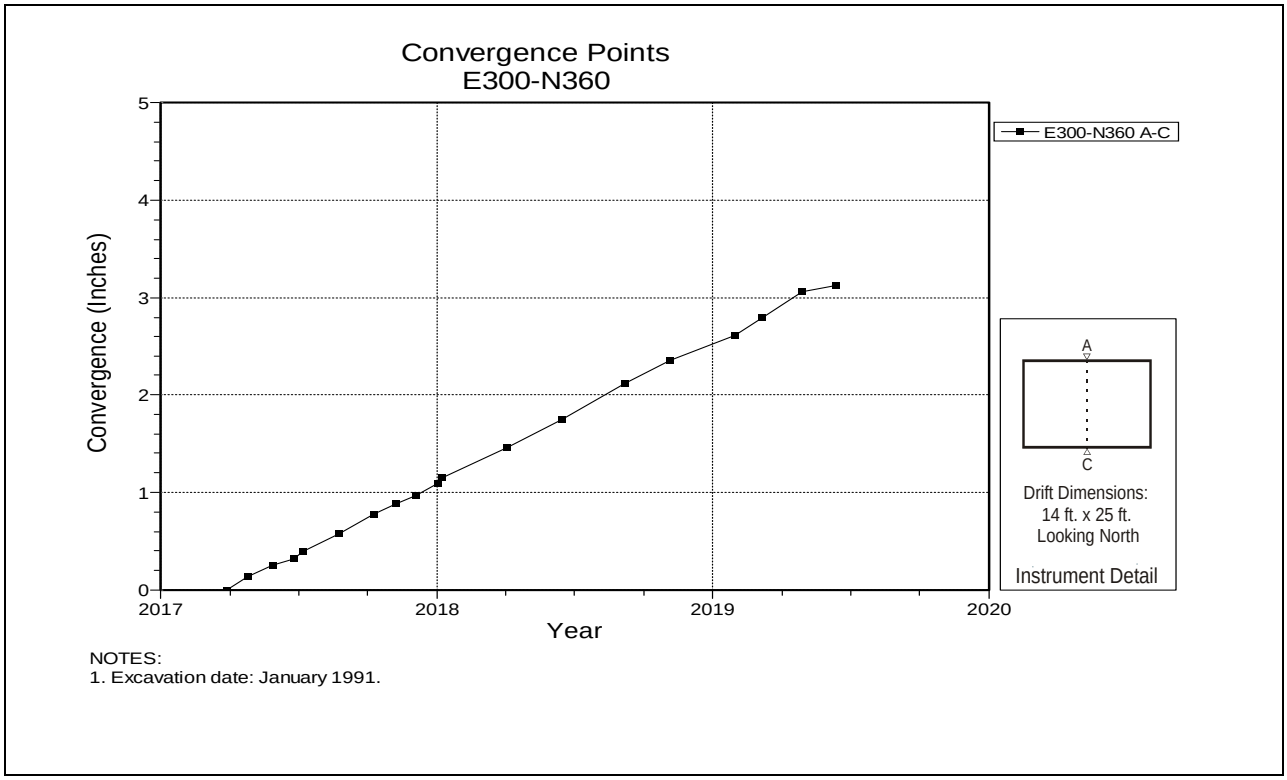

Figure 4-108 Convergence Point Array – E300 N360 – Roof to Floor – Centerline

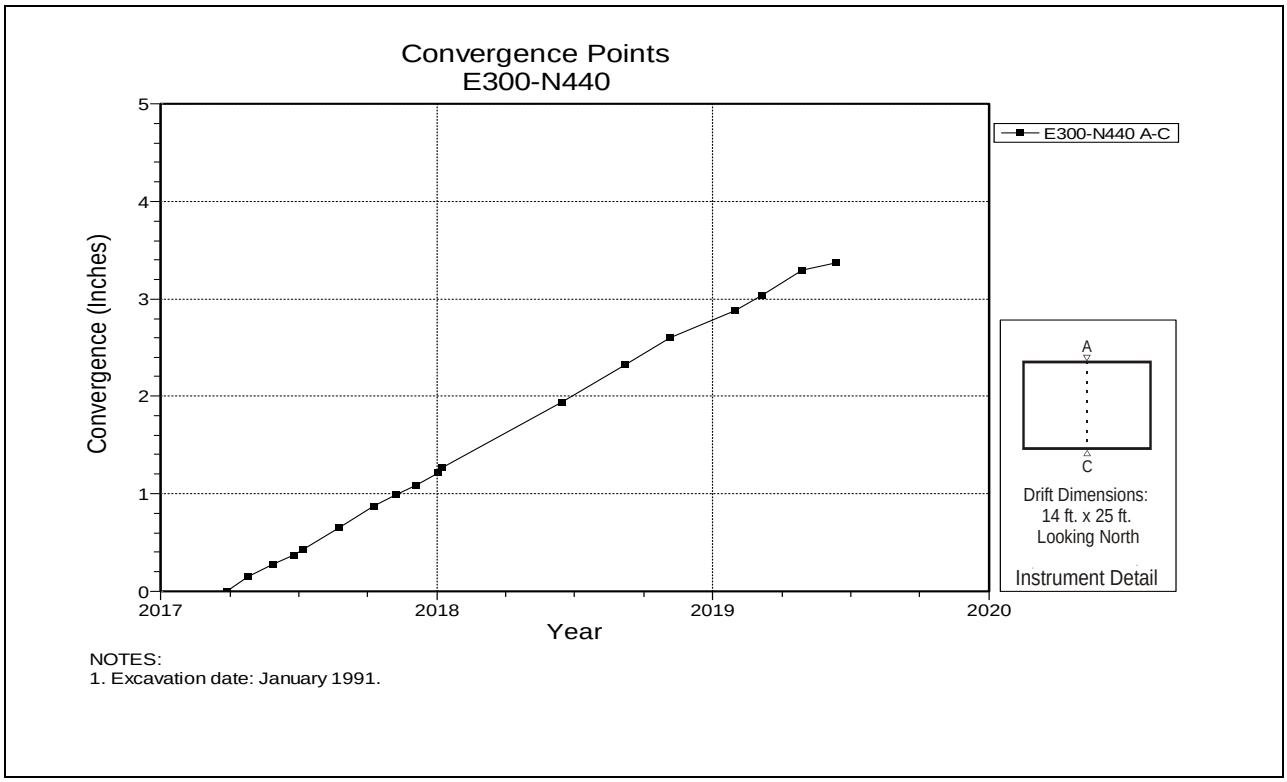

Figure 4-109 Convergence Point Array – E300 N440 – Roof to Floor – Centerline

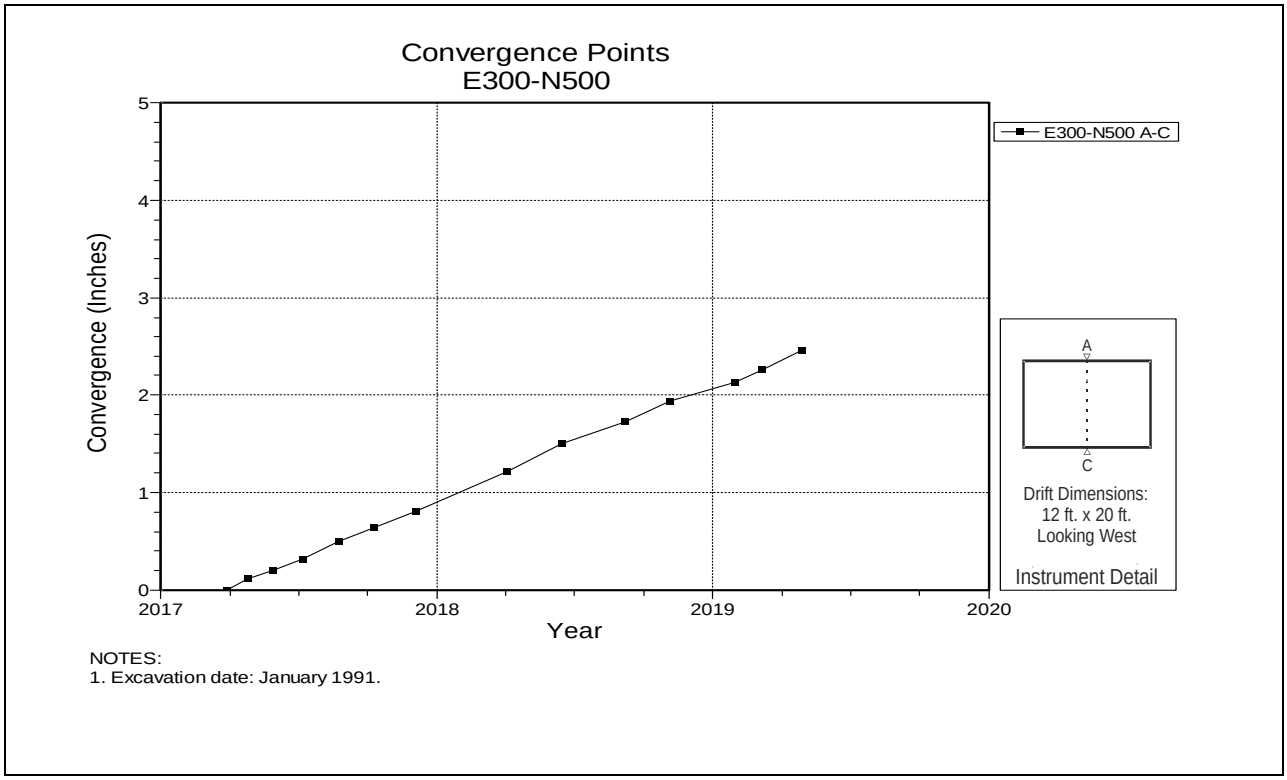

Figure 4-110 Convergence Point Array – E300 N500 – Roof to Floor – Centerline

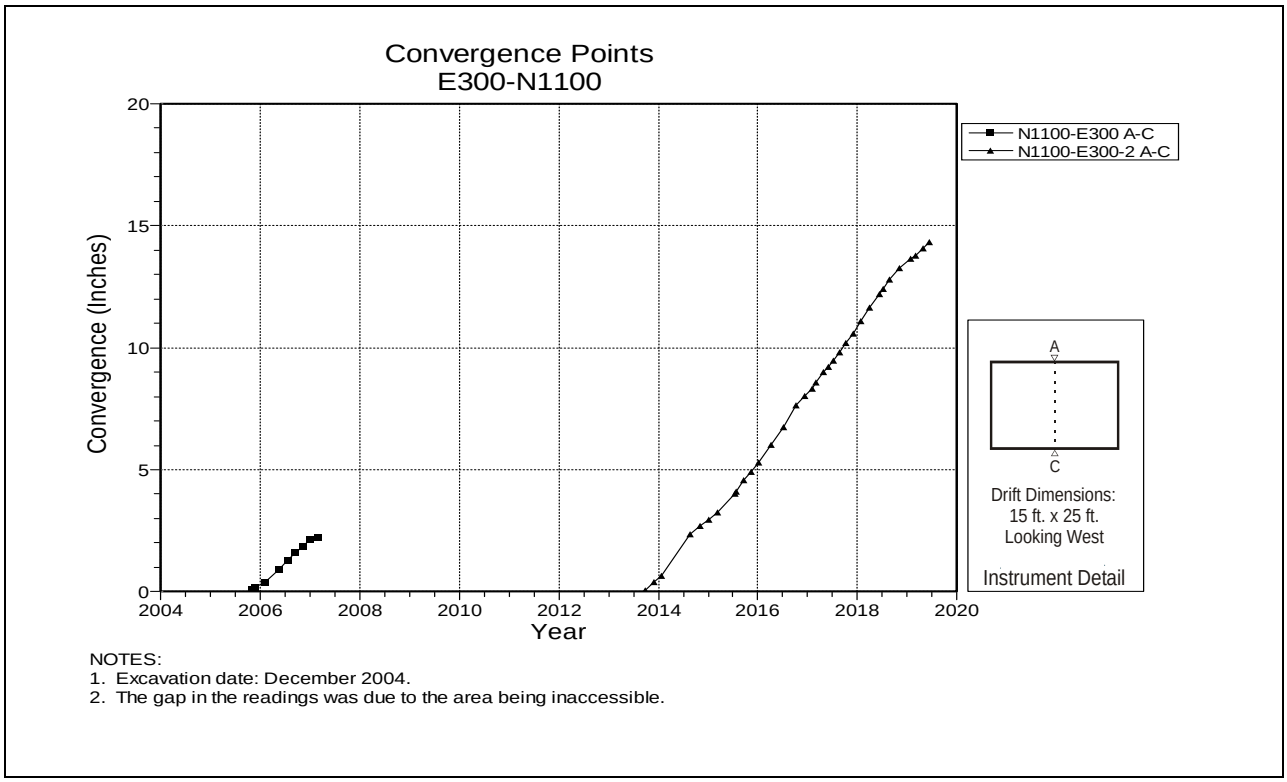

NOTES:
1. Excavation date: December 2004.
2. The gap in the readings was due to the area being inaccessible.

Figure 4-111 Convergence Point Array – E300 N1100 – Roof to Floor – Centerline

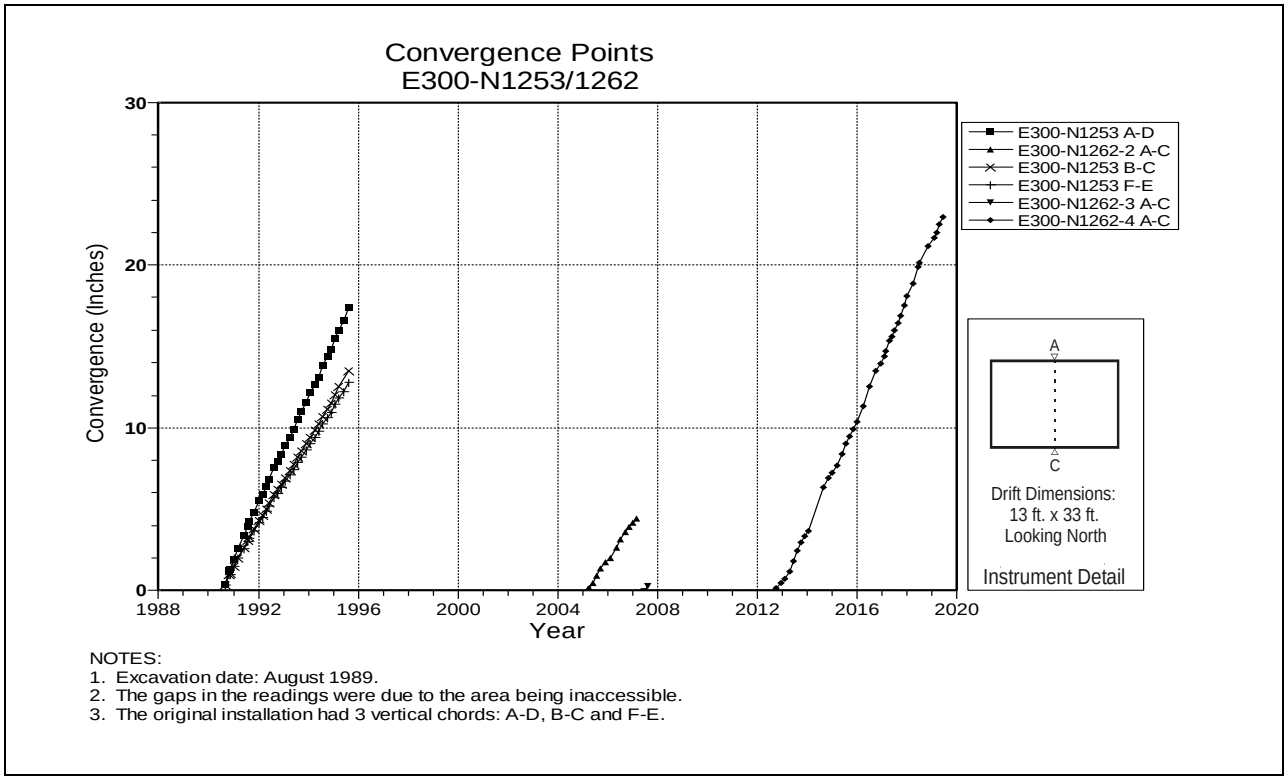

NOTES:
1. Excavation date: August 1989.
2. The gaps in the readings were due to the area being inaccessible.
3. The original installation had 3 vertical chords: A-D, B-C and F-E.

Figure 4-112 Convergence Point Array – E300 N1262 – All Chords

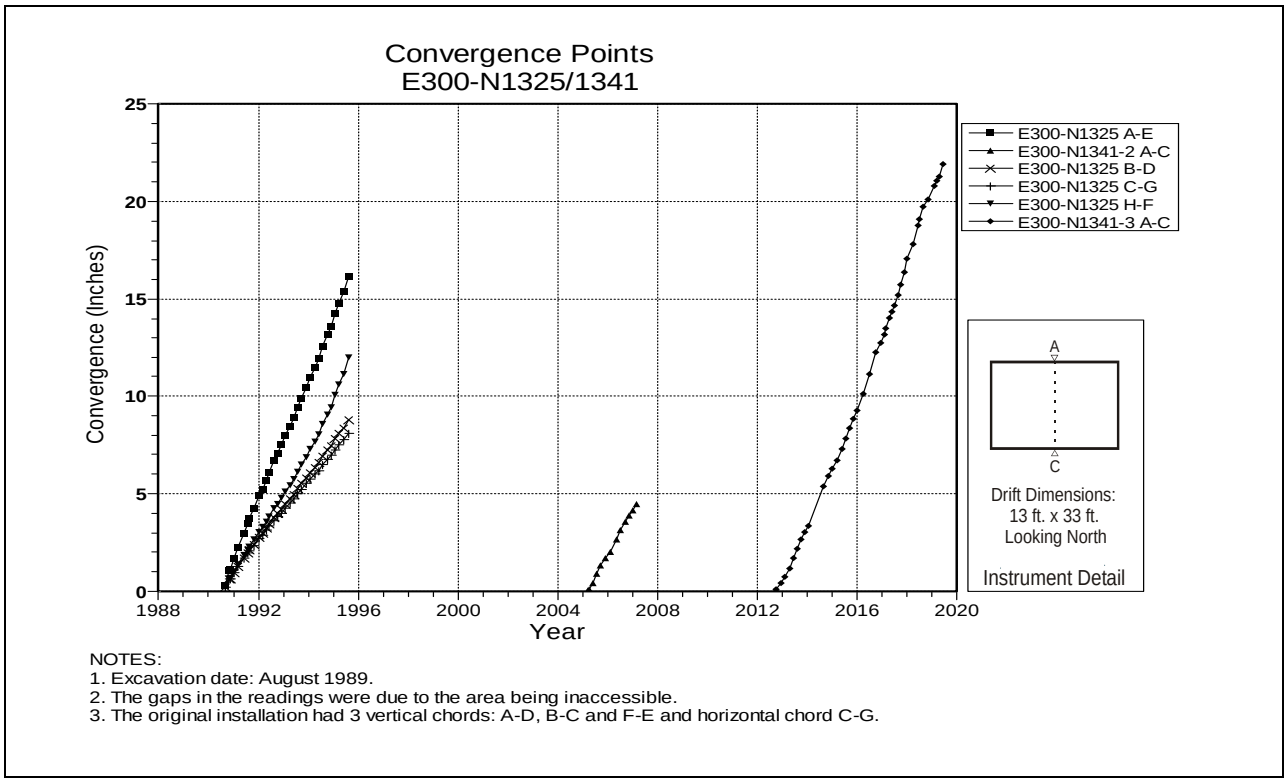

NOTES:
1. Excavation date: August 1989.
2. The gaps in the readings were due to the area being inaccessible.
3. The original installation had 3 vertical chords: A-D, B-C and F-E and horizontal chord C-G.

Figure 4-113 Convergence Point Array – E300 N1341 – All Chords

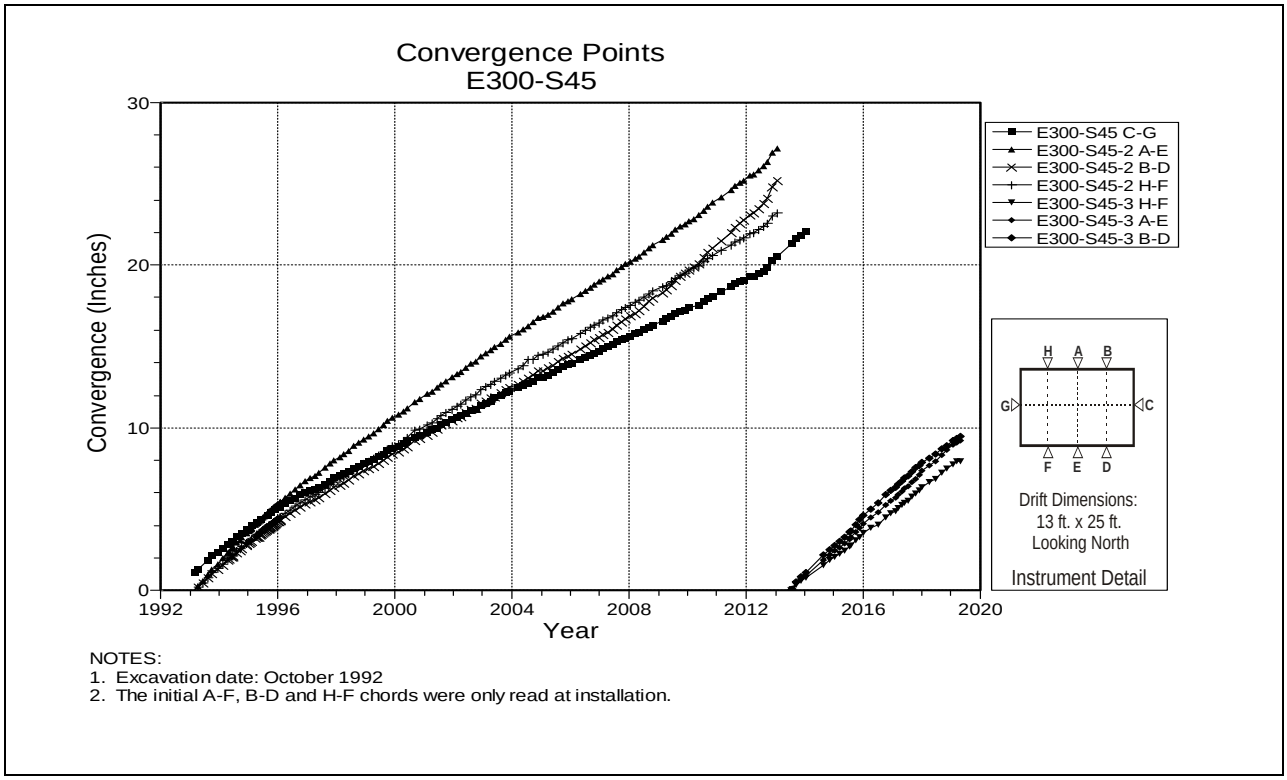

NOTES:
1. Excavation date: October 1992
2. The initial A-F, B-D and H-F chords were only read at installation.

Figure 4-114 Convergence Point Array – E300 S45 – Roof to Floor – All Chords

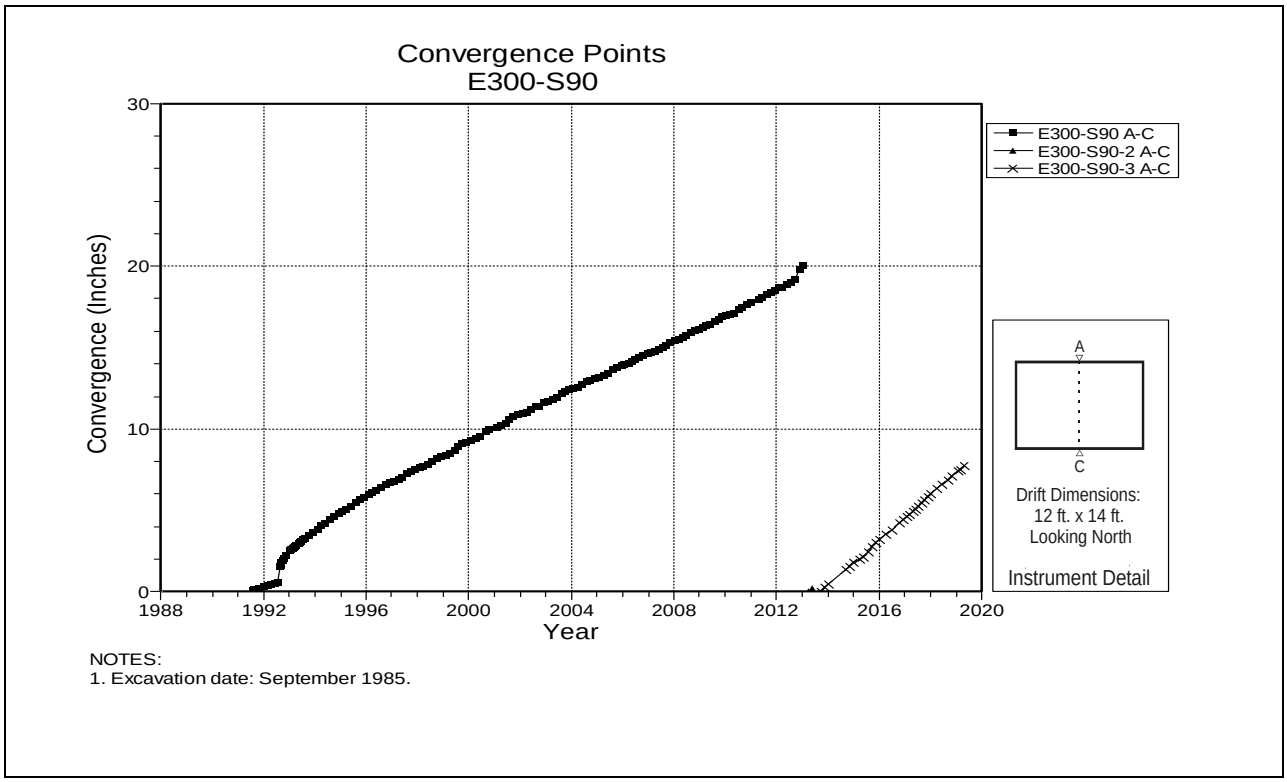

Figure 4-115 Convergence Point Array – E300 S90 – Roof to Floor – Centerline

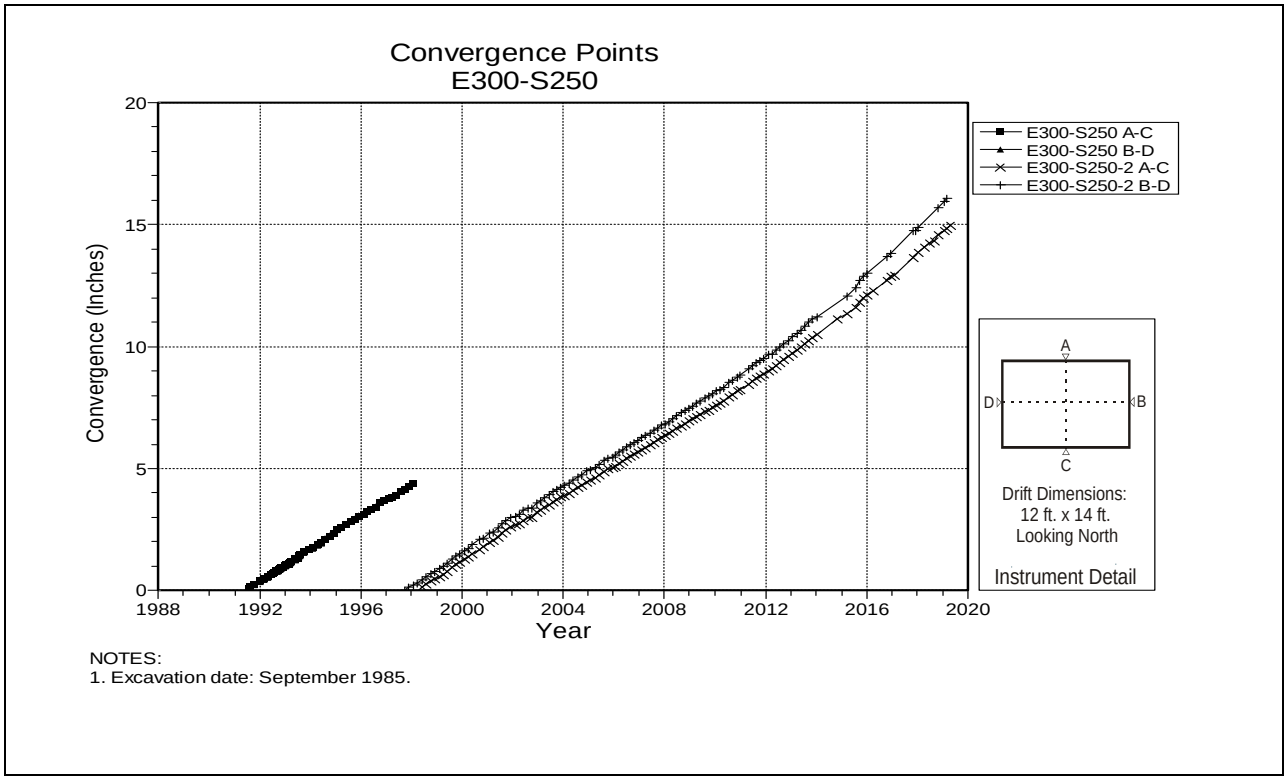

Figure 4-116 Convergence Point Array – E300 S250 – All Chords

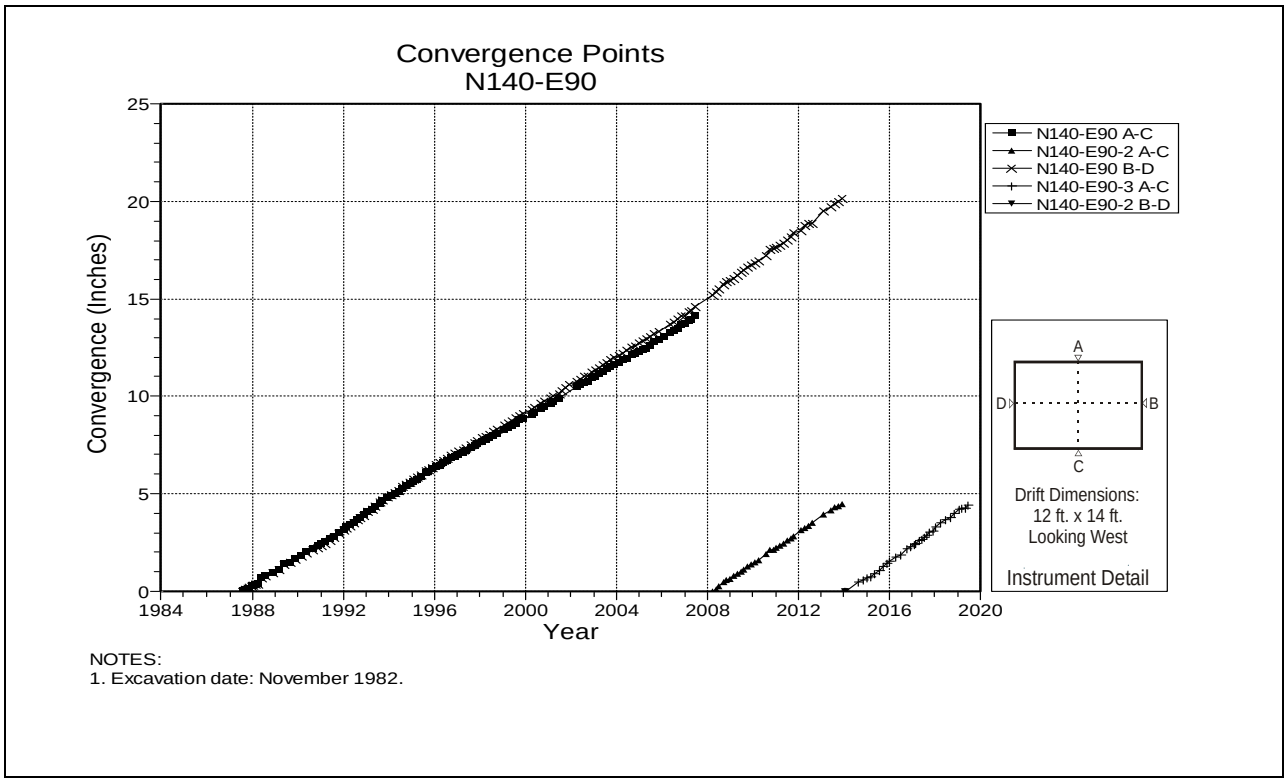

NOTES:
1. Excavation date: November 1982.

Figure 4-117 Convergence Point Array – N140 E90 – All Chords

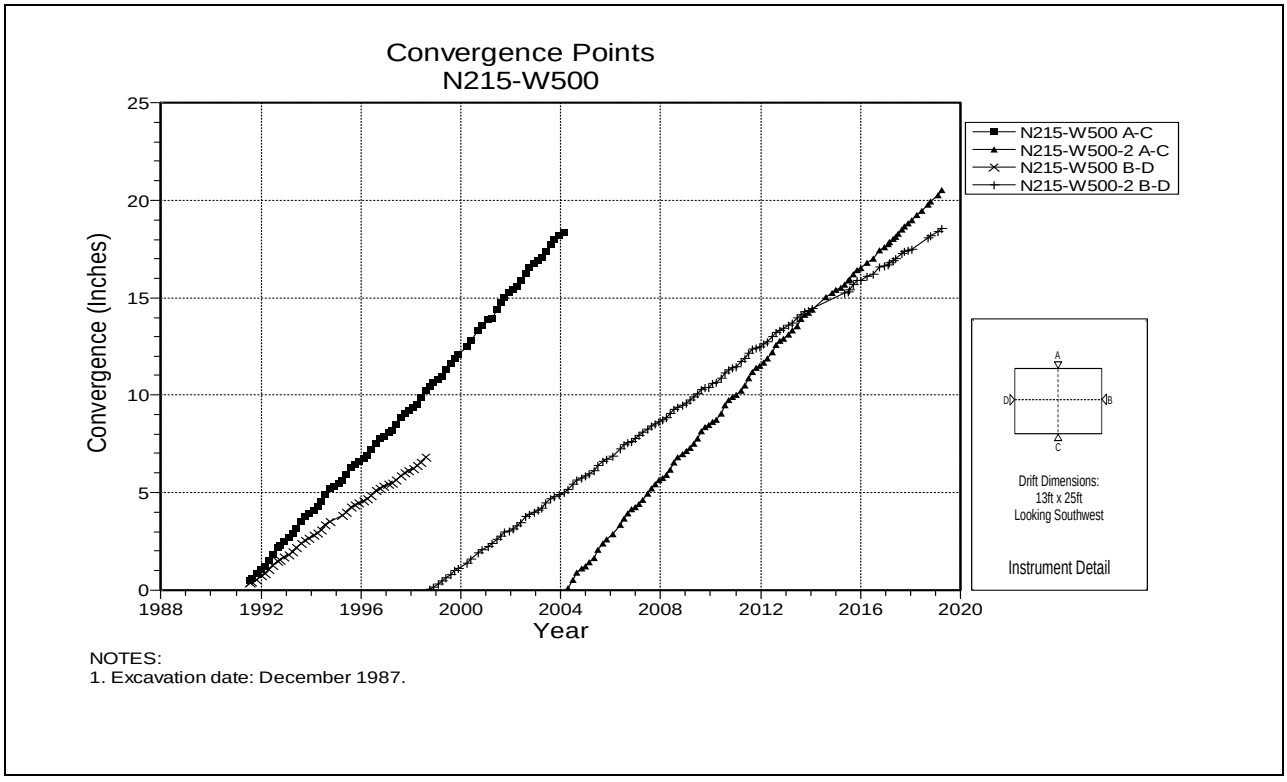

NOTES:
1. Excavation date: December 1987.

Figure 4-118 Convergence Point Array – N215 W500 – All Chords

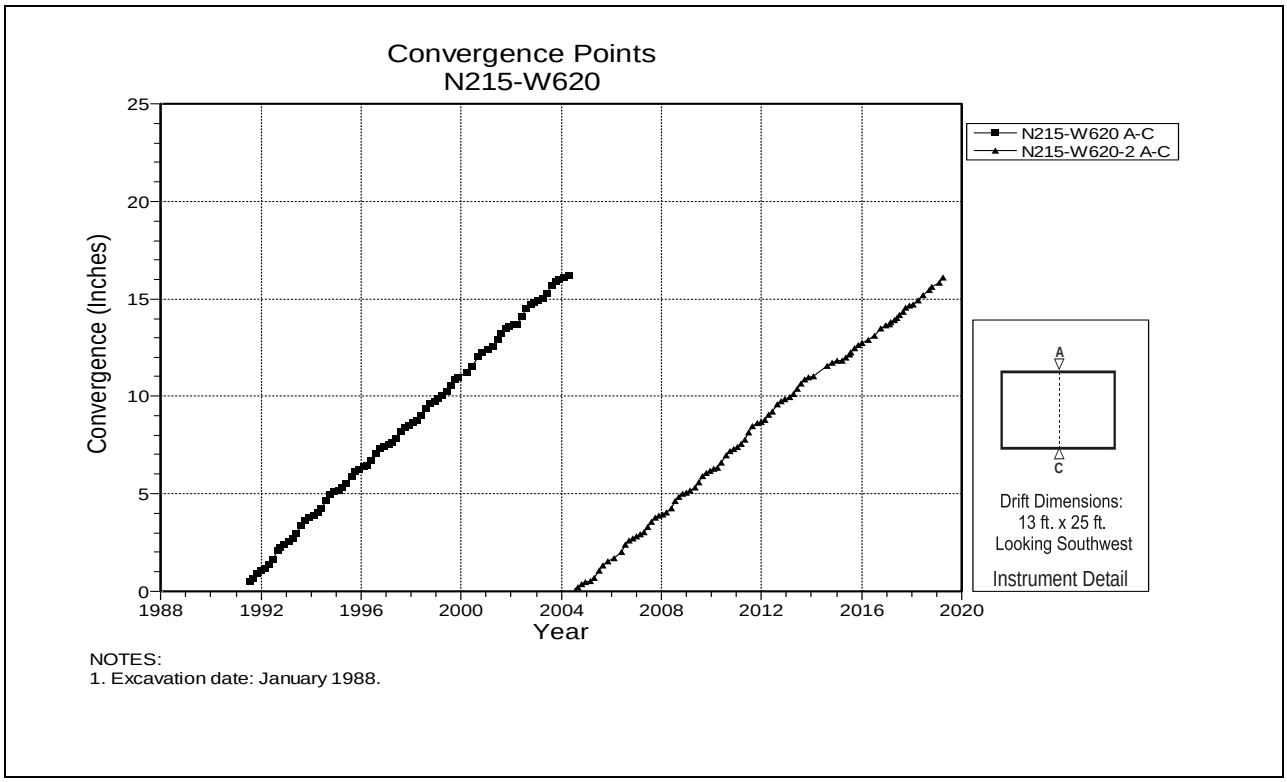

Figure 4-119 Convergence Point Array – N215 W620 – Roof to Floor – Centerline

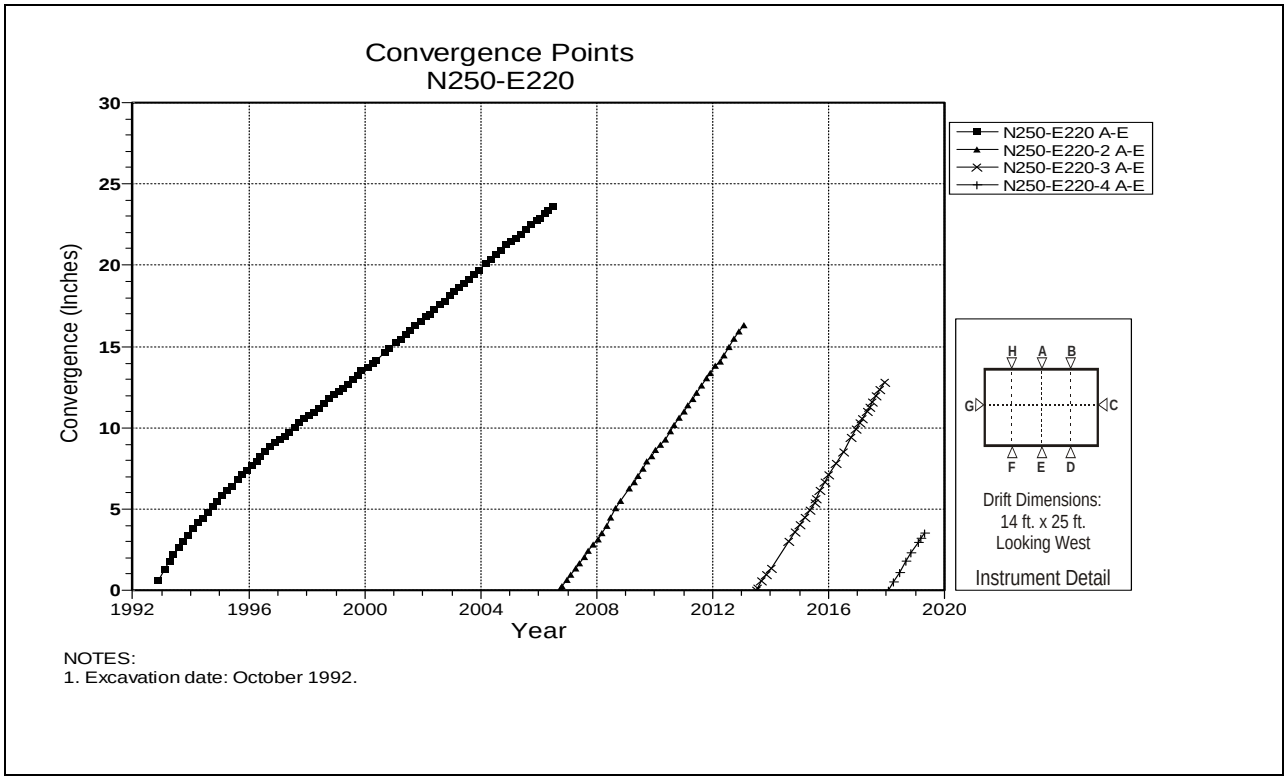

Figure 4-120 Convergence Point Array – N250 E220 – Roof to Floor – Centerline

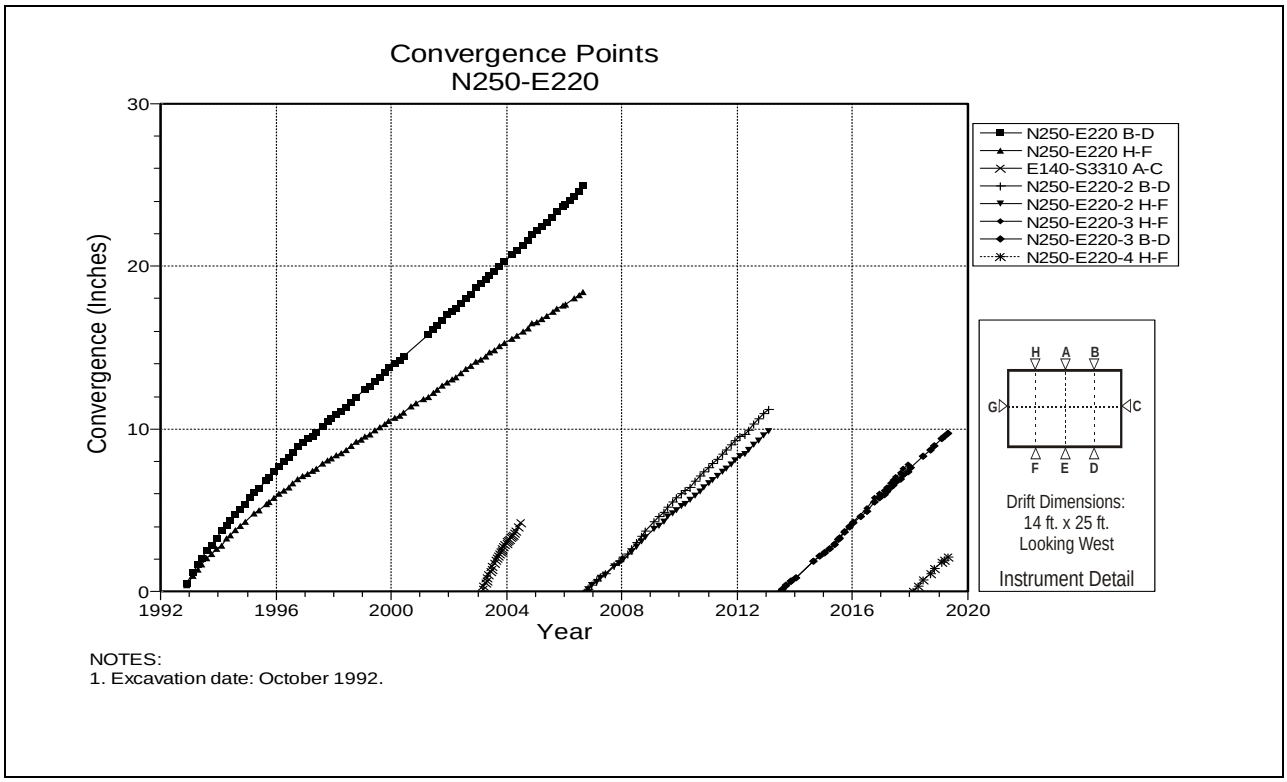

Figure 4-121 Convergence Point Array – N250 E220 – Roof to Floor – Quarter Points

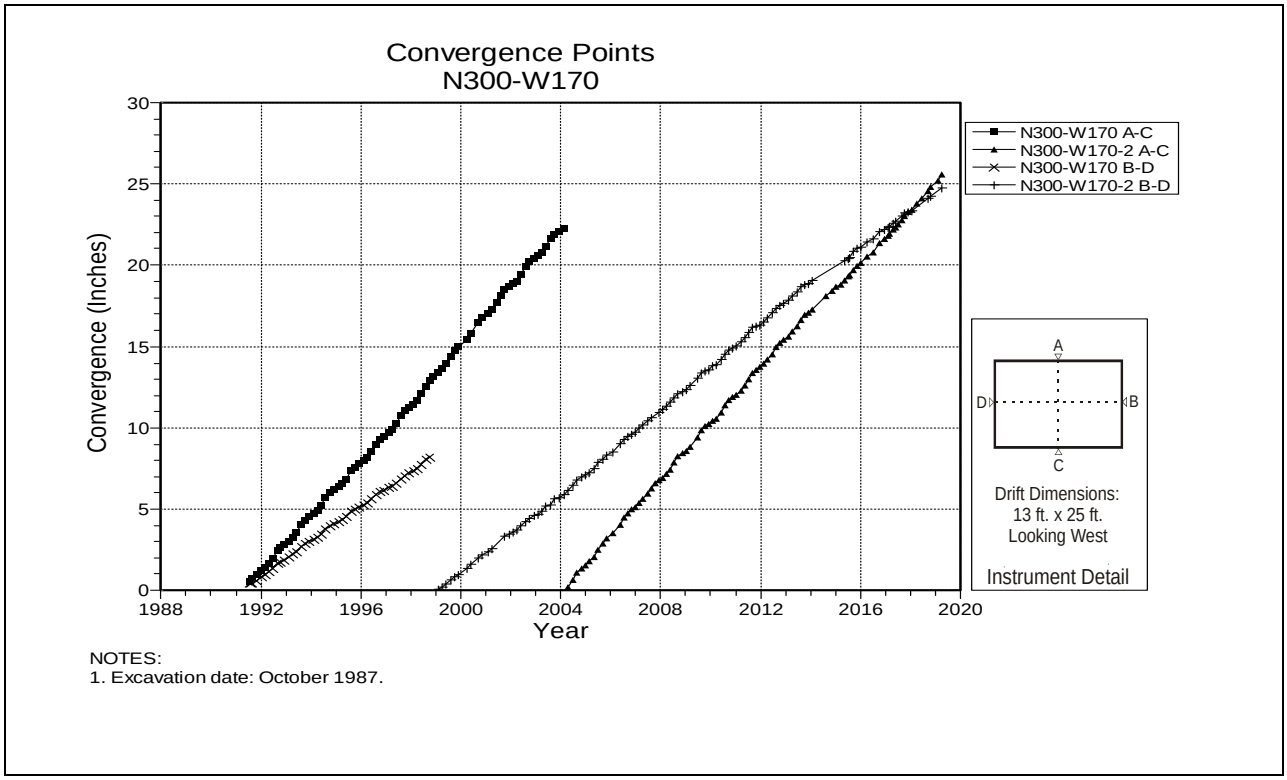

Figure 4-122 Convergence Point Array – N300 W170 – All Chords

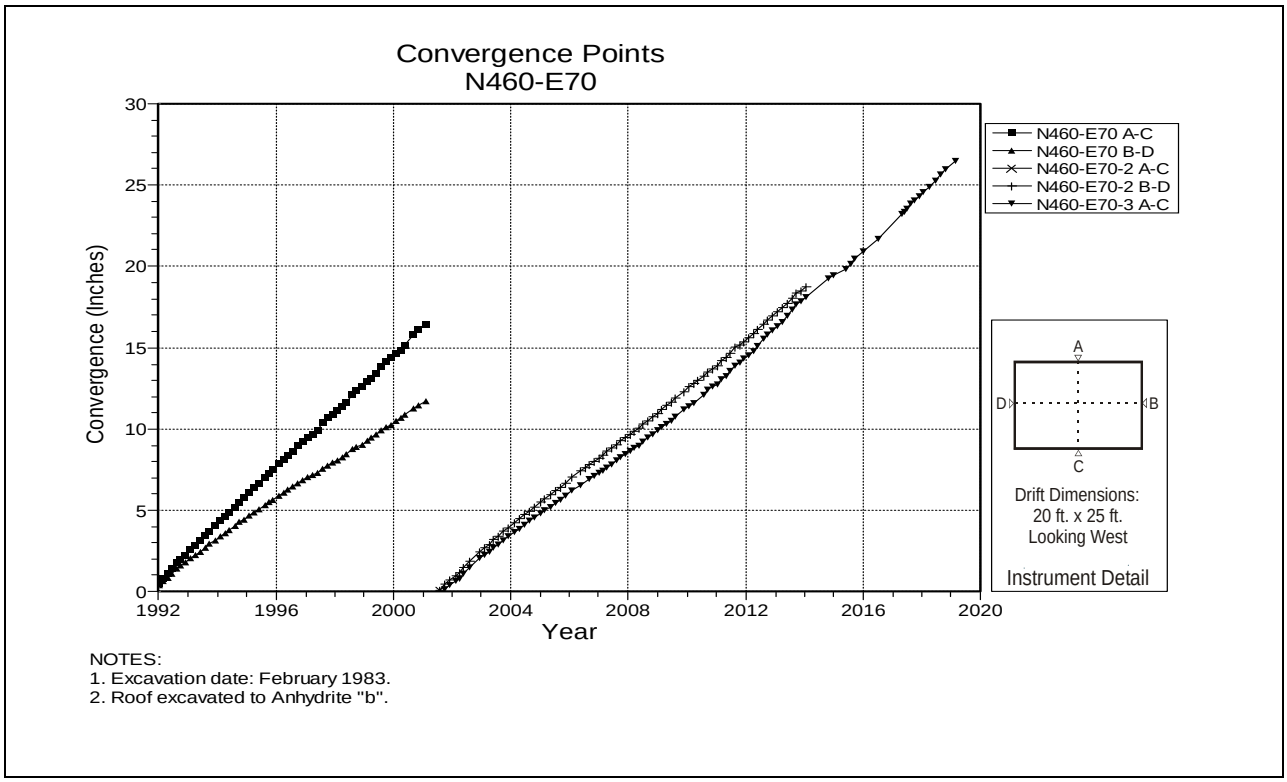

Figure 4-123 Convergence Point Array – N460 E70 – All Chords

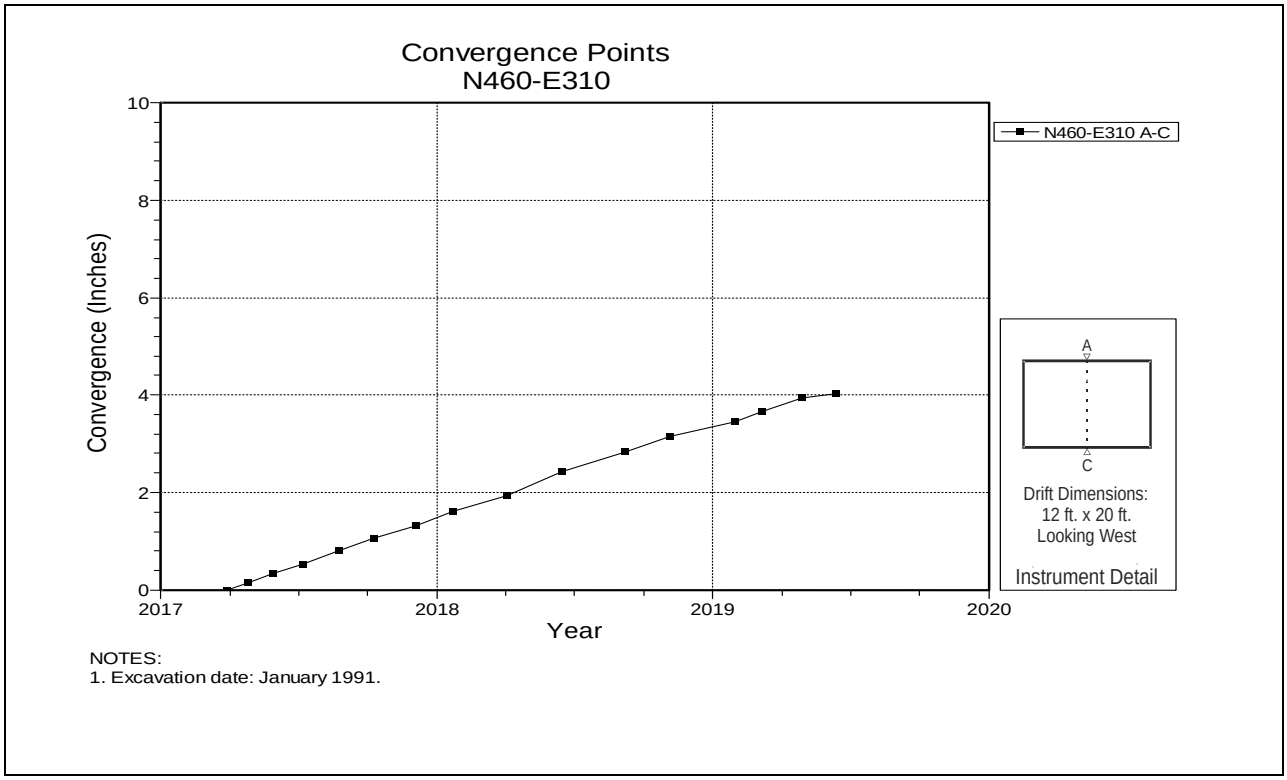

Figure 4-124 Convergence Point Array – N460 E310 – Roof to Floor – Centerline

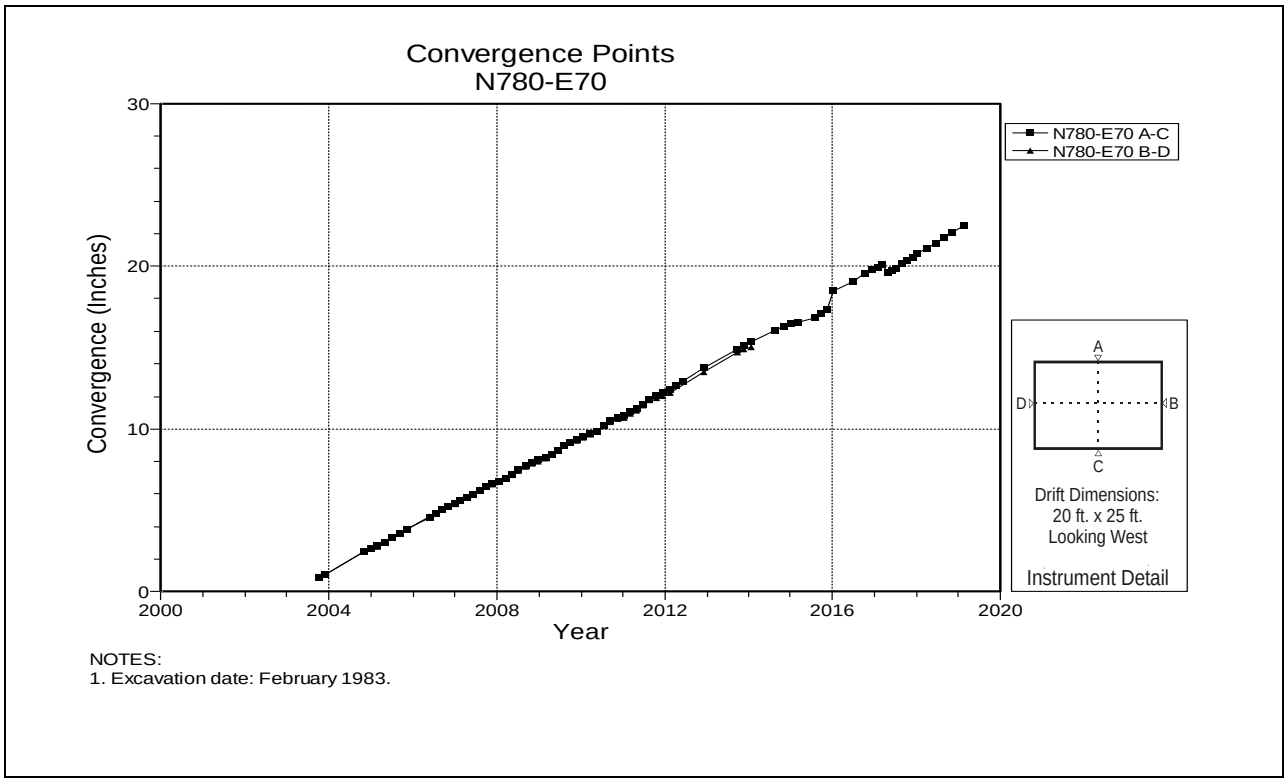

NOTES:
1. Excavation date: February 1983.

Figure 4-125 Convergence Point Array – N780 E70 – All Chords

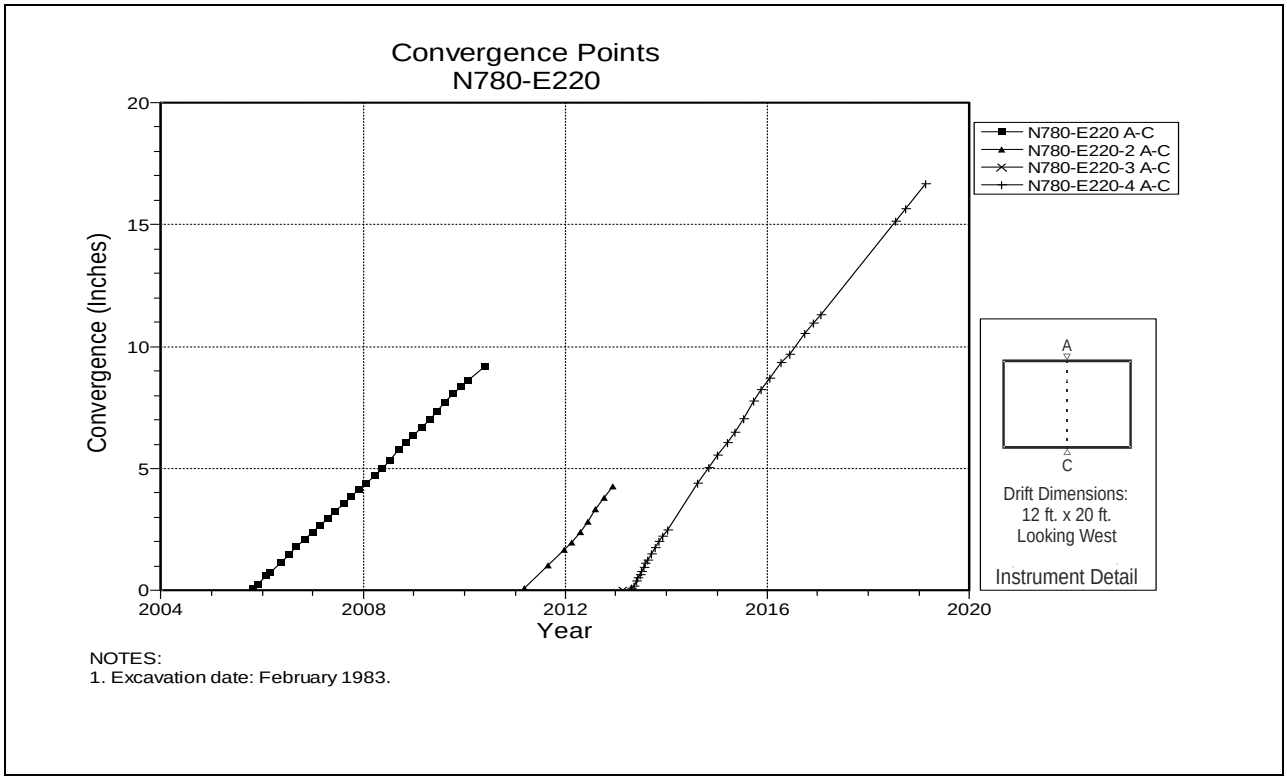

NOTES:
1. Excavation date: February 1983.

Figure 4-126 Convergence Point Array – N780 E220 – Roof to Floor – Centerline

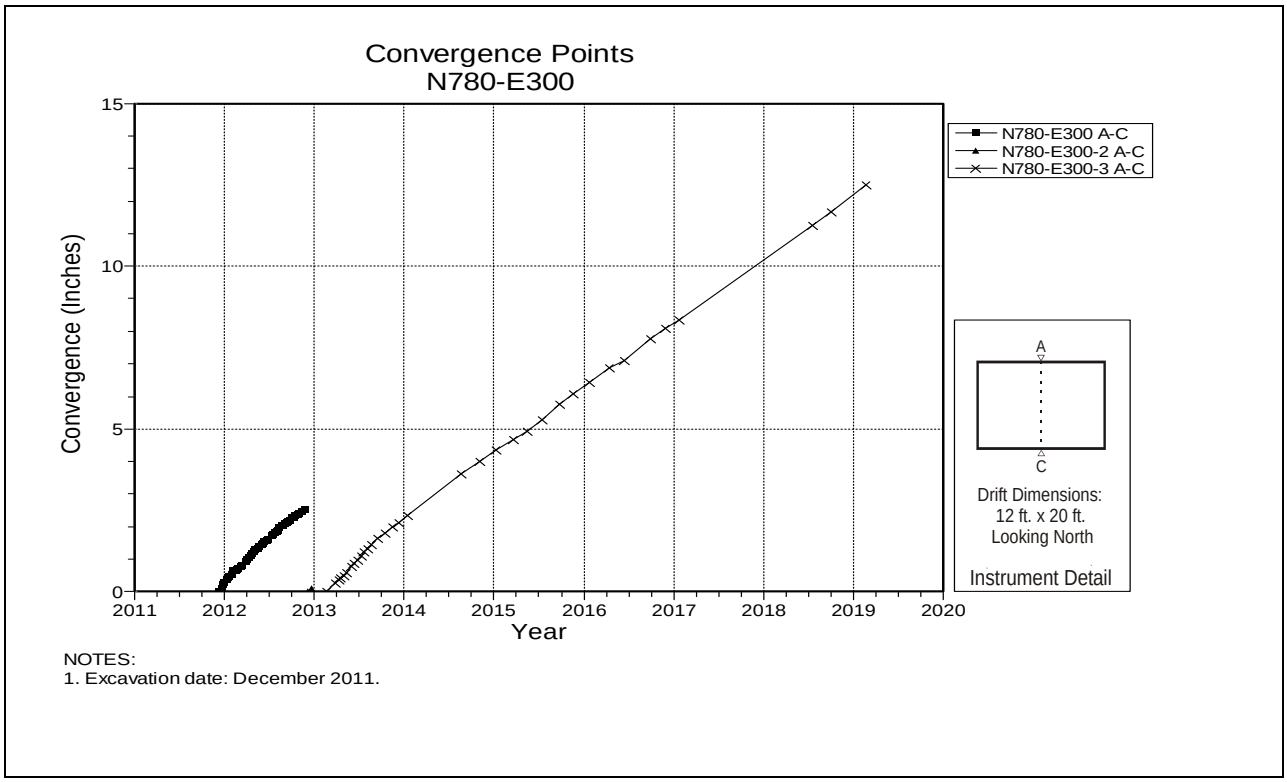

Figure 4-127 Convergence Point Array – N780 E300 – Roof to Floor – Centerline

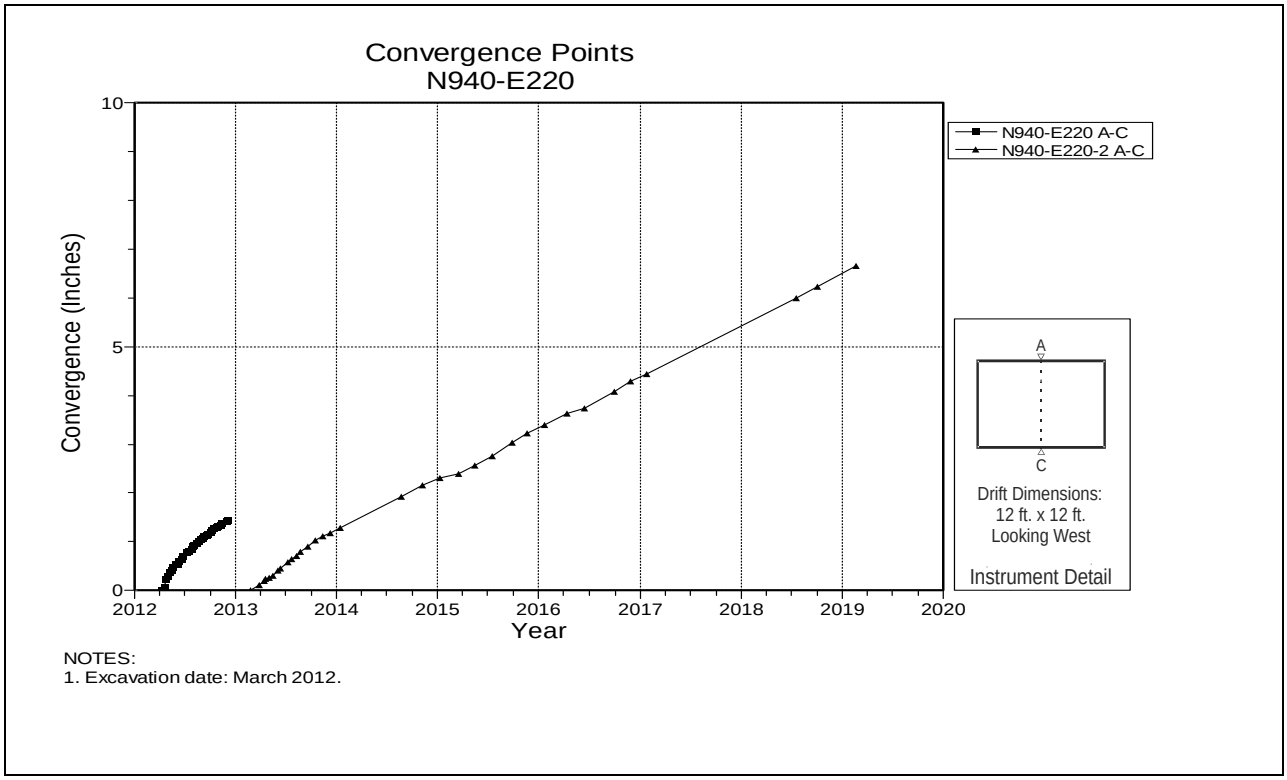

Figure 4-128 Convergence Point Array – N940 E220 – Roof to Floor – Centerline

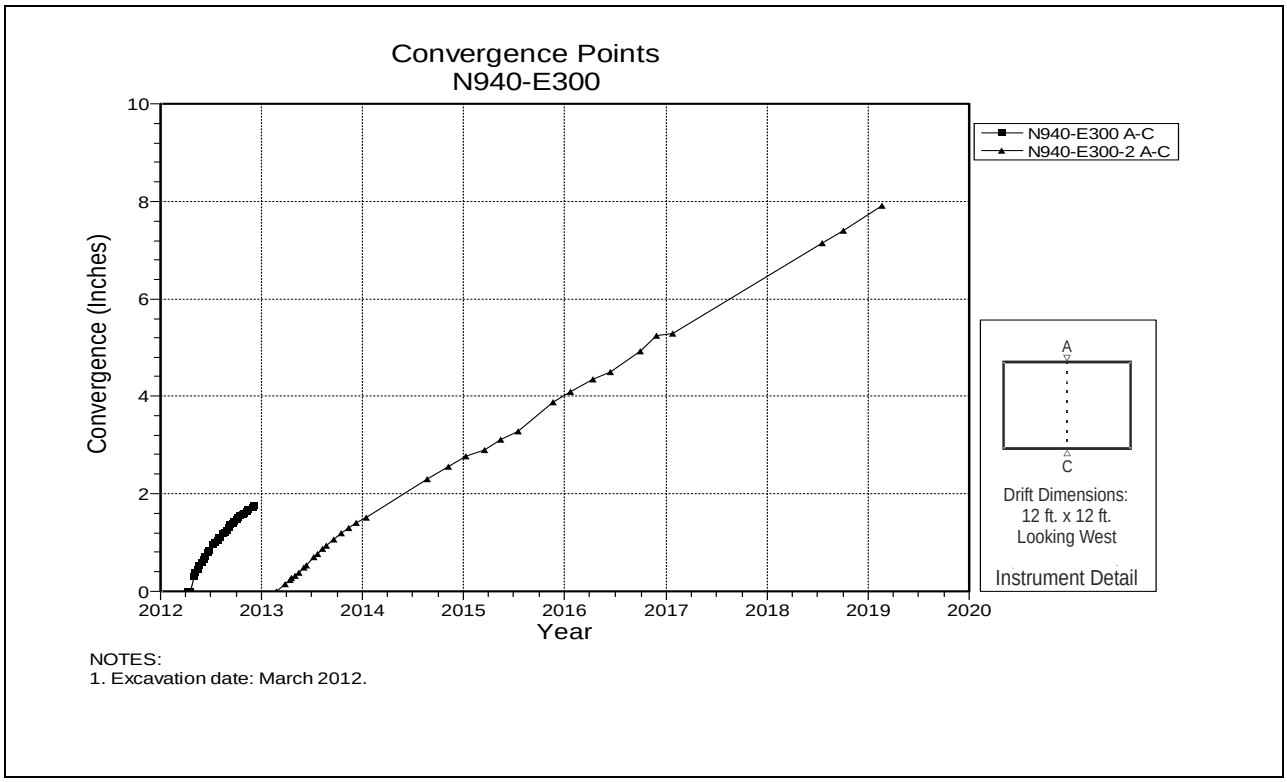

Figure 4-129 Convergence Point Array – N940 E300 – Roof to Floor – Centerline

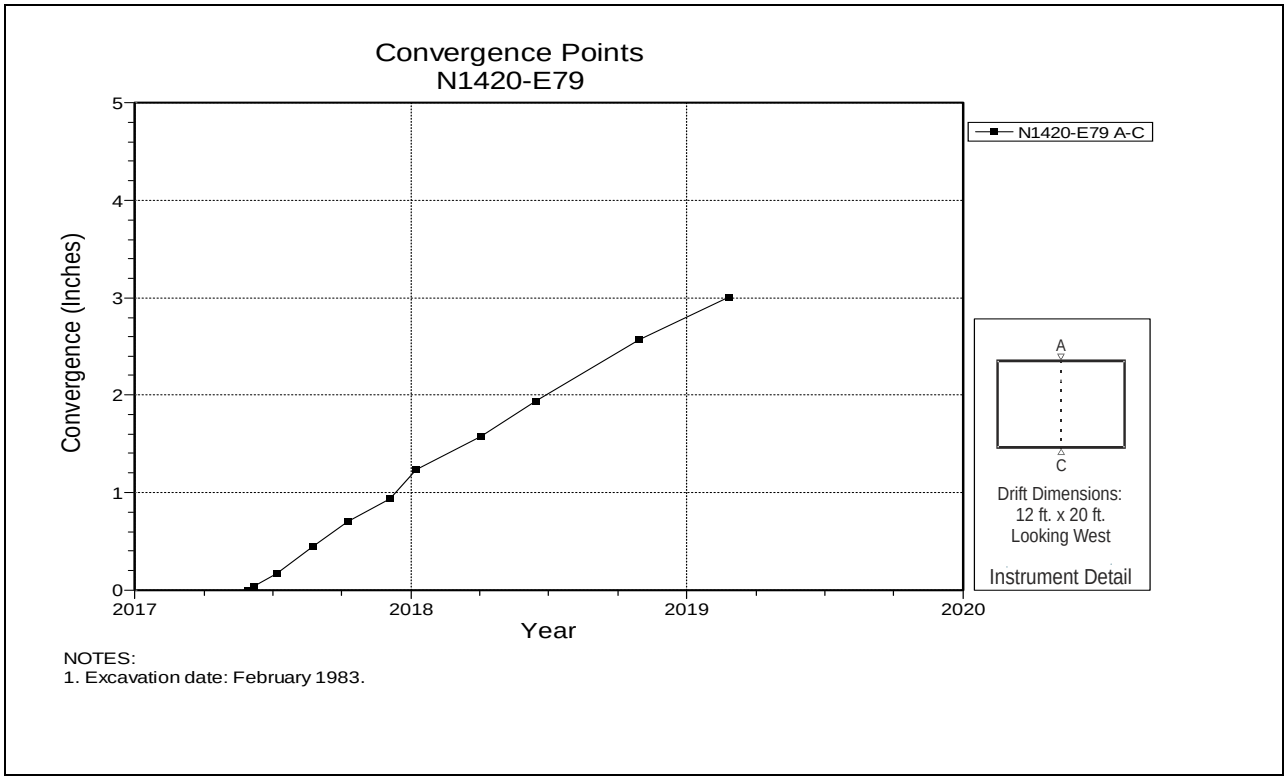

Figure 4-130 Convergence Point Array – N1420 E79 – Roof to Floor – Centerline

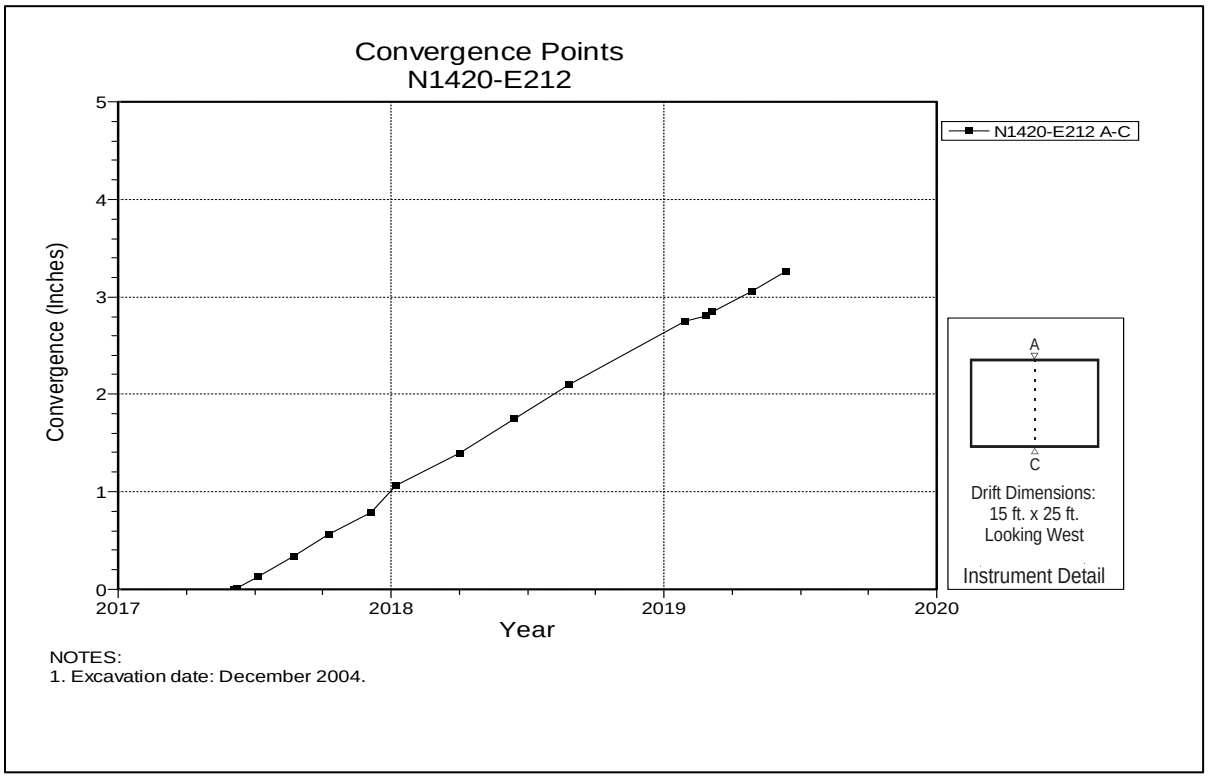

Figure 4-131 Convergence Point Array – N1420 E212 – Roof to Floor – Centerline

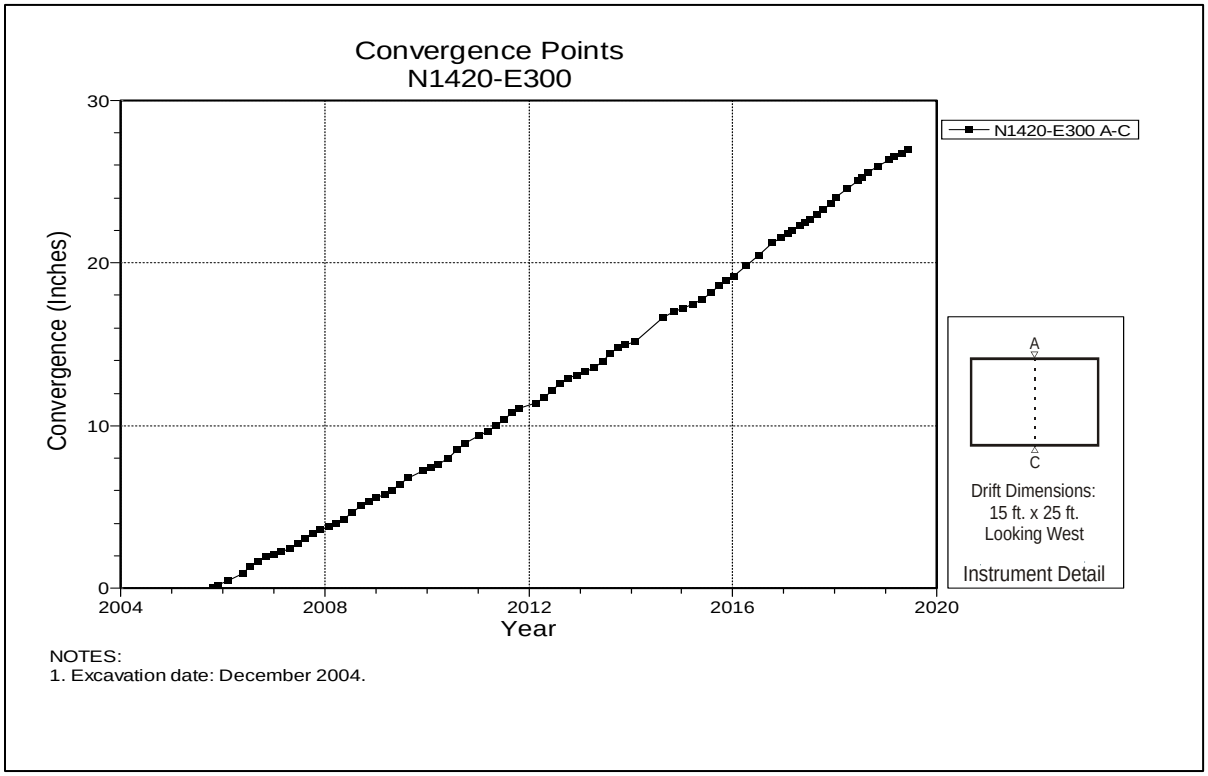

Figure 4-132 Convergence Point Array – N1420 E300 – Roof to Floor – Centerline

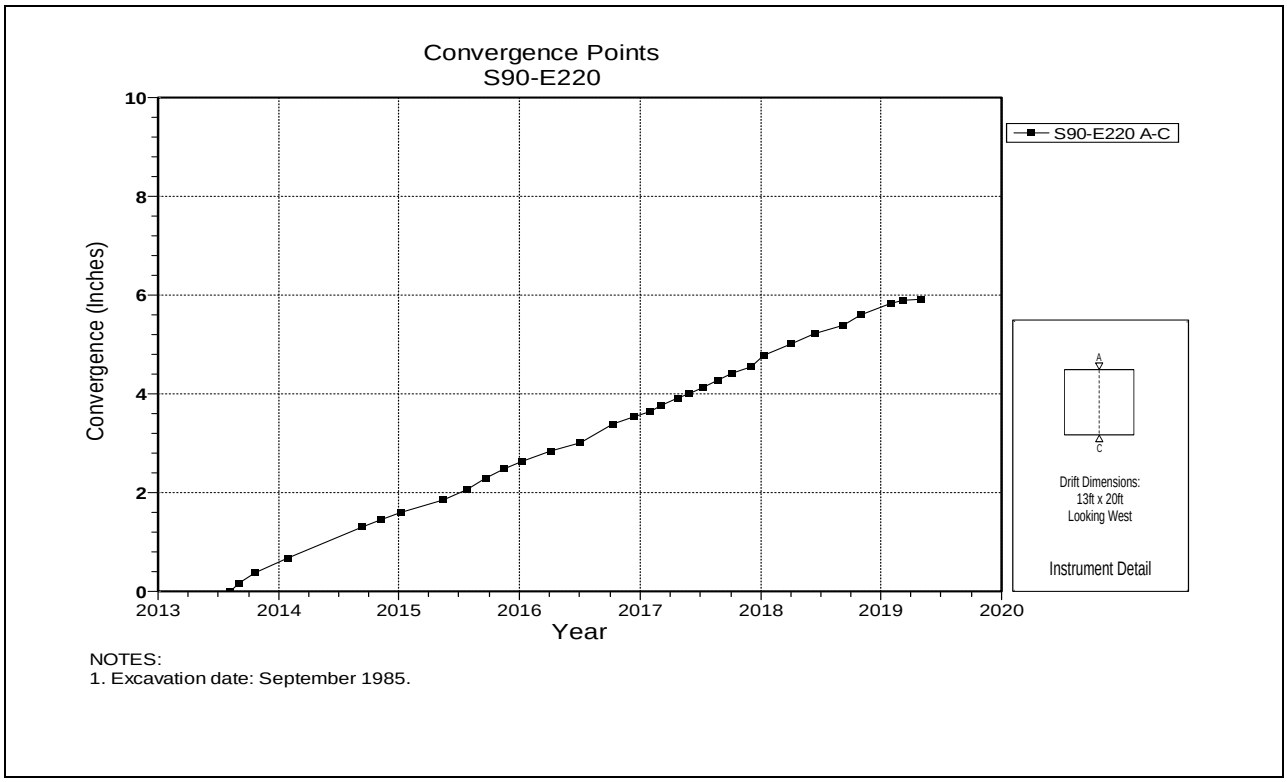

Figure 4-133 Convergence Point Array – S90 E220 – Roof to Floor – Centerline

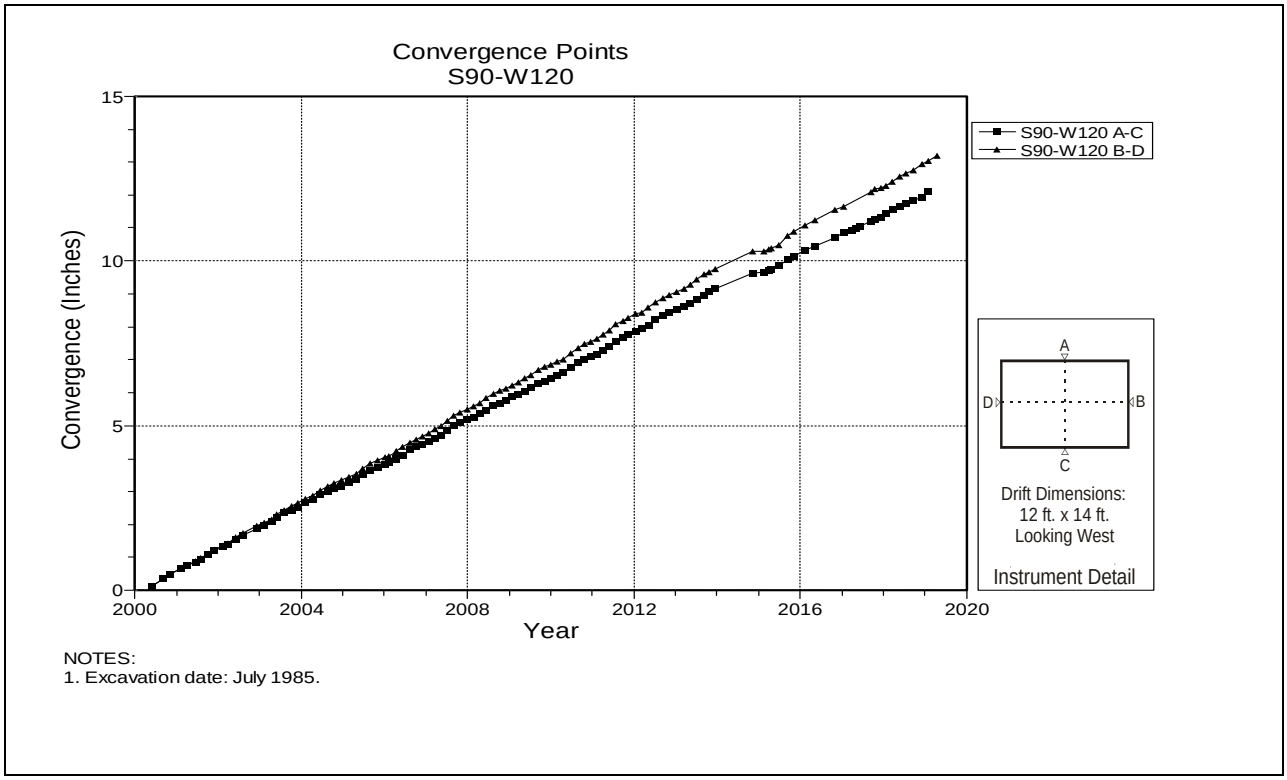

Figure 4-134 Convergence Point Array – S90 W120 – All Chords

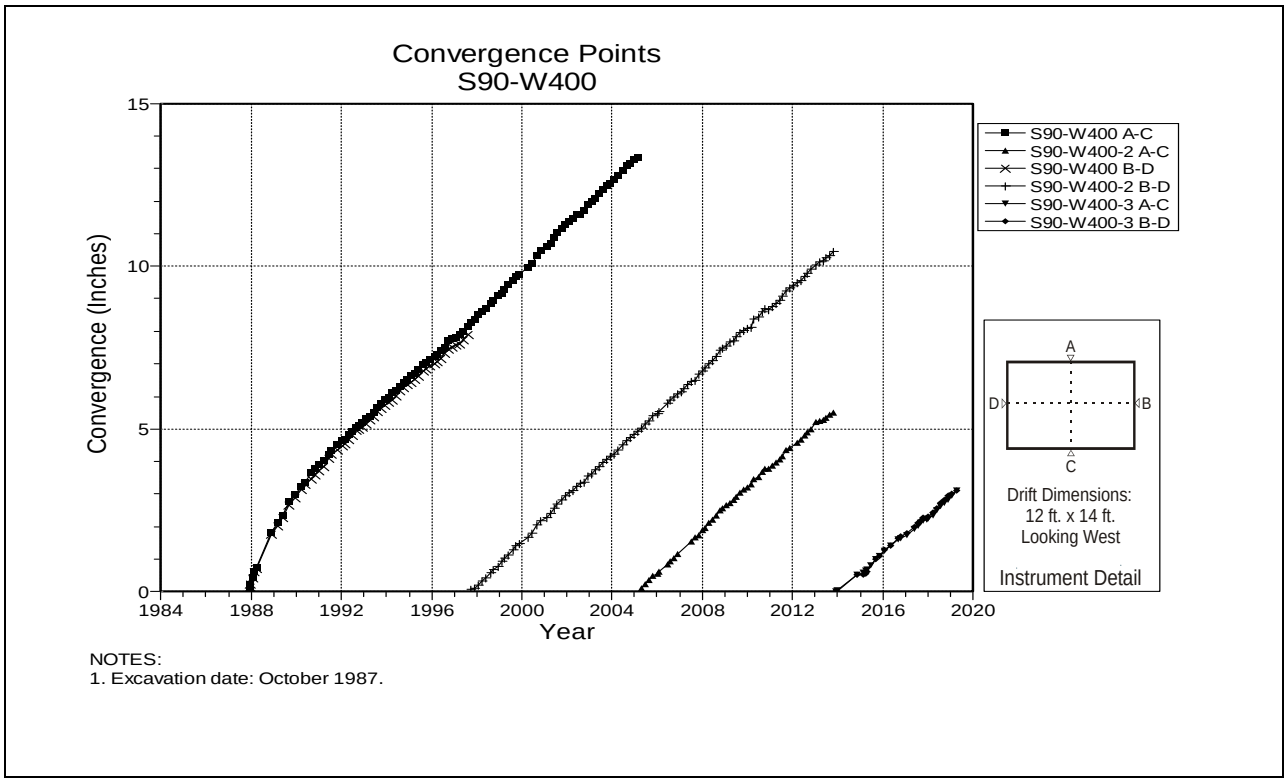

Figure 4-135 Convergence Point Array – S90 W400 – All Chords

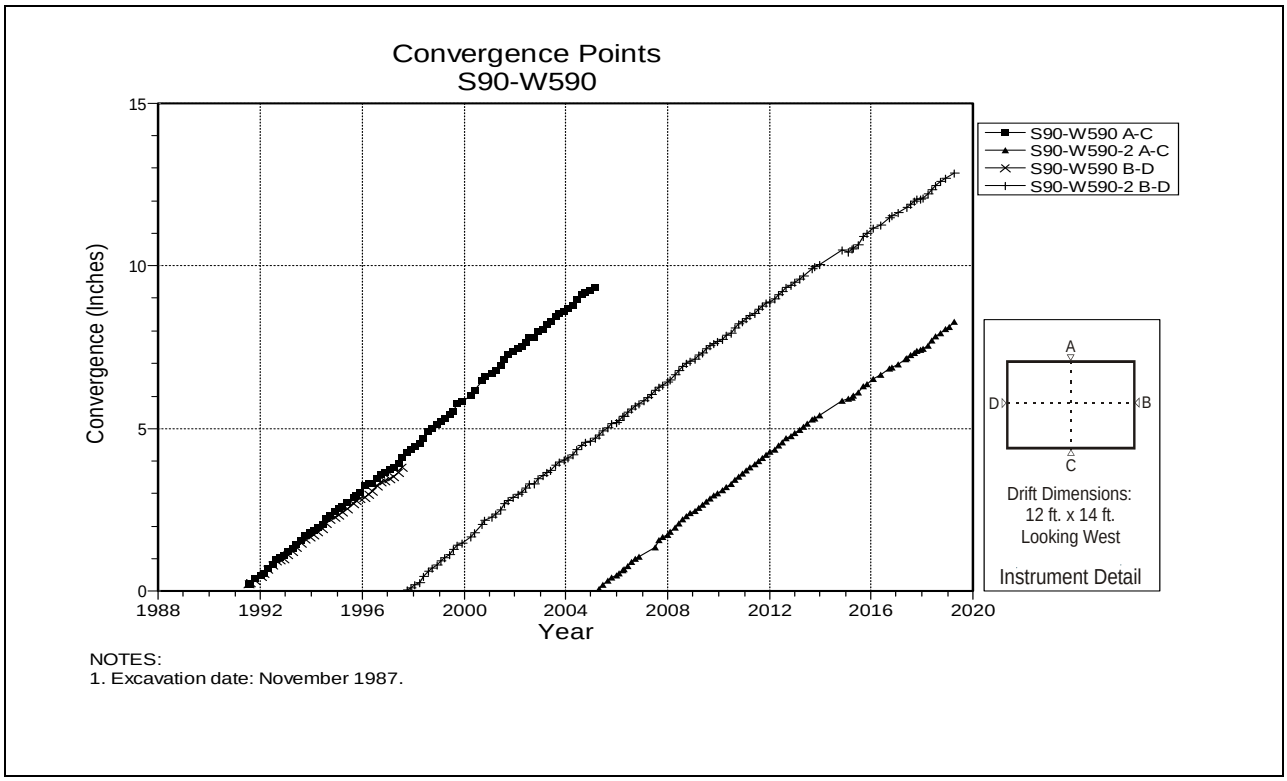

Figure 4-136 Convergence Point Array – S90 W590 – All Chords

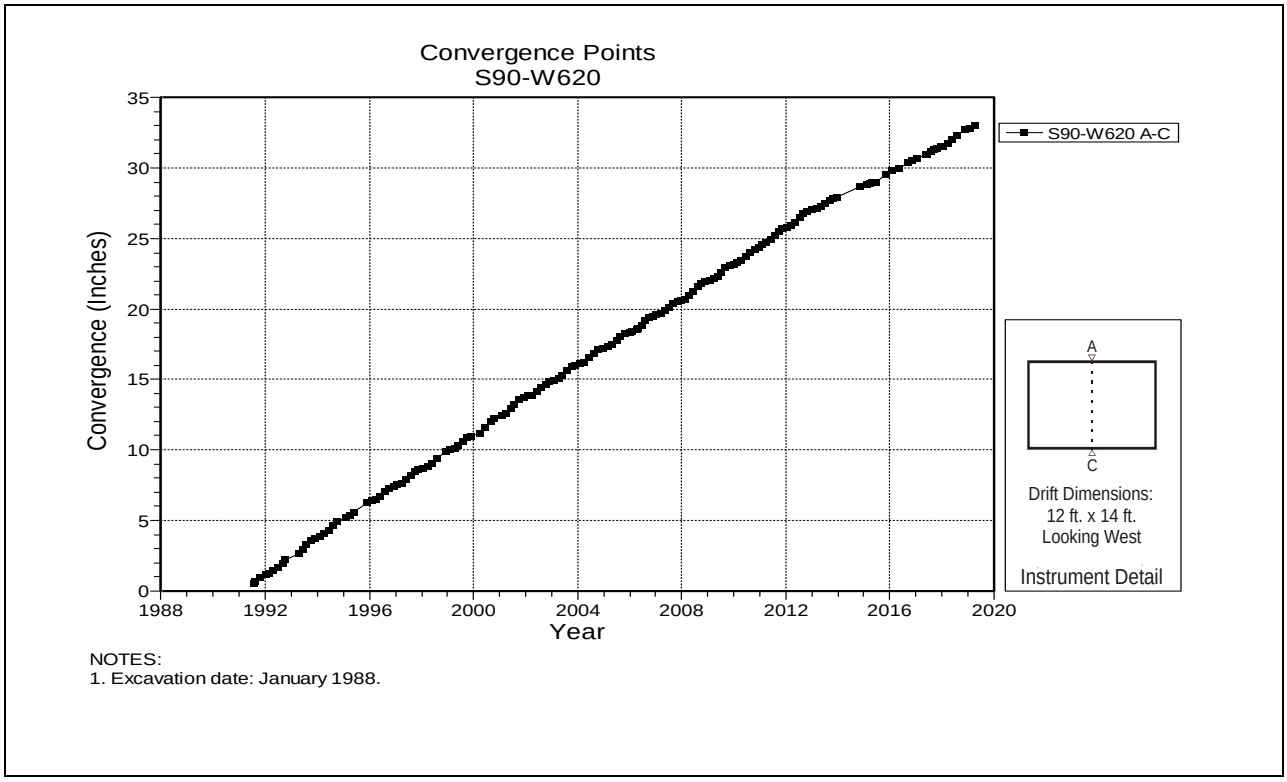

NOTES:
1. Excavation date: January 1988.

Figure 4-137 Convergence Point Array – S90 W620 – Roof to Floor – Centerline

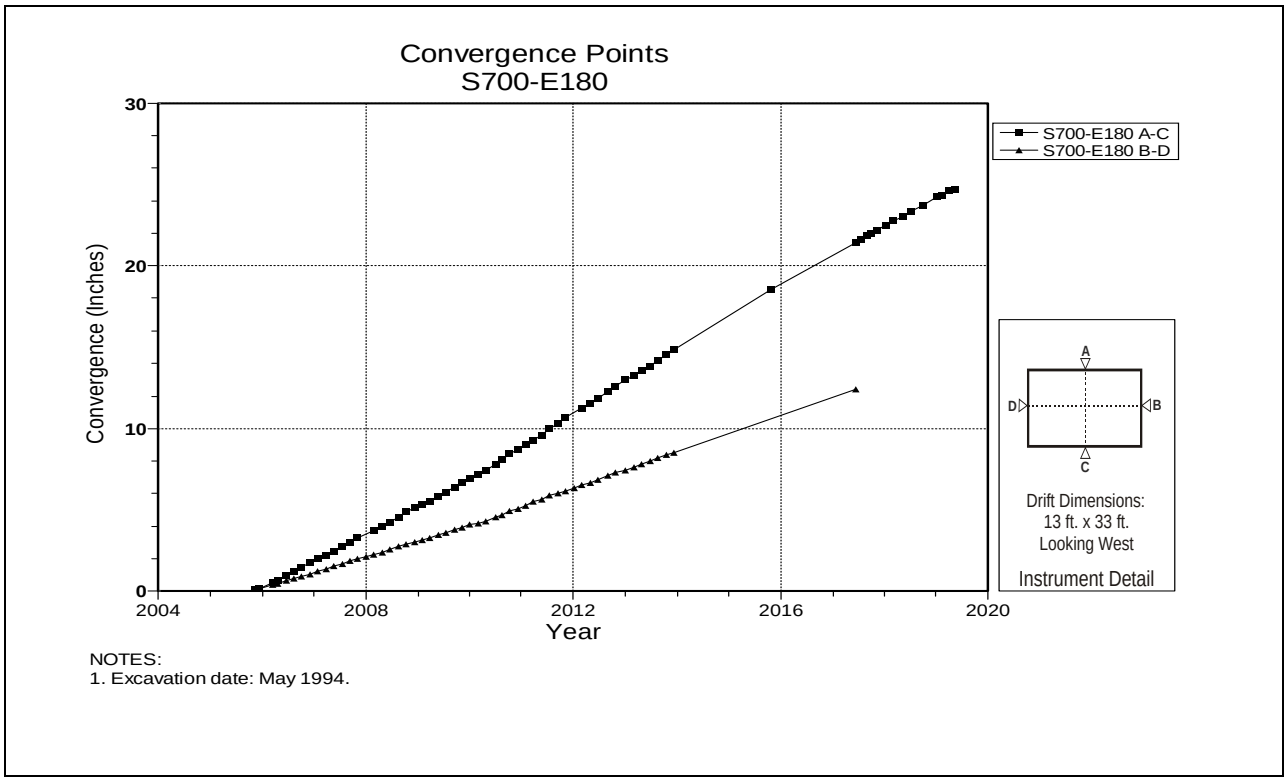

NOTES:
1. Excavation date: May 1994.

Figure 4-138 Convergence Point Array – S700 E180 – All Chords

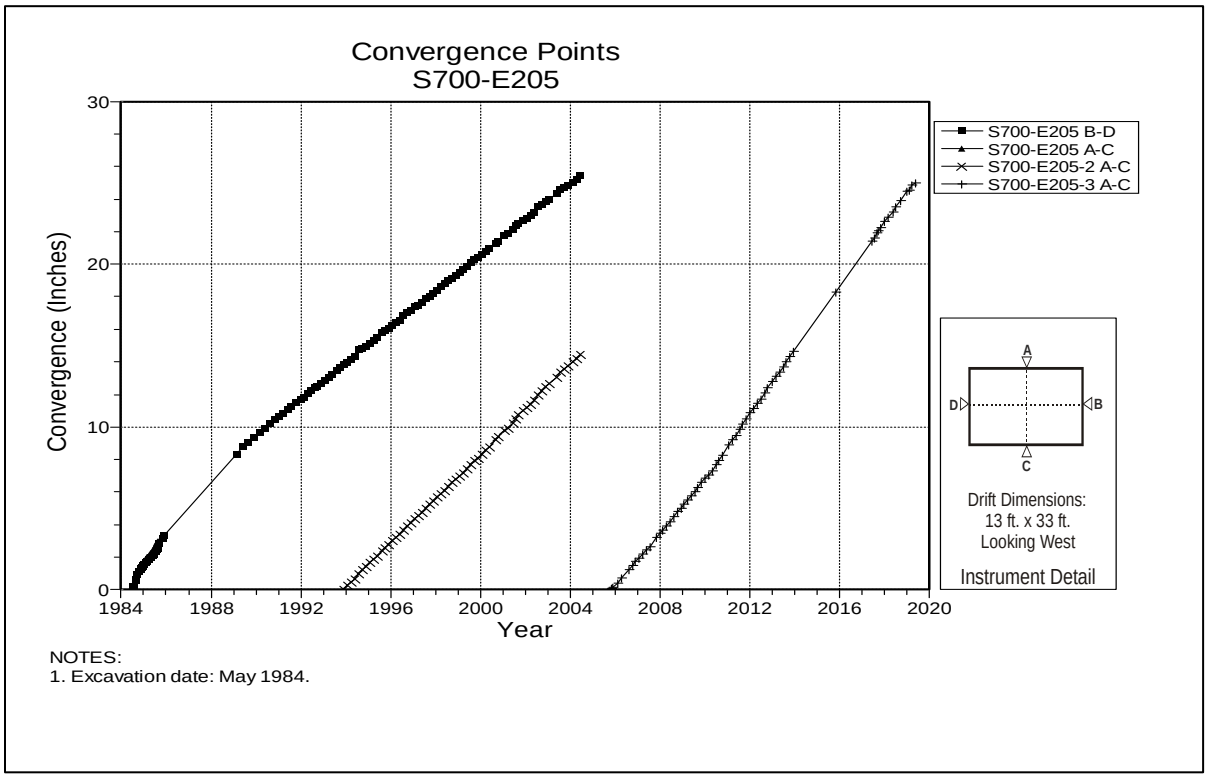

Figure 4-139 Convergence Point Array – S700 E205 – All Chords

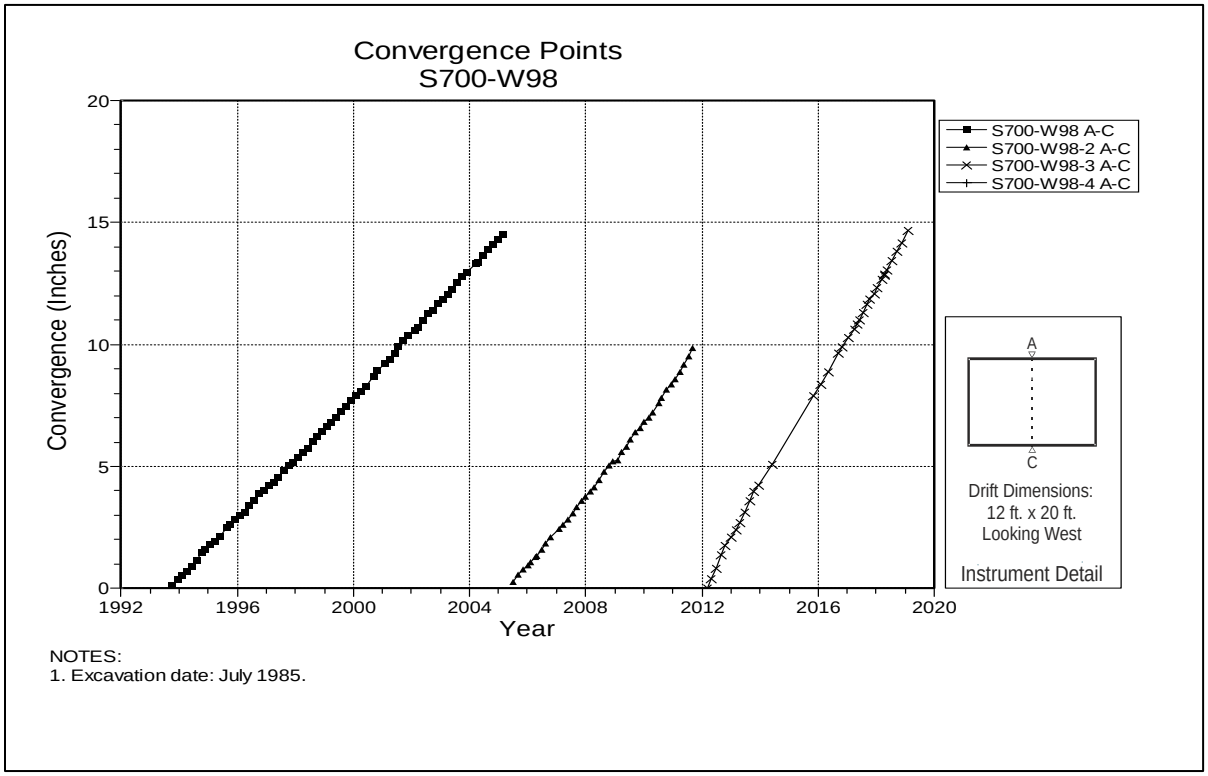

Figure 4-140 Convergence Point Array – S700 W98 – Roof to Floor – Centerline

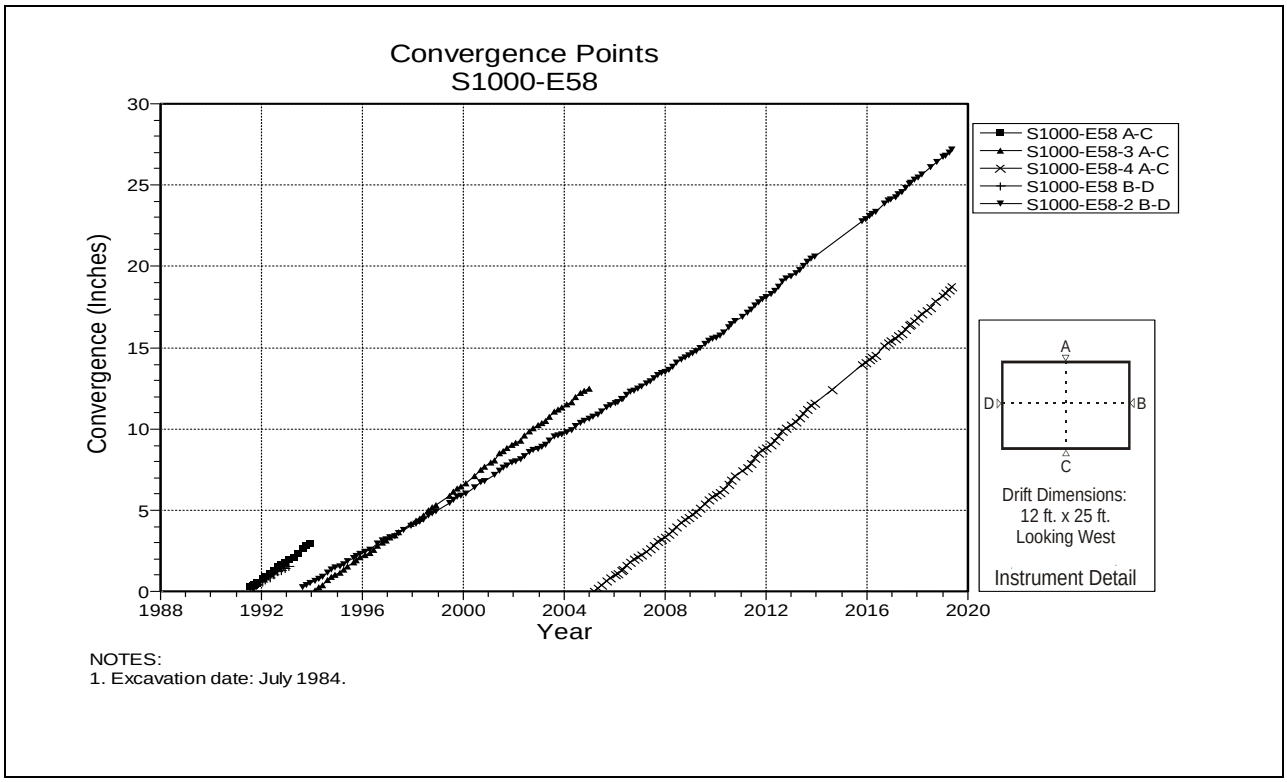

Figure 4-141 Convergence Point Array – S1000 E58 – All Chords

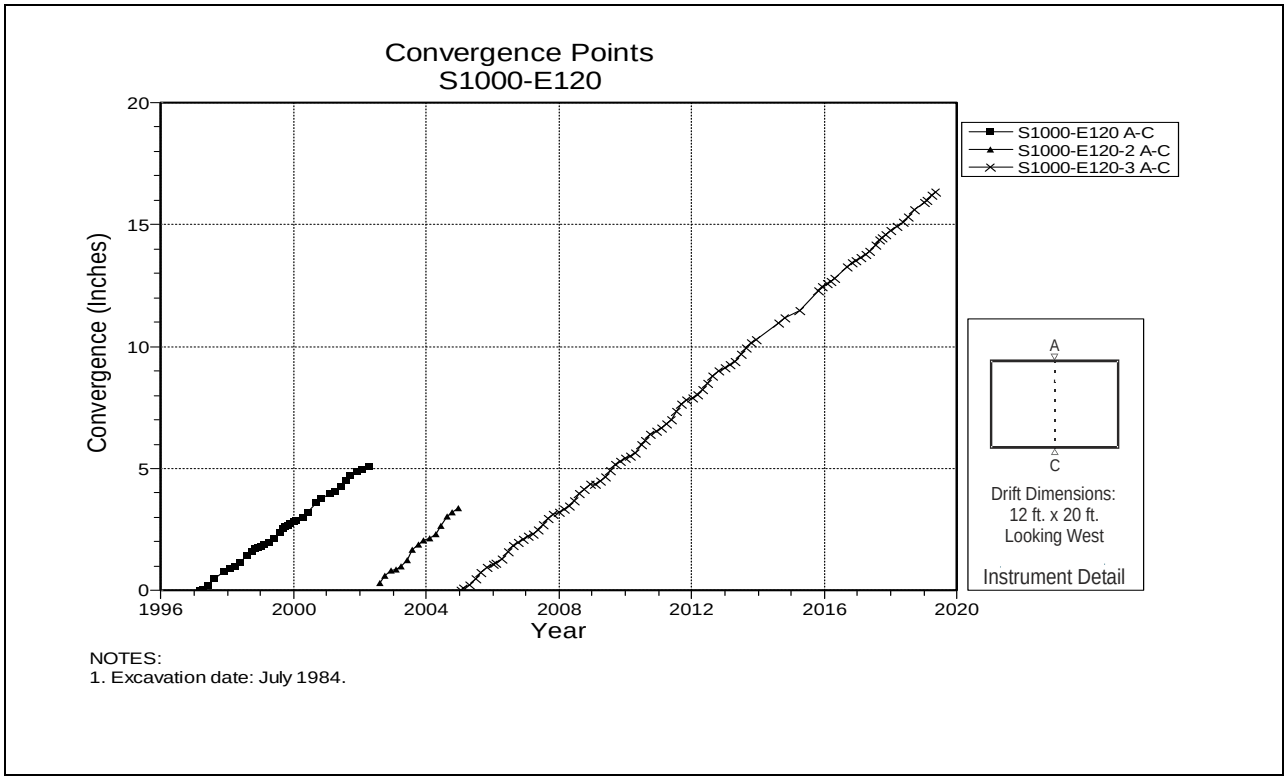

Figure 4-142 Convergence Point Array – S1000 E120 – Roof to Floor – Centerline

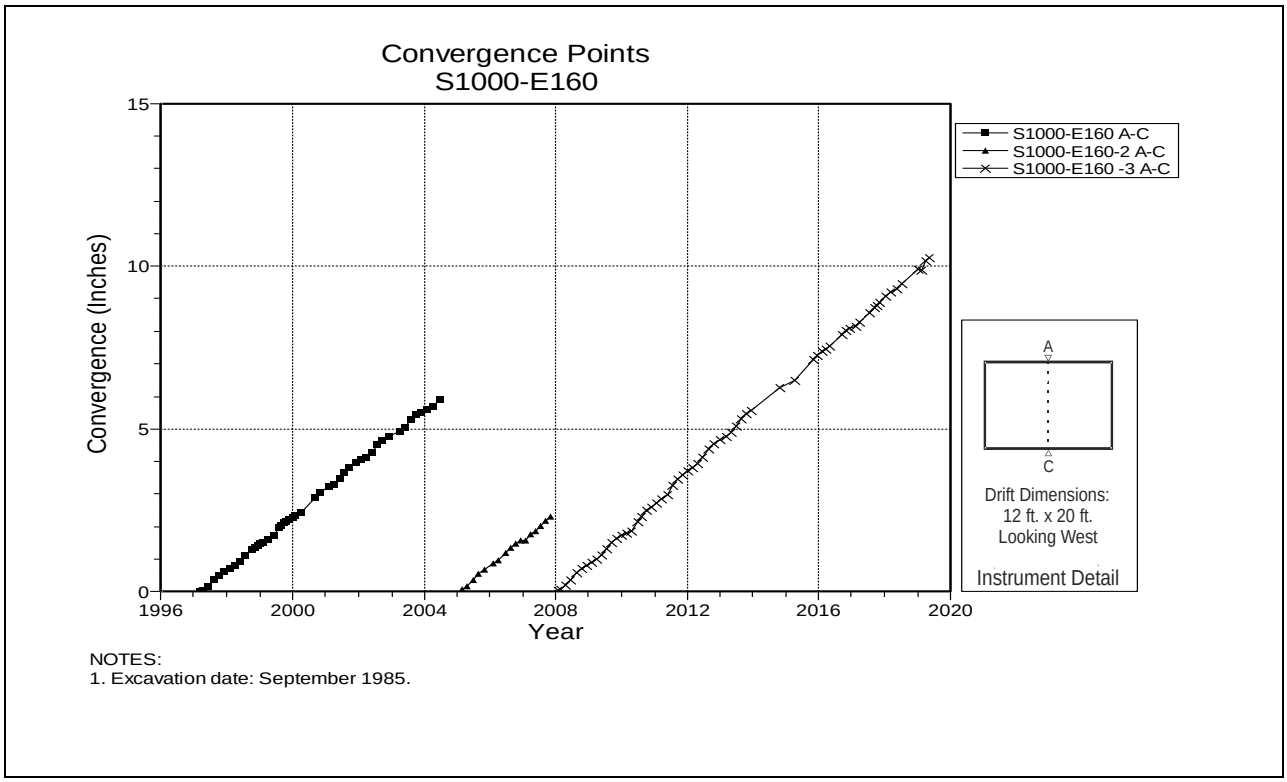

Figure 4-143 Convergence Point Array – S1000 E160 – Roof to Floor – Centerline

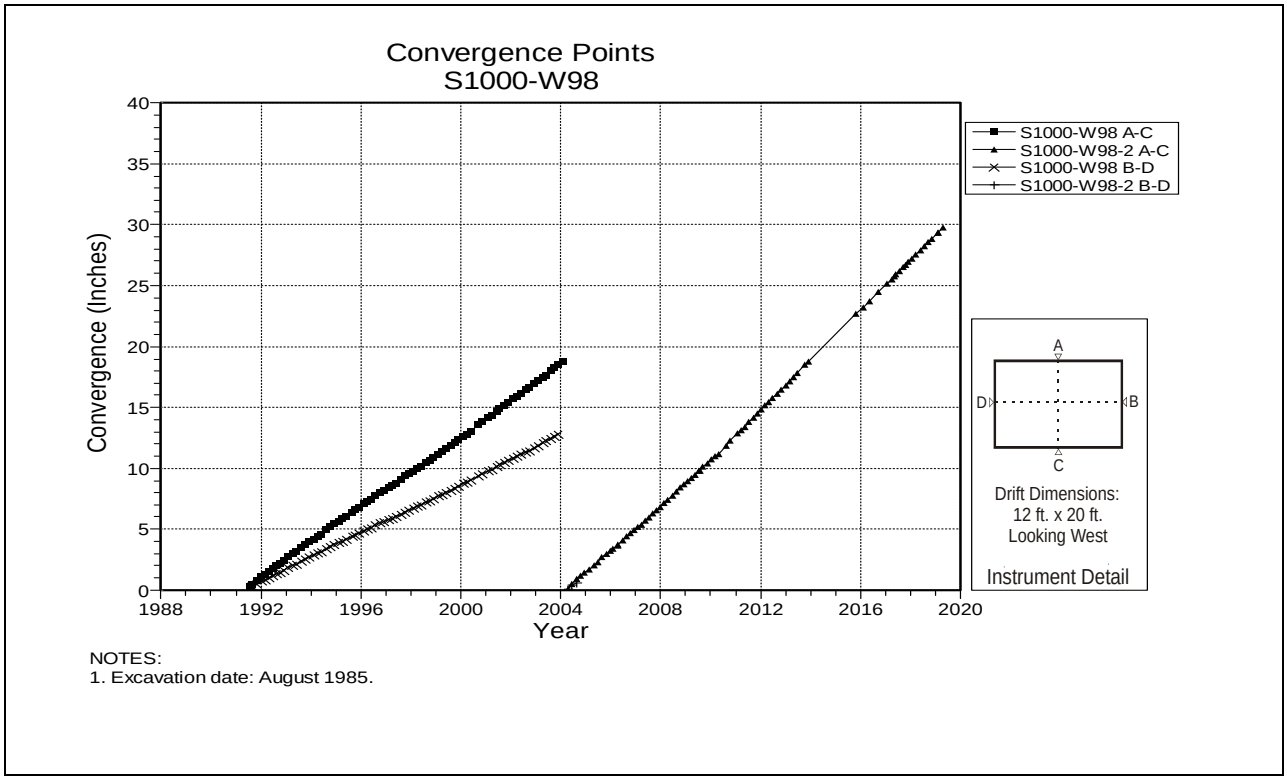

Figure 4-144 Convergence Point Array – S1000 W98 – All Chords

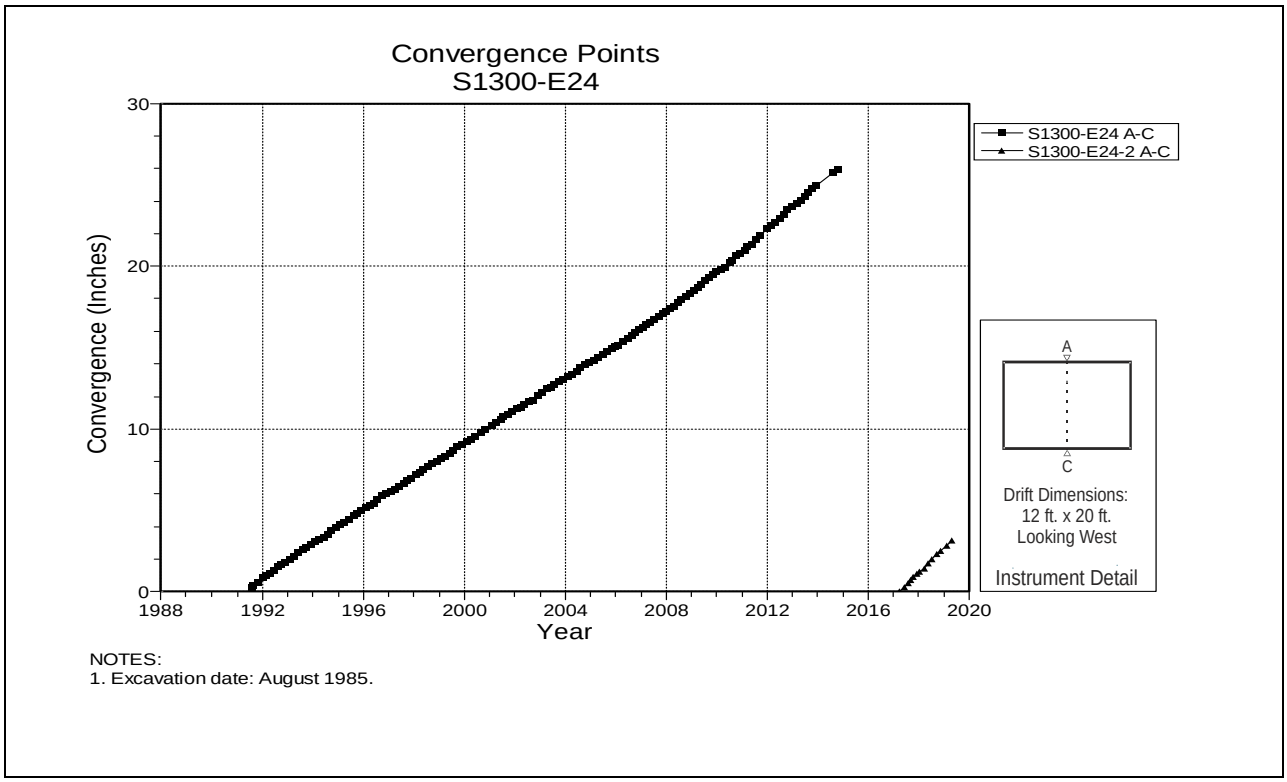

Figure 4-145 Convergence Point Array – S1300 E24 – Roof to Floor – Centerline

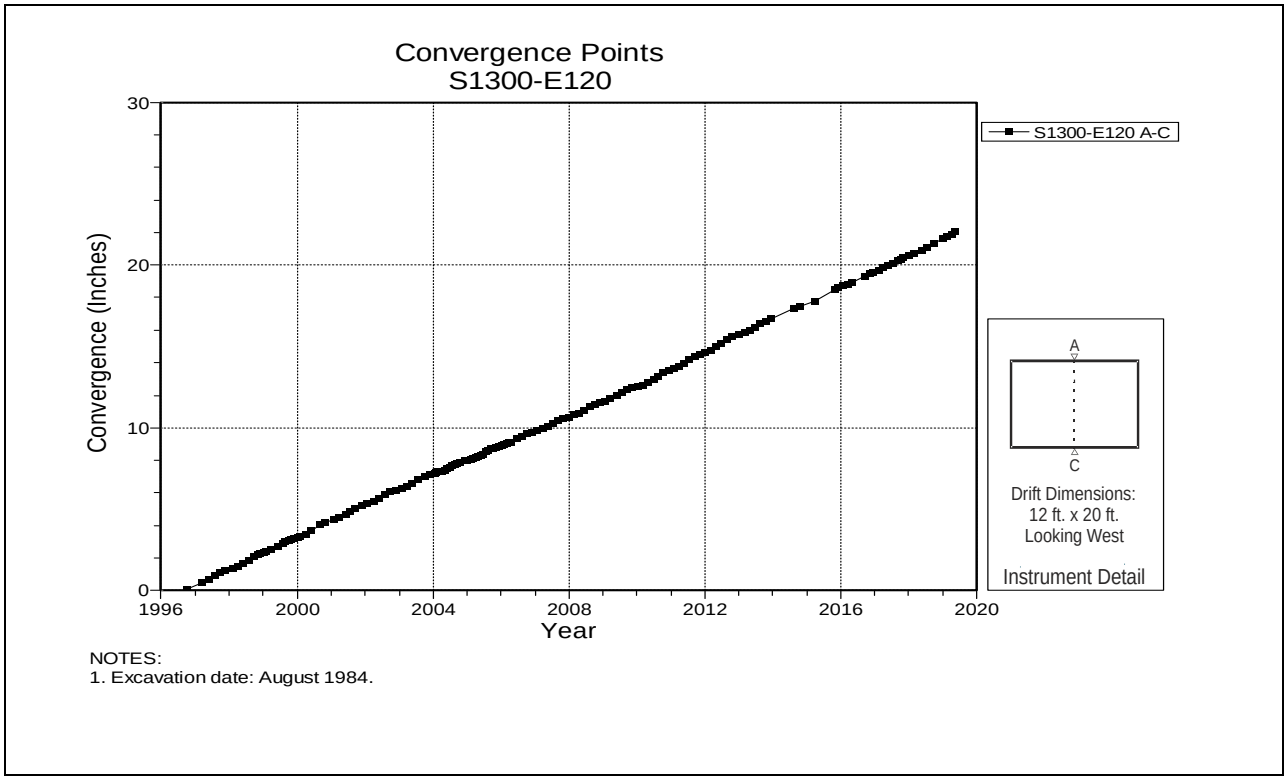

Figure 4-146 Convergence Point Array – S1300 E120 – Roof to Floor – Centerline

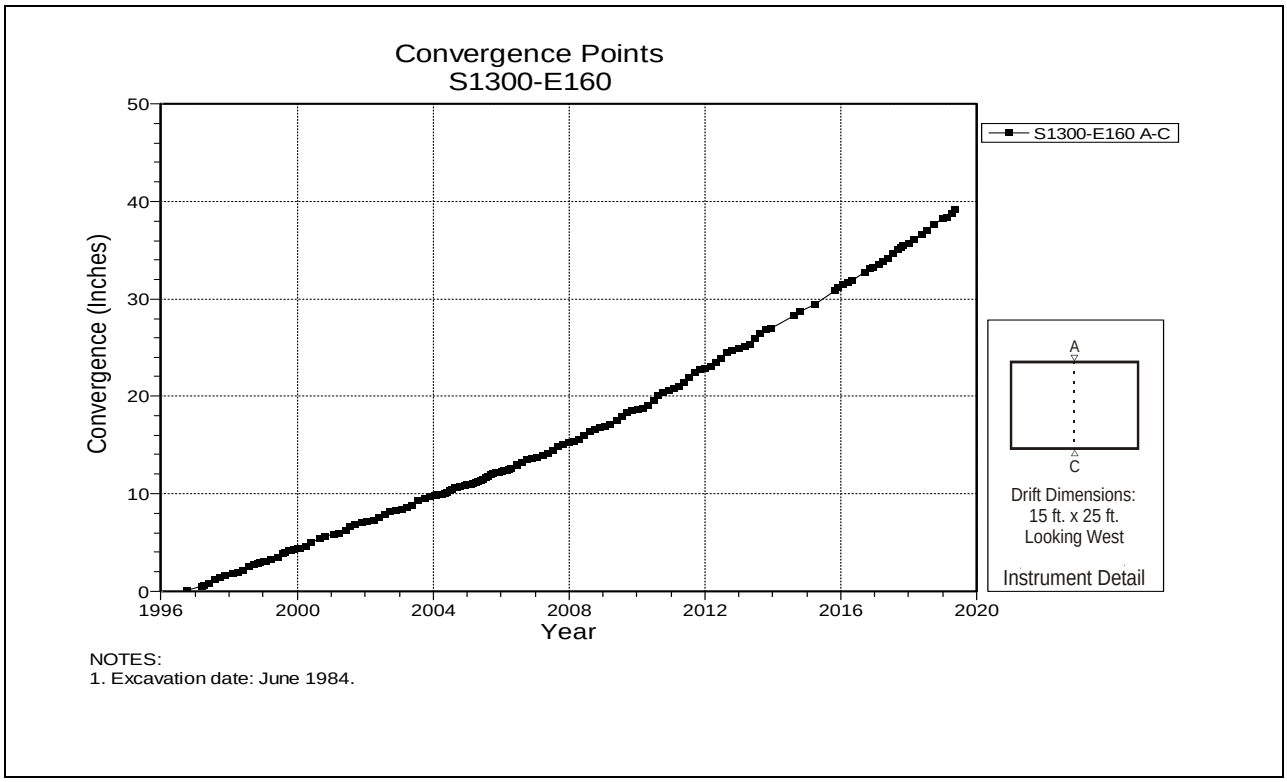

Figure 4-147 Convergence Point Array – S1300 E160 – Roof to Floor – Centerline

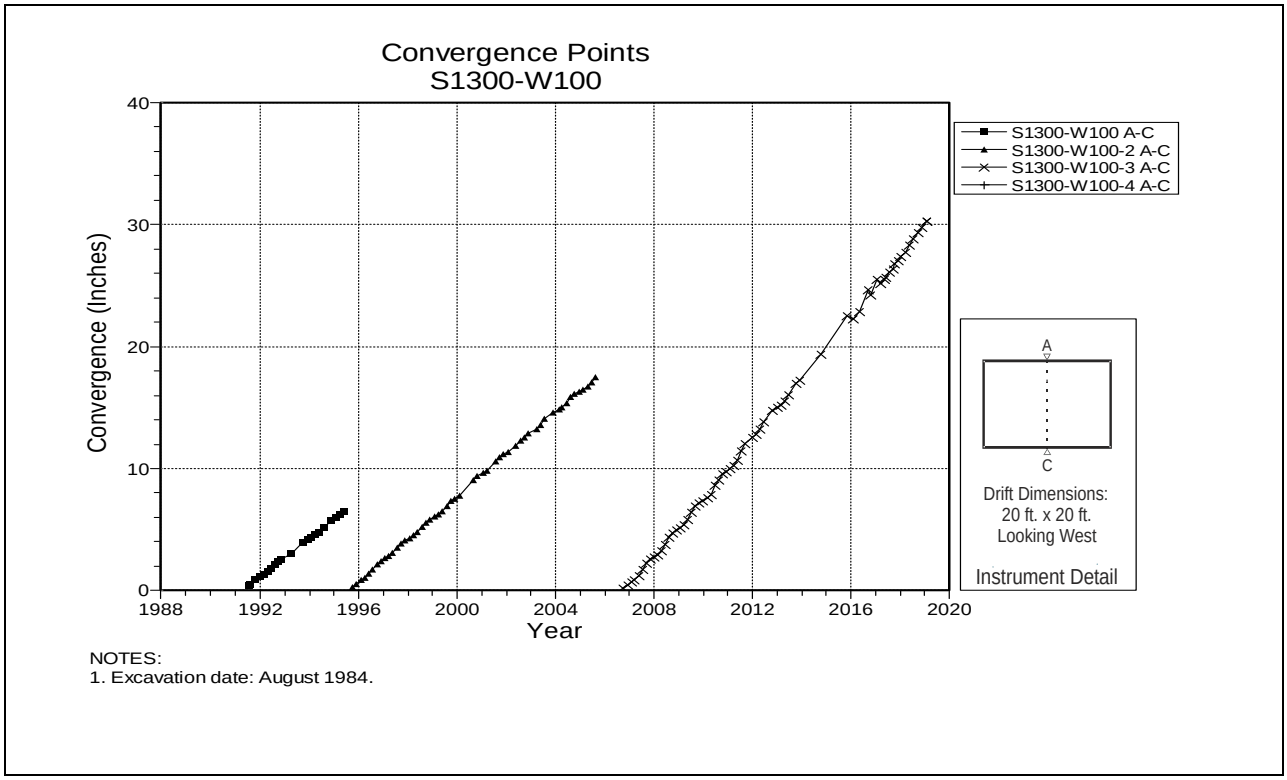

Figure 4-148 Convergence Point Array – S1300 W100 – Roof to Floor – Centerline

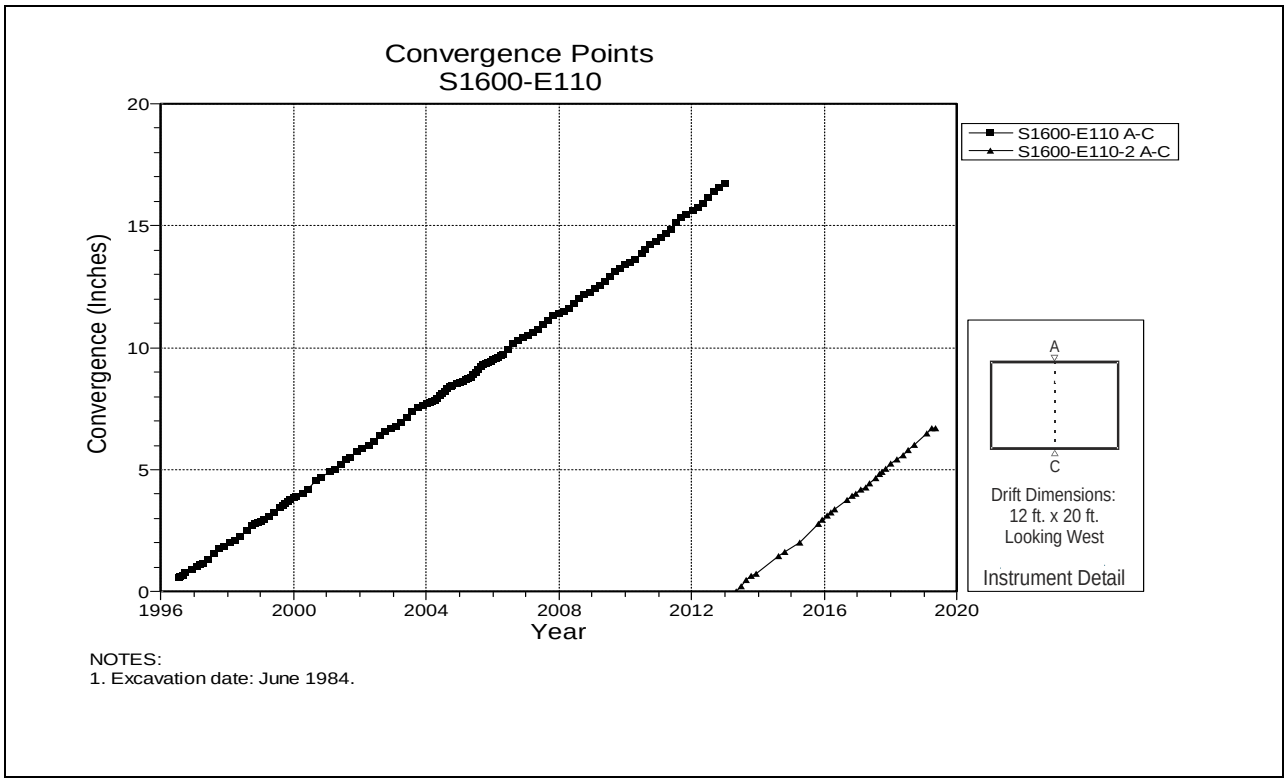

Figure 4-149 Convergence Point Array – S1600 E110 – Roof to Floor – Centerline

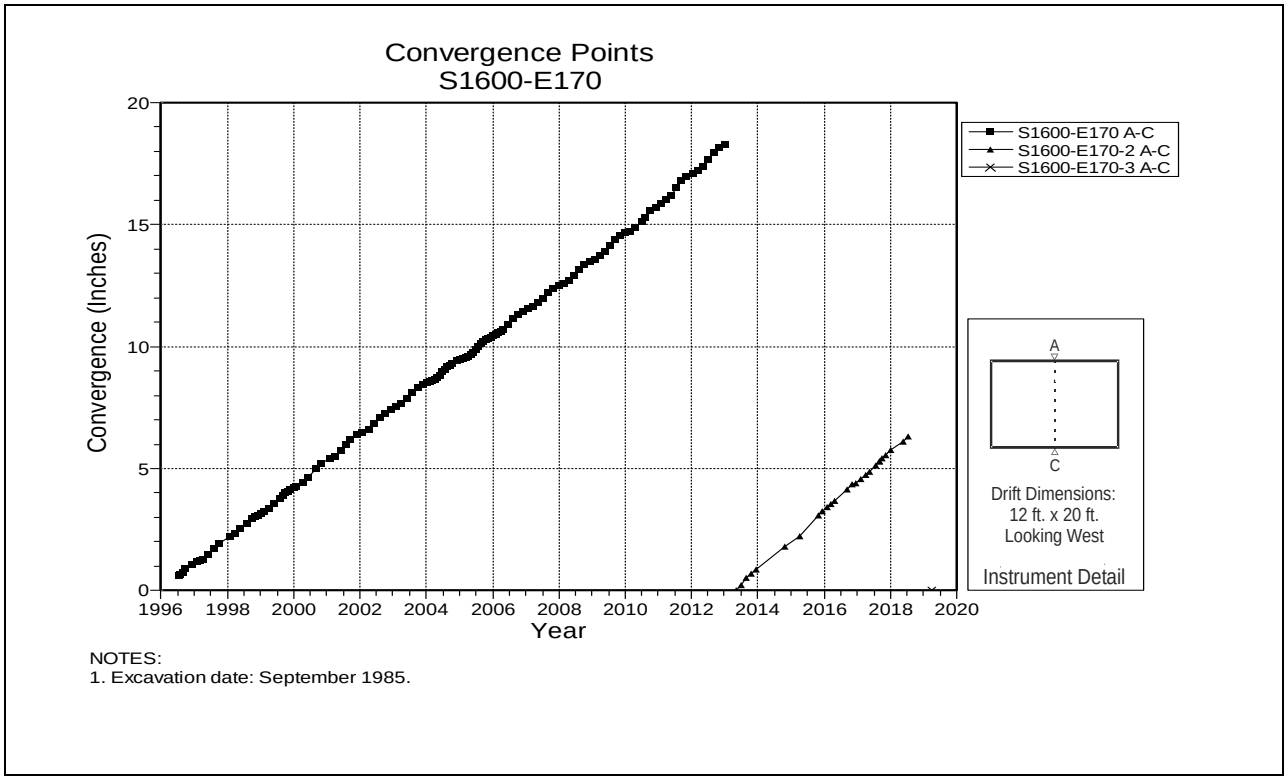

Figure 4-150 Convergence Point Array – S1600 E170 – Roof to Floor – Centerline

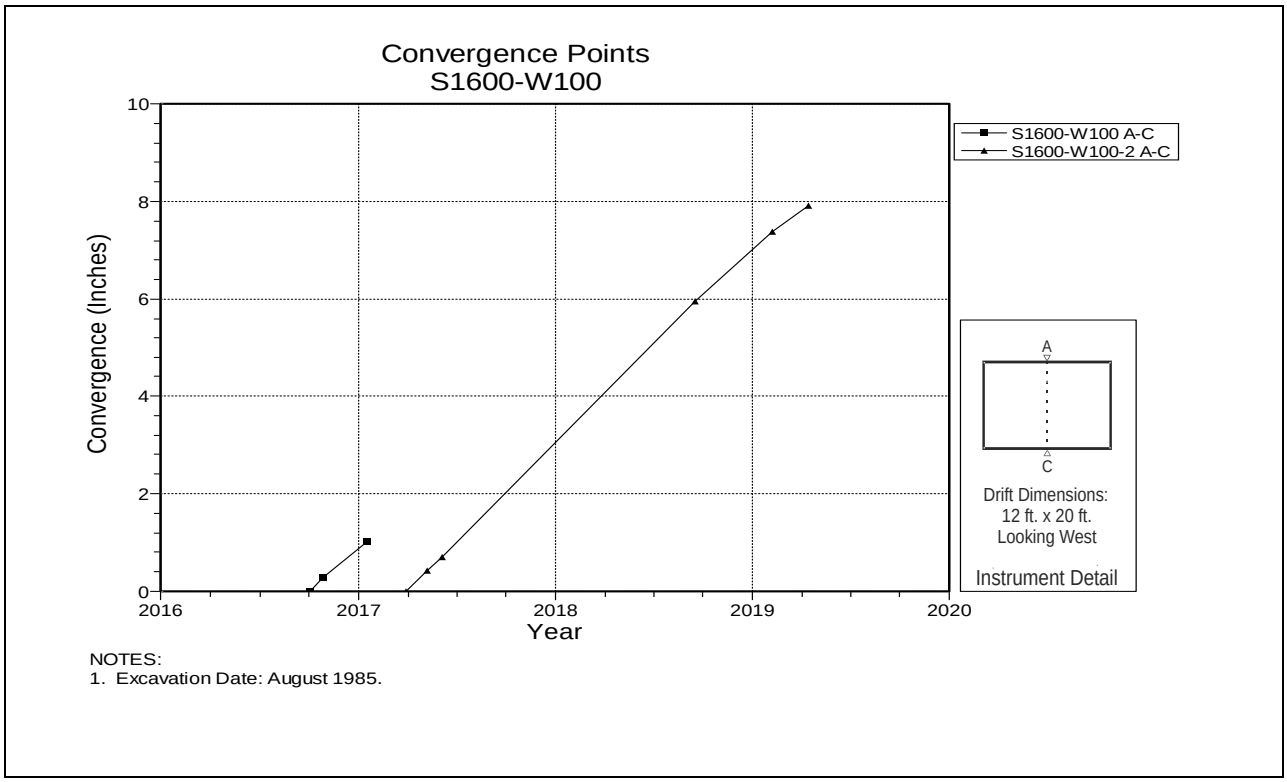

Figure 4-151 Convergence Point Array – S1600 W100 – Roof to Floor – Centerline

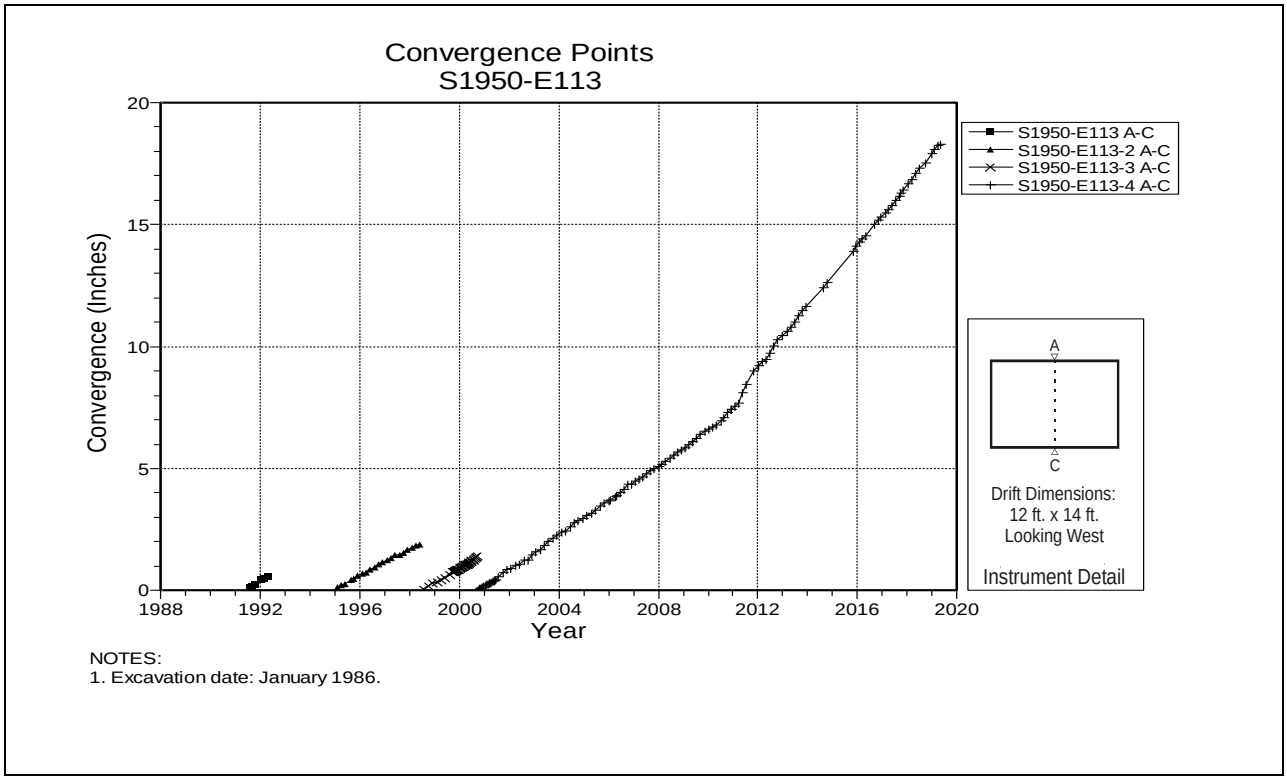

Figure 4-152 Convergence Point Array – S1950 E113 – Roof to Floor – Centerline

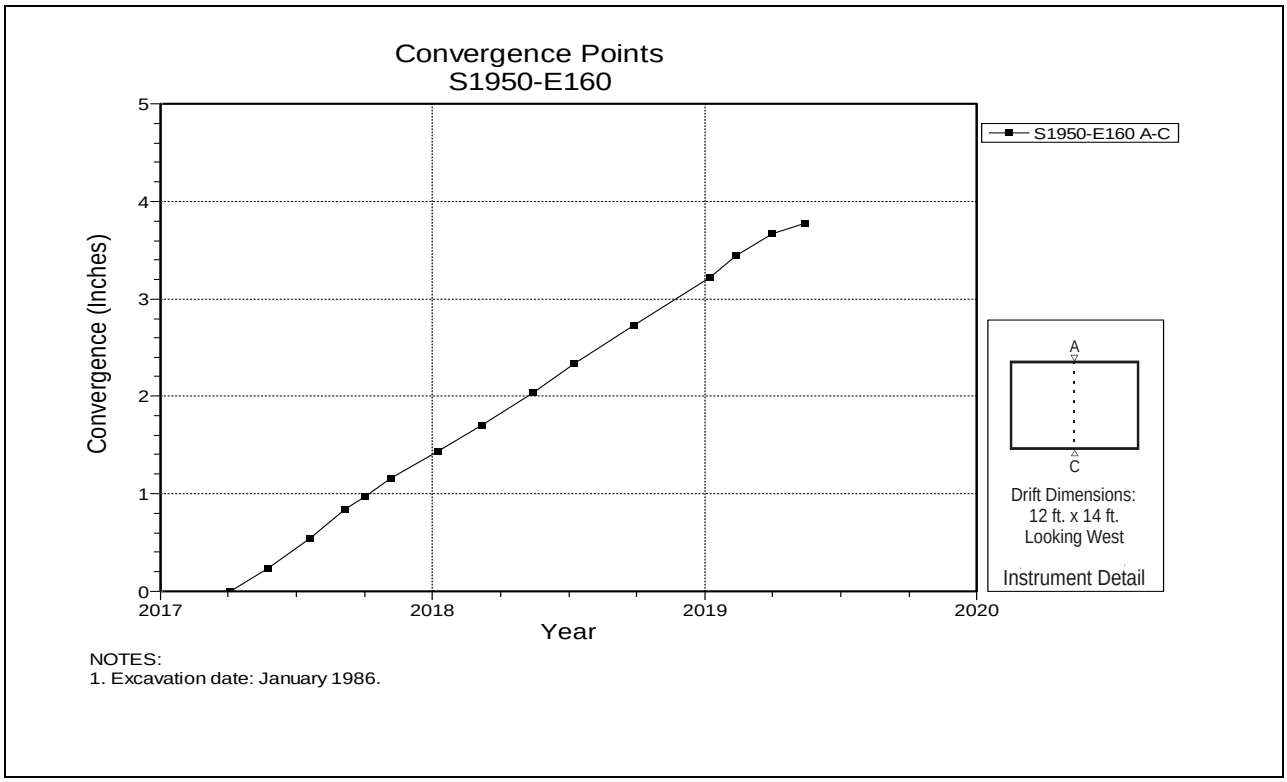

Figure 4-153 Convergence Point Array – S1950 E160 – Roof to Floor – Centerline

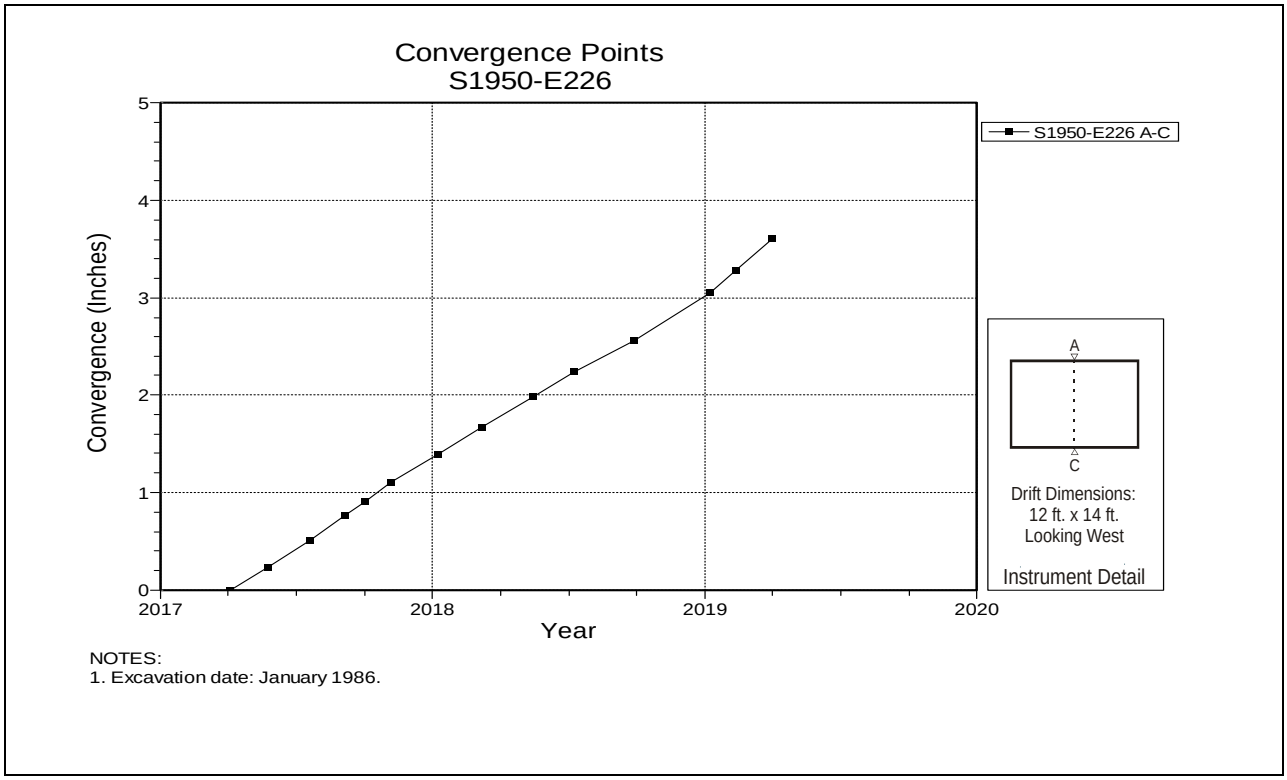

Figure 4-154 Convergence Point Array – S1950 E226 – Roof to Floor – Centerline

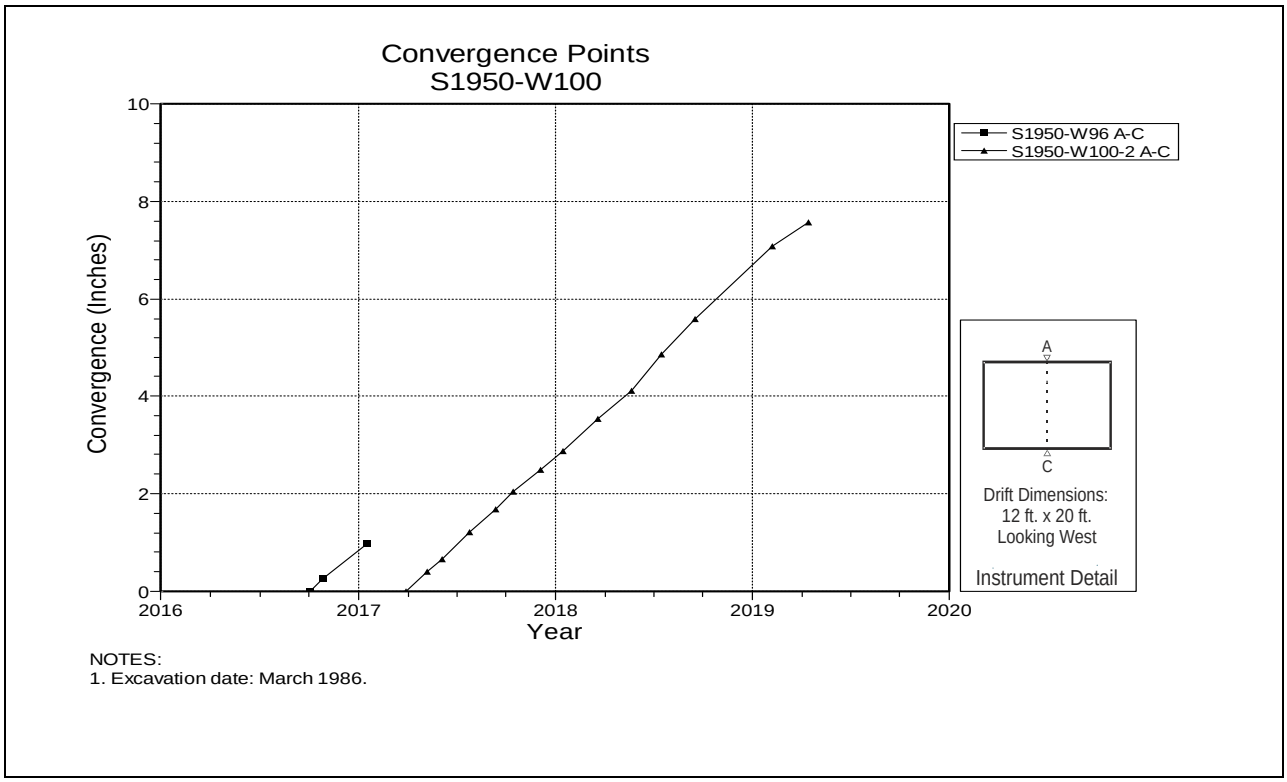

Figure 4-155 Convergence Point Array – S1950 W100 – Roof to Floor – Centerline

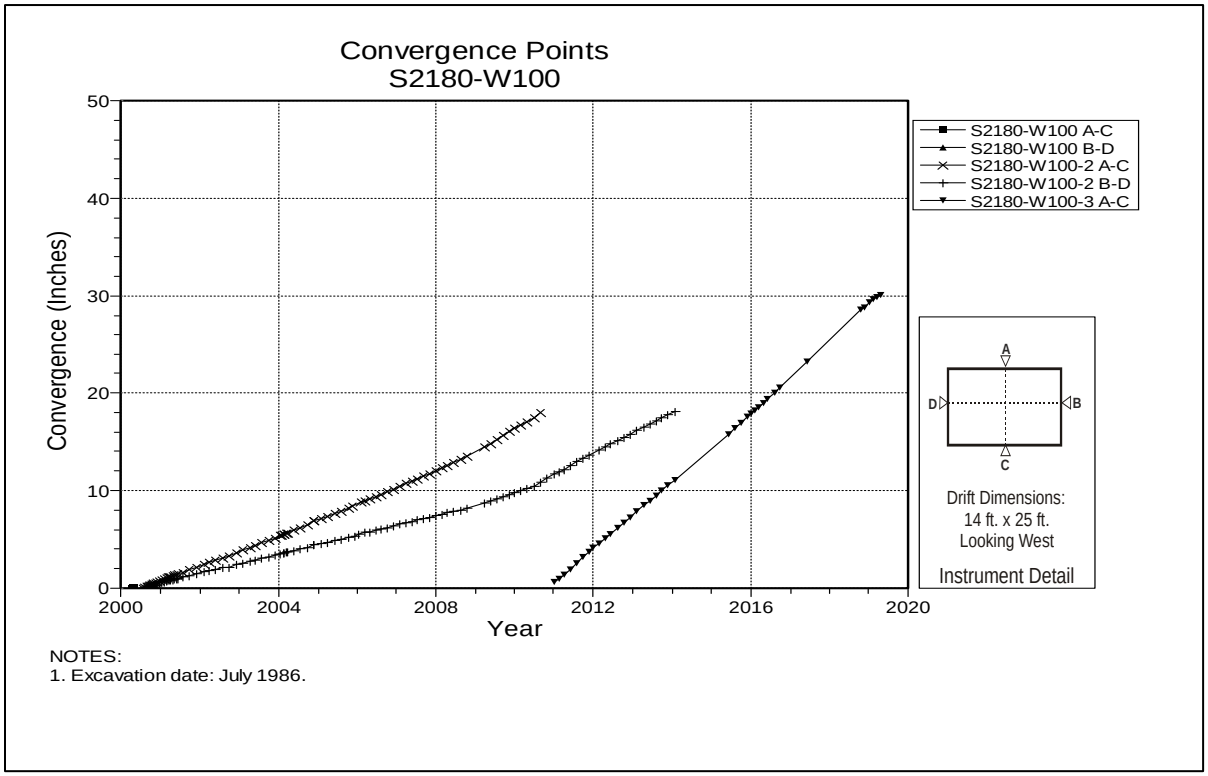

Figure 4-156 Convergence Point Array – S2180 W100 – All Chords

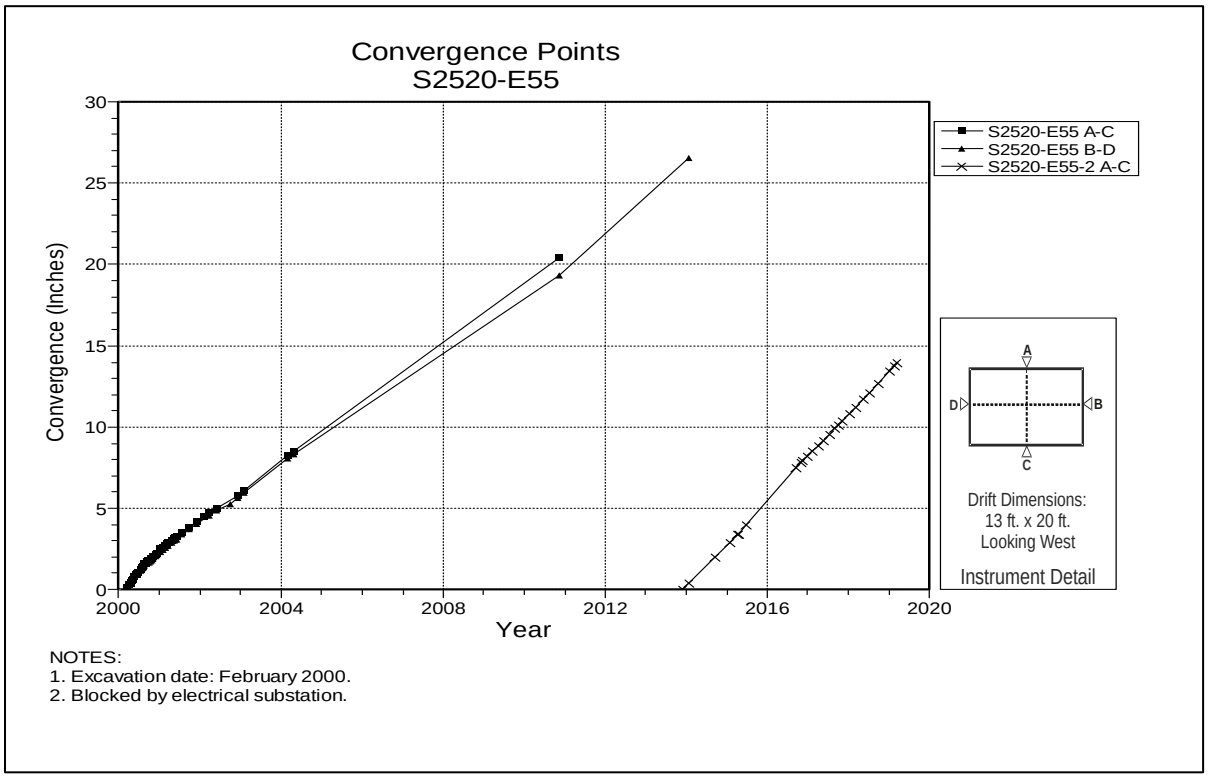

Figure 4-157 Convergence Point Array – S2520 E55 – All Chords

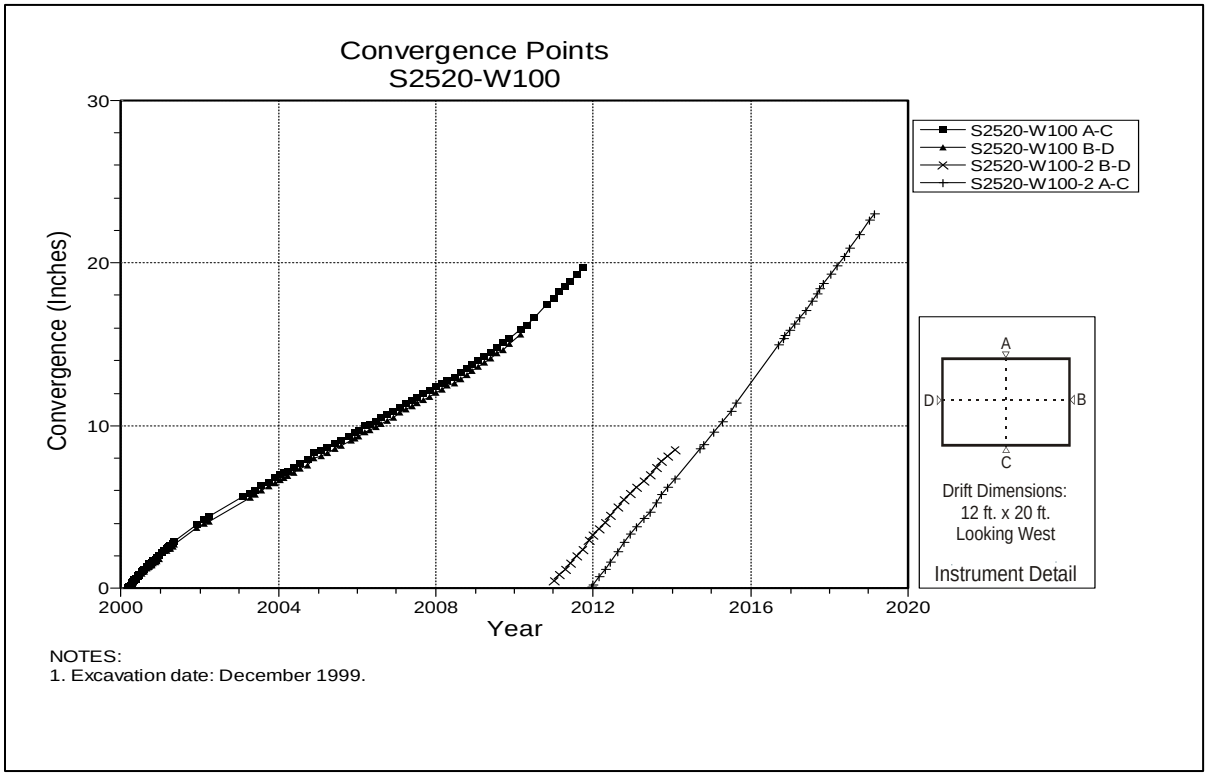

Figure 4-158 Convergence Point Array – S2520 W100 – All Chords

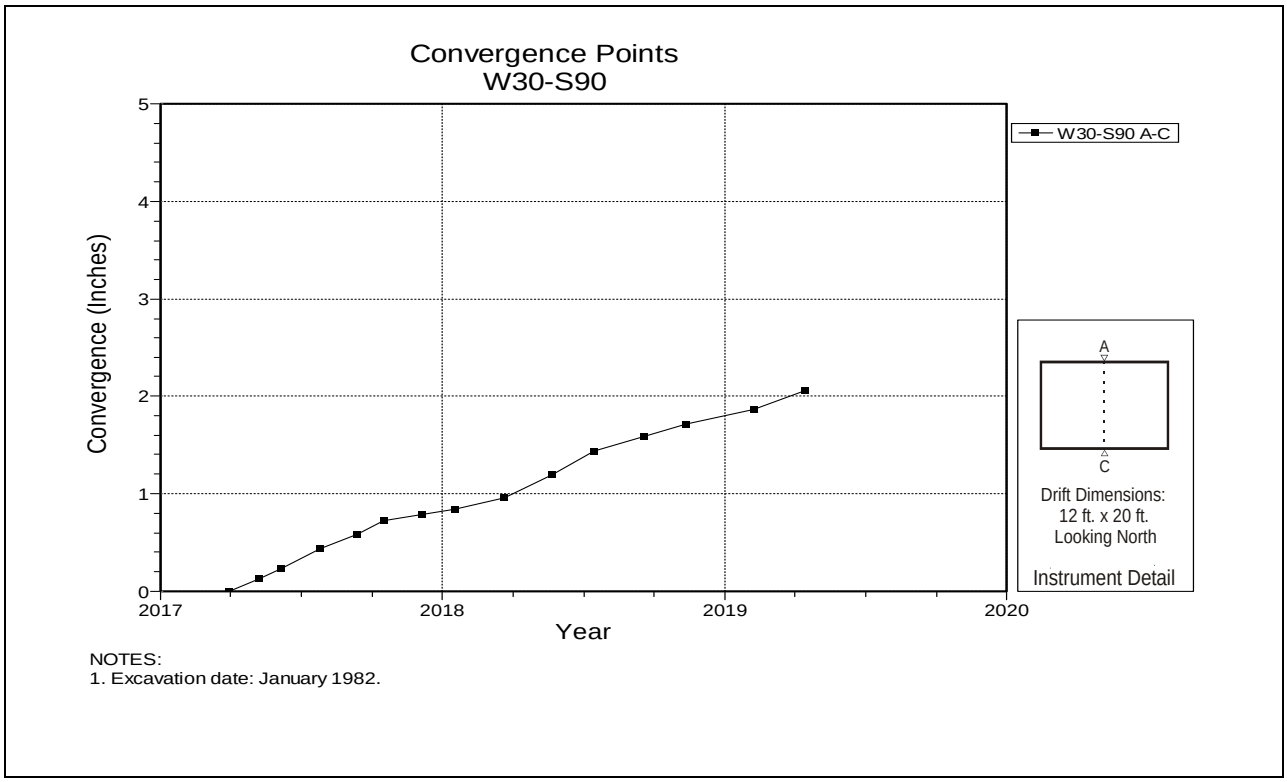

Figure 4-159 Convergence Point Array – W30 S90 – Roof to Floor – Centerline

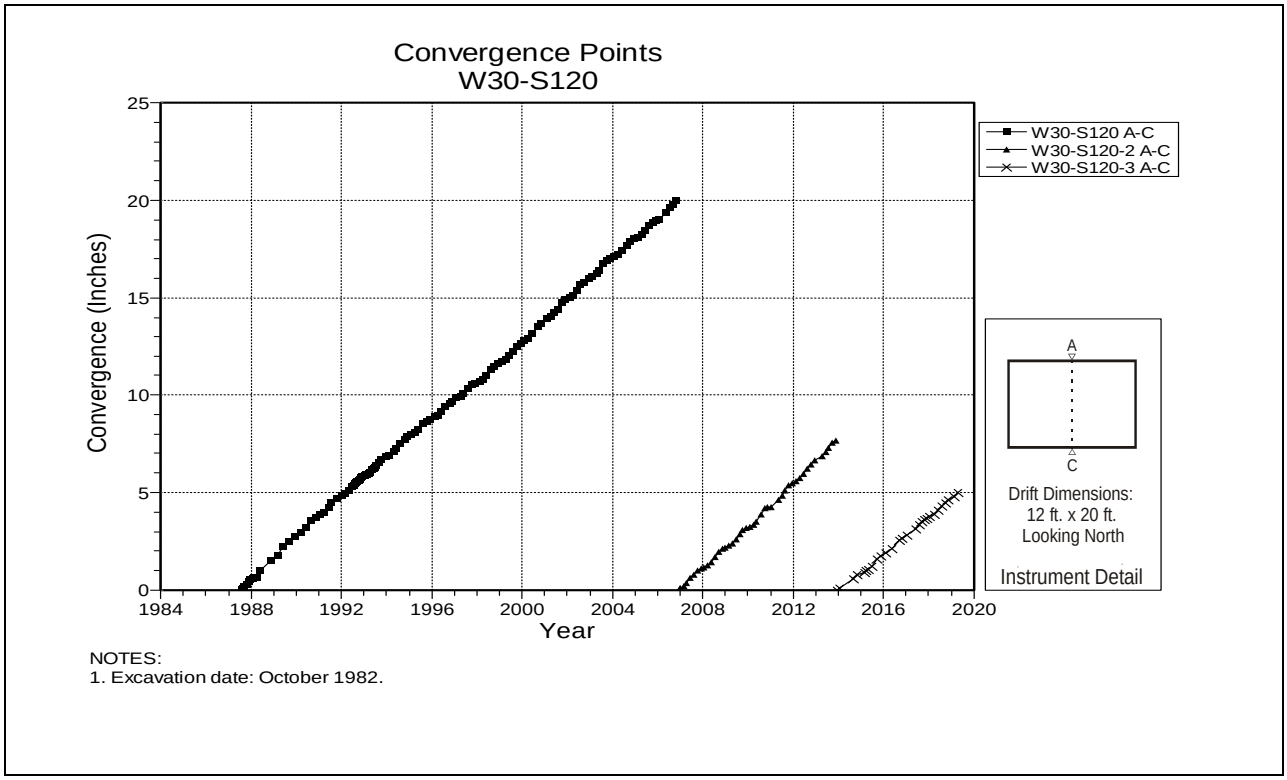

Figure 4-160 Convergence Point Array – W30 S120 – Roof to Floor – Centerline

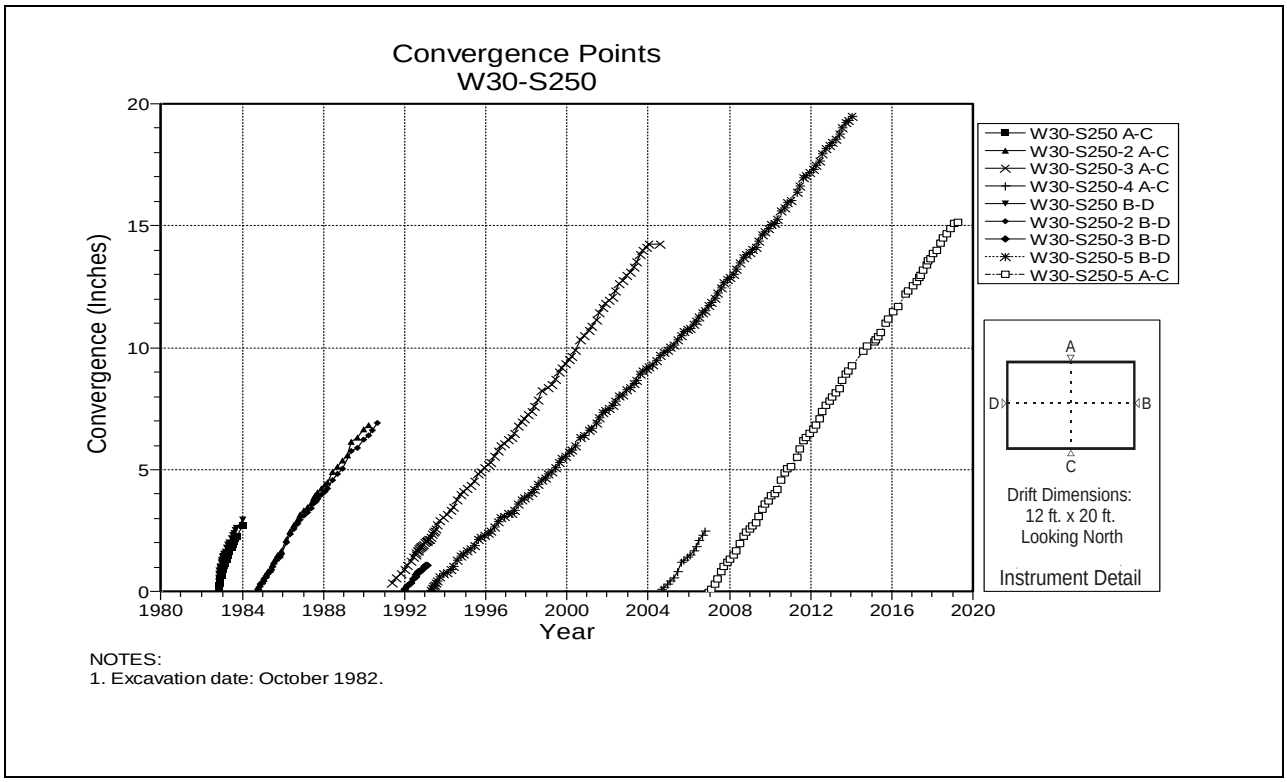

NOTES:
1. Excavation date: October 1982.

Figure 4-161 Convergence Point Array – W30 S250 – All Chords

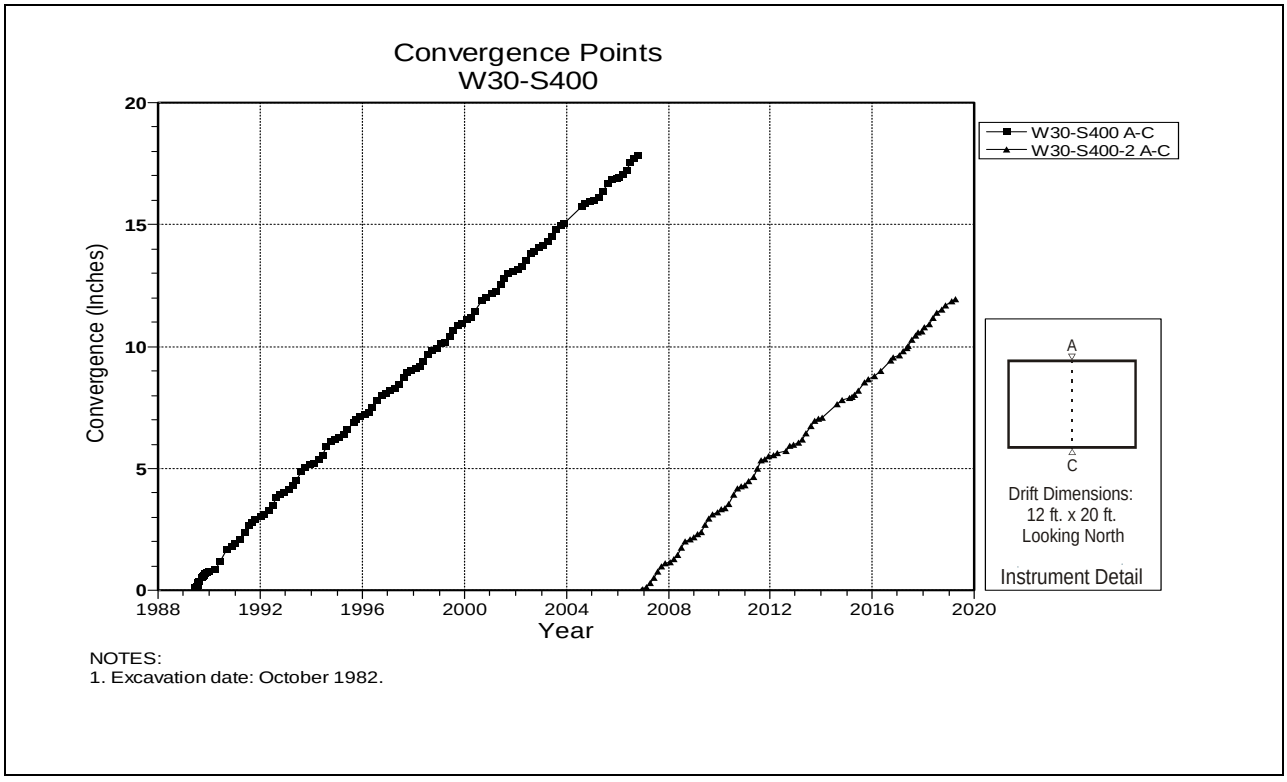

NOTES:
1. Excavation date: October 1982.

Figure 4-162 Convergence Point Array – W30 S400 – Roof to Floor – Centerline

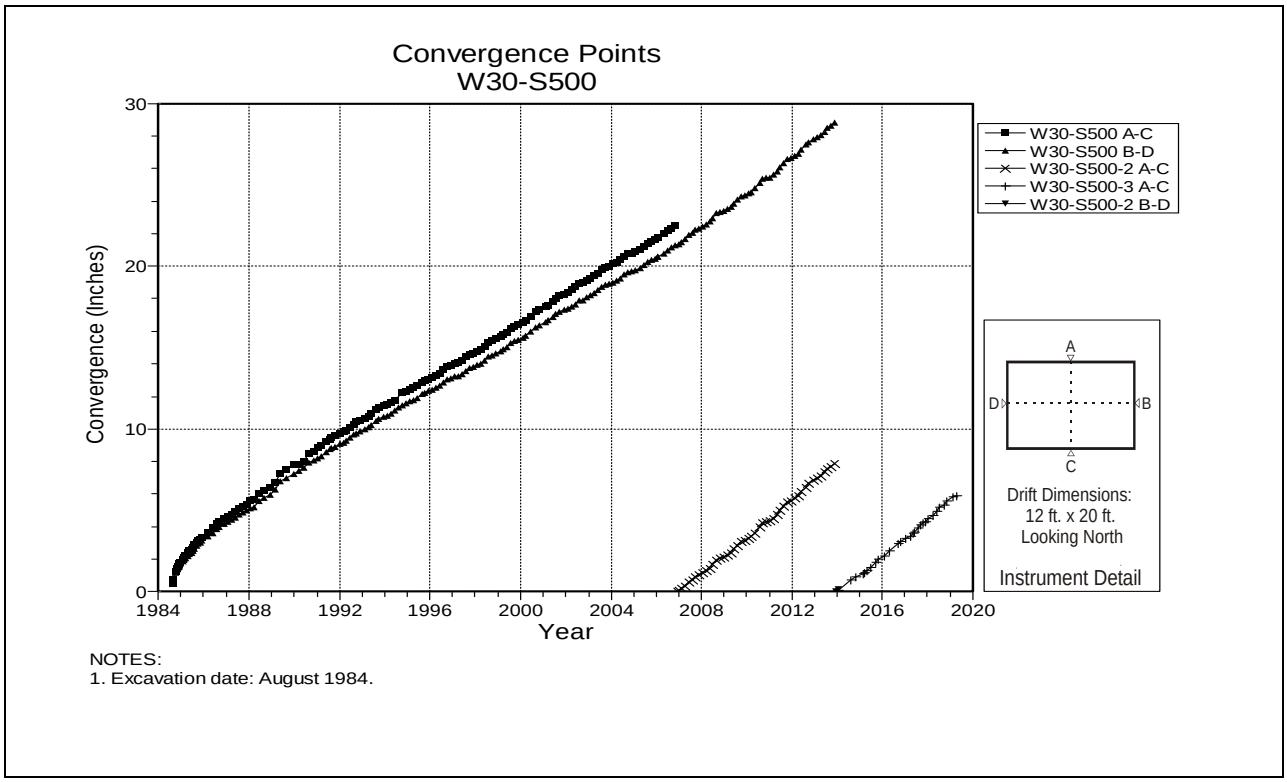

Figure 4-163 Convergence Point Array – W30 S500 – All Chords

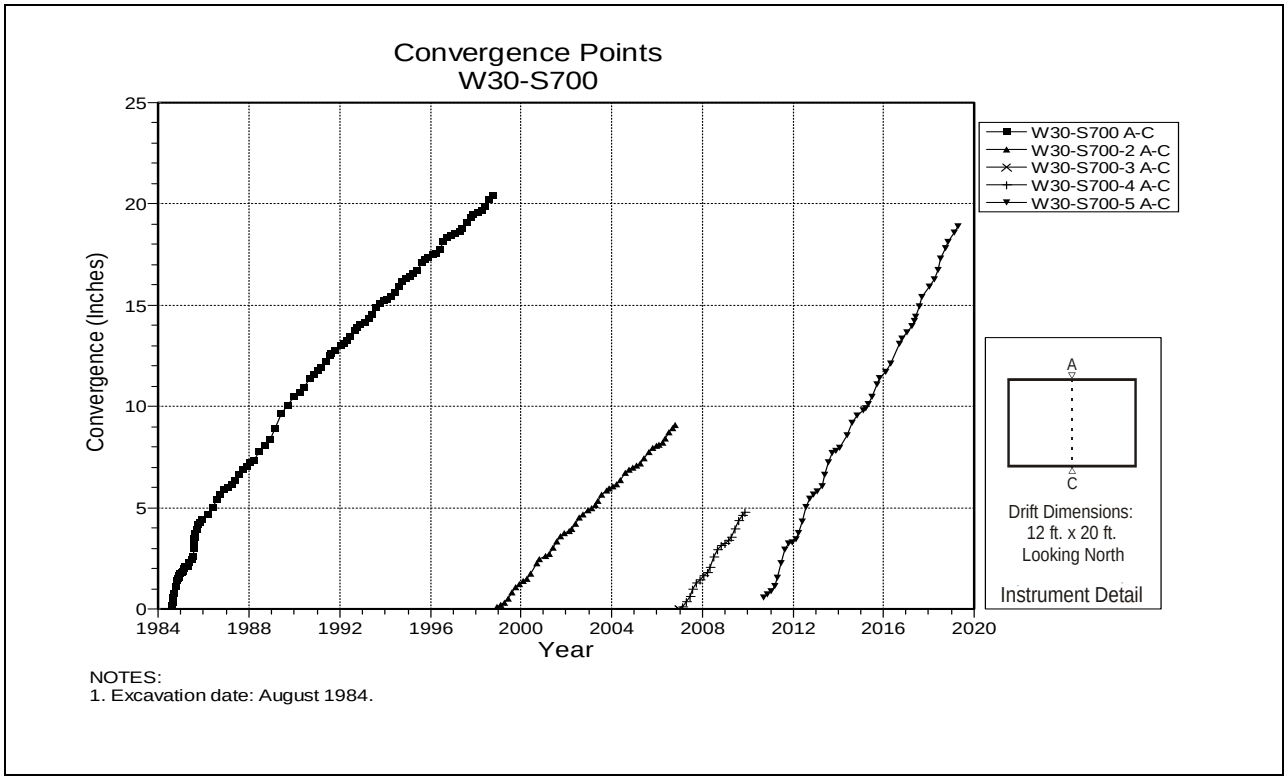

Figure 4-164 Convergence Point Array – W30 S700 – Roof to Floor – Centerline

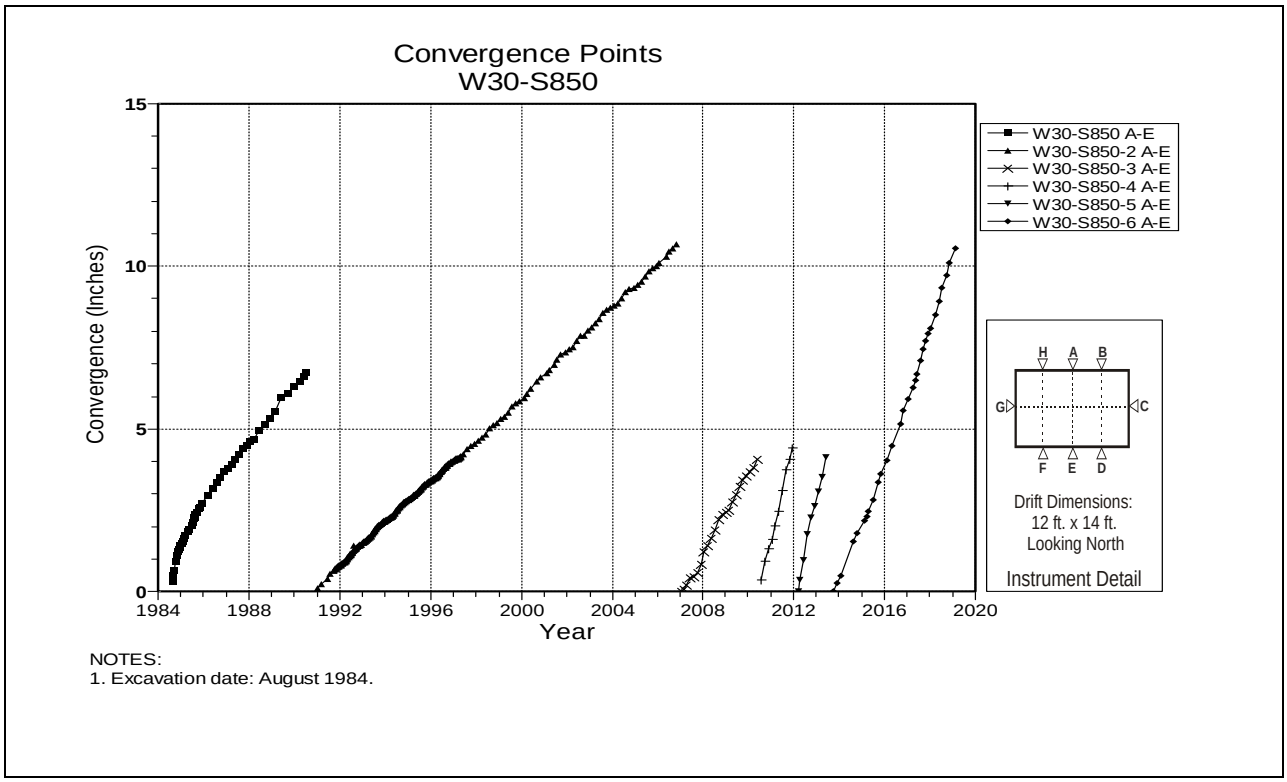

Figure 4-165 Convergence Point Array – W30 S850 – Roof to Floor – Centerline

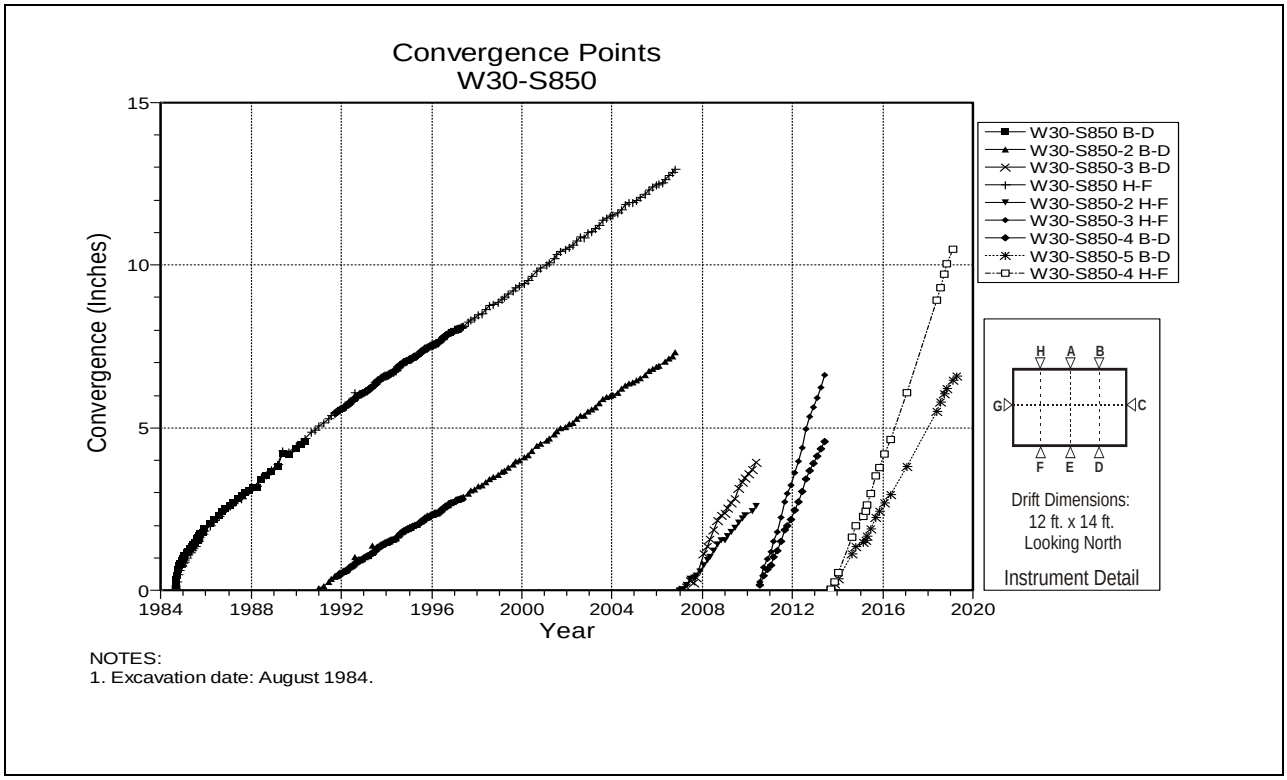

Figure 4-166 Convergence Point Array – W30 S850 – Quarter Points

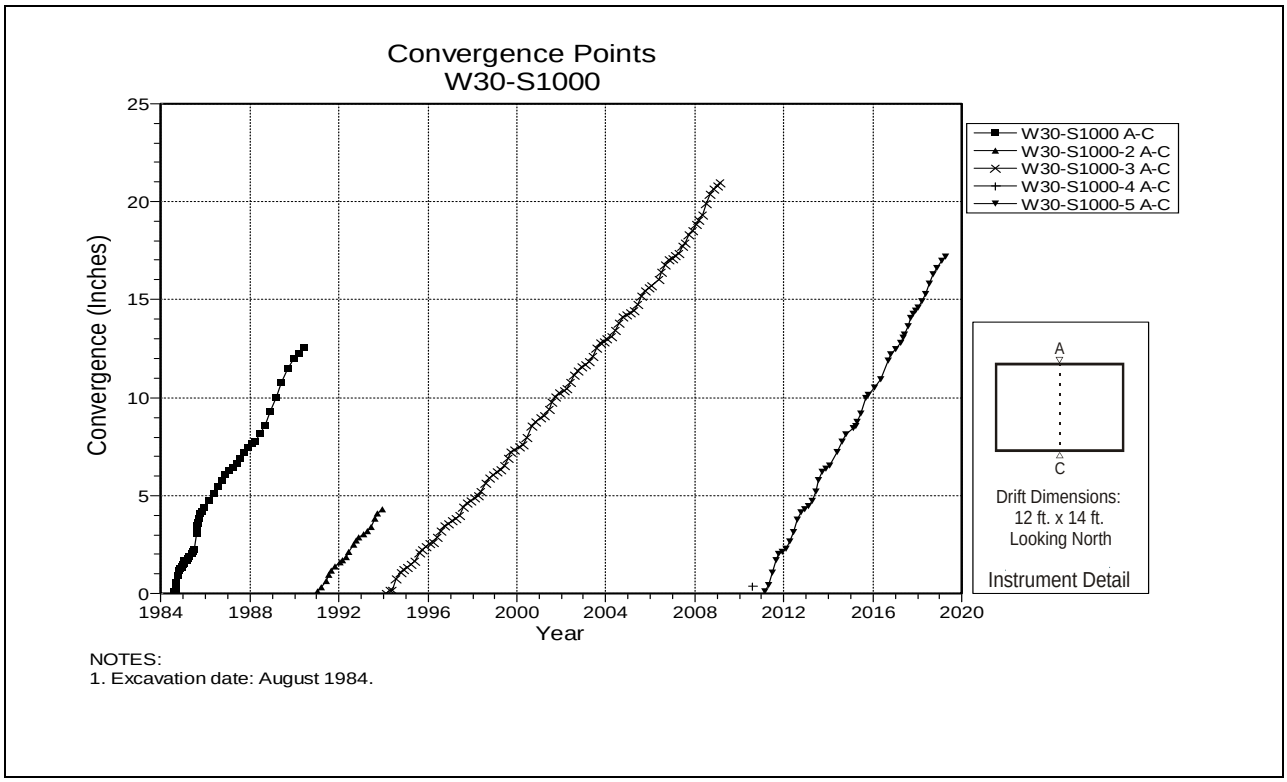

Figure 4-167 Convergence Point Array – W30 S1000 – Roof to Floor – Centerline

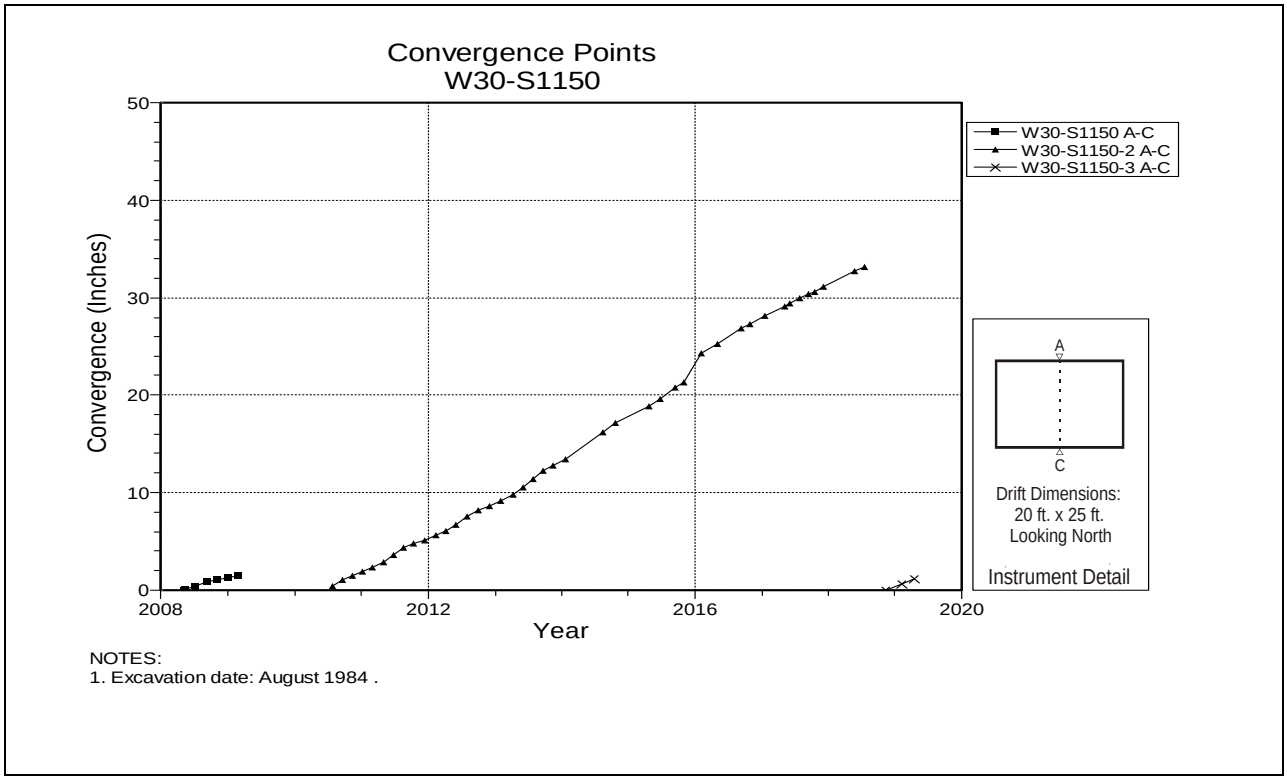

Figure 4-168 Convergence Point Array – W30 S1150 – Roof to Floor – Centerline

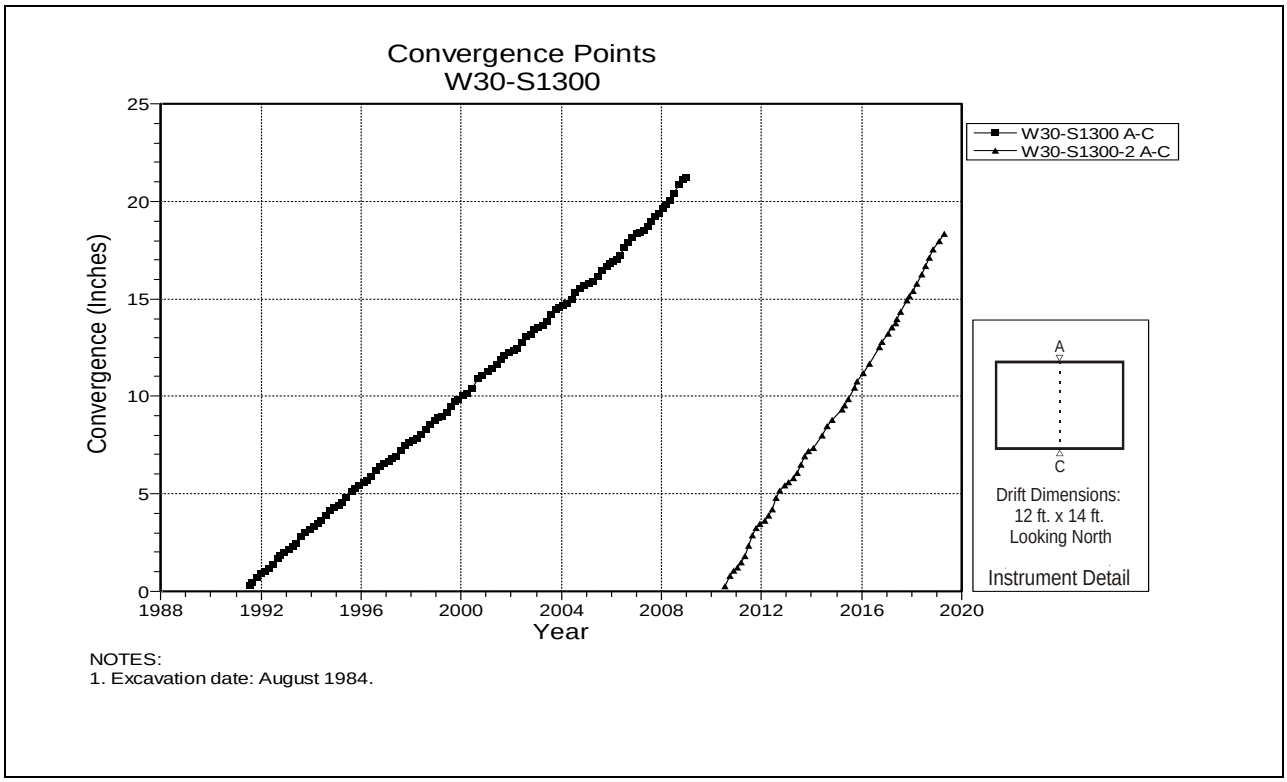

Figure 4-169 Convergence Point Array – W30 S1300 – Roof to Floor – Centerline

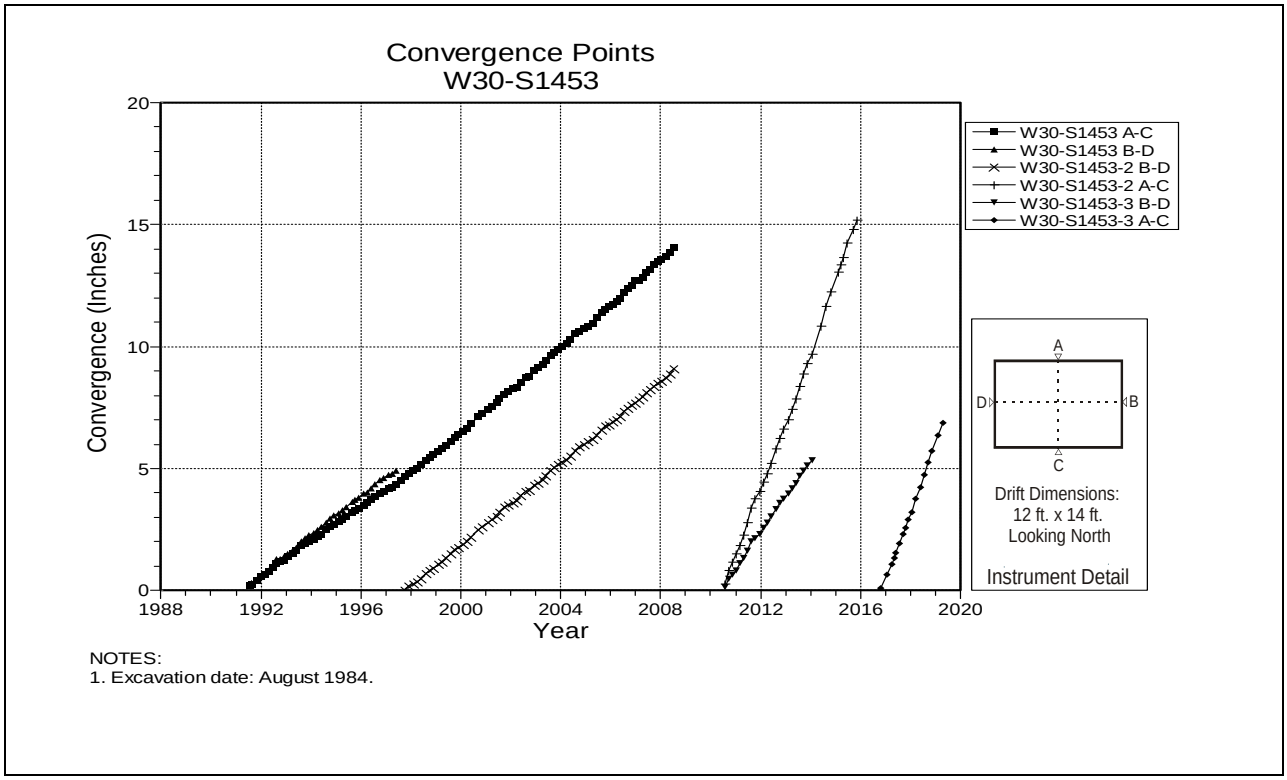

Figure 4-170 Convergence Point Array – W30 S1453 – All Chords

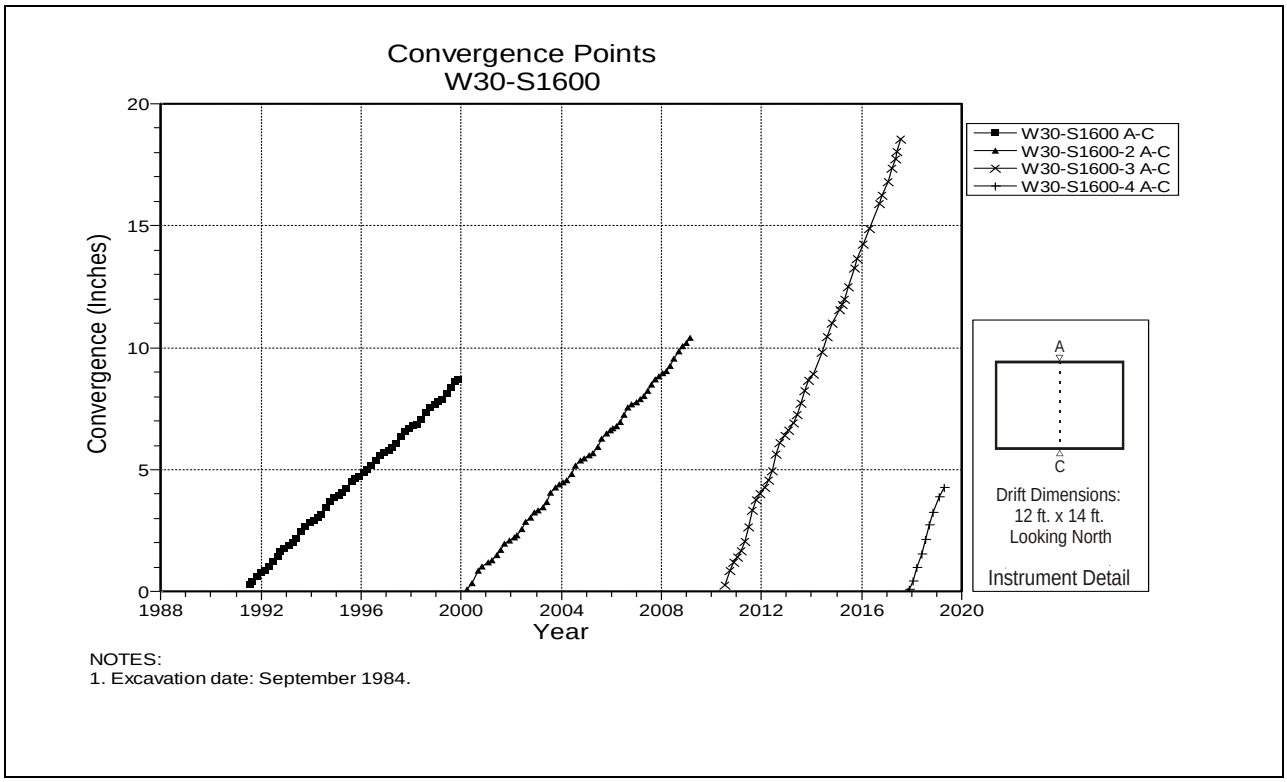

Figure 4-171 Convergence Point Array – W30 S1600 – Roof to Floor – Centerline

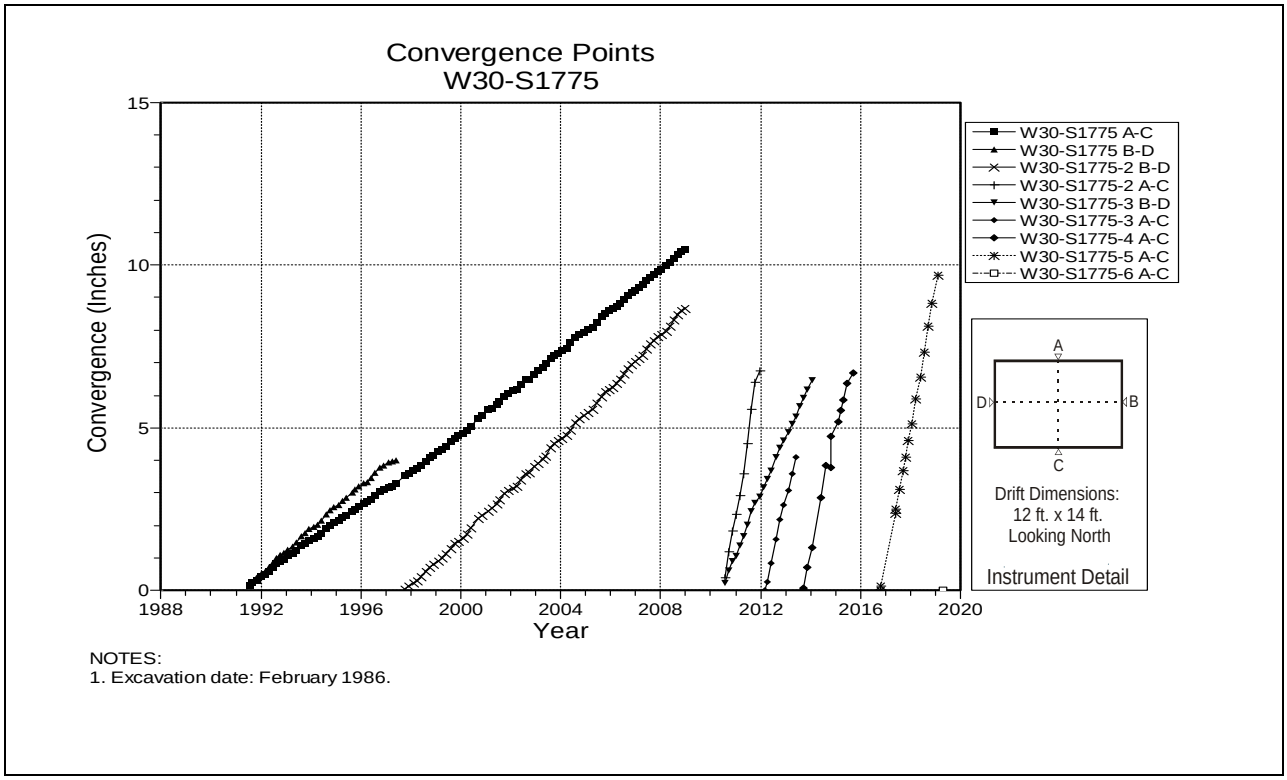

Figure 4-172 Convergence Point Array – W30 S1775 – All Chords

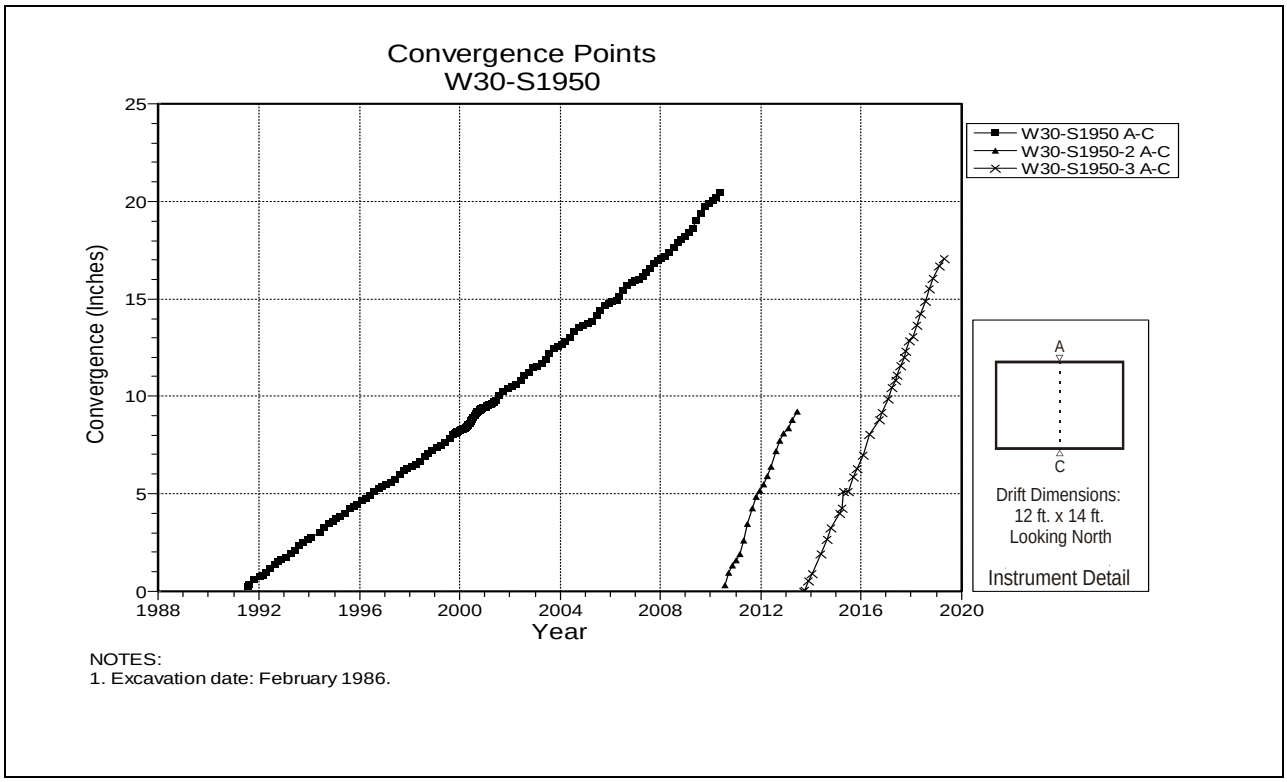

Figure 4-173 Convergence Point Array – W30 S1950 – Roof to Floor – Centerline

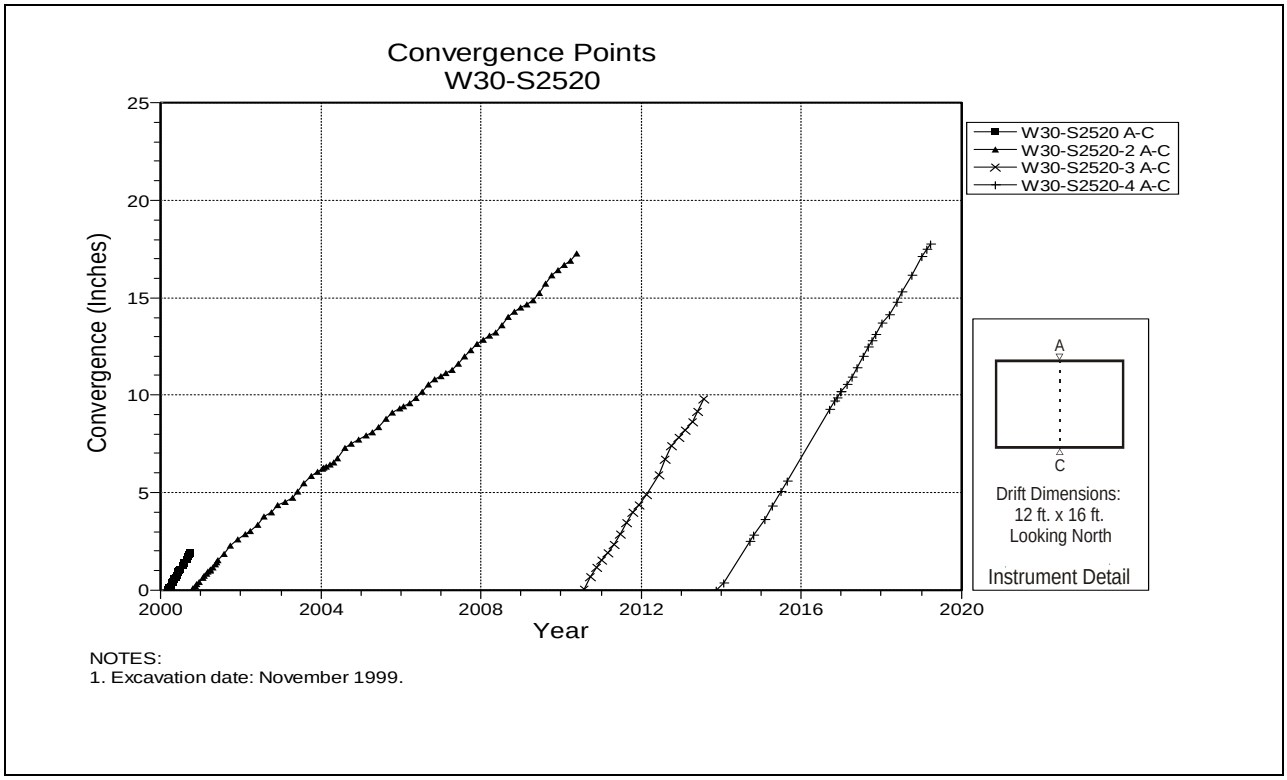

Figure 4-174 Convergence Point Array – W30 S2520 – Roof to Floor – Centerline

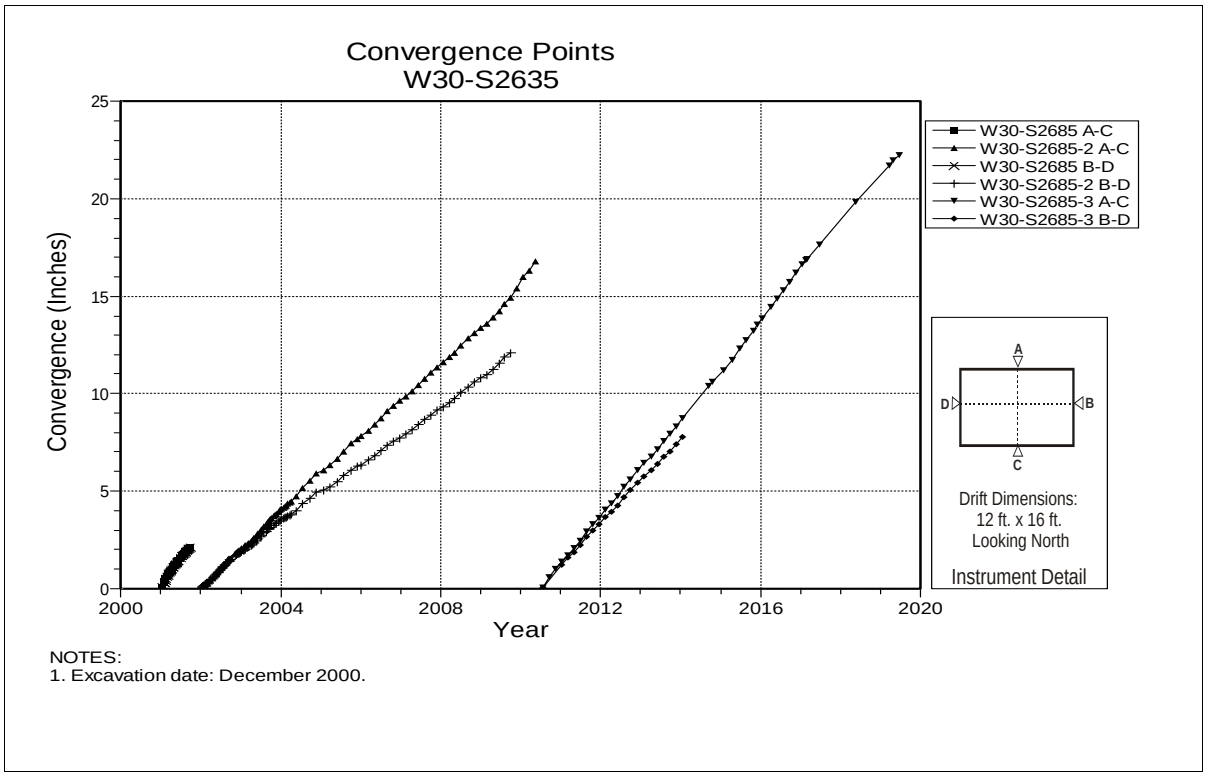

Figure 4-175 Convergence Point Array – W30 S2635 – All Chords

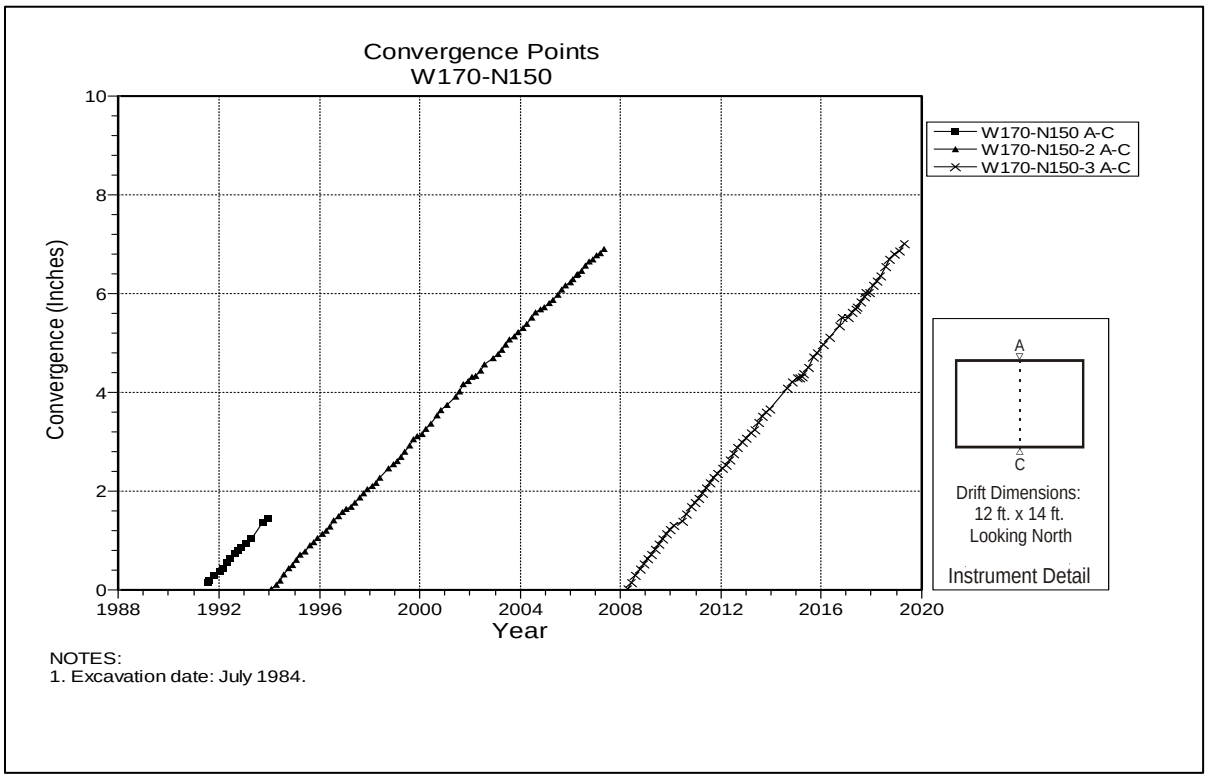

Figure 4-176 Convergence Point Array – W170 N150 – Roof to Floor – Centerline

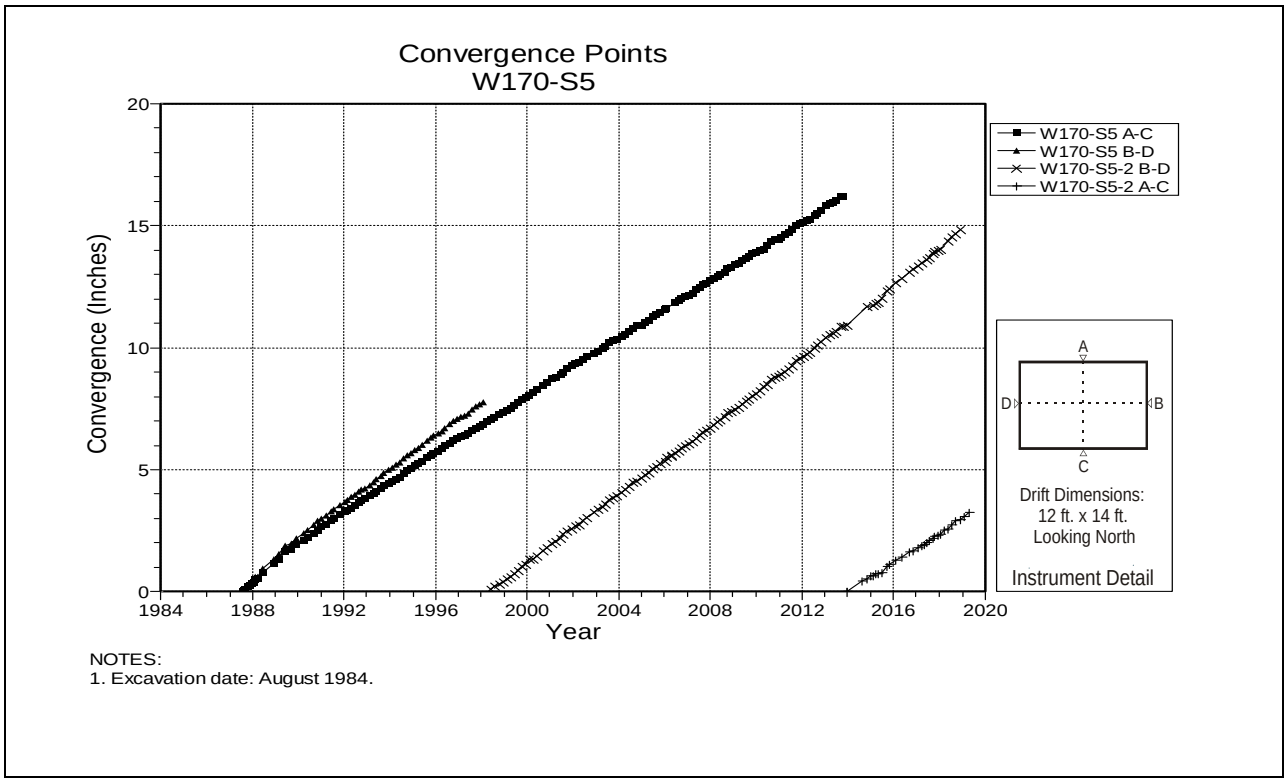

Figure 4-177 Convergence Point Array – W170 S5 – All Chords

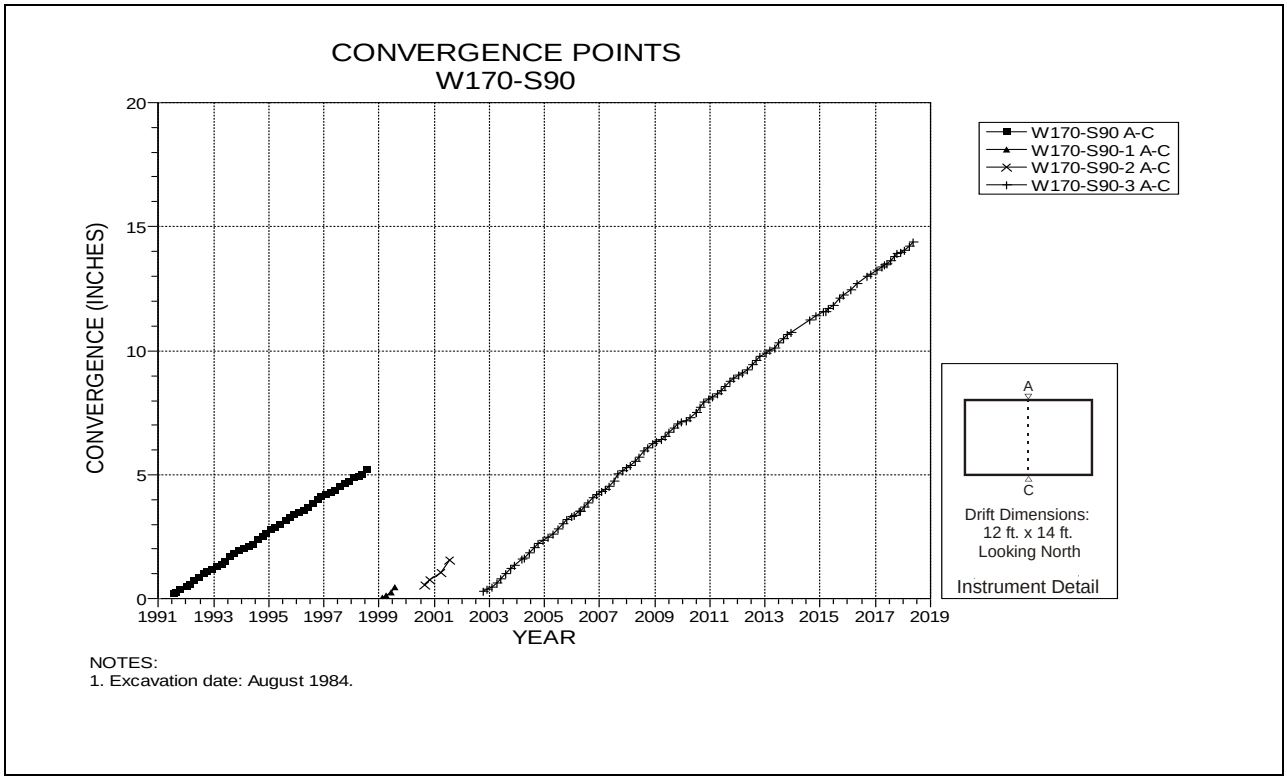

Figure 4-178 Convergence Point Array – W170 S90 – Roof to Floor – Centerline

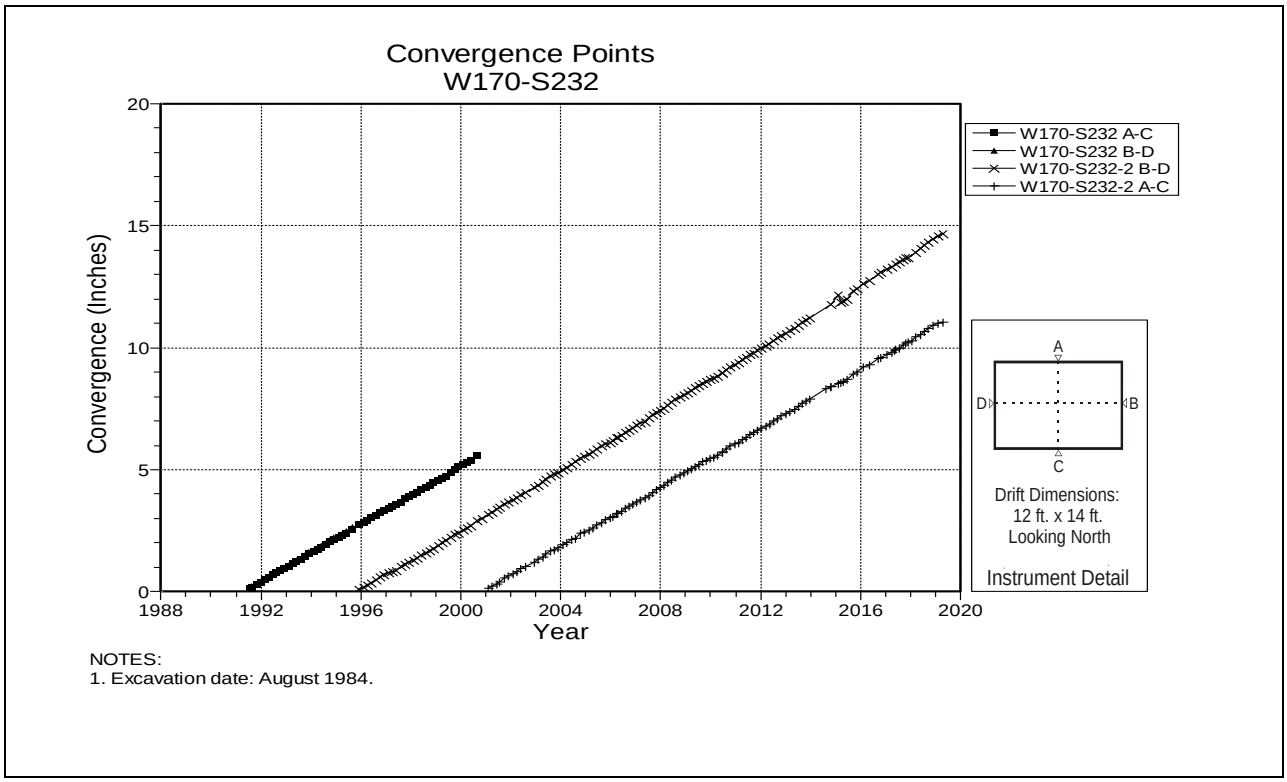

Figure 4-179 Convergence Point Array – W170 S232 – All Chords

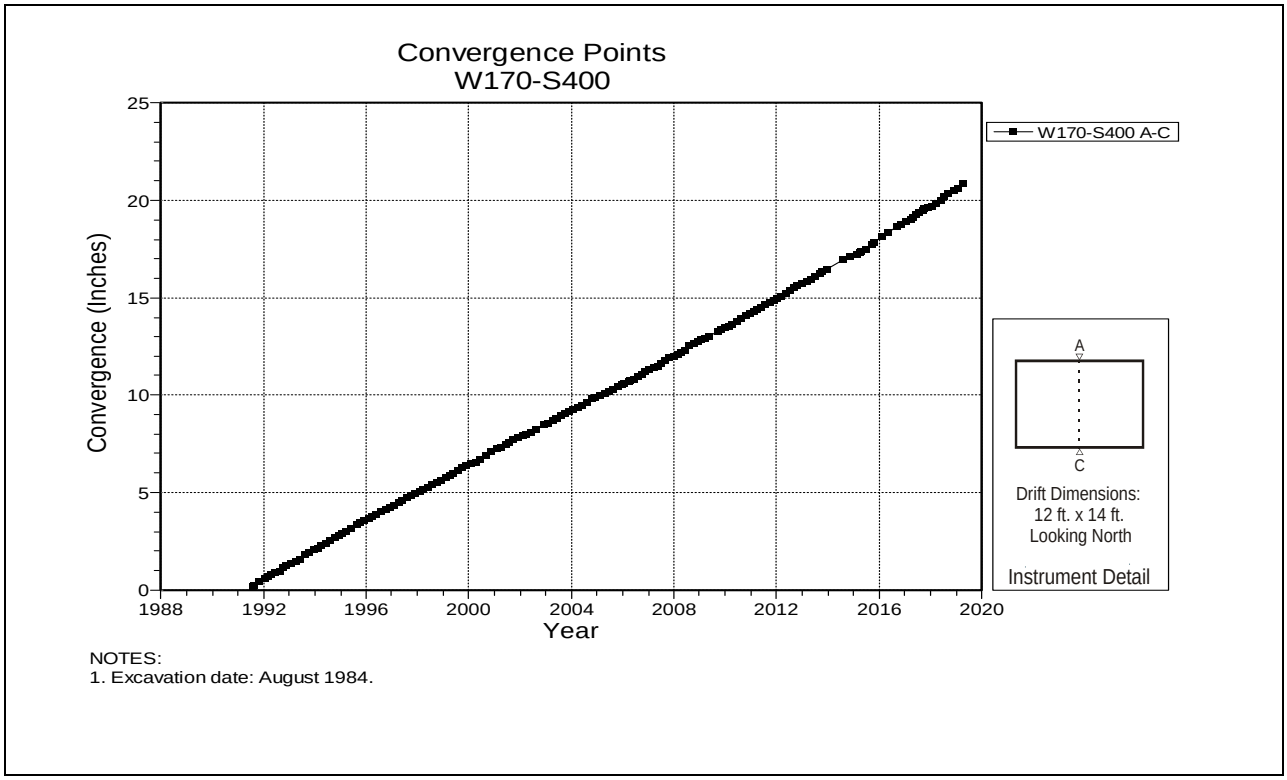

Figure 4-180 Convergence Point Array – W170 S400 – Roof to Floor – Centerline

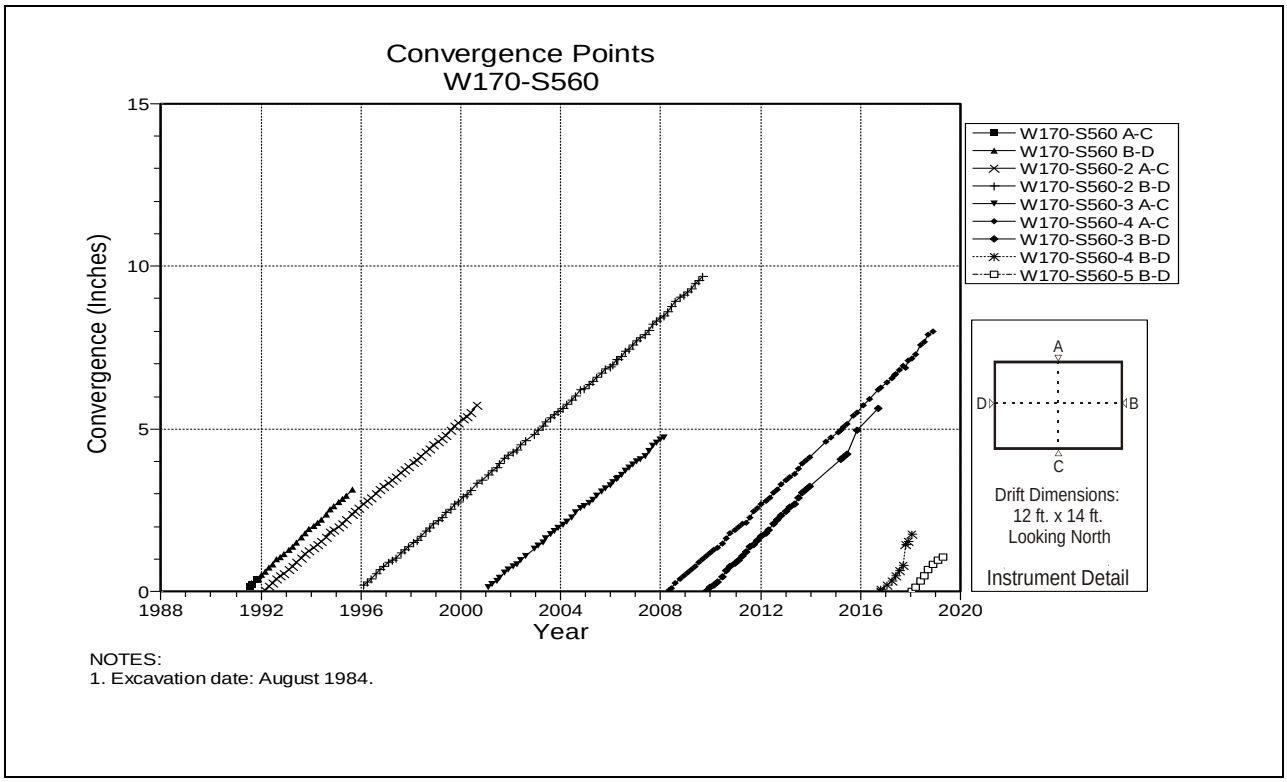

Figure 4-181 Convergence Point Array – W170 S560 – All Chords

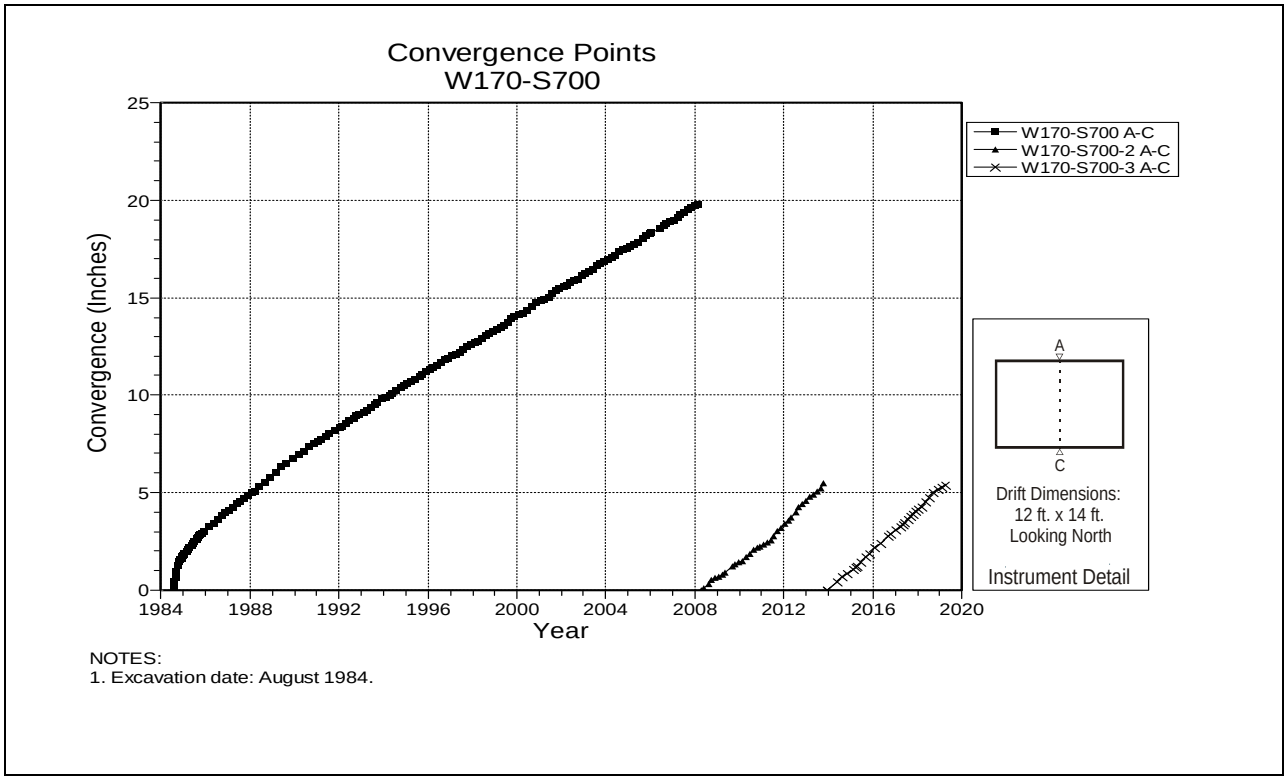

Figure 4-182 Convergence Point Array – W170 S700 – Roof to Floor – Centerline

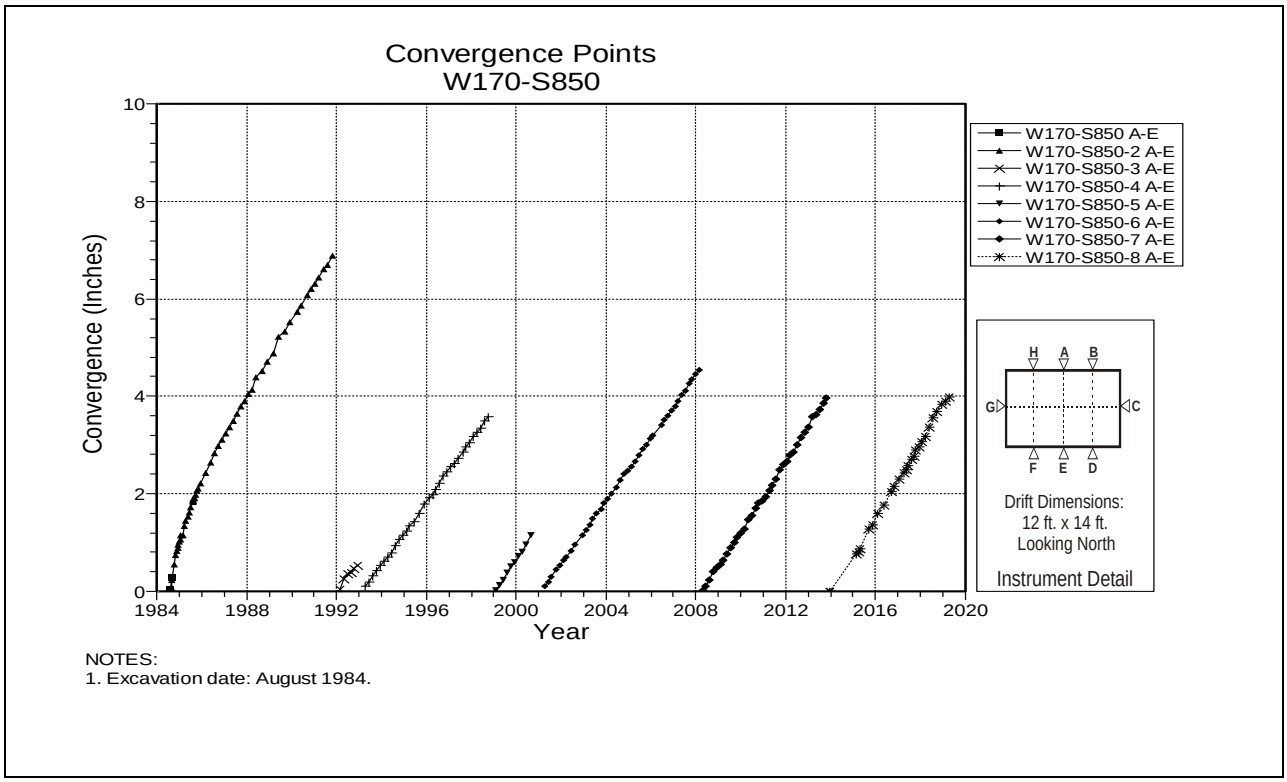

Figure 4-183 Convergence Point Array – W170 S850 – Roof to Floor – Centerline

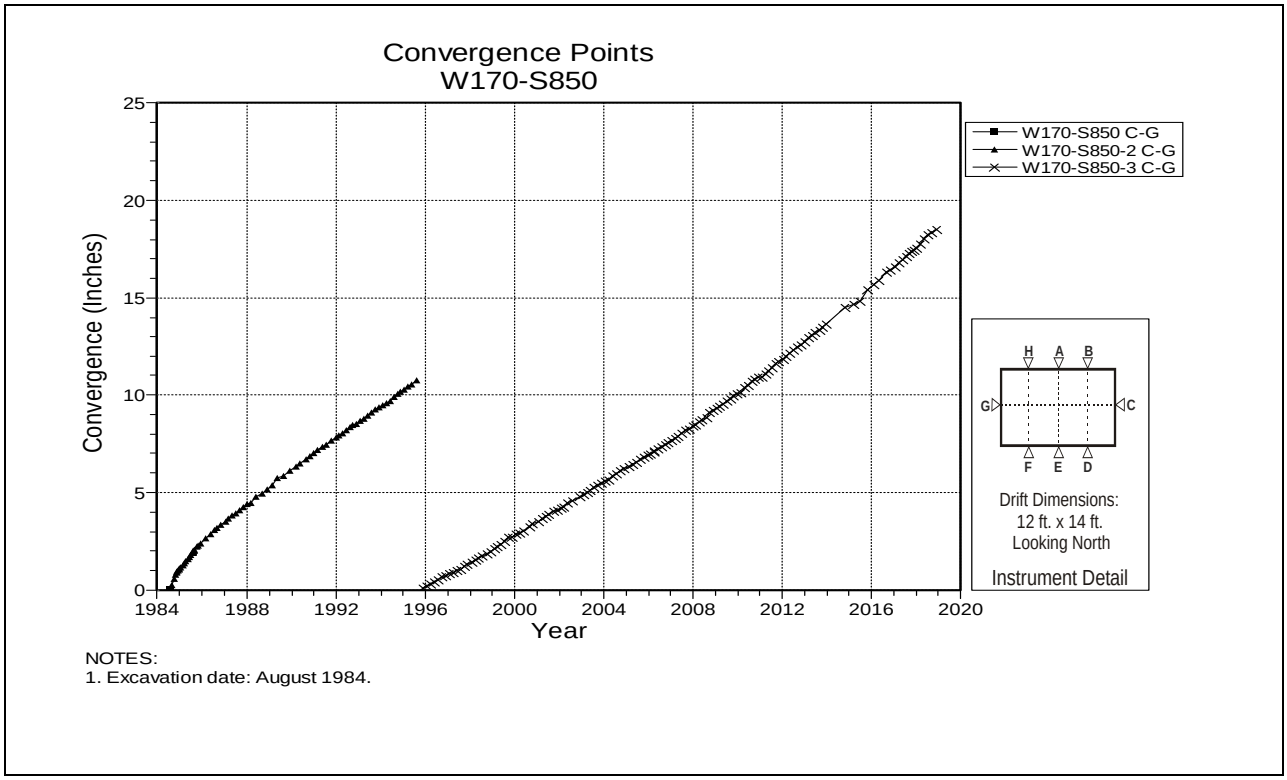

Figure 4-184 Convergence Point Array – W170 S850 – Rib to Rib

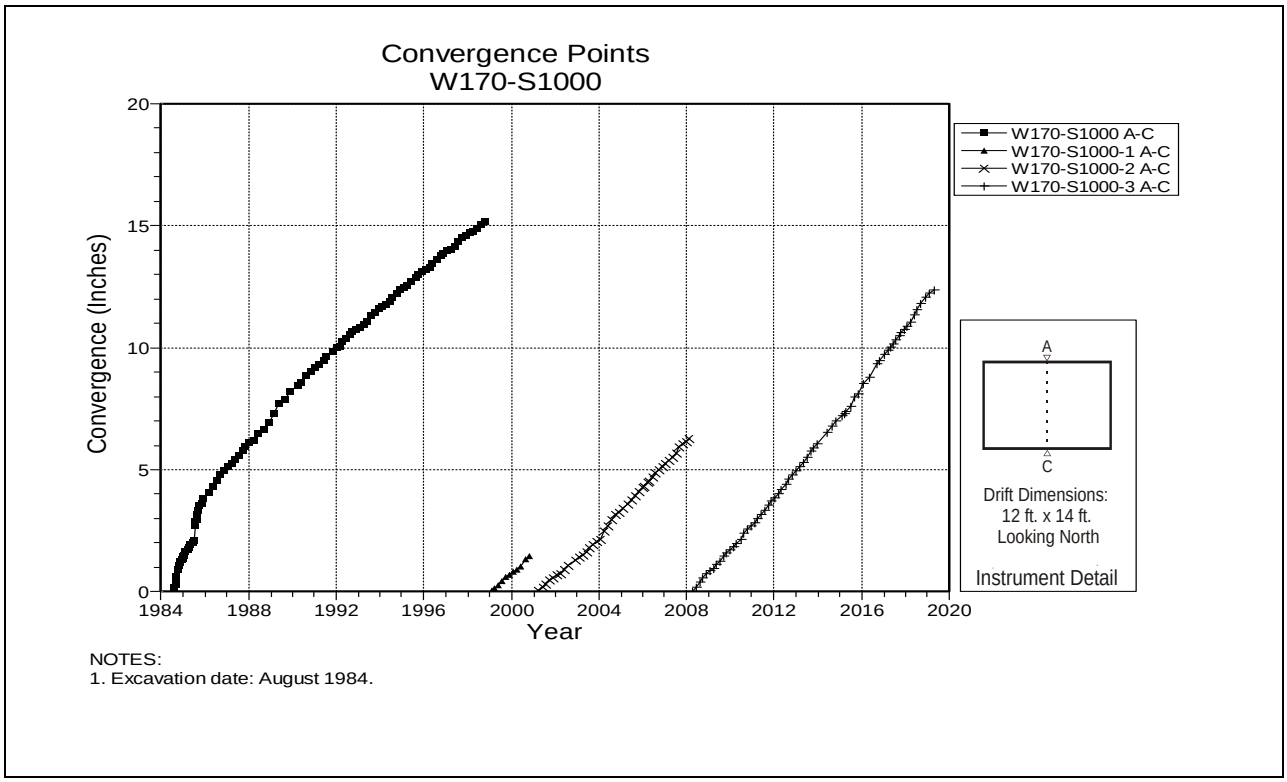

Figure 4-185 Convergence Point Array – W170 S1000 – Roof to Floor – Centerline

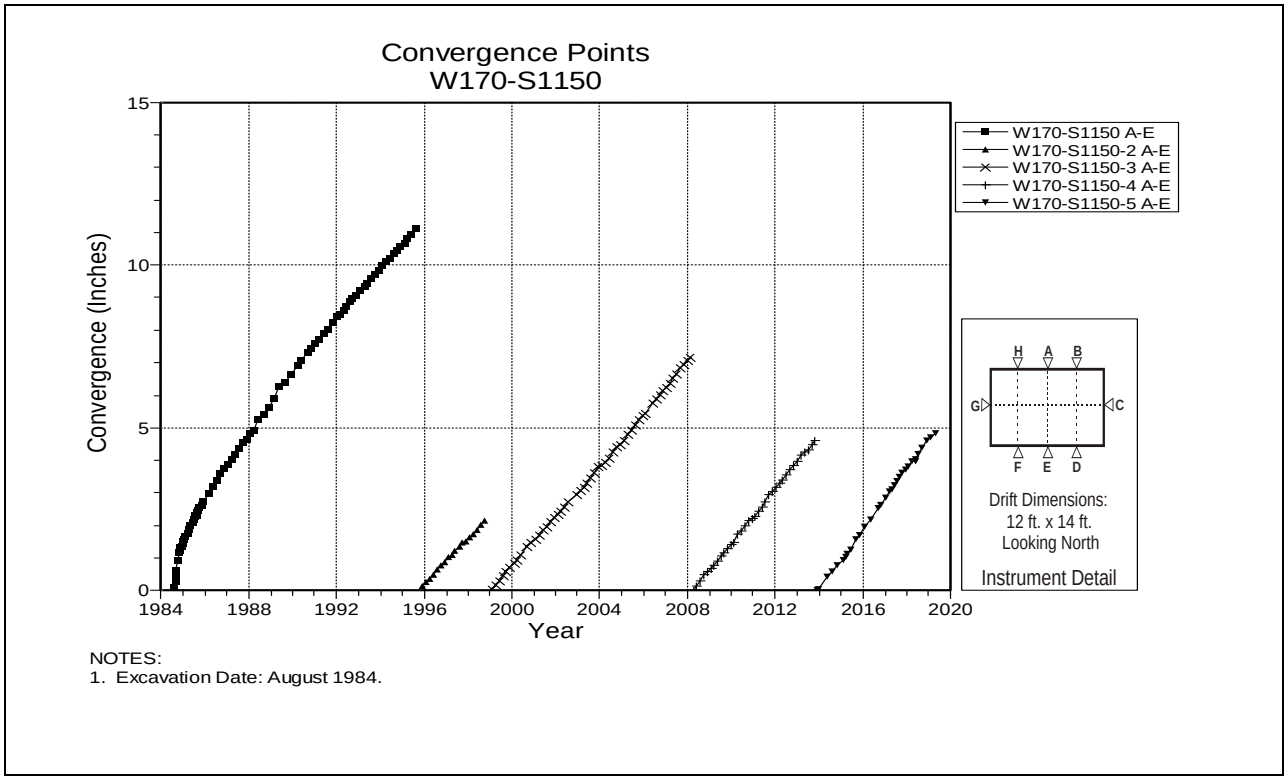

Figure 4-186 Convergence Point Array – W170 S1150 – Roof to Floor – Centerline

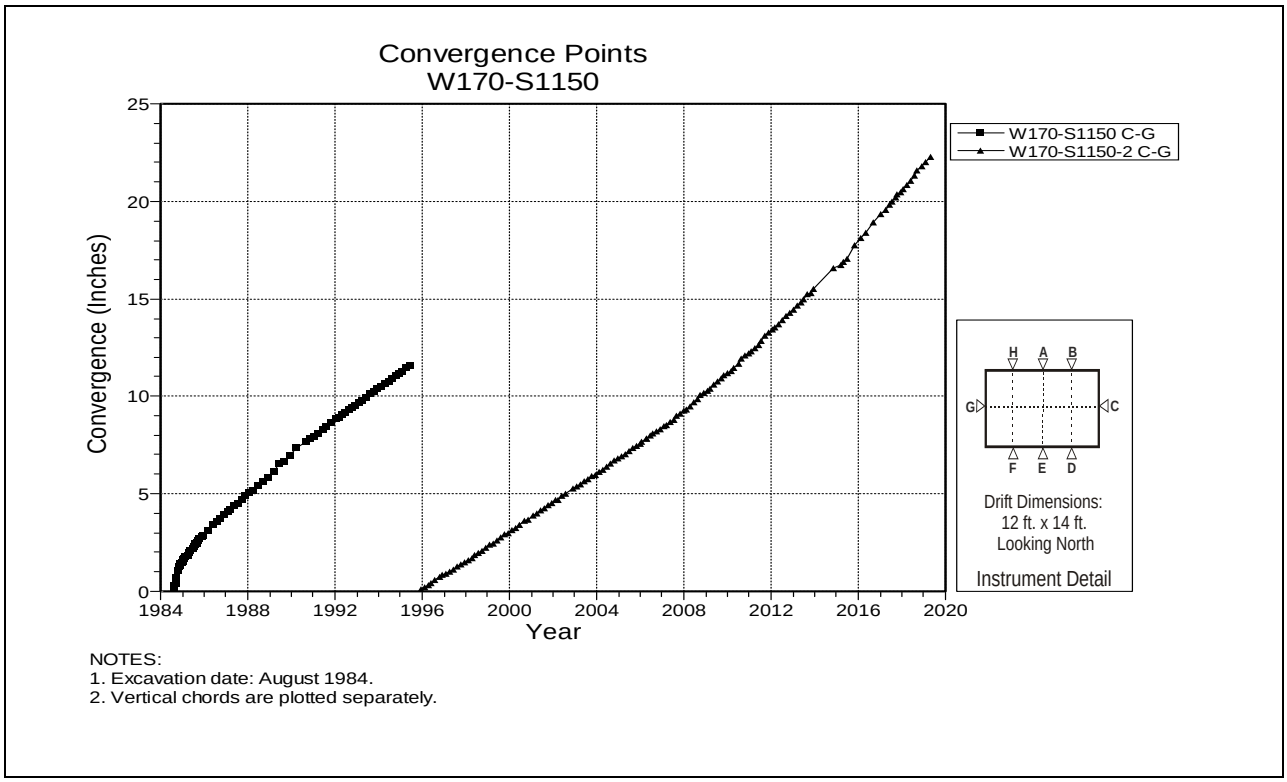

Figure 4-187 Convergence Point Array – W170 S1150 – Rib to Rib

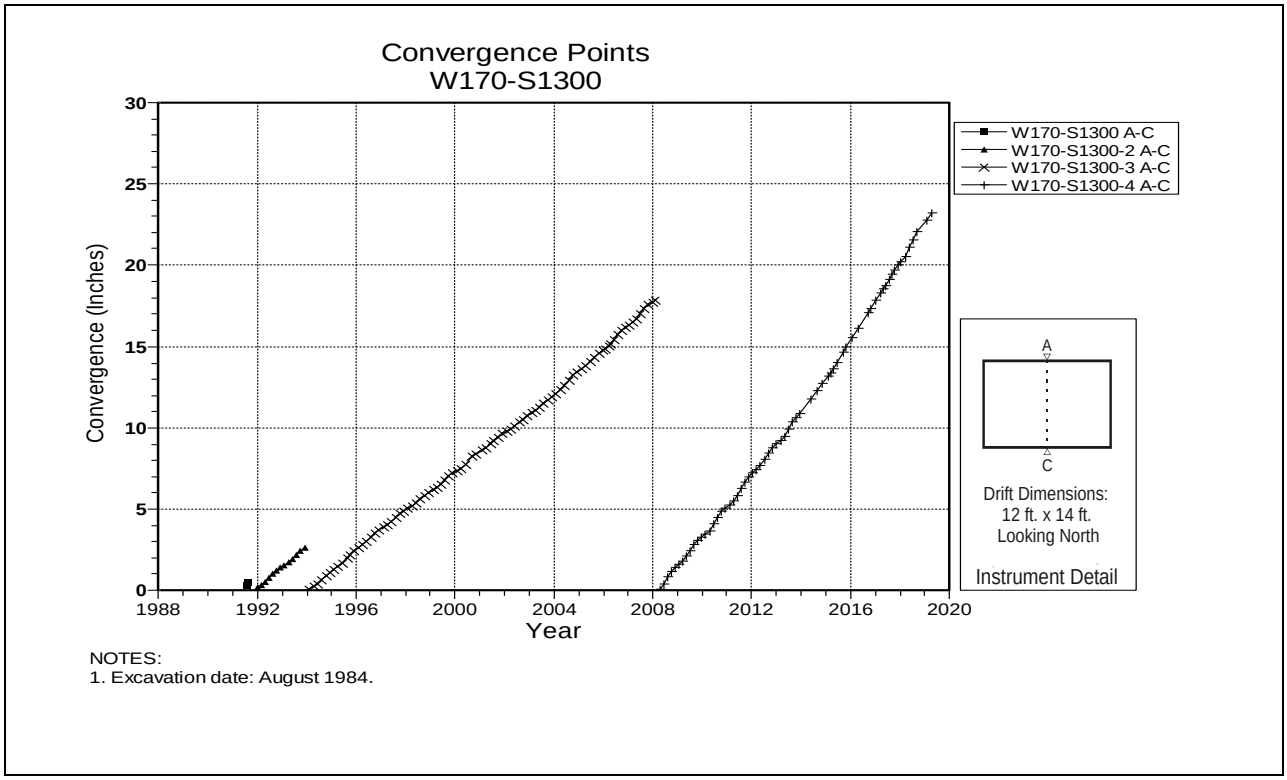

Figure 4-188 Convergence Point Array – W170 S1300 – Roof to Floor – Centerline

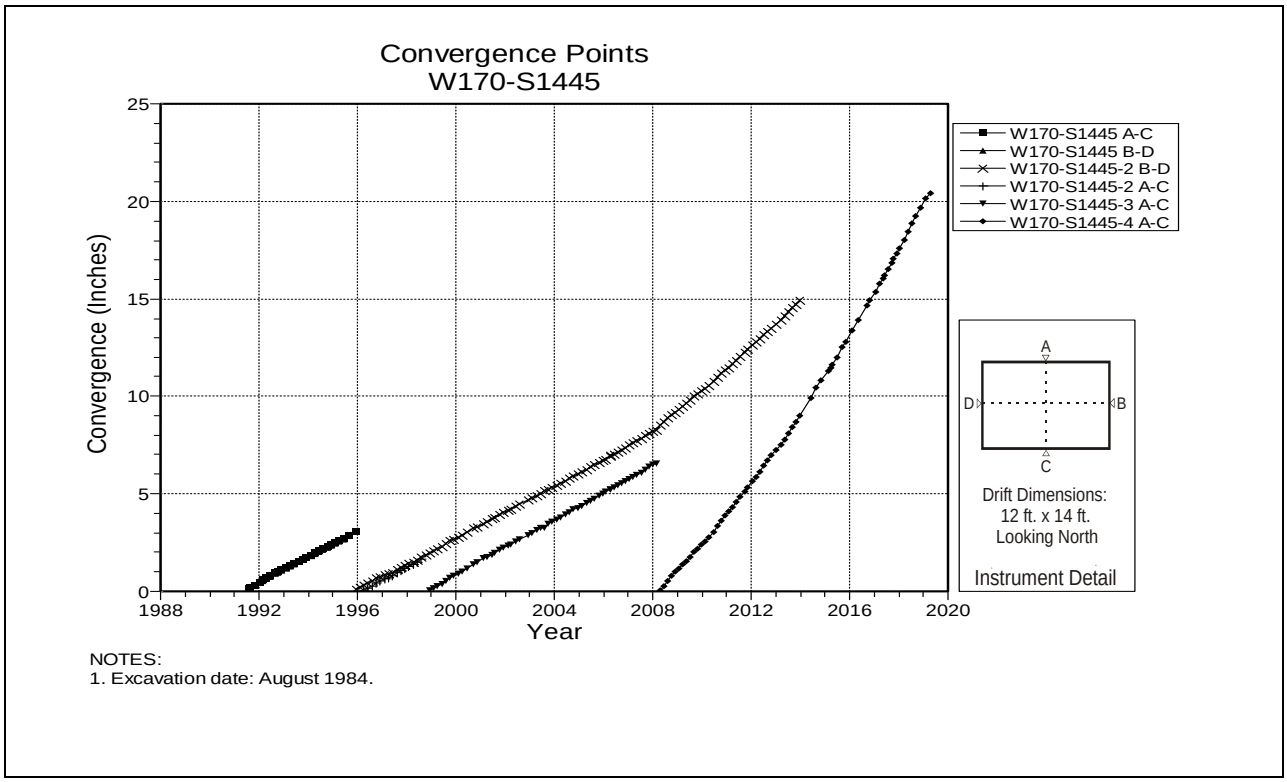

Figure 4-189 Convergence Point Array – W170 S1445 – All Chords

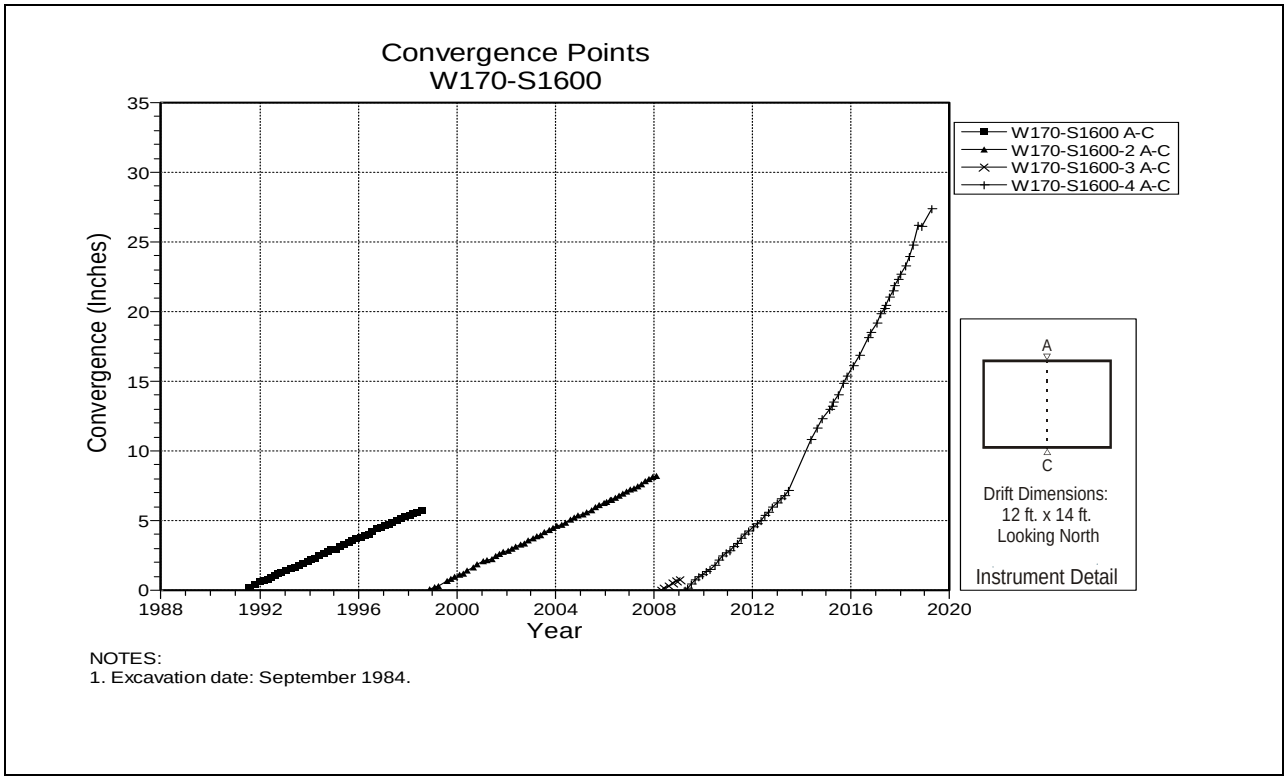

Figure 4-190 Convergence Point Array – W170 S1600 – Roof to Floor – Centerline

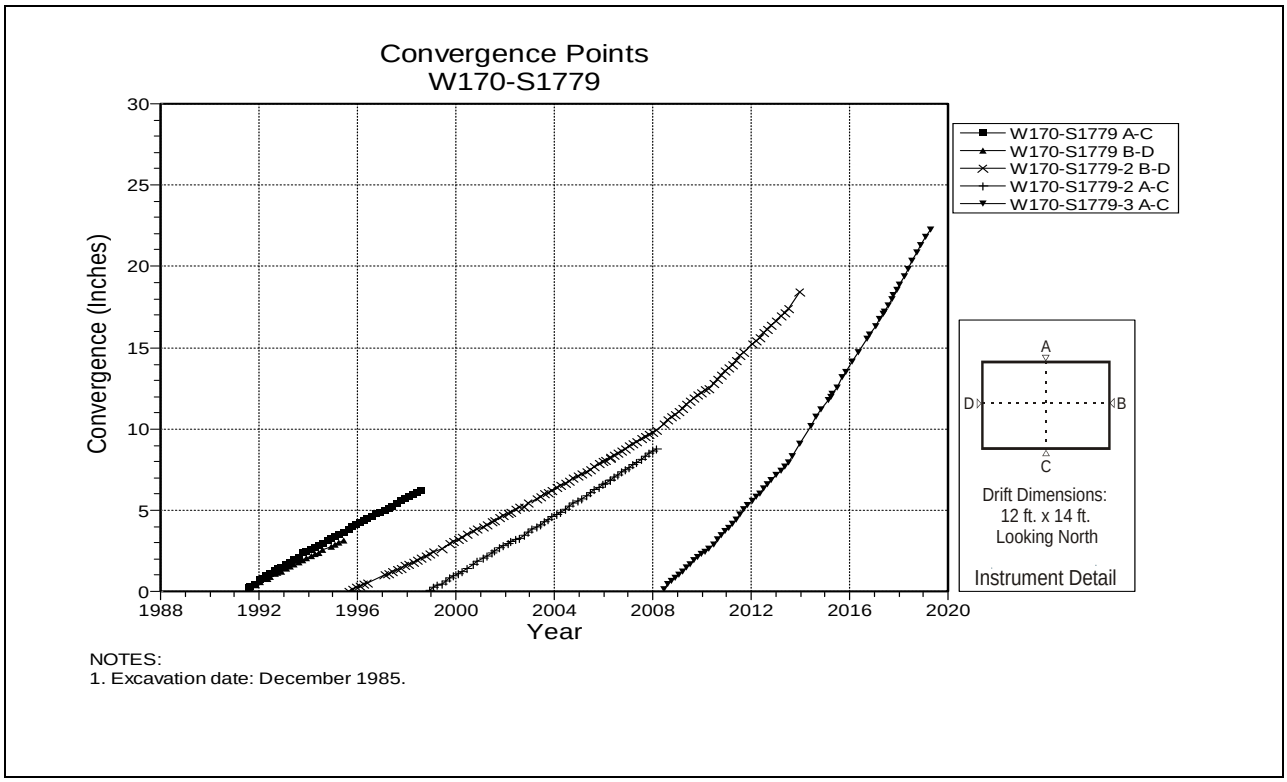

Figure 4-191 Convergence Point Array – W170 S1779 – All Chords

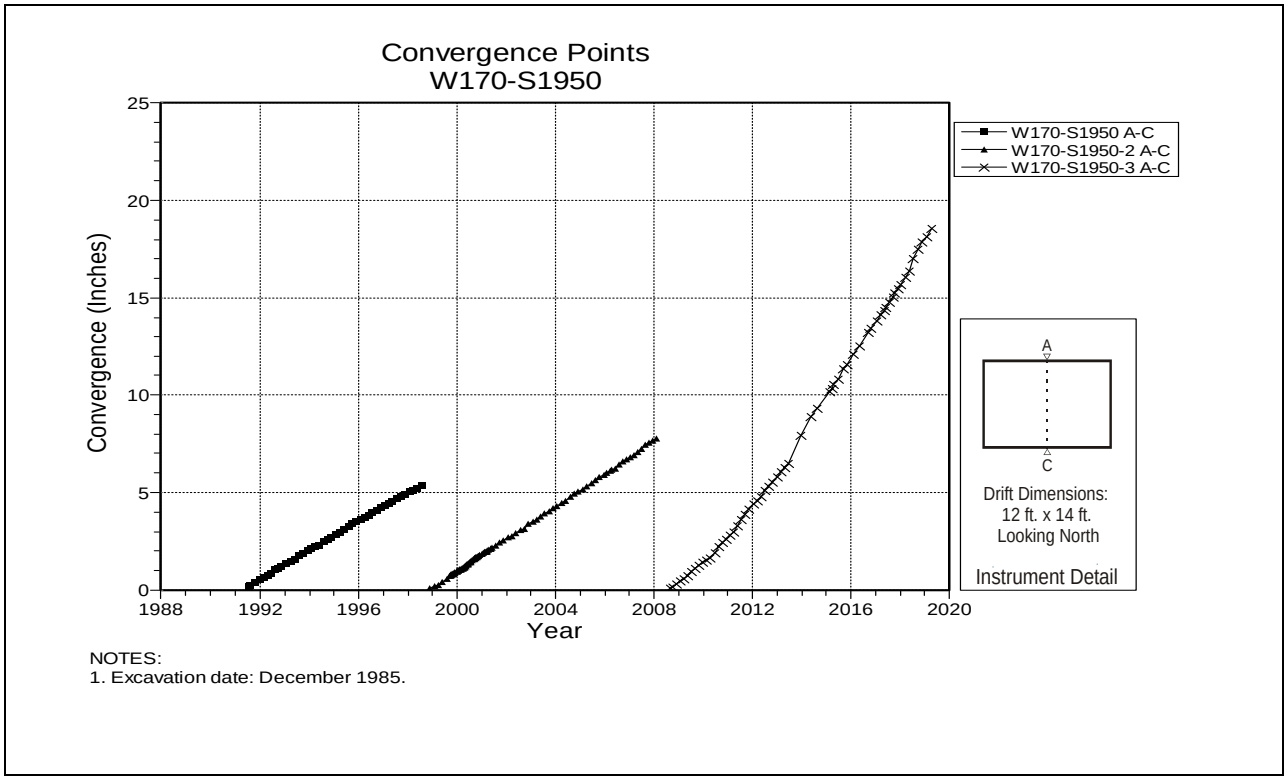

Figure 4-192 Convergence Point Array – W170 S1950 – Roof to Floor – Centerline

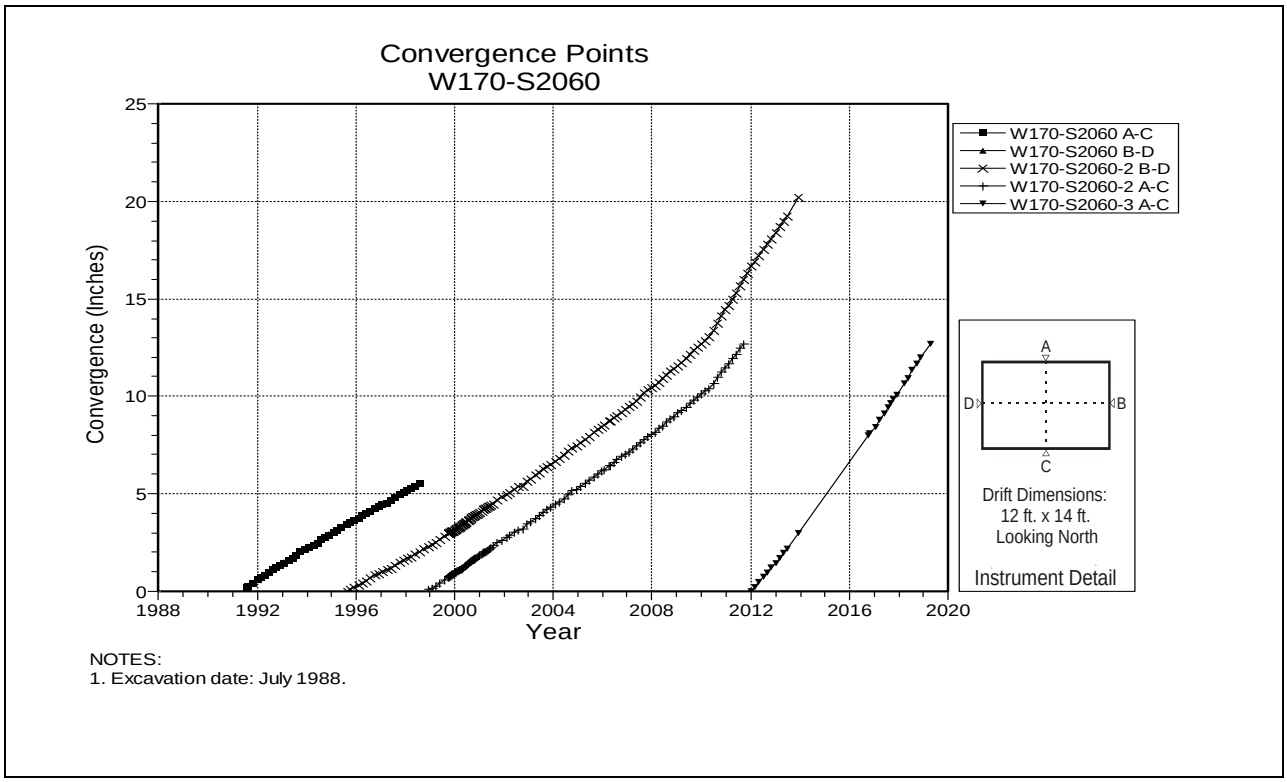

Figure 4-193 Convergence Point Array – W170 S2060 – All Chords

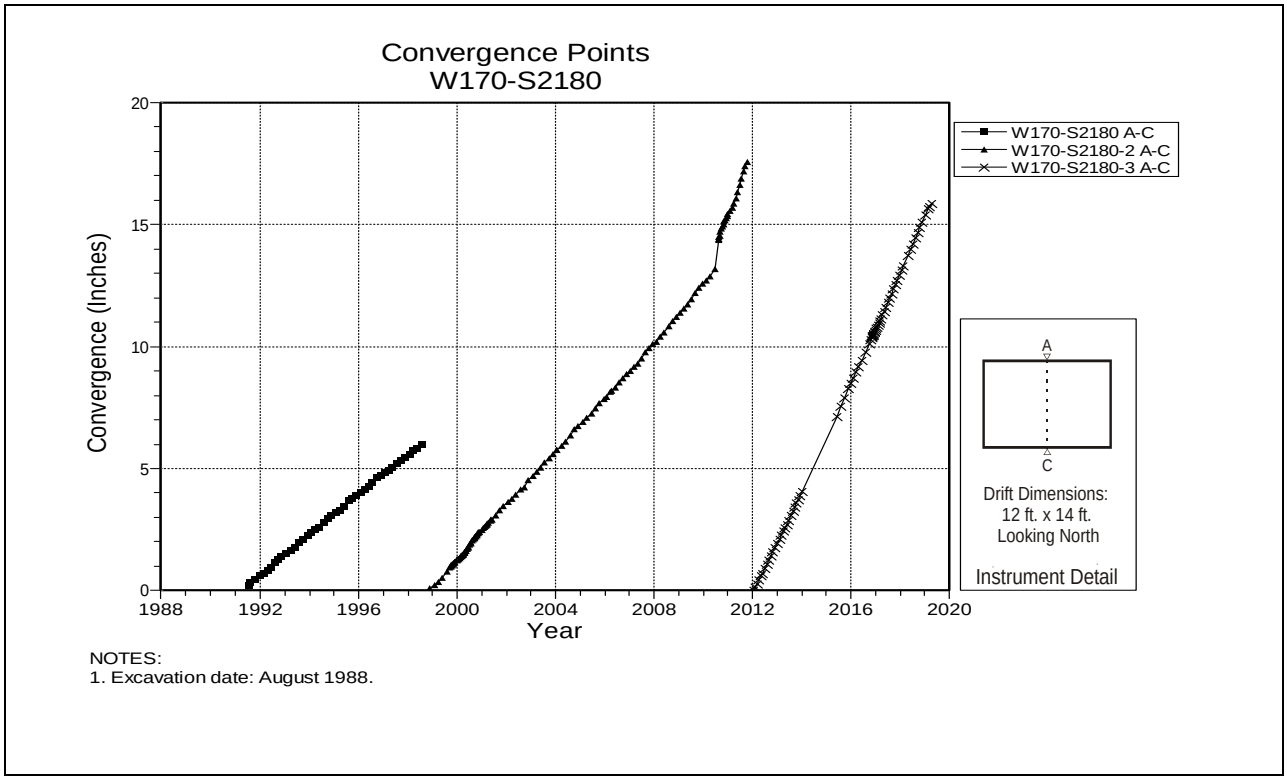

Figure 4-194 Convergence Point Array – W170 S2180 – Roof to Floor – Centerline

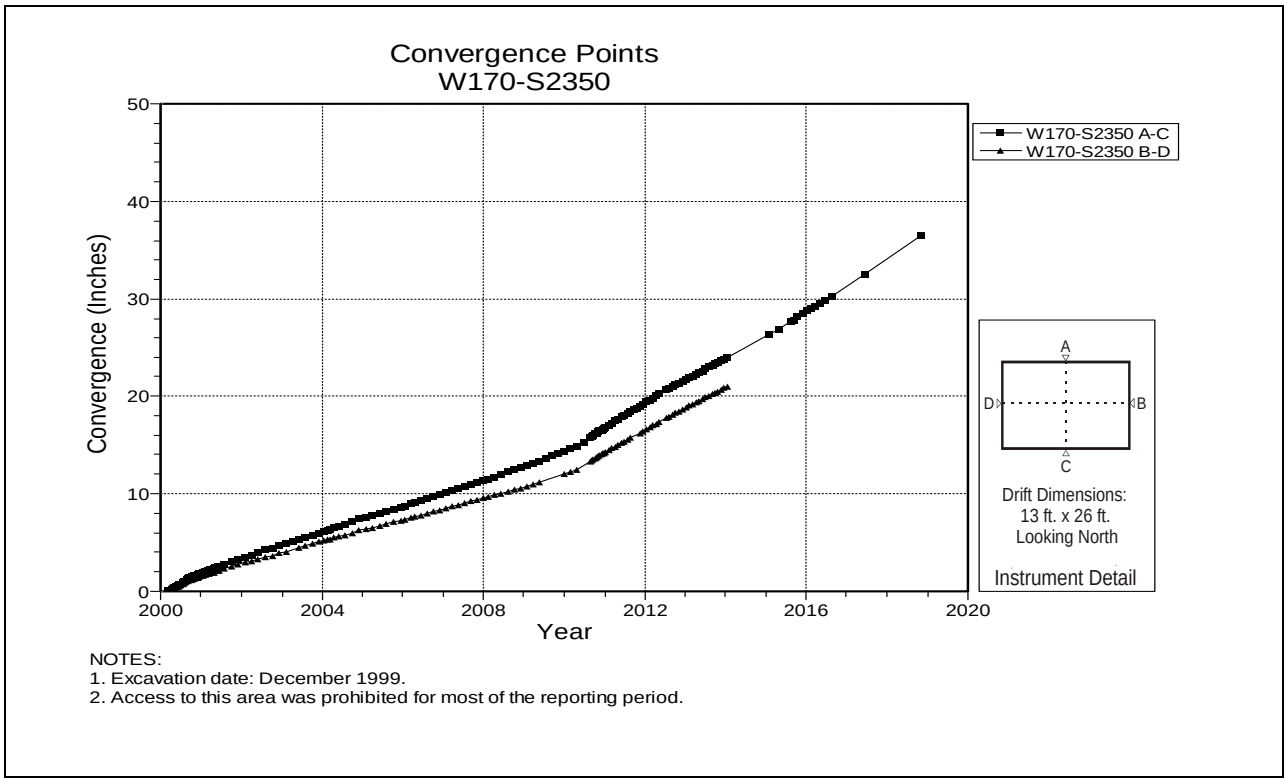

NOTES:
1. Excavation date: December 1999.
2. Access to this area was prohibited for most of the reporting period.

Figure 4-195 Convergence Point Array – W170 S2350 – All Chords

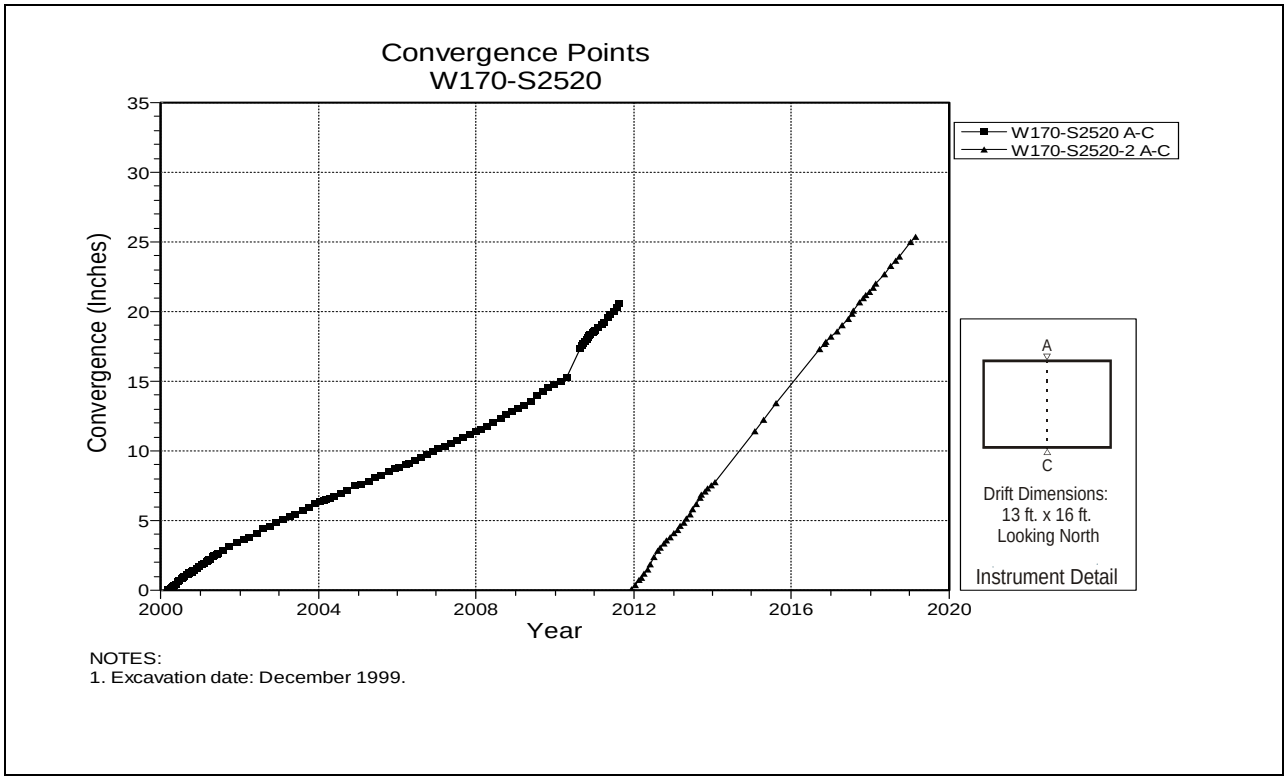

NOTES:
1. Excavation date: December 1999.

Figure 4-196 Convergence Point Array – W170 S2520 – Roof to Floor – Centerline

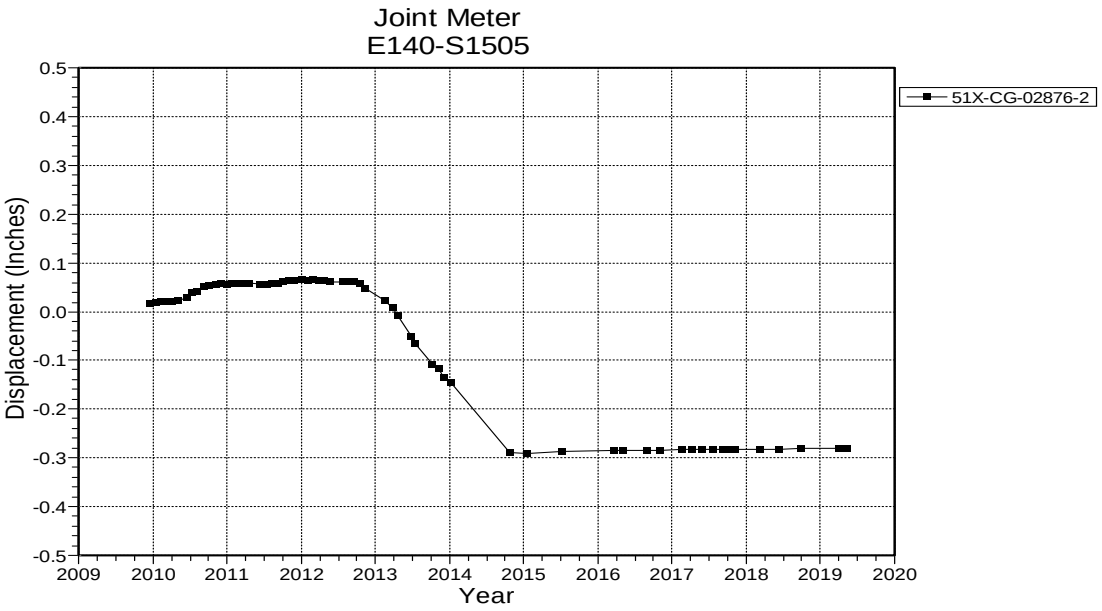

NOTES:
1. Excavation date: December 1982.

Figure 4-197 Joint Meter – E140 S1505

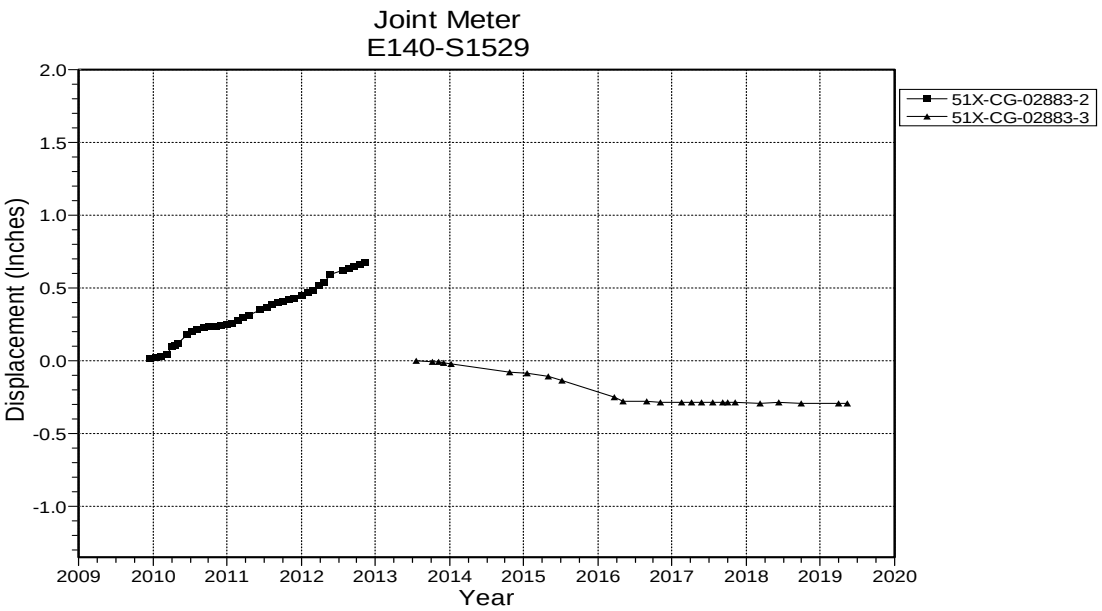

NOTES:
1. Excavation date: December 1982.
2. This instrument was damaged and replaced July 2013.

Figure 4-198 Joint Meter – E140 S1529

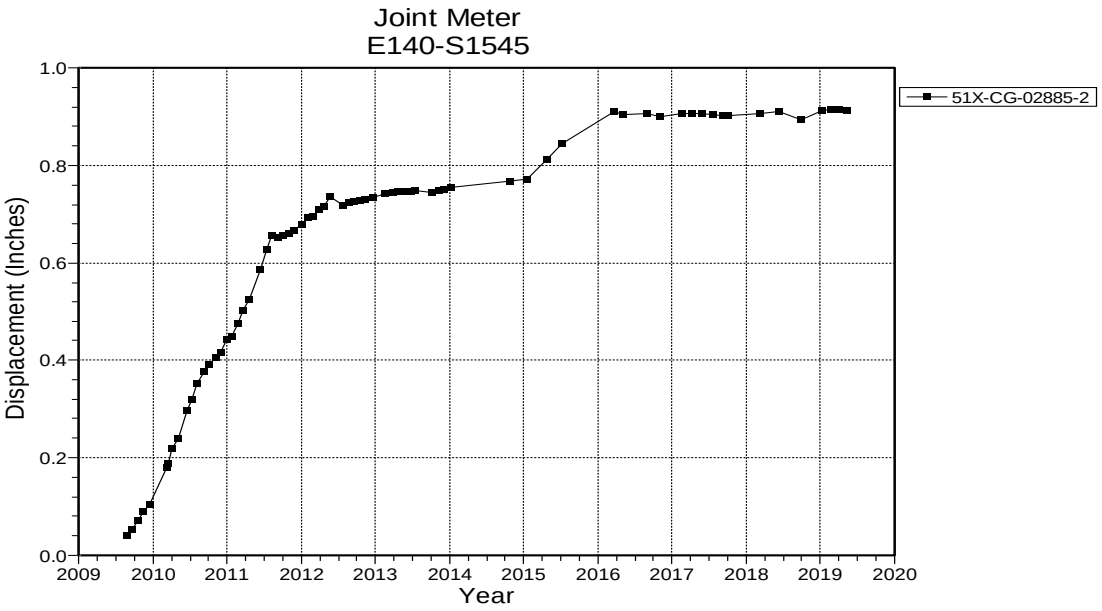

NOTES:
1. Excavation date: December 1982.

Figure 4-199 Joint Meter – E140 S1545

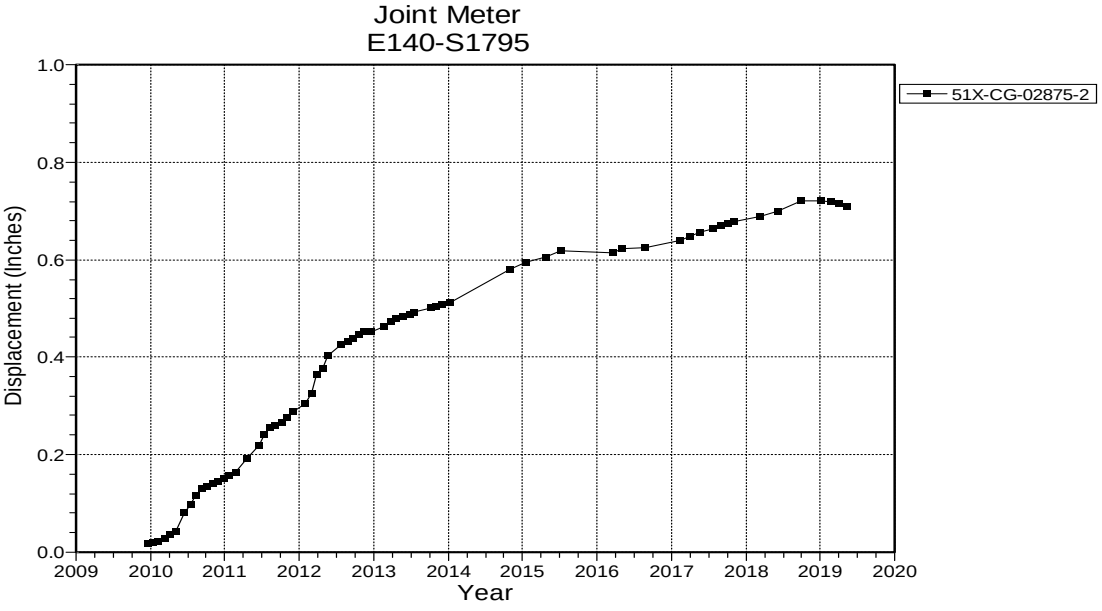

NOTES:
1. Excavation date: December 1982.

Figure 4-200 Joint Meter – E140 S1795

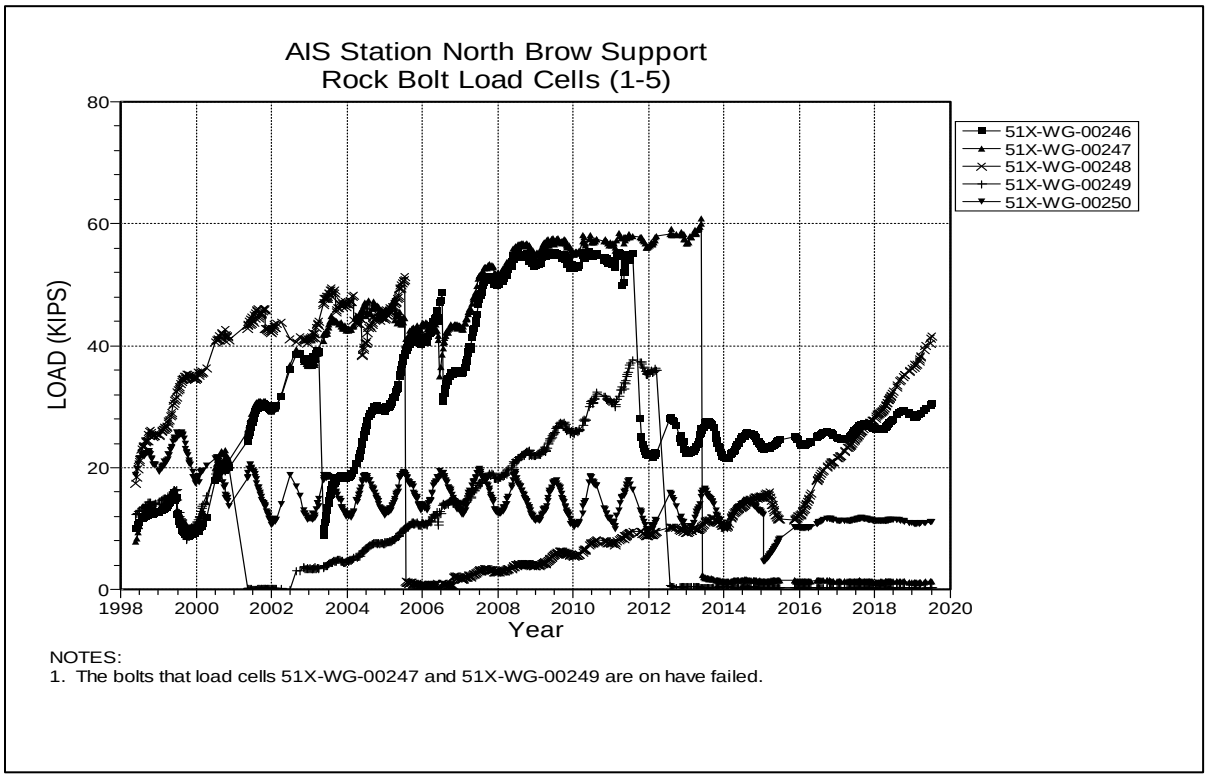

Figure 4-201 Rock Bolt Load Cells 1-5 – AIS North Brow

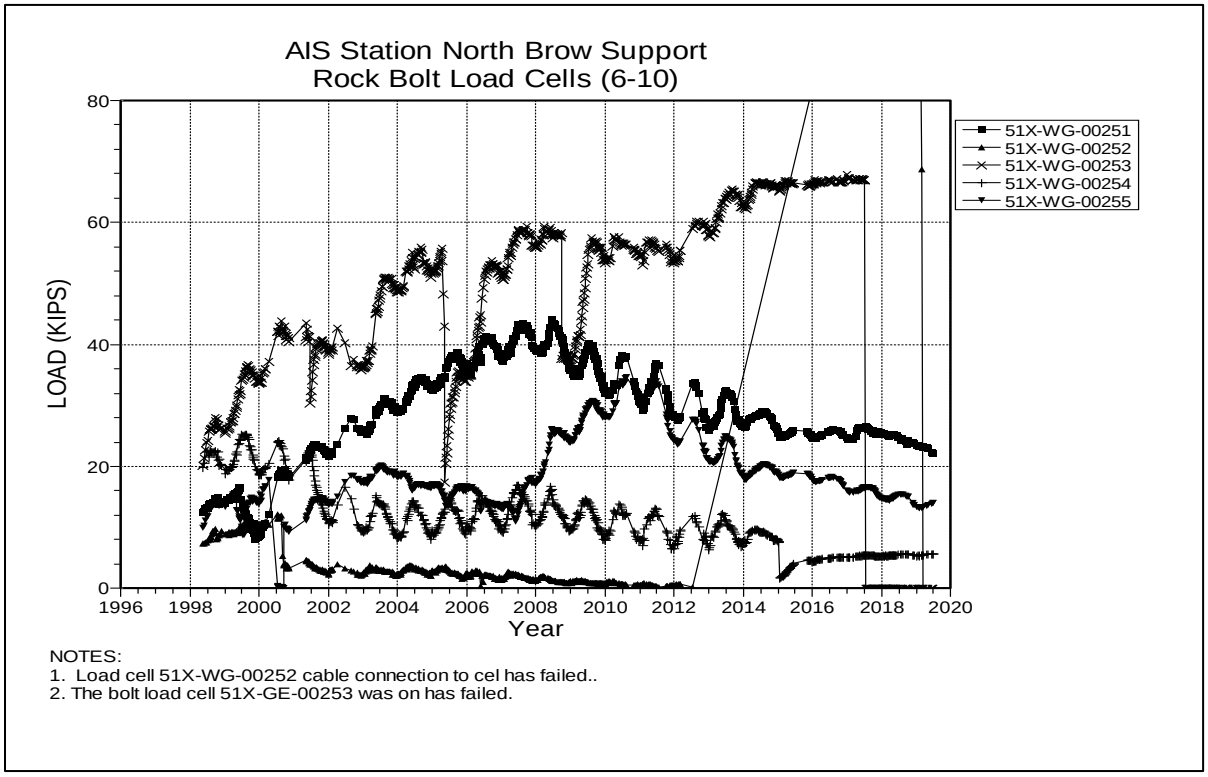

Figure 4-202 Rock Bolt Load Cells 6-10 – AIS North Brow

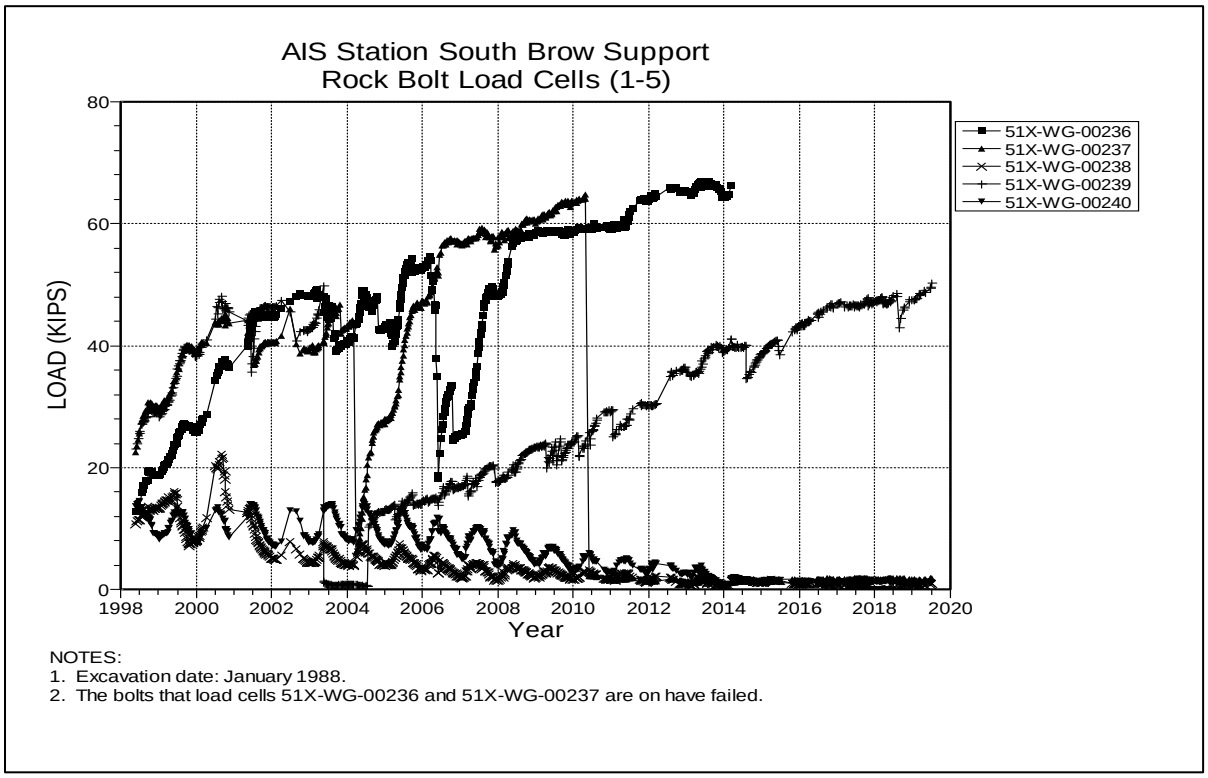

Figure 4-203 Rock Bolt Load Cells 1-5 – AIS South Brow

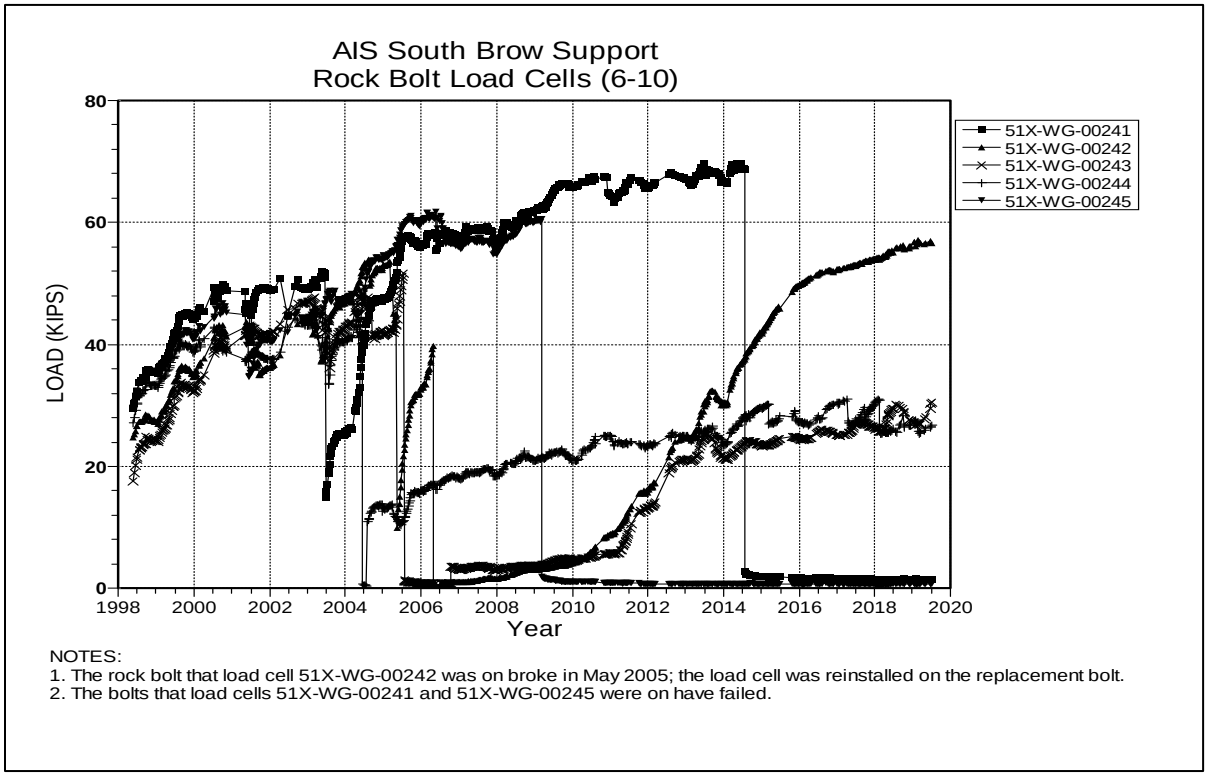

Figure 4-204 Rock Bolt Load Cells 6-10 – AIS South Brow

5.0 INSTRUMENTATION SUMMARY FOR THE WASTE DISPOSAL AREA

This chapter presents a summary of the data collected from instruments located in the Waste Disposal Area at the WIPP. Table 5-1 presents data and analysis of the instrumentation associated with Panel 7. Plots of the instrument data are presented as Figures 5-1 through 5-33. Table 5-2 presents instrument data from Panel 8. Plots of the instrument data are presented as Figures 5-34 through 5-38.

Table 5-1
Panel 7 Data Analysis

Extensometers

Field Tag	Location	Figure Number	Date of Last Reading	Collar Displacement Relative to Deepest Anchor (inches)	Displacement Rate 2018 to 2019 (in/year)	Displacement Rate 2017 to 2018 (in/year)	Rate Change Percent	Comments
51X-GE-00416	S2180-W585	5-1	06/24/19	11.036	0.5	0.5	0	
51X-GE-00417	S2180-W985	5-2	06/24/19	1.440	0.8	0.6	33	
51X-GE-00423	S2520-W585	5-3	05/13/19	13.304	1.9	2.0	-5	
51X-GE-00424	S2520-W985	5-4	08/10/18	12.506	1.7	1.7	0	
51X-GE-00425	W390-S2350	5-5	05/13/19	10.159	1.5	1.5	0	
51X-GE-00426-2	W520-S2350	5-6	06/24/19	0.105	1.0	2.9	-66	
51X-GE-00418	W660-S2350	5-7	06/24/19	2.687	1.6	1.2	33	
51X-GE-00420-1	W920-S2350	5-8	06/24/19	2.784	1.8	1.0	80	

Convergence Points

Field Tag	Location	Figure Number	Last Reading 2018 to 2019		Cumulative Displacement (inches)	Closure Rate 2018 to 2019 (in/year)	Closure Rate 2017 to 2018 (in/year)	Rate Change Percent	Comments
			Date	Inches					
S2180-W285-2 A-C	S2180-W285	5-9	04/24/19	12.571	13.017	1.1	1.6	-31	
S2180-W390-5 A-C	S2180-W390	5-10	04/24/19	0.441	31.046	3.3	4.0	-18	
S2180-W460-5 A-C	S2180-W460	5-11	04/24/19	0.365	36.574	2.7	4.7	-43	
S2180-W520-7 A-C	S2180-W520	5-12	04/24/19	0.391	39.086	2.9	4.2	-31	
S2180-W585-4 A-C	S2180-W585	5-13	11/28/18	29.994	39.971	4.7	5.2	-10	
S2180-W660-4 A-C	S2180-W660	5-14	04/24/19	27.725	37.134	2.8	3.5	-20	
W390-S2275-3 A-C	W390-S2275	5-15	04/24/19	32.919	40.853	4.1	4.9	-16	
W390-S2350-3 A-C	W390-S2350	5-16	04/24/19	25.060	31.624	3.6	4.0	-10	
W390-S2425-4 A-C	W390-S2425	5-17	04/24/19	8.269	31.325	3.1	3.3	-6	
W520-S2275-3 A-C	W520-S2275	5-18	01/11/19	35.523	43.975	4.7	4.7	0	
W520-S2350-3 A-C	W520-S2350	5-19	01/11/19	23.820	36.689	3.3	3.6	-8	
W520-S2425-4 A-C	W520-S2425	5-20	02/13/19	6.859	37.725	2.9	3.6	-19	

Table 5-1
Panel 7 Data Analysis, continued

Convergence Points, continued									
Field Tag	Location	Figure Number	Last Reading 2018 to 2019		Cumulative Displacement (inches)	Closure Rate 2018 to 2019 (in/year)	Closure Rate 2017 to 2018 (in/year)	Rate Change Percent	Comments
			Date	Inches					
W660-S2275-5 A-C	W660-S2275	5-21	03/20/19	0.165	34.394	2.2	3.9	-44	4/24/19 reading was erroneous.
W660-S2350-4 A-C	W660-S2350	5-22	04/24/19	0.329	42.712	1.9	3.5	-46	
W660-S2425-5 A-C	W660-S2425	5-23	04/24/19	0.265	37.715	1.6	5.6	-71	
S2520-W285-5 A-C	S2520-W285	5-24	04/24/19	10.731	33.720	4.6	4.6	0	
S2520-W390-4 A-C	S2520-W390	5-25	04/24/19	8.851	31.455	3.8	3.7	3	
S2520-W455-3 A-C	S2520-W455	5-26	04/24/19	26.318	34.008	3.1	3.6	-14	
S2520-W520-3 A-C	S2520-W520	5-27	04/24/19	28.634	41.412	3.6	3.9	-8	
S2520-W585-5 A-C	S2520-W585	5-28	04/24/19	8.112	30.288	3.3	3.6	-8	
S2520-W660-4 A-C	S2520-W660	5-29	04/24/19	0.259	43.772	2.7	5.1	-47	
S2520-W725-5 A-C	S2520-W725	5-30	01/11/19	25.747	34.698	3.2	3.3	-3	
S2520-W790-5 A-C	S2520-W790	5-31	08/17/18	5.455	30.670	3.2	3.4	-6	
S2520-W855-3 A-C	S2520-W855	5-32	08/17/18	24.647	38.580	3.3	3.5	-6	
S2520-W920-5 A-C	S2520-W920	5-33	08/17/18	4.134	27.405	2.4	2.8	-14	

Table 5-2
Panel 8 Data Analysis

Extensometers								
Field Tag	Location	Figure Number	Date of Last Reading	Collar Displacement Relative to Deepest Anchor (inches)	Displacement Rate 2018 to 2019 (in/year)	Displacement Rate[3] 2017 to 2018 (in/year)	Rate Change Percent[3]	Comments
51X-GE-00443	W390-S1775	5.34	04/23/19	0.353	1.03	N/A	N/A	

Table 5-2
Panel 8 Data Analysis, continued

Convergence Points									
Field Tag	Location	Figure Number	Last Reading 2018 to 2019		Cumulative Displacement (inches)	Closure Rate 2018 to 2019 (in/year)	Closure Rate[3] 2017 to 2018 (in/year)	Rate Change Percent[3]	Comments
			Date	Inches					
W390-S1700 A-C	W390-S1700	5-35	03/19/19	1.127	1.127	2.8	N/A	N/A	
W390-S1775 A-C	W390-S1775	5-36	03/19/19	1.466	1.466	3.6	N/A	N/A	
S1600-W455-2 A-C	S1600-W455	5-37	04/30/19	0.885	18.630	2.5	4.7	-48	
S1600-W520-2 A-C	S1600-W520	5-38	04/30/19	0.781	20.750	2.2	4.3	-49	

[3] N/A – Insufficient data available to perform the calculation. This is usually due to the inability to read the instruments because of activities such as the removal of an instrument due to floor, rib, or back trimming; locations blocked by equipment or waste disposal; installation timing, access issues, etc.

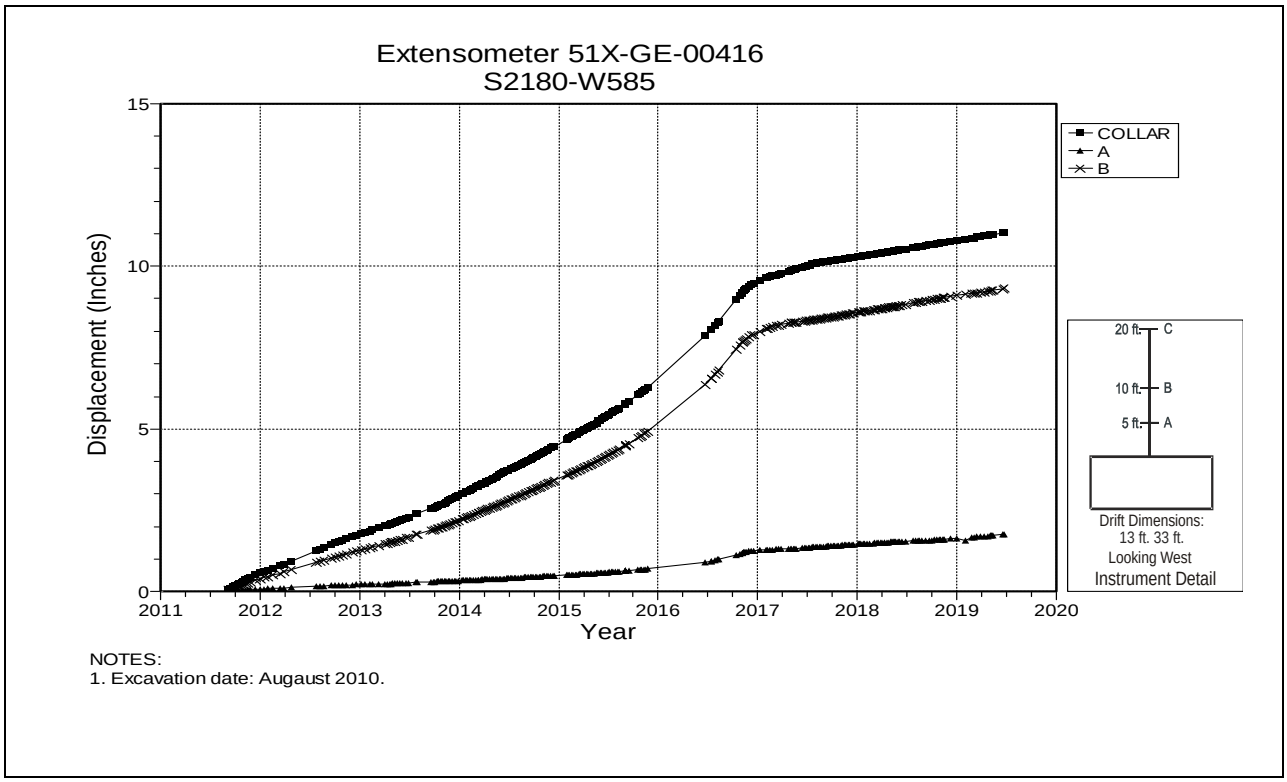

Figure 5-1 Extensometer 51X-GE-00416 – S2180 W585 – Roof

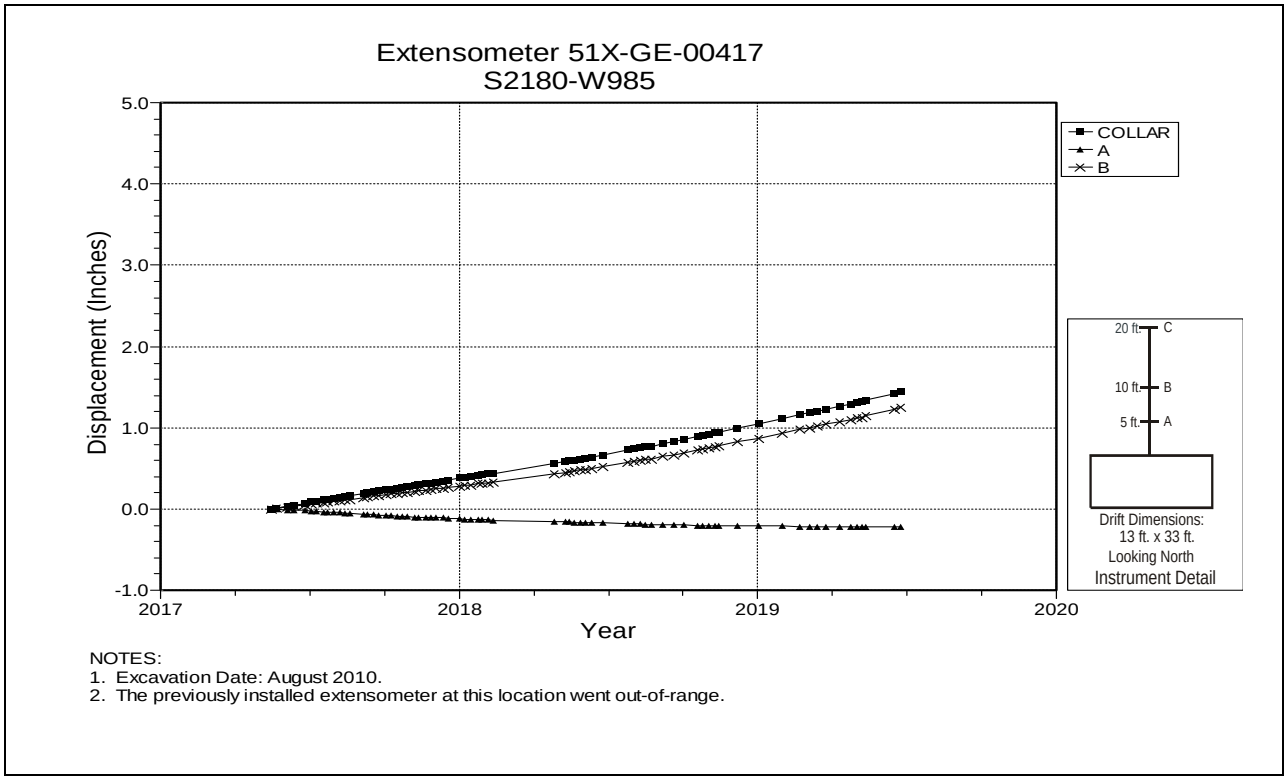

Figure 5-2 Extensometer 51X-GE-00417 – S2180 W985 – Roof

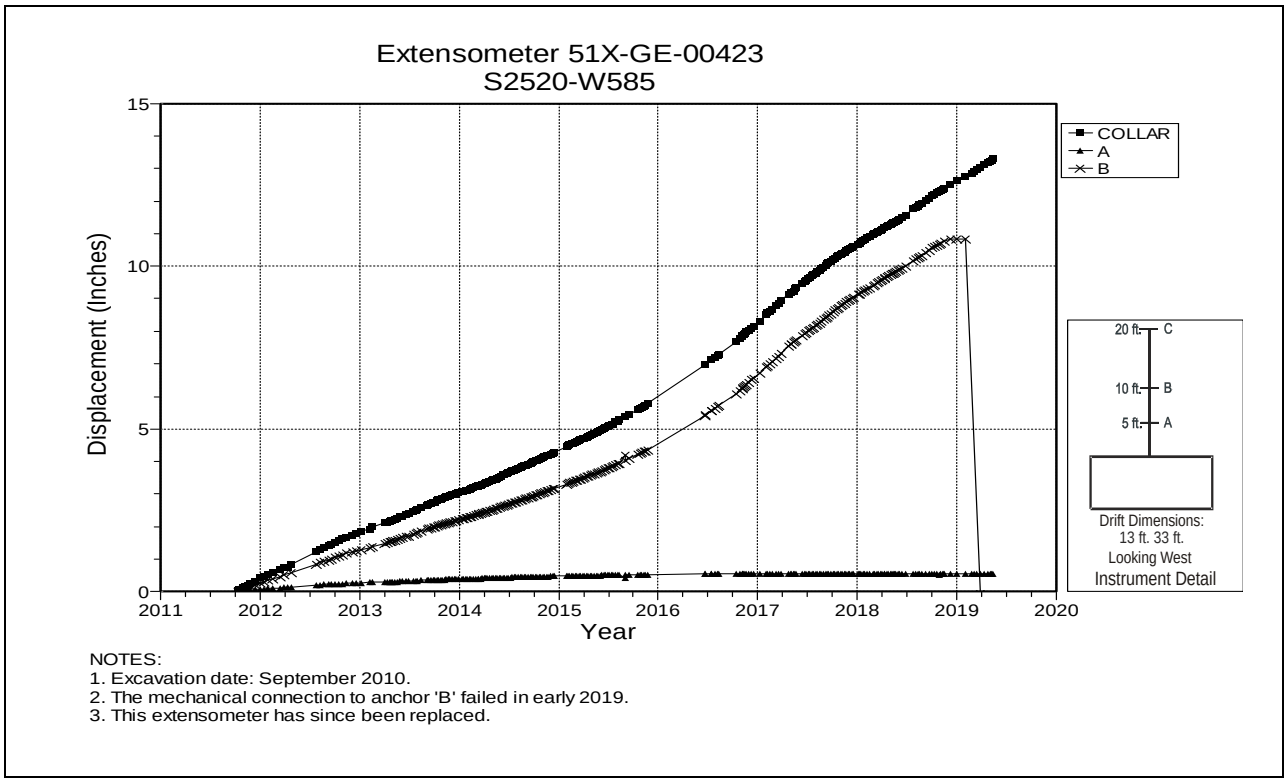

NOTES:
1. Excavation date: September 2010.
2. The mechanical connection to anchor 'B' failed in early 2019.
3. This extensometer has since been replaced.

Figure 5-3 Extensometer 51X-GE-00423 – S2520 W585 – Roof

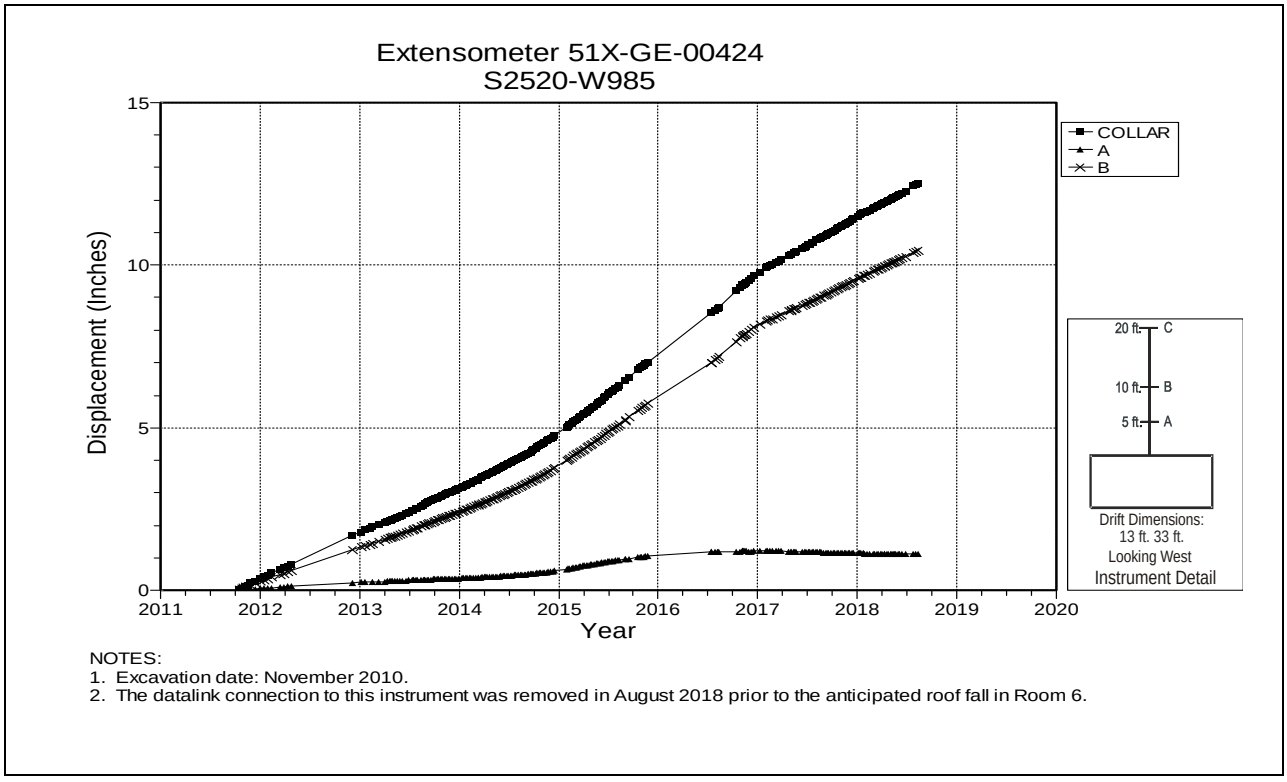

NOTES:
1. Excavation date: November 2010.
2. The datalink connection to this instrument was removed in August 2018 prior to the anticipated roof fall in Room 6.

Figure 5-4 Extensometer 51X-GE-00424 – S2520 W985 – Roof

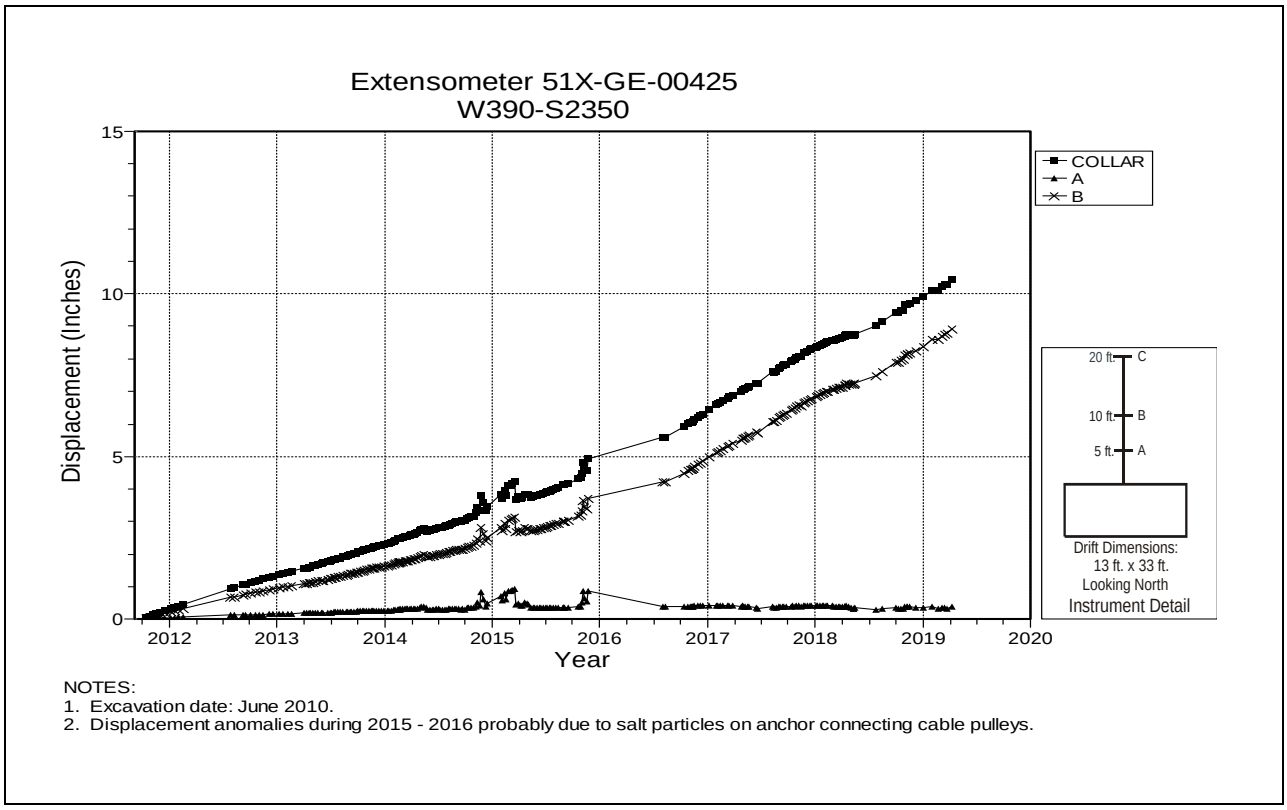

NOTES:
1. Excavation date: June 2010.
2. Displacement anomalies during 2015 - 2016 probably due to salt particles on anchor connecting cable pulleys.

Figure 5-5 Extensometer 51X-GE-00425 – W390-S2350 – Roof

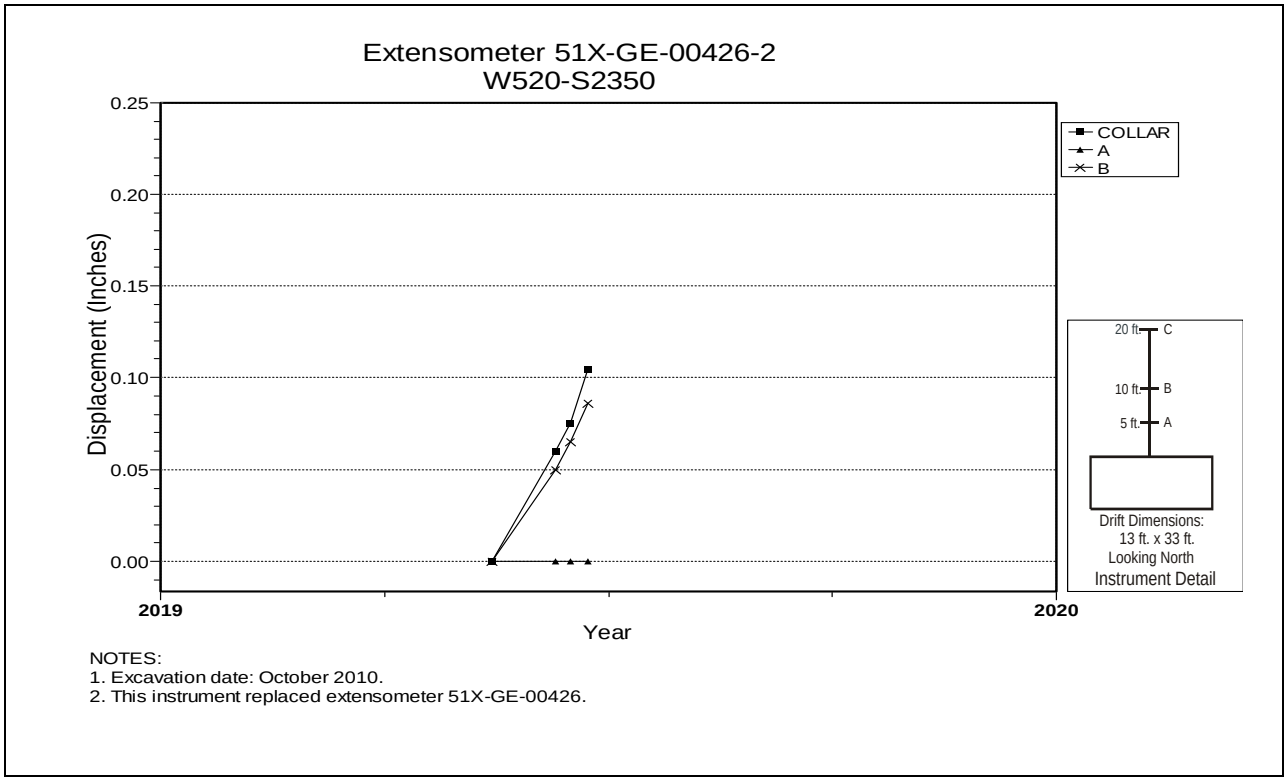

NOTES:
1. Excavation date: October 2010.
2. This instrument replaced extensometer 51X-GE-00426.

Figure 5-6 Extensometer 51X-GE-00426-2 – W520-S2350 – Roof

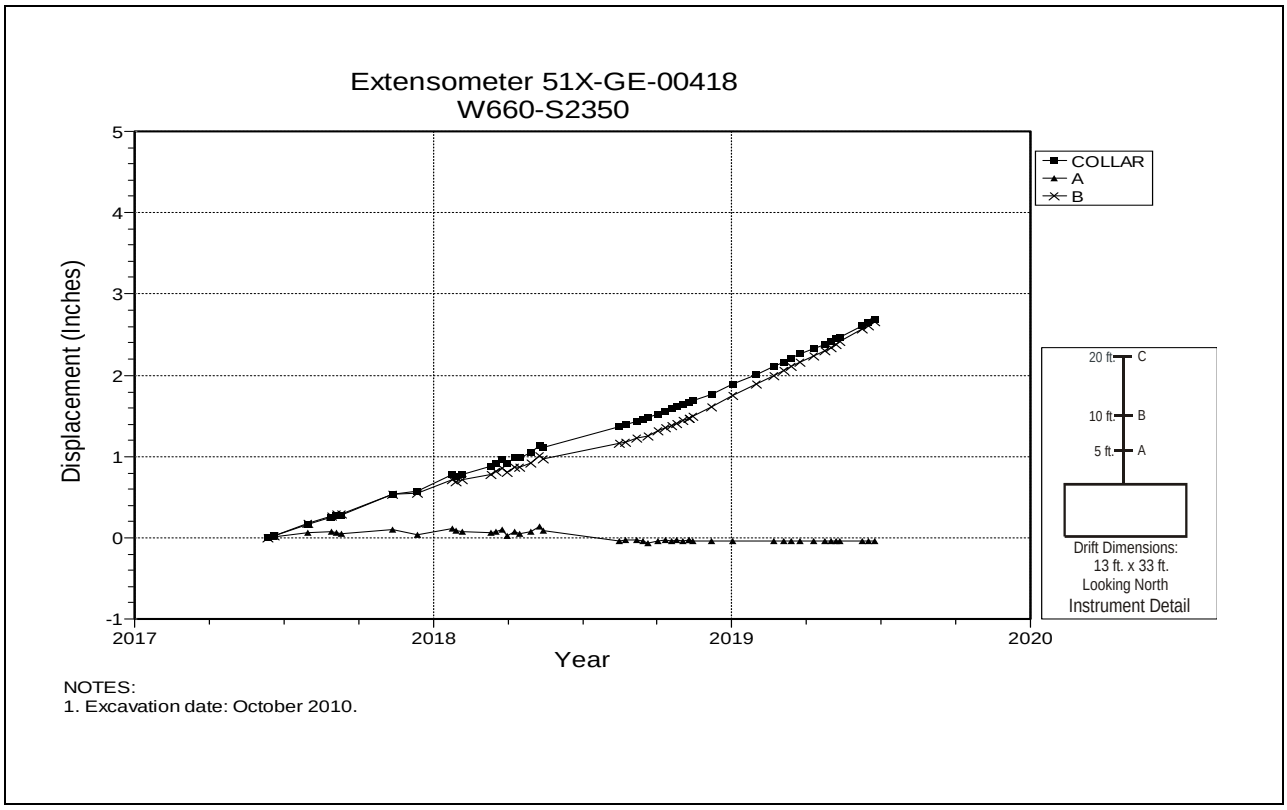

Figure 5-7 Extensometer 51X-GE-00418 – W660-S2350 – Roof

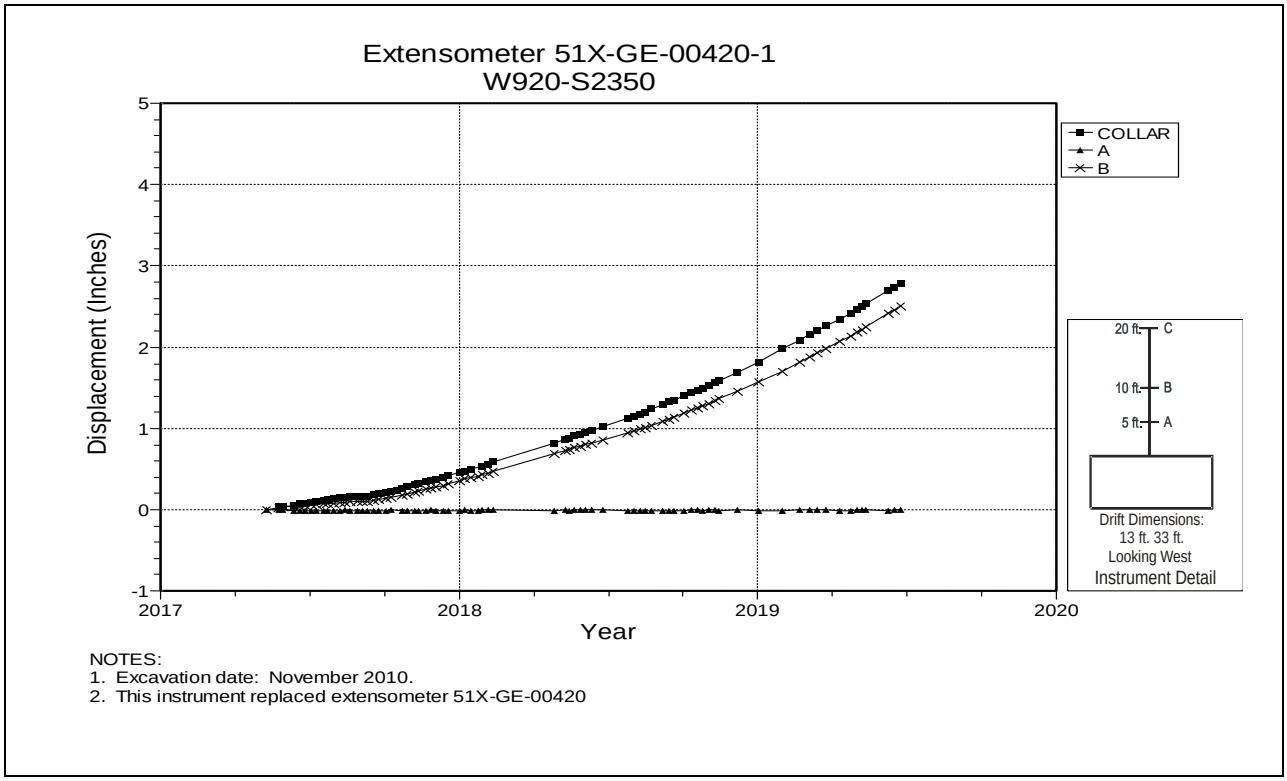

Figure 5-8 Extensometer 51X-GE-00420-1 – W920 S2350 – Roof

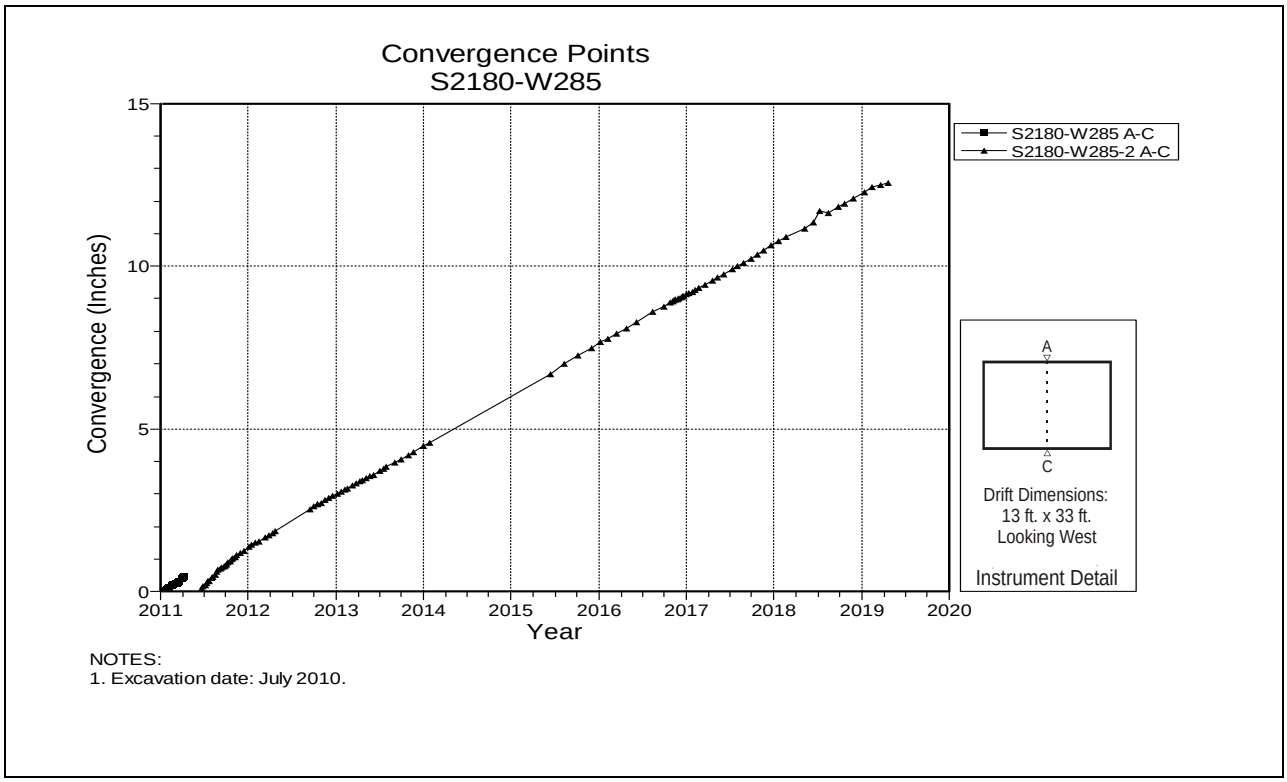

Figure 5-9 Convergence Point Array – S2180 W285 – Roof to Floor

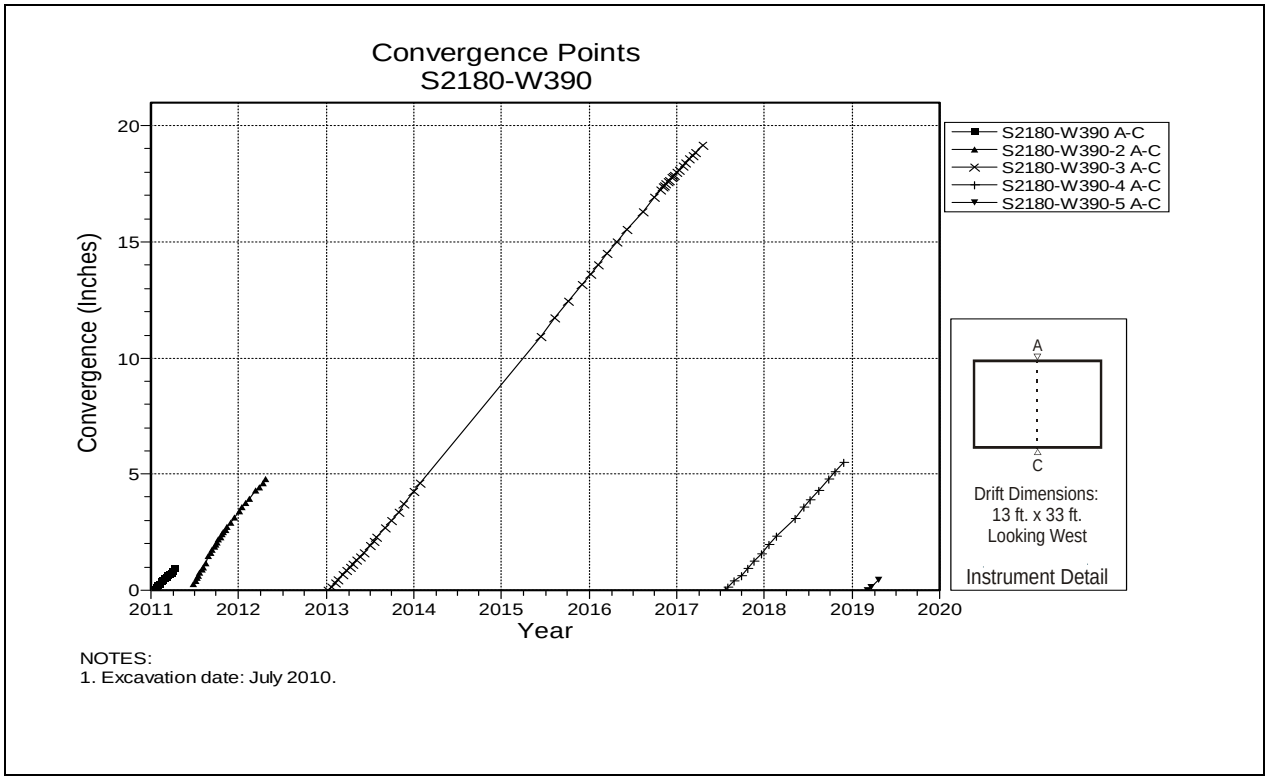

Figure 5-10 Convergence Point Array – S2180 W390 – Roof to Floor

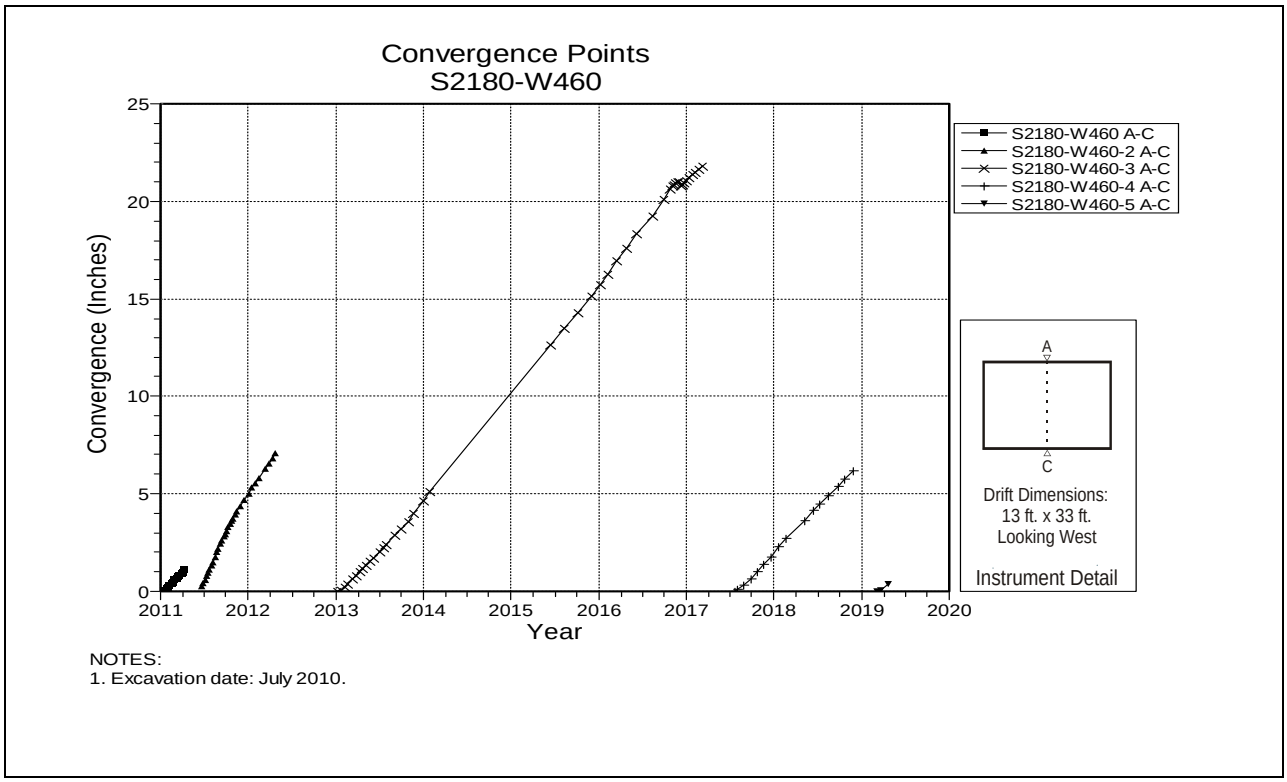

Figure 5-11 Convergence Point Array – S2180 W460 – Roof to Floor

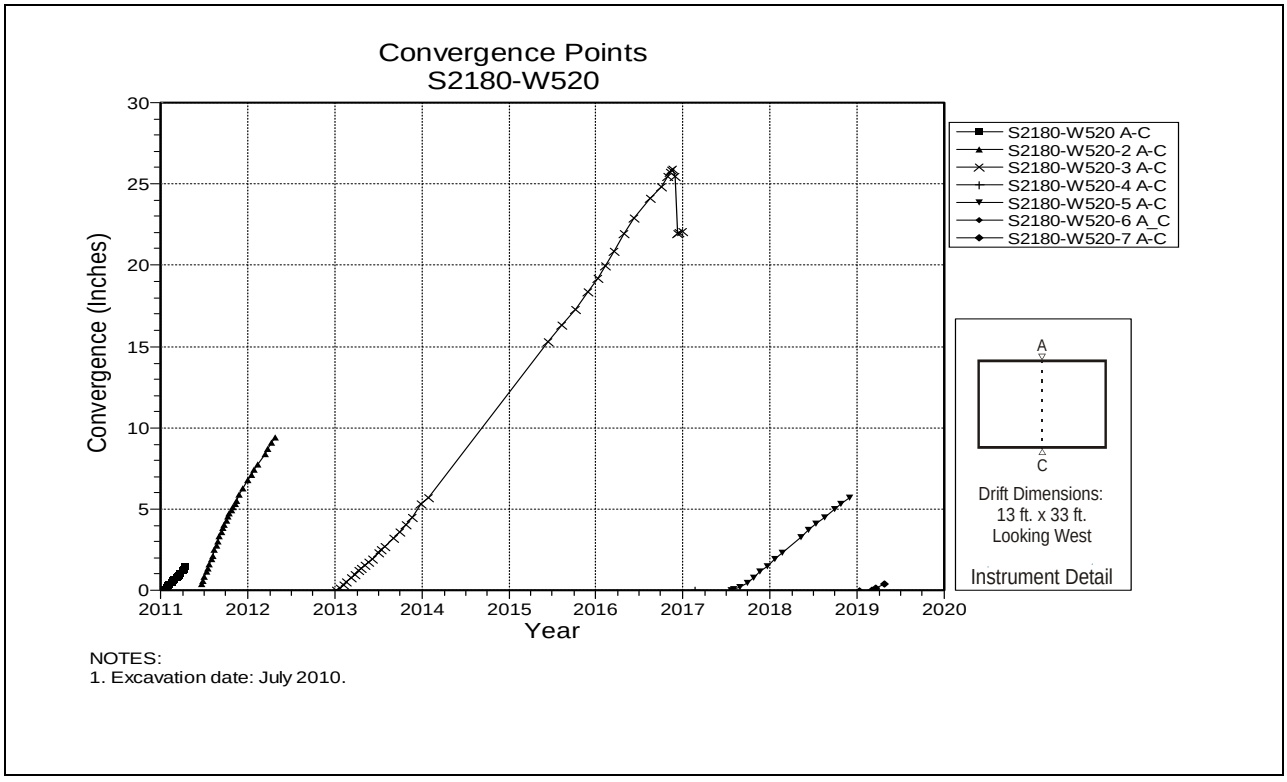

Figure 5-12 Convergence Point Array – S2180 W520 – Roof to Floor

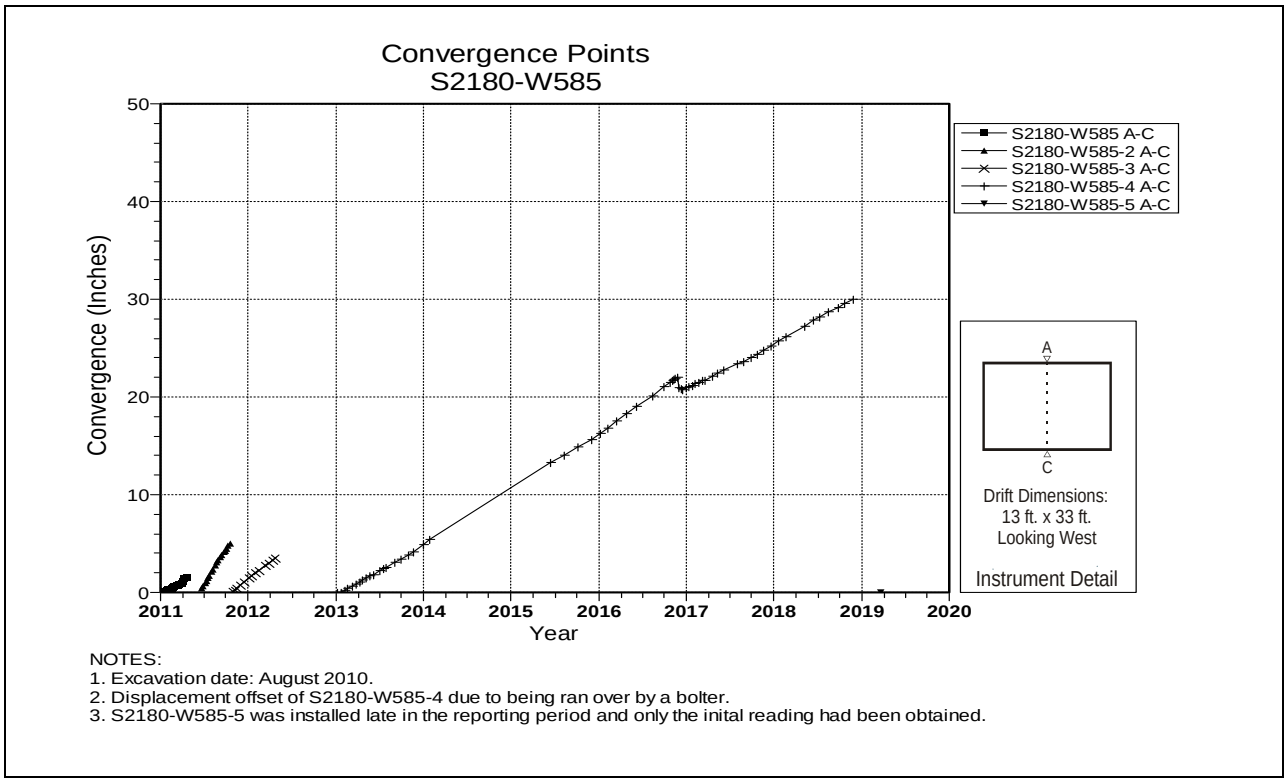

NOTES:
1. Excavation date: August 2010.
2. Displacement offset of S2180-W585-4 due to being ran over by a bolter.
3. S2180-W585-5 was installed late in the reporting period and only the inital reading had been obtained.

Figure 5-13 Convergence Point Array – S2180 W585 – Roof to Floor

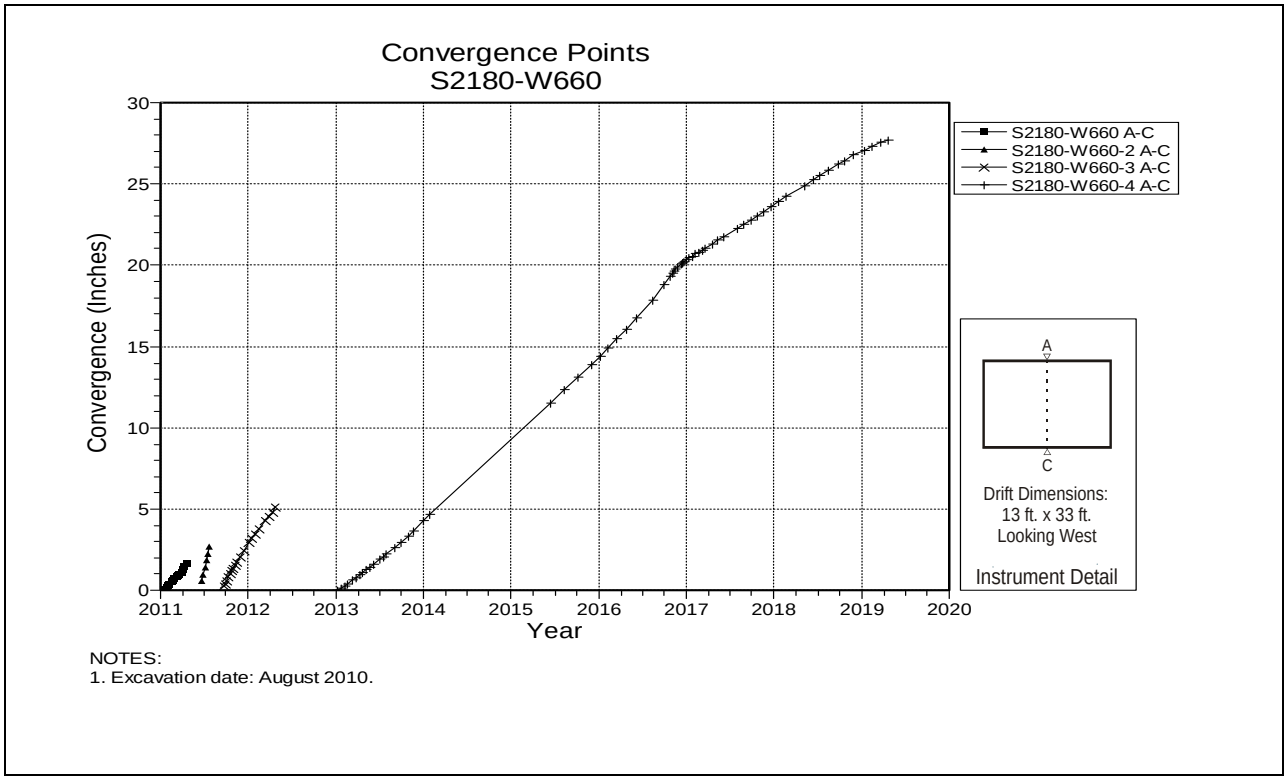

NOTES:
1. Excavation date: August 2010.

Figure 5-14 Convergence Point Array – S2180 W660 – Roof to Floor

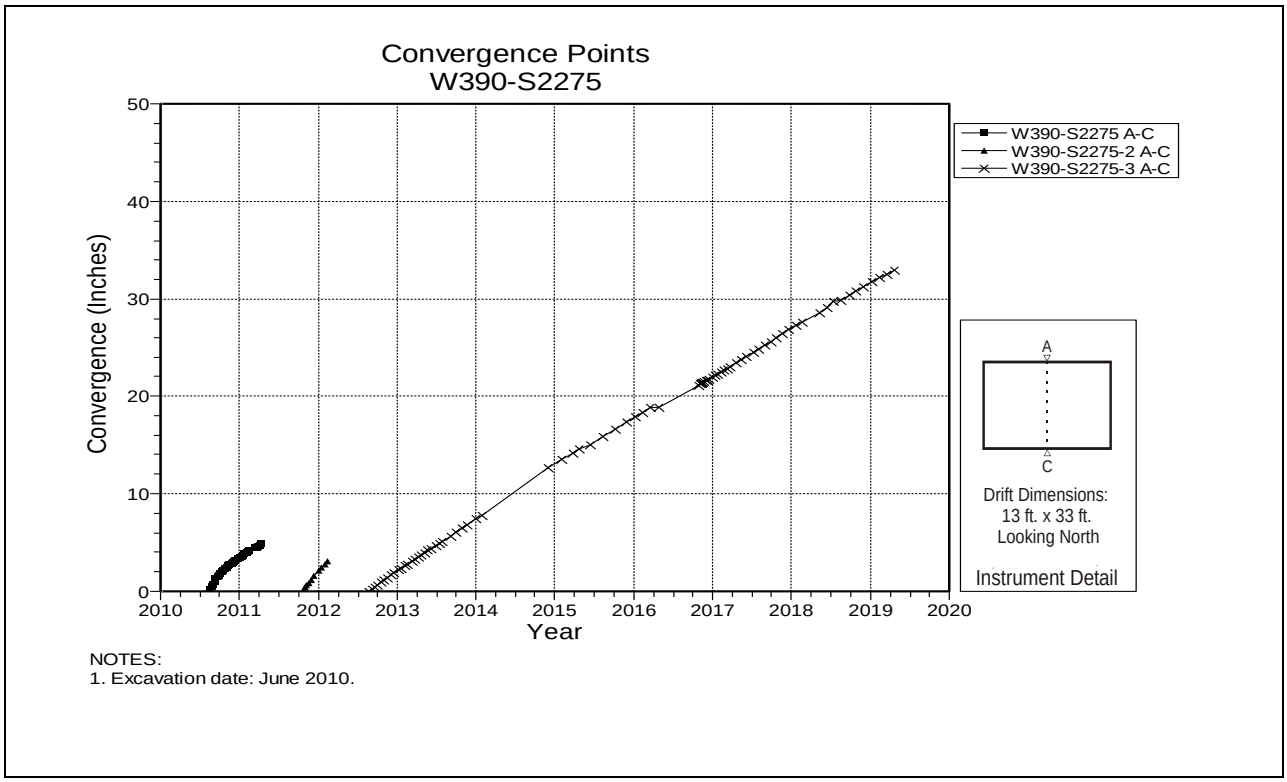

Figure 5-15 Convergence Point Array – W390 S2275 – Roof to Floor

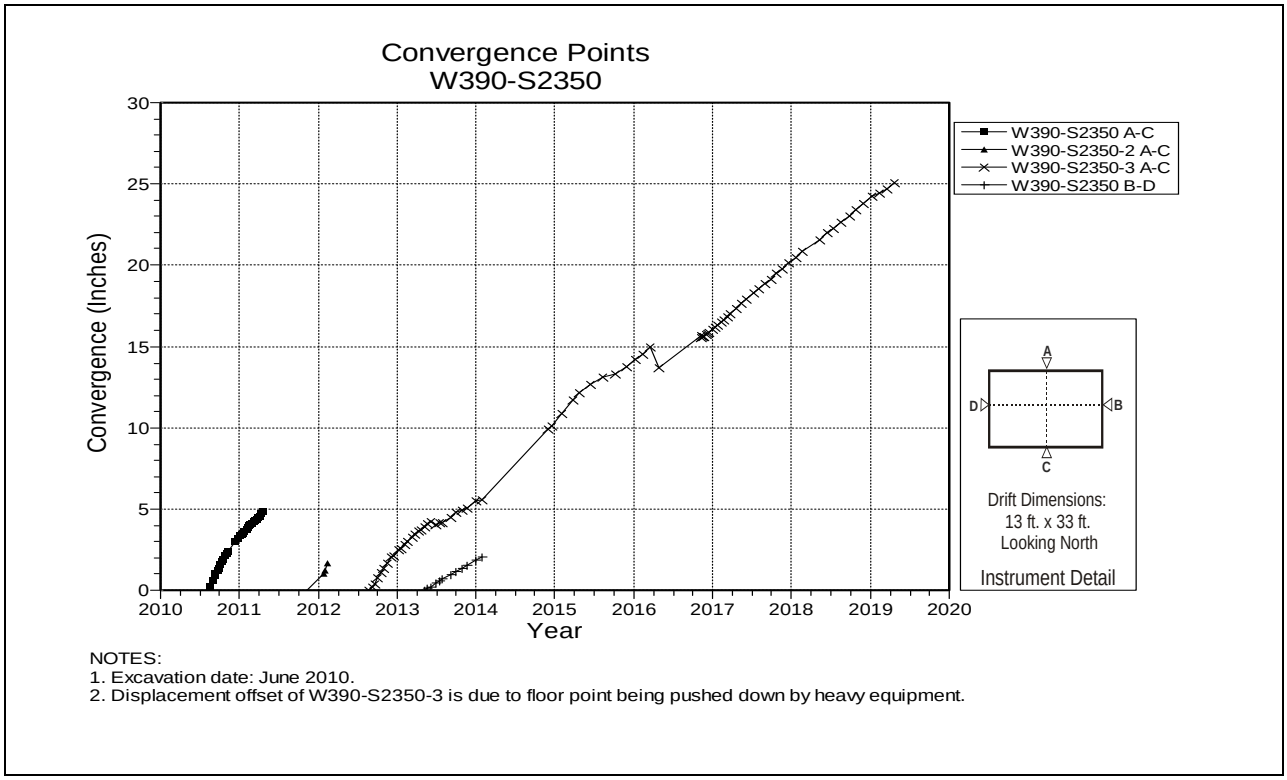

Figure 5-16 Convergence Point Array – W390 S2350 – Roof to Floor

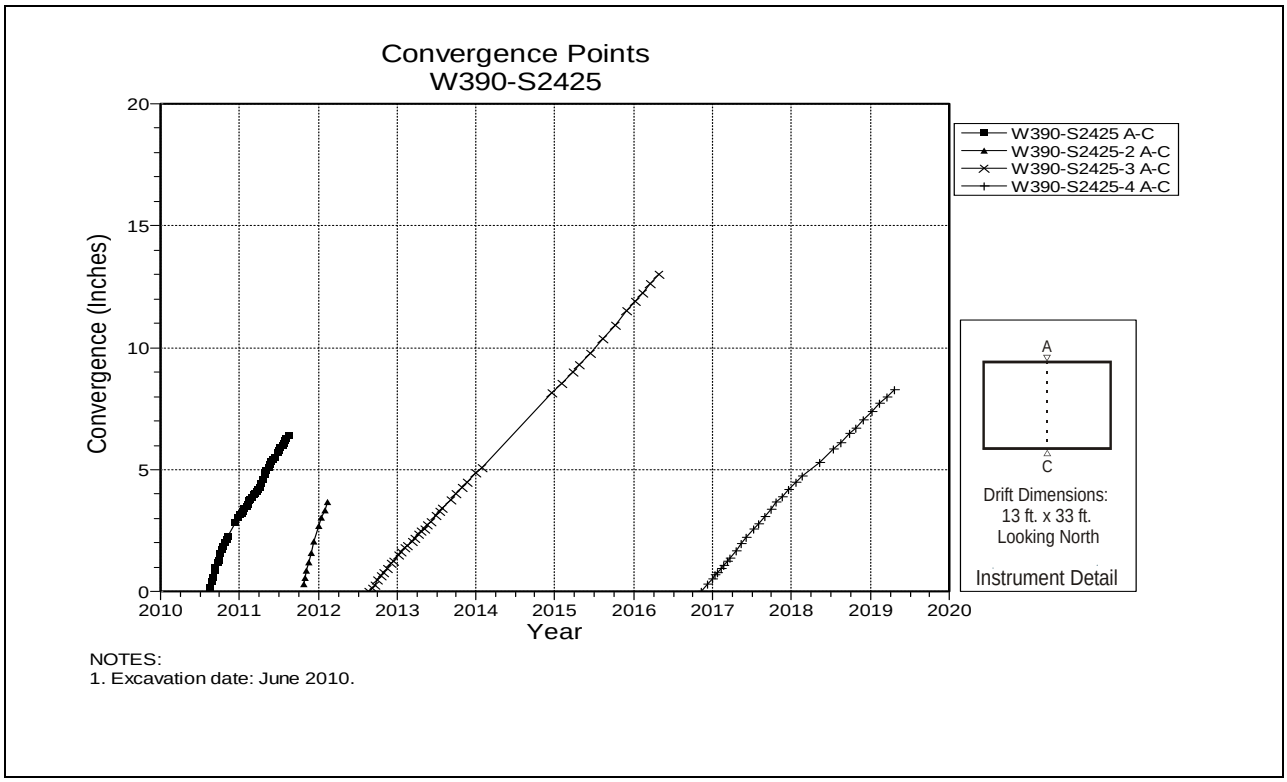

Figure 5-17 Convergence Point Array – W390 S2425 – Roof to Floor

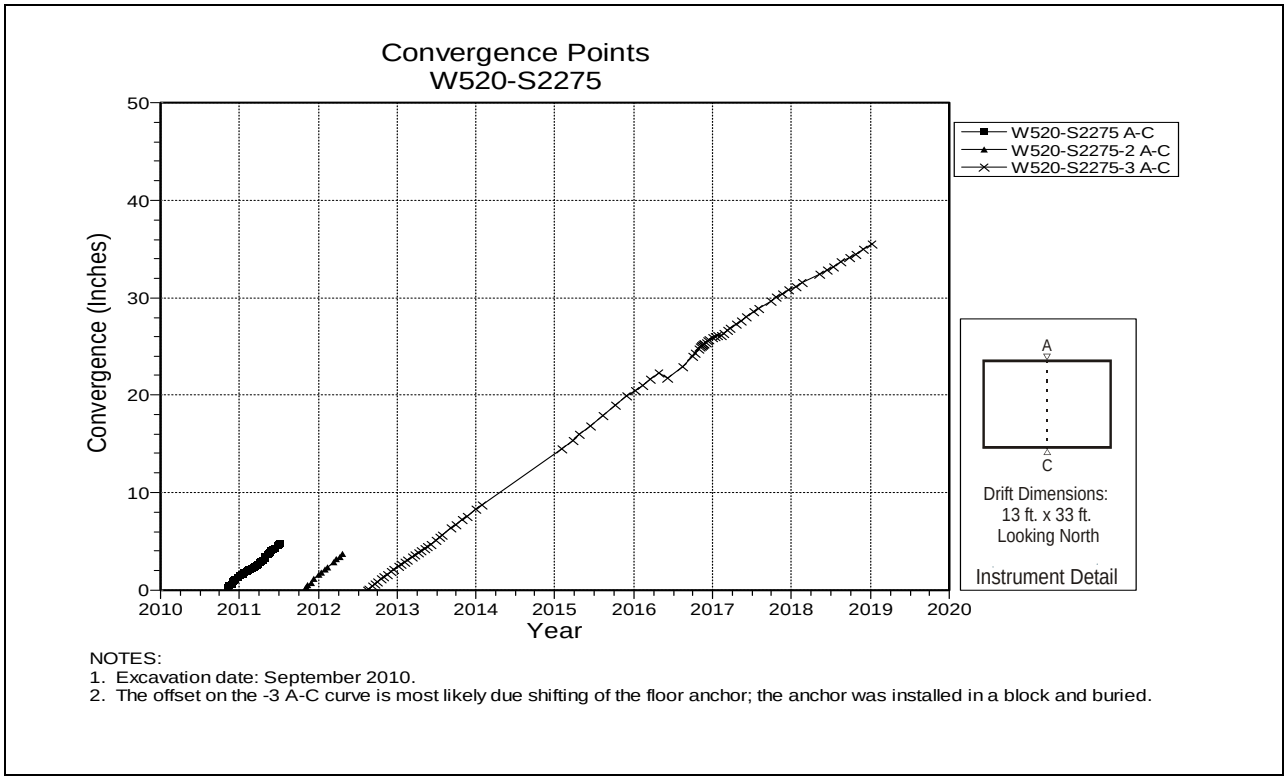

Figure 5-18 Convergence Point Array – W520 S2275 – Roof to Floor

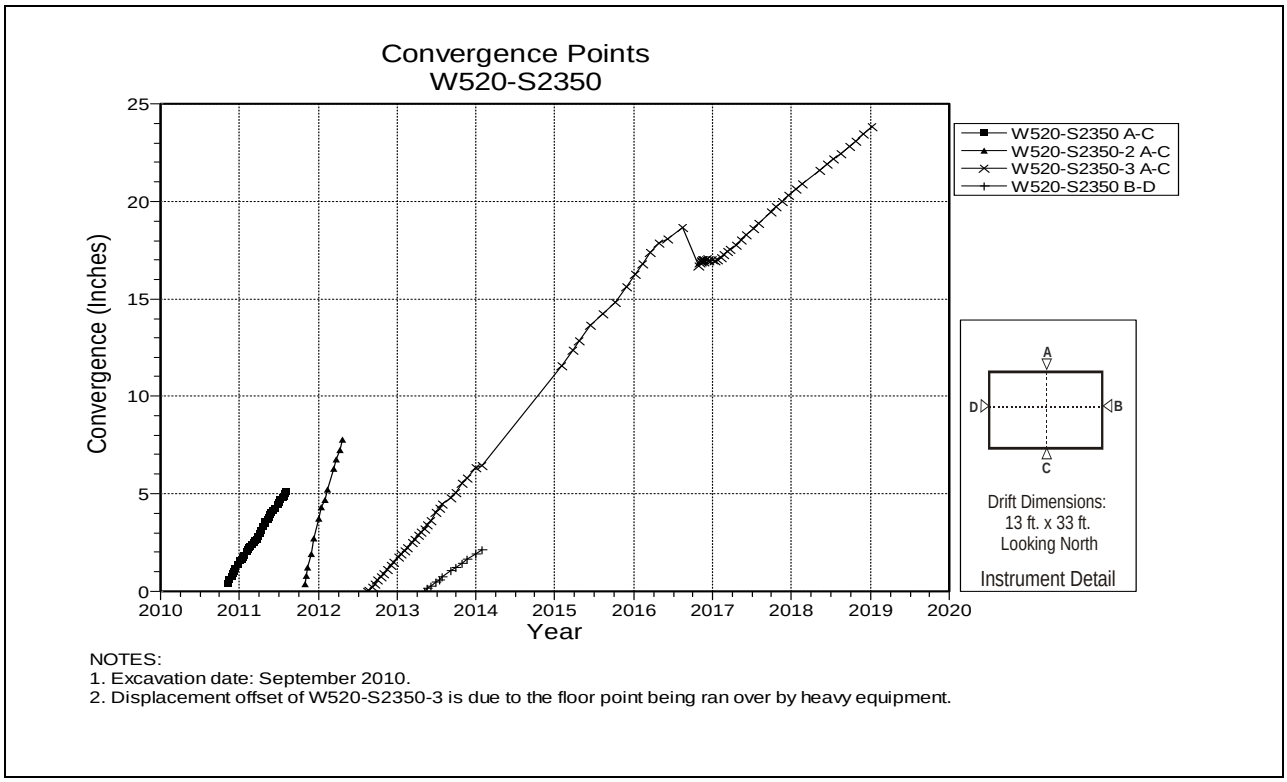

NOTES:
1. Excavation date: September 2010.
2. Displacement offset of W520-S2350-3 is due to the floor point being ran over by heavy equipment.

Figure 5-19 Convergence Point Array – W520 S2350 – All Chords

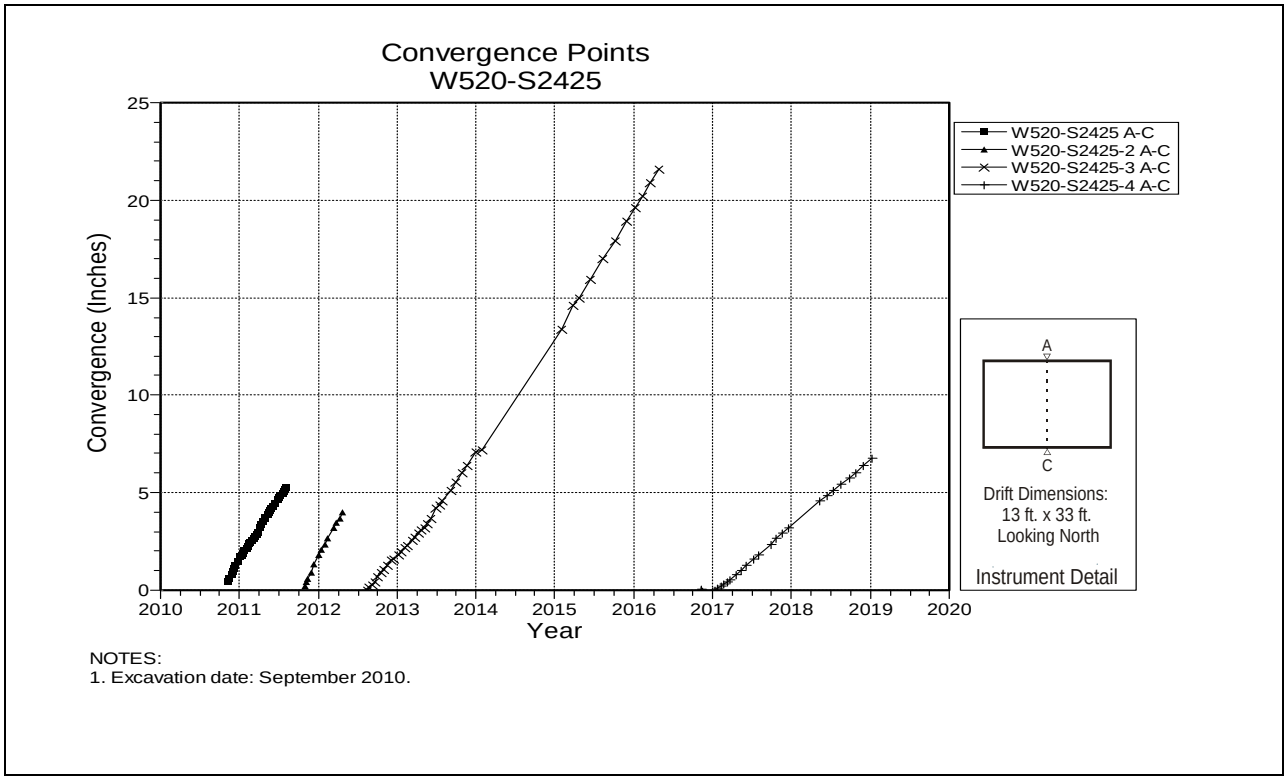

NOTES:
1. Excavation date: September 2010.

Figure 5-20 Convergence Point Array – W520 S2425 – Roof to Floor

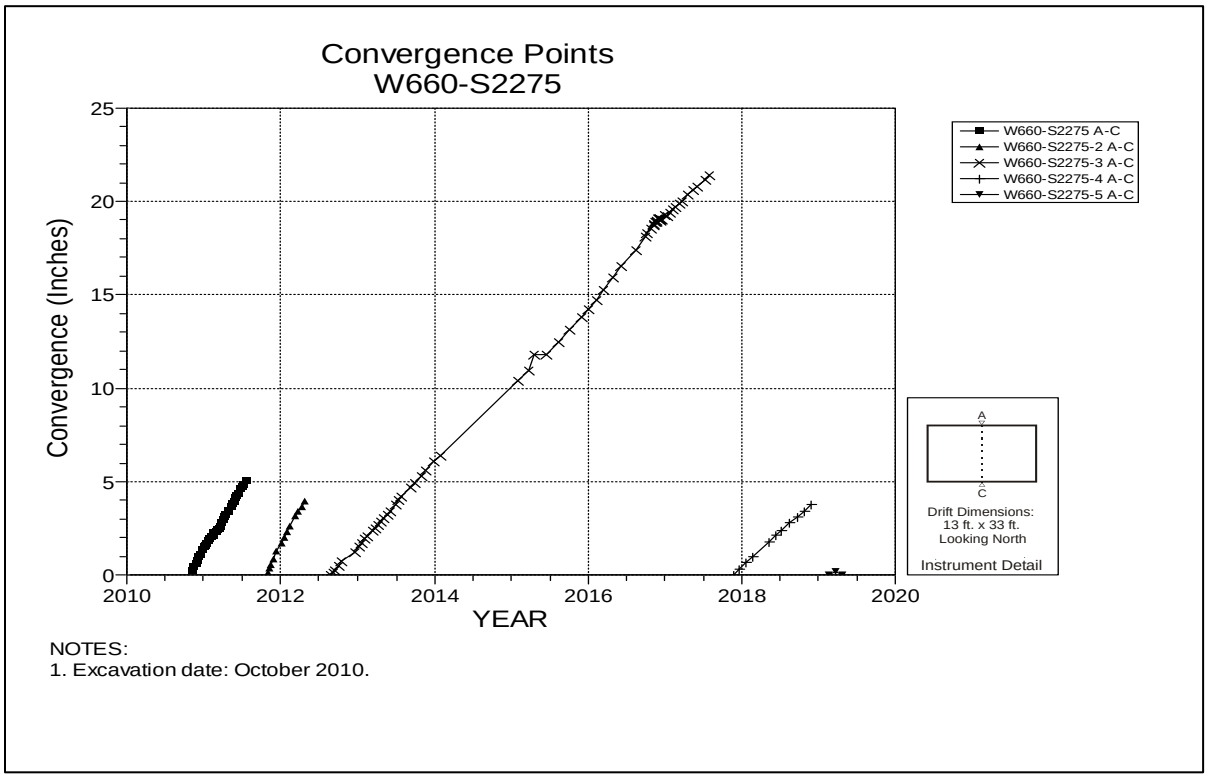

Figure 5-21 Convergence Point Array – W660 S2275 – Roof to Floor

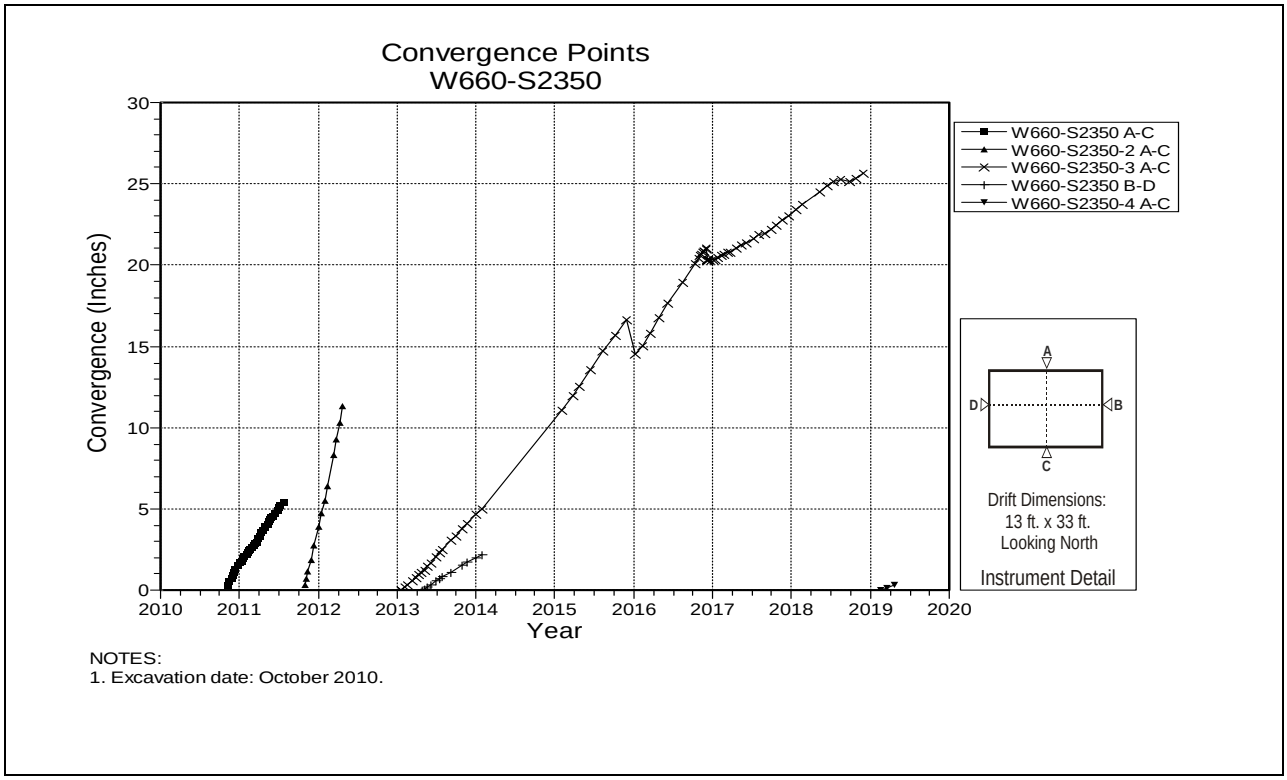

Figure 5-22 Convergence Point Array – W660 S2350 – Roof to Floor

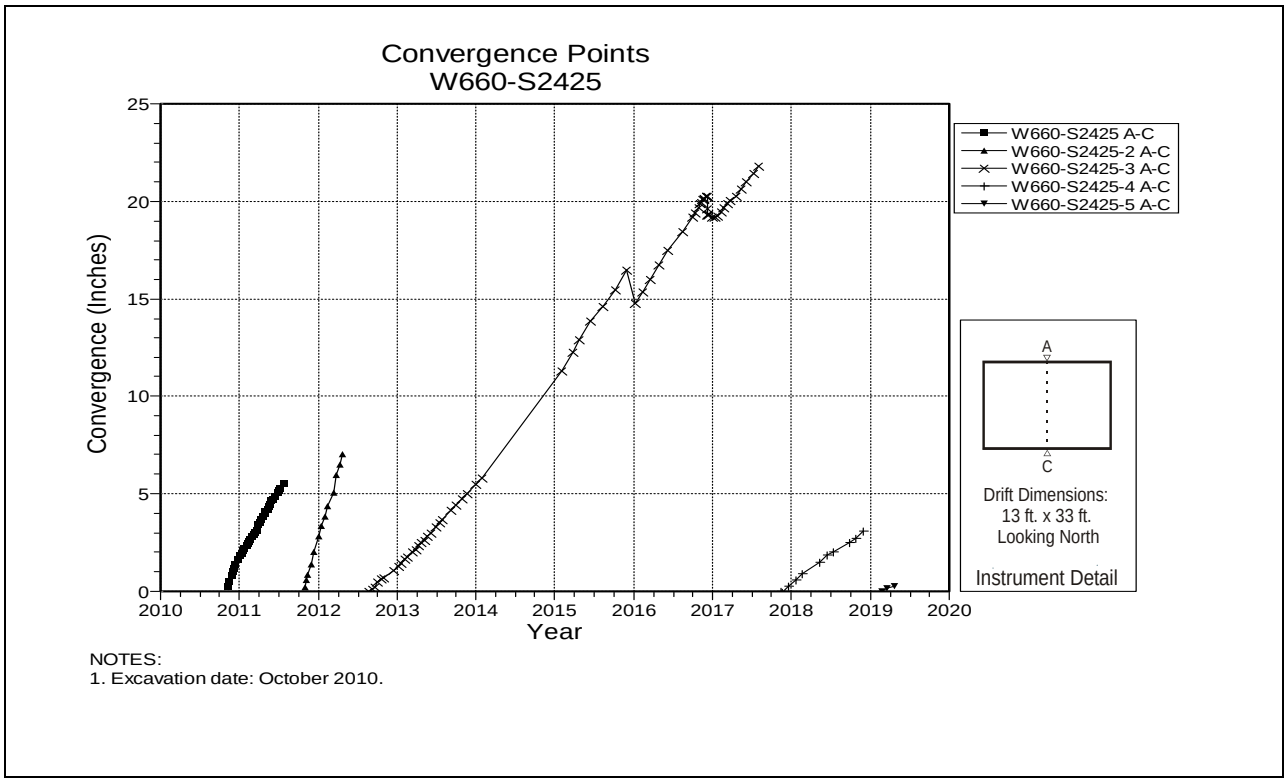

Figure 5-23 Convergence Point Array – W660 S2425 – Roof to Floor

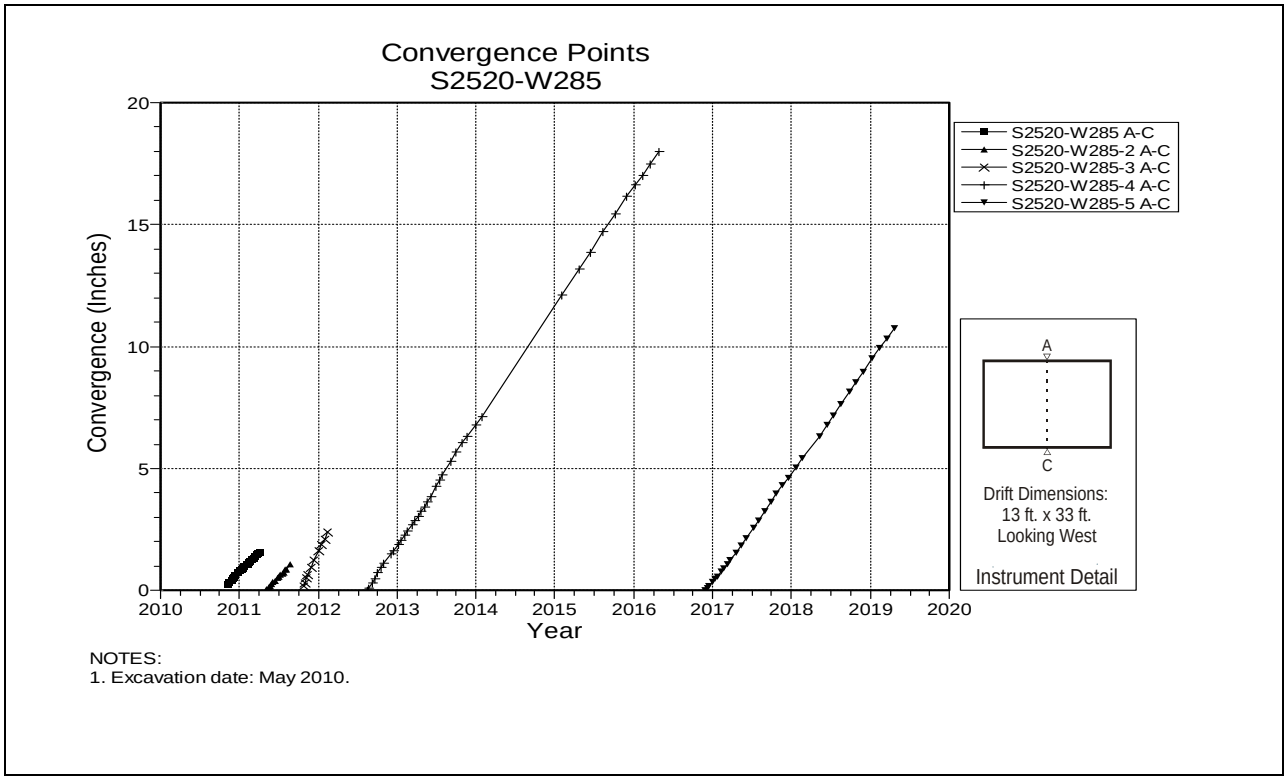

Figure 5-24 Convergence Point Array – S2520 W285 – Roof to Floor

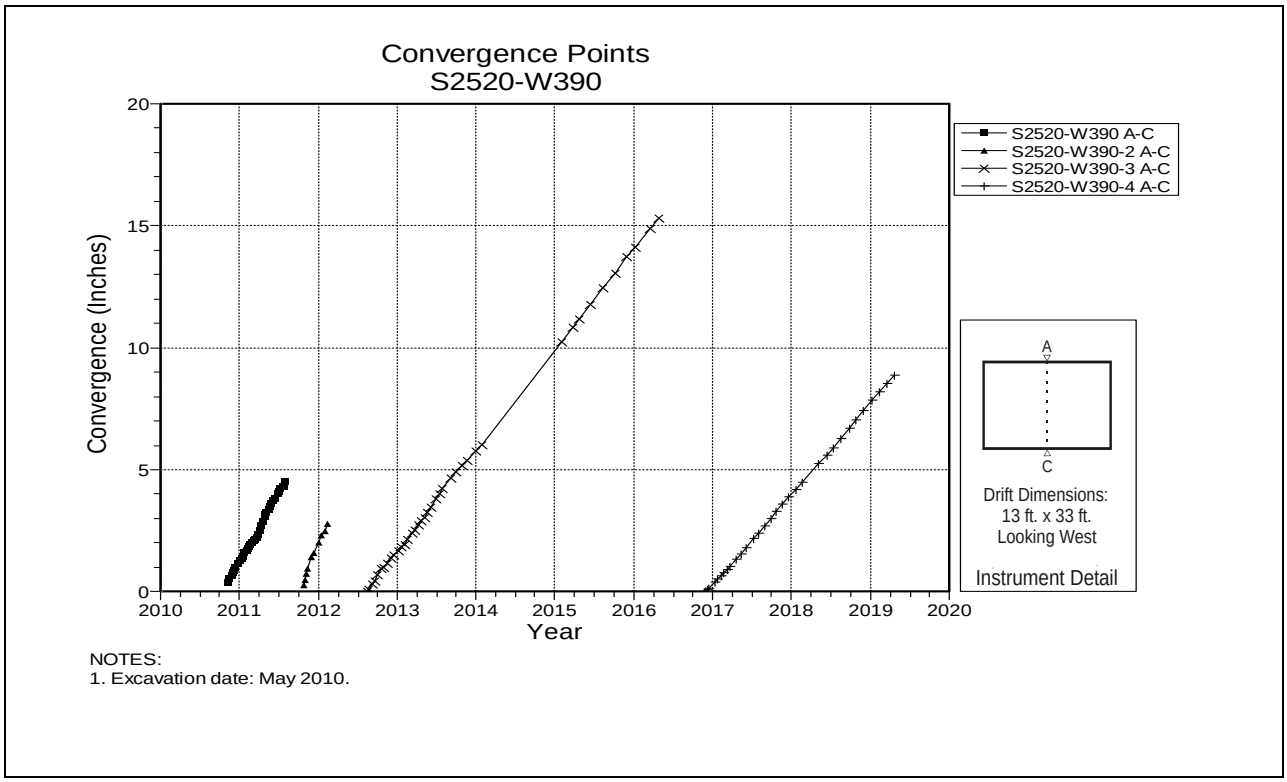

Figure 5-25 Convergence Point Array – S2520 W390 – Roof to Floor

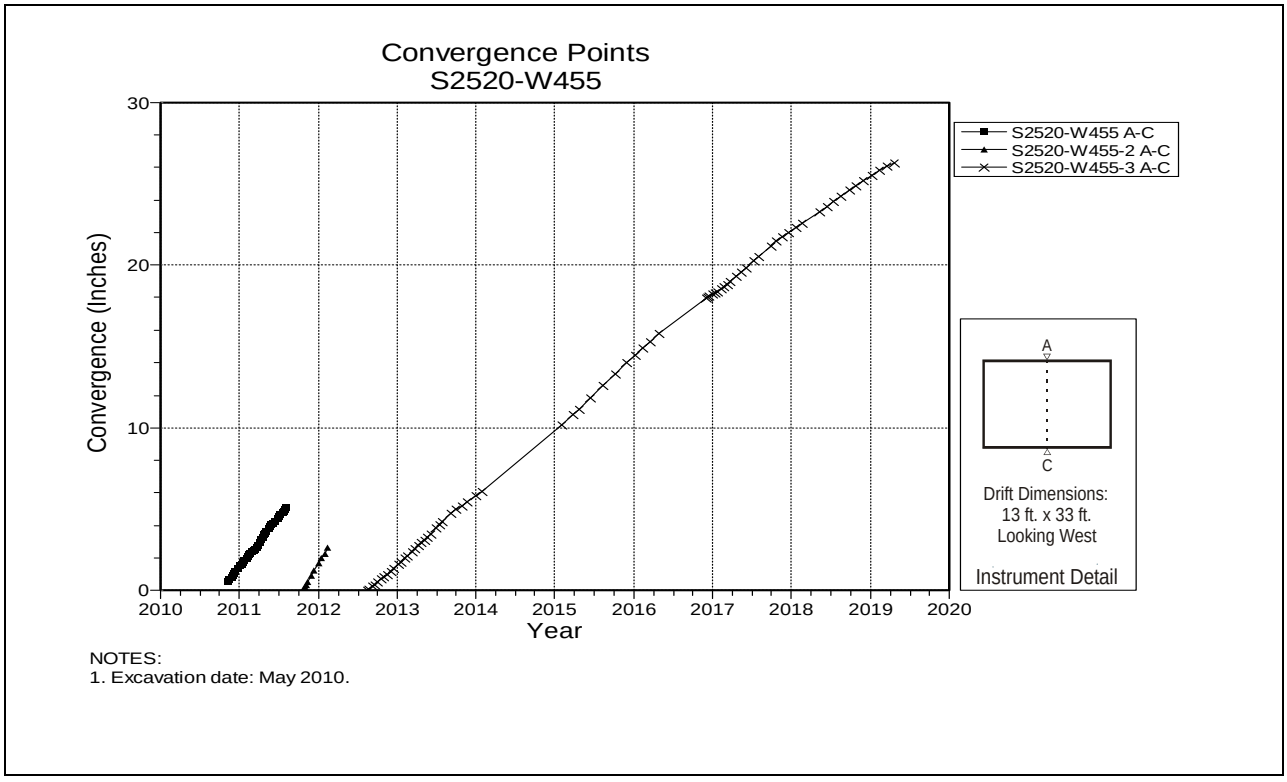

Figure 5-26 Convergence Point Array – S2520 W455 – Roof to Floor

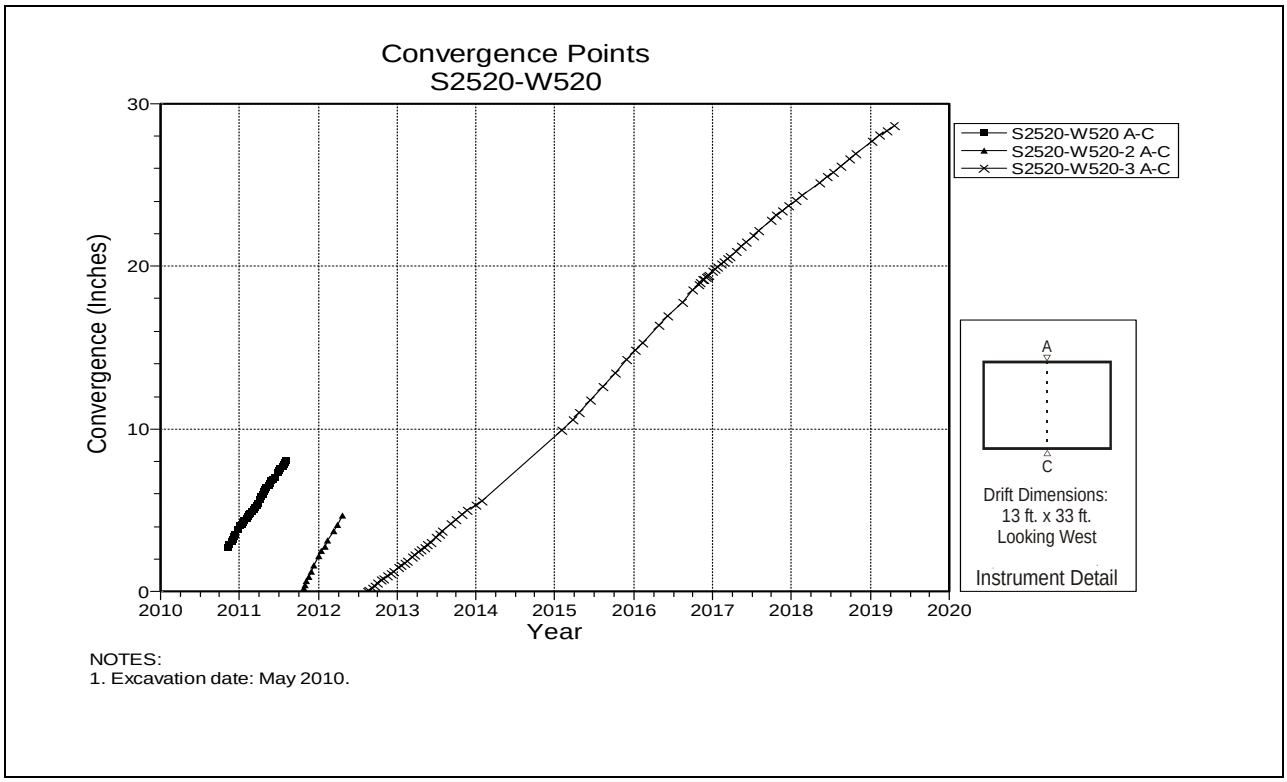

Figure 5-27 Convergence Point Array – S2520 W520 – Roof to Floor

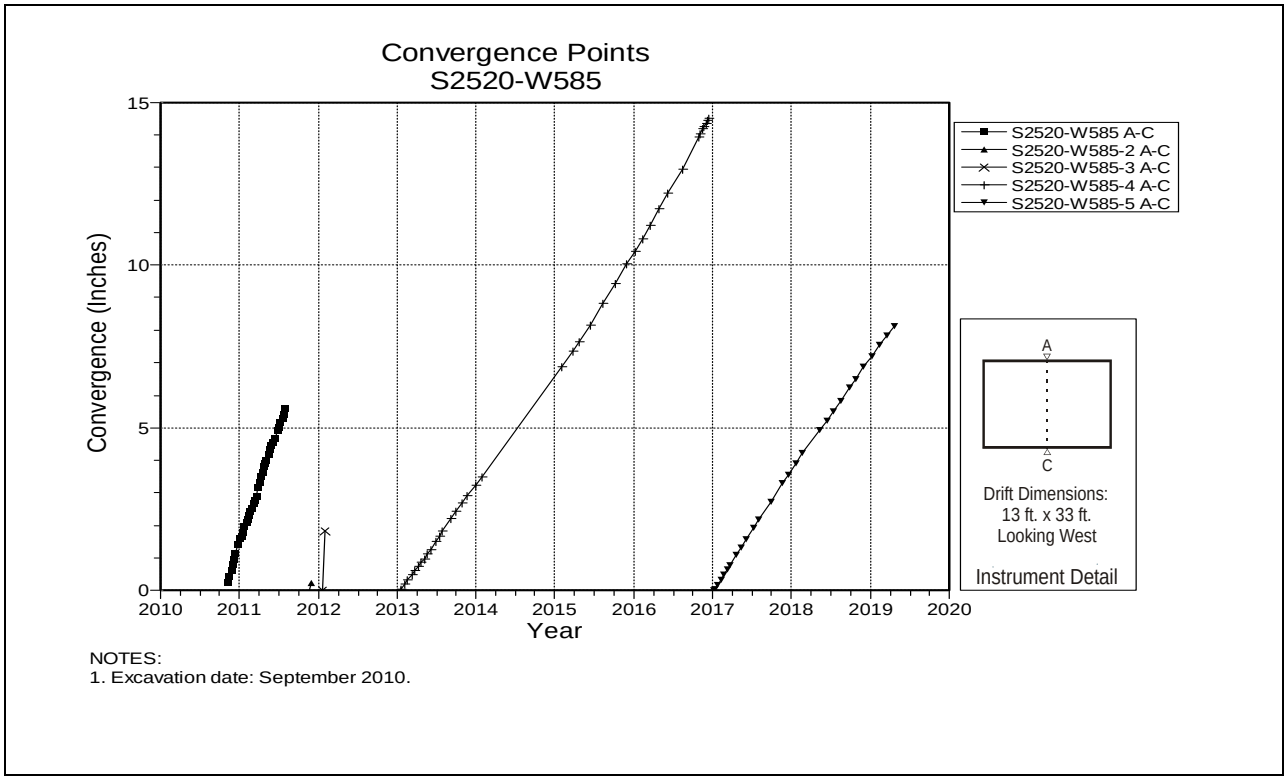

Figure 5-28 Convergence Point Array – S2520 W585 – Roof to Floor

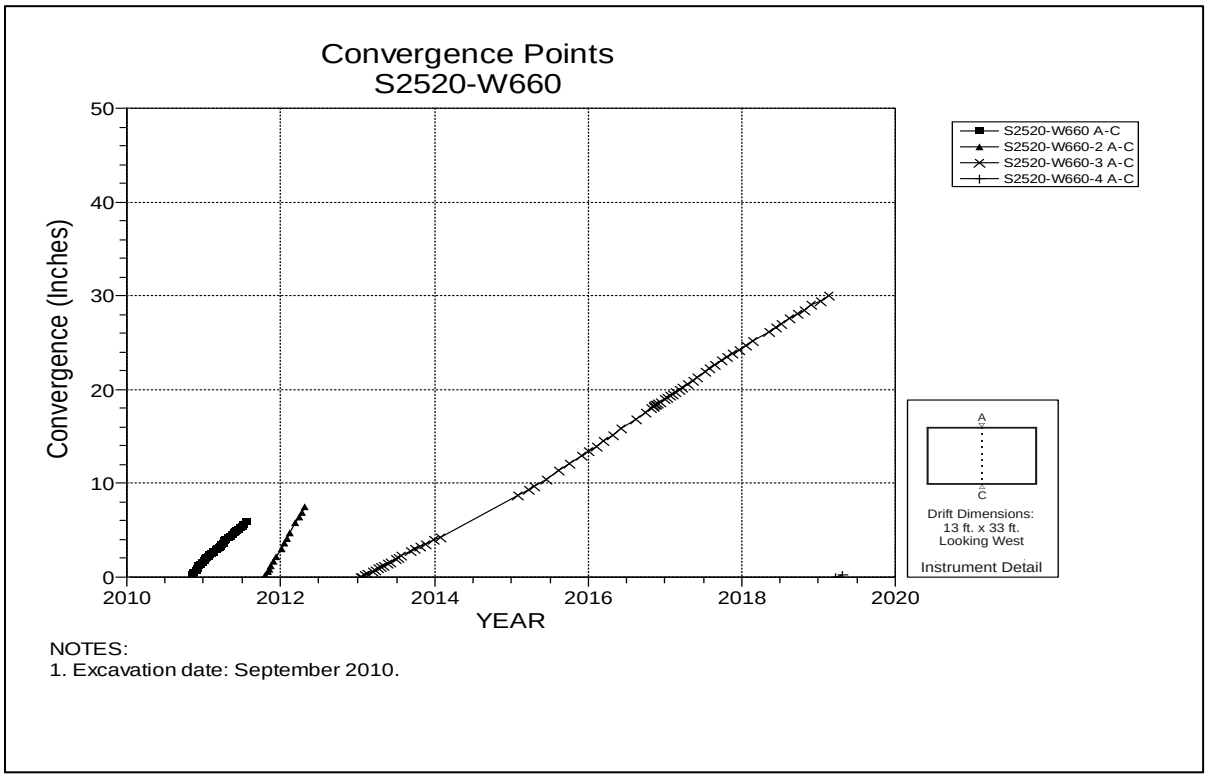

Figure 5-29 Convergence Point Array – S2520 W660 – Roof to Floor

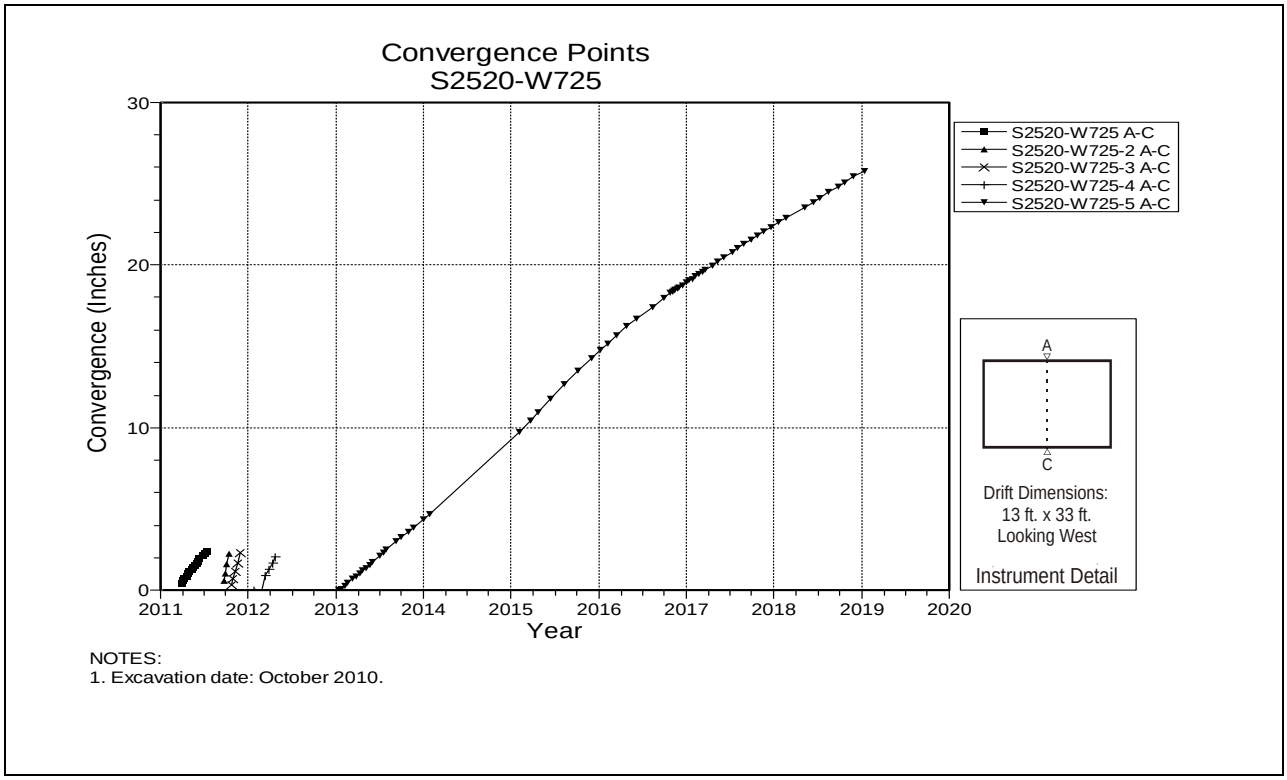

Figure 5-30 Convergence Point Array – S2520 W725 – Roof to Floor

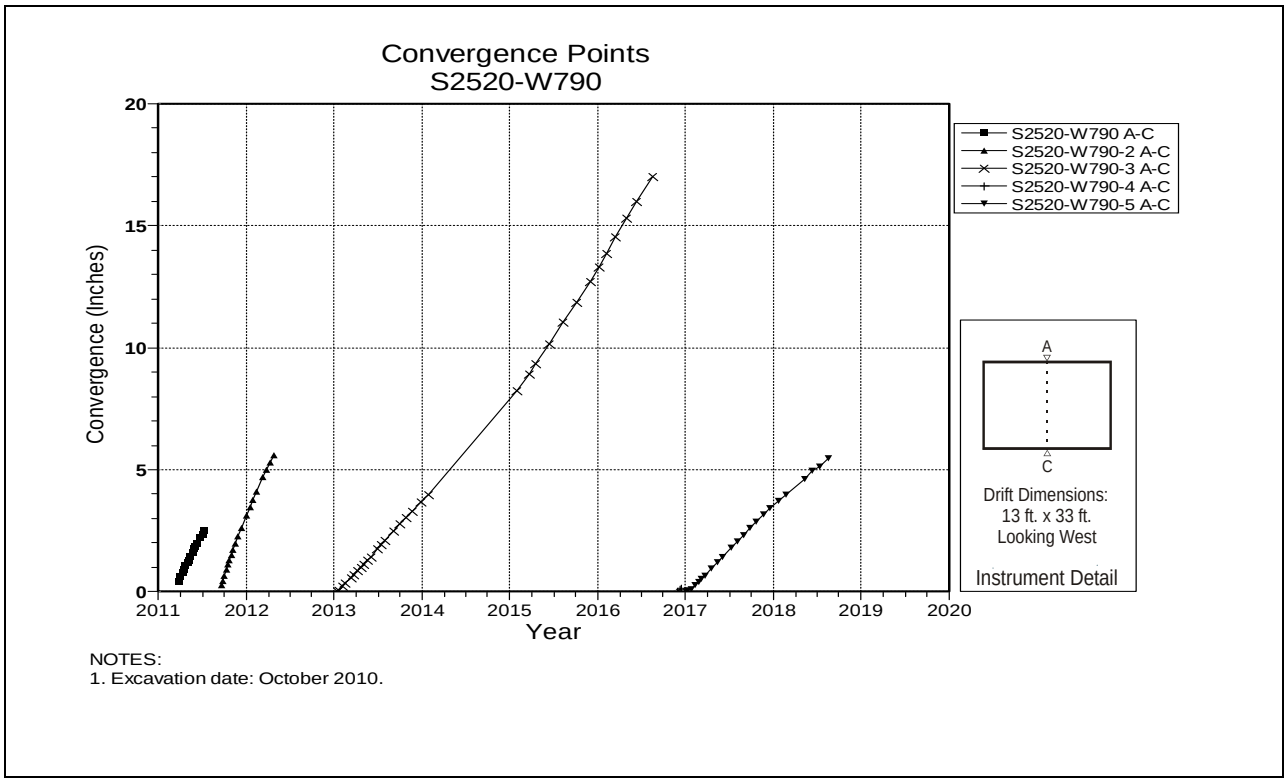

Figure 5-31 Convergence Point Array – S2520 W790 – Roof to Floor

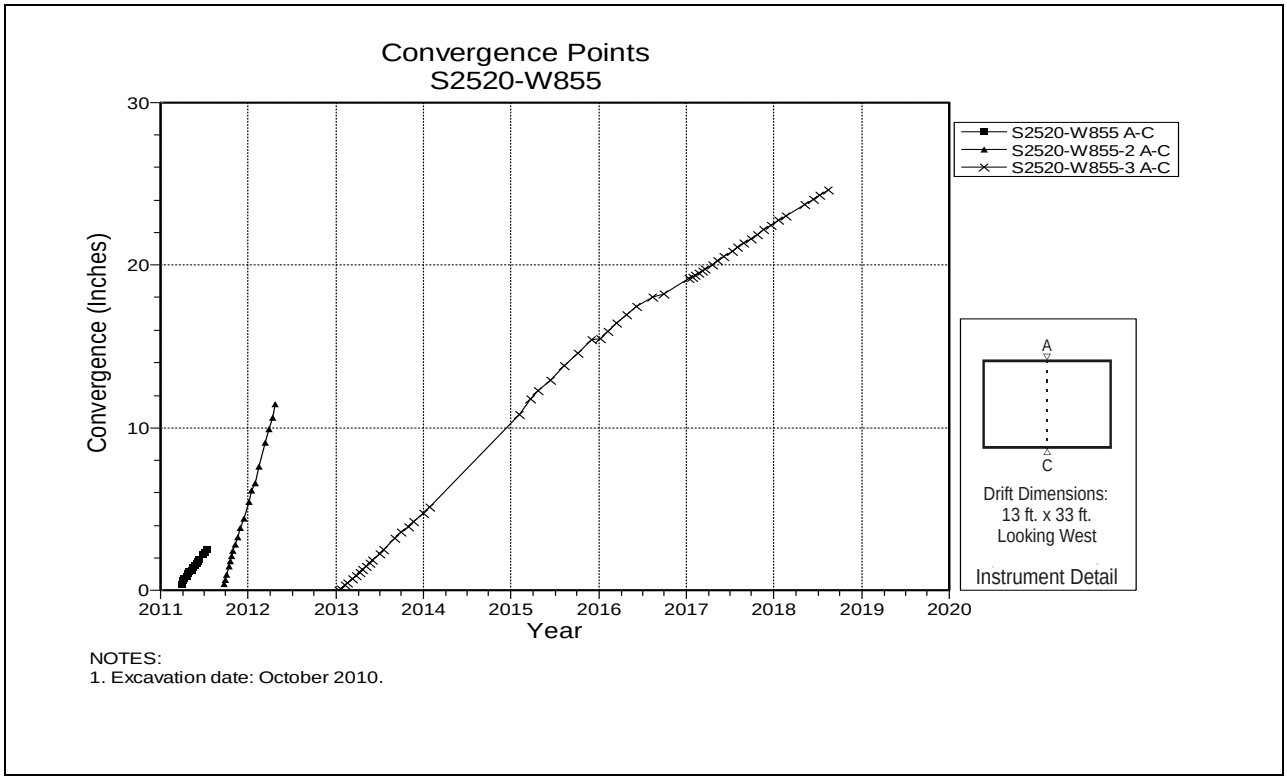

Figure 5-32 Convergence Point Array – S2520 W855 – Roof to Floor

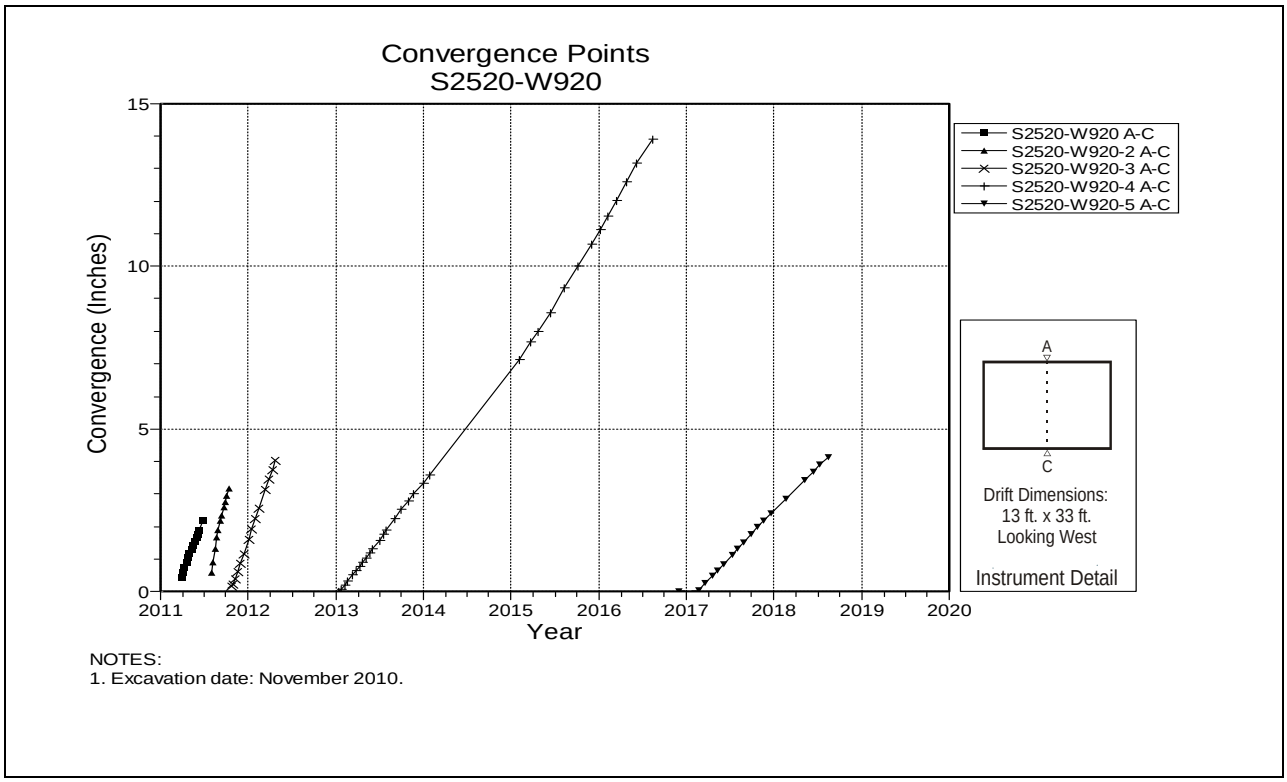

NOTES:
1. Excavation date: November 2010.

Figure 5-33 Convergence Point Array – S2520 W920 – Roof to Floor

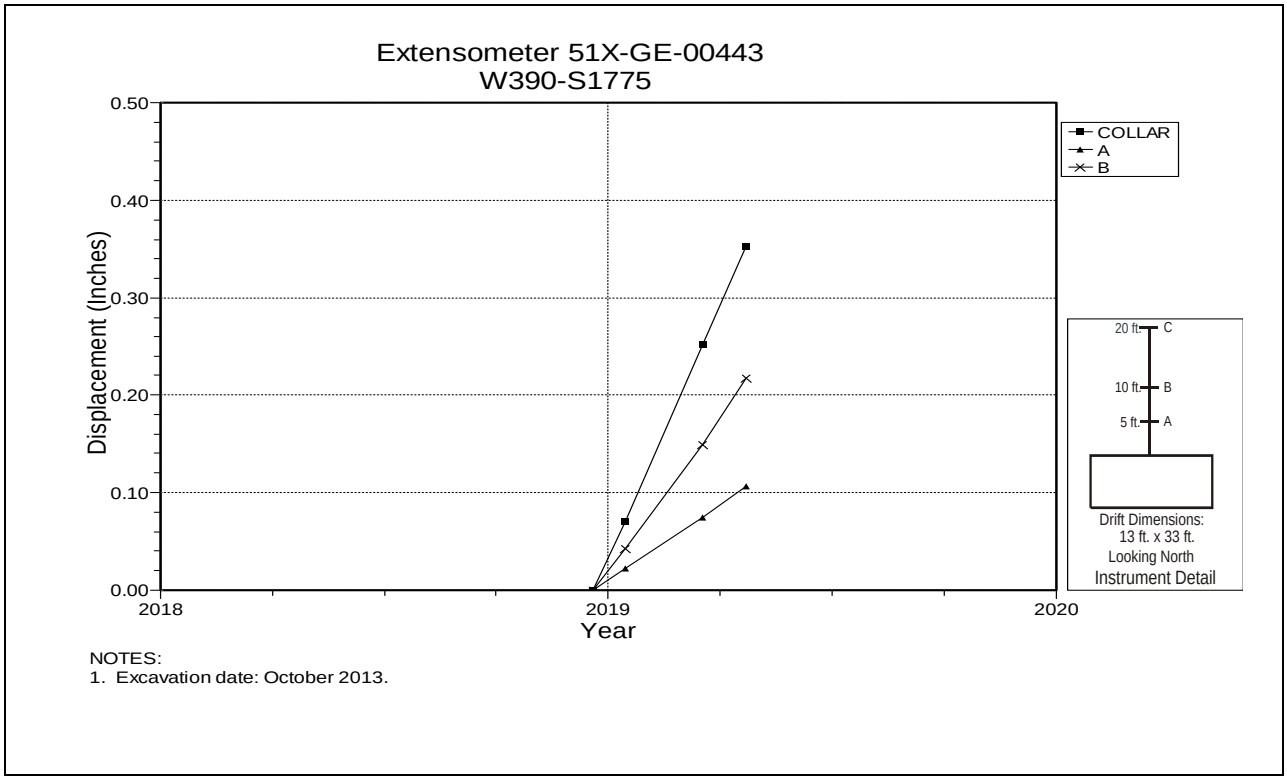

NOTES:
1. Excavation date: October 2013.

Figure 5-34 Extensometer 51X-GE-00443 – W390 S1775

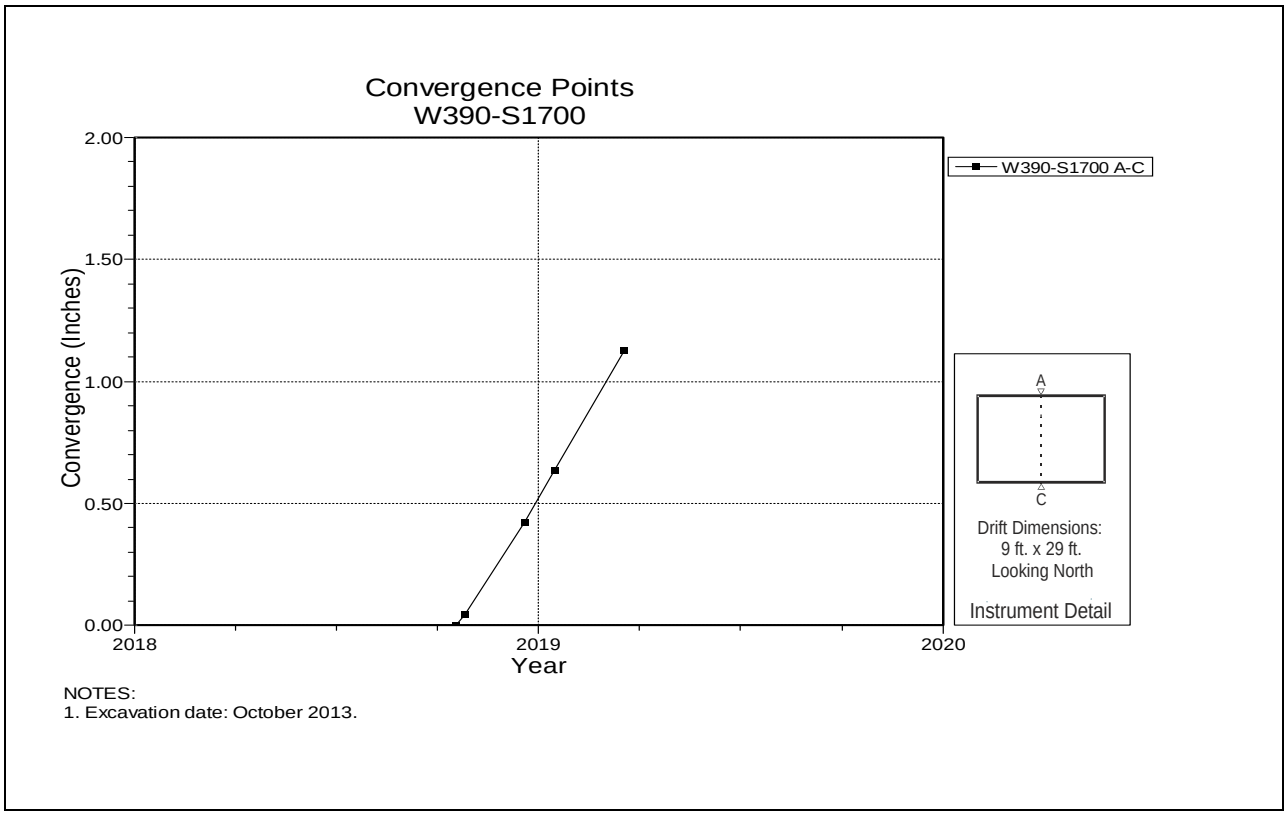

NOTES:
1. Excavation date: October 2013.

Figure 5-35 Convergence Point Array – W390-S1700 – Roof to Floor

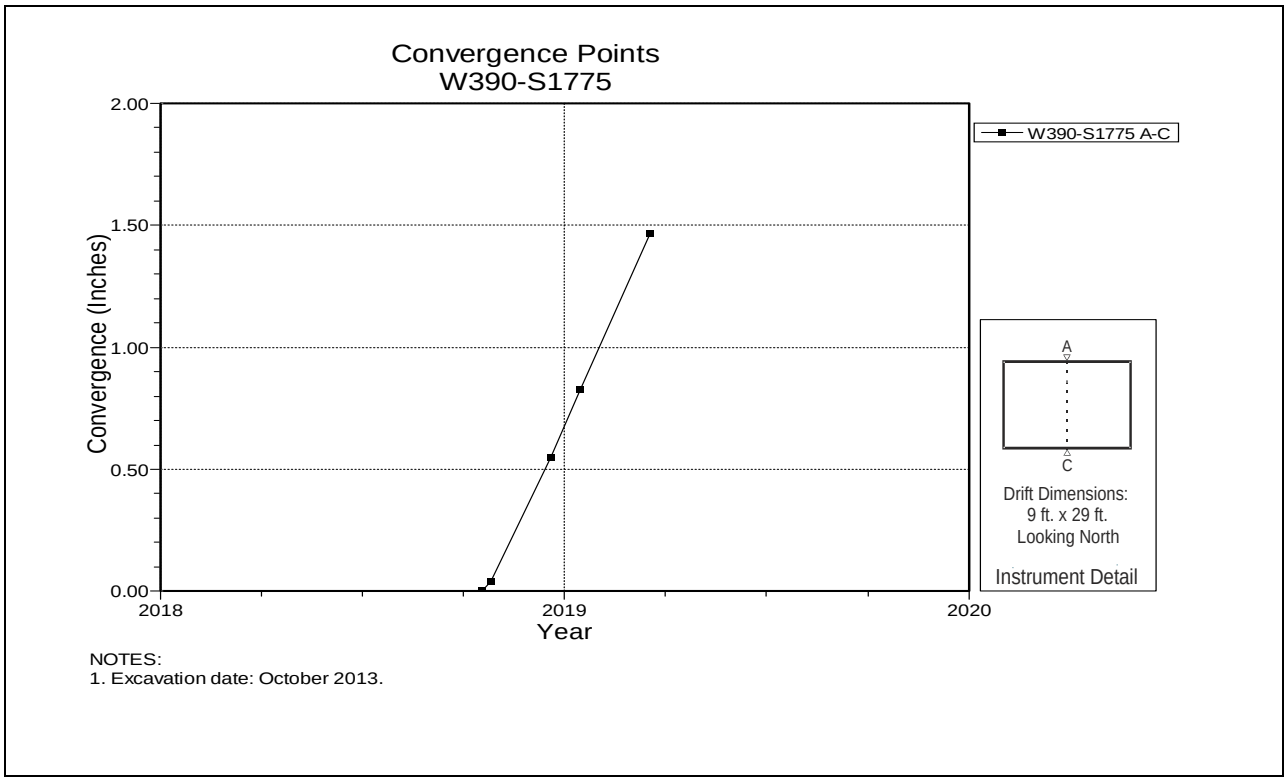

NOTES:
1. Excavation date: October 2013.

Figure 5-36 Convergence Point Array – W390-S1775 – Roof to Floor

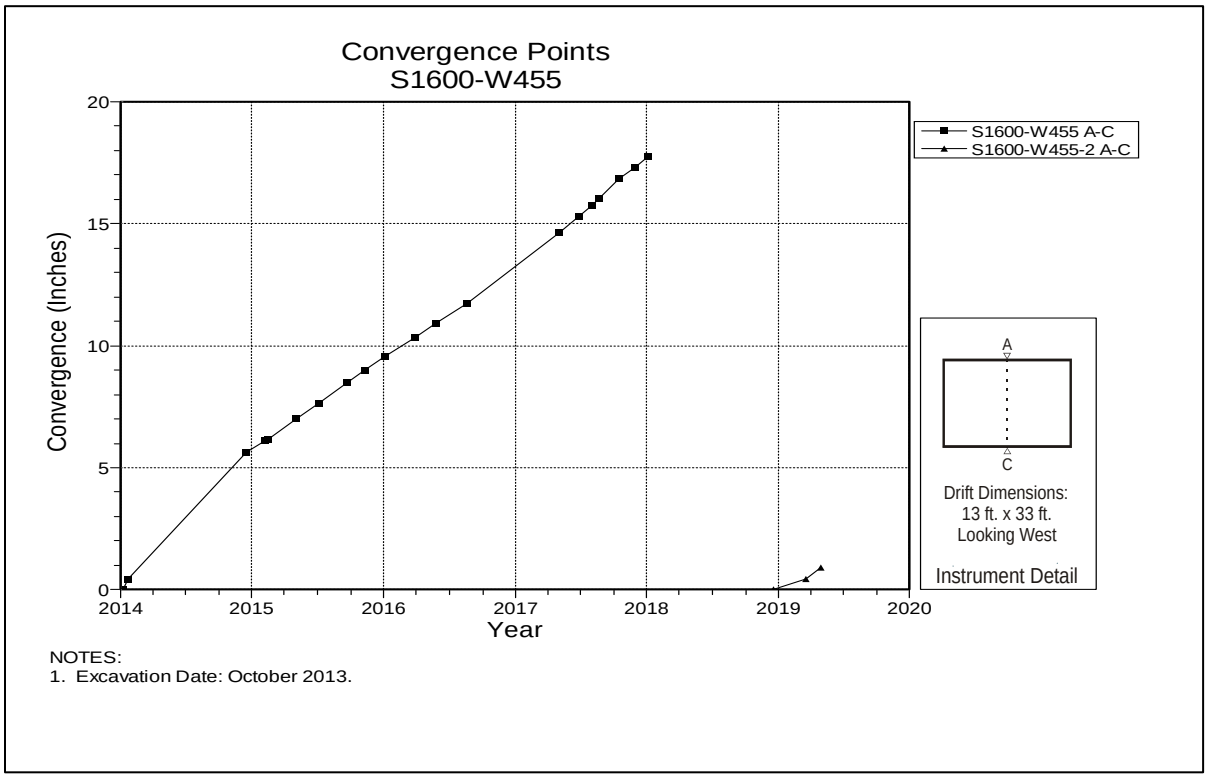

Figure 5-37 Convergence Point Array – S1600-W455 – Roof to Floor

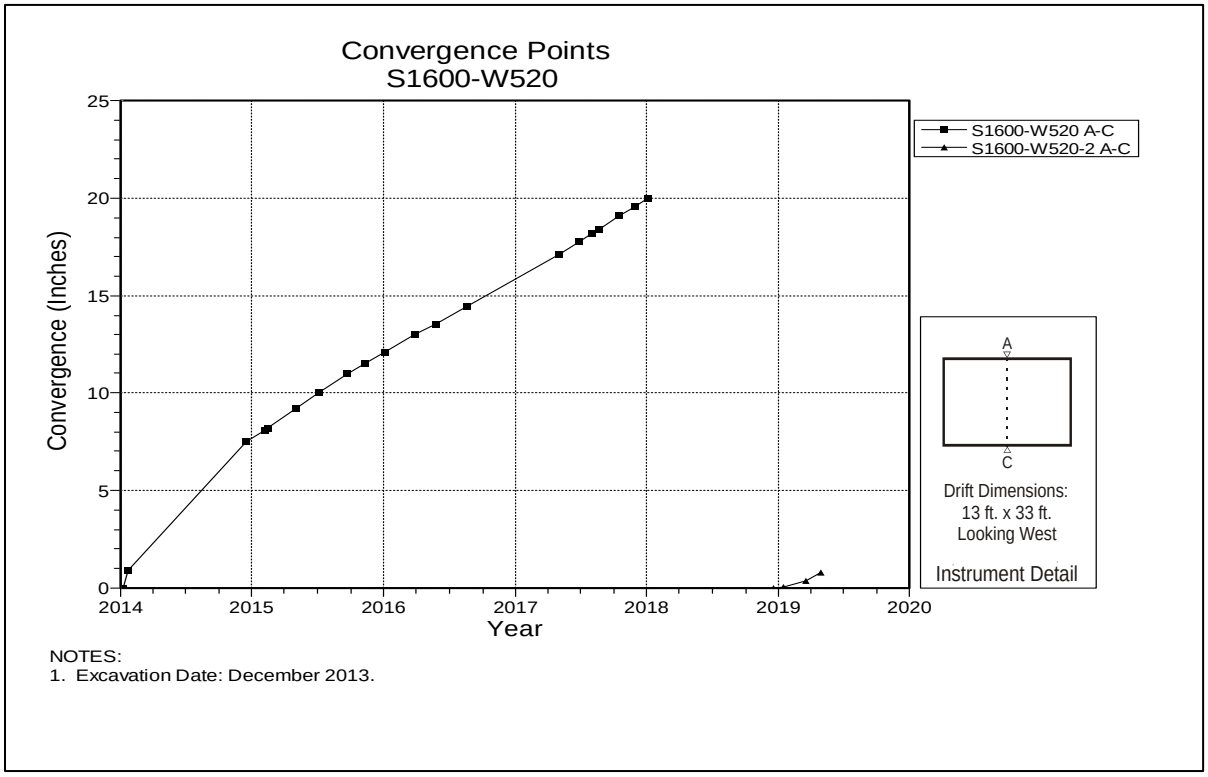

Figure 5-38 Convergence Point Array – S1600-W520 – Roof to Floor

6.0 INSTRUMENTATION SUMMARY FOR THE SDI AREA

This chapter presents a summary of the data collected from the fifty-five radial convergence stations located in the SDI area at the WIPP. A combination of ground control, and to some extent ventilation challenges, led the Operations Department to prohibit access to the SDI area during the previous reporting period. This allowed the resources to be channeled to address more significant ground control remediation in other areas. The same operational challenges apply to this reporting period, although, the inaccessibility is primarily limited to twenty-seven convergence stations in the areas in SDI south of the N-780 drift.

Data from the remaining twenty-eight convergence stations are presented in tabular and graphical format on the following pages.

Table 6-1
SDI Data Analysis

Convergence Points									
Field Tag	Location	Figure Number	Last Reading 2018 to 2019		Cumulative Displacement (inches)	Closure Rate 2018 to 2019 (in/year)	Closure Rate 2016 to 2017[4] (in/year)	Rate Change Percent	Comments
			Date	Inches					
E1300-N860 A-C	E1300-N860	6-1	2/19/2019	6.802	6.802	1.0	0.8	25	
N780-E420-2 A-C	N780-E420	6-2	2/19/2019	10.658	14.484	1.7	1.4	21	
N780-E540-2 A-C	N780-E540	6-3	2/19/2019	14.025	18.445	2.1	1.9	11	
N780-E615-2 A-C	N780-E615	6-4	2/19/2019	10.817	14.035	1.6	1.4	14	
N780-E690-2 A-C	N780-E690	6-5	2/19/2019	14.313	19.663	2.1	1.9	11	
N780-E768 A-C	N780-E768	6-6	2/19/2019	12.200	12.200	1.6	1.5	7	
N780-E845 A-C	N780-E845	6-7	2/19/2019	13.441	13.441	1.7	1.6	6	
N780-E922 A-C	N780-E922	6-8	2/19/2019	13.698	13.698	1.6	1.6	0	
N780-E1050 A-C	N780-E1050	6-9	2/19/2019	13.230	13.230	1.4	1.4	0	
N780-E1100 A-C	N780-E1100	6-10	2/19/2019	13.424	13.424	1.4	1.4	0	
N780-E1150 A-C	N780-E1150	6-11	2/19/2019	12.239	12.239	1.4	1.4	0	
N780-E1200 A-C	N780-E1200	6-12	2/19/2019	12.057	12.057	1.3	1.3	0	
N780-E1250 A-C	N780-E1250	6-13	2/19/2019	9.984	9.984	1.1	1.1	0	
N780-E1300 A-C	N780-E1300	6-14	2/19/2019	6.130	6.130	0.9	0.8	13	
N940-E420-2 A-C	N940-E420	6-15	2/19/2019	10.768	13.214	1.8	1.6	13	
N940-E540-2 A-C	N940-E540	6-16	2/19/2019	11.340	14.291	1.7	1.6	6	
N940-E615-2 A-C	N940-E615	6-17	2/19/2019	11.275	14.100	1.6	1.6	0	
N940-E690-3 A-C	N940-E690	6-18	2/19/2019	16.624	18.992	2.3	2.3	0	
N940-E768-2 A-C	N940-E768	6-19	2/19/2019	11.057	11.892	1.7	1.7	0	
N940-E845-2 A-C	N940-E845	6-20	2/19/2019	9.954	10.877	1.5	1.5	0	
N940-E922-2 A-C	N940-E922	6-21	2/19/2019	10.330	11.553	1.5	1.5	0	
N940-E1000 A-C	N940-E1000	6-22	2/19/2019	11.777	11.777	1.6	1.9	-16	
N940-E1050-2 A-C	N940-E1050	6-23	2/19/2019	9.574	11.091	1.4	1.4	0	
N940-E1100 A-C	N940-E1100	6-24	2/19/2019	12.129	12.129	1.8	1.9	-5	
N940-E1150 A-C	N940-E1150	6-25	2/19/2019	9.398	9.398	1.0	1.5	-33	
N940-E1200 A-C	N940-E1200	6-26	2/19/2019	10.153	10.153	1.5	1.2	25	
N940-E1250 A-C	N940-E1250	6.27	2/19/2019	7.773	7.773	1.1	1.1	0	
N940-E1300 A-C	N940-E1300	6-28	2/19/2019	8.756	8.756	1.3	1.3	0	

[4] Convergence points in SDI were not read the previous reporting period largely due to ventilation and to some extent, ground control issues. Therefore, a comparison of the closure rate between two consecutive reporting period could not be made. However, a comparison was made between this reporting period and the July 1, 2016 – June 30, 2017 reporting period.

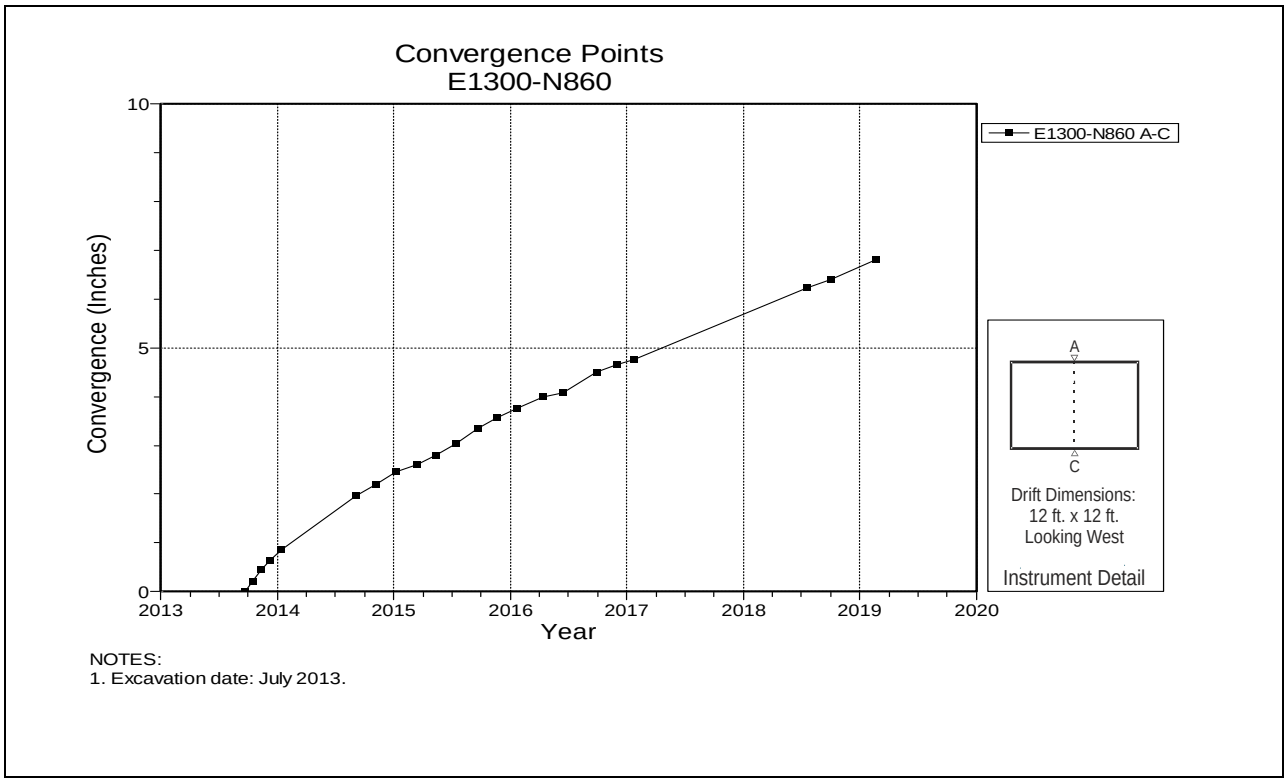

Figure 6-1 Convergence Point Array – E1300 N860 – Roof to Floor

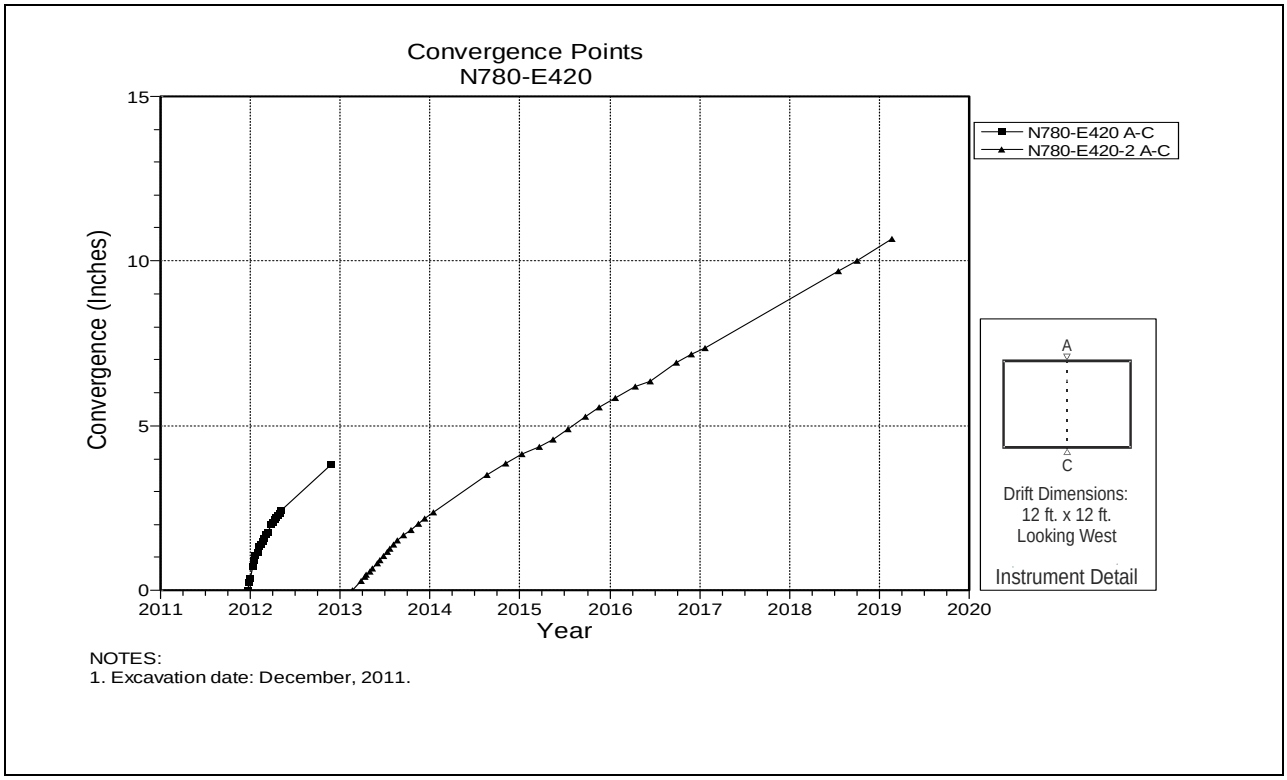

Figure 6-2 Convergence Point Array – N780 E420 – Roof to Floor

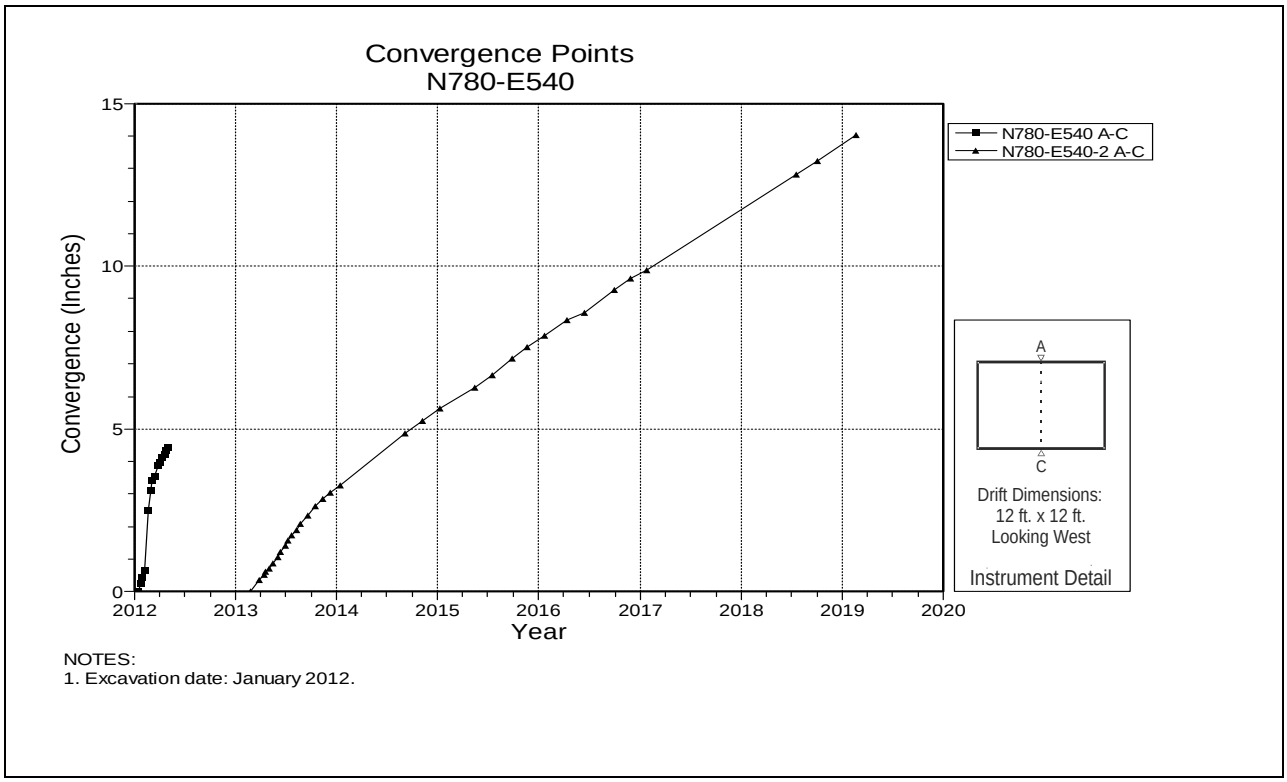

Figure 6-3 Convergence Point Array – N780 E540 – Roof to Floor

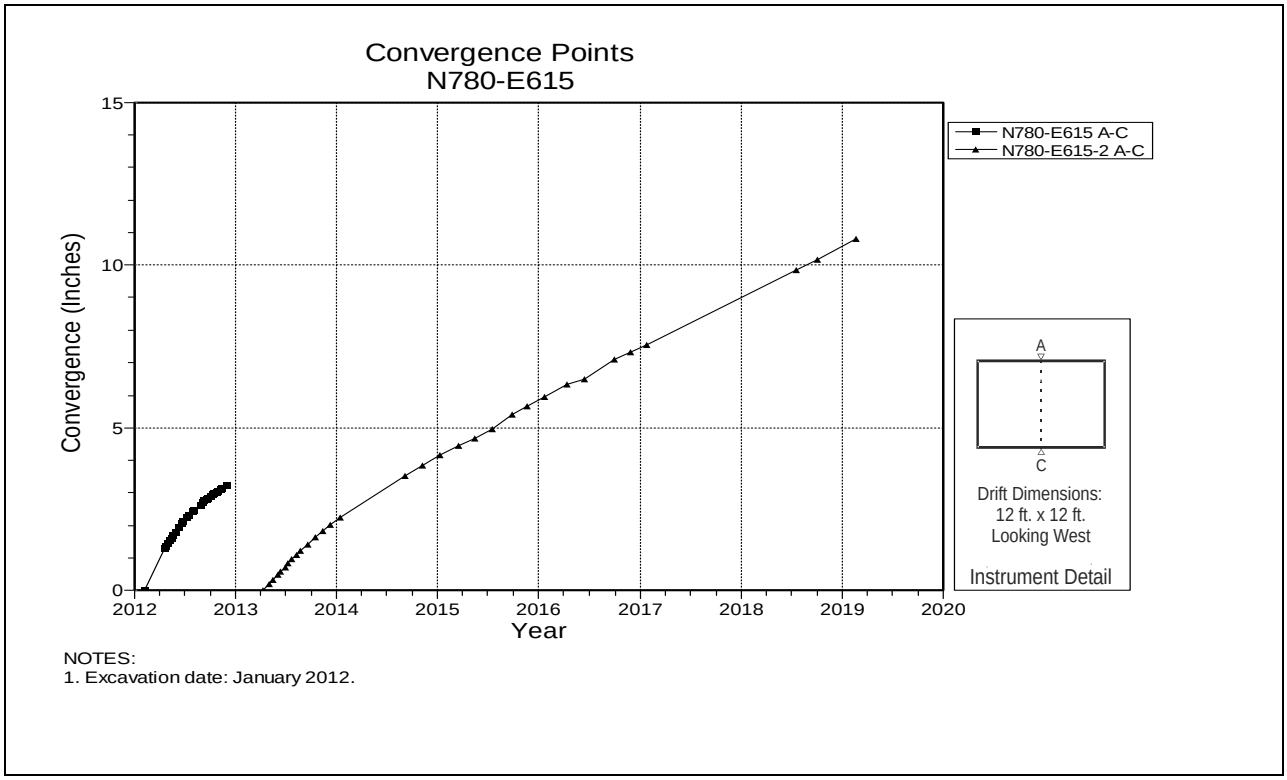

Figure 6-4 Convergence Point Array – N780 E615 – Roof to Floor

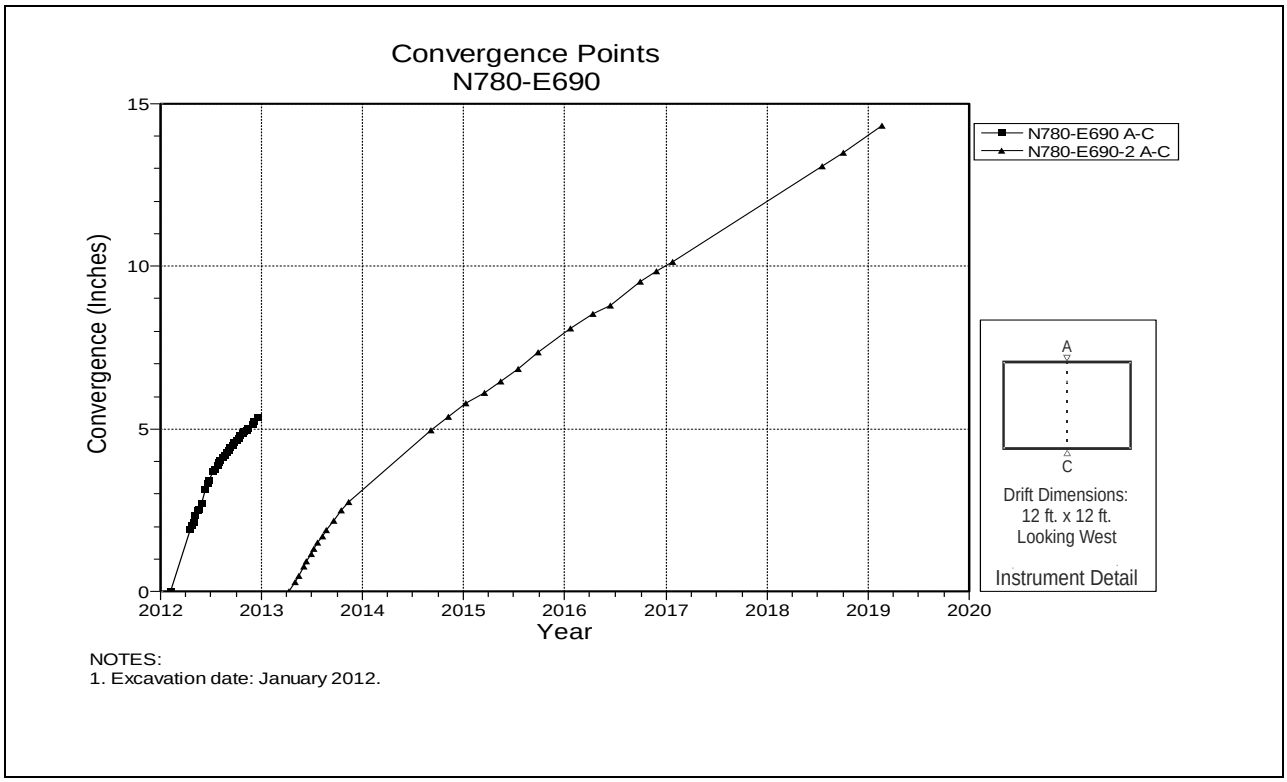

Figure 6-5 Convergence Point Array – N780 E690 – Roof to Floor

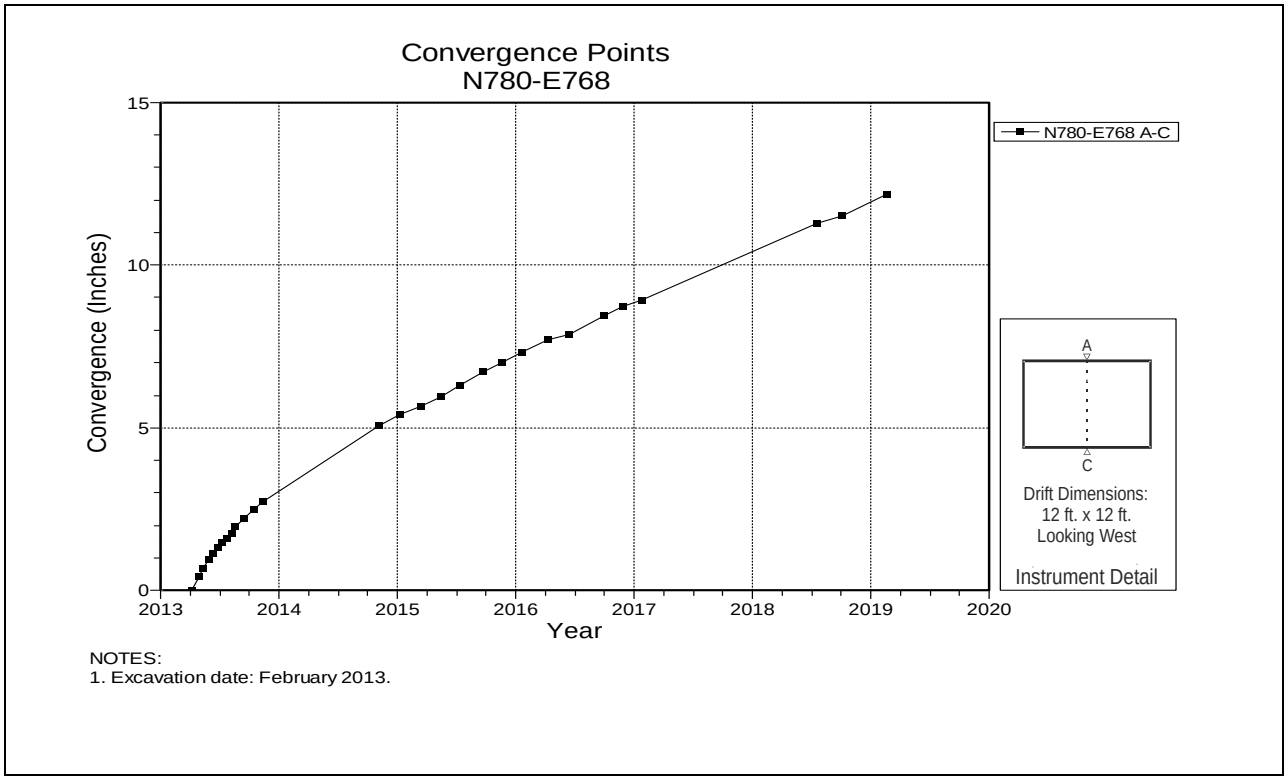

Figure 6-6 Convergence Point Array – N780 E768 – Roof to Floor

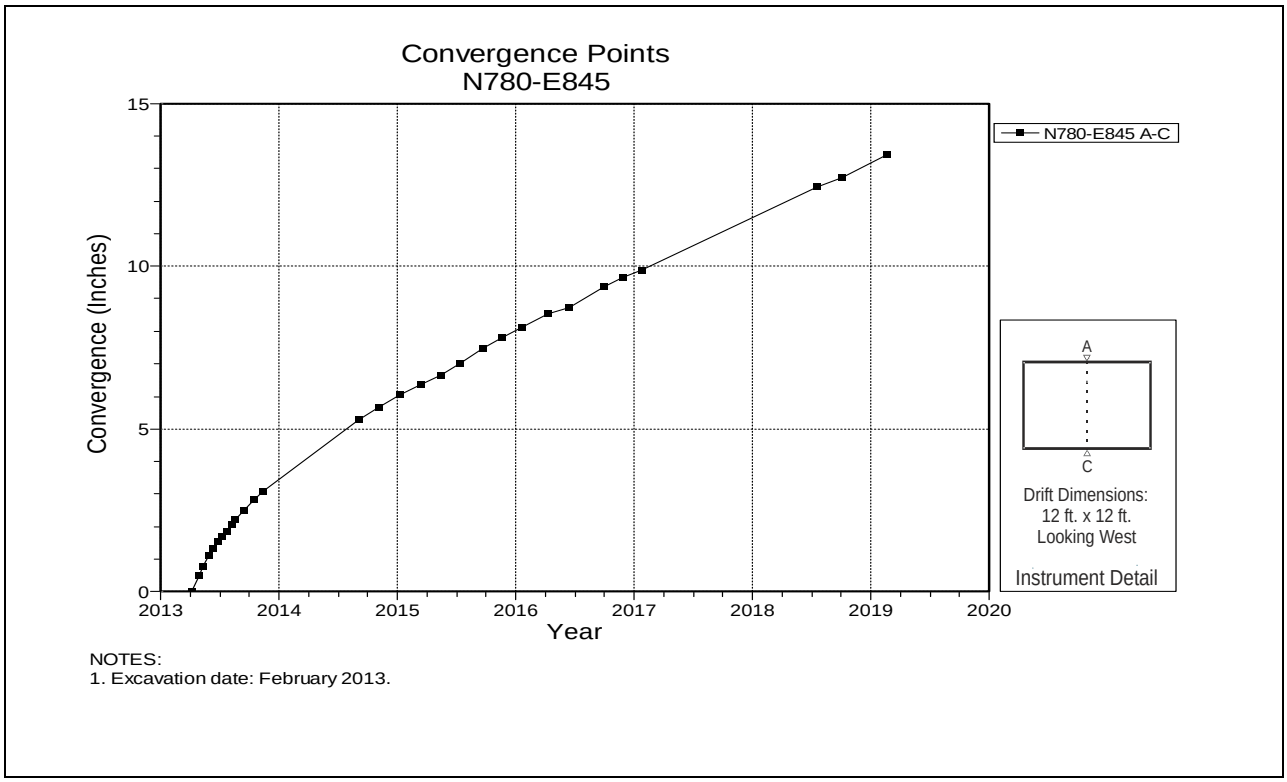

Figure 6-7 Convergence Point Array – N780 E845 – Roof to Floor

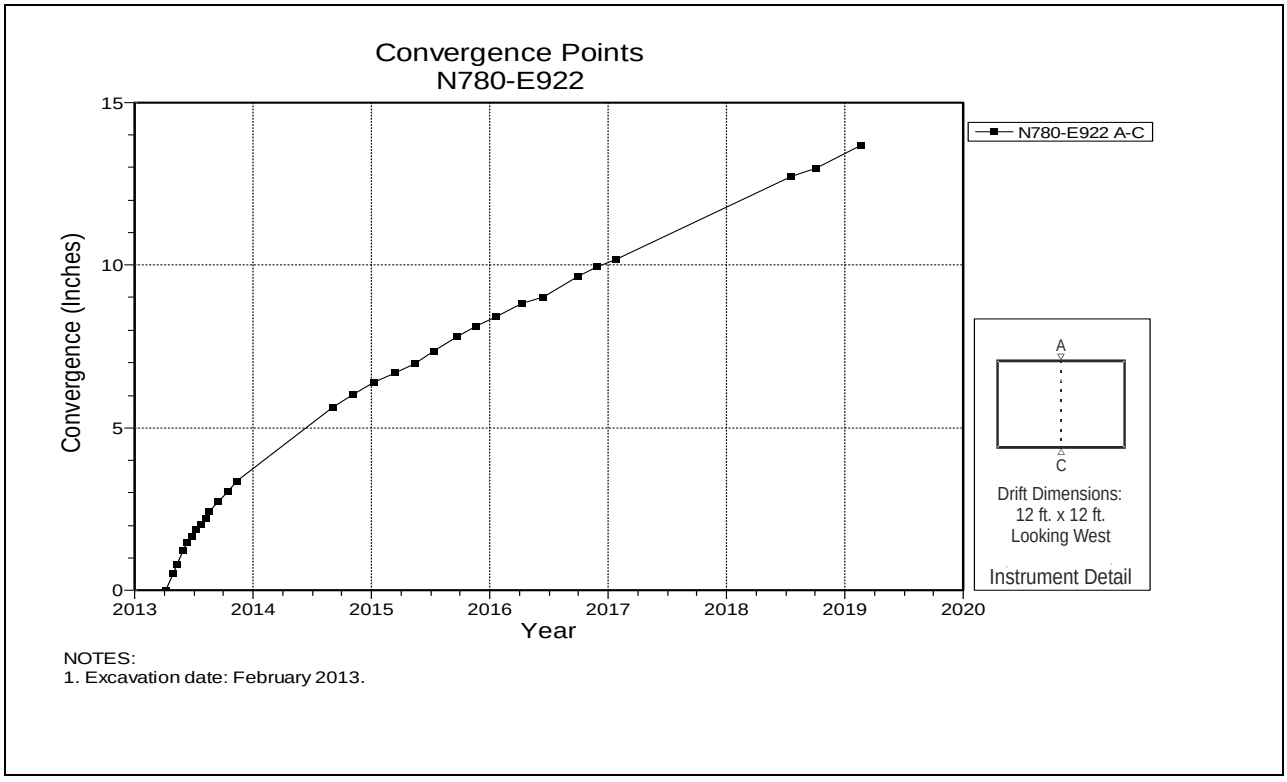

Figure 6-8 Convergence Point Array – N780 E922 – Roof to Floor

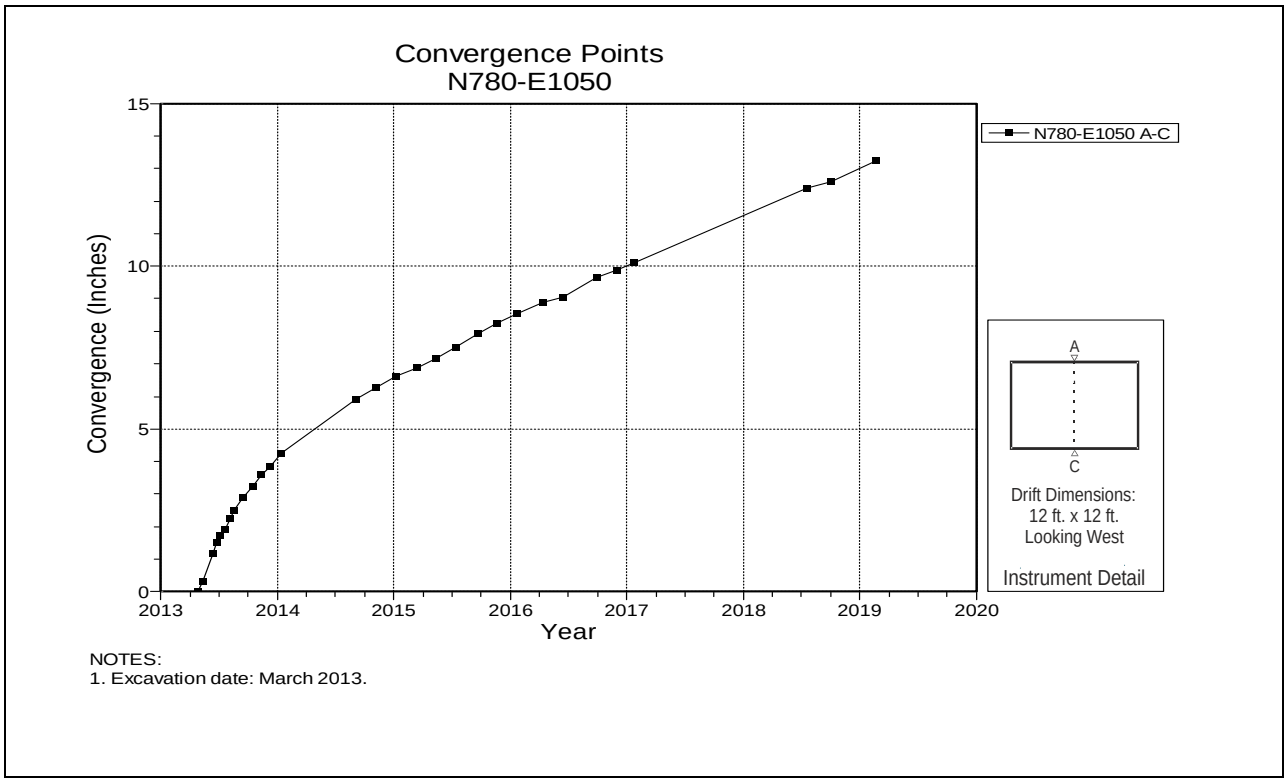

Figure 6-9 Convergence Point Array – N780 E1050 – Roof to Floor

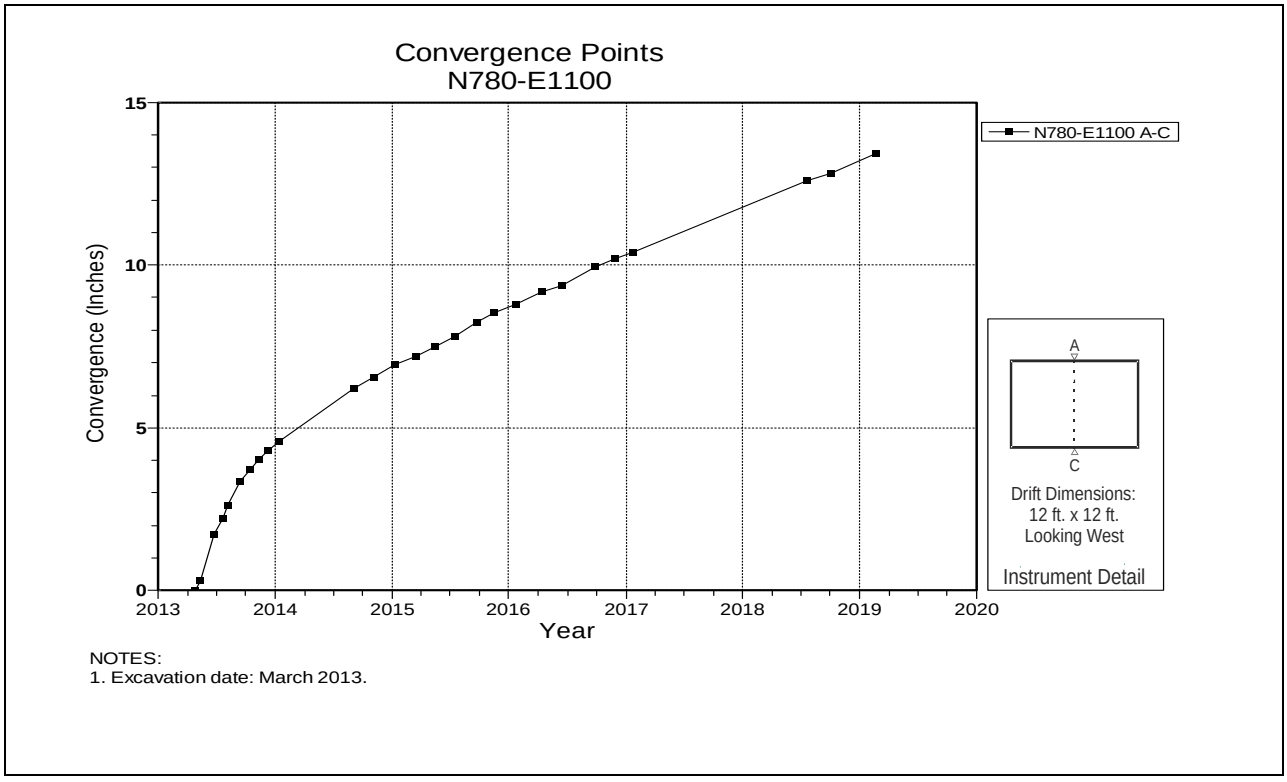

Figure 6-10 Convergence Point Array – N780 E1100 – Roof to Floor

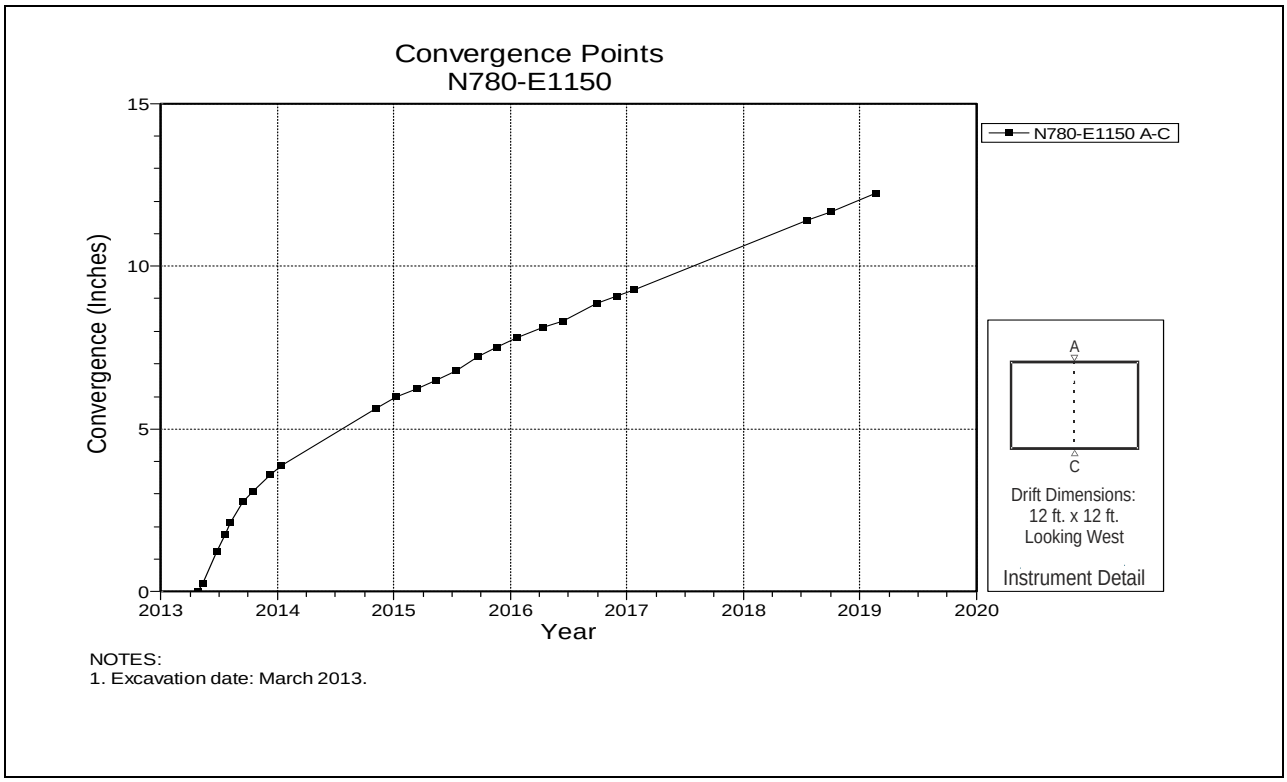

Figure 6-11 Convergence Point Array – N780 E1150 – Roof to Floor

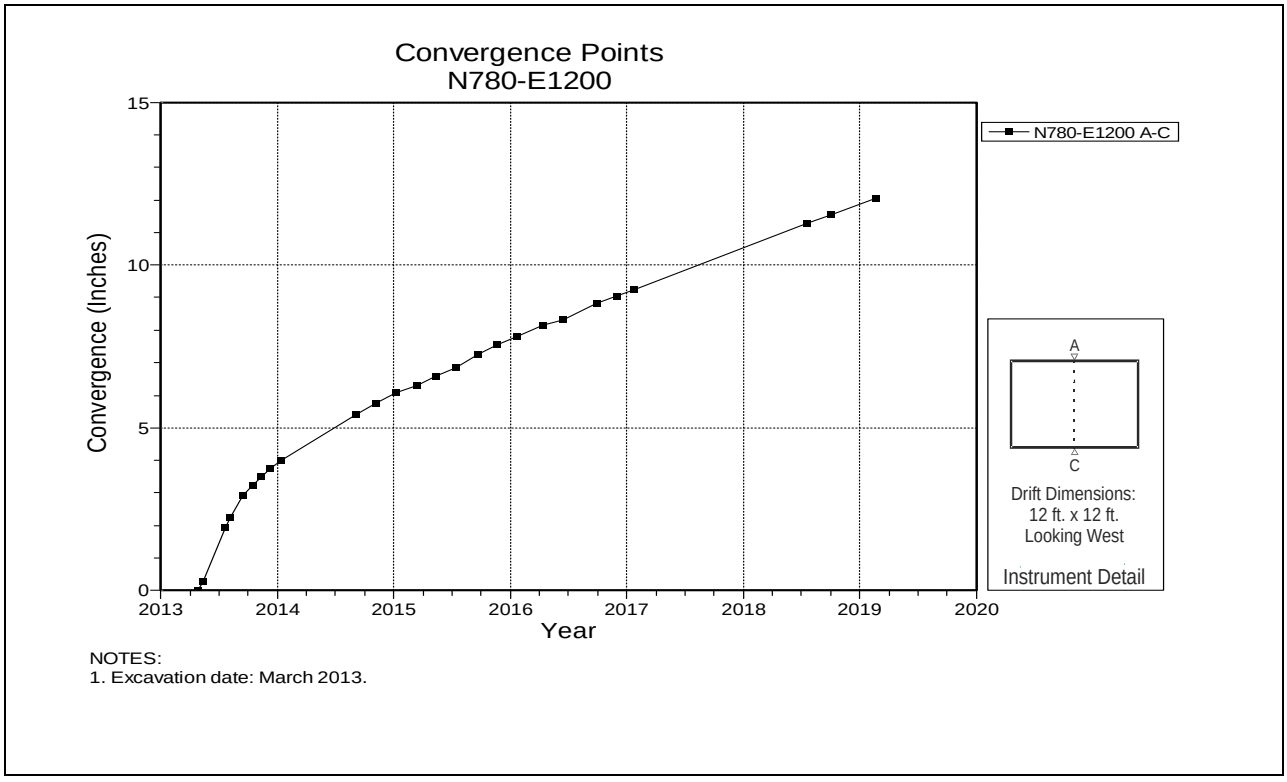

Figure 6-12 Convergence Point Array – N780 E1200 – Roof to Floor

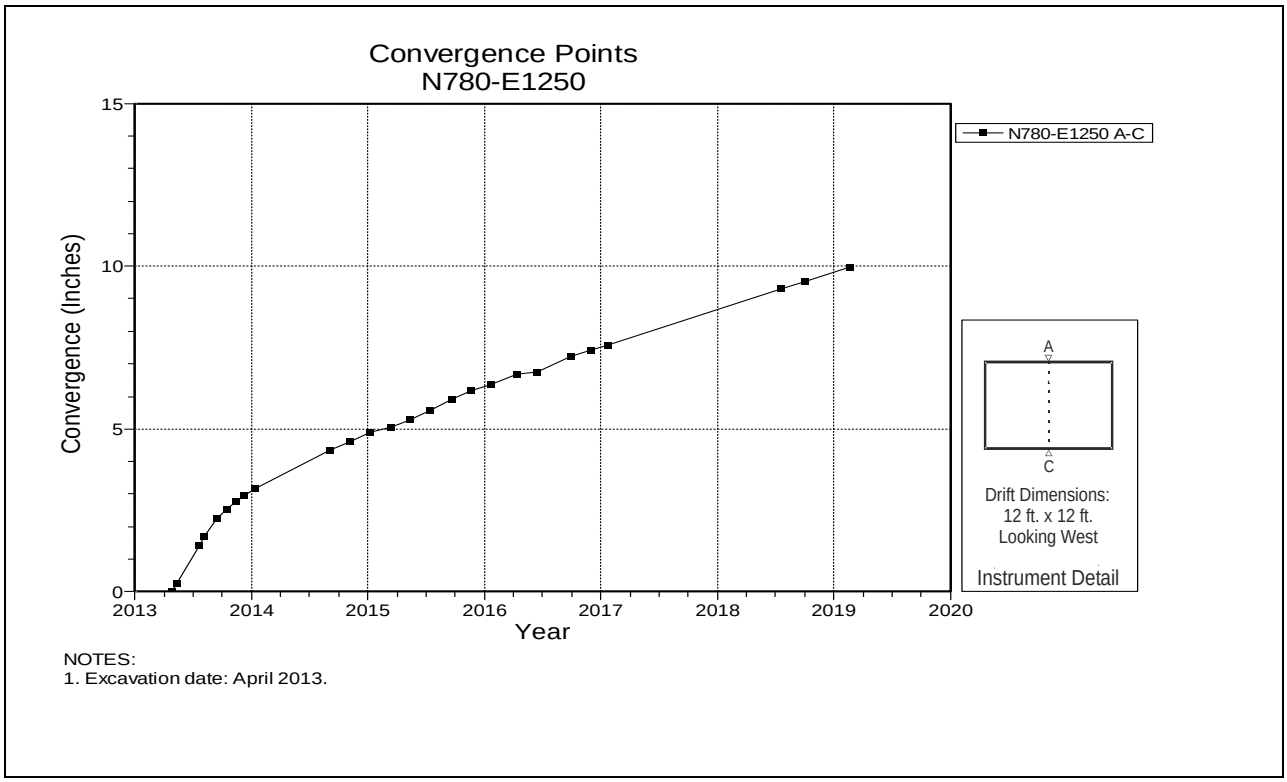

Figure 6-13 Convergence Point Array – N780 E1250 – Roof to Floor

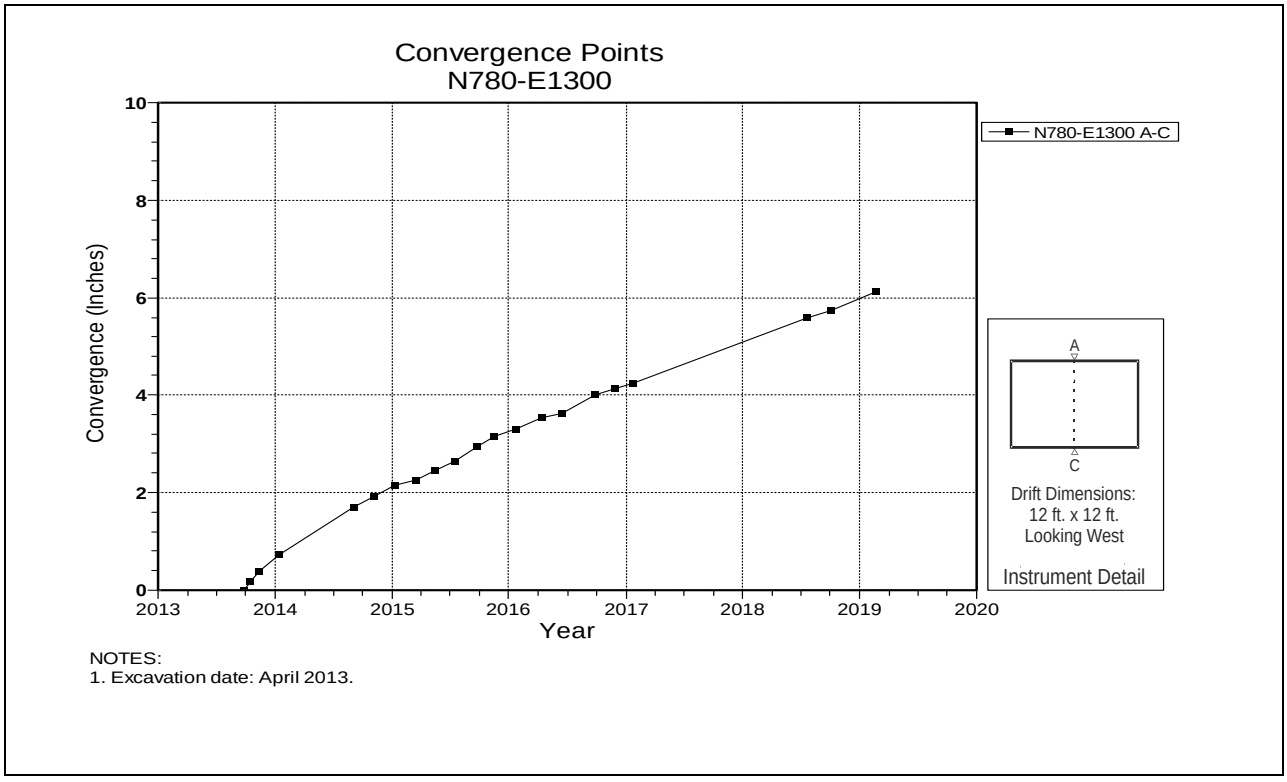

Figure 6-14 Convergence Point Array – N780 E1300 – Roof to Floor

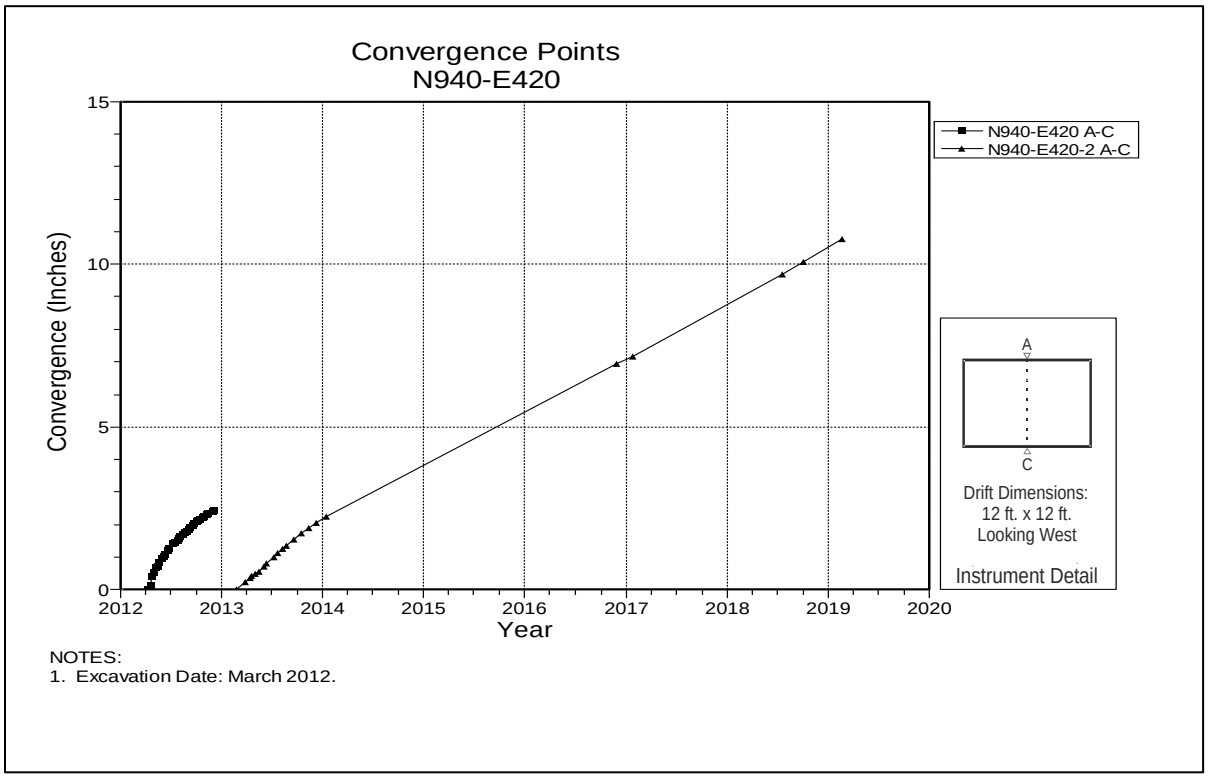

Figure 6-15 Convergence Point Array – N940 E420 – Roof to Floor

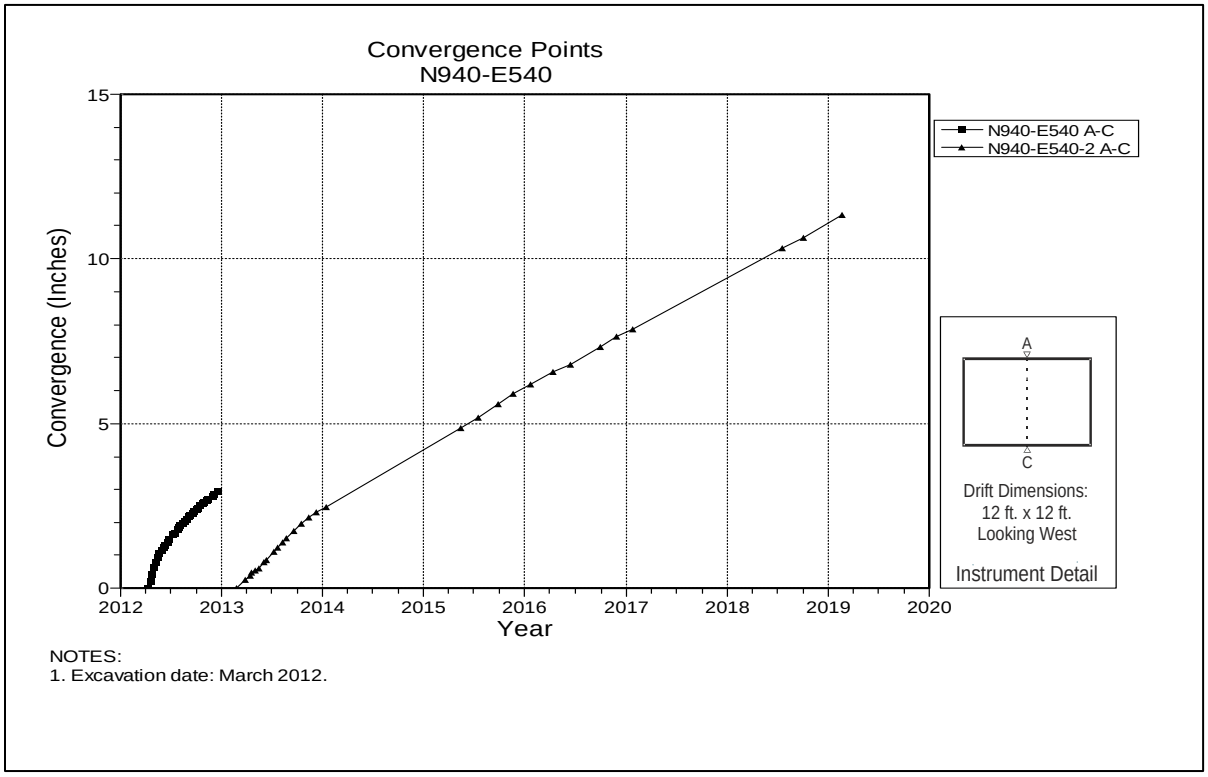

Figure 6-16 Convergence Point Array – N940 E540 – Roof to Floor

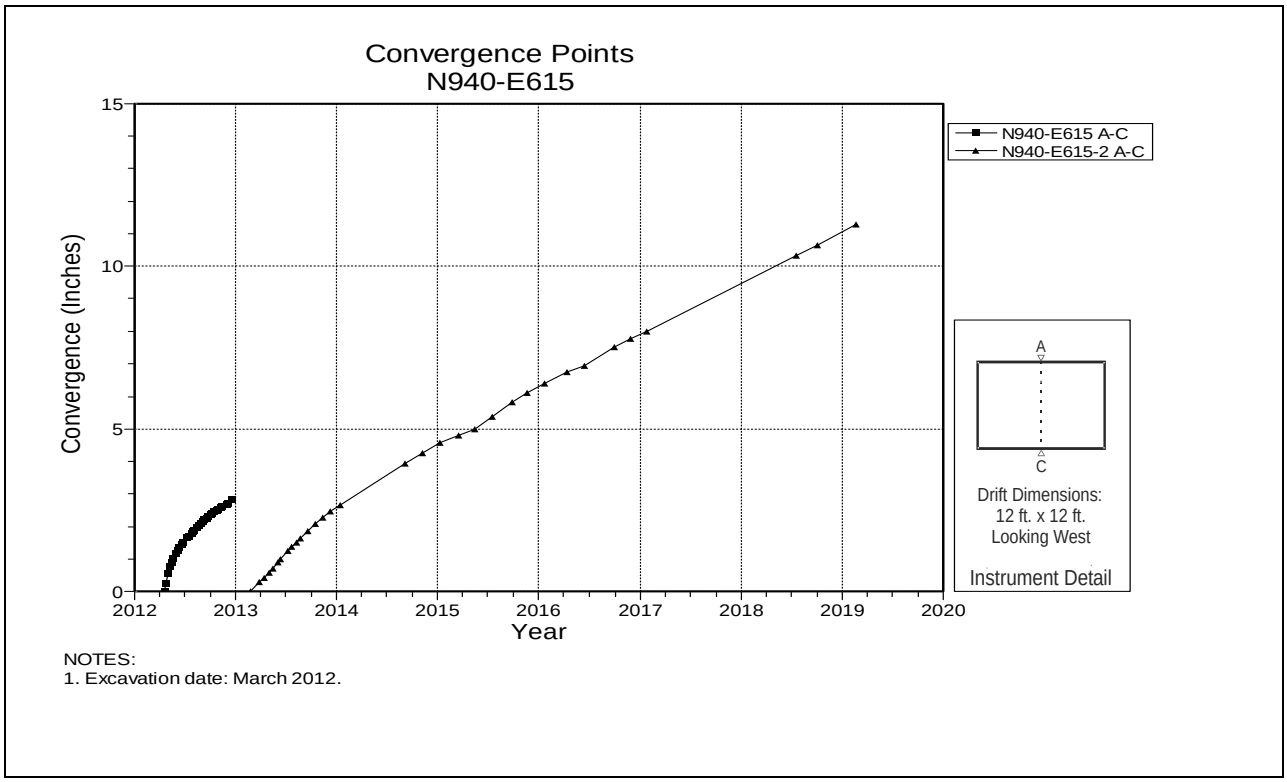

Figure 6-17 Convergence Point Array – N940 E615 – Roof to Floor

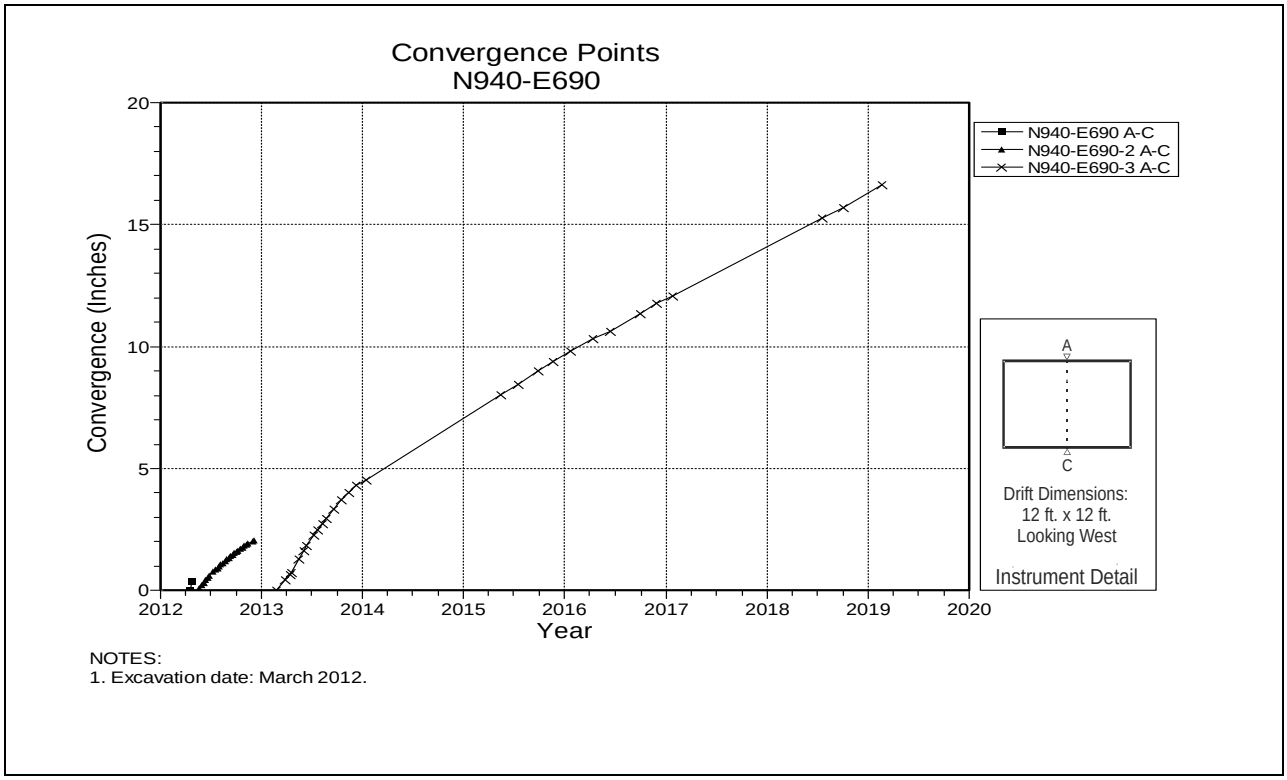

Figure 6-18 Convergence Point Array – N940 E690 – Roof to Floor

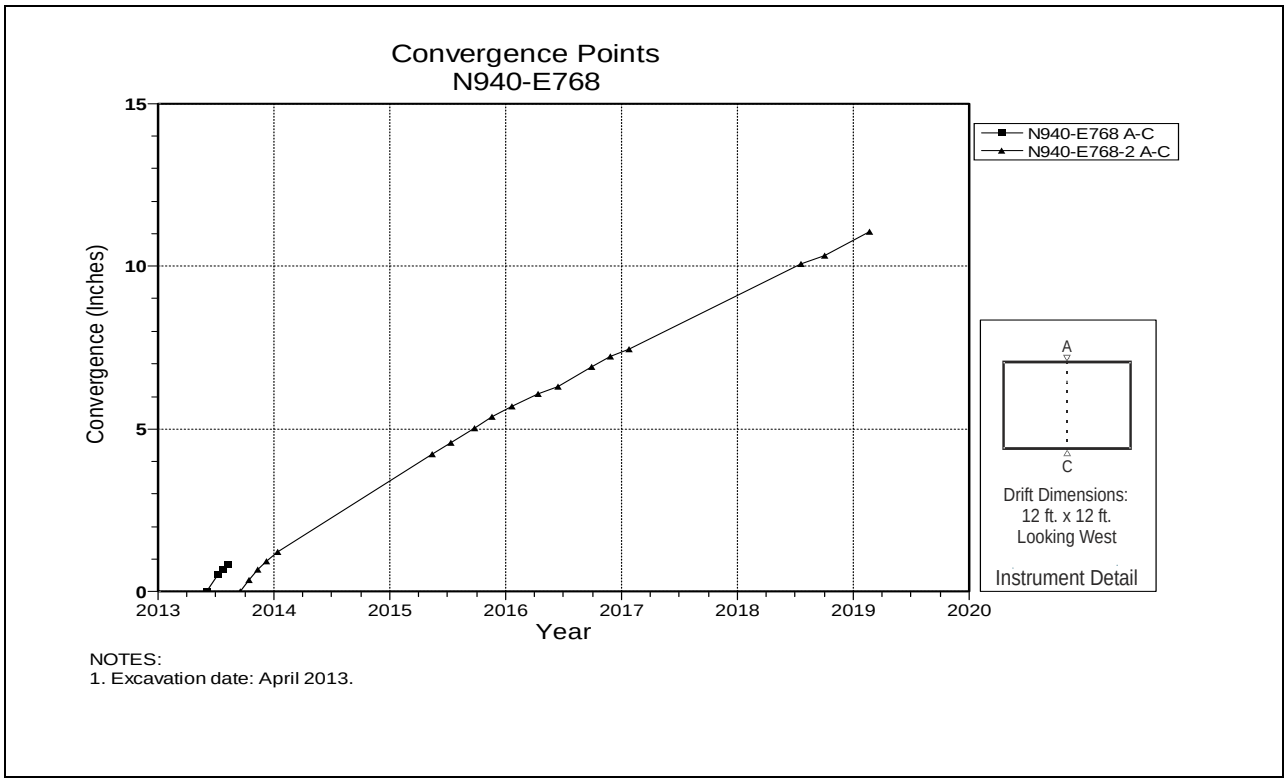

Figure 6-19 Convergence Point Array – N940 E768 – Roof to Floor

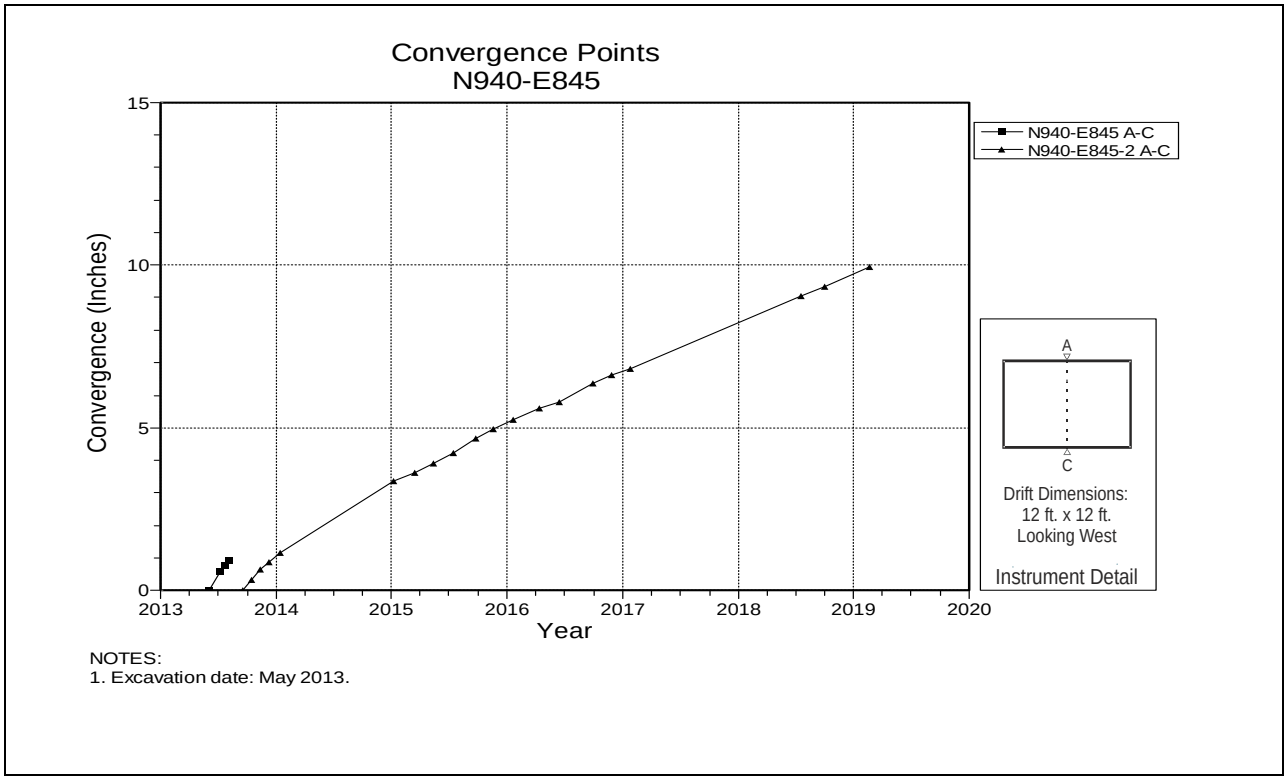

Figure 6-20 Convergence Point Array – N940 E845 – Roof to Floor

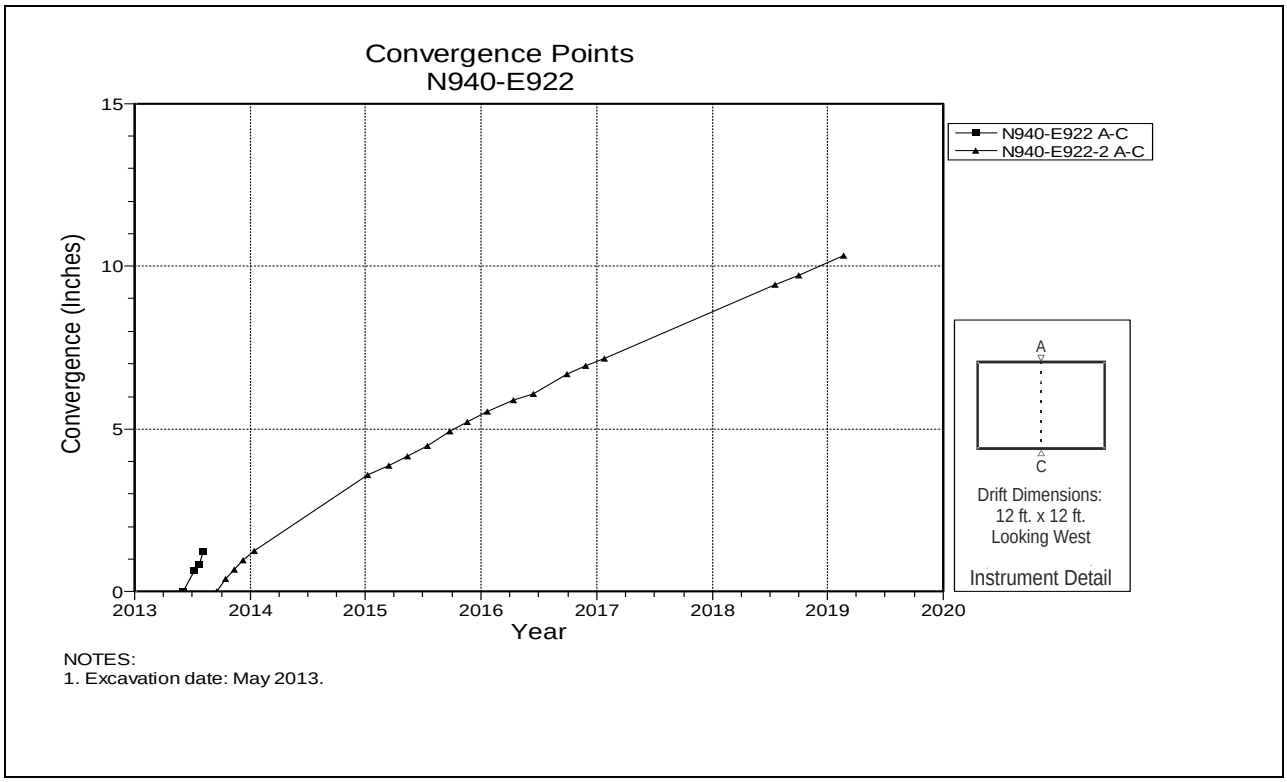

Figure 6-21 Convergence Point Array – N940 E922 – Roof to Floor

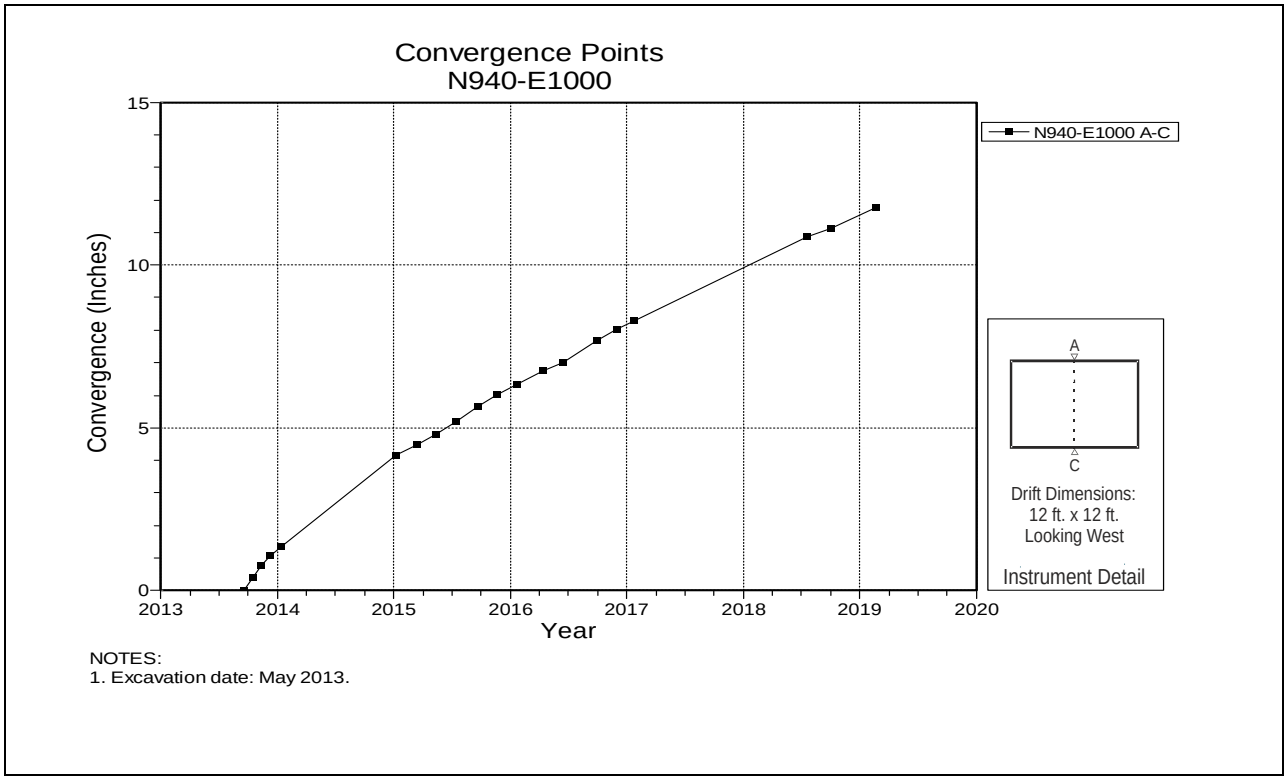

Figure 6-22 Convergence Point Array – N940 E1000 – Roof to Floor

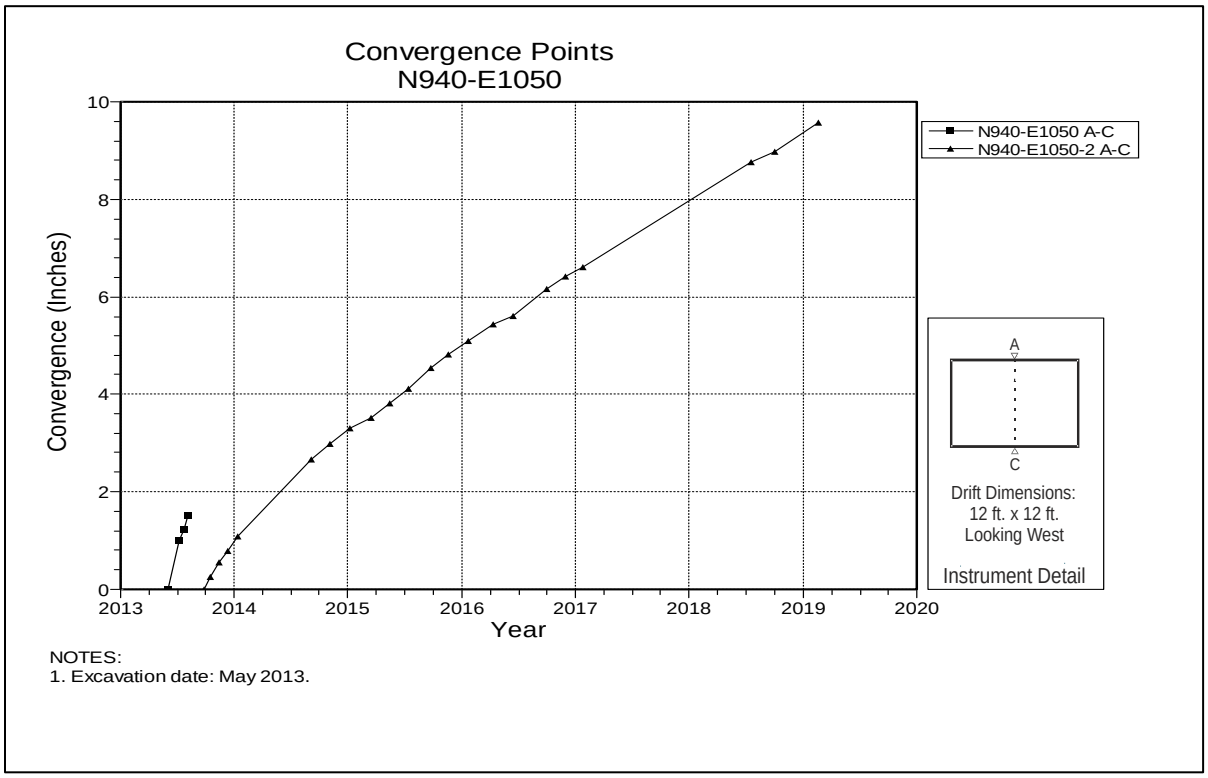

Figure 6-23 Convergence Point Array – N940 E1050 – Roof to Floor

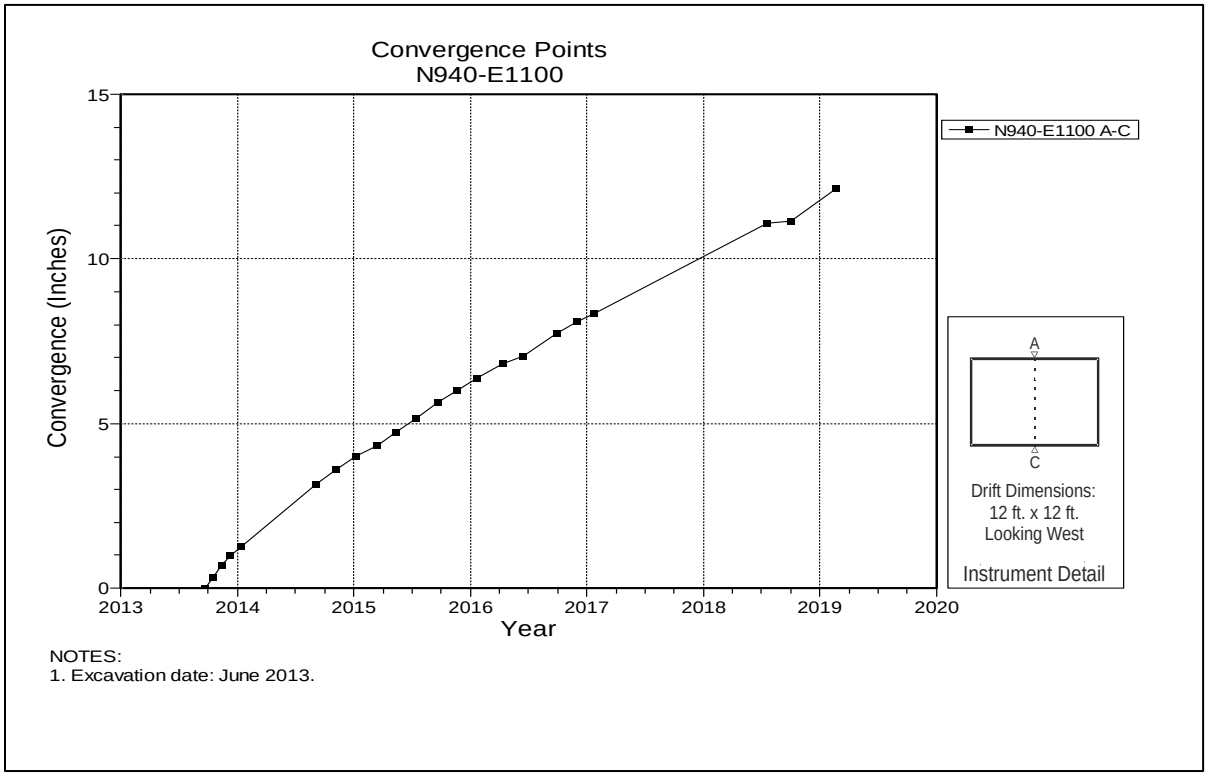

Figure 6-24 Convergence Point Array – N940 E1100 – Roof to Floor

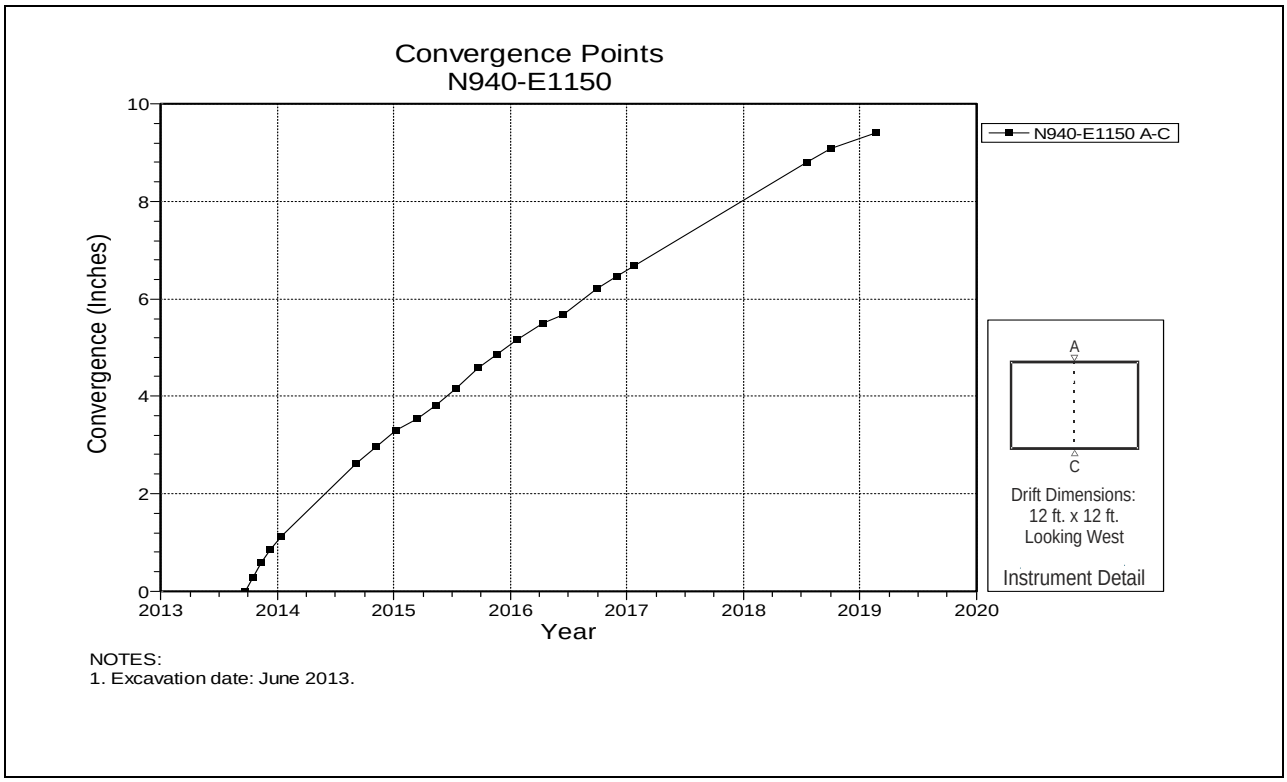

Figure 6-25 Convergence Point Array – N940 E1150 – Roof to Floor

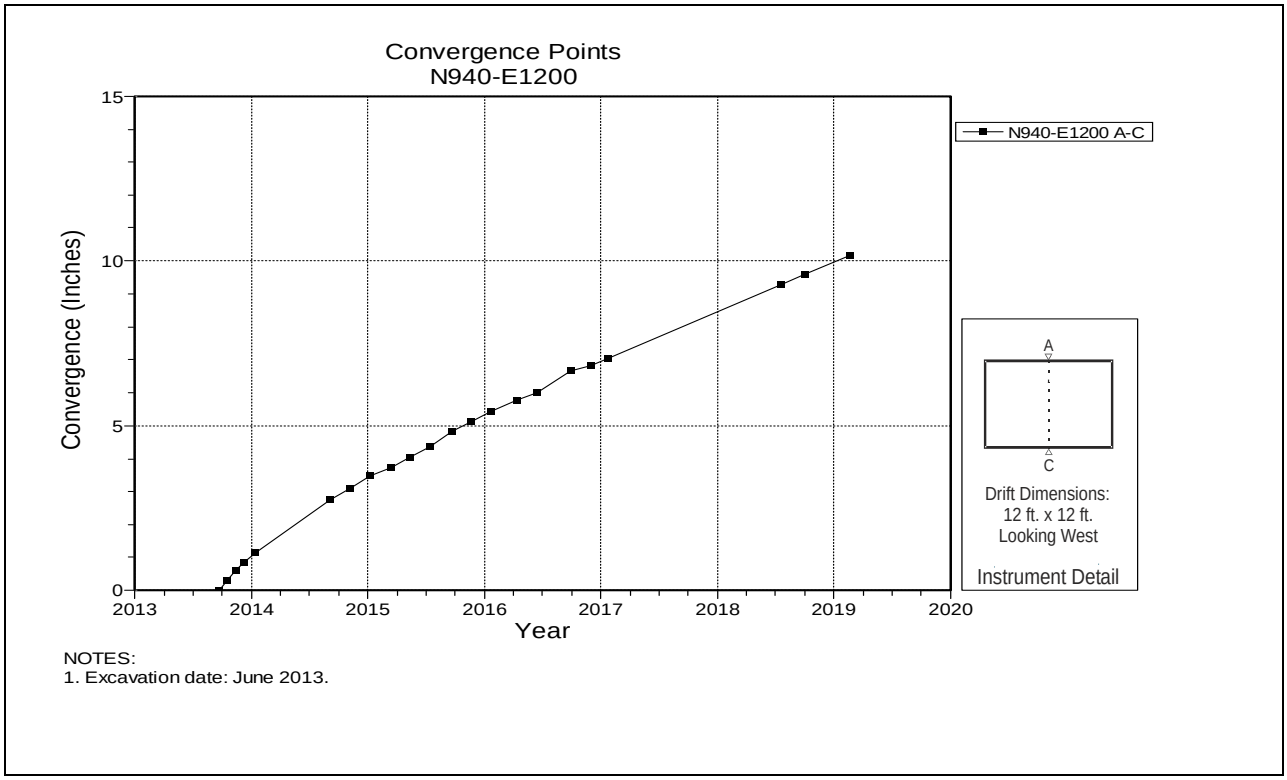

Figure 6-26 Convergence Point Array – N940 E1200 – Roof to Floor

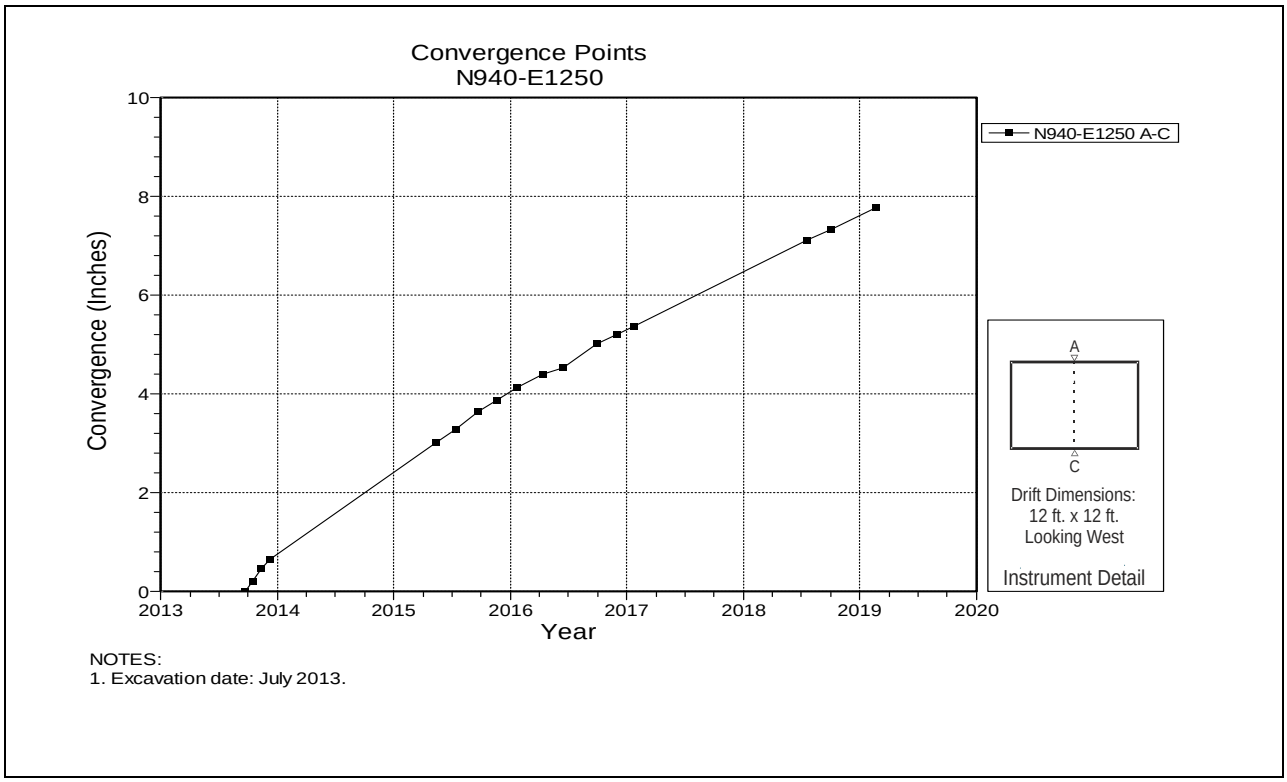

Figure 6-27 Convergence Point Array – N940 E1250 – Roof to Floor

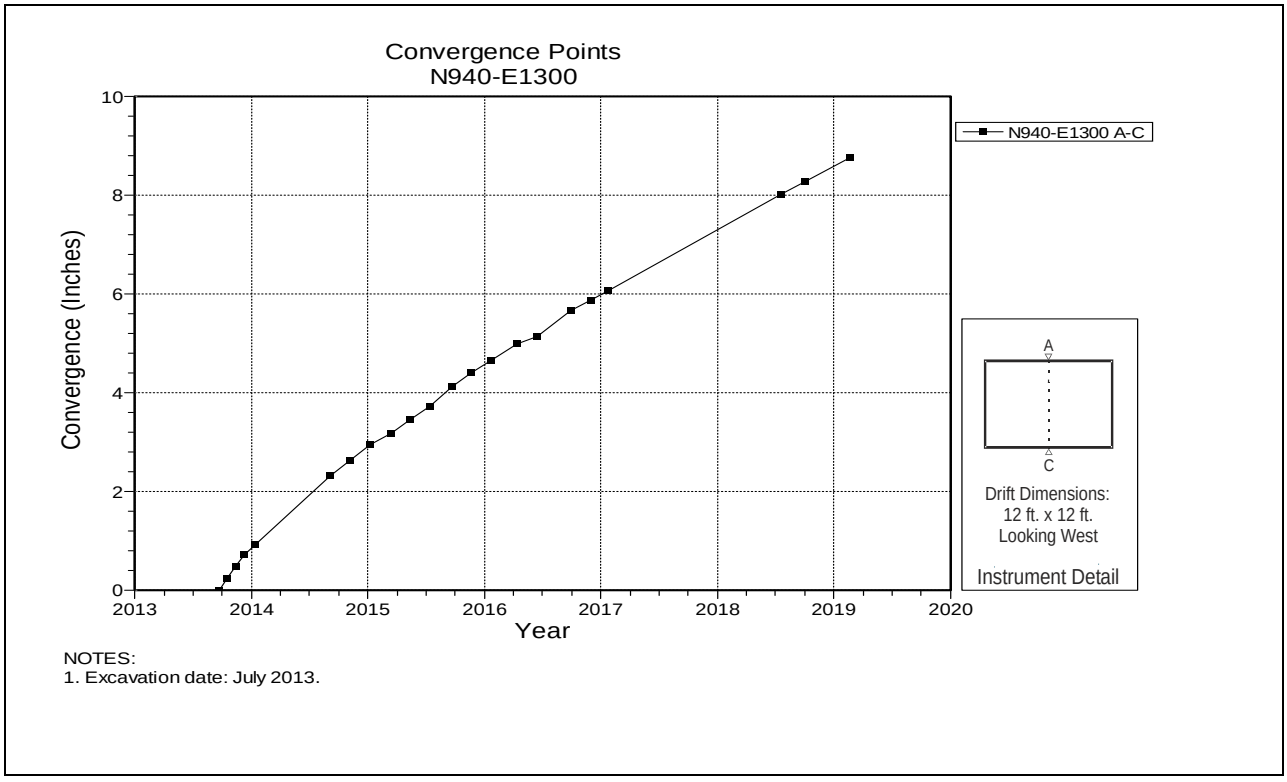

Figure 6-28 Convergence Point Array – N940 E1300 – Roof to Floor

7.0 GEOSCIENCE SUMMARY

Chapter 7 historically presented data acquired to support the WIPP Geoscience Program. This included fracture maps of excavation surfaces, stratigraphic mapping, and drilling vertical observation holes to monitor clay seam displacements and other significant geological features. The significant reduction in ventilation following the radiological release event curtailed the frequent use of man-lifting vehicles to conduct fracture and stratigraphic mapping in the underground. Once liquid fueled vehicles could once again be used in the underground, new fire protection requirements regarding the use of liquid fueled boom lifts added additional difficulties for this program.

The last reporting period where a full complement of routine geoscience activities (fracture mapping, stratigraphic mapping and borehole examinations) were performed was during the July 2013 – June 2014 period. The final activities that period were performed in early February 2014 just days before the fire, followed days later by an unrelated radioactive release.

Although geoscience work could not be performed routinely, activities were and are being performed when necessary to support ground control. For example, during the July 2015 – June 2016 reporting period, ten boreholes were drilled and inspected to support a geotechnical investigation into the rock bolt anchorage horizon in the E140 drift between S700 and S1390.

Unlike instrumentation along with routine visual inspections of the excavated surfaces, and broken bolt counts, the geoscience program does not necessarily provide an early warning as to near term and imminent ground control problems. For example, geoscience program borehole inspections are routinely performed either quarterly or biannually, depending on their location. Fracture mapping is performed quarterly and stratigraphic mapping is performed once following the final excavation of a waste panel or a newly mined area.

However, occasions do occur when geotechnical engineers want timelier observation borehole or fracture data. Such as when an accessible area may experience an increase in rates of roof beam expansion or roof to floor closure. Or, possibly when designing a new bolting pattern. These types of “on demand” inspections are still occurring and will continue to occur during the current absence of routine inspections under the geoscience program as well as when the program resumes.

Collectively, the elements of the geoscience program have produced a body of information, collected over almost 38 years. This information has described both typical and atypical characteristics of deformation at the repository horizon currently excavated. For example, low-angle fracturing, a key component to most of the roof falls that have occurred at WIPP, were first identified and mapped in Site Preliminary and Design Validation (SPDV) Room 1 in the early 1990s as part of the geoscience program.

As of this writing the geoscience program is being revitalized with the drilling and initial inspection of new observation boreholes and training of geotechnical personnel.